Fields Institute Communications 73

The Fields Institute for Research in Mathematical Sciences

Dong Eui Chang
Darryl D. Holm
George Patrick
Tudor Ratiu Editors

Geometry, Mechanics, and Dynamics

The Legacy of Jerry Marsden

FIELDS

Springer

Fields Institute Communications

VOLUME 73

The Fields Institute for Research in Mathematical Sciences

The Fields Institute is a centre for research in the mathematical sciences, located in Toronto, Canada. The Institutes mission is to advance global mathematical activity in the areas of research, education and innovation. The Fields Institute is supported by the Ontario Ministry of Training, Colleges and Universities, the Natural Sciences and Engineering Research Council of Canada, and seven Principal Sponsoring Universities in Ontario (Carleton, McMaster, Ottawa, Queen's, Toronto, Waterloo, Western and York), as well as by a growing list of Affiliate Universities in Canada, the U.S. and Europe, and several commercial and industrial partners.

More information about this series at http://www.springer.com/series/10503

Dong Eui Chang • Darryl D. Holm • George Patrick Tudor Ratiu
Editors

Geometry, Mechanics, and Dynamics

The Legacy of Jerry Marsden

FIELDS The Fields Institute for Research in the Mathematical Sciences

Springer

Editors
Dong Eui Chang
Department of Applied Mathematics
University of Waterloo
Waterloo, ON, Canada

George Patrick
Department of Mathematics and Statistics
University of Saskatchewan
Saskatoon, SK, Canada

Darryl D. Holm
Department of Mathematics
Imperial College London
London, UK

Tudor Ratiu
Section de Mathématiques
Ecole Polytechnique Fédérale de Lausanne
Lausanne, Switzerland

ISSN 1069-5265 ISSN 2194-1564 (electronic)
Fields Institute Communications
ISBN 978-1-4939-2440-0 ISBN 978-1-4939-2441-7 (eBook)
DOI 10.1007/978-1-4939-2441-7

Library of Congress Control Number: 2015933501

Mathematics Subject Classification (2010): 00Bxx, 37-02, 49-02, 53-02, 58-02, 65-02, 70-02

Springer New York Heidelberg Dordrecht London

Cover illustration: Drawing of J.C. Fields by Keith Yeomans

Printed on acid-free paper

Springer Science+Business Media LLC New York is part of Springer Science+Business Media (www.springer.com)

Preface to Fields Volume

Jerrold Eldon Marsden, an eminent mathematician of our time, passed away on September 21, 2010, at the age of 68. This volume contains 20 papers presented at a focus program in honor of Jerry Marsden's legacy in Geometry, Mechanics, and Dynamics held in July 2012 at the Fields Institute for Research in Mathematical Sciences. Marsden helped found the Fields Institute in 1992. It was initially directed by him, and memorable workshops in honor of his 50th and 60th birthday celebrations were held there in 1992 and 2002, respectively. Information about Jerry's contributions, influence, and personal interactions and an overview of the Marsden Legacy focus program at Fields are available at http://www.fields.utoronto.ca/programs/scientific/12-13/Marsden/index.html. Many of Jerry's research publications and more information about him may also be found at http://www.cds.caltech.edu/~marsden/.

No single volume could do justice to the legacy of Jerry Marsden's research and his personal influence on the field of Geometric Mechanics, which he helped create. Many of Jerry's papers and books have received hundreds of citations; some of them have received thousands. The legacy of his influence in mathematics, physics, and computational science, though, is not countable. We miss him dearly.

Waterloo, ON, Canada — Dong Eui Chang
London, UK — Darryl D. Holm
Saskatoon, SK, Canada — George Patrick
Lausanne, Switzerland — Tudor Ratiu

Contents

A Global Version of the Koon-Marsden Jacobiator Formula

Paula Balseiro

Dedicated to the memory of J.E. Marsden

Abstract In this paper we study the Jacobiator (the cyclic sum that vanishes when the Jacobi identity holds) of the almost Poisson brackets describing nonholonomic systems. We revisit the local formula for the Jacobiator established by Koon and Marsden (Rep Math Phys 42:101–134, 1998) using suitable local coordinates and explain how it is related to the global formula obtained in Balseiro (Arch. Ration. Mech. Anal. 214(2):453-501, 2014), based on the choice of a complement to the constraint distribution. We use an example to illustrate the benefits of the coordinate-free viewpoint.

1 Introduction

The geometric approach to nonholonomic systems was among the many research interests of J.E. Marsden, and his contributions to this area were fundamental. A system with nonholonomic constraints can be geometrically described by an almost Poisson bracket [10, 15, 18], whose failure to satisfy the Jacobi identity, measured by the so-called Jacobiator, is precisely what encodes the nonholonomic nature of the system. There is a vast literature on the study of such nonholonomic brackets and their properties, starting with the early work of Chaplygin [6], see e.g. [2, 5, 8–12]. An explicit formula for the Jacobiator of nonholonomic brackets, expressed in suitable local coordinates, was obtained by Koon and Marsden in their 1998 paper [14]. In the present paper, we revisit the Koon-Marsden formula of [14] and explain how it can be derived from the coordinate-free Jacobiator formula for nonholonomic brackets obtained in [1].

We organize the paper as follows. In Section 2, we recall the hamiltonian viewpoint to systems with nonholonomic constraints. For a nonholonomic system

P. Balseiro (✉)
Instituto de Matemática, Universidade Federal Fluminense, Rua Mario Santos Braga S/N, 24020-140 Niteroi, Rio de Janeiro, Brazil
e-mail: pbalseiro@vm.uff.br

D.E. Chang et al. (eds.), *Geometry, Mechanics, and Dynamics*, Fields Institute Communications 73, DOI 10.1007/978-1-4939-2441-7_1

on a configuration manifold Q, determined by a lagrangian $L : TQ \to \mathbb{R}$ and a nonintegrable distribution D on Q (the *constraint distribution*, defining the permitted velocities of the system), we consider the induced *nonholonomic bracket* $\{\cdot,\cdot\}_{\text{nh}}$ defined on the submanifold $\mathcal{M} := \text{Leg}(D)$ of T^*Q, where $\text{Leg} : T^*Q \to TQ$ is the Legendre transform (see Section 2.2). In Section 2.3 (see Theorem 1) we recall the global formula for the Jacobiator of $\{\cdot,\cdot\}_{\text{nh}}$ from [1], which depends on the choice of a complement W of the constraint distribution D such that $TQ = D \oplus W$. As shown in [1], this formula is useful to provide information about properties of reduced nonholonomic brackets in the presence of symmetries.

In Section 3 we recall the choice of coordinates, suitably adapted to the constraints, used by Koon and Marsden in [14], and in terms of which their Jacobiator formula is expressed. We then compare the global and local viewpoints in Section 4, explaining how one can derive the local Jacobiator formula in [14] from the coordinate-free formula in [1].

Since the formula in [1] is coordinate free, it can be used in examples without specific choices of coordinates. We illustrate this fact studying the *snakeboard*, following [14, 17]; here the natural coordinates in the problem are not adapted to the constraints so, in principle, the local formula from [14] cannot be directly applied.

2 Nonholonomic Systems

2.1 The Hamiltonian Viewpoint

A nonholonomic system is a mechanical system on a configuration manifold Q with constraints on the velocities which are not derived from constraints in the positions. Mathematically, it is defined by a lagrangian $L : TQ \to \mathbb{R}$ of mechanical type, i.e., $L = \kappa - U$ where κ is the kinetic energy metric and $U \in C^\infty(Q)$ is the potential energy, and a nonintegrable distribution D on Q determining the constraints, see [3, 7]. If D is an integrable distribution then the system is called *holonomic*.

In order to have an intrinsic formulation of the dynamics of nonholonomic systems, let us consider the Legendre transform $\text{Leg} : TQ \to T^*Q$ associated to the lagrangian L. The Legendre transform is a diffeomorphism since $\text{Leg} = \kappa^\flat$, where $\kappa^\flat : TQ \to T^*Q$ is defined by $\kappa^\flat(X)(Y) = \kappa(X, Y)$. We denote by $\mathcal{H} : T^*Q \to \mathbb{R}$ the hamiltonian function associated to the lagragian L.

We define the constraint submanifold $\mathcal{M}$ of T^*Q by $\mathcal{M} = \kappa^\flat(D)$. Note that $\mathcal{M}$ is a vector subbundle of T^*Q. We denote by $\tau : \mathcal{M} \to Q$ the restriction to $\mathcal{M}$ of the canonical projection $\tau_Q : T^*Q \to Q$.

On $\mathcal{M}$ we have a natural 2-form $\Omega_{\mathcal{M}}$ given by $\Omega_{\mathcal{M}} := \iota^*\Omega_Q$ where $\iota : \mathcal{M} \to T^*Q$ is the inclusion and Ω_Q is the canonical 2-form on T^*Q. The constraints are encoded on a (regular) distribution $\mathcal{C}$ on $\mathcal{M}$ defined, at each $m \in \mathcal{M}$, by

$$\mathcal{C}_m = \{v \in T_m\mathcal{M} \ : \ T\tau(v) \in D_{\tau(m)}\}. \tag{1}$$

It was proven in [2] that the point-wise restriction of the 2-form $\Omega_{\mathcal{M}}$ to $\mathcal{C}$, denoted by $\Omega_{\mathcal{M}}|_{\mathcal{C}}$, is nondegenerate. That is, if $X \in \Gamma(\mathcal{C})$ is such that $\mathbf{i}_X \Omega_{\mathcal{M}}|_{\mathcal{C}} \equiv 0$, then $X = 0$. Therefore, there is a unique vector field X_{nh} on $\mathcal{M}$, called the *nonholonomic vector field*, such that $X_{\text{nh}}(m) \in \mathcal{C}_m$ and

$$\mathbf{i}_{X_{\text{nh}}} \Omega_{\mathcal{M}}|_{\mathcal{C}} = d\mathcal{H}_{\mathcal{M}}|_{\mathcal{C}}, \tag{2}$$

where $\mathcal{H}_{\mathcal{M}} := \iota^* \mathcal{H} : \mathcal{M} \to \mathbb{R}$. The integral curves of X_{nh} are solutions of the nonholonomic dynamics [2].

In order to write (2) in local coordinates, suppose that the constraint distribution D is described (locally) by the annihilators of 1-forms ϵ^a for $a = 1, \ldots, k$, that is $D = \{(q, \dot{q}) : \epsilon^a(q)(\dot{q}) = 0 \text{ for all } a = 1, \ldots, k\}$. If we consider canonical coordinates (q^i, p_i) on T^*Q then the constraints are given by

$$\epsilon_i^a(q) \frac{\partial \mathcal{H}}{\partial p_i} = 0, \qquad \text{for } a = 1, \ldots, k,$$

and (2) becomes

$$\dot{q}^i = \frac{\partial \mathcal{H}}{\partial p_i}, \qquad \dot{p}_i = -\frac{\partial \mathcal{H}}{\partial q^i} + \lambda_a \epsilon^a,$$

where λ_a are functions (called the Lagrange multipliers) which are uniquely determined by the fact that the constraints are satisfied.

2.2 The Nonholonomic Bracket

Recall that an *almost Poisson bracket* on $\mathcal{M}$ is an $\mathbb{R}$-bilinear bracket $\{\cdot, \cdot\} : C^\infty(\mathcal{M}) \times C^\infty(\mathcal{M}) \to C^\infty(\mathcal{M})$ that is skew-symmetric and satisfies the Leibniz condition:

$$\{fg, h\} = f\{g, h\} + \{f, h\}g, \qquad \text{for } f, g, h \in C^\infty(\mathcal{M}).$$

If $\{\cdot, \cdot\}$ satisfies the Jacobi identity, then the bracket is called *Poisson*. The *hamiltonian vector field* X_f on $\mathcal{M}$ associated to a $f \in C^\infty(\mathcal{M})$ is defined by

$$X_f = \{\cdot, f\} \tag{3}$$

and the *characteristic distribution* of $\{\cdot, \cdot\}$ is the distribution on the manifold $\mathcal{M}$ whose fibers are spanned by the hamiltonian vector fields. If the bracket is Poisson, then its characteristic distribution is integrable. However, the converse is not always true.

From the Leibniz identity it follows that there is a one-to-one correspondence between almost Poisson brackets $\{\cdot,\cdot\}$ and bivector fields $\pi \in \bigwedge^2(T\mathcal{M})$ given by

$$\{f,g\} = \pi(df,dg), \qquad f,g, \in C^\infty(\mathcal{M}). \tag{4}$$

Let us denote by $\pi^\sharp : T^*\mathcal{M} \to T\mathcal{M}$ the map defined by $\beta(\pi^\sharp(\alpha)) = \pi(\alpha,\beta)$. Then, using (3), the hamiltonian vector field X_f is also given by $X_f = -\pi^\sharp(df)$ and the characteristic distribution of π is the image of $\pi^\sharp$. The Schouten bracket $[\pi,\pi]$ (see [16]) measures the failure of the Jacobi identity of $\{\cdot,\cdot\}$ through the relation

$$\frac{1}{2}[\pi,\pi](df,dg,dh) = \{f,\{g,h\}\} + \{f,\{g,h\}\} + \{g,\{h,f\}\} + \{h,\{f,g\}\} \tag{5}$$

for $f,g,h \in C^\infty(\mathcal{M})$. So we refer to the trivector $\frac{1}{2}[\pi,\pi]$ as the *Jacobiator* of π, which is zero when π is a Poisson bivector.

Coming back to our context, consider a nonholonomic system on a manifold Q defined by a lagrangian L and a constraint distribution D. Due to the nondegeneracy of $\Omega_{\mathcal{M}}|_{\mathcal{C}}$, there is an induced bivector field $\pi_{\text{nh}} \in \bigwedge^2(T\mathcal{M})$ defined at each $\alpha \in T^*\mathcal{M}$ by

$$\pi_{\text{nh}}^\sharp(\alpha) = X \quad \text{if and only if} \quad \mathbf{i}_X\Omega_{\mathcal{M}}|_{\mathcal{C}} = -\alpha|_{\mathcal{C}}. \tag{6}$$

The characteristic distribution of π_{nh} is the distribution $\mathcal{C}$ defined in (1). Since $\mathcal{C}$ is not integrable, π_{nh} is not Poisson.

The bivector field π_{nh} is called the *nonholonomic bivector field* [10, 15, 18] and it describes the dynamics in the sense that

$$\pi_{\text{nh}}^\sharp(d\mathcal{H}_{\mathcal{M}}) = -X_{\text{nh}}. \tag{7}$$

By (4), the nonholonomic bivector π_{nh} defines uniquely an almost Poisson bracket $\{\cdot,\cdot\}_{\text{nh}}$ on $\mathcal{M}$, called the *nonholonomic bracket*. From (6) we observe that

$$\{f,g\}_{\text{nh}} = \Omega_{\mathcal{M}}(X_f,X_g) \qquad \text{for } f,g \in C^\infty(\mathcal{M}),$$

where $X_f = -\pi_{\text{nh}}^\sharp(df)$ and $X_g = -\pi_{\text{nh}}^\sharp(dg)$. The nonholonomic vector field (7) is equivalently defined through the equation $X_{\text{nh}} = \{\cdot,\mathcal{H}_{\mathcal{M}}\}_{\text{nh}}$.

2.3 The Jacobiator Formula

Recall that $\mathcal{C}$ is a smooth distribution on $\mathcal{M}$. Choose a complement $\mathcal{W}$ of $\mathcal{C}$ on $T\mathcal{M}$ such that, for each $m \in \mathcal{M}$,

$$T_m\mathcal{M} = \mathcal{C}_m \oplus \mathcal{W}_m. \tag{8}$$

Let $P_{\mathcal{C}} : T\mathcal{M} \to \mathcal{C}$ and $P_{\mathcal{W}} : T\mathcal{M} \to \mathcal{W}$ be the projections associated to the decomposition (8). Since $P_{\mathcal{W}} : T\mathcal{M} \to \mathcal{W}$ can be seen as a $\mathcal{W}$-valued 1-form, following [1], we define the $\mathcal{W}$-valued 2-form $\mathbf{K}_{\mathcal{W}}$ given by

$$\mathbf{K}_{\mathcal{W}}(X, Y) = -P_{\mathcal{W}}([P_{\mathcal{C}}(X), P_{\mathcal{C}}(Y)]) \qquad \text{for } X, Y \in \mathfrak{X}(\mathcal{M}). \tag{9}$$

Once a complement $\mathcal{W}$ of $\mathcal{C}$ is chosen, we obtain a coordinate-free formula for the Jacobiator of the nonholonomic bracket.

Theorem 1 ([1]). *The following holds:*

$$\begin{aligned}&\frac{1}{2}[\pi_{\text{nh}}, \pi_{\text{nh}}](\alpha, \beta, \gamma)\\ &= \Omega_{\mathcal{M}}(\mathbf{K}_{\mathcal{W}}(\pi_{\text{nh}}^{\sharp}(\alpha), \pi_{\text{nh}}^{\sharp}(\beta)), \pi_{\text{nh}}^{\sharp}(\gamma)) - \gamma\left(\mathbf{K}_{\mathcal{W}}(\pi_{\text{nh}}^{\sharp}(\alpha), \pi_{\text{nh}}^{\sharp}(\beta))\right) + \text{cyclic.}\end{aligned} \tag{10}$$

for $\alpha, \beta, \gamma \in T^*\mathcal{M}$.

In fact, a more general formula appeared in [1], valid for any bivector field π_B gauge related to π_{nh}. In that context, this formula was used to understand under which circumstances the reduction of π_B by symmetries had an integrable characteristic distribution (even if it was not Poisson).

We will now show how this formula recovers the coordinate Jacobiator formula obtained in [14].

3 The Koon-Marsden Adapted Coordinates

In this section we will recall the Koon-Marsden approach to writing the Jacobiator of a nonholonomic bracket, based on a suitable choice of coordinates of the manifold Q. After this, we will write the objects presented in Section 2 (such as the 2-forms $\Omega_{\mathcal{M}}$ and $\mathbf{K}_{\mathcal{W}}$, and the bivector π_{nh}) in such local coordinates in order to see the equivalence between the local and global viewpoints.

We start by recalling the coordinates chosen in [14]. Consider a nonholonomic system given by a lagrangian L and a nonintegrable distribution D. Let ϵ^a for $a = 1, \ldots, k$ be 1-forms that span the annihilator of D, i.e., $D^\circ = \text{span}\{\epsilon^a\}$. The authors in [14] introduce local coordinates $(q^i) = (r^\alpha, s^a)$ on Q for which each 1-form ϵ^a has the form

$$\epsilon^a = ds^a + A^a_\alpha(r, s)dr^\alpha, \tag{11}$$

where A^a_α are functions on Q for $\alpha = 1, \ldots, n-k$ and $a = 1, \ldots, k$. During the present paper, we refer to the coordinates (r^α, s^a) such that (11) is satisfied as *coordinates adapted to the constraints*.

These coordinates induce a (local) basis of D given by $\{X_\alpha := \frac{\partial}{\partial r^\alpha} - A^a_\alpha \frac{\partial}{\partial s^a}\}$. We complete the basis $\{X_\alpha\}$ and $\{\epsilon^a\}$ in order to obtain dual basis on TQ and T^*Q, that is

$$TQ = \text{span}\left\{X_\alpha, \frac{\partial}{\partial s^a}\right\} \quad \text{and} \quad T^*Q = \text{span}\{dr^\alpha, \epsilon^a\}.$$

Let $(\tilde{p}_\alpha, \tilde{p}_a)$ be the coordinates on T^*Q associated to the basis $\{dr^\alpha, \epsilon^a\}$. Since $\mathcal{M} = \text{span}\{\kappa^\flat(X_\alpha)\} \subset T^*Q$ then

$$\mathcal{M} = \{(q^i, \tilde{p}_a, \tilde{p}_\alpha) \ : \ \tilde{p}_a = [\kappa_{a\alpha}][\kappa_{\alpha\beta}]^{-1}\tilde{p}_\beta = J^\beta_a \tilde{p}_\beta\}, \tag{12}$$

where $[\kappa_{a\alpha}]$ denotes the $(k\times(n-k))$-matrix with entries given by $\kappa_{a\alpha} = \kappa(\frac{\partial}{\partial s^a}, X_\alpha)$, $[\kappa_{\alpha\beta}]^{-1}$ is the inverse matrix associated to the invertible $((n-k)\times(n-k))$-matrix with entries given by $\kappa_{\alpha\beta} = \kappa(X_\alpha, X_\beta)$ and J^β_a are the functions on Q representing the entries of the matrix $[\kappa_{a\alpha}][\kappa_{\alpha\beta}]^{-1}$. Therefore, each element $(r^\alpha, s^a; \tilde{p}_\alpha)$ represents a point on the manifold $\mathcal{M}$.

In [14] the Jacobiator formula is written in terms of the curvature of an Ehresmann connection. The local coordinates (r^α, s^a) induce a fiber bundle with projection given by $\upsilon(r^\alpha, s^a) = r^\alpha$. Let us call W the vertical distribution defined by this projection.

The Ehresmann connection A on $\upsilon : Q = \{r^\alpha, s^a\} \to R = \{r^\alpha\}$ is chosen in such a way that its horizontal space agrees with the distribution D. The connection A is represented by a vector-valued differential form given, at each $X \in TQ$, by

$$A(X) = \epsilon^a(X)\frac{\partial}{\partial s^a}. \tag{13}$$

The *curvature* associated to this connection is a vector-valued 2-form $\mathbf{K}_W$ defined on $X, Y \in \mathfrak{X}(Q)$ by

$$\mathbf{K}_W(X, Y) = -A([P_D(X), P_D(Y)]), \tag{14}$$

where $P_D : TQ \to TQ$ is the projection to D given by $P_D(X) = dr^\alpha(X)X_\alpha$.

In coordinates, the curvature $\mathbf{K}_W$ is given by the following formula [14, Sec. 2.1]:

$$\mathbf{K}_W(X, Y) = d\epsilon^a(P_D(X), P_D(Y))\frac{\partial}{\partial s^a},$$

hence, locally,

$$d\epsilon^a|_D = C^a_{\alpha\beta} dr^\alpha \wedge dr^\beta|_D, \tag{15}$$

where $C^a_{\alpha\beta}(r,s) = \dfrac{\partial A^a_\beta}{\partial r^\alpha} - A^b_\alpha \dfrac{\partial A^a_\beta}{\partial s^b}$. Let us define

$$K^a_{\alpha\beta} = C^a_{\alpha\beta} - C^a_{\beta\alpha}. \tag{16}$$

For each $a = 1,\dots,k$ the coefficients $K^a_{\alpha\beta}$ are skew-symmetric and $d\epsilon^a|_D = K^a_{\alpha\beta} dr^\alpha \wedge dr^\beta|_D$, for $\alpha < \beta$. Therefore, if $X, \bar{X} \in D$ then $d\epsilon^a(X,\bar{X}) = K^a_{\alpha\beta} v^\alpha \bar{v}^\beta$ where $X = v^\alpha X_\alpha$ and $\bar{X} = \bar{v}^\beta X_\beta$.

Remark 1. Observe that in [14], the 1-forms ϵ^a where denoted by ω^a while $\mathbf{K}_W$ was denoted by B and the coefficients $K^a_{\alpha\beta}$ were $-B^a_{\alpha\beta}$. In this case, for $\dot{q} \in D$ then $d\omega^b(\dot{q},\cdot)|_D = -B^b_{\alpha\beta}\dot{r}^\alpha dr^\beta|_D$ (observe the correction in the sign with respect to the equation in [14, Sec. 2.1]).

Finally, in [14, Theorem 2.1] the almost Poisson bracket $\{\cdot,\cdot\}_{\mathcal{M}}$ describing the dynamics of a nonholonomic system was written following [18] but in local coordinates on Q adapted to the constraints (11). That is, $\{\cdot,\cdot\}_{\mathcal{M}}$ was computed from the canonical Poisson bracket on T^*Q but written in terms of the adapted coordinates $(r^\alpha, s^a, \tilde{p}_\alpha, \tilde{p}_a)$. As a result, the almost Poisson bracket $\{\cdot,\cdot\}_{\mathcal{M}}$ on $\mathcal{M}$, written in local coordinates $(r^\alpha, s^a, \tilde{p}_\alpha)$, has the following form [14]

$$\{q^i, q^j\}_{\mathcal{M}} = 0, \quad \{r^\alpha, \tilde{p}_\beta\}_{\mathcal{M}} = \delta^\beta_\alpha, \quad \{s^a, \tilde{p}_\alpha\}_{\mathcal{M}} = -A^a_\alpha, \quad \{\tilde{p}_\alpha, \tilde{p}_\beta\}_{\mathcal{M}} = K^b_{\alpha\beta} J_b^\gamma \tilde{p}_\gamma \tag{17}$$

4 The Coordinate Version of the Jacobiator Formula

4.1 Interpretation of the Adapted Coordinates

In this section, we will relate the choice of the coordinates proposed in [14] with the choice of a complement $\mathcal{W}$ done in [1] (see (11) and (8), respectively). We will also connect the *curvature* (14) with the 2-form (9), and the nonholonomic bivector π_{nh} with the bracket $\{\cdot,\cdot\}_{\mathcal{M}}$ given in (6) and (17), respectively.

Consider a nonholonomic system on a manifold Q given by a lagrangian L and a nonintegrable distribution D. Let us consider local coordinates (r^α, s^a) adapted to the constraints as in (11).

Lemma 1. *The choice of coordinates (r^α, s^a) adapted to the constraints (11), induce a complement W of D on TQ such that*

$$TQ = D \oplus W, \qquad \textit{where} \quad W = \operatorname{span}\left\{\frac{\partial}{\partial s^a}\right\}. \tag{18}$$

The projection $P_W : TQ \to W$ associated to the decomposition (18) is interpreted in [14] as the Ehresmann connection A (13). In this context we compare the curvature $\mathbf{K}_W$ defined in (14) (see [14]) with the $\mathcal{W}$-valued 2-form $\mathbf{K}_\mathcal{W}$ defined in (9).

Recall that the submanifold $\mathcal{M} = \kappa^\flat(D) \subset T^*Q$ is described by local coordinates $(r^\alpha, s^a; \tilde{p}_\alpha)$ (see (12)). Locally $T^*\mathcal{M}$ is generated by the basis $\mathfrak{B}_{T^*\mathcal{M}} = \{dr^\alpha, \epsilon^a, d\,\tilde{p}_\alpha\}$. During the rest of the paper, when there is no risk of confusion, we will use the same notation for 1-forms on Q and their pull back to $\mathcal{M}$ and T^*Q, (i.e., $\tau^* dr^\alpha = dr^\alpha$ and $\tau^*\epsilon^a = \epsilon^a$ where $\tau : \mathcal{M} \to Q$ is the canonical projection).

Since τ-projectable vector fields generate $T\mathcal{M}$ at each point, we can consider a complement $\mathcal{W}$ of $\mathcal{C}$ generated by τ-projectable vector fields Z_a such that $T\tau(Z_a) \in W$. That is,

$$\mathcal{C} = \operatorname{span}\left\{ X_\alpha, \frac{\partial}{\partial \tilde{p}_\alpha} \right\} \quad \text{and} \quad \mathcal{W} = \operatorname{span}\left\{ Z_a \ : \ T\tau(Z_a) = \frac{\partial}{\partial s^a} \right\}. \tag{19}$$

Lemma 2. *Let $\mathcal{W}$ be a complement of $\mathcal{C}$ as in (19) where W is the complement of D induced by the coordinates (r^α, s^a) as in Lemma 1.*

(i) The $\mathcal{W}$-valued 2-form $\mathbf{K}_\mathcal{W}$ and the curvature $\mathbf{K}_W$, defined in (9) and (14) respectively, are related, at each $X, Y \in T\mathcal{M}$, by $\mathbf{K}_W(T\tau(X), T\tau(Y)) = T\tau(\mathbf{K}_\mathcal{W}(X, Y))$. In local coordinates (r^α, s^a) adapted to the constraints (11), the following holds:

$$\mathbf{K}_\mathcal{W}|_\mathcal{C} = (C^a_{\alpha\beta} dr^\alpha \wedge dr^\beta|_\mathcal{C}) \otimes Z_a.$$

(ii) Let $\bar{\mathcal{W}}$ be a different complement of $\mathcal{C}$ such that $T\tau(\mathcal{W}) = T\tau(\bar{\mathcal{W}}) = W$. For $X, Y \in \Gamma(\mathcal{C})$ we have

$$\mathbf{K}_\mathcal{W}(X, Y) - \mathbf{K}_{\bar{\mathcal{W}}}(X, Y) \in \Gamma(\mathcal{C}).$$

Proof.

(i) During this proof and to avoid confusion, we will work with the basis $\{\tau^* dr^\alpha, \tau^*\epsilon^a, d\,\tilde{p}_\alpha\}$ of $T^*\mathcal{M}$, keeping dr^α and ds^a to denote 1-forms on Q. Let us consider the basis $\mathfrak{B} = \{X_\alpha, \frac{\partial}{\partial \tilde{p}_\alpha}, Z_a\}$ of $T\mathcal{M}$ adapted to $\mathcal{C} \oplus \mathcal{W}$ and its dual $\mathfrak{B}^* = \{\tau^* dr^a, \Psi_\alpha, \tau^*\epsilon^a\}$ where $\Psi_\beta(X_\alpha) = \Psi_\beta(Z_a) = 0$ and $\Psi_\beta(\frac{\partial}{\partial \tilde{p}_\alpha}) = \delta_{\alpha\beta}$. Then, for $X, Y \in \Gamma(\mathcal{C})$,

$$\begin{aligned} \mathbf{K}_\mathcal{W}(X, Y) &= -P_\mathcal{W}([X, Y]) = -\tau^*\epsilon^a([X, Y])Z_a \\ &= d\tau^*\epsilon^a(X, Y)Z_a = d\epsilon^a(T\tau(X), T\tau(Y))Z_a. \end{aligned}$$

Therefore, $T\tau(\mathbf{K}_\mathcal{W}(X, Y)) = d\epsilon^a(T\tau(X), T\tau(Y)) \otimes \frac{\partial}{\partial s^a} = \mathbf{K}_W(T\tau(X), T\tau(Y))$.

Finally, since $T\tau(X), T\tau(Y) \in \Gamma(D)$ (see (1)) and using (15) we obtain

$$\mathbf{K}_{\mathcal{W}}|_{\mathcal{C}} = (C^a_{\alpha\beta}\tau^* dr^\alpha \wedge \tau^* dr^\beta|_{\mathcal{C}}) \otimes Z_a.$$

Using our simplified notation ($\tau^* dr^\alpha = dr^\alpha$) we obtain the desired formula.

(*ii*) Let $\mathfrak{B}$ and $\mathfrak{B}^*$ be the basis as in item (*i*). Consider also $\bar{\mathfrak{B}} = \{X_\alpha, \frac{\partial}{\partial \tilde{p}_\alpha}, \bar{Z}_a\}$ a basis of $T\mathcal{M}$ adapted to $T\mathcal{M} = \mathcal{C} \oplus \bar{\mathcal{W}}$ such that $T\tau(\bar{Z}_a) = \frac{\partial}{\partial s^a}$ and its dual $\bar{\mathfrak{B}}^* = \{dr^\alpha, \bar{\Psi}_\alpha, \epsilon^a\}$, such that $\bar{\Psi}_\beta(X_\alpha) = \bar{\Psi}_\beta(\bar{Z}_a) = 0$ and $\bar{\Psi}_\beta(\frac{\partial}{\partial \tilde{p}_\alpha}) = \delta_{\alpha\beta}$. Then we have that, for $X, Y \in \mathcal{C}$,

$$\begin{aligned}\mathbf{K}_{\bar{\mathcal{W}}}(X,Y) &= -P_{\bar{\mathcal{W}}}([X,Y]) \\ &= \epsilon^a([X,Y])\bar{Z}_a = \mathbf{K}_{\mathcal{W}}(X,Y) + \epsilon^a([X,Y]) \otimes (\bar{Z}_a - Z_a).\end{aligned}$$

Since $\bar{Z}_a - Z_a \in \operatorname{Ker} T\tau \subset \mathcal{C}$ then $\mathbf{K}_{\mathcal{W}}(X,Y) - \mathbf{K}_{\bar{\mathcal{W}}}(X,Y) \in \mathcal{C}$. □

Remark 2. Note that the coordinates description of $\mathbf{K}_{\mathcal{W}}$ shows that it is semi-basic with respect to the bundle projection $\tau : \mathcal{M} \to Q$, i.e., $\mathbf{i}_X \mathbf{K}_{\mathcal{W}} = 0$ if $T\tau(X) = 0$. This is in agreement with [1, Prop. 3.1]

In order to write the nonholonomic bivector π_{nh} using (6) but in local coordinates $(r^\alpha, s^a; \tilde{p}_\alpha)$ on $\mathcal{M}$ we study the local description of the 2-section $\Omega_{\mathcal{M}}|_{\mathcal{C}}$.

The canonical 1-form Θ_Q on T^*Q is given, in local coordinates $(r^\alpha, s^a; \tilde{p}_\alpha, \tilde{p}_a)$, by $\Theta_Q = \tilde{p}_\alpha dr^\alpha + \tilde{p}_a \epsilon^\alpha$. Then, it is straightforward to see that the canonical 2-form Ω_Q is written locally as

$$\Omega_Q = dr^\alpha \wedge d\,\tilde{p}_\alpha + \epsilon^a \wedge d\,\tilde{p}_a - \tilde{p}_a d\epsilon^a.$$

Recall that $\iota : \mathcal{M} \to T^*Q$ is the natural inclusion, so the pull back of Ω_Q to $\mathcal{M}$ is given by

$$\Omega_{\mathcal{M}} = \iota^*\Omega_Q = dr^\alpha \wedge d\,\tilde{p}_\alpha + \iota^*\epsilon^a \wedge d\iota^*(\tilde{p}_a) - \iota^*(\tilde{p}_a) d(\iota^*\epsilon^a), \tag{20}$$

where dr^α and $d\,\tilde{p}_\alpha$ are considered as 1-forms on $\mathcal{M}$.

Therefore,

$$\begin{aligned}\Omega_{\mathcal{M}}|_{\mathcal{C}} &= dr^\alpha \wedge d\,\tilde{p}_\alpha - \iota^*(\tilde{p}_a)\iota^*(d\epsilon^a)|_{\mathcal{C}} \\ &= dr^\alpha \wedge d\,\tilde{p}_\alpha - J^\delta_a \tilde{p}_\delta C^a_{\alpha\beta} dr^\alpha \wedge dr^\beta|_{\mathcal{C}},\end{aligned} \tag{21}$$

where in the last equation we use (12) and the coordinate version of $d\epsilon|_D$ given in (15). Applying (6) to the 2-form $\Omega_{\mathcal{M}}$ and $\mathcal{C}$, given in (20) and (19) respectively, we compute the nonholonomic bivector field π_{nh} on $\mathcal{M}$:

$$\pi^\sharp_{\text{nh}}(dr^\alpha) = \frac{\partial}{\partial \tilde{p}_\alpha}, \quad \pi^\sharp_{\text{nh}}(ds^a) = -A^a_\alpha \frac{\partial}{\partial \tilde{p}_\alpha}, \quad \pi^\sharp_{\text{nh}}(d\,\tilde{p}_\alpha) = -X_\alpha + J^\delta_a \tilde{p}_\delta K^a_{\alpha\beta} \frac{\partial}{\partial \tilde{p}_\beta}. \tag{22}$$

Lemma 3. *The almost Poisson bracket* $\{\cdot,\cdot\}_{\mathcal{M}}$ *given in* (17) *(see [14, Theorem 2.1]) is the coordinate version of the nonholonomic bracket* $\{\cdot,\cdot\}_{\text{nh}}$ *associated to the bivector field* π_{nh} *obtained from* (6).

4.2 The Jacobiator in Adapted Coordinates

Consider a nonholonomic system on a manifold Q given by a lagrangian L and a constraint distribution D such that ϵ^a, for $a = 1,\dots,k$, are 1-forms generating D°. Consider local coordinates (r^α, s^a) on Q adapted to the constraints as in (11). Let $(r^\alpha, s^a; \tilde{p}_\alpha)$ be the coordinates on the manifold $\mathcal{M} = \kappa^\flat(D)$. By Lemma 3, the almost Poisson bracket $\{\cdot,\cdot\}_{\mathcal{M}}$ (17) is the coordinate version of the bivector field π_{nh} given in (6), and thus Koon-Marsden formula for the Jacobiator can be written directly with respect to $\{\cdot,\cdot\}_{\text{nh}}$.

Theorem 2 ([14, Sec. 2.5]). *The Jacobiator of the nonholonomic bracket* $\{\cdot,\cdot\}_{\text{nh}}$, *in coordinates* $(r^a, s^a; \tilde{p}_\alpha)$ *on* $\mathcal{M}$, *is given by the following formula*

$$
\begin{aligned}
\{\tilde{p}_\gamma,\{r^\alpha,\tilde{p}_\beta\}_{\text{nh}}\}_{\text{nh}} + \text{cyclic} &= J_b^\alpha K_{\beta\gamma}^b,\\
\{\tilde{p}_\beta,\{s^a,\tilde{p}_\alpha\}_{\text{nh}}\}_{\text{nh}} + \text{cyclic} &= -K_{\alpha\beta}^a - A_\gamma^a J_b^\gamma K_{\alpha\beta}^b,\\
\{\tilde{p}_\gamma,\{\tilde{p}_\alpha,\tilde{p}_\beta\}_{\text{nh}}\}_{\text{nh}} + \text{cyclic} &= \tilde{p}_\tau J_a^\tau \frac{\partial A_\gamma^a}{\partial s^b} K_{\alpha\beta}^b + \tilde{p}_\tau J_a^\tau K_{\delta\gamma}^a J_b^\delta K_{\alpha\beta}^b\\
&\quad - \tilde{p}_\tau K_{\alpha\beta}^b \left(\frac{\partial J_b^\tau}{\partial r^\gamma} - A_\gamma^a \frac{\partial J_b^\tau}{\partial s^a}\right) + \text{cyclic},
\end{aligned}
\tag{23}
$$

with all other combinations equal to zero and where J_b^α, $K_{\alpha\beta}^a$ *and* A_α^a *are the functions on* Q *defined in* (12), (16) *and* (11), *respectively.*

The next result relates the coordinate formula (23) of the Jacobiator with the coordinate-free formula given in Theorem 1.

Theorem 3. *Let* (r^α, s^a) *be coordinates on* Q *adapted to the constraints as in* (11) *and let* W *be the complement of* D *induced by the coordinates (Lemma 1). The Koon-Marsden Jacobiator formula* (23) *for the nonholonomic bracket* $\{\cdot,\cdot\}_{\text{nh}}$ *is the coordinate version of the Jacobiator formula given in Theorem 1 for* $\mathcal{W}$ *any complement of* $\mathcal{C}$ *as in* (19).

Proof. In order to prove the equivalence we write the Schouten bracket $[\pi_{\text{nh}}, \pi_{\text{nh}}]$ using Theorem 1 evaluated on the elements $\{dr^\alpha, ds^a, d\tilde{p}_\alpha\}$.

First, observe that by Remark 2, the 2-form $\mathbf{K}_{\mathcal{W}}$ defined in (9) is annihilated by any of the elements $\pi_{\text{nh}}^\sharp(dr^\alpha)$ or $\pi_{\text{nh}}^\sharp(ds^\alpha)$ (see (22)). On the other hand, by Lemma 2(*ii*), we have that $\mathbf{K}_{\mathcal{W}}(\pi_{\text{nh}}^\sharp(d\tilde{p}_\alpha), \pi_{\text{nh}}^\sharp(d\tilde{p}_\beta)) = K_{\alpha\beta}^a Z_a$, where $Z_a \in T\mathcal{M}$ such that $T\tau(Z_a) = \frac{\partial}{\partial s^a}$. Moreover, observe that $\epsilon^a(Z_b) = \delta_{\alpha\beta}$ and $dr^\alpha(Z_a) = 0$.

Therefore, using the coordinate version of $\Omega_{\mathcal{M}}$ (20) in Theorem 1 we obtain

$$\begin{aligned}\frac{1}{2}[\pi_{\mathrm{nh}},\pi_{\mathrm{nh}}](dr^\alpha, d\tilde{p}_\beta, d\tilde{p}_\gamma) &= \Omega_{\mathcal{M}}(\mathbf{K}_{\mathcal{W}}(\pi_{\mathrm{nh}}^\sharp(d\tilde{p}_\beta),\pi_{\mathrm{nh}}^\sharp(d\tilde{p}_\gamma)),\pi_{\mathrm{nh}}^\sharp(dr^\alpha))\\ &\quad - dr^\alpha(\mathbf{K}_{\mathcal{W}}(\pi_{\mathrm{nh}}^\sharp(d\tilde{p}_\beta),\pi_{\mathrm{nh}}^\sharp(d\tilde{p}_\gamma)))\\ &= J_a^\alpha K_{\beta\gamma}^a,\\ \frac{1}{2}[\pi_{\mathrm{nh}},\pi_{\mathrm{nh}}](ds^a, d\tilde{p}_\alpha, d\tilde{p}_\beta) &= \Omega_{\mathcal{M}}(\mathbf{K}_{\mathcal{W}}(\pi_{\mathrm{nh}}^\sharp(d\tilde{p}_\alpha),\pi_{\mathrm{nh}}^\sharp(d\tilde{p}_\beta)),\pi_{\mathrm{nh}}^\sharp(ds^a))\\ &\quad - ds^a(\mathbf{K}_{\mathcal{W}}(\pi_{\mathrm{nh}}^\sharp(d\tilde{p}_\alpha),\pi_{\mathrm{nh}}^\sharp(d\tilde{p}_\beta)))\\ &= -K_{\alpha\beta}^b A_\gamma^a J_b^\gamma - K_{\alpha\beta}^a.\end{aligned}$$

Finally, let $Y_a := Z_a - \frac{\partial}{\partial s^a} \in \operatorname{Ker} T\tau \subset \mathcal{C}$. Then, we have that

$$\begin{aligned}\frac{1}{2}[\pi_{\mathrm{nh}},\pi_{\mathrm{nh}}](d\tilde{p}_\alpha, d\tilde{p}_\beta, d\tilde{p}_\gamma) &= \Omega_{\mathcal{M}}(K_{\alpha\beta}^a Z_a, \pi_{\mathrm{nh}}^\sharp(d\tilde{p}_\gamma)) - d\tilde{p}_\gamma(K_{\alpha\beta}^a Z_a) + \text{cyclic}\\ &= \Omega_{\mathcal{M}}(K_{\alpha\beta}^a \frac{\partial}{\partial s^a}, \pi_{\mathrm{nh}}^\sharp(d\tilde{p}_\gamma)) + \Omega_{\mathcal{M}}(K_{\alpha\beta}^a Y_a, \pi_{\mathrm{nh}}^\sharp(d\tilde{p}_\gamma))\\ &\quad - d\tilde{p}_\gamma(K_{\alpha\beta}^a Y_a) + \text{cyclic}\\ &= \Omega_{\mathcal{M}}(K_{\alpha\beta}^a \frac{\partial}{\partial s^a}, \pi_{\mathrm{nh}}^\sharp(d\tilde{p}_\gamma)) + \text{cyclic}\\ &= \tilde{p}_\tau J_a^\tau \frac{\partial A_\gamma^a}{\partial s^b} K_{\alpha\beta}^b + \tilde{p}_\tau J_a^\tau K_{\delta\gamma}^a J_b^\delta K_{\alpha\beta}^b\\ &\quad - \tilde{p}_\tau K_{\alpha\beta}^b \left(\frac{\partial J_b^\tau}{\partial r^\gamma} - A_\gamma^a \frac{\partial J_b^\tau}{\partial s^a}\right) + \text{cyclic}.\end{aligned}$$

The Jacobiator on the other combinations of elements of the basis $\{dr^\alpha, ds^a, d\tilde{p}_\alpha\}$ is zero. Thus, the relation (5) implies that the Jacobiator formula in Theorem 1 evaluated in coordinates (11) gives the Koon-Marsden formula (23).

Observe that in this proof we are implicitly using Lemma 2 for $\mathcal{W}$ and $\bar{\mathcal{W}} = \operatorname{span}\left\{\frac{\partial}{\partial s^a}\right\}$.

Remark 3. From (10) it is straightforward to see that if the 2-form $\mathbf{K}_{\mathcal{W}}$ is zero then the bivector π_{nh} is Poisson. On the other hand, it was observed in [14] that if the curvature $\mathbf{K}_W$ is zero then the Jacobi identity of $\{\cdot,\cdot\}_{\mathrm{nh}}$ is satisfied. Using the equivalence between $\mathbf{K}_{\mathcal{W}}$ and $\mathbf{K}_W$ (Lemma 2(i)) we see that both 2-forms are zero when D is involutive, i.e., the system is holonomic.

Remark 4 (Symmetries). If the nonholonomic system admits a group of symmetries G then π_{nh} is G-invariant with respect to the induced (lifted) action on $\mathcal{M}$. As a consequence, the orbit projection $\mathcal{M} \to \mathcal{M}/G$ induces a reduced bivector field $\pi_{\mathrm{red}}^{\mathrm{nh}}$ on $\mathcal{M}/G$ describing the reduced dynamics. Let V (respectively $\mathcal{V}$) be the tangent

space to the orbit of the G-action on Q (respect. on $\mathcal{M}$). If $W \subset V$ then there is a unique choice of the complement $\mathcal{W}$ contained in $\mathcal{V}$:

$$\mathcal{W} := (T\tau|_{\mathcal{V}})^{-1}(W).$$

With this choice of $\mathcal{W}$, Theorem 1 induces a formula for the Jacobiator of the reduced bivector $\pi_{\text{red}}^{\text{nh}}$ (see [1, Sec. 4]).

There are a number of examples of systems verifying that the complement W induced by the coordinates adapted to the constraints (11) (as in Lemma 1) is vertical with respect to a G-symmetry, including the vertical rolling disk, the nonholonomic particle and the Chaplygin sphere, see [1, Sec. 7].

On the other hand, it may happen that a given example is described in coordinates that are not adapted to the constraints. Then, it is better to use the coordinate free formula of Theorem 1.

5 Example: The Snakeboard

The snakeboard describes the dynamics of a board with two sets of actuated wheels, one on each end of the board. A human rider generates forward motion by twisting his body back and forth, and thus producing a movement on the wheels. This effect is modeled as a momentum wheel which sits in the middle of the board and is allowed to spin about the vertical axis. The configuration of the snakeboard is given by the position and orientation of the board in the plane, the angle of the momentum wheel and the angles of the back and front wheels. Therefore, the configuration manifold Q is given by $Q = SE(2) \times (-\pi/2, \pi/2) \times S^1$ with local coordinates $q = (x, y, \theta, \psi, \phi)$, where (x, y, θ) represents the position and orientation of the center of the board, ψ is the angle of the momentum wheel relative to the board and ϕ is the angle of the front and back wheel as in [17] (for details see [4] and [14]).

The Lagrangian is given by

$$L(q, \dot{q}) = \frac{m}{2}(\dot{x}^2 + \dot{y}^2) + \frac{mr^2}{2}\dot{\theta}^2 + \frac{J_0}{2}\dot{\psi}^2 + J_0\dot{\psi}\dot{\theta} + J_1\dot{\phi}^2,$$

where m the total mass of the board, r is the distance between the center of the board and the wheels, J_0 is the inertia of the rotor and J_1 is the inertia of each wheel.

The (nonintegrable) constraint distribution D is given by the annihilator of the following 1-forms:

$$\begin{aligned} \epsilon^1 &= -\sin(\theta + \phi)dx + \cos(\theta + \phi)dy - r\cos\phi d\theta \\ \epsilon^2 &= -\sin(\theta - \phi)dx + \cos(\theta - \phi)dy + r\cos\phi d\theta. \end{aligned} \tag{24}$$

Remark 5. The coordinates $(x, y, \theta, \psi, \phi)$ on Q are not adapted to the 1-forms of constraints ϵ^1, ϵ^2. In [13] a simplified version is considered where, taking $\phi \neq 0$, it is possible to write the 1-forms of constraints in such a way that $(x, y, \theta, \psi, \phi)$ are adapted coordinates as in (11). In this paper, we will work with the 1-forms given in (24), so, our coordinates in Q are not adapted to the constraints, even though these are the coordinates chosen in [14] to study the reduction by the group of symmetries $SE(2)$.

The distribution D on Q is given by

$$D = \text{span}\left\{ X_\psi := \frac{\partial}{\partial \psi},\ X_\phi := \frac{\partial}{\partial \phi},\ X_s := -2r\cos^2\phi\cos\theta\frac{\partial}{\partial x} \right.$$
$$\left. -2r\cos^2\phi\sin\theta\frac{\partial}{\partial y} + \sin(2\phi)\frac{\partial}{\partial \theta} \right\}.$$

We choose the complement W of D generated by $\{X_1, X_2\}$ so that $\epsilon^a(X_b) = \delta^a_b$ for $a, b = 1, 2$, that is

$$W = \text{span}\left\{ X_1 := -\frac{1}{2}\sin\theta\sec\phi\frac{\partial}{\partial x} + \frac{1}{2}\cos\theta\sec\phi\frac{\partial}{\partial y} - \frac{1}{2r}\sec\phi\frac{\partial}{\partial \theta}, \right.$$
$$\left. X_2 := -\frac{1}{2}\sin\theta\sec\phi\frac{\partial}{\partial x} + \frac{1}{2}\cos\theta\sec\phi\frac{\partial}{\partial y} + \frac{1}{2r}\sec\phi\frac{\partial}{\partial \theta} \right\}.$$

Consider the dual basis $\mathfrak{B}_{TQ} = \{X_\psi, X_\phi, X_s, X_1, X_2\}$ and $\mathfrak{B}_{T^*Q} = \{d\psi, d\phi, \alpha_s, \epsilon^1, \epsilon^2\}$ where

$$\alpha_s = -\frac{1}{2r}\cos\theta\sec^2\phi dx - \frac{1}{2r}\sin\theta\sec^2\phi dy.$$

Let us denote by $(q; v_\psi, v_\phi, v_s, v_1, v_2)$ the coordinates on TQ associated with the basis $\mathfrak{B}_{TQ}$ while $(q; \tilde{p}_\psi, \tilde{p}_\phi, \tilde{p}_s, \tilde{p}_1, \tilde{p}_2)$ denote the coordinates on T^*Q associated to $\mathfrak{B}_{T^*Q}$.

The submanifold $\mathcal{M} = \kappa^\flat(D) = \text{span}\{\kappa^\flat(X_\psi), \kappa^\flat(X_\phi), \kappa^\flat(X_s)\}$ is defined in coordinates by

$$\mathcal{M} = \{(q; \tilde{p}_\psi, \tilde{p}_\phi, \tilde{p}_s, \tilde{p}_1, \tilde{p}_2) \ :\ \tilde{p}_1 = -\tilde{p}_2 = J_1(\phi)\tilde{p}_s + J_2(\phi)\tilde{p}_\psi\}, \tag{25}$$

where

$$J_1(\phi) = \frac{mr}{4(r^2m - J_0\sin^2\phi)}\sin\phi\sec^2\phi \qquad \text{and} \qquad J_2(\phi) = -J_1(\phi)\sin(2\phi).$$

In order to compute the nonholonomic bivector π_{nh} describing the dynamics, we write the 2-form $\Omega_{\mathcal{M}}$ and the 2-section $\Omega_{\mathcal{M}}|_{\mathcal{C}}$ in our local coordinates. The canonical 1-form Θ_Q on T^*Q is given by $\Theta_Q = \tilde{p}_\psi d\psi + \tilde{p}_\phi d\phi + \tilde{p}_s \alpha_s + \tilde{p}_a \epsilon^a$. Then,

$$\begin{aligned}\Omega_Q = & d\psi \wedge d\,\tilde{p}_\psi + d\phi \wedge d\,\tilde{p}_\phi + \alpha_s \wedge d\,\tilde{p}_s - \tilde{p}_s d\alpha_s + \epsilon^1 \wedge d\,\tilde{p}_1 \\ & + \epsilon^2 \wedge d\,\tilde{p}_2 - \tilde{p}_1 d\epsilon^1 - \tilde{p}_2 d\epsilon^2,\end{aligned}$$

Let us consider the basis $\mathfrak{B}_{T^*\mathcal{M}} = \{d\phi, d\psi, \alpha_s, \epsilon^1, \epsilon^2, d\,\tilde{p}_\phi, d\,\tilde{p}_\psi, d\,\tilde{p}_s\}$ of $T^*\mathcal{M}$ (here we are using the same notation for the pullbacks of the forms to $\mathcal{M}$). Recall that, on $\mathcal{M}$, $\tilde{p}_1$ and $\tilde{p}_2$ are given by (25) and denoting $J_i = J_i(\phi)$ for $i = 1, 2$ we obtain

$$\begin{aligned}\Omega_{\mathcal{M}} = & d\psi \wedge d\,\tilde{p}_\psi + d\phi \wedge d\,\tilde{p}_\phi + \alpha_s \wedge d\,\tilde{p}_s - \tilde{p}_s d\alpha_s + J_1 \epsilon^1 \wedge d\,\tilde{p}_s + J_2 \epsilon^1 \wedge d\,\tilde{p}_\psi \\ & + \tilde{p}_s J_1' \epsilon^1 \wedge d\phi + \tilde{p}_\psi J_2' \epsilon^1 \wedge d\phi - J_1 \epsilon^2 \wedge d\,\tilde{p}_s - J_2 \epsilon^2 \wedge d\,\tilde{p}_\psi \\ & - \tilde{p}_s J_1' \epsilon^2 \wedge d\phi - \tilde{p}_\psi J_2' \epsilon^2 \wedge d\phi - (J_1 \tilde{p}_s + J_2 \tilde{p}_\psi)(d\epsilon^1 - d\epsilon^2).\end{aligned} \tag{26}$$

On $T\mathcal{M}$ consider the dual basis $\mathfrak{B}_{T\mathcal{M}} = \left\{X_\psi, X_\phi, X_s, X_1, X_2, \frac{\partial}{\partial \tilde{p}_\psi}, \frac{\partial}{\partial \tilde{p}_\phi}, \frac{\partial}{\partial p_s}\right\}$ associated to $\mathfrak{B}_{T^*\mathcal{M}}$. Therefore, we can decompose $T\mathcal{M} = \mathcal{C} \oplus \mathcal{W}$ such that

$$\mathcal{C} = \text{span}\left\{X_\psi\,,\ X_\phi\,,\ X_s\,,\ \frac{\partial}{\partial \tilde{p}_\psi}\,,\ \frac{\partial}{\partial \tilde{p}_\phi}\,,\ \frac{\partial}{\partial p_s}\right\} \qquad \mathcal{W} = \text{span}\,\{X_1\,,\ X_2\}\,. \tag{27}$$

Therefore, using that $d\epsilon^a|_{\mathcal{C}} = (-1)^a 2r\cos\phi\alpha_s \wedge d\phi|_{\mathcal{C}}$ for $a = 1, 2$ and that $d\alpha_s|_{\mathcal{C}} = 2\tan\phi d\phi \wedge \alpha_s|_{\mathcal{C}}$, the 2-section $\Omega_{\mathcal{M}}|_{\mathcal{C}}$ is given by

$$\begin{aligned}\Omega_{\mathcal{M}}|_{\mathcal{C}} = & d\psi \wedge d\,\tilde{p}_\psi + d\phi \wedge d\,\tilde{p}_\phi + \alpha_s \wedge d\,\tilde{p}_s \\ & - \tilde{p}_s 2\tan\phi d\phi \wedge \alpha_s + (J_1 \tilde{p}_s + J_2 \tilde{p}_\psi) 4r\cos\phi\alpha_s \wedge d\phi\,|_{\mathcal{C}}.\end{aligned}$$

Now, we compute the nonholonomic bracket π_{nh} using (6)

$$\begin{aligned}\pi_{\text{nh}} = & \frac{\partial}{\partial\psi} \wedge \frac{\partial}{\partial \tilde{p}_\psi} + \frac{\partial}{\partial\phi} \wedge \frac{\partial}{\partial \tilde{p}_\phi} + X_s \wedge \frac{\partial}{\partial \tilde{p}_s} \\ & - (\tilde{p}_s 2\tan\phi + 4r(J_1 \tilde{p}_s + J_2 \tilde{p}_\psi)\cos\phi) \frac{\partial}{\partial \tilde{p}_s} \wedge \frac{\partial}{\partial \tilde{p}_\phi}.\end{aligned} \tag{28}$$

Therefore, the hamiltonian vector fields are

$$\begin{aligned}&\pi_{\text{nh}}^\sharp(d\psi) = \frac{\partial}{\partial \tilde{p}_\psi}, \qquad \pi_{\text{nh}}^\sharp(d\phi) = \frac{\partial}{\partial \tilde{p}_\phi}, \\ &\pi_{\text{nh}}^\sharp(\alpha_s) = \frac{\partial}{\partial \tilde{p}_s}, \qquad \pi_{\text{nh}}^\sharp(\epsilon^i) = 0, \qquad \pi_{\text{nh}}^\sharp(d\,\tilde{p}_\psi) = -\frac{\partial}{\partial\psi},\end{aligned} \tag{29}$$

$$\pi_{\text{nh}}^{\sharp}(d\,\tilde{p}_\phi) = -\frac{\partial}{\partial\phi} + (2\tan\phi\,\tilde{p}_s + 4r\cos\phi(J_1\tilde{p}_s + J_2\tilde{p}_\psi))\frac{\partial}{\partial\tilde{p}_s},$$
$$\pi_{\text{nh}}^{\sharp}(d\,\tilde{p}_s) = -X_s - (2\tan\phi\,\tilde{p}_s + 4r\cos\phi(J_1\tilde{p}_s + J_2\tilde{p}_\psi))\frac{\partial}{\partial\tilde{p}_\phi}.$$

In order to apply Theorem 1 to compute the Jacobiator of π_{nh} we study the $\mathcal{W}$-valued 2-form $\mathbf{K}_{\mathcal{W}}$ defined in (9) for $\mathcal{W}$ in (27). For $X, Y \in \mathcal{C}$ and using the dual basis $\mathfrak{B}_{T\mathcal{M}}$ and $\mathfrak{B}_{T^*\mathcal{M}}$ we have that

$$\begin{aligned}\mathbf{K}_{\mathcal{W}}(X,Y) &= -P_{\mathcal{W}}([X,Y]) = -\epsilon^1([X,Y])X_1 - \epsilon^2([X,Y])X_2\\ &= d\epsilon^1(X,Y)X_1 + d\epsilon^2(X,Y)X_2.\end{aligned}$$

Therefore,

$$\mathbf{K}_{\mathcal{W}}|_{\mathcal{C}} = -2r\cos(\phi)(\alpha_s \wedge d\phi\,|_{\mathcal{C}}) \otimes (X_1 - X_2). \tag{30}$$

Finally, we consider the 2-forms $\Omega_{\mathcal{M}}$ and $\mathbf{K}_{\mathcal{W}}$, described in (26) and (30) and the vector fields (29), to obtain, by (10), that

$$\begin{aligned}&[\pi_{\text{nh}}, \pi_{\text{nh}}](d\,\tilde{p}_\phi, d\,\tilde{p}_s, d\psi) = 4r\cos(\phi)J_2(\phi),\\ &[\pi_{\text{nh}}, \pi_{\text{nh}}](d\,\tilde{p}_\phi, d\,\tilde{p}_s, \alpha) = 4r\cos(\phi)J_1(\phi)\\ &[\pi_{\text{nh}}, \pi_{\text{nh}}](d\,\tilde{p}_\phi, d\,\tilde{p}_s, \epsilon^i) = (-1)^i 2r\cos(\phi), \quad i = 1,2,\end{aligned} \tag{31}$$

while on other combination of elements the Jacobiator is zero.

This example admits a symmetry given by the Lie group $SE(2)$, see [14]. The reduced manifold $\mathcal{M}/G$ is $S^1\times S(-\pi/2,-\pi/2)\times\mathbb{R}^3$ and the nonholonomic bivector field π_{nh} is invariant by the orbit projection $\rho : \mathcal{M} \to \mathcal{M}/G$. Thus, on $\mathcal{M}/G$ we have the reduced nonholonomic bivector defined at each $\alpha \in T^*(\mathcal{M}/G)$ by

$$(\pi_{\text{red}}^{\text{nh}})^{\sharp}(\alpha) = T\rho\,\pi_{\text{nh}}^{\sharp}(\rho^*\alpha).$$

The Jacobiator of the reduced nonholonomic bivector field $\pi_{\text{red}}^{\text{nh}}$ satisfies

$$[\pi_{\text{red}}^{\text{nh}}, \pi_{\text{red}}^{\text{nh}}](\alpha,\beta,\gamma) = T\rho\left([\pi_{\text{nh}}, \pi_{\text{nh}}](\rho^*\alpha, \rho^*\beta, \rho^*\gamma)\right)$$

for $\alpha, \beta, \gamma \in T^*(\mathcal{M}/G)$. So, in our example it is simple to compute the Jacobiator of $\pi_{\text{red}}^{\text{nh}}$. Taking into account that, in local coordinates, the orbit projection $\rho : \mathcal{M} \to \mathcal{M}/G$ is given by $\rho(\psi,\phi,\theta,x,y,\tilde{p}_\psi,\tilde{p}_\phi,\tilde{p}_s) = (\psi,\phi,\tilde{p}_\psi,\tilde{p}_\phi,\tilde{p}_s)$, the Jacobiator of the reduced bivector $\pi_{\text{red}}^{\text{nh}}$ describing the dynamics is given by

$$[\pi_{\text{red}}^{\text{nh}}, \pi_{\text{red}}^{\text{nh}}](d\,\tilde{p}_\phi, d\,\tilde{p}_s, d\psi) = 4r\cos(\phi)J_2(\phi)$$

while on other elements of $T^*(\mathcal{M}/G)$ is zero.

Just to complete the example we can write, in our coordinates, the reduced bivector field $\pi_{\text{red}}^{\text{nh}}$ on $\mathcal{M}/G$:

$$\pi_{\text{nh}}^{\text{red}} = \frac{\partial}{\partial\psi}\wedge\frac{\partial}{\partial\tilde{p}_\psi}+\frac{\partial}{\partial\phi}\wedge\frac{\partial}{\partial\tilde{p}_\phi}-(\tilde{p}_s 2\tan\phi+4r(J_1\tilde{p}_s+J_2\tilde{p}_\psi)\cos(\phi))\frac{\partial}{\partial\tilde{p}_s}\wedge\frac{\partial}{\partial\tilde{p}_\phi}.$$

Acknowledgements I thank the organizers of the *Focus Program on Geometry, Mechanics and Dynamics, the Legacy of Jerry Marsden*, held at the Fields Institute in Canada, for their hospitality during my stay. I also benefited from the financial support given by Mitacs (Canada), and I am specially grateful to Jair Koiller for his help. I also thank FAPERJ (Brazil) and the GMC Network (projects MTM2012-34478, Spain) for their support. I finally acknowledge CAPES (Brazil) for the financial support through the grant CsF PVE 11/2012.

References

1. Balseiro, P. The Jacobiator of nonholonomic systems and the geometry of reduced nonholonomic brackets, Arch. Ration. Mech. Anal. **214(2)**, 453–501 (2014)
2. Bates, L., Sniatycki, J.: Nonholonomic reduction. Rep. Math. Phys. **32**, 99–115 (1993)
3. Bloch, A.M.: Non-holonomic Mechanics and Control. Springer, New York (2003)
4. Bloch, A.M., Krishnapasad, P.S., Marsden, J.E., Murray, R.M.: Nonholonomic mechanical systems with symmetry. Arch. Ration. Mech. Anal. **136**, 21–99 (1996)
5. Borisov, A.V., Mamaev, I.S.: Conservation laws, hierarchy of dynamics and explicit integration of nonholonomic systems. Regular Chaotic Dyn. **13**, 443–490 (2008)
6. Chaplygin, S.A.: On the theory of the motion of nonholonomic systems. The reducing-multiplier theorem. Translated from Matematicheskiĭ sbornik (Russian) **28** (1911), no. 1 by A. V. Getling. Regular Chaotic Dyn. **13**, 369–376 (2008)
7. Cushman, R.H., Duistermaat, H., Šniatycki, J.: Geometry of Nonholonomically Constrained Systems. World Scientific, Singapore (2010)
8. Fernandez, O., Mestdag, T., Bloch, A.: A generalization of Chaplygin's reducibility theorem. Regul. Chaotic Dyn. **14**, 635–655 (2009)
9. García-Naranjo, L.C.: Reduction of almost Poisson brackets and Hamiltonization of the Chaplygin sphere. Discrete Continuous Dyn. Syst. Ser. S **3**, 37–60 (2010)
10. Ibort, A., de León, M., Marrero, J.C., Martín de Diego, D.: Dirac brackets in constrained dynamics. Fortschr. Phys. **47**, 459–492 (1999)
11. Jovanović, B.: Hamiltonization and integrability of the Chaplygin sphere in $\mathbb{R}^n$. J. Nonlinear Sci. **20**, 569–593 (2010)
12. Koiller, J., Rios, P.P.M., Ehlers, K.M.: Moving frames for cotangent bundles. Rep. Math. Phys. **49**(2), 225–238 (2002)
13. Koon, W.S., Marsden, J.E.: The Hamiltonian and lagrangian approaches to the dynamics of nonholonomic systems. Rep. Math. Phys. **40**, 21–62 (1997)
14. Koon, W.S., Marsden, J.E.: The poisson reduction of nonholonomic mechanical systems. Rep. Math. Phys. **42**, 101–134 (1998)
15. Marle, Ch.M.: Various approaches to conservative and nonconservative nonholonomic systems. Rep. Math. Phys. **42**, 211–229 (1998)

16. Marsden, J.E., Ratiu, T.S.: Introduction to Mechanics and Symmetry. A Basic Exposition of Classical Mechanical Systems. Texts in Applied Mathematics, vol. 17, 2nd edn. Springer, New York (1999)
17. Ostrowski, J.: Geometric Perspectives on the Mechanics and Control of Undulatory Locomotion. Ph.D. thesis, California Institute of Technology (1995)
18. van der Schaft, A.J., Maschke, B.M.: On the Hamiltonian formulation of nonholonomic mechanical systems. Rep. Math. Phys. **34**, 225–233 (1994)

Geometry of Image Registration: The Diffeomorphism Group and Momentum Maps

Martins Bruveris and Darryl D. Holm

Abstract These lecture notes explain the geometry and discuss some of the analytical questions underlying image registration within the framework of *large deformation diffeomorphic metric mapping* (LDDMM) used in computational anatomy.

1 Introduction

The goal of computational anatomy is to model and study the variability of anatomical shape. The ideas of computational anatomy originate in the seminal book "Growth and Form" by D'Arcy Thompson [66].

> In a very large part of morphology, our essential task lies in the comparison of related forms rather than in the precise definition of each; and the *deformation* of a complicated figure may be a phenomenon easy of comprehension, though the figure itself have to be left unanalysed and undefined. This process of comparison [. . .] finds its solution in the elementary use of a certain method of the mathematician. This method is the Method of Coordinates, on which is based the Theory of Transformations. [66, p. 1032]

More recently Grenander [25, 26, 28] generalized these ideas to encompass a diverse collection of real-world situations and formulated the principles of pattern theory. The following formulation is adapted from [51]:

1. A wide variety of signals result from observing the world, all of which show patterns of many kinds. These patterns are caused by laws present in the world, but at least partially hidden from direct observation.
2. Observations are affected by many variables that are not conveniently modelled deterministically because they are too complex or too difficult to observe.

M. Bruveris (✉)
Department of Mathematics, Brunel University London, Uxbridge UB8 3PH, UK
e-mail: martins.bruveris@brunel.ac.uk

D.D. Holm
Department of Mathematics, Imperial College London, London SW7 2AZ, UK
e-mail: d.holm@imperial.ac.uk

D.E. Chang et al. (eds.), *Geometry, Mechanics, and Dynamics*, Fields Institute Communications 73, DOI 10.1007/978-1-4939-2441-7_2

3. Patterns can be described as precise *pure patterns* distorted and transformed by a limited family of *deformations*.

To have a specific example in mind, we will consider computational neuroanatomy; i.e., the study of the form and shape of the brain [27]. The observations in this case are the diagnostic tools accessible to the clinician; of particular interest to us are noninvasive imaging techniques like computed tomography (CT), magnetic resonance imaging (MRI), functional MRI and diffusion tensor imaging (DTI). The hidden laws behind the observations are all the processes taking place at cellular, organ and environmental level, which together influence and form the anatomical shape of the brain.

To avoid having to model the brain from first principles, we observe instead that topologically all brains are very similar. If we take the MRI scans of two patients—volumetric grey-scale images of two brains—then we will be able to deform the contour surfaces of one image to approximately match the other. The study of shape and variability of brains within the framework of pattern theory, thus reduces to estimating the transformations that deform one brain image into an other. Given two images, the problem of finding this transformation is called the problem of *image registration*. One then compares these transformations in order to infer information about shape and variability.

1.1 Outline of the Notes

The purpose of these lecture notes is to explain the geometry that underlies image registration within the LDDMM framework and to show how it is used in computational anatomy. Section 1 introduces the main objectives of computational anatomy. Section 2 explains the Lie group concepts and Riemannian geometry underlying the image registration problem. Finally, Sect. 3 sketches some of the analytical problems that arise in image registration within the LDDMM framework. The references are not exhaustive. Throughout, we rely on the fundamental texts [51, 75].

1.2 Image Registration with LDDMM

Mathematically we model a volumetric grey-scale image I as a function $I : \mathbb{R}^3 \to \mathbb{R}$ and we denote by $\mathscr{F}(\mathbb{R}^3)$ the collection of all such functions, subject to certain smoothness assumptions. We model transformations φ as smooth, invertible maps $\varphi : \mathbb{R}^3 \to \mathbb{R}^3$ with smooth inverses. Such maps are called *diffeomorphisms*. Invertibility ensures that tissue is not torn apart or collapsed to single points. The set of all transformations is denoted by $\mathrm{Diff}(\mathbb{R}^3)$ and since it is closed under composition and taking the inverse, it forms a group, called the

diffeomorphism group. Deforming an image I by the transformation φ corresponds to the change of coordinates $I \circ \varphi^{-1}$. In the transformed image $I \circ \varphi^{-1}$ the voxel $\varphi(x)$ has the same grey-value as the voxel x of the original image.

Given two images $I_0, I_1 \in \mathscr{F}(\mathbb{R}^3)$, the first approach to the image registration problem would be to search for $\varphi \in \mathrm{Diff}(\mathbb{R}^3)$, such that $I_0 \circ \varphi^{-1} = I_1$. Two things can go wrong. First, such a φ may not exist and second, if it exists, it may not be unique. To address these problems, we can introduce a distance $d_1(\varphi, \psi)$ on the set of transformations and a distance $d_2(I, J)$ on the set of images and search for the minimizer of

$$\operatorname*{argmin}_{\varphi} d_1(\mathrm{Id}, \varphi)^2 + \tfrac{1}{\sigma^2} d_2(I_0 \circ \varphi, I_1)^2. \tag{1}$$

The first term addresses the problem of uniqueness by ensuring that among all the transformations that deform I_0 into I_1 we pick the simplest one, by which we mean the one closest to the identity transformation. The second term allows us to compare images for which an exact solution to the registration problem does not exist, by requiring that the transformed image is close but not necessarily equal to I_1. Taken together (1) represents a balance between finding a simple transformation and one that reproduces the given image. The parameter σ^2 controls this balance between simplicity or regularity of the transformation and the registration accuracy.

There are many possible definitions of a distance $d_1(\mathrm{Id}, \varphi)$ on the space of smooth invertible maps. We shall concentrate on the definition used in the *large deformation diffeomorphic metric mapping* (LDDMM) approach [10, 47, 49, 67], which generates the transformation $\varphi = \varphi_1$ as the flow of a time-dependent vector field. That is, $t \mapsto \varphi_t$ is a solution to the flow equation

$$\partial_t \varphi_t(x) = u_t(\varphi_t(x)), \qquad \varphi_0(x) = x.$$

The distance $d_1(\mathrm{Id}, \varphi)$ is measured using a norm on the vector field u_t,

$$d_1(\mathrm{Id}, \varphi)^2 = \inf_{\{u_t \,:\, \varphi = \varphi_1\}} \int_0^1 |u_t|^2 \, \mathrm{d}t.$$

Regarding the distance $d_2(I, J)$ on images, the simplest choice is the L^2-norm, i.e. $d_2(I, J) = |I - J|_{L^2(\mathbb{R}^3)}$, which will be used throughout these notes. The problem of image registration via LDDMM will form the basis of the following discussion.

Definition 1 (Image Registration via LDDMM). Given two images $I_0, I_1 \in V$, find a time-dependent vector field $t \mapsto u_t \in \mathfrak{X}(\mathbb{R}^3)$ that minimizes the energy

$$E(u) = \frac{1}{2} \int_0^1 |u_t|^2 \, \mathrm{d}t + \frac{1}{2\sigma^2} \left| I_0 \circ \varphi_1^{-1} - I_1 \right|^2_{L^2(\mathbb{R}^3)}, \tag{2}$$

where $\varphi_t \in \mathrm{Diff}(\mathbb{R}^3)$ is the flow of u_t, i.e.

$$\partial_t \varphi_t(x) = u_t(\varphi_t(x)), \qquad \varphi_0(x) = x \ ,$$

The vector field $t \mapsto u_t$ and the transformation φ_1 are the solutions of the image registration problem.

This is not the only possible approach to image registration. In fact, a large literature about image registration exists. An overview of the available methods can be found, e.g. in [29, 36]. The LDDMM method, whilst being computationally more expensive than others, is among the most accurate [6] registration methods. Here we will concentrate on the geometric structure of the LDDMM solutions. In particular, we will sketch some applications in which the geometry behind LDDMM helps illuminate relationships between anatomical shape and neurological functions.

Data structures other than images can be registered within the LDDMM framework. These include landmarks [23, 35], curves [17, 24], surfaces [68], tensor fields [2, 14] or functional data on a manifold [46, 54]. In fact the abstract formulation of LDDMM in Sect. 2 encompasses all these examples. Instead of the L^2-norm one can use other similarity metrics to measure the distance between images, e.g. mutual information [39]. The biggest departure from LDDMM would be to change the way diffeomorphisms are generated. Possible approaches are stationary vector fields [5], free-form deformations [62], only affine transformations [34] or demons [65, 69]. Common to all these methods however is the loss of geometric structure.

1.3 Anatomical Shape and Function

Alzheimer's disease (AD) is a neurodegenerative disease and is the most frequent type of dementia in the elderly [19]. Related to AD is mild cognitive impairment (MCI), an intermediate cognitive state between healthy ageing and dementia. Although most patients who develop AD are first diagnosed with MCI, not all of those with MCI will develop AD. There is considerable variability among the prognoses of patients with MCI: some develop into AD, while others remain stable, revert back to normal cognitive status or develop other forms of dementia. It is therefore of interest to find methods of predicting the prognosis of patients with MCI. One approach is to look for manifestations of AD and MCI in the anatomical shape and to find connections between anatomical shape and clinical measures of cognitive status that are used to diagnose and distinguish between AD, MCI and normal cognitive state (NCS) [73].

1.3.1 Alzheimer's Disease and the Shape of Subcortical Structures

In [59] a population $(I_j)_{1\le j\le 383}$ of 383 subjects, both healthy and diseased, was registered to a common template I_{templ}; i.e., for each pair I_j, I_{templ} a deformation φ_j, satisfying $I_{\text{templ}} \circ \varphi_j^{-1} \approx I_j$, was computed by solving the registration problem in Def. 1. Seven subcortical structures $S^1, \dots, S^7$ were extracted from each image and the log-Jacobian $f_j^k = \log\left(\det D\varphi_j\right)|_{\partial S^k}$ of the estimated transformation φ_j, restricted to the boundary of the structure S^k, was used to measure the shape variation with respect to the template. These maps f_j^k were called "surface deformation maps". After performing principal component analysis on these maps followed by linear regression with the diagnosis (AD, MCI or NCS), it was found for example that AD and MCI, when compared to NCS is associated with a pronounced surface inward deformation in areas of the amygdala and the hippocampus and with a simultaneous outward deformation in the body and inferior lateral ventricles. These results are in agreement with previous neuroimaging findings and show that LDDMM can be used to highlight local shape variations related to AD.

1.4 Analysis of Longitudinal Data

A more accurate assessment of disease states can be obtained by comparing two different scans of one patient, taken at two different times. Let I_{b}^j and I_{f}^j denote the baseline scan and the follow-up scan taken a few years later of the jth patient respectively. Registering I_{b}^j to I_{f}^j via LDDMM computes a transformation φ_j such that $I_{\text{b}}^j \circ \varphi_j^{-1} \approx I_{\text{f}}^j$, and also its generating vector field u_t^j. Sect. 2 shows that the entire vector field u_t^j can be recovered from its value at $t = 0$ via the *Euler-Poincaré equation on the diffeomorphism group*, also called *EPDiff* and introduced in equation (13). This means that the initial vector field u_0^j can be determined from the initial *deformation momentum*, p^j. Thus, the shape differences between I_{b}^j and I_{f}^j are encoded in the deformation momentum p^j.

To compare the deformation momenta p^j, $j = 1, 2, \dots$, for a set of different patients all baseline scans I_{b}^j are registered in a second step to a common template I_{templ}. Then it is necessary to transport each of the deformation momenta p^j from I_{b}^j to the common template and thereby obtain the corresponding $\tilde{p}^j$. Thus it is possible to compare the evolution between the baseline and the follow-up scans, by its nature a very nonlinear object, by comparing the computed momenta $\tilde{p}^j$, which are elements of a vector space (Figure 1).

Regarding the transport operation several methods have been proposed. From a geometrical point of view, parallel transport from Riemannian geometry is the most natural operation and this has been used in [57, 74, 76]. Since computing the parallel transport of the momentum along geodesics is numerically quite challenging, a first-order approximation called Schild's ladder was proposed in [38] as an alternative.

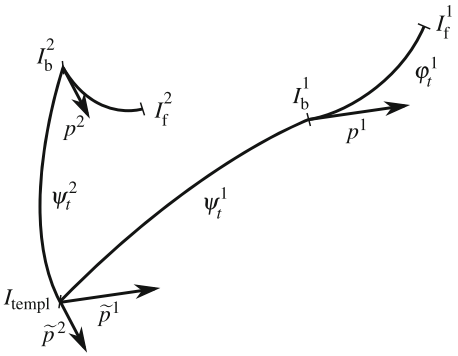

Fig. 1 The use of parallel transport in a longitudinal study AD. The baseline scan I_b^1 is registered to the follow-up scan I_f^1 via φ_t^1 and the baseline scan is registered to the template image I_{templ} via ψ_t^1. The deformation φ^1 is encoded in the initial momentum p^1, which is parallel transported along the path ψ_t^1 to $I_{\mathrm{templ.}}$ to obtain $\tilde{p}^1$. In this way the changed between baseline and follow-up scans can be compared across a population of patients

Other methods that depend only on the end-deformation and not on the whole geodesic path were considered and compared in [20]. From the viewpoint of applications, there is, as of now, no consensus about which is the most appropriate method for the transport of deformation momenta.

Longitudinal Study of the Shape of Hippocampi

Parallel transport was used in [56] as the transport method to compare deformations of the hippocampus in subjects with early AD and healthy controls across a time span of two years. It was shown that the conversion from normal cognitive function to early AD in the time span between the baseline scan and the follow-up scan is associated with an inward deformation of the hippocampal tail. Subjects who were already diagnosed with AD at the time of the baseline scan on the other hand exhibited an inward deformation of the whole hippocampal body.

1.5 Propagation of Anatomical Information

Registering two images I_0 and I_1 via a transformation φ gives us a voxel-to-voxel correspondence between these two images. Assuming that we are given a manual segmentation of the template image I_0, in which some or all voxels of I_0 are assigned membership to a labelled anatomical structure, we can propagate this segmentation via φ to the image I_1. This is the idea of registration-based or

atlas-based segmentation, see [15, 22, 48]. To remove the bias inherent in the choice of the template I_0, one can use multi-template registration techniques and replace I_0 with a collection $(I^j_{\text{templ}})_{j=1,\dots,N}$ of several manually segmented images. Each template I^j_{templ} is registered to I_1 and the transformation is used to propagate the segmentation of I^j_{templ} to I_1. Now there are N potentially contradicting segmentations of I_1, that have to be combined using some *classifier fusion* technique, such as majority voting [4], Bayesian modelling [72] or Markov random fields [21]. For subcortical structures of the brain, this sort of atlas-based segmentation was shown to outperform other methods [7]. It is possible to use atlas-based registration with a variety of image registration methods. However, a study that involved segmenting brain scans of mice [8] has shown that the choice of the registration method is more important than the choice of fusion method. Thus in applications where accuracy is important, LDDMM may be preferred, despite having higher computational cost than some other registration methods.

Automatic Labelling via Ontologies

In the same spirit, Steinert-Threlkeld et al. [64] combined an ex-vivo scan of the left ventricle, manually parcellated and labelled, with the LDDMM registration method and an ontology query language to allow the medical practitioner to obtain quantitative and qualitative answers to questions like: "In which region was significant tissue volume expansion observed between systole and diastole?" and "What was the average rate of expansion per region of interest?" The ability to automatically answer these questions is a key step toward automating the diagnostic process.

Patient-Specific Models for Atrial Fibrillation [41]

Atrial fibrillation is a cardiac arrhythmia, characterized by the irregular propagation of electrocardial waves across the atrium. Advances in late-gadolinium enhanced MRI, allows the in-vivo localization of fibrotic tissue in the atrium, by diffusion tensor imaging (DTI). Although the DTI approach does not yet have the necessary resolution to determine the fibre orientation of the muscle fibres in-vivo, there already exist atlases with information about fibre orientation, obtained ex-vivo. Image registration can be used to propagate the fibre orientations from the atlas to the patient and thus obtain a patient-specific model of the atrium that includes both locations of fibrotic tissue and orientation of the muscle fibres. The resulting model can then be used to simulate the propagation of electrocardial waves and to predict the occurrence of arrhythmia in the patient's atrium.

1.6 Other Applications

We cannot hope to give an exhaustive description of all the applications of LDDMM and its associated geometry to computational medicine in these notes. Among the omitted topics are: estimating the dimensionality of the anatomical shape variations [60]; generalizing geodesic regression to the anatomical shape manifold and computing the mean aging process of the brain across a population [16]; the use of parallel transport not only for longitudinal studies, but also to characterize the left-right asymmetry of subcortical structures [58]; applications to other diseases like schizophrenia [55] or cerebral palsy [18]; addition of functional data to anatomical shapes [46]. There are also applications outside the medical field to the study of variations of cell shape [61] and to construct generative models for cells [53].

2 Geometry of Matching Problems

In order to better see the geometric properties of image registration with LDDMM, we will first formulate an abstract version of it. As we study this abstract problem, we will at each step show how it relates to the concrete example of image registration.

2.1 Abstract Formulation

In the spirit of pattern theory we can formulate image registration as follows: a group of transformations acts on a space of objects and we are searching for the transformation that deforms a template object to a target object. The presentation here follows [12].

Let us model the group of transformations by a Lie group G and the space of objects by a vector space V. We will in this section assume that both G and V are finite-dimensional in order to avoid questions about topologies, smoothness and dual spaces that arise when dealing with infinite-dimensional spaces. The process of deforming objects $I \in V$ by transformations $g \in G$ is modelled by a smooth map

$$\ell : G \times V \to V, \qquad (g, I) \mapsto g.I.$$

Note that $g.I$ is simply a notation for $\ell(g, I)$, i.e. the object I transformed under g. Let $e \in G$ denote the neutral element of the group. We require ℓ to satisfy the following axioms

- $\ell(e, I) = I$ or $e.I = I$ for $I \in V$ and
- $\ell(g, \ell(h, I)) = \ell(gh, I)$ or $g.(h.I) = (gh).I$ for $g, h \in G$ and $I \in V$,

The first axiom tells us that the identity transformation doesn't change the object while the second is an associativity axiom and allows us to write simply $gh.I$ for either $g.(h.I)$ or $(gh).I$. Such a map ℓ is called a *left action of the group G on the vector space V*. An in-depth treatment of group actions, beyond what we will need for our purposes, can be found, e.g. in [43].

Example 2. Consider the rotation group $SO(3)$ and the vector space $\mathbb{R}^3$. The action

$$\ell : SO(3) \times \mathbb{R}^3 \to \mathbb{R}^3, \qquad (R, x) \mapsto Rx$$

is given by matrix multiplication. The rules of matrix algebra imply that this is indeed a left action.

To generate deformations and to measure their "size" or "energy", we use the linearization of the Lie group G. The *Lie algebra* $\mathfrak{g}$ *of* G is the tangent space of G at the identity, i.e. $\mathfrak{g} = T_eG$. Intuitively $\mathfrak{g}$ consists of "infinitesimal deformations". The following points of view are equivalent:

- Given a smooth curve $t \mapsto u_t \in \mathfrak{g}$ of infinitesimal deformations, there exists a curve $t \mapsto g_t \in G$ in the group, which is the solution of the differential equation

$$\partial_t g_t = u_t g_t, \qquad g_0 = e.$$

  The curve g_t is called the *flow* or *integral curve of* u_t.
- Given a smooth curve $t \mapsto g_t \in G$ of deformations, its velocity is $\partial_t g_t \in T_{g_t}G$ and it defines a curve $u_t := (\partial_t g_t)g_t^{-1} \in T_eG$ of infinitesimal deformations. The curve u_t is called the *right-trivialized velocity of* g_t.

To complete the modelling of the matching problem we assume that both the Lie algebra $\mathfrak{g}$ and the space V of objects are endowed with inner products $\langle ., . \rangle_{\mathfrak{g}}$ and $\langle ., . \rangle_V$ respectively. The kinetic energy of a curve g_t of deformations is measured via its right-trivialized velocity

$$E_{\mathrm{KE}}(u) = \tfrac{1}{2} \int_0^1 |u_t|_{\mathfrak{g}}^2 \, \mathrm{d}t \ ,$$

where $|u|_{\mathfrak{g}} = \sqrt{\langle u, u \rangle_{\mathfrak{g}}}$ is the norm induced by the inner product. The inner product on V will be used to measure the distance between objects. The matching problem can now we stated as follows.

Definition 3 (Abstract Registration Problem). Given two objects $I_0, I_1 \in V$ find a curve $t \mapsto u_t \in \mathfrak{g}$ that minimizes the energy

$$E(u) = \tfrac{1}{2} \int_0^1 |u_t|_{\mathfrak{g}}^2 \, \mathrm{d}t + \tfrac{1}{2\sigma^2} |g_1.I_0 - I_1|_V^2 \ , \tag{3}$$

where $g_1 \in G$ is the endpoint of the flow of u_t, i.e.

$$\partial_t g_t = u_t g_t, \qquad g_0 = e.$$

The transformation g_1 then matches I_0 to I_1.

We defer questions about existence of minimizers to Sect. 3. Our goal now is to study properties of the minimizing curves u_t. In particular, we want to see which properties of the minimizer are fixed by the group and what features of it are affected by the choice of the space of objects. We assume all objects to be sufficiently smooth. Thus, minima of E are also critical points; so we will be interested in calculating the derivative $DE(u)$. In order to do that we need some more tools from geometry.

2.2 The Adjoint Action

On the group G we fix an element $g \in G$ and consider the map

$$\operatorname{conj}_g : G \to G, \qquad \operatorname{conj}_g(h) = ghg^{-1},$$

called *conjugation*. It satisfies $\operatorname{conj}_g(e) = e$ and we denote its tangent map by

$$\operatorname{Ad}_g := T_e \operatorname{conj}_g : T_e G \to T_e G.$$

This map is called the *adjoint representation* of G. The following properties of conj can be easily verified,

$$\operatorname{conj}_g \circ \operatorname{conj}_h = \operatorname{conj}_{gh}$$
$$\operatorname{conj}_{g^{-1}} = \left(\operatorname{conj}_g\right)^{-1}.$$

These properties imply the following differential versions,

$$\operatorname{Ad}_g \operatorname{Ad}_h = \operatorname{Ad}_{gh}$$
$$\operatorname{Ad}_{g^{-1}} = \left(\operatorname{Ad}_g\right)^{-1}.$$

Considered as a map of both variables, the operation $\operatorname{Ad} : G \times \mathfrak{g} \to \mathfrak{g}$ defines a left action of G on its Lie algebra $\mathfrak{g}$. We also see that Ad is a group homomorphism $\operatorname{Ad} : G \to GL(\mathfrak{g})$ between G and the group $GL(\mathfrak{g})$ of invertible linear maps on $\mathfrak{g}$. This property is the reason for the name adjoint representation.

2.3 The Coadjoint Action

Again keeping $g \in G$ fixed we consider the linear map $\mathrm{Ad}_g : \mathfrak{g} \to \mathfrak{g}$. This map has a transpose $\mathrm{Ad}^* : \mathfrak{g}^* \to \mathfrak{g}^*$ in the sense of linear algebra, defined via

$$\left\langle \mathrm{Ad}_g^* \, \mu, u \right\rangle_{\mathfrak{g}^* \times \mathfrak{g}} = \left\langle \mu, \mathrm{Ad}_g \, u \right\rangle_{\mathfrak{g}^* \times \mathfrak{g}} \ ,$$

for $\mu \in \mathfrak{g}^*$ and $u \in \mathfrak{g}$. This map Ad^* is called the *coadjoint representation* of G. Similarly to Ad it satisfies

$$\begin{aligned} \mathrm{Ad}_g^* \, \mathrm{Ad}_h^* &= \mathrm{Ad}_{hg}^* \\ \mathrm{Ad}_{g^{-1}}^* &= \left(\mathrm{Ad}_g^* \right)^{-1} . \end{aligned}$$

Considered as a map of both variables, the map $\mathrm{Ad}^* : G \times \mathfrak{g}^* \to \mathfrak{g}^*$ defines a right action of G on $\mathfrak{g}^*$. It is not a left action, because in the associativity rule the order of the multiplication is changed. To make it into a left action we can consider the map $(g, \mu) \mapsto \mathrm{Ad}_{g^{-1}}^* \, \mu$. The name coadjoint representation stems from the way of looking at Ad^* as a group antihomomorphism $\mathrm{Ad}^* : G \to GL(\mathfrak{g}^*)$.

2.4 Variations of the Flow

Why is this interlude necessary? In order to differentiate the term $|g_1.I_0 - I_1|_V^2$ in (3) we need to know how to differentiate g_1 with respect to u_t, since g_1 is defined as the flow

$$\partial_t g_t = u_t g_t, \qquad g_0 = e \ ,$$

of u_t at time $t = 1$. This is given in the following lemma, the proof of which is adapted from [10, 70].

Lemma 4. *Let $t \mapsto u_t \in \mathfrak{g}$ be a smooth curve and $(\varepsilon, t) \mapsto u_t^\varepsilon$ a smooth variation of this curve. Denote by $\delta u_t := \partial_\varepsilon|_{\varepsilon=0} \left(u_t^\varepsilon \right)$ an infinitesimal variation of u_t. Then*

$$\delta g_t := \partial_\varepsilon|_{\varepsilon=0} \left(g_t^\varepsilon \right) = g_t \int_0^t \mathrm{Ad}_{g_s^{-1}} \, \delta u_s \, \mathrm{d}s.$$

Proof. For all ε we have

$$\partial_t g_t^\varepsilon = u_t^\varepsilon g_t^\varepsilon, \qquad g_0^\varepsilon = e.$$

Taking the ε-derivative of this equality yields the ODE

$$\partial_t \partial_\varepsilon|_{\varepsilon=0} \left(g_t^\varepsilon\right) = \delta u_t g_t + u_t \delta g_t \ ,$$

and so we obtain

$$\begin{aligned} \partial_t \left(g_t^{-1} \delta g_t\right) &= -g_t^{-1} u_t g_t g_t^{-1} \delta g_t + g_t^{-1} \left(\delta u_t g_t + u_t \delta g_t\right) \\ &= g_t^{-1} \delta u_t g_t \\ &= \mathrm{Ad}_{g_t^{-1}} \delta u_t . \end{aligned}$$

Now we integrate both sides from 0 to t and multiply by g_t from the left to obtain

$$\delta g_t = g_t \int_0^t \mathrm{Ad}_{g_s^{-1}} \delta u_s \, \mathrm{d}s \ ,$$

as required. □

The second tool we will need to compute the derivative $DE(u)$ is a map that describes the relation between the group G and the space V it acts upon. This map is called the *momentum map*.

2.5 The Momentum Map

Starting with the action $\ell : G \times V \to V$ of a Lie group G on a vector space V, we fix $I \in V$ and consider the map $\ell^I : G \to V$ given by $\ell^I(g) = \ell(g, I)$. The derivative of this map at $e \in G$ is $T_e \ell^I : \mathfrak{g} \to T_I V$ and it may be interpreted, if we allow I to vary, as a vector field on V, i.e. now keep $u \in \mathfrak{g}$ fixed and consider

$$\zeta_u : V \to TV, \qquad I \mapsto T_e \ell^I . u. \tag{4}$$

Thus $\zeta : \mathfrak{g} \to \mathfrak{X}(V)$ assigns to each Lie algebra element u a vector field ζ_u on V. These are called the *fundamental vector fields* of the G-action. We will also use the notation $\zeta_u(I) = u.I$.

The tangent bundle TV of V can be identified via $TV \cong V \times V$ with two copies of V, the first containing basepoints and the second the tangent vectors. Similarly we can identify the cotangent bundle T^*V with the product $T^*V \cong V \times V^*$. Now take an element $(I, \pi) \in T^*V$. The pairing

$$\langle \pi, \zeta_u(I) \rangle_{V^* \times V} \ ,$$

is linear in $u \in \mathfrak{g}$ as can be seen from (4) and thus $u \mapsto \langle \pi, \zeta_u(I) \rangle_{V^* \times V}$ is a linear form on $\mathfrak{g}$ or equivalently an element of $\mathfrak{g}^*$. Denote this element by $I \diamond \pi$. The defining equation for $I \diamond \pi \in \mathfrak{g}^*$ is

$$\langle I \diamond \pi, u \rangle_{\mathfrak{g}^* \times g} = \langle \pi, \zeta_u(I) \rangle_{V^* \times V} \ ,$$

and $\diamond$ is a map $\diamond : T^*V \to \mathfrak{g}^*$, called the *momentum map* of the cotangent lifted action of G on T^*V. We shall explain the action of G on T^*V in the following paragraph.

2.6 Momentum Maps in Geometric Mechanics

In geometric mechanics, momentum maps generalize the notions of linear and angular momenta. For a mechanical system, whose configuration space is a manifold M acted on by a Lie group G, the momentum map $\diamond : T^*M \to \mathfrak{g}^*$ assigns to each element of the phase space T^*M a *generalized momentum* $I \diamond \pi$ in the dual $\mathfrak{g}^*$ of the Lie algebra. For example, the momentum map for spatial translations is the linear momentum, and for rotations it is the angular momentum.

One important feature of the momentum map in geometric mechanics is due to Noether's theorem. Noether's theorem states that if the Hamiltonian of the system under consideration is invariant under the action of G, then the generalized momentum $I \diamond \pi$ is a constant of motion. This theorem enables one generate conservation laws from symmetries. See [33, 40] for more details on momentum maps and geometric mechanics.

2.7 Tangent and Cotangent Lifted Actions

The action of a Lie group G on the vector space V is a map $\ell : G \times V \to V$. Fixing an element $g \in G$ we obtain a map $\ell_g : V \to V$, which we can differentiate to obtain $T\ell_g : TV \to TV$. It can be checked that the map of both variables

$$T_2\ell : G \times TV \to TV \ ,$$

is a left action of G on the space TV. Here $T_2\ell$ denotes the derivative of ℓ with respect to the second variable. The map $T\ell_g : V \times V \to V \times V$, being a derivative, is linear in the second variable, i.e. for each I the map

$$T_I\ell_g : V \cong T_IV \to T_{g.I}V \cong V \ ,$$

is linear and thus has a transpose

$$T_I^*\ell_g : V^* \cong T_{g.I}^*V \to T_I^*V \cong V^*.$$

This allows us to define the *cotangent lifted action* of G on the cotangent bundle $T^*V \cong V \times V^*$ via

$$g.(I,\pi) = \left(\ell(g,I), T^*_{g.I}\ell_{g^{-1}}.\pi\right) ,$$

for $(I,\pi) \in T^*V$. Note that the presence of the inverse makes this a left action. The following lemma shows that the momentum map is *equivariant* with respect to the cotangent lifted action.

Lemma 5. *For $g \in G$, $u \in \mathfrak{g}$, $I \in V$ and $\pi \in V^*$ we have*

- $g.\zeta_u(g^{-1}.I) = \zeta_{\mathrm{Ad}_g u}(I)$, *and*
- $g.I \diamond g.\pi = \mathrm{Ad}^*_{g^{-1}}(I \diamond \pi)$.

Proof. First note that $g.\zeta_u(g^{-1}.I)$ is a slightly informal way to denote g acting on $\zeta_u(g^{-1}.I)$ via the tangent lifted action; i.e.,

$$g.\zeta_u(g^{-1}.I) = T_{g^{-1}.I}\ell_g.\zeta_u(g^{-1}.I).$$

To prove the first identity take a curve $h(t) \in G$ with $h(0) = e$ and $\partial_t g|_{t=0} = u$. Via associativity, we have

$$\ell(g, h(t).g^{-1}.I) = \ell(gh(t)g^{-1}, I) ,$$

and by differentiating this identity we obtain

$$\begin{aligned} T_{g^{-1}.I}\ell_g.\zeta_u(g^{-1}.I) &= T_e\ell^I.\,\mathrm{Ad}_g\, u \\ g.\zeta_u(g^{-1}.I) &= \zeta_{\mathrm{Ad}_g u}(I). \end{aligned}$$

For the second identity note that $g.I \diamond g.\pi$ is a short way of writing

$$g.I \diamond g.\pi = \diamond(g.(I,\pi)) = \diamond(g.I, T^*_{g.I}\ell_{g^{-1}}.\pi) = g.I \diamond T^*_{g.I}\ell_{g^{-1}}.\pi .$$

Now take any $u \in \mathfrak{g}$ and consider the pairing

$$\begin{aligned} \langle g.I \diamond g.\pi, u\rangle_{\mathfrak{g}^*\times\mathfrak{g}} &= \langle T^*_{g.I}\ell_{g^{-1}}.\pi, \zeta_u(g.I)\rangle_{V^*\times V} = \\ &= \langle \pi, T_{g.I}\ell_{g^{-1}}.\zeta_u(g.I)\rangle_{V^*\times V} = \langle \pi, \zeta_{\mathrm{Ad}_{g^{-1}}u}(I)\rangle_{V^*\times V} = \\ &= \langle \mathrm{Ad}^*_{g^{-1}}(I \diamond \pi), u\rangle_{\mathfrak{g}^*\times\mathfrak{g}} . \end{aligned}$$

This concludes the proof. □

2.8 The $\flat$-Map

The final piece of notation is the $\flat$-map of a vector space associated to an inner product. On the vector space V the $\flat$-map is defined as

$$\flat : V \to V^*, \qquad \langle u^\flat, v\rangle_{V^*\times V} = \langle u, v\rangle_V,$$

where the pairing on the left side is the canonical pairing between V^* and V and on the right side we have the inner product $\langle ., .\rangle_V$. Each inner product gives rise to a $\flat$-map and we have two of them in our framework, one on $\mathfrak{g}$ and one on V. As there is no risk of confusion between them, we will use the same notation for both. Inspired by their appearance in physics, the elements $u \in \mathfrak{g}$ are called *velocities* while the dual objects $u^\flat \in \mathfrak{g}^*$ are called *momenta*.

2.9 Derivative of the Matching Energy

We now have assembled all the tools we need to calculate the derivative $DE(u)$.

Theorem 6. *Consider the matching energy*

$$E(u) = \frac{1}{2}\int_0^1 |u_t|^2_{\mathfrak{g}}\, \mathrm{d}t + \frac{1}{2\sigma^2}\,|g_1.I_0 - I_1|^2_V\,.$$

Its derivative is given by

$$DE(u)(t) = u_t^\flat + g_t I_0 \diamond g_t g_1^{-1}\pi\ , \tag{5}$$

with $\pi = \frac{1}{\sigma^2}(g_1 I_0 - I_1)^\flat \in V^* \cong T^*_{g_1.I_0}V$.

Proof. The derivative is a curve $t \mapsto DE(u)(t) \in \mathfrak{g}^*$ and the pairing between $DE(u)$ and a variation δu is given by

$$\langle DE(u), \delta u\rangle = \int_0^1 \langle DE(u)(t), \delta u_t\rangle_{\mathfrak{g}^*\times\mathfrak{g}}\, \mathrm{d}t.$$

From

$$\left\langle D\left(\frac{1}{2}\int_0^1 |u_t|^2_{\mathfrak{g}}\, \mathrm{d}t\right), \delta u\right\rangle = \int_0^1 \langle u_t, \delta u_t\rangle_{\mathfrak{g}}\, \mathrm{d}t = \int_0^1 \left\langle u_t^\flat, \delta u_t\right\rangle_{\mathfrak{g}^*\times\mathfrak{g}} \mathrm{d}t\ ,$$

we see that the derivative of the kinetic energy part is simply $u_t^\flat$. Now for the matching term,

$$\left\langle D\left(\frac{1}{2\sigma^2}\,|g_1.I_0 - I_1|^2_V\right), \delta u\right\rangle = \frac{1}{\sigma^2}\,\langle g_1.I_0 - I_1, \delta g_1.I_0\rangle_{V^*\times V} = \langle \pi, \delta g_1.I_0\rangle_{V^*\times V}\,.$$

We apply Lem. 4 to express δg_1 via δu and the we use adjoint operations to isolate δu. Consequently, we find

$$\begin{aligned}
\langle \pi, \delta g_1 . I_0 \rangle_{V^* \times V} &= \left\langle \pi, g_1 . \int_0^1 \operatorname{Ad}_{g_t^{-1}} \delta u_t \, \mathrm{d}t . I_0 \right\rangle_{V^* \times V} \\
&= \int_0^1 \left\langle g_1^{-1} . \pi, \left(\operatorname{Ad}_{g_t^{-1}} \delta u_t \right) . I_0 \right\rangle_{V^* \times V} \mathrm{d}t \\
&= \int_0^1 \left\langle I_0 \diamond g_1^{-1} . \pi, \operatorname{Ad}_{g_t^{-1}} \delta u_t \right\rangle_{\mathfrak{g}^* \times \mathfrak{g}} \mathrm{d}t \\
&= \int_0^1 \left\langle \operatorname{Ad}^*_{g_t^{-1}} \left(I_0 \diamond g_1^{-1} . \pi \right), \delta u_t \right\rangle_{\mathfrak{g}^* \times \mathfrak{g}} \mathrm{d}t \\
&= \int_0^1 \left\langle g_t . I_0 \diamond g_t g_1^{-1} . \pi, \delta u_t \right\rangle_{\mathfrak{g}^* \times \mathfrak{g}} \mathrm{d}t .
\end{aligned}$$

And thus we obtain the result. □

2.10 Image Matching

In image matching the group of transformations is taken to be the group $\operatorname{Diff}(\mathbb{R}^3)$ of diffeomorphisms of $\mathbb{R}^3$, i.e., smooth invertible maps $\varphi : \mathbb{R}^3 \to \mathbb{R}^3$ with smooth inverses. The space of objects is $\mathscr{F}(\mathbb{R}^3)$, the space of real-valued smooth functions on $\mathbb{R}^3$, and the action is given by

$$\ell : \operatorname{Diff}(\mathbb{R}^3) \times \mathscr{F}(\mathbb{R}^3) \to \mathscr{F}(\mathbb{R}^3), \qquad (\varphi, I) \mapsto I \circ \varphi^{-1}.$$

Due to the inverse in the definition, the voxel $\varphi(x)$ of the transformed image has the same grey-value as the voxel x of the original image. We will postpone the discussion of analytical aspects of $\operatorname{Diff}(\mathbb{R}^3)$ to Sect. 3 and for now assume all objects are sufficiently smooth for the necessary operations.

Remark 7 (Convenient Calculus). The discussion here can be made rigorous by considering the group

$$\operatorname{Diff}_{H^\infty}(\mathbb{R}^3) = \left\{ \varphi \,:\, \operatorname{Id} - \varphi \in H^\infty(\mathbb{R}^3) \right\}$$

of all diffeomorphisms φ, such that $\operatorname{Id} - \varphi$ lies in the intersection $H^\infty(\mathbb{R}^3)$ of all Sobolev spaces. The group $\operatorname{Diff}_{H^\infty}(\mathbb{R}^3)$ is a smooth regular Fréchet-Lie group. For the space of images we can take either $\mathscr{F}(\mathbb{R}^3) = H^\infty(\mathbb{R}^3)$ functions with square-integrable derivatives or $\mathscr{F}(\mathbb{R}^3) = C_c^\infty(\mathbb{R}^3)$ compactly supported functions. Then the action $\ell : \operatorname{Diff}_{H^\infty}(\mathbb{R}^3) \times C_c^\infty(\mathbb{R}^3) \to C_c^\infty(\mathbb{R}^3)$ is smooth in the sense of

convenient calculus [37] and all the operations described below can be interpreted in that framework. See [45] for details on diffeomorphism groups with other decay properties.

The Lie algebra of $\mathrm{Diff}(\mathbb{R}^3)$ is $\mathfrak{X}(\mathbb{R}^3)$, the space of vector fields on $\mathbb{R}^3$. Given a time-dependent vector field $t \mapsto u_t \in \mathfrak{X}(\mathbb{R}^3)$ its flow is defined by the differential equation

$$\partial_t \varphi_t(x) = u_t\left(\varphi_t(x)\right), \qquad \varphi_0(x) = x, \qquad x \in \mathbb{R}^3.$$

Let us assume that we are given a norm on $\mathfrak{X}(\mathbb{R}^3)$, defined via a positive, self-adjoint differential operator L as follows,

$$\langle u, v\rangle_L = \int_{\mathbb{R}^3} u(x) \cdot Lv(x)\,\mathrm{d}x. \tag{6}$$

For example the H^1-norm

$$\langle u, v\rangle_{H^1} = \int_{\mathbb{R}^3} u(x)\cdot v(x) + \alpha^2 \sum_{i=1}^{3} \nabla u^i(x)\cdot \nabla v^i(x)\,\mathrm{d}x\ ,$$

can be defined via the operator $Lu = u - \alpha^2 \Delta u$, where the Laplace operator is understood to act componentwise on u.

The dual space of $\mathfrak{X}(\mathbb{R}^3)$ is the space of distributions. We consider only the smooth dual, that is the space $\mathfrak{X}(\mathbb{R}^3)^* := \left\{Lu : u \in \mathfrak{X}(\mathbb{R}^3)\right\}$ generated by the $\flat$-map. As the duality pairing between $\mathfrak{X}^*(\mathbb{R}^3)$ and $\mathfrak{X}(\mathbb{R}^3)$ we choose the L^2-pairing, i.e.

$$\langle \alpha, u\rangle_{\mathfrak{X}(\mathbb{R}^3)^*\times\mathfrak{X}(\mathbb{R}^3)} = \int_{\mathbb{R}^3} \alpha(x)\cdot u(x)\,\mathrm{d}x.$$

Thus we see that the $\flat$-map of the $\langle .,.\rangle_L$-inner product is given by $u^\flat = Lu$.

On the space of images we use the L^2-inner product $\langle I, J\rangle_{L^2} = \int_{\mathbb{R}^3} I(x)J(x)\,\mathrm{d}x$. Again we don't look at the whole dual space, but only at the subspace generated by functionals of the form $I \mapsto \int_{\mathbb{R}^3} \pi I\,\mathrm{d}x$ with $\pi \in \mathscr{F}(\mathbb{R}^3)$. Thus the canonical pairing is given by

$$\langle \pi, I\rangle_{\mathscr{F}(\mathbb{R}^3)^*\times\mathscr{F}(\mathbb{R}^3)} = \int_{\mathbb{R}^3} \pi(x) I(x)\,\mathrm{d}x.$$

The $\flat$-map in this case is the identity, $I^\flat = I$. However the distinction between $\mathscr{F}(\mathbb{R}^3)$ and its dual $\mathscr{F}(\mathbb{R}^3)^*$ is still important, because $\mathrm{Diff}(\mathbb{R}^3)$ will act differently on the two spaces.

The infinitesimal action of $u \in \mathfrak{X}(\mathbb{R}^3)$ on $I \in \mathscr{F}(\mathbb{R}^3)$ can be computed via

$$\zeta_u(I) = \partial_t|_{t=0}\varphi_t.I\ ,$$

where $t \mapsto \varphi_t$ is a curve with $\varphi_0 = \mathrm{Id}$ and $\partial_t|_{t=0}\varphi_t = u$. Then

$$\zeta_u(I) = \partial_t|_{t=0}\left(I \circ \varphi_t^{-1}\right) = -\nabla I \cdot u.$$

This allows us to compute the momentum map

$$\begin{aligned}\langle I \diamond \pi, u\rangle_{\mathfrak{X}(\mathbb{R}^3)^*\times\mathfrak{X}(\mathbb{R}^3)} &= \langle \pi, \zeta_u(I)\rangle_{\mathscr{F}(\mathbb{R}^3)^*\times\mathscr{F}(\mathbb{R}^3)} \\ &= -\int_{\mathbb{R}^3} \pi(x)\nabla I(x)\cdot u(x)\,\mathrm{d}x \\ &= \langle -\pi\nabla I, u\rangle_{\mathfrak{X}(\mathbb{R}^3)^*\times\mathfrak{X}(\mathbb{R}^3)}.\end{aligned}$$

Thus, in this case, $I \diamond \pi = -\pi\nabla I$.

The last pieces of the geometrical framework are the lifted tangent and cotangent actions. The action of $\mathrm{Diff}(\mathbb{R}^3)$ on $\mathscr{F}(\mathbb{R}^3)$ is linear, i.e. $\varphi.(aI + bJ) = a(\varphi.I) + b(\varphi.J)$ and so the tangent action on $T\mathscr{F}(\mathbb{R}^3) \cong \mathscr{F}(\mathbb{R}^3)\times\mathscr{F}(\mathbb{R}^3)$ coincides with the action on $\mathscr{F}(\mathbb{R}^3)$,

$$\varphi.(I, U) = (I \circ \varphi^{-1}, U \circ \varphi^{-1}).$$

In particular we don't have to keep track of the basepoint. To compute the dual action on $\mathscr{F}(\mathbb{R}^3)^*$ we use the definition

$$\begin{aligned}\langle \varphi.\pi, U\rangle_{\mathscr{F}(\mathbb{R}^3)^*\times\mathscr{F}(\mathbb{R}^3)} &= \langle \pi, \varphi^{-1}.U\rangle_{\mathscr{F}(\mathbb{R}^3)^*\times\mathscr{F}(\mathbb{R}^3)} \\ &= \int_{\mathbb{R}^3} \pi(x)U(\varphi(x))\,\mathrm{d}x \\ &= \int_{\mathbb{R}^3} \left|\det D\varphi^{-1}(x)\right| \pi\left(\varphi^{-1}(x)\right) U(x)\,\mathrm{d}x \\ &= \left\langle \left|\det D\varphi^{-1}(x)\right| \pi\circ\varphi^{-1}, U\right\rangle_{\mathscr{F}(\mathbb{R}^3)^*\times\mathscr{F}(\mathbb{R}^3)}\end{aligned}$$

with $\pi \in \mathscr{F}(\mathbb{R}^3)^*$ and $U \in \mathscr{F}(\mathbb{R}^3)$. Thus the cotangent lifted action is given by

$$\varphi.(I, \pi) = \left(I \circ \varphi^{-1}, \left|\det D\varphi^{-1}(x)\right| \pi \circ \varphi^{-1}\right),$$

and we see that the objects dual to images transform as densities.

Now we can compute the criticality condition from Thm. 6,

$$DE(u)(t) = u_t^\flat + \varphi_t.I_0 \diamond \varphi_t\varphi_1^{-1}.\pi,$$

with $\pi = \frac{1}{\sigma^2}\left(\varphi_1.I_0 - I_1\right)^\flat$. To simplify the formulas, let us define $\varphi_{t,1} := \varphi_t \circ \varphi_1^{-1}$, which denotes the flow of u_t from time 1 backwards to t. In general $\varphi_{t,s} := \varphi_t \circ \varphi_s^{-1}$ is the solution of

$$\partial_t\varphi_{t,s}(x) = u_t\left(\varphi_{t,s}(x)\right), \qquad \varphi_{s,s}(x) = x.$$

So we have

$$DE(u)(t) = Lu^t - \left|\det D\varphi_{t,1}^{-1}(x)\right| \left(\pi \circ \varphi_{t,1}^{-1}\right) \nabla \left(\varphi_t.I_0\right) \ ,$$

and

$$\pi \circ \varphi_{t,1}^{-1} = \frac{1}{\sigma^2} \left(I_0 \circ \varphi_1^{-1} - I_1\right) \circ \varphi_1 \circ \varphi_t^{-1} =$$

$$= \frac{1}{\sigma^2} \left(I_0 \circ \varphi_t^{-1} - I_1 \circ \varphi_1 \circ \varphi_t^{-1}\right) = \frac{1}{\sigma^2} \left(\varphi_t.I_0 - \varphi_{t,1}.I_1\right).$$

Hence the derivative is given by

$$DE(u)(t) = Lu_t - \frac{1}{\sigma^2} \left|\det D\varphi_{t,1}^{-1}(x)\right| \left(\varphi_t.I_0 - \varphi_{t,1}.I_1\right) \nabla \left(\varphi_t.I_0\right) \ ,$$

and critical points of E satisfy

$$Lu_t = \frac{1}{\sigma^2} \left|\det D\varphi_{t,1}^{-1}(x)\right| \left(\varphi_t.I_0 - \varphi_{t,1}.I_1\right) \nabla \left(\varphi_t.I_0\right).$$

This formula was first derived in [10], where it was used to implement a gradient descent method for E, which enabled computation of a numerical solution of the registration problem.

2.11 Conservation of Momentum

Returning to the general framework let us have a closer look at the equation (5) for the derivative and the information contained therein. Let u_t be a critical point of the registration problem in Def. 3. Then

$$u_t^\flat = -g_t.I_0 \diamond g_t g_1^{-1}.\pi \ , \tag{7}$$

which we can reformulate as

$$u_t^\flat = -\operatorname{Ad}^*_{g_t^{-1}} \left(I_0 \diamond g_1^{-1}.\pi\right) \tag{8}$$

$$\operatorname{Ad}^*_{g_t} u_t^\flat = I_0 \diamond g_1^{-1}.\pi. \tag{9}$$

Now note that the right hand side of (9) does not depend on time any more while the left hand side doesn't depend on V any more. As the right hand side is independent of t, we can differentiate the identity to obtain

$$\partial_t \left(\operatorname{Ad}^*_{g_t} u_t^\flat\right) = 0. \tag{10}$$

2.12 *Differentiating* Ad *and* Ad*

It is time to introduce some more tools from geometry related to the derivatives of the adjoint and coadjoint representations. Differentiating (10) with respect to $u_t^\flat$ is not a problem, because $\mathrm{Ad}^*_{g_t}$ is a linear transformation. What we need to know, is how to differentiate the expression with respect to g_t.

We know from the definition of Ad, that it can be interpreted as a map $\mathrm{Ad} : G \to GL(\mathfrak{g})$. The group $GL(\mathfrak{g})$ of invertible linear transformations of $\mathfrak{g}$ is also a Lie group. If $\dim \mathfrak{g} = n$, then we can identify $GL(\mathfrak{g}) \cong GL(\mathbb{R}^n)$ with invertible $n \times n$-matrices. Because invertible matrices form an open subset of all matrices, the tangent space $T_e GL(\mathbb{R}^n)$ at the identity is the space of all matrices. Thus the Lie algebra of $GL(\mathfrak{g})$ is $\mathfrak{gl}(\mathfrak{g})$, the space of all linear transformations of $\mathfrak{g}$. Hence the derivative of Ad at $e \in G$ is a map

$$\mathrm{ad} := T_e \,\mathrm{Ad} : \mathfrak{g} \to \mathfrak{gl}(\mathfrak{g}), \qquad u \mapsto \mathrm{ad}_u \,,$$

and is called the *adjoint representation* of $\mathfrak{g}$. The map ad figures in the following differentiation formula.

Lemma 8. *Let $t \mapsto g_t \in G$ be a smooth curve and $v \in \mathfrak{g}$. Then*

$$\partial_t \left(\mathrm{Ad}_{g_t} \, v \right) = \mathrm{ad}_{\partial_t g_t g_t^{-1}} \mathrm{Ad}_{g_t} \, v.$$

Proof. We obtain this formula by writing

$$\begin{aligned} \partial_t|_{t=t_0} \left(\mathrm{Ad}_{g_t} \, v \right) &= \partial_t|_{t=t_0} \left(\mathrm{Ad}_{g_t g_{t_0}^{-1}} \mathrm{Ad}_{g_{t_0}} \, v \right) \\ &= \mathrm{ad}_{\partial_t|_{t=t_0} g_t g_{t_0}^{-1}} \mathrm{Ad}_{g_{t_0}} \, v \,. \end{aligned}$$

□

However we will need the transposed version of it. For each $u \in \mathfrak{g}$ fixed, the transpose ad^*_u is defined by

$$\left\langle \mathrm{ad}^*_u \, \mu, v \right\rangle_{\mathfrak{g}^* \times \mathfrak{g}} = \left\langle \mu, \mathrm{ad}_u \, v \right\rangle_{\mathfrak{g}^* \times \mathfrak{g}} \,,$$

and thus ad^* defines a map

$$\mathrm{ad}^* : \mathfrak{g} \to \mathfrak{gl}(\mathfrak{g}^*).$$

This map is called the *coadjoint representation* of $\mathfrak{g}$. The transposed version of Lem. 8 is given in the following lemma.

Lemma 9. *Let $t \mapsto g_t \in G$ be a smooth curve and $\mu \in \mathfrak{g}^*$. Then*

$$\partial_t \left(\mathrm{Ad}^*_{g_t} \, \mu \right) = \mathrm{Ad}^*_{g_t} \, \mathrm{ad}^*_{\partial_t g_t g_t^{-1}} \, \mu.$$

Proof. Take $u \in \mathfrak{g}$ and consider

$$\begin{aligned}\partial_t \langle \mathrm{Ad}^*_{g_t}\, \mu, u\rangle &= \langle \mu, \partial_t\, \mathrm{Ad}_{g_t}\, u\rangle \\ &= \langle \mu, \mathrm{ad}^*_{\partial_t g_t g_t^{-1}}\, \mathrm{Ad}_{g_t}\, u\rangle \\ &= \langle \mathrm{Ad}^*_{g_t}\, \mathrm{ad}^*_{\partial_t g_t g_t^{-1}}\, \mu, u\rangle\,,\end{aligned}$$

from which the statement follows. □

2.13 The Euler-Poincaré Equation

Lemma 9 allows us to express equation (10) as,

$$\begin{aligned}0 = \partial_t \left(\mathrm{Ad}^*_{g_t}\, u_t^\flat\right) &= \mathrm{Ad}^*_{g_t}\, \partial_t u_t^* + \mathrm{Ad}^*_{g_t}\, \mathrm{ad}^*_{\partial_t g_t g_t^{-1}}\, u_t^\flat \\ &= \mathrm{Ad}^*_{g_t}\left(\partial_t u_t^* + \mathrm{ad}^*_{\partial_t g_t g_t^{-1}}\, u_t^\flat\right)\,,\end{aligned}$$

and because $\mathrm{Ad}^*_{g_t}$ is invertible we obtain the equation

$$\partial_t u_t^\flat = -\,\mathrm{ad}^*_{u_t}\, u_t^\flat.$$

Let us state this result as a theorem.

Theorem 10. *Let $t \mapsto u_t \in \mathfrak{g}$ be a solution of the registration problem from Def. 3. Then it satisfies the equation*

$$\partial_t u_t^\flat = -\,\mathrm{ad}^*_{u_t}\, u_t^\flat. \tag{11}$$

This equation is called the Euler-Poincaré equation *on the Lie group G.*

Remark 11. The Euler-Poincaré equation is an evolution equation on the dual $\mathfrak{g}^*$ of the Lie algebra $\mathfrak{g}$, independent of I_0, I_1. Discussion of the history and some applications of the Euler-Poincaré equation can be found in [31, 40].

Now let us discuss the interplay between the group of transformations and the objects that are being matched. Let $t \mapsto u_t$ be a solution of the matching problem. Then u_t satisfies the Euler-Poincaré equation, which depends only on the geometry of the group, as encoded by ad^*, and on the chosen metric $\langle .,.\rangle_{\mathfrak{g}}$ via the $\flat$-operator. The Euler-Poincaré equation does not see the space of objects, the action of the transformation group thereon or the particular objects I_0, I_1, we are trying to match. How is this possible? In order to compute u_t via the Euler-Poincaré equation we need to supply initial conditions and these do depend I_0, I_1, the group action, and the inner product $\langle .,.\rangle_V$ we chose on V. From (7) we see that

$$u_0^\flat = -I_0 \diamond g_1^{-1}.\pi \ , \tag{12}$$

with $\pi = \frac{1}{\sigma^2}(g_1.I_0 - I_1)^\flat$. So the initial value $u_0^\flat$ depends on the given objects I_0, I_1, on the inner product $\langle ., . \rangle_V$ via the $\flat$-map and on the group action via the momentum map.

The momentum map has yet another role to play. It allows us to reduce the dimensionality of the matching problem. Let us assume that both G and V are finite-dimensional. If $\dim G$ is much bigger than $\dim V$, then there must be a redundancy in the action of G on V. The momentum map $\diamond : V \times V^* \to \mathfrak{g}^*$ tells us that the initial condition $u_0^\flat$ will lie in the space $\mathrm{Im}(I_0 \diamond .)$, whose dimension is at most $\dim V$. Even more, we see from (7) that for each time t we have $u_t^\flat \in \mathrm{Im}\,(g_t.I_0 \diamond .)$. The same thing happens for infinite dimensional spaces, as we will see in the case of image matching.

2.14 The EPDiff Equation

To write the Euler-Poincaré equation on the diffeomorphism group we first need to calculate the operators Ad, ad and ad^*. Differentiating the conjugation $\mathrm{conj}_\varphi(\psi) = \varphi \circ \psi \circ \varphi^{-1}$ gives

$$\mathrm{Ad}_\varphi u = T_{\mathrm{Id}}(\mathrm{conj}_\varphi).u = (D\varphi.u) \circ \varphi^{-1} \ ,$$

with $\varphi \in \mathrm{Diff}(\mathbb{R}^3)$ and $u \in \mathfrak{X}(\mathbb{R}^3)$. Now we differentiate once more, which leads to

$$\mathrm{ad}_u v = T_{\mathrm{Id}} \left(\varphi \mapsto \mathrm{Ad}_\varphi v\right).u = Du.v - Dv.u = -[u, v] \, ;$$

where $[u, v]$ is the commutator bracket of vector fields. Next we need the coadjoint action ad^*. To compute it, we take $m \in \mathfrak{X}(\mathbb{R}^3)^*$ and pair it with $\mathrm{ad}_u v$ as in [31],

$$\begin{aligned}
\langle m, \mathrm{ad}_u v \rangle_{L^2} &= \int_{\mathbb{R}^3} m \cdot (Du.v - Dv.u) \, \mathrm{d}x \\
&= \int_{\mathbb{R}^3} m^k \partial_i u^k v^i - m^k \partial_i v^k u^i \, \mathrm{d}x \\
&= \int_{\mathbb{R}^3} m^i \partial_k u^i v^k + \partial_i (m^k u^i) v^k \, \mathrm{d}x \\
&= \langle Du^T.m + Dm.u + m \, \mathrm{div}\, u, v \rangle_{L^2} \, .
\end{aligned}$$

We can thus write the *Euler-Poincaré equation on the diffeomorphism group*, also called *EPDiff*. It has the form

$$\partial_t m + Dm.u + Du^T.m + \mathrm{div}(u)m = 0 \ , \qquad m = u^\flat = Lu. \tag{13}$$

The EPDiff equation (13) first appeared in the context of unidirectional propagation of shallow water waves [13]. In the context of planar image registration, the crests of the shallow water waves correspond to the contour lines of the image [32]. To improve readability in (13), we have omitted the subscript t for the time-dependence. For the sake of completeness, we also include the coadjoint action,

$$\mathrm{Ad}^*_\varphi m = (\det D\varphi)\, D\varphi^T.(m \circ \varphi).$$

2.15 Momentum Map for Image Matching

The momentum map for the action of $\mathrm{Diff}(\mathbb{R}^3)$ on the space $\mathscr{F}(\mathbb{R}^3)$ of images is $I \diamond \pi = -\pi \nabla I$. Thus (12) tells us that the initial momentum is of the form

$$Lu_0 = (\varphi_1^{-1}.\pi)\nabla I_0. \tag{14}$$

As I_0 is fixed this means that we only have to look for the initial momenta in the subspace

$$\mathrm{Im}\,(I_0 \diamond .) = \left\{P \nabla I_0 \,:\, P \in \mathscr{F}(\mathbb{R}^3)\right\}\ ,$$

elements of which are specified using only one real-valued function P, while the vector field u_0 or equivalently the momentum Lu_0 needs 3 functions. This reduction strategy was employed in [50, 71] to solve the matching problem by estimating the initial momentum and using the EPDiff equation to reconstruct the path.

The momentum map also allows for an intuitive interpretation. Equation (14) tells us that the optimal momentum will point in the direction of the gradient of I_0, that is Lu_0 will be orthogonal to the contour lines of I_0. Indeed we see from

$$Lu_t = \varphi_{t,1}.\pi \nabla\, (\varphi_t.I_0)\ ,$$

that for all times the momentum is orthogonal to the contour lines of the image $\varphi_t.I_0$ at time t. A vector field that is parallel to the contour lines will leave the image constant and since we are interested in deforming the images with the least amount of energy it is natural that the momentum wants to be orthogonal the contour lines.

2.16 Evolution Equations on T^*V

We have seen that the solution u_t of the matching problem from Def. 3 can be expressed via the momentum map

$$u_t^\flat = -g_t\, I_0 \diamond g_{t,1}.\pi\ ,$$

and it satisfies the Euler-Poincaré evolution equation on $\mathfrak{g}^*$:

$$\partial_t u_t^\flat = -\operatorname{ad}_{u_t}^* u_t^\flat. \tag{15}$$

The momentum map representation can now be used to reduce the dimensionality of the problem by writing the evolution equation (15) directly on T^*V. Let us define the variables

$$I_t := g_t.I_0, \qquad P_t := g_{t,1}.\pi.$$

Geometrically we have $I_t \in V$ and $P_t \in T^*_{I_t}V \cong V^*$ so that the pair (I_t, P_t) describes an element of T^*V. Computing the time-derivative of I_t gives

$$\partial_t I_t = \partial_t (g_t.I_0) = (\partial_t g_t).I_0 = u_t g_t.I_0 = u_t.I_t = \zeta_{u_t}(I_t).$$

To simplify the derivation of the evolution equation for P_t we will assume that the action of G on V is linear, as in the case of image matching. In that case the lifted actions of G on TV and T^*V do not depend on the basepoint. Take $U \in V \cong T_{I_t}V$ and consider

$$\begin{aligned}
\partial_t \langle P_t, U\rangle_{V^*\times V} &= \partial_t \langle g_{t,1}.\pi, U\rangle_{V^*\times V} \\
&= \partial_t \left\langle g_1^{-1}.\pi, g_t^{-1}.U\right\rangle_{V^*\times V} \\
&= \left\langle g_1^{-1}.\pi, -g_t^{-1}(\partial_t g_t) g_t^{-1}.U\right\rangle_{V^*\times V} \\
&= -\langle P_t, u_t.U\rangle_{V^*\times V} \\
&= \left\langle -u_t^T.P_t, U\right\rangle_{V^*\times V}.
\end{aligned}$$

The geometrically correct expression, which holds for a general G-action, not just a linear one, is

$$\partial_t P_t = -T^*_{I_t}\zeta_{u_t}.P_t.$$

In case of a linear action the fundamental vector field ζ_{u_t} is linear and thus we can omit the derivative and write simply u_t^T for the transpose map $T^*_{I_t}\zeta_{u_t}$ in the last line of the calculation above. Thus we obtain the following system of evolution equations on T^*V,

$$\begin{aligned}
\partial_t I_t &= \zeta_{u_t}(I_t) \\
\partial_t P_t &= -T^*_{I_t}\zeta_{u_t}.P_t \\
u_t^\flat &= I_t \diamond P_t.
\end{aligned} \tag{16}$$

Note that, while we cannot completely avoid computing the vector field u_t, it only needs to be updated at each time step using the variables (I_t, P_t) on T^*V.

2.17 Evolution Equations for Image Matching

Let us write out the evolution equations in the case of image matching. The action is linear and the fundamental vector fields are given by

$$\zeta_u(I) = -\nabla I \cdot u.$$

Now we compute the transpose

$$\begin{aligned}\langle P, \zeta_u(I)\rangle_{\mathscr{F}(\mathbb{R}^3)^*\times\mathscr{F}(\mathbb{R}^3)} &= -\int_{\mathbb{R}^3} P(x)\nabla I(x)\cdot u(x)\,\mathrm{d}x \\ &= \int_{\mathbb{R}^3} \operatorname{div}(Pu)(x) I(x)\,\mathrm{d}x \\ &= \langle \operatorname{div}(Pu), I\rangle_{\mathscr{F}(\mathbb{R}^3)^*\times\mathscr{F}(\mathbb{R}^3)}.\end{aligned}$$

Thus the evolution equations have the form

$$\begin{aligned}\partial_t I_t + \nabla I_t \cdot u_t &= 0 \\ \partial_t P_t + \operatorname{div}(P_t u_t) &= 0 \\ L u_t &= -P_t \nabla I_t.\end{aligned} \tag{17}$$

See also [77] for a direct derivation and [30] for an explanation and classification of the cotangent lift momentum maps associated with EPDiff.

2.18 Matching via Initial Momentum

The evolution equations in (17) allow for a reformulation of the matching problem from Def. 3. Instead of searching for paths $t \mapsto u_t \in \mathfrak{g}$, we see that any solution of the registration problem is completely determined by the initial momentum $P_0 = g_1^{-1}.\pi$. Thus we can formulate the following equivalent matching problem.

Definition 12 (Registration Problem via Initial Momentum). Given $I_0, I_\mathrm{T} \in V$ find $P_0 \in V^* \cong T^*_{I_0}V$ which minimizes

$$E(P_0) = \frac{1}{2}\,|I_0 \diamond P_0|^2_{\mathfrak{g}} + \frac{1}{2\sigma^2}\,|I_1 - I_\mathrm{T}|^2_V \ ,$$

where I_1 is defined as the solution of

$$\begin{aligned}\partial_t I_t &= \zeta_{u_t}(I_t)\\ \partial_t P_t &= -T^*_{I_t}\zeta_{u_t}.P_t\\ u_t^\flat &= I_t \diamond P_t.\end{aligned}$$

Remark 13. We replaced in the Def. 12 of the registration problem the integral $\int_0^1 |u_t|^2_{\mathfrak{g}}\,\mathrm{d}t$ over the whole time interval by $|u_0|^2_{\mathfrak{g}} = |I_0 \diamond P_0|^2_{\mathfrak{g}}$. This is justified, because if $t \mapsto u_t \in \mathfrak{g}$ is a solution of the registration problem from Def. 3, then its norm $|u_t|^2_{\mathfrak{g}}$ is constant in time. It is possible to prove this result directly, by using the evolution equations for (I_t, P_t) as follows,

$$\begin{aligned}\partial_t|_{t=t_0}\left(\frac{1}{2}|u_t|^2_{\mathfrak{g}}\right) &= \langle \partial_t|_{t=t_0}(I_t \diamond P_t), u_{t_0}\rangle_{\mathfrak{g}^*\times\mathfrak{g}}\\ &= \partial_t|_{t=t_0}\left\langle P_t, \zeta_{u_{t_0}}(I_t)\right\rangle_{\mathfrak{g}^*\times\mathfrak{g}}\\ &= -\left\langle T^*_{I_{t_0}}\zeta_{u_{t_0}}.P_{t_0}, \zeta_{u_{t_0}}(I_{t_0})\right\rangle_{\mathfrak{g}^*\times\mathfrak{g}} + \left\langle P_{t_0}, T_{I_{t_0}}\zeta_{u_{t_0}}.\zeta_{u_{t_0}}(I_{t_0})\right\rangle_{\mathfrak{g}^*\times\mathfrak{g}}\\ &= 0.\end{aligned}$$

In order to find minima for the registration problem from Def. 12, we would need to compute the derivative of the energy $E(P_0)$ with respect to P_0, which would require us to differentiate the solution I_1 with respect to P_0. This can be done using a technique called *adjoint equations* and is slightly more involved than the computation of the derivative in Thm. (3). Further details as well as a discussion of the numerical discretization can be found in [71].

2.19 Interpretation via Riemannian Geometry

Many of the derivations, theorems and properties discussed in this section are familiar from Riemannian geometry. Let us start with the Euler-Poincaré equation and discuss why it arises. The registration problem in Def. 3 asks us to find curves $t \mapsto u_t \in \mathfrak{g}$, that are minima of

$$E(u) = \frac{1}{2}\int_0^1 |u_t|^2_{\mathfrak{g}}\,\mathrm{d}t + \frac{1}{2\sigma^2}|g_1.I_0 - I_1|^2_V\,. \tag{18}$$

How does Riemannian geometry arise here? A Riemannian metric γ on a manifold is an inner product on each tangent space that varies smoothly with the basepoint. On the group G we have an inner product $\langle .,. \rangle_{\mathfrak{g}}$ on $\mathfrak{g} = T_eG$ and we can use right-multiplication to define the following Riemannian metric on the whole group,

$$\gamma_g(X_g, Y_g) := \left\langle X_g g^{-1}, Y_g g^{-1} \right\rangle_{\mathfrak{g}}, \qquad X_g, Y_g \in T_g G. \tag{19}$$

Let $t \mapsto u_t \in \mathfrak{g}$ be a curve and $t \mapsto g_t \in G$ be its flow, i.e. $\partial_t g_t = u_t g_t$, $g_0 = e$. Then (18) is equivalent to

$$E(g) = \frac{1}{2} \int_0^1 \gamma_{g_t} (\partial_t g_t, \partial_t g_t) \, \mathrm{d}t + \frac{1}{2\sigma^2} |g_1.I_0 - I_1|_V^2 \ ,$$

where we look for the minimum over all curves $t \mapsto g_t \in G$ with $g_0 = e$. Let $t \mapsto \tilde{g}_t$ be a minimum. Then this curve also must be a minimum of

$$E_{\mathrm{KE}}(g) = \frac{1}{2} \int_0^1 \gamma_{g_t} (\partial_t g_t, \partial_t g_t) \, \mathrm{d}t \ ,$$

over the set $\{t \mapsto g_t : g_0 = e, \ g_1 = \tilde{g}_1\}$ of all curves with fixed endpoints. This is exactly the definition of a geodesic in Riemannian geometry. That is, the Euler-Poincaré equation in the general form

$$\partial_t u_t^\flat = -\operatorname{ad}_{u_t}^* u_t^\flat \ ,$$

is the geodesic equation for right-invariant metrics on Lie groups. The property used in Rem. 13, that the norm $t \mapsto |u_t|_{\mathfrak{g}}^2$ is constant is also a general result for geodesics in Riemannian geometry. It can be shown using the Euler-Poincaré equation in the following way,

$$\partial_t \left(\frac{1}{2} |u_t|_{\mathfrak{g}}^2 \right) = \left\langle \partial_t u_t^\flat, u_t \right\rangle_{\mathfrak{g}^* \times \mathfrak{g}} = \left\langle -\operatorname{ad}_{u_t}^* u_t^\flat, u_t \right\rangle_{\mathfrak{g}^* \times \mathfrak{g}} = -\left\langle u_t^\flat, \operatorname{ad}_{u_t} u_t \right\rangle_{\mathfrak{g}^* \times \mathfrak{g}} .$$

Now we use the property that $\operatorname{ad}_u v$ is antisymmetric, i.e. $\operatorname{ad}_u v = -\operatorname{ad}_v u$, which implies $\operatorname{ad}_{u_t} u_t = 0$, and conclude that $|u_t|_{\mathfrak{g}}^2$ is constant in time.

2.20 *Riemannian Geometry on V*

Let us consider the left action $\ell : G \times V \to V$ of G on V. Assume for now that the action is *transitive*, i.e. for any two $I, J \in V$ there exists $g \in G$ such that $g.I = J$. Equivalently this means that for any $I \in V$ the map $\ell^I : G \to V$ is onto. If the action is not onto, we can restrict ourselves to an orbit $G.I = \{g.I : g \in G\}$ and proceed as below.

We have an inner product $\langle ., . \rangle_{\mathfrak{g}}$ on the Lie algebra, which we can extend to a right-invariant Riemannian metric γ^G on the whole group G via (19). We want to project this metric to a Riemannian metric γ^V on V. Fix $I_0 \in V$ and let $J \in V$ be

any element. Then we can write $J = g.I_0$ for some $g \in G$, not necessarily unique, due to the transitivity of the action. If $U \in T_J V$ is a tangent vector, we can write it in the form $U = X_g.I_0 = T_g \ell^{I_0}.X_g$ with some $X_g \in T_g G$ and again X_g is not necessarily unique.

Theorem 14. *The expression*

$$\gamma_J^V(U,U) = \inf_{U = X_g.I_0} \gamma_g^G(X_g, X_g) \,, \tag{20}$$

defines a well-defined Riemannian metric on V that is independent of the choice of I_0.

Proof. Two things need to be proven. First, the expression on the right side must not depend on g and second we have to show that γ^V is independent of I_0. As a first step we note that any $X_g \in T_g G$ is of the form Xg with $X \in \mathfrak{g}$ and thus we can rewrite the condition in the infimum of (20) as

$$U = X_g.I_0 = Xg.I_0 = \zeta_X(J) \,,$$

as well as

$$\gamma_g^G(X_g, X_g) = \gamma_g^G(Xg, Xg) = \langle X, X \rangle_{\mathfrak{g}} \,,$$

and hence

$$\gamma_J^V(U,U) = \inf_{U = X_g.I_0} \gamma_g^G(X_g, X_g) = \inf_{U = \zeta_X(J)} \langle X, X \rangle_{\mathfrak{g}} \,.$$

This shows that the metric γ^V is independent of both the group element g used to represent J as well as the choice of I_0 and thus everything is proven. □

Associated to the map $\ell^{I_0} : G \to V$ is a splitting of the Lie algebra $\mathfrak{g}$ into two orthogonal subspaces. Denote by $\mathrm{Ver}(g) = \left(\ker T_g \ell^{I_0}\right) g^{-1} \subseteq \mathfrak{g}$ the vertical subspace. In fact $\mathrm{Ver}(g)$ depends only on the element $J = g.I_0$ and can be described by

$$\mathrm{Ver}(J) = \{X \in \mathfrak{g} : \zeta_X(J) = 0\} \,.$$

The orthogonal complement of $\mathrm{Ver}(J)$ with respect to the inner product $\langle ., . \rangle_{\mathfrak{g}}$ is called the *horizontal subspace*,

$$\mathrm{Hor}(J) = \mathrm{Ver}(J)^{\perp}.$$

For each $J \in V$ the momentum map gives an identification between $T_J V$ and $\mathrm{Hor}(J)$ via

$$T_I U \ni U \mapsto (I \diamond U^\flat)^\sharp \in \mathrm{Hor}(J) \ ,$$

where $\sharp : \mathfrak{g}^* \to \mathfrak{g}$ denotes the inverse of the $\flat$-map. To see that $(J \diamond U^\flat)^\sharp \in \mathrm{Hor}(J)$ take any $X \in \mathrm{Ver}(J)$ and look at

$$\langle J \diamond U^\flat, X \rangle_{\mathfrak{g}^* \times \mathfrak{g}} = \langle U^\flat, \zeta_X(J) \rangle_{V^* \times V} = 0.$$

Surjectivity follows in finite dimensions via dimension counting and is a more delicate matter in infinite dimensions. The momentum map has the following property: for each $U \in T_J V$ the element $(J \diamond U^\flat)^\sharp \in \mathfrak{g}$ realizes the infimum in (20); i.e.,

$$\gamma^J(U, U) = \langle (J \diamond U^\flat)^\sharp, (J \diamond U^\flat)^\sharp \rangle_{\mathfrak{g}}.$$

The Riemannian interpretation of the matching problem may now be given, as follows: A solution $t \mapsto u_t$ or $t \mapsto g_t$ of the registration problem is a solution of the Euler-Poincaré equation (11) and thus a geodesic on the group G with respect to the metric γ^G. Furthermore the velocity at all times satisfies $u_t \in \mathrm{Hor}(g_t.I_0)$. Such geodesics are called *horizontal geodesics*. It follows from Riemannian geometry that the projected curve $I_t = g_t.I_0$ is a geodesic with respect to the Riemannian metric γ^V. The set of evolution equations (16) are the geodesic equations on V with respect to the metric γ^V, written in the Hamiltonian form [71].

Let us come back to (1) from the introduction, which described registration as the minimization of

$$E(g) = d_1(e, g)^2 + \tfrac{1}{\sigma^2} d_2(g.I_0, I_1)^2 \ ,$$

where $d_1(.,.)$ is a distance function on G and $d_2(.,.)$ a distance function on V. The LDDMM framework chose $d_1(.,.)$ to be the geodesic distance with respect to the metric γ^G. What the above discussion shows is that we can replace it with $d^V(.,.)$, the geodesic distance with respect to γ^V; i.e. we can minimize

$$E(J) = d^V(I_0, J)^2 + \tfrac{1}{\sigma^2} d_2(J, I_1)^2 \ ,$$

with $d_2(.,.)$ being some other metric on V.

For further details on the background from Riemannian geometry and the theory of group actions consult [43]. The Hamiltonian approach to Riemannian geometry, including the infinite dimensional case is described in [44]. Riemannian metrics induced by group actions, especially the diffeomorphism group, in the context of shape matching are discussed in [9, 42].

3 Existence of Solutions for Image Registration

In this section we want to present a framework that allows us to prove the existence of minimizers for the image registration problem, that is for the energy

$$E(u) = \frac{1}{2}\int_0^1 |u_t|_L^2 \,\mathrm{d}t + \frac{1}{2\sigma^2}\|I_0 \circ \varphi^{-1} - I_1\|_{L^2}^2 ,$$

where $I_0, I_1 : \mathbb{R}^3 \to \mathbb{R}$ are grey-value images, $u : [0, 1] \to \mathfrak{X}(\mathbb{R}^3)$ a time-dependent vector field and φ_1 its flow at time 1.

There are two competing tendencies in the mathematical modelling for image registration. We want the diffeomorphism group to be an (infinite-dimensional) Lie group. That is, we want the group operations to be smooth, so that we can rigorously apply the geometric framework of Sect. 2. In addition, we want the Lie algebra of the diffeomorphism group with the norm $\langle ., . \rangle_L$ to be a Hilbert space, so that we can use completeness to show the existence of minimizers. Unfortunately the following theorem by Omori [52] shows that these two requirements are incompatible.

Theorem 15 ([52]). *If a connected Banach-Lie group G acts effectively, transitively and smoothly on a compact manifold, then G must be a finite dimensional Lie group.*

The action of a Lie group G on a manifold M is called effective, if

$$g.x = h.x \text{ for all } x \in M \text{ implies } g = h.$$

This means that we can distinguish group elements based on how they act on the manifold. The action of the diffeomorphism group $\mathrm{Diff}(M)$ on the base manifold M, given by $\varphi.x = \varphi(x)$ is by definition effective. The theorem thus implies that the diffeomorphism group of a compact manifold cannot be made into a Banach-Lie group. For noncompact manifolds the argument is a bit more complicated, but also follows from results in [52].

Since we cannot have both smooth group operations and a Hilbert space as a Lie algebra, we will now describe a framework that gives up the structure of a Lie group to gain completeness. For more detailed exposition and full proofs, we refer to [75].

Since none of the arguments in this section are specific to three dimensions, we will consider the case of d-dimensional images. Also images are not necessarily defined on the whole of $\mathbb{R}^d$. So let $\Omega \subseteq \mathbb{R}^d$ be an open subset of $\mathbb{R}^d$, where the image $I : \Omega \to \mathbb{R}$ is defined. We consider a certain class of spaces of vector fields, called *admissible vector spaces*, to serve as the equivalent of a Lie algebra. The following introduction is taken from [11].

Definition 16. A Hilbert space $\mathscr{H}$, consisting of vector fields on the domain Ω, is called *admissible*, if it is continuously embedded in $C_0^1(\Omega, \mathbb{R}^d)$, i.e. there exists a constant $C > 0$ such that

$$|u|_{1,\infty} \leq C\,|u|_{\mathscr{H}}.$$

Here $C_0^1(\Omega, \mathbb{R}^d)$ is the space of all C^1-vector fields on Ω that vanish on the boundary $\partial\Omega$ and at infinity with the norm

$$|u|_{1,\infty} := \sup_{x\in\Omega} |u(x)| + \sum_{i=1}^{d} |\nabla u^i(x)|.$$

An admissible vector space $\mathscr{H}$ falls into the class of reproducing kernel Hilbert spaces.

Definition 17. A Hilbert space $\mathscr{H}$, consisting of functions $u : \Omega \to \mathbb{R}^d$ is called a *reproducing kernel Hilbert space (RKHS)*, if for all $x \in \Omega$ and $a \in \mathbb{R}^d$ the directional point-evaluation $\mathrm{ev}_x^a : \mathscr{H} \to \mathbb{R}$ defined as $\mathrm{ev}_x^a(u) := a \cdot u(x)$ is a continuous linear functional.

In this case the relation

$$\langle u, K(., x)a\rangle = a \cdot u(x), \qquad u \in \mathscr{H},\ a \in \mathbb{R}^d\ ,$$

defines a function $K : \Omega \times \Omega \to \mathbb{R}^{d\times d}$, called the *kernel of* $\mathscr{H}$.

If we denote by $L : \mathscr{H} \to \mathscr{H}^*$ the canonical isomorphism between a Hilbert space and its dual, then we have the relation

$$K(y, x)a = L^{-1}(\mathrm{ev}_x^a)(y).$$

In order for the RHKS to be admissible, the kernel K has to satisfy the following properties:

- K is twice continuously differentiable with bounded derivatives, i.e. $K \in C^2(\Omega \times \Omega, \mathbb{R}^{d\times d})$ and $|K|_{2,\infty} < \infty$.
- K vanishes on the boundary of $\Omega \times \Omega$, i.e. $K(x, y) = 0$ whenever $x \in \partial\Omega$ or $y \in \partial\Omega$.

Further exposition of the theory of RKHS can be found, e.g. in [3, 63].

Example 18. The Sobolev embedding theorem (see e.g. [1, Chapter 6]) states that for $\Omega \subseteq \mathbb{R}^d$ there is an embedding

$$H^{k+m}(\Omega) \hookrightarrow C^k(\Omega), \qquad m > \frac{d}{2}\ ,$$

of the Sobolev space $H^{k+m}(\Omega)$ into the space of k-times continuously differentiable functions $C^k(\Omega)$. Therefore for $m > \frac{d}{2} + 1$, the space $H^m(\Omega)$ is an admissible space. The corresponding kernel is the Green's function of the operator $L = \mathrm{Id} + \sum_{j=1}^{m} (-1)^j \Delta^j$.

We fix an admissible vector space $\mathscr{H}$ with kernel K and let $u \in L^2([0, 1], \mathscr{H})$ be a time-dependent vector field. In Sect. 2 we assumed the vector fields to be smooth in

time, but since we want to minimize over the space of time-dependent vector fields, we work here with the space $L^2([0,1],\mathscr{H})$ of vector fields that are only square-integrable in time. This space is a Hilbert space with the inner product given by

$$\langle u, v\rangle_{L^2_{\mathscr{H}}} = \int_0^1 \langle u_t, v_t\rangle^2_{\mathscr{H}}\, \mathrm{d}t.$$

We want to define the flow φ_t of the vector field u, as before via the differential equation

$$\partial_t \varphi_t = u_t \circ \varphi_t, \qquad \varphi_0(x) = x. \tag{21}$$

If u_t were smooth or at least continuous in time, we could apply standard existence theorems for ODEs. Note that the theorem of Picard-Lindelöf requires vector fields that are continuous in time and Lipschitz continuous in space. In our case u_t is continuously differentiable in space, but only square-integrable in time. We have the following result concerning the existence and uniqueness of a flow for such a vector field.

Theorem 19. *Let $\mathscr{H}$ be an admissible space and $u \in L^2([0,1],\mathscr{H})$ a time-dependent vector field. Then (21) has a unique solution $\varphi \in C^1([0,1]\times\Omega,\Omega)$, such that for each $t \in [0,1]$, the map $\varphi_t : \Omega \to \Omega$ is a C^1-diffeomorphism of Ω.*

Proof. See [75, Appendix C.2] for the existence of a solution and [75, Thm. 8.7] for properties of φ_t. □

For matching purposes we will work with all diffeomorphisms that can be obtained as flows of such vector fields. Define the group $G_{\mathscr{H}}$ to be

$$G_{\mathscr{H}} := \left\{\varphi_1 : \varphi_t \text{ is a solution of (21) for some } u \in L^2([0,1],\mathscr{H})\right\}. \tag{22}$$

It can be equipped with the following distance, which is modelled after the geodesic distance on Riemannian manifolds,

$$d_{\mathscr{H}}(\psi_0,\psi_1)^2 = \inf_{u\in L^2([0,1],\mathscr{H})} \left\{ \int_0^1 |u_t|^2_{\mathscr{H}}\, \mathrm{d}t \;:\; \psi_1 = \psi_0 \circ \varphi_1^u \right\}. \tag{23}$$

The set $G_{\mathscr{H}}$ has the following properties

Theorem 20. *Let $\mathscr{H}$ be an admissible space and $G_{\mathscr{H}}$ defined via (22). Then*

- *$G_{\mathscr{H}}$ is a group.*
- *(Trouvé) The function $d_{\mathscr{H}}$ is a distance on $G_{\mathscr{H}}$ and $(G_{\mathscr{H}}, d_{\mathscr{H}})$ is a complete metric space.*
- *For each $\psi_0, \psi_1 \in G_{\mathscr{H}}$ there exists $u \in L^2([0,1],\mathscr{H})$ realizing the infimum in (23), i.e. $d_{\mathscr{H}}(\psi_0,\psi_1) = |u|_{L^2_{\mathscr{H}}}$.*

Proof. See [75, Thm. 8.14] for a proof that $G_{\mathscr{H}}$ is closed under group operations, see [75, Thm. 8.15] for the completeness of $d_{\mathscr{H}}$ and see [75, Thm. 8.20] for the existence of a minimum. □

Note that we have not said anything about the structure of $G_{\mathscr{H}}$ as a manifold or a Lie group. In an informal way the space $\mathscr{H}$ acts as a "Lie algebra" of the "Lie group" $\mathscr{G}_{\mathscr{H}}$, but all the statements of Sect. 2 are to be interpreted only formally in this framework.

The main advantage of working with admissible spaces and the group $G_{\mathscr{H}}$ is the following theorem.

Theorem 21. *Let $\mathscr{H}$ be an admissible space and $I_0, I_1 \in L^2(\Omega)$. Then there exists a minimizer for the registration energy*

$$E(u) = \frac{1}{2}\int_0^1 |u_t|^2_{\mathscr{H}}\,\mathrm{d}t + \frac{1}{2\sigma^2}\|I_0 \circ \varphi^{-1} - I_1\|^2_{L^2}\,, \tag{24}$$

i.e. there exists $\tilde{u} \in L^2([0,1],\mathscr{H})$ such that $E(\tilde{u}) = \inf_{u\in L^2([0,1],\mathscr{H})} E(u)$.

Proof (Sketch). Let us introduce the notation $U(\varphi) = \frac{1}{2\sigma^2}\|I_0 \circ \varphi^{-1} - I_1\|^2_{L^2}$. This allows us to write $E(u) = \frac{1}{2}|u|^2_{L^2_{\mathscr{H}}} + U(\varphi_1)$. Consider a minimizing sequence $u^n \in L^2([0,1],\mathscr{H})$, such that $E(u^n) \to \inf_u E(u)$. As the functional $U(.)$ is bounded from below, the sequence $(u^n)_{n\in\mathbb{N}}$ is bounded in the Hilbert space $L^2([0,1],\mathscr{H})$. Since bounded sets in Hilbert spaces are weakly compact, we can extract a subsequence, again denoted by $(u^n)_{n\in\mathbb{N}}$, that converges weakly to some $\tilde{u}$. What remains to show now is that this $\tilde{u}$ is indeed the minimizer. The inequality $\inf_u E(u) \le E(\tilde{u})$ is trivial and it remains to show the converse.

From

$$\langle u^n, \tilde{u}\rangle \le |u^n|_{L^2}|\tilde{u}|_{L^2}$$

we see by passing to the lim inf that $|\tilde{u}|_{L^2} \le \liminf_{n\to\infty}|u^n|_{L^2}$. Concerning $U(\varphi_1^n)$ we will use the following property:

$$\text{If } u^n \to \tilde{u} \text{ weakly in } L^2([0,1],\mathscr{H}), \text{ then } U(\varphi_1^n) \to U(\tilde{\varphi}_1).$$

This implication can be split up into two steps.

1. Let $u^n \to \tilde{u}$ weakly. Then the sequence $(\varphi_1^n)_{n\in\mathbb{N}}$ of flows satisfies
   - $\varphi_1^n \to \tilde{\varphi}_1$ and $(\varphi_1^n)^{-1} \to \tilde{\varphi}_1^{-1}$ uniformly on compact sets and
   - the sequence $(|D\varphi^n|_\infty)_{n\in\mathbb{N}}$ is bounded.
2. Under the above conditions on the sequence $(\tilde{\varphi}_1^n)_{n\in\mathbb{N}}$ of flows, we have convergence $U(\varphi_1^n) \to U(\tilde{\varphi}_1)$.

The proof for the first step is a combination of [75, Thm. 8.11] and Gronwall's lemma [75, Thm. C.8]. An explicit proof for the second step can be found in [11, Thm. 2.7]. Putting all pieces together we get

$$\begin{aligned} E(\tilde{u}) &= \tfrac{1}{2}|\tilde{u}|^2_{L^2_{\mathscr{H}}} + U(\tilde{\varphi}_1) \\ &\leq \liminf_{n\to\infty} \tfrac{1}{2}|u^n|^2_{L^2_{\mathscr{H}}} + \lim_{n\to\infty} U(\varphi_1^n) = \lim_{n\to\infty} E(u^n) \\ &\leq \inf_{u\in L^2} E(u) \ , \end{aligned}$$

Hence $\tilde{u}$ is a minimizer. □

To make the connection back to the general framework, we will show that, if the images I_0, I_1 are sufficiently smooth, then the minimizer will also be smooth, both in space and in time. Thus the smooth geometric framework on Sect. 2 retains some use. It may not be sufficient to show existence of a minimizer or its properties, but if existence has been established, the minimizer does reside in the smooth framework.

Theorem 22. *Let $\mathscr{H}$ be an admissible space. Let $I_0 \in C^1_0(\Omega)$ and $I_1 \in C_0(\Omega)$. Then the minimizer u of the registration energy (24) satisfies*

$$Lu_t = \frac{1}{\sigma^2} \left|\det D\varphi_{t,1}^{-1}(x)\right| \left(I_0 \circ \varphi_t^{-1} - I_1 \circ \varphi_{t,1}^{-1}\right) \nabla \left(I_0 \circ \varphi_t^{-1}\right) \ ,$$

and the equation

$$Lu_t = \mathrm{Ad}^*_{\varphi_t^{-1}} Lu_0. \tag{25}$$

Proof. See [75, Thm. 11.5] and [75, Thm. 11.6]. □

We did encounter equation (25) in the smooth setting as well in the form (10). Now however we see that the right hand side is differentiable in t, because φ_t, being the solution of a differential equation, is differentiable in t and so is u_t. Differentiating (25) with respect to t leads to the EPDiff equation (13). Finally we can state the following theorem, which brings us back to the smooth framework.

Theorem 23. *Let $\mathscr{H}$ be an admissible space with $\Omega = \mathbb{R}^3$. Then $H^\infty(\mathbb{R}^3, \mathbb{R}^3) \subset \mathscr{H}$ and $\mathrm{Diff}_{H^\infty}(\mathbb{R}^3) \subset G_{\mathscr{H}}$. If $I_0, I_1 \in C^\infty_c(\mathbb{R}^3)$, then the minimizer $t \mapsto u_t$ of (24) from Thm. 21 satisfies*

$$u \in C^\infty([0,1], H^\infty(\mathbb{R}^3, \mathbb{R}^3)).$$

This theorem closes the loop between the geometric and analytic settings for image registration.

Acknowledgements Both authors gratefully acknowledge partial support by Advanced Grant 267382 from the European Research Council.

References

1. Adams, R.A.: Sobolev Spaces. Academic, New York (1975)
2. Alexander, D.C., Pierpaoli, C., Basser, P.J., Gee, J.C.: Spatial transformations of diffusion tensor magnetic resonance images. IEEE Trans. Med. Imaging **20**(11), 1131–1139 (2001)
3. Aronszajn, N.: Theory of reproducing kernels. Trans. Am. Math. Soc. **68**, 337–404 (1950)
4. Artaechevarria, X., Munoz-Barrutia, A., Ortiz-de Solorzano, C.: Combination strategies in multi-atlas image segmentation: application to brain MR data. IEEE Trans. Med. Imaging **28**(8), 1266–1277 (2009)
5. Ashburner, J.: A fast diffeomorphic image registration algorithm. NeuroImage **38**(1), 95–113 (2007)
6. Ashburner, J., Friston, K.J.: Diffeomorphic registration using geodesic shooting and Gauss-Newton optimisation. NeuroImage **55**(3), 954–967 (2011)
7. Babalola, K.O., Patenaude, B., Aljabar, P., Schnabel, J., Kennedy, D., Crum, W., Smith, S., Cootes, T., Jenkinson, M., Rueckert, D.: An evaluation of four automatic methods of segmenting the subcortical structures in the brain. NeuroImage **47**(4), 1435–1447 (2009)
8. Bai, J., Trinh, T.L.H., Chuang, K.H., Qiu, A.: Atlas-based automatic mouse brain image segmentation revisited: model complexity vs. image registration. Magn. Reson. Imaging **30**(6), 789–798 (2012)
9. Bauer, M., Bruveris, M., Michor, P.W.: Overview of the geometries of shape spaces and diffeomorphism groups. J. Math. Imaging Vis. **50**, 60–97 (2014). doi:10.1007/s10851-013-0490-z
10. Beg, M.F., Miller, M.I., Trouvé, A., Younes, L.: Computing large deformation metric mappings via geodesic flows of diffeomorphisms. Int. J. Comput. Vis. **61**(2), 139–157 (2005)
11. Bruveris, M.: Geometry of diffeomorphism groups and shape matching. Ph.D. thesis, Imperial College, London (2012)
12. Bruveris, M., Gay-Balmaz, F., Holm, D.D., Ratiu, T.: The momentum map representation of images. J. Nonlinear Sci. **21**, 115–150 (2011)
13. Camassa, R., Holm, D.D.: An integrable shallow water equation with peaked solitons. Phys. Rev. Lett. **71**(11), 1661–1664 (1993). doi:10.1103/PhysRevLett.71.1661. http://dx.doi.org/10.1103/PhysRevLett.71.1661
14. Cao, Y., Miller, M.I., Winslow, R.L., Younes, L.: Large deformation diffeomorphic metric mapping of vector fields. IEEE Trans. Med. Imaging **24**(9), 1216–1230 (2005)
15. Collins, D.L., Peters, T.M., Dai, W., Evans, A.C.: Model-based segmentation of individual brain structures from MRI data. In: Robb, R.A. (ed.) Society of Photo-Optical Instrumentation Engineers (SPIE) Conference Series, vol. 1808, pp. 10–23 (1992)
16. Davis, B.C., Fletcher, P.T., Bullitt, E., Joshi, S.: Population shape regression from random design data. Int. J. Comput. Vis. **90**, 255–266 (2010)
17. Durrleman, S., Pennec, X., Trouvé, A., Ayache, N.: Statistical models on sets of curves and surfaces based on currents. Med. Image Anal. **13**(5), 793–808 (2009)
18. Faria, A.V., Hoon, A., Stashinko, E., Li, X., Jiang, H., Mashayekh, A., Akhter, K., Hsu, J., Oishi, K., Zhang, J., Miller, M.I., van Zijl, P.C., Mori, S.: Quantitative analysis of brain pathology based on MRI and brain atlases—applications for cerebral palsy. NeuroImage **54**(3), 1854–1861 (2011)
19. Ferri, C.P., Prince, M., Brayne, C., Brodaty, H., Fratiglioni, L., Ganguli, M., Hall, K., Hasegawa, K., Hendrie, H., Huang, Y., Jorm, A., Mathers, C., Menezes, P.R., Rimmer, E., Scazufca, M.: Global prevalence of dementia: a Delphi consensus study. Lancet **366**(9503), 2112–2117 (2006)
20. Fiot, J.B., Risser, L., Cohen, L.D., Fripp, J., Vialard, F.X.: Local vs global descriptors of hippocampus shape evolution for Alzheimer's longitudinal population analysis. In: Durrleman, S., Fletcher, T., Gerig, G., Niethammer, M. (eds.) Spatio-Temporal Image Analysis for Longitudinal and Time-Series Image Data. Lecture Notes in Computer Science, vol. 7570, pp. 13–24. Springer, Berlin/Heidelberg (2012)

21. Fischl, B., Salat, D.H., Busa, E., Albert, M., Dieterich, M., Haselgrove, C., van der Kouwe, A., Killiany, R., Kennedy, D., Klaveness, S., Montillo, A., Makris, N., Rosen, B., Dale, A.M.: Whole brain segmentation: automated labeling of neuroanatomical structures in the human brain. Neuron **33**(3), 341–355 (2002)
22. Gee, J.C., Reivich, M., Bajcsy, R.: Elastically deforming a three-dimensional atlas to match anatomical brain images. J. Comput. Assist. Tomogr. **17**(2), 225–236 (1993)
23. Glaunès, J., Vaillant, M., Miller, M.I.: Landmark matching via large deformation diffeomorphisms on the sphere. J. Math. Imaging Vis. **20**, 179–200 (2004)
24. Glaunès, J., Qiu, A., Miller, M.I., Younes, L.: Large deformation diffeomorphic metric curve mapping. Int. J. Comput. Vis. **80**, 317–336 (2008)
25. Grenander, U.: Regular Structure. Lectures in Pattern Theory III. Applied Mathematical Science, vol. 33. Springer, Berlin/Heidelberg (1981)
26. Grenander, U.: General Pattern Theory. Oxford University Press, Oxford (1993)
27. Grenander, U., Miller, M.I.: Computational anatomy: an emerging discipline. Q. Appl. Math. **56**, 617–694 (1998)
28. Grenander, U., Miller, M.I.: Pattern Theory: From Representation to Inference. Oxford University Press, Oxford (2007)
29. Holden, M.: A review of geometric transformations for nonrigid body registration. IEEE Trans. Med. Imaging **27**(1), 111–128 (2008)
30. Holm, D.D., Marsden, J.E.: Momentum maps and measure-valued solutions (peakons, filaments, and sheets) for the EPDiff equation. In: Marsden, J.E., Ratiu, T. (eds.) The Breadth of Symplectic and Poisson Geometry. Progress in Mathematics, vol. 232, pp. 203–235. Birkhäuser, Basel (2005)
31. Holm, D.D., Marsden, J.E., Ratiu, T.S.: The Euler-Poincaré equations and semidirect products with applications to continuum theories. Adv. Math. **137**, 1–81 (1998)
32. Holm, D.D., Rathanather, J.T., Trouvé, A., Younes, L.: Soliton dynamics in computational anatomy. NeuroImage **23**, 170–178 (2004)
33. Holm, D.D., Schmah, T., Stoica, C.: Geometric Mechanics and Symmetry: From Finite to Infinite Dimension. Clarendon Press, Oxford (2009)
34. Jenkinson, M., Smith, S.: A global optimisation method for robust affine registration of brain images. Med. Image Anal. **5**(2), 143–156 (2001)
35. Joshi, S., Miller, M.I.: Landmark matching via large deformation diffeomorphisms. IEEE Trans. Image Process. **9**(8), 1357–1370 (2000)
36. Klein, A., Andersson, J., Ardekani, B.A., Ashburner, J., Avants, B., Chiang, M.C., Christensen, G.E., Collins, D.L., Gee, J., Hellier, P., Song, J.H., Jenkinson, M., Lepage, C., Rueckert, D., Thompson, P., Vercauteren, T., Woods, R.P., Mann, J.J., Parsey, R.V.: Evaluation of 14 nonlinear deformation algorithms applied to human brain MRI registration. NeuroImage **46**(3), 786–802 (2009)
37. Kriegl, A., Michor, P.W.: The Convenient Setting of Global Analysis. Mathematical Surveys and Monographs, vol. 53. American Mathematical Society, Providence (1997)
38. Lorenzi, M., Ayache, N., Pennec, X.: Schild's ladder for the parallel transport of deformations in time series of images. In: Székely, G., Hahn, H. (eds.) Information Processing in Medical Imaging. Lecture Notes in Computer Science, vol. 6801, pp. 463–474. Springer, New York (2011)
39. Maes, F., Collignon, A., Vandermeulen, D., Marchal, G., Suetens, P.: Multimodality image registration by maximization of mutual information. IEEE Trans. Med. Imaging **16**(2), 187–198 (1997)
40. Marsden, J.E., Ratiu, T.S.: Introduction to Mechanics and Symmetry. Texts in Applied Mathematics, vol. 17, 2nd edn. Springer, New York (1999)
41. McDowell, K.S., Vadakkumpadan, F., Blake, R., Blauer, J., Plank, G., MacLeod, R.S., Trayanova, N.A.: Methodology for patient-specific modeling of atrial fibrosis as a substrate for atrial fibrillation. J. Electrocardiol. **45**(6), 640–645 (2012)
42. Micheli, M., Michor, P.W., Mumford, D.: Sobolev metrics on diffeomorphism groups and the derived geometry of spaces of submanifolds. Izv. Math. **77**(3), 541–570 (2013). doi:10.1070/IM2013v077n03ABEH002648

43. Michor, P.W.: Topics in Differential Geometry. Graduate Studies in Mathematics, vol. 93. American Mathematical Society, Providence (2008)
44. Michor, P.W., Mumford, D.: An overview of the Riemannian metrics on spaces of curves using the Hamiltonian approach. Appl. Comput. Harmon. Anal. **23**(1), 74–113 (2007)
45. Michor, P.W., Mumford, D.: A zoo of diffeomorphism groups on $\mathbb{R}^n$. Ann. Glob. Anal. Geom. **44**(4), 529–540 (2013). doi:10.1007/s10455-013-9380-2
46. Miller, M.I., Qiu, A.: The emerging discipline of computational functional anatomy. NeuroImage **45**(1, Suppl. 1), S16–S39 (2009)
47. Miller, M.I., Younes, L.: Group actions, homeomorphisms, and matching: a general framework. Int. J. Comput. Vis. **41**, 61–84 (2001)
48. Miller, M.I., Christensen, G.E., Amit, Y., Grenander, U.: Mathematical textbook of deformable neuroanatomies. Proc. Natl. Acad. Sci, **90**(24), 11944–11948 (1993)
49. Miller, M.I., Trouvé, A., Younes, L.: On the metrics and Euler-Lagrange equations of computational anatomy. Annu. Rev. Biomed. Eng. **4**, 375–405 (2002)
50. Miller, M., Trouvé, A., Younes, L.: Geodesic shooting for computational anatomy. J. Math. Imaging Vis. **24**, 209–228 (2006)
51. Mumford, D., Desolneux, A.: Pattern Theory: The Stochastic Analysis of Real-World Signals. A K Peters, Natick (2010)
52. Omori, H.: On Banach-Lie groups acting on finite dimensional manifolds. Tôhoku Math. J. **30**(2), 223–250 (1978)
53. Peng, T., Wang, W., Rohde, G., Murphy, R.: Instance-based generative biological shape modeling. In: IEEE International Symposium on Biomedical Imaging: From Nano to Macro, 2009. ISBI '09, pp. 690–693 (2009)
54. Qiu, A., Bitouk, D., Miller, M.: Smooth functional and structural maps on the neocortex via orthonormal bases of the Laplace-Beltrami operator. IEEE Trans. Med. Imaging **25**(10), 1296–1306 (2006)
55. Qiu, A., Younes, L., Wang, L., Ratnanather, J.T., Gillepsie, S.K., Kaplan, G., Csernansky, J., Miller, M.I.: Combining anatomical manifold information via diffeomorphic metric mappings for studying cortical thinning of the cingulate gyrus in schizophrenia. NeuroImage **37**(3), 821–833 (2007)
56. Qiu, A., Younes, L., Miller, M.I., Csernansky, J.G.: Parallel transport in diffeomorphisms distinguishes the time-dependent pattern of hippocampal surface deformation due to healthy aging and the dementia of the alzheimer's type. NeuroImage **40**(1), 68–76 (2008)
57. Qiu, A., Albert, M., Younes, L., Miller, M.I.: Time sequence diffeomorphic metric mapping and parallel transport track time-dependent shape changes. NeuroImage **45**(1, Suppl. 1), S51–S60 (2009)
58. Qiu, A., Wang, L., Younes, L., Harms, M.P., Ratnanather, J.T., Miller, M.I., Csernansky, J.G.: Neuroanatomical asymmetry patterns in individuals with schizophrenia and their non-psychotic siblings. NeuroImage **47**(4), 1221–1229 (2009)
59. Qiu, A., Fennema-Notestine, C., Dale, A.M., Miller, M.I.: Regional shape abnormalities in mild cognitive impairment and Alzheimer's disease. NeuroImage **45**(3), 656–661 (2009)
60. Qiu, A., Younes, L., Miller, M.: Principal component based diffeomorphic surface mapping. IEEE Trans. Med. Imaging **31**(2), 302–311 (2012)
61. Rohde, G.K., Ribeiro, A.J.S., Dahl, K.N., Murphy, R.F.: Deformation-based nuclear morphometry: capturing nuclear shape variation in HeLa cells. Cytometry A **73A**(4), 341–350 (2008)
62. Rueckert, D., Sonoda, L.I., Hayes, C., Hill, D.L.G., Leach, M.O., Hawkes, D.J.: Nonrigid registration using free-form deformations: application to breast MR images. IEEE Trans. Med. Imaging **18**(8), 712–721 (1999)
63. Saitoh, S.: Theory of Reproducing Kernels and Its Applications. Pitman Research Notes in Mathematics. Longman, England (1988)
64. Steinert-Threlkeld, S., Ardekani, S., Mejino, J.L., Detwiler, L.T., Brinkley, J.F., Halle, M., Kikinis, R., Winslow, R.L., Miller, M.I., Ratnanather, J.T.: Ontological labels for automated location of anatomical shape differences. J. Biomed. Inform. **45**(3), 522–527 (2012)

65. Thirion, J.P.: Image matching as a diffusion process: an analogy with Maxwell's demons. Med. Image Anal. **2**(3), 243–260 (1998)
66. Thompson, D.W.: On Growth and Form. Dover, New York (1992). Reprint of 1942 2nd edn. (1st edn. 1917)
67. Trouvé, A.: Diffeomorphic groups and pattern matching in image analysis. Int. J. Comput. Vis. **28**, 213–221 (1998)
68. Vaillant, M., Glaunes, J.: Surface matching via currents. In: Christensen, G., Sonka, M. (eds.) IPMI. Lecture Notes in Computer Science, vol. 3565, pp. 381–392. Springer, Berlin (2005)
69. Vercauteren, T., Pennec, X., Perchant, A., Ayache, N.: Symmetric log-domain diffeomorphic registration: a demons-based approach. In: Metaxas, D., Axel, L., Fichtinger, G., Székely, G. (eds.) Medical Image Computing and Computer-Assisted Intervention MICCAI 2008. Lecture Notes in Computer Science, vol. 5241, pp. 754–761. Springer, New York (2008)
70. Vialard, F.X.: Hamiltonian approach to shape spaces in a diffeomorphic framework: from the discontinuous image matching problem to a stochastic growth model. Ph.D. thesis, École Normale Supérieure de Cachan (2009)
71. Vialard, F.X., Risser, L., Rueckert, D., Cotter, C.J.: Diffeomorphic 3D image registration via geodesic shooting using an efficient adjoint calculation. Int. J. Comput. Vis. **97**, 229–241 (2012)
72. Warfield, S., Zou, K., Wells, W.: Simultaneous truth and performance level estimation (STAPLE): an algorithm for the validation of image segmentation. IEEE Trans. Med. Imaging **23**(7), 903–921 (2004)
73. Weiner, M.W., Veitch, D.P., Aisen, P.S., Beckett, L.A., Cairns, N.J., Green, R.C., Harvey, D., Jack, C.R., Jagust, W., Liu, E., Morris, J.C., Petersen, R.C., Saykin, A.J., Schmidt, M.E., Shaw, L., Siuciak, J.A., Soares, H., Toga, A.W., Trojanowski, J.Q.: The Alzheimer's disease neuroimaging initiative: a review of papers published since its inception. Alzheimers Dement. **8**(1 Suppl.), S1–S68 (2012)
74. Younes, L.: Jacobi fields in groups of diffeomorphisms and applications. Q. Appl. Math. **65**(1), 113–134 (2007)
75. Younes, L.: Shapes and Diffeomorphisms. Springer, Berlin (2010)
76. Younes, L., Qiu, A., Winslow, R., Miller, M.I.: Transport of relational structures in groups of diffeomorphisms. J. Math. Imaging Vis. **32**, 41–56 (2008)
77. Younes, L., Arrate, F., Miller, M.I.: Evolution equations in computational anatomy. NeuroImage **45**, 40–50 (2009)

Multisymplectic Geometry and Lie Groupoids

Henrique Bursztyn, Alejandro Cabrera, and David Iglesias

In memory of Jerry Marsden

Abstract We study higher-degree generalizations of symplectic groupoids, referred to as *multisymplectic groupoids*. Recalling that Poisson structures may be viewed as infinitesimal counterparts of symplectic groupoids, we describe "higher" versions of Poisson structures by identifying the infinitesimal counterparts of multisymplectic groupoids. Some basic examples and features are discussed.

1 Introduction

Multisymplectic structures are higher-degree analogs of symplectic forms which arise in the geometric formulation of classical field theory much in the same way that symplectic structures emerge in the hamiltonian description of classical mechanics, see [17, 21, 26] and references therein. This symplectic approach to field theory was explored in a number of Marsden's publications, which treated (as it was typical in Marsden's work) theoretical as well as applied aspects of the subject, see e.g. [18, 19, 30, 31]. Multisymplectic geometry (as in [8, 9]) also arises in other settings, such as the study of homotopical structures [35], categorified symplectic geometry [2], and geometries defined by closed forms [28].

H. Bursztyn (✉)
IMPA, Estrada Dona Castorina 110, 22460-320 Rio de Janeiro, Brazil
e-mail: henrique@impa.br

A. Cabrera
Departamento de Matematica Aplicada, Instituto de Matematica, Universidade Federal do Rio de Janeiro. Caixa Postal 68530, Rio de Janeiro RJ 21941-909, Brasil
e-mail: acabrera@labma.ufrj.br

D. Iglesias
Departamento de Matemáticas, Estadística e Investigación Operativa, Universidad de la Laguna, Santa Cruz de Tenerife, Spain
e-mail: diglesia@ull.es

D.E. Chang et al. (eds.), *Geometry, Mechanics, and Dynamics*, Fields Institute Communications 73, DOI 10.1007/978-1-4939-2441-7_3

Poisson structures are generalizations of symplectic structures which are central to geometric mechanics[1] and permeate Marsden's work. A natural problem in multisymplectic geometry is the identification of "higher" analogs of Poisson structures bearing a relation to multisymplectic forms that extends the way Poisson geometry generalizes symplectic geometry. In this note we discuss one possible approach to tackle this issue.

Our viewpoint relies on the relationship between Poisson geometry and objects known as *symplectic groupoids* [11, 37]. This relationship is part of a generalized Lie theory in which Poisson structures arise as infinitesimal, or linearized, counterparts of symplectic groupoids, in a way analogous to how Lie algebras correspond to Lie groups. In order to find higher analogs of Poisson structures the route we take is to first consider higher-degree versions of symplectic groupoids, referred to as *multisymplectic groupoids*, and then to identify the geometric objects arising as their infinitesimal counterparts. Recalling that symplectic groupoids are Lie groupoids equipped with a symplectic structure that is compatible with the groupoid multiplication, in the sense that the symplectic form is *multiplicative* (see (5) below), multisymplectic groupoids are defined analogously, as Lie groupoids endowed with a multiplicative multisymplectic structure. Our identification of the infinitesimal objects corresponding to multisymplectic groupoids builds on the infinitesimal description of general multiplicative differential forms obtained in [1, 4].

For a manifold M, our "higher-degree" analogs of Poisson structures can be conveniently expressed (in the spirit of Dirac geometry [12]) in terms of subbundles

$$L \subset TM \oplus \wedge^k T^*M \tag{1}$$

satisfying suitable properties, including an involutivity condition with respect to the "higher" Courant-Dorfman bracket on the space of sections of $TM \oplus \wedge^k T^*M$ (see e.g. [22, Sec. 2]). Related geometric objects have been recently considered in the study of higher analogs of Dirac structures in [38] (see also [36]). But, as it turns out, the higher Poisson structures that arise from multisymplectic groupoids are not particular cases of the higher Dirac structures of [38] (for example, comparing with [38, Def. 3.1], the higher Poisson structures (1) considered here are not necessarily lagrangian subbundles, though always isotropic). An alternative characterization of these objects, more in the spirit of the bivector-field description of Poisson structures, is presented in Prop. 3.

Another perspective on higher Poisson structures relies on the view of Poisson structures as Lie brackets on the space of smooth functions of a manifold. A natural issue in this context is finding an appropriate extension of the Poisson bracket defined by a symplectic form (see (4)) to multisymplectic manifolds. This problem involves notorious difficulties and much work has been done on it, see e.g. [16, 25, 35]. The approach to higher Poisson structures in this note follows a different path and does not address any of the issues involved in the algebraic study of higher Lie-type brackets.

[1] For example, in the description of the interplay between hamiltonian dynamics and symmetries [29], and in the transition from classical to quantum mechanics [7].

The paper is structured as follows. We review Poisson structures and their connection with symplectic groupoids in Section 2. In Section 3 we recall the basics of multisymplectic forms. The main results are presented in Section 4, in which we introduce multisymplectic groupoids and identify their infinitesimal counterparts. In Section 5 we give different descriptions of these objects and explain some of their properties, while examples are discussed in Section 6.

As one should expect, higher Poisson structures naturally arise in connection with symmetries in multisymplectic geometry. This aspect of the subject is not treated here, though we hope to explore it, as well as its relations with field theory, in future work. Parallel ideas to those in this note can be also carried out in the context of polysymplectic geometry, see [24, 32].

2 Poisson Structures and Symplectic Groupoids

We start by recalling a few different viewpoints to Poisson structures.

A *Poisson structure* on a smooth manifold M is Lie bracket $\{\cdot,\cdot\}$ on $C^\infty(M)$ which is compatible with the pointwise product of functions via the Leibniz rule:

$$\{f,gh\} = \{f,g\}h + \{f,h\}g, \quad f,g,h \in C^\infty(M). \tag{2}$$

The Leibniz condition (2) implies that $\{\cdot,\cdot\}$ is necessarily defined by a bivector field $\pi \in \Gamma(\wedge^2 TM)$ via

$$\pi(df,dg) = \{f,g\}, \quad f,g \in C^\infty(M).$$

This leads to the alternative description of Poisson structures on M as bivector fields $\pi \in \Gamma(\wedge^2 TM)$ satisfying $[\pi,\pi] = 0$, where $[\cdot,\cdot]$ is the Schouten-Nijenhuis bracket on multivector fields. (The vanishing of $[\pi,\pi]$ accounts for the Jacobi identity of $\{\cdot,\cdot\}$.) We denote Poisson manifolds by either (M,π) or $(M,\{\cdot,\cdot\})$.

Symplectic manifolds are naturally equipped with Poisson structures. Given a symplectic manifold (M,ω), and denoting by X_f the hamiltonian vector field associated with $f \in C^\infty(M)$ via

$$i_{X_f}\omega = df, \tag{3}$$

the Poisson bracket on M is given by

$$\{f,g\} = \omega(X_g, X_f). \tag{4}$$

A more recent perspective on Poisson structures, which is the guiding principle of this note, relies on another type of connection between Poisson structures and symplectic manifolds. It is based on the fact that Poisson geometry fits into a generalized Lie theory, naturally expressed in terms of Lie algebroids and groupoids,

see e.g. [11]. In this context, Poisson manifolds are seen as infinitesimal counterparts of global objects called *symplectic groupoids* [37], analogously to how Lie algebras are regarded as infinitesimal versions of Lie groups. We will briefly recall the main aspects of the theory.

Let $\mathcal{G} \rightrightarrows M$ be a Lie groupoid (the reader can find definitions and further details in [7]). We use the following notation for its structure maps: $\mathsf{s}, \mathsf{t} : \mathcal{G} \to M$ for the source, target maps, $m : \mathcal{G}_{\mathsf{s}}\times_{\mathsf{t}}\mathcal{G} \to \mathcal{G}$ for the multiplication map,[2] $\epsilon : M \hookrightarrow \mathcal{G}$ for the unit map, and $\mathsf{inv} : \mathcal{G} \to \mathcal{G}$ for the groupoid inversion. We will often identify M with its image under ϵ (the submanifold of $\mathcal{G}$ of identity arrows).

A differential form $\omega \in \Omega^r(\mathcal{G})$ is called *multiplicative* if it satisfies

$$m^*\omega = \mathrm{pr}_1^*\omega + \mathrm{pr}_2^*\omega, \tag{5}$$

where $\mathrm{pr}_i : \mathcal{G}_{\mathsf{s}}\times_{\mathsf{t}}\mathcal{G} \to \mathcal{G}$, $i = 1, 2$, is the natural projection onto the i-th factor.[3] A *symplectic groupoid* is a Lie groupoid $\mathcal{G} \rightrightarrows M$ equipped with a multiplicative symplectic form $\omega \in \Omega^2(\mathcal{G})$. In this case, condition (5) is equivalent to the graph of the multiplication map m being a lagrangian submanifold of $\mathcal{G} \times \mathcal{G} \times \overline{\mathcal{G}}$, where $\overline{\mathcal{G}}$ is equipped with the opposite symplectic form $-\omega$. Symplectic groupoids first arose in symplectic geometry in the context of quantization (see e.g. [3, Sec. 8.3]) but turn out to provide a convenient setting for the study of symmetries and reduction [34].

In order to explain how symplectic groupoids are related to Poisson structures, recall that a *Lie algebroid* is a vector bundle $A \to M$ equipped with a bundle map $\rho : A \to TM$, called the *anchor*, and a Lie bracket $[\cdot, \cdot]$ on $\Gamma(A)$ such that

$$[u, fv] = f[u, v] + (\mathcal{L}_{\rho(u)} f)v,$$

for $u, v \in \Gamma(A)$, $f \in C^\infty(M)$. Lie algebroids are infinitesimal versions of Lie groupoids: for a Lie groupoid $\mathcal{G} \rightrightarrows M$, its associated Lie algebroid is defined by $A = \ker(d\mathsf{s})|_M$, with anchor map $d\mathsf{t}|_A : A \to TM$ and Lie bracket on $\Gamma(A)$ induced by the Lie bracket of right-invariant vector fields on $\mathcal{G}$. Much of the usual theory relating Lie algebras and Lie groups carries over to Lie algebroids and groupoids, a notorious exception being Lie's third theorem, i.e., not every Lie algebroid arises as the Lie algebroid of a Lie groupoid (see [13] for a thorough discussion of this issue).

The first indication of a connection between Poisson geometry and Lie algebroids/groupoids is the fact that, if (M, π) is a Poisson manifold, then its cotangent bundle $T^*M \to M$ inherits a Lie algebroid structure, with anchor map given by

$$\pi^\sharp : T^*M \to TM, \quad \pi^\sharp(\alpha) = i_\alpha \pi, \tag{6}$$

[2] Here the fibred product $\mathcal{G}_{\mathsf{s}}\times_{\mathsf{t}}\mathcal{G} = \{(g, h) \in \mathcal{G} \times \mathcal{G} \,|\, \mathsf{s}(g) = \mathsf{t}(h)\}$ represents the space of composable arrows.

[3] For a function $f \in \Omega^0(\mathcal{G}) = C^\infty(\mathcal{G})$, condition (5) becomes $f(gh) = f(g) + f(h)$, i.e., it says that f is a groupoid morphism into $\mathbb{R}$ (viewed as an abelian group).

and Lie bracket on $\Gamma(T^*M) = \Omega^1(M)$ given by

$$[\alpha, \beta] = \mathscr{L}_{\pi^\sharp(\alpha)}\beta - \mathscr{L}_{\pi^\sharp(\beta)}\alpha - d(\pi(\alpha, \beta)). \tag{7}$$

The precise relation between Poisson structures and symplectic groupoids is as follows. First, given a symplectic groupoid $(\mathscr{G} \rightrightarrows M, \omega)$, its space of units M inherits a natural Poisson structure π, uniquely determined by the fact that the target map $\mathsf{t} : \mathscr{G} \to M$ is a Poisson map (while $\mathsf{s} : \mathscr{G} \to M$ is anti-Poisson); moreover, denoting by A the Lie algebroid of $\mathscr{G}$, there is a canonical identification between A and the Lie algebroid structure on T^*M induced by π, explicitly given by

$$\mu : A \xrightarrow{\sim} T^*M, \quad \mu(u) = i_u\omega|_{TM}.$$

Here we view TM as a subbundle of $T\mathscr{G}|_M$ via $\epsilon : M \hookrightarrow \mathscr{G}$, so that we can write

$$T\mathscr{G}|_M = TM \oplus A. \tag{8}$$

In other words, the Lie groupoid $\mathscr{G}$ integrates the Lie algebroid T^*M defined by π.

Conversely, given a Poisson manifold (M, π) and assuming that its associated Lie algebroid is integrable (i.e., can be realized as the Lie algebroid of a Lie groupoid[4]), then its s-simply-connected integration $\mathscr{G} \rightrightarrows M$ inherits a symplectic groupoid structure [27]. (As shown in [10], one can obtain $\mathscr{G}$ by means of an infinite-dimensional Marsden-Weinstein reduction.)

The upshot of this discussion is that *Poisson manifolds are the infinitesimal versions of symplectic groupoids.*

Some of the prototypical examples of symplectic groupoids are traditional phase spaces in mechanics. For example, any cotangent bundle T^*Q, equipped with its canonical symplectic form, is a symplectic groupoid over Q with respect to the groupoid structure given by fibrewise addition of covectors; in this case, source and target maps coincide, both being the bundle projection $T^*Q \to Q$, and the corresponding Poisson structure on Q is trivial: $\pi = 0$. A more interesting example is given by the cotangent bundle of a Lie group G. In this case, besides the symplectic groupoid structure over G that we just described, T^*G is also a symplectic groupoid over $\mathfrak{g}^*$, where $\mathfrak{g}$ denotes the Lie algebra of G. The groupoid structure

$$T^*G \rightrightarrows \mathfrak{g}^*$$

is induced by the co-adjoint action of G on $\mathfrak{g}^*$ (see e.g. [34]); source and target maps are given by the momentum maps for the cotangent lifts of the actions of G on itself by left and right translations, while the corresponding Poisson structure on $\mathfrak{g}^*$ is just its natural Lie-Poisson structure. The fact that the target map is a Poisson map may

[4] See e.g. [37] for a nonintegrable example and [14] for a discussion of obstructions to integrability.

be viewed as the *Lie-Poisson reduction theorem* (see e.g. [29, Sec. 13.1]), another one of Marsden's favorite topics. The correspondence between Poisson structures and symplectic groupoids extends much of the theory relating $\mathfrak{g}^*$ and T^*G to more general settings.

3 Multisymplectic Structures

A *multisymplectic structure* [8, 9] on a manifold M is a differential form $\omega \in \Omega^{k+1}(M)$ which is closed and nondegenerate, in the sense that $i_X\omega = 0$ implies that $X = 0$, for $X \in \Gamma(TM)$. Equivalently, the nondegeneracy condition says that the bundle map

$$\omega^\sharp : TM \to \wedge^k T^*M, \quad X \mapsto i_X\omega, \tag{9}$$

is injective. As in [2, 35], we refer to a multisymplectic form of degree $k+1$ as a *k-plectic* form. Hence a 1-plectic form ω is a usual symplectic structure, in which case the map (9) is necessarily surjective; note that the wedge powers ω^r, $r = 2, \ldots, \dim(M)$, are natural examples of higher degree multisymplectic forms. For completeness, we briefly recall some other examples, see e.g. [9].

For a manifold Q, the total space of the exterior bundle $\wedge^k T^*Q$ carries a canonical k-plectic form ω_{can}, generalizing the canonical symplectic structure on T^*Q. Indeed, there is a "tautological" k-form θ on $\wedge^k T^*Q$ given by

$$\theta_\xi(X_1, \ldots, X_k) = \xi(dp(X_1), \ldots, dp(X_k)),$$

where $p : \wedge^k T^*Q \to Q$ is the natural bundle projection, $\xi \in \wedge^k T^*Q$, and X_i, $i = 1, \ldots, k$, are tangent vectors to $\wedge^k T^*Q$ at ξ. Then

$$\omega_{can} = d\theta \tag{10}$$

is a k-plectic form on $\wedge^k T^*Q$. These k-plectic manifolds are closely related to the multi-phase spaces in field theory (see e.g. [18, 21] and references therein).

Other examples of k-plectic manifolds include $(k+1)$-dimensional orientable manifolds equipped with volume forms. An important class of 2-plectic manifolds is given by compact, semi-simple Lie groups G, equipped with the Cartan 3-form $H \in \Omega^3(G)$, i.e., the bi-invariant 3-form uniquely defined by the condition $H(u, v, w) = \langle u, [v, w]\rangle$, where $u, v, w \in \mathfrak{g}$ and $\langle \cdot, \cdot \rangle$ is the Killing form (see e.g. [2, 9]). Hyper-Kähler manifolds are examples of 3-plectic manifolds: if $\omega_1, \omega_2, \omega_3$ are the three Kähler forms on a hyper-Kähler manifold M, then the form $\omega_1 \wedge \omega_1 + \omega_2 \wedge \omega_2 + \omega_3 \wedge \omega_3 \in \Omega^4(M)$ is 3-plectic [9, 28].

In physical applications (such as quantization), an important issue concerns the identification of an appropriate analog of the Poisson bracket (4) on a k-plectic manifold (M, ω); there is an extensive literature on this problem, see [8, 16, 25, 35].

As a starting point, one usually considers forms $\alpha \in \Omega^{k-1}(M)$ for which there exists a (necessarily unique) vector field X_α such that $i_{X_\alpha}\omega = d\alpha$; such forms are called *hamiltonian*. Then, on the space of hamiltonian $(k-1)$-forms, one defines the bracket

$$\{\alpha, \beta\} = i_{X_\alpha} i_{X_\beta} \omega, \tag{11}$$

which is a direct generalization of the Poisson bracket (4) when $k = 1$. This skew-symmetric bracket turns out to be well defined on the space of hamiltonian $(k-1)$-forms, but the Jacobi identity usually fails (see e.g. [8, 35]):

$$\{\alpha, \{\beta, \gamma\}\} + \{\gamma, \{\alpha, \beta\}\} + \{\beta, \{\gamma, \alpha\}\} = -d i_{X_\alpha} i_{X_\beta} i_{X_\gamma} \omega. \tag{12}$$

Much work has been done to deal with this "defect" on the jacobiator of (11), either by forcing its elimination or by somehow making sense of it. One approach relies on noticing that closed $(k-1)$-forms are automatically hamiltonian, so one can consider the quotient space of hamiltonian forms modulo closed forms (see e.g. [8]); the bracket (11) descends to this quotient and, since the right-hand side of (12) is exact, the quotient inherits a genuine Lie-algebra structure.[5] By using multivector fields, one can also consider hamiltonian forms of other degrees and show that these Lie algebras fit into larger graded Lie algebras. A more recent approach, see [2, 35], shows that, without taking quotients (so as to force the vanishing of the jacobiator), the bracket (11) on hamiltonian forms can be naturally understood in terms of structures from homotopy theory; namely, this bracket is part of a Lie k-algebra (a special type of L_∞-algebra). A missing ingredient in these generalizations of the Poisson bracket (4) is a corresponding analog of the Leibniz rule (2). For a discussion in this direction, see e.g. [23, 25].

Just as symplectic manifolds are particular cases of Poisson manifolds, one could wonder about the analog of Poisson manifolds in multisymplectic geometry. As recalled in Section 2, the Leibniz rule is central for the general definition of a Poisson structure. So, as indicated by the previous discussion on Poisson brackets on k-plectic manifolds, it is not evident how to define such analogs in terms of algebraic/Lie-type structures on spaces of forms. A different, more geometric, perspective to this problem will be discussed next.

[5] In the case of exact k-plectic manifolds, a different way to eliminate the jacobiator defect is presented in [16], based on a modification of the bracket (11) using the k-plectic potential.

4 Multisymplectic Groupoids and Their Infinitesimal Versions

We start with a straightforward generalization of symplectic groupoids to multisymplectic geometry: A *multisymplectic groupoid* is a Lie groupoid equipped with a multisymplectic form that is multiplicative, in the sense of (5). We will also use the terminology *k-plectic groupoid* when the multisymplectic form has degree $k+1$.

Recalling that Poisson structures arise as infinitesimal versions of symplectic groupoids, as briefly explained in Section 2, we will now identify the infinitesimal objects corresponding to multisymplectic groupoids.

Let $\mathcal{G} \rightrightarrows M$ be an s-simply-connected Lie groupoid, let $A \to M$ be its Lie algebroid, with anchor map $\rho : A \to TM$. The following result is established in [1, 4]: there is a 1-1 correspondence between closed, multiplicative forms $\omega \in \Omega^{k+1}(\mathcal{G})$ and vector-bundle maps $\mu : A \to \wedge^k T^*M$ (covering the identity map on M) satisfying:

$$i_{\rho(u)}\mu(v) = -i_{\rho(v)}\mu(u), \tag{13}$$

$$\mu([u,v]) = \mathscr{L}_{\rho(u)}\mu(v) - i_{\rho(v)}d(\mu(u)), \tag{14}$$

for $u, v \in \Gamma(A)$. Such maps μ are called (closed) *IM* $(k+1)$*-forms* (where IM stands for *infinitesimally multiplicative*). Using (8), one can write the explicit relation between ω and μ as

$$i_{X_k} \ldots i_{X_1}\mu_x(u) = \omega_x(u, X_1, \ldots, X_k), \tag{15}$$

for $u \in A|_x$ and $X_i \in TM|_x$, $x \in M$.

We now discuss a slight refinement of this result taking into account the nondegeneracy condition of multisymplectic forms. We will need a few properties of multiplicative forms on Lie groupoids, all of which follow from (5). If ω is a multiplicative form on $\mathcal{G}$, then the following holds:

$$\epsilon^*\omega = 0, \qquad \mathsf{inv}^*\omega = -\omega, \tag{16}$$

and

$$i_{u^r}\omega = \mathsf{t}^*\mu(u), \quad \forall u \in \Gamma(A), \tag{17}$$

where u^r is the vector field on $\mathcal{G}$ determined by $u \in \Gamma(A)$ via right translations; see [6, Sec. 3] for the proofs of these identities (the proofs there work in any degree, though the statements refer to 2-forms). Using the second equation in (16) and (17), we also obtain

$$i_{\overline{u}^l}\omega = -\mathsf{s}^*\mu(u), \tag{18}$$

where $\overline{u}^l = \mathsf{inv}_*(u^r)$ (note that this vector field coincides with the one defined by left translations of $\overline{u} = d\,\mathsf{inv}(u) \in \Gamma(\ker(d\mathsf{t})|_M)$).

Proposition 1. *A closed, multiplicative form $\omega^{k+1}(\mathcal{G})$ is nondegenerate if and only if its corresponding IM form $\mu : A \to \wedge^k T^*M$ satisfies*

1. $\ker \mu = \{0\}$,
2. $(\mathrm{Im}(\mu))^\circ = \{X \in TM \mid i_X \mu(u) = 0 \ \forall u \in A\} = \{0\}$.

Proof. Assume that ω is nondegenerate, and let us verify that (1) and (2) hold. If $u \in \ker \mu$, then (by (17)) $i_u \omega = \mathsf{t}^* \mu(u) = 0$, so $u = 0$ and (1) follows. Let now $X \in (\mathrm{Im}(\mu))^\circ|_x$, $x \in M$. Then $i_u i_X \omega = -i_X \mathsf{t}^* \mu(u) = \mathsf{t}^* i_X \mu(u) = 0$ for all $u \in A|_x$. We claim that this implies that $i_X \omega = 0$, so that $X = 0$ by nondegeneracy, and hence (2) holds. To see that, it suffices to check that $i_{Z_k} \dots i_{Z_1} i_X \omega = 0$ for arbitrary $Z_i \in T\mathcal{G}|_x$, $i = 1, \dots, k$. Using (8), we write $Z_i = X_i + u_i$, for $X_i \in TM|_x$ and $u_i \in A|_x$. Expanding out $i_{Z_k} \dots i_{Z_1} i_X \omega$ using multilinearity, we see that the term $i_{X_k} \dots i_{X_1} i_X \omega$ vanishes by the first condition in (16), and all the other terms vanish as a consequence of the fact that $i_u i_X \omega = 0 \ \forall u \in A$.

Conversely, suppose that (1) and (2) hold, and let $X \in T_g \mathcal{G}$ be such that $i_X \omega = 0$. Then

$$i_{u^r} i_X \omega = 0 = -i_X(\mathsf{t}^* \mu(u))$$

for all $u \in \Gamma(A)$, which means that $d\mathsf{t}(X) \in (\mathrm{Im}(\mu))^\circ$, so $d\mathsf{t}(X) = 0$ by (2). Hence X is tangent to the t-fiber at g, and we can find $v \in \Gamma(A)$ so that $\mathsf{inv}_*(v^r)|_g = \overline{v}^l|_g = X$. By (18), at the point g we have

$$i_X \omega = i_{\overline{v}^l} \omega = -\mathsf{s}^* \mu(v),$$

so $i_X \omega = 0$ implies that $\mu(v) = 0$, hence $v = 0$ by (1), and $X = \overline{v}^l|_g = 0$.

It follows that the infinitesimal counterpart of a k-plectic groupoid is a closed IM $(k+1)$-form $\mu : A \to \wedge^k T^*M$ additionally satisfying conditions (1) and (2) of Prop. 1. A natural terminology for the resulting object is *IM k-plectic form*. In this paper, we will alternatively refer to them as *higher Poisson structures of degree k*, or simply *k-Poisson structures* (being aware that this may clash with the terminology for different objects in the literature). Before giving different characterizations of k-Poisson structures and examples, we briefly explain how 1-Poisson structures are the same as ordinary Poisson structures.

4.1 The Case $k = 1$

For a bundle map $\mu : A \to T^*M$, note that condition (1) in Prop. 1 says that μ is injective, while (2) says that μ is surjective. It follows that a 1-Poisson structure is a bundle map $\mu : A \to T^*M$ satisfying (13), (14) (i.e., a closed IM 2-form), and that is an isomorphism.

Note that given a Poisson structure π on M, if we consider the associated Lie algebroid $A = T^*M$, see (6) and (7), it is clear that

$$\mu = \mathrm{id} : A \to T^*M \tag{19}$$

is a 1-Poisson structure. It turns out that any 1-Poisson structure is equivalent[6] to one of this type. To justify this claim, it will be convenient to view Poisson structures from the broader perspective of Dirac geometry [12].

Let us consider the bundle $\mathbb{T}M := TM \oplus T^*M \to M$ equipped with the non-degenerate, symmetric fibrewise bilinear pairing $\langle \cdot, \cdot \rangle$ given at each $x \in M$ by

$$\langle (X, \alpha), (Y, \beta) \rangle := \beta(X) + \alpha(Y), \tag{20}$$

for $X, Y \in T_xM$, $\alpha, \beta \in T_x^*M$, and with the Courant-Dorfman bracket $[\![\cdot, \cdot]\!] : \Gamma(\mathbb{T}M) \times \Gamma(\mathbb{T}M) \to \Gamma(\mathbb{T}M)$,

$$[\![(X, \alpha), (Y, \beta)]\!] := ([X, Y], \mathscr{L}_X \beta - i_Y d\alpha). \tag{21}$$

Poisson structures on M are equivalent to subbundles $L \subset \mathbb{T}M$ satisfying

(d1) $L = L^\perp$, i.e., L is *lagrangian* with respect to $\langle \cdot, \cdot \rangle$,
(d2) $L \cap TM = \{0\}$,
(d3) $[\![\Gamma(L), \Gamma(L)]\!] \subseteq \Gamma(L)$.

Condition (d1) is equivalent to L being isotropic, i.e., $L \subseteq L^\perp$, and the dimension condition $\mathrm{rank}(L) = \dim(M)$. Using the exact sequence

$$L \cap TM \to L \to T^*M$$

induced by the natural projection $\mathrm{pr}_2 : \mathbb{T}M \to T^*M$, we see that (d2) is equivalent to saying that L projects isomorphically onto T^*M. It follows that conditions (d1) and (d2) can be alternatively written as

(d1′) $L \subseteq L^\perp$,
(d2′) $\mathrm{pr}_2|_L : L \to T^*M$ is an isomorphism.

Given a subbundle $L \subset \mathbb{T}M$, conditions (d1′) and (d2′) are equivalent to L being the graph of a skew-adjoint bundle map $T^*M \to TM$; such maps are always of the form $\alpha \mapsto i_\alpha \pi$, where π is a bivector field. The involutivity condition (d3) amounts to $[\pi, \pi] = 0$.

[6] We say that two IM $(k+1)$-forms $\mu_1 : A_1 \to \wedge^k T^*M$ and $\mu_2 : A_2 \to \wedge^k T^*M$ are *equivalent* if there is a Lie-algebroid isomorphism $\phi : A_1 \to A_2$ such that $\mu_2 \circ \phi = \mu_1$; these are infinitesimal versions of isomorphism of Lie groupoids preserving multiplicative forms.

Let $\mu : A \to T^*M$ be a 1-Poisson structure, and let us consider the bundle map

$$(\rho, \mu) : A \to \mathbb{T}M, \tag{22}$$

where $\rho : A \to TM$ is the anchor. Since μ is an isomorphism, the map (22) is injective, and its image is a subbundle $L \subset \mathbb{T}M$ satisfying (d2′). Note that condition (13) for μ amounts to condition (d1′) for L, while (14) becomes (d3). It follows that L represents a Poisson structure on M, explicitly given by

$$\pi(\alpha, \beta) = i_{\rho(\mu^{-1}(\alpha))}\beta, \qquad \alpha, \beta \in T^*M.$$

It is clear from (14) that $\mu : A \to T^*M$ is an isomorphism of Lie algebroids, where T^*M has the Lie-algebroid structure induced by π (as in (6) and (7)), showing the equivalence between μ and the 1-Poisson structure (19) associated with π.

As we see next, one has a similar interpretation of general k-Poisson structures in terms of higher Courant-Dorfman brackets (as in [22, Sec. 2]), leading to objects closely related to those studied in [38].

5 Descriptions of k-Poisson Structures

Let us consider the vector bundle

$$\mathbb{T}M^{(k)} := TM \oplus \wedge^k T^*M;$$

we denote by $\mathrm{pr}_1 : \mathbb{T}M^{(k)} \to TM$ and $\mathrm{pr}_2 : \mathbb{T}M^{(k)} \to \wedge^k T^*M$ the natural projections. The same expressions as in (20) and (21) lead to a symmetric $\wedge^{k-1}T^*M$-valued pairing $\langle \cdot, \cdot \rangle$ on the fibres of $\mathbb{T}M^{(k)}$ and a bracket $[\![\cdot, \cdot]\!]$ on $\Gamma(\mathbb{T}M^{(k)})$, that we will keep referring to as the Courant-Dorfman bracket.

Given a subbundle $L \subset \mathbb{T}M^{(k)}$, we keep denoting by $L^\perp$ its orthogonal relative to $\langle \cdot, \cdot \rangle$; note that, for $k > 1$, it may happen that $L^\perp$ does not have constant rank (see Section 6). We will keep calling L *isotropic* if $L \subset L^\perp$, and *involutive* if its space of sections $\Gamma(L)$ is closed under $[\![\cdot, \cdot]\!]$. For a subbundle $D \subseteq \wedge^k T^*M$, we let

$$D^\circ := \{X \in TM \mid i_X\alpha = 0 \; \forall \alpha \in D\}$$

be its annihilator.

Whenever $L \subset \mathbb{T}M^{(k)}$ is an isotropic and involutive subbundle, it inherits a Lie-algebroid structure with anchor map $\mathrm{pr}_1|_L : L \to TM$ and Lie bracket $[\![\cdot, \cdot]\!]|_{\Gamma(L)}$ on $\Gamma(L)$. In particular, it follows that the distribution

$$\mathrm{pr}_1(L) \subseteq TM \tag{23}$$

is integrable and its integral leaves (the "orbits" of the Lie algebroid) define a singular foliation on M, see [15, Sec. 8.1]. One may also directly check that

$$\mathrm{pr}_2|_L : L \to \wedge^k T^*M \tag{24}$$

is a closed IM k-form. Since $\ker(\mathrm{pr}_2|_L) = L \cap TM$ and

$$(\mathrm{pr}_2(L))^\circ = L^\perp \cap TM \supseteq L \cap TM,$$

it is clear that (24) is a k-Poisson structure if and only if

$$L^\perp \cap TM = \{0\}. \tag{25}$$

By considering the bundle map (24), we will think of any isotropic, involutive subbundle $L \subseteq \mathbb{T}M^{(k)}$ satisfying (25) as a k-Poisson structure. It turns out that all k-Poisson structures on M are of this type.

Proposition 2. *Any k-Poisson structure $\mu : A \to \wedge^k T^*M$ is equivalent to a subbundle $L \subset \mathbb{T}M^{(k)}$ that is isotropic, involutive, and satisfies (25).*

Proof. Let $\mu : A \to \wedge^k T^*M$ be a k-Poisson structure. The bundle map $(\rho, \mu) : A \to \mathbb{T}M$ is an isomorphism onto its image (due to condition (1) in Prop. 1), which is a subbundle $L \subset \mathbb{T}M^{(k)}$ that is isotropic, involutive, and satisfies (25) (as a result of (13), (14) and condition (2) in Prop. 1, respectively). It is clear that $(\rho, \mu) : A \to L$ is an isomorphism of Lie algebroids, which establishes the desired equivalence.

We conclude that the infinitesimal versions of k-plectic groupoids can be seen as isotropic, involutive subbundles $L \subset \mathbb{T}M^{(k)}$ satisfying (25). Note that the condition $L = L^\perp$ (see (d1)) may not hold for $k > 1$ (we will see simple examples in Section 6); in the case $k = 1$, the condition $L^\perp \cap TM = (\mathrm{pr}_2(L))^\circ = \{0\}$ implies that $\mathrm{pr}_2(L) = T^*M$, so that $L = L^\perp$.

Another characterization of k-Poisson structures, closer in spirit to the description of Poisson structures via bivector fields, is as follows.

Proposition 3. *There is a one-to-one correspondence between subbundles $L \subset \mathbb{T}M^{(k)}$ as in Prop. 2 and pairs (D, λ), where $D \subseteq \wedge^k T^*M$ is a subbundle and $\lambda : D \to TM$ is a bundle map (covering the identity) satisfying the following conditions: (a) $D^\circ = \{0\}$, (b) $i_{\lambda(\alpha)}\beta = -i_{\lambda(\beta)}\alpha$, for $\alpha, \beta \in D$, and (c) the space $\Gamma(D)$ is involutive with respect to the bracket (c.f. (7))*

$$[\alpha, \beta]_\lambda := \mathscr{L}_{\lambda(\alpha)}\beta - i_{\lambda(\beta)}d\alpha = \mathscr{L}_{\lambda(\alpha)}\beta - \mathscr{L}_{\lambda(\beta)}\alpha - d(i_{\lambda(\alpha)}\beta), \tag{26}$$

and $\lambda : \Gamma(D) \to \Gamma(TM)$ preserves brackets.

Proof. Given a k-Poisson structure $L \subset TM \oplus \wedge^k T^*M$, note that $\mathrm{pr}_2|_L : L \to \wedge^k T^*M$ is injective (since $\ker(\mathrm{pr}_2|_L) = L \cap TM \subseteq L^\perp \cap TM = \{0\}$). Setting

$D = \mathrm{pr}_2(L)$ and $\lambda = \mathrm{pr}_1 \circ (\mathrm{pr}_2|_L)^{-1}$, we see that $L = \{(\lambda(\alpha), \alpha) \,|\, \alpha \in D\}$. Then (25) is equivalent to condition (a), while (b) means that L is isotropic. The involutivity of L is equivalent to condition (c).

For $k = 1$, as previously remarked, $D = T^*M$ (as a result of (a)), while (b) says that $\lambda = \pi^\sharp$, for a bivector field π. The involutivity condition in (c) is automatically satisfied, and the bracket-preserving property is equivalent to the Poisson condition $[\pi, \pi] = 0$ (see e.g. [5, Lem. 2.3]).

For a k-Poisson structure defined by (D, λ) as in Prop. 3, D acquires a Lie algebroid structure with bracket (26) and anchor λ, in such a way that $\mathrm{pr}_2|_L : L \to D$ is an isomorphism of Lie algebroids. In terms of (D, λ), the singular foliation on M determined by the k-Poisson structure (see (23)) is given by the integral leaves of the distribution $\lambda(D) \subseteq TM$. Moreover, each leaf $\mathscr{O}$ inherits a $(k+1)$-form ω by

$$\omega(Y_0, Y_1, \ldots, Y_k) = i_{Y_k} \ldots i_{Y_1} \alpha, \tag{27}$$

where $Y_i \in \lambda(D)|_{\mathscr{O}} = T\mathscr{O}$, and $\alpha \in D$ is such that $Y_0 = \lambda(\alpha)$; indeed, property (b) in Prop. 3 assures that ω is well defined. One may also verify, using (c) in Prop. 3, that ω is closed. For $k = 1$, one recovers the symplectic foliation that underlies any Poisson structure and completely determines it. However, for $k > 1$, it is no longer true that the leafwise closed $(k+1)$-forms are nondegenerate, nor that a k-Poisson structure is uniquely determined by them, see Remark 1 (c.f. [38, Prop. 3.8]).

The description of k-Poisson structures in Prop. 3 also makes the notion of morphism of k-Poisson manifolds more evident: if (D_i, λ_i) is a k-Poisson structure on M_i, $i = 1, 2$, then a map $\phi : M_1 \to M_2$ is a *k-Poisson morphism* if, for all $x \in M_1$, $\phi^*(D_2|_{\phi(x)}) \subseteq D_1|_x$ and $d\phi(\lambda_1(\phi^*\alpha)) = \lambda_2(\alpha)$, for all $\alpha \in D_2|_{\phi(x)}$.

6 Some Examples and Final Remarks

We now give some examples of k-Poisson structures. The first two examples are from [38].

Example 1. Let $\omega \in \Omega^{k+1}(M)$ be a k-plectic form. Then its graph

$$L = \{(X, i_X\omega),\ X \in TM\} \subset \mathbb{T}M^{(k)}$$

satisfies $L = L^\perp$ and is involutive (as a consequence of ω being closed, see [38, Prop. 3.2]). Also, $L^\perp \cap TM = L \cap TM = \ker(\omega) = \{0\}$ by nondegeneracy. In terms of Prop. 3, $D = \mathrm{Im}(\omega^\sharp)$ and $\lambda = (\omega^\sharp)^{-1} : D \to TM$. So, just as any symplectic structure is a Poisson structure, any k-plectic form is a particular type of k-Poisson structure. A k-plectic groupoid integrating this k-Poisson structure is the pair groupoid $M \times M$, with k-plectic structure $p_1^*\omega - p_2^*\omega$ where p_i, $i = 1, 2$, denote the two natural projections from $M \times M$ to M.

Considering a k-plectic groupoid $\mathscr{G} \rightrightarrows M$ with the k-Poisson structure of Example 1, one may use (17) to check that the target map $\mathsf{t} : \mathscr{G} \to M$ is a k-Poisson morphism, extending the well-known property of symplectic groupoids, see Section 2.

We saw in Section 4.1 that Poisson bivector fields are the same as 1-Poisson structures. Other types of higher Poisson structures are obtained from top-degree multivector fields as follows.

Example 2. Let $\pi \in \Gamma(\wedge^{k+1} TM)$ be a multivector field of top degree, i.e., $k = \dim(M) - 1$. Then its graph

$$L = \{(i_\alpha \pi, \alpha) \mid \alpha \in \wedge^k T^*M\} \subseteq \mathbb{T}M^{(k)}$$

is isotropic and involutive – and, besides Poisson bivector fields, these are the only examples of non-zero multivector fields whose graphs have these properties, see [38, Prop. 3.4]. Also, since $\mathrm{pr}_2(L) = \wedge^k T^*M$, it is clear that $\mathrm{pr}_2(L)^\circ = L^\perp \cap TM = \{0\}$, so L is a k-Poisson structure. The foliations defined by these k-Poisson structures are usually singular: leaves are either open subsets of M or singular points (where π vanishes). The restriction of π to each open leaf is nondegenerate, and the induced $(k+1)$-forms ω on these leaves (see (27)) are the volume forms dual to π, i.e., they are defined by $i_{(i_\alpha \pi)}\omega = \alpha, \forall \alpha \in \wedge^k T_x^*M$. The groupoids integrating these k-Poisson structures have been mostly studied when $\dim(M) = 2$ (so π is a bivector field), see [20, 33].

The fact that the particular k-Poisson structures of Examples 1 and 2 are infinitesimal versions of k-plectic groupoids was observed in [38, Prop. 3.7].

In the preceding examples, the bundle L always satisfied $L = L^\perp$. For examples where this condition fails, consider subbundles

$$L \subseteq \wedge^k T^*M \subset \mathbb{T}M^{(k)}. \tag{28}$$

These are automatically isotropic and involutive. Note that

$$L^\perp = L^\circ \oplus \wedge^k T^*M, \quad \text{and} \quad L^\perp \cap TM = L^\circ.$$

So L is a k-Poisson structure as long as $L^\circ = \{0\}$, and $L \subsetneq L^\perp$ as long as L is properly contained in $\wedge^k T^*M$. A k-plectic groupoid integrating it is L itself, viewed as a vector bundle (with groupoid structure given by fibrewise addition), equipped with the k-plectic form given by the pullback of the canonical multisymplectic form on $\wedge^k T^*M$ (see (10)); the fact that this pullback is nondegenerate boils down to the condition $L^\perp \cap TM = L^\circ = \{0\}$.

Example 3. For $L = \wedge^k T^*M$, note that $L^\circ = \{0\}$ (and hence L is a k-Poisson structure on M) if and only if $\dim(M) \geq k$.

Example 4. Let ξ be a nondegenerate k-form on M, and let $L \subset \wedge^k T^*M$ be the line bundle generated by ξ,

$$L|_x = \{c\xi_x \mid c \in \mathbb{R}\}, \quad x \in M.$$

Then $L^\circ = \ker(\xi) = 0$, so L is a k-Poisson structure.

Remark 1. Note that all k-Poisson structures of the type (28) determine the same foliation, the leaves of which are the points of M.

A general observation is that one can take direct products of k-Poisson structures: if L_1 and L_2 are k-Poisson structures on M_1 and M_2, respectively, we define their product by

$$L := \{(X + Y, \alpha + \beta) \mid (X, \alpha) \in L_1,\ (Y, \beta) \in L_2\} \subseteq TM \oplus \wedge^k T^*M,$$

where $M = M_1 \times M_2$ and we simplify the notation by identifying forms on M_i with their pullbacks to M via the projections. One may directly verify that L is a k-Poisson structure on M. Moreover, if $(\mathscr{G}_i \rightrightarrows M_i, \omega_i)$ is a k-symplectic groupoid integrating L_i, $i = 1, 2$, the direct product $\mathscr{G}_1 \times \mathscr{G}_2 \rightrightarrows M_1 \times M_2$ (equipped with the k-plectic form $\omega_1 + \omega_2$) is a k-plectic groupoid that integrates L. The following is a concrete example.

Example 5. Let (M, ω) be a k-plectic manifold, and let N be a manifold with $\dim(N) \geq k$. Then the subbundle

$$L = \{(X, i_X\omega + \alpha) \mid X \in TM, \alpha \in \wedge^k T^*N\} \subset T(M \times N) \oplus \wedge^k T^*(M \times N)$$

is a k-Poisson structure on $M \times N$ (c.f. [38, Thm. 3.12]), the direct product of the k-plectic form on M with the k-Poisson structure $L = \wedge^k T^*N$ on N (see Example 3). The leaves of L are $M \times \{t\}$, $t \in N$, with induced $(k+1)$-form (as in (27)) given by ω.

The next observation illustrates that k-Poisson structures become more rigid than Poisson structures when $k > 1$.

Remark 2. Let M and N be as is Example 5, let $f \in C^\infty(N)$, and consider the smooth family $\omega_t = f(t)\omega$, $t \in N$, of k-plectic forms on M. For $k = 1$, this family defines a Poisson structure on $M \times N$, uniquely determined by the fact that its symplectic leaves are $(M \times \{t\}, \omega_t)$. A higher generalization of this Poisson structure is given by the (isotropic) subbundle $L \subset T(M \times N) \oplus \wedge^k T^*(M \times N)$ defined by

$$L|_{(x,t)} = \{(X, i_X\omega_t + \alpha) \mid X \in T_xM, \alpha \in \wedge^k T_t^*N\}.$$

As it turns out, for $k > 1$, one may verify that such L is involutive if and only if $df = 0$, i.e., f is (locally) constant.

We finally mention another product-type operation for multisymplectic manifolds leading to higher Poisson structures that are not multisymplectic.

Example 6. Let (M_i, ω_i) be a k_i-plectic manifold, $i = 1, 2$. Let $M = M_1 \times M_2$ and $\omega = \omega_1 \wedge \omega_2 \in \Omega^{k_1+k_2+2}(M)$ (we keep the simplified notation of identifying forms on M_i with their pullbacks to M via the projections $M \to M_i$). Then

$$L = \{(X, i_X\omega) = (X, (i_X\omega_1) \wedge \omega_2) \mid X \in TM_1\} \subset TM \oplus \wedge^{k_1+k_2+1} T^*M$$

can be checked to be a $(k_1 + k_2 + 1)$-Poisson structure. Its leaves are of the form $M_1 \times \{y\}$, for $y \in M_2$, and the induced $(k_1 + k_2 + 2)$-form on each leaf is zero. An integrating k-plectic groupoid is given by the direct product of the pair groupoid $M_1 \times M_1$ (see Example 1) and the trivial groupoid over M_2, endowed with the multiplicative $(k_1 + k_2 + 2)$-form given by $(p_1^*\omega_1 - p_2^*\omega_1) \wedge \omega_2$.

Acknowledgements H.B. and A.C. thank the organizers of the *Focus Program on Geometry, Mechanics and Dynamics: the Legacy of Jerry Marsden*, held at the Fields Institute in July of 2012, for their hospitality during the program, as well as MITACS for travel support (for which we also thank J. Koiller). H. B. and A. C. were partly funded by CNPq, Faperj and Capes (through the grant PVE 11/2012) D. I. thanks MICINN (Spain) for a "Ramón y Cajal" research contract; he is partially supported by MICINN grants MTM2012-34478 and MTM2009-08166-E and Canary Islands government project SOLSUB200801000238. We have benefited from many stimulating conversations with M. Forger, J.C. Marrero, N. Martinez, C. Rogers and M. Zambon. We also thank the referees for several useful comments that improved the presentation of this note.

References

1. Arias Abad, C., Crainic, M.: The Weil algebra and the Van Est isomorphism. Ann. Inst. Fourier (Grenoble) **61**, 927–970 (2011)
2. Baez, J., Hoffnung, H., Rogers, C.: Categorified symplectic geometry and the classical string. Commun. Math. Phys. **293**, 701–715 (2010)
3. Bates, S., Weinstein, A.: Lectures on the Geometry of Quantization. Berkeley Mathematics Lecture Notes, vol. 8. American Mathematical Society/Berkeley Center for Pure and Applied Mathematics, Providence, RI/Berkeley, CA (1997)
4. Bursztyn, H., Cabrera, A.: Multiplicative forms at the infinitesimal level. Math. Ann. **353**, 663–705 (2012)
5. Bursztyn, H., Crainic, M.: Dirac structures, moment maps and quasi-Poisson manifolds. In: The Breadth of Symplectic and Poisson Geometry. Progress in Mathematics, vol. 232, pp. 1–40. Birkhauser, Boston (2005)
6. Bursztyn, H., Crainic, M., Weinstein, A., Zhu, C.: Integration of twisted Dirac brackets. Duke Math. J. **123**, 549–607 (2004)
7. Cannas da Silva, A., Weinstein, A.: Geometric Models for Noncommutative Algebras. Berkeley Mathematics Lecture Notes, vol. 10. American Mathematical Society/Berkeley Center for Pure and Applied Mathematics, Providence, RI/Berkeley, CA (1999)
8. Cantrijn, F., Ibort, A., de Leon, M.: Hamiltonian structures on multisymplectic manifolds. Rend. Sem. Mat. Univ. Pol. Torino **54**, 225–236 (1996). Geom. Struc. Phys. Theories, I
9. Cantrijn, F., Ibort, A., de Leon, M.: On the geometry of multisymplectic manifolds. J. Aust. Math. Soc. A **66**, 303–330 (1999)
10. Cattaneo, A., Felder, G.: Poisson sigma models and symplectic groupoids. In: Quantization of Singular Symplectic Quotients. Progress in Mathematics, vol. 198, pp. 61–93. Birkhauser, Basel (2001)

11. Coste, A., Dazord, P., Weinstein, A.: Groupoïdes symplectiques. Publications du Département de Mathématiques. Nouvelle Série. A, vol. 2, i–ii, 1–62, Publ. Dép. Math. Nouvelle Sér. A, 87-2, Univ. Claude-Bernard, Lyon (1987)
12. Courant, T.: Dirac manifolds. Trans. Am. Math. Soc. **319**, 631–661 (1990)
13. Crainic, M., Fernandes, R.: Integrability of Lie brackets. Ann. Math. **157**, 575–620 (2003)
14. Crainic, M., Fernandes, R.: Integrability of Poisson brackets. J. Differ. Geom. **66**, 71–137 (2004)
15. Dufour, J.-P., Zung, N.-T.: Poisson Structures and Their Normal Forms. Progress in Mathematics, vol. 242. Birkhauser, Boston (2005)
16. Forger, M., Paufler, C., Römer, H.: The Poisson bracket for poisson forms in multisymplectic field theory. Rev. Math. Phys. **15**, 705–743 (2003)
17. Gotay, M.: A multisymplectic framework for classical field theory and the calculus of variations. I. Covariant Hamiltonian formalism. In: Mechanics, Analysis and Geometry: 200 Years After Lagrange, pp. 203–235. Elsevier, New York (1991)
18. Gotay, M., Isenberg, J., Marsden, J., Montgomery, R.: Momentum maps and classical relativistic fields. Part I: covariant field theory. ArXiv: physics/9801019 (1998)
19. Gotay, M., Isenberg, J., Marsden, J.: Momentum maps and classical relativistic fields. Part II: canonical analysis of field theories. ArXiv: math-ph/0411032 (2004)
20. Gualtieri, M., Li, S.: Symplectic groupoids of log symplectic manifolds, Int. Math. Res. Not. **11**, 3022–3074 (2014)
21. Hélein, F.: Multisymplectic formalism and the covariant phase space. In: Variational Problems in Differential Geometry. London Mathematical Society Lecture Note Series, vol. 394, pp. 94–126. Cambridge University Press, Cambridge (2012)
22. Hitchin, N.: Generalized Calabi-Yau manifolds. Q. J. Math. **54**, 281–308 (2003)
23. Hrabak, S.P.: On a multisymplectic formulation of the classical BRST symmetry for first order field theories. Part I: algebraic structures. ArXiv:math-ph/9901012 (1999)
24. Iglesias Ponte, D., Marrero, J.C., Vaquero, M.: Poly-Poisson structures. Lett. Math. Phys. **103**, 1103–1133 (2013)
25. Kanatchikov, I.V.: On field theoretic generalizations of a Poisson algebra. Rep. Math. Phys. **40**, 225–234 (1997)
26. Kijowski, J., Szczyrba, W.: A canonical structure for classical field theories. Commun. Math. Phys. **46**, 183–206 (1976)
27. Mackenzie, K., Xu, P.: Integration of Lie bialgebroids. Topology **39**, 445–467 (2000)
28. Madsen, T., Swann, A.: Closed forms and multi-moment maps. Geom. Dedicata **165**, 25–52 (2013)
29. Marsden, J., Ratiu, T.: Introduction to Mechanics and Symmetry. Text in Applied Mathematics, vol. 17. Springer, New York (1994)
30. Marsden, J.E., Patrick, G., Shkoller, S.: Multisymplectic geometry, variational integrators and nonlinear PDEs. Commun. Math. Phys. **199**, 351–395 (1998)
31. Marsden, J.E., Pekarsky, S., Shkoller, S., West, M.: Variational methods, multisymplectic geometry and continuum mechanics. J. Geom. Phys. **38**, 253–284 (2001)
32. N. Martínez: Poly-symplectic groupoids and poly-Poisson structures, arXiv:1409.0695 [math.SG] (2014)
33. Martinez-Torres, D.: A note on the separability of canonical integrations of Lie algebroids. Math. Res. Lett. **17**, 69–75 (2010)
34. Mikami, K., Weinstein, A.: Moments and reduction for symplectic groupoid actions. Publ. Res. Inst. Math. Sci. **24**, 121–140 (1988)
35. Rogers, C.: L_∞-algebras from multisymplectic geometry. Lett. Math. Phys. **100**, 29–50 (2012)
36. Vankerschaver, J. Yoshimura, H., Leok, M.: The Hamilton-Pontryagin principle and multi-Dirac structures for classical field theories. J. Math. Phys. 53, 072903 (2012)
37. Weinstein, A.: Symplectic groupoids and Poisson manifolds. Bull. Am. Math. Soc. (N.S.) **16**, 101–104 (1987)
38. Zambon, M.: L_∞-algebras and higher analogues of Dirac structures and Courant algebroids. J. Symplectic Geom. **10**, 563–599 (2012)

The Topology of Change: Foundations of Probability with Black Swans

Graciela Chichilnisky

Abstract Classic probability theory treats rare events as 'outliers' that are disregarded and underestimated. In a moment of change however rare events can become frequent, and frequent events rare. We postulate new axioms for probability theory that require a balanced treatment of rare and frequent events, based on what we call "the topology of change". The axioms extend the foundation of probability to integrate rare but potentially catastrophic events or *black swans:* natural hazards, market crashes, catastrophic climate change and episodes of species extinction. The new results include a characterization of a family of purely finitely additive measures that are—somewhat surprisingly—absolutely continuous with respect to the Lebesgue measure. This is a new development from an earlier characterization of probability measures implied by the new axioms, which where countably additive measures created in Chichilnisky (2000), Wiley, Chichester (2002), Chichilnisky (2009, 2009a). The results are contrasted to the axioms of Kolmogorov (1933/1950), De Groot (1970/2004), Arrow (1971), Dubins and Savage (1965), Savage (1972), Von Neumann and Morgernstern (1944), and Hernstein and Milnor.

1 Introduction

Classic probability theory treats rare events as 'outliers' and often disregards them. This is an unavoidable shortcoming of classic theory and has been known for some time. It conflicts with observations about the distribution of rare events in natural and human systems, such as earthquakes and financial markets. It is now known that the shortcoming originates from the axioms created by Kolmogorov [21] to provide a foundation for probability theory [1, 7, 8]. It turns out that the same phenomenon that underestimates rare events leads classic probability theory to underestimate the likelihood of change. In a situation of change, events that are rare become frequent and frequent events become rare. By ignoring rare events we tend to underestimate the possibility of change. In a slight abuse of language it could be said that classic probability theory leads us to 'ignore' change. The change we refer to includes rare

G. Chichilnisky (✉)
Columbia University, New York, NY 10027, USA
e-mail: chichilnisky@columbia.edu

D.E. Chang et al. (eds.), *Geometry, Mechanics, and Dynamics*, Fields Institute Communications 73, DOI 10.1007/978-1-4939-2441-7_4

events of great importance that should not be underestimated, for example *black swans* such as catastrophic climate change and major episodes of species extinction.

Sensitivity to change is a topological issue at its core. It measures how likelihoods change with changes in measurements or observations. If we are sensitive to change our responses change in harmony with the signals. To disregard change means that our response "needle" is either insensitive to, or at odds with, the observed signals. In mathematical terms this is all about continuity of the response and as such it is defined and measured by topology. In a recent discovery it was found that an important continuity axiom of classic probability theory is responsible for its insensitivity to rare events. De Groot (1970, 2004) calls this axiom SP4, Arrow called it "monotone continuity" (Arrow (1971), and similar continuity axioms appear in the work of Hernstein and Milnor, see Chichilnisky [6–8]). The continuity that these axioms provide is coarse, and it was shown to be responsible for insensitivity to rare events [9] (Chichilnisky (2009, 2009a)). In that sense classic axioms lead to insensitivity about the likelihood of change. A single continuity axiom explains why classic probability theory is insensitive to rare events and why it ignores change.

To overcome this limitation, new axioms for probability theory were created that balance the treatment of rare and frequent events, based on a more sensitive notion of continuity or a 'finer' topology—and new types of probability distributions have been identified as emerging from the new axioms [7, 8]. In order to be sensitive to rare events, the new axioms have to use a different continuity criterion, a topology finer than that implicit in axiom SP4 or in the "monotone continuity" axiom, both of which involve averages. The new topology is about extremes not averages, and it is appropriately called "the topology of change" because it is more sensitive to the measurement of rare events that are often at stake in a situation of change. This topology is the $sup\ norm$ topology on L_∞ that, while new in this area, has been used earlier by Debreu [14] to formalize Adam Smith's theorem on the Invisible Hand, and in [7, 8] to axiomatize choice under uncertainty. The sup norm provides a finer notion of continuity than "monotone continuity" and SP4. This sensitivity tallies with the experimental evidence of how people react to rare events [9, 22]. Using the topology of change, the new axioms of probability theory extend the classic foundations of probability, treating rare and frequent events in a more balanced fashion and providing a more balanced view on the likelihood of change.

The article provides new results in this framework, as follows. We introduce the Swan Axiom, a new axiom that is based on continuity in the topology of change. We show how the old and the new topologies differ, namely how continuity in the sense of monotone continuity and SP4 does not imply continuity in the topology of change and how this changes the probability distributions from countably additive to a combination of countably additive and purely finitely additive measures. We also identify a new family of purely finitely additive measures that is continuous with respect to the "topology of change". Somewhat surprisingly, we show that the change in topology—from probability distributions that satisfy Monotone Continuity to those who satisfy the topology of change—does not necessarily give rise to discontinuity with respect to the Lebesgue measure on R, such as 'delta functions' nor to measures with "atoms". Indeed the new

results presented in this article show the opposite: each of the measures in the family we provide of purely finitely additive measures satisfying the new axioms is *absolutely continuous* with respect to the Lebesgue measure. Therefore the notion of continuity that derives from the new axioms does not imply atoms nor assigns positive weights to sets of Lebesgue measure zero. These new results tally with the earlier characterization of probabilities measures satisfying the new axioms as combinations of purely finitely additive and countably additive measures, [7–9] Chichilnisky (2008). We contrast the new measures with the those defined by Kolmogorov [21], De Groot [15], Arrow [2], Dubins and Savage [17], Savage (1954), Von Neumann Morgernstern (1954), and Hernstein and Milnor (1972). Finally we show that the new results rather than contradicting classic theory can be seen as an extension of it. The new theory of probability offered here is an extension of the old since the probability distributions implied by the new axioms coincide with classic countably additive distributions when the sample is populated only by frequent events. As already stated in general the new probability measures consist of a convex combination of countable and finitely additive measures with strictly positive elements of both which, in practical terms, assign more weight to black swans than do normal distributions, and predict more realistically the emergence of change and generally the incidence of 'outliers'.[1] When applied to decision theory under uncertainty, this gives rise to a new type of rationality that changes and updates Bayesian updating rules and also Von Neumann Morgernstern foundations of game theory [5, 7, 9] (Chichilnisky, 2010, 2011), appearing to coincide with observations [22] of how the brain makes decisions using both the amigdala and the cortex (LeDoux 1996).

The article is organized as follows. First we show how the standard notion of continuity or topology that is used in classic probability theory—"monotone continuity" as defined by Arrow [2], and in Hernstein and Milnor 1972, [15]—implies *countably additive measures* that are by nature insensitive to rare events and hence to change*:* these probability measures assign a negligible weight to rare events, no matter how important these may be, treating such events as outliers, [9, 10]. On the other hand the *purely finitely additive measures* defined by Dubins and Savage (1972) assign no weight to frequent events, which is equally troubling, as illustrated in the Appendix. Our new axiomatization for probability theory is shown through a representation theorem (Chichilnisky 2008) to balance the two approaches and to extend both, requiring sensitivity to rare as well as to frequent events. This as we saw requires a notion of continuity that is defined with respect to a finer topology that is sensitive to rare as well as to frequent events, the topology of change. The results presented here highlight the classic role of topology and continuity, which have always been at the core of the axioms of probability theory [2, 25].

[1]The theory presented here explains also Jump-Diffusion processes (Chichilnisky 2012), the existence of 'heavy tails' in power law distributions, and the lumpiness of most of the physical systems that we observe and measure.

2 The Mathematics of Uncertainty

Uncertainty is described by a distinctive and exhaustive set of **events** represented by sets $\{U_\alpha\}$ whose union describes a universe $\mathscr{U}$. An event is identified with its **characteristic function** $\phi_U : U \to R$.[2] The relative likelihood or probability of an event[3] is a real number $W(U)$ that measures how likely it is to occur. The probability of the universe is 1 and that of the empty set is zero. Classic axioms for subjective probability (respectively likelihoods) were introduced by Kolmogorov [21], see Savage (1954) and De Groot [15]. The relative likelihood or probability of two disjoint events is the sum of their probabilities: $W(U_1 \cup U_2) = W(U_1) + W(U_2)$ when $U_1 \cap U_2 = \emptyset$. This corresponds to the definition of a probability as a *measure* on a family ($\sigma-$algebra) of measurable sets of $\mathscr{U}$.[4]

A measure is a continuous linear function that assigns to each event U a real number. The space of events can therefore be identified with the space of characteristic functions, which are measurable and essentially bounded functions. When $\mathscr{U} = R$, the characteristic functions are in $L_\infty(R)$, the space of Lebesgue measurable and essentially bounded real valued functions on R, which we endow with the *"topology of change"*, defined as the sup norm on the space of functions $f : R \to R$, namely $\| f \| = ess \sup_R | f(x) |$. Recall that the functions in L_∞ are defined a.e. with respect to the Lebesgue measure on R, and each is absolutely continuous with respect to the Lebesgue measure on R. Since measures are continuous real valued functions on L_∞, they are by definition in the dual space of L_∞ , denoted L^*_∞, namely in the space of all continuous real valued functions on L_∞. A measure μ therefore satisfies the usual conditions (1) $\mu(A \cup B) = \mu(a) + \mu(B)$ if A and B are disjoint, and $\mu(\varnothing) = 0$. A *countably additive measure* is an element of L^*_∞ that satisfies in addition (2) $\mu(\sum A_i) = \sum_i \mu(A_i)$ $i = 1, \ldots \infty$, when the sets A_i are disjoint pairwise. A *purely finitely additive measure* is an element of L^*_∞ that satisfies condition (1) but not condition (2); therefore for a purely finitely additive measure there are cases where the measure of an infinite sequence of disjoint sets is not the sum of the sequence of their measures. The *space of all purely finitely additive measures* is denoted PA.

It is well known that $L^*_\infty = L_1 + PA$ where L_1 is the space of integrable functions on R with respect to the Lebesgue measure; this is a classic representation theorem by Yosida (1974), Yosida and Hewitt (1952), Chichilnisky (2000). Indeed, each countably additive measure can be represented by an integrable continuous function on $L_\infty(R)$ namely a function $g : R \to R$ in $L_1(R)$, where the representation takes the form $\mu(A) = \int_A g(x)dx$. This representation does not apply to purely finitely additive measures.[5] A *vanishing sequence of events* $\{E_\alpha\}_{=1,2...}$ is

[2] $\phi_U(x) = 1$ when $x \in U$ and $\phi_U(x) = 0$ when $x \notin U$.

[3] In this article for simplicity we make no difference between probabilities and relative likelihoods.

[4] This is Savage's (1972) definition of probability, see also Kadane and O'Hagan (1995).

[5] Savage's probabilities can be either purely finitely additive or countably additive. In that sense they include all the probabilities in this article. However this article will exclude probabilities that

defined as one satisfying $\forall\alpha,\ E_{\alpha+1} \subset E_\alpha$ and $\cap_{\alpha=1}^{\infty} E_\alpha = \emptyset$ a.e. The following two continuity axioms were introduced in [25], see also Arrow (1971), Hernstein and Milnor (Chichilnisky 2009a) and DeGroot (1970–2004), in each case for the purpose of ensuring countable additivity:

Axiom 1 (Monotone Continuity Axiom (MC)) *For every **vanishing** sequence of events* $\{E_\alpha\}_{=1,2...}$ *the probability* $W(E_i) \to 0$ *as* $i \to \infty$.

In words, this axiom requires that the probability of the sets along a vanishing sequence goes to zero. For example consider the decreasing sequence made of infinite intervals of the form (n, ∞) for $n = 1, 2...$ This is a vanishing sequence. Monotone continuity implies that the likelihood the sets of this sequence of events goes to zero even though all its sets are unbounded and essentially identical. A similar example can be constructed with a decreasing sequence of bounded sets, $(-1/n, 1/n)$ for $n = 1, 2 \ldots$, which is also a vanishing sequence as it is a decreasing sequence and their intersection is a single point $\{0\}$: observe that the set consisting of a single point $\{0\}$ is almost everywhere (a.e.) equal to the empty set on R, and that the events in this section are always defined a.e. with respect to the Lebesgue measure of R.[6]

Axiom 2 (De Groot's Axiom SP_4[7]**)** *If* $A_1 \supset A_2 \supset \ldots$ *is a decreasing sequence of events and* B *is some fixed event that is less likely than* A_i *for all* i, *then the probability or likelihood of the intersection* $\cap_i^{\infty} A_i$ *is larger than the probability or likelihood of the event* B.

The following proposition establishes that the two axioms presented above, Monotone Continuity and SP_4, are equivalent and that both imply countable additivity:

Proposition 1. *A relative likelihood (or probability measure) satisfies the **Monotone Continuity** Axiom if and only if it satisfies Axiom* SP_4, *and each of the two axioms implies countable additivity of the corresponding relative likelihood.*

Proof. Assume that Axiom SP_4 is satisfied. When the intersection of a decreasing (nested) vanishing sequence of events $\{A_i\}$ is empty namely $\cap_i A_i = \emptyset$ and the set B is less likely to occur than every set A_i, then the subset B must be as likely as the empty set, namely its probability must be zero. In other words, if B is more likely than the empty set, then regardless of how small is the set B, it is impossible for every set A_i to be as likely as B. Equivalently, the probability of the

---

are either purely finitely additive, or those that are countably additive, requiring elements of both, and therefore our characterization of a probability is strictly finer than that Savage's (1954), and different from the view of a measure as a countably additive set function in [15].

[6] An equivalent definition of Monotone Continuity is that for every two events E_1 and E_2 in $\{E_\alpha\}_{=1,2...}$ with $W(E_1) > W(E_2)$, there exists N such that altering arbitrarily the events E_1 and E_2 on a subset E^i, where $i > N$, does not alter the probability or relative likelihood ranking of the events, namely $W(E_1') > W(E_2')$ where E_1' and E_2' are the altered events.

[7] See [15].

sets that are far away in the vanishing sequence $\{A_i\}$ must go to zero. Therefore SP_4 implies Monotone Continuity (MC). Reciprocally, assume MC is satisfied. Consider a decreasing sequence of events A_i and define a new sequence by subtracting from each set the intersection of the family, namely $A_1 - \cap_i^\infty A_i,\ A_2 - \cap_i^\infty A_i, \ldots$. Let B be a set that is more likely than the empty set but less likely than every A_i. Observe that the intersection of the new sequence is empty, $\cap_i A_i - \cap_i^\infty A_i = \emptyset$ and since $A_i \supset A_{i+1}$ the new sequence is, by definition, a vanishing sequence. Therefore by MC $\lim_i W(A_i - \cap_i^\infty A_i) = 0$. Since $W(B) > 0$, B must be more likely than $A_i - \cap_i^\infty A_i$ for some i onwards. Furthermore, $A_i = (A_i - \cap_i^\infty A_i) \cup (\cap_i^\infty A_i)$ and $(A_i - \cap_i^\infty A_i) \cap (\cap_i^\infty A_i) = \emptyset$, so that $W(A_i) > W(B)$ is equivalent to $W(A_i - \cap_i^\infty A_i) + W((\cap_i^\infty A_i) > W(B)$. Observe that $W(\cap_i^\infty A_i) < W(B)$ would contradict the inequality $W(A_i) = W(A_i - \cap_i^\infty A_i) + W((\cap_i^\infty A_i) > W(B)$, since as we saw above, by MC, $\lim_i W(A_i - \cap_i^\infty A_i) = 0$, and $W(A_i - \cap_i^\infty A_i) + W((\cap_i^\infty A_i) > W(B)$. It follows that $W(\cap_i^\infty A_i) > W(B)$, which establishes De Groots's Axiom SP_4. Therefore Monotone Continuity is equivalent to De Groot's Axiom SP_4. A proof that each of the two axioms implies countable additivity is in [2, 15, 25].

The next section shows that the two classic axioms, Monotone Continuity and SP_4, are biased against or neglect rare events, no matter how important these may be.

3 Rare Events and Change

The axioms presented in this article originate from Chichilnisky [5, 7, 8], except for one new axiom—**the Swan Axiom**—that is introduced here and represents the essence of the new probability theory. Below we explain how the Swan Axiom relates to standard theory and its connection with Godel's incompleteness theorem and the Axiom of Choice that are at the foundation of Mathematics.

To explain how the new theory intersects with standard probability or relative likelihood, we compare the results presented here with Savage's (1972) axiomatization of probability measures as finitely additive measures, as well as with [2, 25] classic work that is based instead on countably additive measures. Savage (1972) axiomatizes subjective probabilities as finitely additive measures representing the decision makers' beliefs, an approach that can ignore frequent events as shown in the Appendix. To overcome this, Villegas and Arrow [2, 25] introduced their additional continuity axiom ('Monotone Continuity') that ensures as we saw above the countably additivity of the measures. However this requirement of monotone continuity has unusual implications when the subject is confronted with rare events. A practical example it discussed below: it predicts that in exchange for a couple of cents, one should be willing to accept a small risk of death, a possibility that Arrow himself described as 'outrageous' [2, p. 48 and 49]. The issue of course is the "smallness" of the risk or "how rare is the risk", and here is where topology enters. Monotone continuity has a low bar for smallness while the sup norm has

a higher bar as we shall see below. This article defines a realistic solution, and it implies that for some very large payoffs and in certain special situations, one may be willing to accept a small risk of death—but not in others. This means that Monotone Continuity holds in some cases but not in others, a possibility that leads to the axiomatization proposed in this article, which is the logical negation of Monotone Continuity—one that is consistent with recent experimental observations for example those reported in Chanel and Chichilnisky [9, 10].

This section explains in what sense standard probability theory is biased against—or disregards—rare events. The next section defines new axioms for relative likelihood or probabilities, and compares them with the classic axioms. In this section the definitions and results are given for a general measure space of events; the definitions are refined below when the events are Borel measurable sets in the real line R.

Definition 1. A probability W is said to be **biased against rare events** or **insensitive to rare events** when it neglects events that are 'vanishing' according to the definition provided in Section 3 above. Formally, a probability is insensitive to rare events when given two events A and B and any vanishing sequence of events $(E_j), \exists\, N = N(f,g) > 0$, such that $W(A) > W(B) \Leftrightarrow W(A') > W(B')\ \forall\ A', B'$ satisfying $A' = A$ and $B' = B$ a.e. on $E_j^c \subset R$ when $j > N$.[8] As already discussed this implies a bias against the likelihood of change.

Proposition 2. *A probability satisfies Monotone Continuity if and only if it is biased against rare events and underestimates the likelihood of change.*

Proof. [7] Chichilnisky (2000).

Corollary 1. *Countably additive probabilities are biased against rare events and underestimate change.*

Proof. It follows from Propositions 1 and 2 and Chichilnisky [7].

Proposition 3. *Purely finitely additive probabilities are biased against frequent events.*

Proof. See Appendix.

The following example illustrates the role of Monotone Continuity and SP_4 in introducing a bias against rare events. The best way to explain the role of Monotone Continuity is by means of the example provided by Kenneth Arrow, Arrow [2, p. 48 and 49] . He explains that if a is an action that involves receiving one cent, b is another that involves receiving zero cents, and c is a third action involving receiving one cent and facing a small probability of death, then *Monotone Continuity* requires that the third action involving death and one cent should be preferred to the action with zero cents when the probability of death is small enough. One accepts a small chance of death in exchange for one cent. Even Arrow says 'this

[8] Here E^c denotes the complement of the set E, $A' = A$ a.e. on $E_j^c \Leftrightarrow A' \cap E_j^c = A \cap E_j^c$ a.e.

may sound outrageous at first blush…' [2, p. 48 and 49]. Outrageous or not, Monotone Continuity (MC) leads to neglect rare events that involve change with major consequences, like death. It can be said that death is a black swan: this is the content of Proposition 2 above.

4 New Axioms for Probability Theory: The Topology of Change

This section presents the new axiomatic foundation for probability theory that is neither biased against rare nor against frequent events [7, 8].

The new axioms for probability—or relative likelihoods—are as follows:

Axiom 3 *Probabilities are additive and continuous in the topology of change.*

Axiom 4 *Probabilities are unbiased against rare events.*

Axiom 5 *Probabilities are unbiased against frequent events.*

Additivity is a natural condition and **continuity** captures the notion that 'nearby' events are thought as being similarly likely to occur; this property is important to ensure that 'sufficient statistics' exist and it is based on a finer topology than Monotone Continuity—the sup norm of L_∞ that we called the "topology of change". Axiom 3 defines continuity with respect to a finer topology Axioms 4 and 5 together are equivalent to the Swan Axiom defined in the previous section, which is required to avoid a bias against rare and frequent events as shown in Section 3. The concept of continuity bears further elaboration. Topology provides the notion of what is meant by 'nearby'; different topologies define different notions of 'nearby' and therefore different notions of what is meant by 'continuity.' For example, 'nearby' was defined in [25] and [2] as follows: two events are **close** or **nearby** when they differ on a **small set—**thus reducing the problem to determine what is a small set. As stated in Arrow [2, p. 48]: "An event that is far out on a *vanishing sequence* is 'small' by any reasonable standards" [2, p. 48] . As the sets (n, ∞) are all similar, there is no reason why they become "small" for large enough n, according to Villegas and Arrow.

To overcome the bias against rare events, we introduce a new axiom that is the logical negation of MC: this means that sometimes MC holds and other times it does not. We call this the **Swan Axiom,** and is stated formally below:

Axiom 6 (Swan Axiom) *There exist vanishing sequences of sets* $\{U_i\}$*—namely,* $\forall i, U_{i+1} \subset U_i$ *and* $\cap U_i = \varnothing$*— where the limit of the measures* $\mu(U_i)$ *as* $i \to \infty$ *is not zero.*

Observe that in some cases the measures of the sets in a vanishing family may converge to zero and in other cases they do not. In words, this axiom is the logical negation of Monotone Continuity and can be equivalently described as follows:

"There exist events A and B with $W(A) > W(B)$, and for every vanishing sequence of events $\{E_\alpha\}_{=1,2...}$ an $N > 0$ such that altering arbitrarily the events A and B on the set E^i, where $i > N$, alters the probability ranking of the events, namely $W(B') > W(A')$, where B' and A' are the altered events."

Proposition 4. *A probability that satisfies the Swan Axiom is neither biased against rare events, nor biased against frequent events.*

Proof. This is immediate from the definition.

Example: To illustrate how this axiom works in practice consider an experiment where the subjects are offered a certain amount of money to choose and ingest a pill at random from a pile of pills that contains one pill that causes death [3, 4]. Experimentally, it is observed that in some cases people accept a sum of money and choose a pill provided the pile is large enough—namely when the probability of death is small enough—thus satisfying the Monotone Continuity axiom and in the process determining a statistical value for their lives. But there are also cases where the subjects will not accept to choose any pill, no matter how large is the pile. Some people refuse a payment if it involves a small probability of death, no matter how small the probability may be [3, 4]. This conflicts with the Monotone Continuity axiom, as explicitly presented by Arrow [2]. Our Axiom provides a reasonable resolution to this dilemma that is realistic and consistent with the experimental evidence. It implies that there exist catastrophic outcomes such as the risk of death, so terrible that one is unwilling to face a small probability of death to obtain one cent versus half a cent, no matter how small the probability may be. According to our Swan Axiom, no probability of death may be acceptable when only one cent and half a cent are involved. Our Axiom also implies that in other cases there may be a small enough probability that the lottery involving death may be acceptable, or that the payoff is large enough to justify the small risk. This is a possibility discussed by Arrow [2], where he explains that for large payoffs (for example, one billion US dollars), one may be willing to accept a small probability of death. In other words: sometimes one is willing to take a risk of death with a small enough probability of a catastrophe, and in other cases one is not. This is the content of the Swan Axiom.

We saw in Proposition 2 that the notion of continuity defined by Villegas and Arrow—namely Monotone Continuity—conflicts with the Swan Axiom and neglects rare events. Indeed Proposition 1 shows that countably additive measures are biased against rare events. On the other hand, Proposition 3 and the Example in the Appendix show that purely finitely additive measures can also be biased, in this case against frequent events. A natural question is whether it is possible to eliminate simultaneously both biases. The following theorem addresses this issue:

Theorem 1. *A probability that satisfies the Swan Axiom is neither biased against frequent nor against rare events. The resulting measures are neither purely finitely additive nor countably additive. They are a strict convex combinations of both.*

Proof. The next Section contains a proof of Theorem 1 and provides examples when the events are Borel sets in R or within an interval $(a, b) \subset R$.

Theorem 1 establishes that neither Savage's approach, nor Villegas' and Arrow's approaches, satisfy the three new axioms stated above. These three axioms require more than the additive probabilities of Savage, since purely finitely additive probabilities are finitely additive and yet they must be excluded here; at the same time the axioms require less than the countably additivity of Villegas and Arrow, since countably additive probabilities are biased against rare events. Theorem 1 above shows that a strictly convex combination of both does the job.

Theorem 1 shows how the Swan Axiom resolves the bias problem against frequent and rare events, but it does not by itself prove the existence of likelihoods that satisfy all three axioms. What is missing is an appropriate definition of 'nearby', namely of topology and continuity, that does not conflict with the Swan Axiom. The following shows that this can be achieved.

We now specialize the space of measurable sets so they are Borel measurable subsets of the real line R, and consider the Lebesgue measure on R. In this context a probability or likelihood function $W : L_\infty \to R$ is called **biased against rare events**, or **insensitive to rare events** when it neglects events that are small according to a probability measure μ on R that is absolutely continuous with respect to the Lebesgue measure. Formally:

Definition 2. A probability is insensitive to rare events when given two events f and $g, \exists \varepsilon = \varepsilon(f, g) > 0$, such that $W(f) > W(g) \Leftrightarrow W(f') > W(g') \forall f', g'$ satisfying $f' = f$ and $g' = g$ a.e. on $A \subset R$ and $\mu(A^c) < \varepsilon$. Here A^c denotes the complement of the set A.

Definition 3. A probability or likelihood function $W : L \to R$ is said to be **insensitive to frequent events** when given any two events $f, g, \exists \varepsilon(f, g) > 0$ such that $W(f) > W(g) \Leftrightarrow W(f') > W(g') \forall f', g'$ satisfying $f' = f$ and $g' = g$ a.e. on $A \subset R$ and $\mu(A^c) > 1 - \varepsilon$.

Definition 4. W is called **sensitive** to rare (or frequent) events when it is **not insensitive** to rare (or frequent) events.

Below we identify an event with its characteristic function, so that events are contained in the space of bounded real valued functions on the universe space $\mathscr{U}$, $L_\infty(\mathscr{R})$, and endow this space with the sup norm rather than with the notion of smallness and continuity defined by Arrow and Villegas as described above. In this case the probability or likelihood $W : L_\infty(\mathscr{U}) \to R$ is taken to be continuous with respect to the sup norm. Events are elements of the Borel measurable sets of the real line R or an interval (a, b), they are identified with the characteristic functions, denoted f, g etc, and 'continuity' is based on a topology used earlier in Debreu [14]and in Chichilnisky [7–10], the sup norm $\| f \| = \operatorname{ess\,sup}_{x \in R} | f(x) |$. This is a sharper and more stringent definition of closeness than the one used by Villegas and Arrow, since an event can be small under the Villegas-Arrow definition but not under ours, see the Appendix for examples. The difference in the use of topologies as shown below achieves sensitivity to rare events. To simply notation, a probability that satisfies the classic axioms in De Groot [15] is from now on called

a **standard probability**, and is therefore countably additive. As already mentioned, a classic representation result is that for any event $f \in L_\infty$ a standard (countably additive) probability has the form $W(f) = \int_R f(x).\phi(x)d\mu$, where $\phi \in L_1(R)$ is an integrable function.

The next step is to show existence and characterize all the likelihoods or probability distributions that satisfy the 3 new axioms. The following three axioms are identical to the three axioms above, specialized to the case at hand, Borel sets of R, and measures in L_∞ with the topology defined by the $sup\ norm$ on $L_\infty(R)$, which we called "the topology of change"

Axiom 7 *$W : L_\infty \to R$ is linear and continuous.*

Axiom 8 *$W : L_\infty \to R$ is sensitive to frequent events.*

Axiom 9 *$W : L_\infty \to R$ is sensitive to rare events.*

The first and the second axiom agree with classic theory (except for the choice of topology) and standard likelihoods satisfy them. The third axiom is new.

Lemma 1. *A standard probability satisfies Axioms 7 and 8, but it is biased against rare events and therefore does not satisfy Axiom 9.*

Proof. Consider $W(f) = \int_R f(x)\phi(x)dx,\ \int_R \phi(x)dx = K < \infty$. Then

$$W(f) + W(g) = \int_R f(x)\phi(x)dx + \int_R g(x)\phi(x)dx = \int_R f(x) + g(x).\phi(x)dx = W(f+g),$$

and therefore W is linear. It is **continuous** with respect to the L_1 norm $\parallel f \parallel_1 = \int_R \mid f(x) \mid \phi(x)d\mu$ because $\parallel f \parallel_\infty < \varepsilon$ implies

$$W(f) = \int_R f(x).\phi(x)dx \leq \int_R \mid f(x) \mid .\phi(x)dx \leq \varepsilon \int \phi(x)dx = \varepsilon K.$$

Since the sup norm is finer than the L_1 norm, continuity in L_1 implies continuity with respect to the sup norm [18]. Thus a standard probability satisfies Axiom 1. It is obvious that for every two events f, g, with $W(f) > W(g)$, the inequality is reversed namely $W(g') > W(f')$ when f' and g' are appropriate variations of f and g that differ from f and g on sets of sufficiently large Lebesgue measure. Therefore Axiom 2 is satisfied. A standard probability is however not sensitive to rare events, as shown in Chichilnisky [7–10, 13] (Chichilnisky 2008).

5 Existence and Representation Theorems

Theorem 2. *There exists a probability distribution or likelihood function $W : L_\infty \to R$ satisfying the new Axioms 7, 8, and 9. A probability distribution satisfies Axioms 7, 8, and 9 if and only if there exist two continuous linear functions on L_∞*

denoted ϕ_1 and ϕ_2, *and a real number* λ, $0 < \lambda < 1$, *such that for any observable event* $f \in L_\infty$ *the likelihood*

$$W(f) = \lambda \int_{x \epsilon R} f(x)\phi_1(x)dx + (1-\lambda)\phi_2(f) \tag{1}$$

where $\phi_1 \in L_1(R, \mu)$ *defines a countably additive measure on* R *and where* ϕ_2 *is a purely finitely additive measure.*

Proof. This result follows from the representation Theorem in Chichilnisky [7, 8].

Corollary 2. *Absent rare events, a probability that satisfies Axioms 7, 8, and 9 is consistent with classic axioms and yields a countably additive measure.*

Proof. Axiom 9 is an empty requirement when there are no rare events while, as shown above, Axioms 7 and 8 are consistent with standard relative likelihood.

6 Heavy Tails and Families of Purely Finitely Additive Measures

This section presents new results adding to the introduction of the Swan Axiom 6 defined in Section 4 above: it examines the different notions of continuity, how heavy tails originate from the new axioms and defines a family of purely finitely additive measures that are each absolutely continuous with respect to the Lebesgue measure on R.

A main difference introduced by the new axioms is the use of a finer topology—the "topology of change", which is the sup norm on L_∞, and defines the continuity properties of probability distributions. In the classic axioms a probability distribution is continuous if it satisfies Monotone Continuity or equivalently SP4. Here the continuity required is with respect to the topology of change, which is a finer topology: the following example explains the difference that this makes on the concept of continuity of probability distributions:

6.1 Contrasting Monotone Continuity and the Topology of Change

Different topologies define different approaches to 'continuity'. Consider the family $\{E^i\}$ where $E^i = [i, \infty)$, $i = 1, 2, \ldots$. This is a vanishing family because $\forall i \; E^i \supset E^{i+1}$ and $\bigcap_{i=1}^{\infty} E^i = \varnothing$. Consider now the events $f^i(t) = K > 0$ when $t \in E^i$ and $f^i(t) = 0$ otherwise, and $g^i(t) = 2K$ when $t \in E^i$ and $g^i(t) = 0$ otherwise. Then for all i, $\sup_{E^i} \mid f^i(t) - g^i(t) \mid = K$. In the sup norm topology this implies that f^i and g^i are **not** 'close' to each other, as the difference $f^i - g^i$ does not converge

to zero. No matter how far along we are along the vanishing sequence E^i the two events f^i, g^i differ by at least the number K. Yet since the events f^i, g^i differ from $f \equiv 0$ and $g \equiv 0$ respectively only in the set E^i, and $\{E^i\}$ is a vanishing sequence, for large enough i they are as 'close' as desired according to Villegas-Arrow's definition of 'nearby' events.

6.2 Heavy Tails

The following illustrates the additional weight that the new axioms assign to rare events; in this example in the form of 'heavy tails' (e.g. [7]. The finitely additive measure ϕ_2 appearing in the second term in (1) can be illustrated as follows. On the subspace of events with limiting values at infinity, $L'_\infty = \{f \epsilon L_\infty : \lim_{x\to\infty}(x) < \infty\}$, define $\phi_2(f) = \lim_{x\to\infty} f(x)$ and extend this to a function on all of L_∞ using Hahn Banach's theorem. The difference between a standard probability and the likelihood defined in (1) is the second term ϕ_2, which focuses all the weight at infinity. This can be interpreted as a 'heavy tail' namely a part of the distribution that is not part of the standard density function ϕ_1 and gives more weight to the sets that contain *terminal* events namely sets of the form (x, ∞).

6.3 The Family PA of Purely Finitely Additive Measures on R

This section provides a new family of purely finitely additive measures that are absolutely continuous with respect to the Lebesgue measure, and studies its properties [16, 23].

Definition 5. An *open neighborhood* of a real number $x \in R$ has the standard meaning under the usual topology of the line R. An *'open neighborhood of* ∞' is defined to be a set of the form $\{x \in R : x. > r$ for $r \in R\}$. As already stated, the word "essentially" means a.e. with respect to the Lebesgue measure on R that has been used to define the space L_∞.

We now define a property on measures in the space L^*_∞ :

Definition 6 (Property (P)). A measure in L^*_∞ is said to satisfy Property (P) at x if it assigns measure zero to any set that is essentially contained in the complement of an open neighborhood of x. A measure in L^*_∞ is said to satisfy Property (P) at ∞, if it assigns measure 0 to any measurable set that is essentially contained in the complement of an open neighborhood of ∞ as defined above. A measure is said to satisfy Property (P) if it satisfies Property (P) either at ∞ or at any $x \in R$.

Lemma 2. *A measure satisfying property* (P)*is always purely finitely additive.*

Proof. Consider first the case where the measure has property (P) at ∞. Define a countable family of disjoint sets $F = \{A_1, A_2 \ldots\}$ recursively as follows: $A_1 = \{x : -1 < x < 1\}$ and for all n, $A_n = \{x : -n < x < n\} - A_{n-1}$. Observe that each set A_n has measure zero, since by assumption μ satisfies property (P), and that each of the sets in the family F is bounded. The sets in the family F are also disjoint by construction. If μ was countably additive, then we should have $\mu(\cup F) = \mu(\cup_{n=1}^{\infty} A_n) = \sum_{n=1}^{\infty} \mu(A_n) = 0$. Yet the measure of the union of the countable family F is not 0, because $\cup F = R$, the entire real line, so that $\mu(\cup F) = 1$. Therefore μ fails to be countably additive on the countable and disjoint family F. Since by definition μ is a measure, and it fails to be countably additive, it must be a purely finitely additive measure.

A similar argument can be given for the case where the measure has property (P) at a finite number $x \in R$. Define now $F = \{A_n\}_{n=1,2,\ldots}$ recursively as follows: $A_1 = [x-1, x+1]^c$ where the super-index c denotes the complement of a set, and for all $n \geq 1$, $A_n = [x - 1/n, x + 1/n]^c - A_{n-1}$. Observe that each set in the family F has measure 0. The union of the family is not the whole space as before—since the point $\{x\}$ is not in the union; yet the entire space minus $\{x\}$ should have the same measure than the space as a whole, because by definition a measure is a continuous linear function on L_∞, the space of measurable and essentially bounded functions with the Lebesgue measure on R, which means that the measure must provide the same value to functions in L_∞ that are essentially equal, in the sense of differing only in a set of Lebesgue measure 0. The characteristic functions of two measurable sets differing in a set of measure zero, must therefore be are assigned the same value by a measure, so the union of the family F must be assigned the same measure as the entire space, namely $\mu(\cup F) = 1$. Therefore the measure μ fails to be countably additive, and since it is a measure it must be purely finitely additive.

Observe that in Lemma 1 the same argument applies for a measure that has property (P) at x for a finite $x \in R$, or one that has property (P) at $\{\infty\}$. The "test" family F is defined similarly in both cases, where for a finite x, $A_1 = \{x : -\epsilon < x < \varepsilon\}$, and $A_n = \{x : -n < x < n\} - A_{n-1}$. The only difference in the argument arises from the fact that, for a finite $\{x\}$, the union of the family $\cup F$ is not all of R, but rather $R - \{x\}$. But $R - \{x\}$ is essentially the same as R in the Lebesgue measure used to define $L\infty$.

Lemma 3. *Using Hahn-Banach's theorem it is possible to define purely finitely additive measures on R.*

Proof. Lemma 1 started from assuming the existence of a measure in L_∞^* that satisfies property (P) at ∞. Using Hahn Banach's theorem we now define the desired measure, namely a continuous linear function h from L_∞ to R, and show that it satisfies (P) at ∞. Therefore by Lemma 1, the function h is a purely finitely additive measure, as we wished to prove.

Consider the subspace CL_∞ of all functions f in L_∞ that are continuous and have an essential limit at ∞. CL_∞ is a closed linear subspace of the Banach space $L\infty$. On the subspace CL_∞ define the function $h(f) = ess \lim_{x \to \infty} f(x)$. By

construction the function h is well defined on CL_∞; this function is continuous, linear and has norm 1. The function h can therefore be extended by using Hahn-Banach's theorem to all of L_∞, as a continuous, linear function that preserves the norm of h. Since h has norm 1 the extension is not the zero function. Call this extension h as well; by construction, $h \in L_\infty^*$. Therefore by definition, the extended function h defines a measure. Now observe that $h : L_\infty \rightarrow R$ satisfies Property (P) since when applied to characteristics functions of bounded sets, it assigns to them measure zero. A similar argument can be replicated to show the existence of purely finite measures that satisfy property (P) at any $x \in R$.

We have mentioned that it is not possible to construct or represent a purely finitely additive measure on R the same way as one constructs or represents a countably additive measure on R. This is not surprising since the Hanh-Banach Theorem that is used to define a purely finitely additive measure in Lemma 2 is itself not constructible. The next and last section show the connection between the new axioms for probability (or relative likelihoods) presented here, the Axiom of Choice and Godel's [19] work.

7 The Axiom of Choice and Godel's Incompleteness Theorem

There is a connection between Axioms 3, 4, and 5 presented here and the Axiom of Choice that is at the foundation of mathematics [19]. The Axiom of Choice postulates that there exists a universal and consistent fashion to select an element from every set.

The best way to describe the situation is by means of an example, see also [12, 18, 27, 28] and [20].

Example: Representing a purely finitely additive measure.

Define a measure ρ as follows: for every Borel measurable set $A \subset R$, $\rho(A) = 1$ if $A \supset \{x : x > a$, for some $a \in R\}$, and otherwise $\rho(A) = 0$. Then ρ is not countably additive, because the family of countably many disjoint sets $\{V_i\}_{i=0,1,...}$ defined as $V_i = (i, i+1] \bigcup (-i-1, -i]$, satisfy $V_i \bigcap V_i = \varnothing$ when $i \neq j$, and $\bigcup_{i=0}^{\infty} V_i = \bigcup_{i=0}^{\infty} (i, i+1] \bigcup (-i-1, -i] = R$, so that $\rho(\bigcup_{i=0}^{\infty} V_i) = 1$,while $\sum_{i=0}^{\infty} \rho(V_i) = 0$, which contradicts countable additivity. Since the contradiction arises from assuming that ρ is countably additive, ρ must be purely finitely additive. Observe that ρ assigns zero measure to any bounded set, and a positive measure only to unbounded sets that contain a 'terminal set' of the form

$$\{x \in R : x > a \text{ for some } a \in R\}.$$

One can define a function on L_∞ that represents this purely finitely additive measure ρ if we restrict our attention to the closed subspace L'_∞ of L_∞ consisting of those

functions $f(x)$ in L_∞ that have a limit when $x \to \infty$, by the formula $\rho(f) = \lim_{x\to\infty} f(x)$, as in Lemma 3 of the previous section. The function $\rho(.)$ can be seen as a limit of a sequence of delta functions whose support increases without bound. The problem is now to extend the function ρ to another defined on the entire space L_∞. This could be achieved in various ways but as we will see, each of them requires the Axiom of Choice.

One can use Hahn - Banach's theorem [18] to extend the function ρ from the closed subspace $L'_\infty \subset L_\infty$ to the entire space L_∞ preserving its norm. However, in its general form Hahn - Banach's theorem requires the Axiom of Choice [18]. Alternatively, one can extend the notion of a *limit* to encompass all functions in L_∞ including those with no standard limit. This can be achieved by using the notion of convergence along a *free ultrafilter* arising from compactifying the real line R as in Chichilnisky and Heal [12]. However the existence of a *free ultrafilter* also requires the Axiom of Choice.

This illustrates why the attempts to construct *purely finitely additive measures* that are representable as functions on L_∞, require the Axiom of Choice. Since our criteria require purely finitely additive measures, this provides a connection between the Axiom of Choice and our axioms for relative likelihood. It is somewhat surprising that the consideration of rare events that are neglected in standard statistical theory conjures up the Axiom of Choice, which is independent from the rest of mathematics [19].

Acknowledgements This article is an expression of gratitude to the memory of Jerry Marsden, a great mathematician and a wonderful man. As his first PhD student in pure Mathematics when he was a professor at the Mathematics Department of UC Berkeley, the author is indebted to Jerry Marsden for counseling and support in obtaining the first of her two PhDs at UC Berkeley, in pure Mathematics. The second PhD in Economics at UC Berkeley was obtained by the author with the counseling of the Nobel Laureate economist, Gerard Debreu. Jerry Marsden was critical to encourage the growth of the research in this article on new and more realistic axiomatic foundations of probability theory; he invited the author to organize a Workshop on Catastrophic Risks at the Fields Institute in 1996 where this research was introduced, and strongly encouraged since 1996 the continuation and growth of this research.

The author is Director, Columbia Consortium for Risk Management (CCRM) Columbia University, and Professor of Economics and of Mathematical Statistics, Columbia University, New York 10027, 335 Riverside Drive, NY 10025, tel. 212 678 1148, chichilnisky@columbia.edu; website: www.chichilnisky.com. We acknowledge support from Grant No 5222-72 of the US Air Force Office of Research directed by Professor Jun Zheng, Washington DC from 2009 to 2012. Initial results on Sustainable Development were presented at Stanford University's 1993 Seminar on Reconsideration of Values, organized by Kenneth Arrow, at the National Bureau of Economic Research Conference *Mathematical Economics: The Legacy of Gerard Debreu* at UC Berkeley, October 21, 2005, the Department of Economics of the University of Kansas National Bureau of Economic Research General Equilibrium Conference, September 2006, at the Departments of Statistics of the University of Oslo, Norway, Fall 2007, at a seminar organized by the former Professor Christopher Heyde at the Department of Statistics of Columbia University, Fall 2007, at seminars organized by Drs. Charles Figuieres and Mabel Tidball at LAMETA Universite de Montpellier, France December 19 and 20, 2008, and by Professor Alan Kirman at GREQAM Universite de Marseille, December 18 2008. In December 8 2012, the work presented here and its applications were presented at an invited Plenary Key Note Presentation by the author to the Annual Meetings of the Canadian Mathematical Society Montreal Canada, December 8 2012. The work

presented in this article is also the subject of a forthcoming Plenary Key Note Presentation to the Annual Meeting of the Australian Mathematical Society in Sidney, Australia, December 18, 2013. We are grateful to the above institutions and individuals for supporting the research, and for helpful comments and suggestions.

Appendix

Example: A Probability that is Biased Against Frequent Events

Consider $W(f) = \liminf_{x \epsilon R}(f(x))$. This is insensitive to frequent events of arbitrarily large Lebesgue measure [18] and therefore does not satisfy Axiom 2. In addition it is not linear, failing Axiom 1.

Example: The Dual Space L^*_∞ Consists of Countably Additive and Finitely Additive Measures

The space of continuous linear functions on L_∞ is the 'dual' of L_∞, and is denoted L^*_∞. It has been characterized e.g. in Yosida [27, 28]. L^*_∞ consists of the sum of two subspaces $(i) L_1$ functions g that define countably additive measures ν on R by the rule $\nu(A) = \int_A g(x)dx$ where $\int_R \mid g(x) \mid dx < \infty$ so that υ is *absolutely continuous* with respect to the Lebesgue measure, and (ii) a subspace consisting of purely finitely additive measure. A countable measure can be identified with an L_1 function, called its 'density,' but purely finitely additive measures cannot be identified by such functions.

Example: A Finitely Additive Measure that is Not Countably Additive

See Example in Section 7.

References

1. Anscombe, F.J., Aumann, R.J.: A definition of subjective probability. Ann. Math. Stat. **43**, 199–295 (1963)
2. Arrow, K.: Essays in the Theory of Risk Bearing. North Holland, Amsterdam (1971)
3. Chanel, O., Chichilnisky, G.: The influence of fear in decisions: experimental evidence. J. Risk Uncertain. **39**(3), 271–298 (2009)

4. Chanel, O., Chichilnisky, G.: The value of life: theory and experiments working paper, GREQE. Universite de Marseille and Columbia University, New York (2009)
5. Chichilnisky, G.: An axiomatic approach to sustainable development. Soc. Choice Welf. **13**, 321–257 (1996)
6. Chichilnisky, G.: Updating Von Neumann Morgenstern axioms for choice under uncertainty. In: Proceedings of a Conference on Catastrophic Risks. The Fields Institute for Mathematical Sciences, Toronto (1996)
7. Chichilnisky, G.: An axiomatic approach to choice under uncertainty with catastrophic risks. Resour. Energy Econ. **22**, 221–231 (2000)
8. Chichilnisky, G.: Catastrophic risk. In: El-Shaarawi, A.H., Piegorsch, W.W. (eds.) Encyclopedia of Environmetrics, vol. 1, pp. 274–279. Wiley, Chichester (2002)
9. Chichilnisky, G.: The limits of econometrics: non parametric estimation in Hilbert spaces. Econ. Theory **25**(4), 1070–1086 (2009)
10. Chichilnisky, G.: The topology of fear. J. Math. Econ. **45**(12), 807–816 (2009a)
11. Chichilnisky, G.: Choice under uncertainty: the work and legacy of Kenneth Arrow. In: Cont, R. (ed.) Encyclopedia of Quantitative Finance. Wiley, Chichester (2009)
12. Chichilnisky, G., Heal, G, M.: Social choice with infinite populations. Soc. Choice Welf. **14**, 303–319 (1997)
13. Chichilnisky, G., Wu, H-M.: General equilibrium with endogenous uncertainty and default. J. Math. Econ. **42**, 499–524 (2006)
14. Debreu, G.: Valuation equilibrium and pareto optimum. Proc. Natl. Acad. Sci. **40**, 588–592 (1953)
15. De Groot, M.H.: Optimal Statistical Decisions. Wiley, Hoboken, NJ (1970/2004)
16. Dubins, L.: Finitely additive conditional probabilities, conglomerability and disintegration. Ann. Probab. **3**, 89–99 (1975)
17. Dubins, L., Savage, L.: How to Gamble if you Must. McGraw Hill, New York (1965)
18. Dunford, N., Schwartz, J.T.: Linear Operators, Part I. Interscience, New York (1958)
19. Godel, K.: The Consistency of the Continuum Hypothesis. Annals of Mathematical Studies, vol. 3. Princeton University Press, Princeton (1940)
20. Kadane, J.B., O'Hagan, A.: Using finitely additive probability: uniform distributions of the natural numbers. J. Am. Stat. Assoc. **90**, 525–631 (1995)
21. Kolmogorov, A.N.: Foundations of the Theory of Probability. Chelsea Publishing Co., New York (1933/1950)
22. Le Doux, J.: The Emotional Brain. Simon and Schuster, New York (1996)
23. Purves, R.W., Sudderth, W.D.: Some finitely additive probability. Ann. Probab. **4**, 259–276 (1976)
24. Savage, L.: The Foundations of Statistics, revised edn. Wiley, New York (1972)
25. Villegas, C.: On quantitative probability σ-algebras. Ann. Math. Stat. **35**, 1789–1800 (1964)
26. Von Neumann, J., Morgernstern, O.: Theory of Games and Economic Behavior. Princeton University Press, New Jersey (1944)
27. Yosida, K.: Functional Analysis, 4th edn. Springer, New York/Heidelberg (1974)
28. Yosida, K., Hewitt, E.: Finitely level independent measures. Trans. Am. Math. Soc. **72**, 46–66 (1952)

Chaos in the Kepler Problem with Quadrupole Perturbations

Gabriela Depetri and Alberto Saa

Abstract We use the Melnikov integral method to prove that the Hamiltonian flow on the zero-energy manifold for the Kepler problem perturbed by a quadrupole moment is chaotic, irrespective of the perturbation being of prolate or oblate type. This result helps to elucidate some recent conflicting works in the physics literature based on numerical simulations.

1 Introduction

The Kepler two-body problem has been a splendid inspiration for physicists and mathematicians for the last three centuries (see, for instance, Chapter 9 of [1]). Many works, in particular, have been devoted to the study of the onset of chaos in the perturbed Kepler problem (see, for a recent review, [2] and the references therein). For astronomical and astrophysical applications, it is natural to consider the weak field approximation in which the gravitational field of a body is decomposed into a multipole expansion. The original Kepler problem corresponds to the case where only the first expansion term, the monopole, is present. The next term in the expansion, the dipole term, is known to give origin to integrable motion, see Chapter 7 of [3] and Section 2 below. The quadrupole term is usually considered as the simplest perturbation to the Newtonian potential which could lead to chaotic motion in the Kepler problem (see, for instance, [4]). By employing the

G. Depetri (✉)
Instituto de Física Gleb Wataghin, Universidade Estadual de Campinas,
13083-859 Campinas, SP, Brazil
e-mail: gdepetri@gmail.com

A. Saa
Departamento de Matemática Aplicada, Universidade Estadual de Campinas,
13083-859 Campinas, SP, Brazil
e-mail: asaa@ime.unicamp.br

D.E. Chang et al. (eds.), *Geometry, Mechanics, and Dynamics*, Fields Institute Communications 73, DOI 10.1007/978-1-4939-2441-7_5

usual cylindrical coordinates (r, z, ϕ) around the gravitational center, the simplest quadrupole perturbation to the Newtonian potential reads

$$U(r,z) = -\frac{\alpha}{\sqrt{r^2+z^2}} - \frac{q}{2}\frac{2z^2-r^2}{(r^2+z^2)^{5/2}}, \tag{1}$$

where α and q stands for, respectively, the monopole intensity (proportional to the total gravitational mass) and the quadrupole intensity. The cylindrical coordinates are assumed to be adjusted to the quadrupole direction. Two qualitative distinct cases can be distinguished for the potential (1). Oblate deformations, as those ones of rotating deformed bodies, correspond to $q < 0$, whereas prolate deformations, as cigar-like mass distributions, to $q > 0$. The study of the integrability of a test body motion under action of the potential (1) is a long standing problem, with substantially relevance to astronomy and astrophysics [5].

In [4], a numerical study of bounded trajectories is reported suggesting that the motion under prolate perturbations would be indeed chaotic while, on the other hand, oblate perturbations would correspond to an integrable case. Such conclusion would be rather puzzling since it is known that, for disk-like perturbation (which could be understood as extreme oblate perturbations), bounded oblique orbits are known to be chaotic [6, 7]. This qualitative difference for the cases $q > 0$ and $q < 0$ is attributed in [4] to some qualitative differences in the saddle points of the effective potential, but it is also known that such kind of local argument leads typically to conditions that are not sufficient neither necessary to the appearance of chaos in theses systems [8]. More recently, a new numerical study suggesting that the oblate perturbations would also give origin to bounded chaotic orbits has appeared [9]. Here, we explore these conflicting results by applying the Melnikov integral method [10] for the parabolic orbits [11] (the zero-energy manifold) of (1). We prove the quadrupole perturbations effectively give rise to chaotic motion on the zero-energy manifold, irrespective of the perturbation being of prolate ($q > 0$) or oblate ($q < 0$) type.

2 The Melnikov Conditions

The Hamiltonian associated to the motion of a test body of unit mass under the action of the potential (1) is given by

$$H = \frac{1}{2}\left(p_r^2 + p_z^2\right) + \frac{L_z^2}{2r^2} + U(r,z), \tag{2}$$

where (r, p_r) and (z, p_z) stands for the usual canonical cylindrical coordinates and L_z is the (conserved) angular momentum around the z axis. The Hamiltonian H is itself a conserved quantity and the integrability of the Hamiltonian flow governed by (2) corresponds to the celebrated problem of the existence of the third isolating

conserved integral of motion [5]. In order the write the quadrupole perturbation in (2) conveniently, let us introduce the new variables (R, θ)

$$\begin{cases} r = R\cos\theta, \\ z = R\sin\theta, \end{cases} \tag{3}$$

which leads to

$$H = H_0 + qW_1(R) + qW_2(R,\theta), \tag{4}$$

where

$$H_0 = \frac{1}{2}\left(p_R^2 + \frac{p_\theta^2}{R^2}\right) + \frac{L_z^2}{2R^2\cos^2\theta} - \frac{\alpha}{R}, \tag{5}$$

with (R, p_R) and (θ, p_θ) standing for the usual canonical coordinates, and

$$-\frac{q}{R^3} + \frac{3q\cos^2\theta}{2R^3} \equiv qW_1(R) + qW_2(R,\theta). \tag{6}$$

Notice that the perturbation (6) corresponds to the case $\beta = 3$ considered in [2], but the unperturbed Hamiltonian (5) is indeed different. Without loss of generality, let us assume hereafter that $\alpha = 1$. Notice that a dipole perturbation would give rise to a Hamiltonian (4) with $W_1 = 0$ and $W_2 = R^{-2}\sin\theta$, which indeed corresponds to a particular case of the integrable case discussed in the Section 48 of [3].

In order to compute the Melnikov integrals [10] for the Kepler problem with quadrupole perturbations, we will adopt the integral method adapted for parabolic orbits presented in [11]. To this purpose, we need to obtain the equivalent of the homoclinic orbit of our problem. The total energy and the total angular momentum are the conserved quantities of our system,

$$H_0 = \frac{\dot{R}^2}{2} + \frac{G^2}{2R^2} - \frac{1}{R}, \tag{7a}$$

$$G^2 = R^4\dot{\theta}^2 + \frac{L_z^2}{\cos^2\theta}, \tag{7b}$$

and from the expressions above, we have

$$\frac{dR}{\sqrt{2\left(H_0 + \frac{1}{R}\right) - \frac{G^2}{R^2}}} = \pm dt, \tag{8a}$$

$$\frac{1}{R^2}\frac{dR}{\sqrt{2\left(H_0 + \frac{1}{R}\right) - \frac{G^2}{R^2}}} = \frac{d\theta}{\sqrt{G^2 - \frac{L_z^2}{\cos^2\theta}}}, \tag{8b}$$

From (7a), we see that the minimum value of R with $H_0 = 0$ satisfies $G^2 = 2R_{min}$. We are interested in the parabolic orbits and, hence, substituting $H_0 = 0$ in (8a) and (8b) and performing the integration, we have

$$\pm t = \frac{\sqrt{2}}{3}\left(R - \frac{R_{min}}{2}\right)\sqrt{R - R_{min}} + \text{const}, \tag{9a}$$

$$\frac{1}{4A}\ln\left|\frac{A + \sin\theta}{A - \sin\theta}\right| + \text{const} = \arctan\sqrt{\frac{R}{R_{min}} - 1}, \tag{9b}$$

where $A = \sqrt{1 - \frac{L_z^2}{G^2}}$. Notice that, from (7b), one has that $0 < A \leq 1$.

Inverting (9a), we have the expression $R(t)$ of the homoclinic orbit, but this is not necessary to our purposes. Also, adjusting the constant in (9b) so that $R = R_{min}$ for $\theta = 0$, we have the following expression for $R(\theta)$

$$R(\theta) = R_{min}\sec^2\left[\frac{1}{4A}\ln\left|\frac{A + \sin\theta}{A - \sin\theta}\right|\right]. \tag{10}$$

From (10), it is clear that $R(\theta)$ is an even function and that the parabolic orbit can be parametrized with $-\theta^* < \theta < \theta^*$, where $R(\theta^*) = \infty$, which leads to

$$\sin\theta^* = A\tanh A\pi. \tag{11}$$

The Melnikov conditions to detect integrability of a Hamiltonian system of the type (2) corresponds to the existence of simple zeros for the quantities [11]

$$M_1(\theta_0) = \int_{-\infty}^{\infty}\{H_0, W_2\}\mathrm{d}t, \qquad M_2(\theta_0) = \int_{-\infty}^{\infty}\{G, W_2\}\mathrm{d}t, \tag{12}$$

where the integrals are taken over the zero-energy manifold. For each value of A, this is a two-dimensional manifold parametrized as $\mathscr{R} = R(t - t_0)$ and $\vartheta = \Theta(t - t_0) + \theta_0$, with arbitrary t_0 and θ_0. We see that

$$M_1(\theta_0) = -\int_{-\infty}^{\infty}\left[\dot{\mathscr{R}}\frac{\partial W_2}{\partial R} + \dot{\Theta}\frac{\partial W_2}{\partial\theta}\right]\mathrm{d}t = -W_2\Big|_{t=-\infty}^{t=\infty} + \int_{-\infty}^{\infty}\frac{\partial W_2}{\partial t}\mathrm{d}t = 0, \tag{13}$$

and, with some trigonometry, that

$$M_2(\theta_0) = -\frac{3}{8R_{min}}\left[I_1\cos(2\theta_0) + I_2\sin(2\theta_0)\right], \tag{14}$$

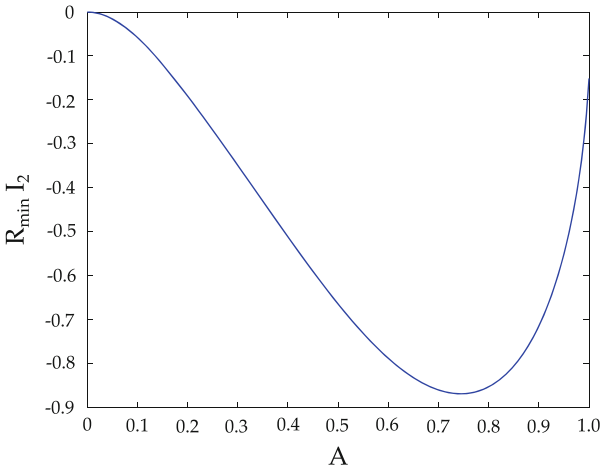

Fig. 1 The integral (16) for different values of A. Notice that $I_2 = 0$ only for $A = 0$ and for $A = 1$, the latter corresponding to $L_z = 0$ and, thus, to the case $\beta = 3$ considered in [2]

where, after changing the integration variable,

$$I_1 = \int_{-\theta^*}^{\theta^*} \frac{\sin(2\theta)}{R(\theta)} \mathrm{d}\theta, \qquad I_2 = \int_{-\theta^*}^{\theta^*} \frac{\cos(2\theta)}{R(\theta)} \mathrm{d}\theta. \tag{15}$$

Since $R(\theta)$ is an even function, we have $I_1 = 0$. Finally, the non identically zero contribution to the Melnikov integral comes from the integral

$$I_2 = \frac{1}{R_{min}} \int_{-\theta^*}^{\theta^*} \cos(2\theta) \cos^2 \left[\frac{1}{4A} \ln \left| \frac{A + \sin\theta}{A - \sin\theta} \right| \right] \mathrm{d}\theta, \tag{16}$$

where θ^* is given by (11). Is is enough to prove that $I_2 \neq 0$ for some value of A to establish that $M_2(\theta_0)$ given by (14) has (infinitely many) simple zeros, which implies the absence of the extra conserved integral of motion and, consequently, that the motion is indeed chaotic, irrespective of the sign of the perturbation parameter q. Figure 1 depicts the integral (16) as a function of A, and we can check that one has indeed $I_2 \neq 0$ for $0 < A < 1$.

3 Final Remarks

By using the Melnikov integral method adapted for parabolic orbits [11], we prove that the Hamiltonian flow on the zero-energy manifold for the Kepler problem perturbed by a quadrupole moment is chaotic, irrespective of the perturbation being of prolate or oblate type. This result favors, in this way, the numerical results obtained in [9], which are in conflict with those ones presented in [4].

Acknowledgements The authors are grateful to FAPESP (2013109357-9), CNPq and CSF11/2012, PVE Darryl Holm, for the financial support, and to the Fields Institute and the Université Libre de Bruxelles, where part of this work was done, for the warm hospitality. GD would like to thank M. Santoprete for the fruitful discussions at the Fields Institute. Both authors thank J. C. Sartorelli for all the help.

References

1. Abraham, R., Marsden, J.E.: Foundations of Mechanics, 2nd edn. AMS, Providence (2008)
2. Diacu, F., Pérez-Chavela, E., Santoprete, M.: The Kepler problem with anisotropic perturbations. J. Math. Phys. **46**, 072701 (2005)
3. Landau, L.D., Lifshitz E.M.: Mechanics. Pergamon Press, Oxford (1969)
4. Gueron, E., Letelier, P.S.: Chaotic motion around prolate deformed bodies. Phys. Rev. E **63**, 035201 (2001)
5. Boccalleti, D., Pucacco, G.: Theory of Orbits. Perturbative and Geometrical Methods, vol. 2. Springer, New York (2004)
6. Saa, A., Venegeroles, R.: Chaos around the superposition of a black-hole and a thin disk. Phys. Lett. **259A**, 201 (1999)
7. Saa, A.: Chaos around the superposition of a monopole and a thick disk. Phys. Lett. **269A**, 204 (2000)
8. Saa, A.: On the viability of local criteria for chaos. Ann. Phys. **314**, 508 (2004)
9. Letelier, P.S., Ramos-Caro, J., López-Suspes, F.: Chaotic motion in axially symmetric potentials with oblate quadrupole deformation. Phys. Lett. **375A**, 3655 (2011)
10. Holmes, P.J., Marsden, J.E.: Melnikov's method and Arnold diffusion for perturbations of integrable Hamiltonian systems. J. Math. Phys. **23**, 669 (1982)
11. Cicogna, G., Santoprete, M.: Mel'nikov method revisited. Regul. Chaotic Dyn. **6**, 377 (2001)

Groups of Diffeomorphisms and Fluid Motion: Reprise

David G. Ebin

Abstract Following Ebin and Marsden (Ann Math 92(1):102–163, 1970) we provide a concise proof of the well-posedness of the equations of perfect fluid motion. We use a construction which casts the equations as an ordinary differential equation on a non-linear function space.

1 Introduction

In 1970 Marsden and the present author published [4], which became an influential paper. According to Google Scholar it is Marsden's second most cited paper and the present author's most cited paper. Also it was translated into Russian and published in the Soviet journal *Matematika* [5] with additional comments and references.

The paper follows the work of [1] and [7] and provides the necessary analytical structure for both.

The main theorem of [4] is the well-posedness of the equations of motion of a perfect (incompressible, homogeneous and inviscid) fluid, but the proof there given is somewhat circuitous and rather long. In the present article we provide a shorter more direct approach.

2 Construction of Equations

One can describe fluid motion as a curve in the group of diffeomorphisms of a region that is filled with fluid. We take the region to be a closed Riemannian manifold. Call it M. Then $\eta(t) : M \to M$ will be the curve of diffeomorphisms. For each $x \in M$, $\eta(t)(x)$ will be the position at time t of that fluid particle which at time zero was at x.

D.G. Ebin (✉)
Department of Mathematics, Stony Brook University, Stony Brook, NY 11794-3651, USA
e-mail: ebin@math.sunysb.edu

D.E. Chang et al. (eds.), *Geometry, Mechanics, and Dynamics*, Fields Institute Communications 73, DOI 10.1007/978-1-4939-2441-7_6

The energy of the fluid moving by $\eta(t)$ is

$$\mathscr{E}(t) = \frac{1}{2}\int_M \langle \dot{\eta}(t), \dot{\eta}(t)\rangle \mu$$

where $\dot{\eta}$ is the time derivative of η, $\langle\ ,\ \rangle$ is the Riemannian metric and μ is the volume element defined by the metric. Using Hamilton's principle we require that the actual fluid motion be a stationary curve of $\int_a^b \mathscr{E}(t)dt$ in the sense that if $\eta(t,s)$ is a one-parameter family of curves with $\eta(t) = \eta(t,0)$, for $t \in [a,b]$, and $s \in (-\epsilon,\epsilon)$ and with $\partial_s\eta(a,s) = \partial_s\eta(b,s) = 0$ then

$$\partial_s \int_a^b \mathscr{E}(t,s)\, dt|_{s=0} = \frac{1}{2}\partial_s \int_a^b \int_M \langle \dot{\eta}(t,s), \dot{\eta}(t,s)\rangle \mu dt|_{s=0} = 0 \tag{1}$$

But since equation (1) must hold for all variations $\eta(t,s)$ we find that:

$$\partial_s \int_a^b \langle \dot{\eta}(t,s)(x), \dot{\eta}(t,s)(x)\rangle\, dt|_{s=0} = 0 \tag{2}$$

for each $x \in M$, so from equation (2) we find that the curve $t \to \eta(t)(x)$ is a geodesic in M. Thus we might think that fluid particles move along geodesics. However since our fluid is incompressible the curve $\eta(t)$ must consist of diffeomorphisms which preserve the volume element. Hence we have the additional requirement:

$$\eta(t,s)^*(\mu) = \mu \tag{3}$$

and with this (1) has a different consequence as we now explain.

$\dot{\eta}(t,s)(x)$ and $\partial_s\eta(t,s)(x)|_{s=0}$ are both tangent vectors at $\eta(t,s)(x)$. We will call them $v(t)(\eta(t,s)(x))$ and $w(t)(\eta(t,s)(x))$ respectively. Then differentiating (3) with respect to t and s, we get:

$$\mathscr{L}_{v(t)}(\mu) = 0 \ \text{ and } \ \mathscr{L}_{w(t)}(\mu) = 0 \tag{4}$$

where $\mathscr{L}$ denotes the Lie derivative. But since μ is the volume element of the Riemannian metric we find that $\mathscr{L}_u(\mu) = \operatorname{div}(u)\mu$ for any vector field u so we get $\operatorname{div} v(t) = \operatorname{div} w(t) = 0$. As is well known, a vector field u can be decomposed into its solonoidal and gradient parts; that is, $u = v + \nabla f$ where ∇f is the gradient of some function f and $\operatorname{div} v = 0$. We also note that:

$$\int_M \langle v, \nabla f\rangle \mu = -\int_M f \operatorname{div} v\, \mu = 0$$

so the decomposition gives summands which are orthogonal with respect to the L^2 inner product on vector fields. We will call the projection onto these summands P and Q, so $Pu = v$ and $Qu = \nabla f$.

Starting from (1), integrating by parts and using $\eta^*(\mu) = \mu$ and letting $v(t)$ and $w(t)$ be defined as above, we get:

$$\int_a^b \left(\int_M \langle \partial_t v + \nabla_v v, w \rangle \mu \right) dt = 0 \tag{5}$$

where ∇ is the covariant derivative defined by the Riemannian metric. Since (5) must hold for any divergence free $w(t)$, this implies that for each t,

$$\int_M \langle \partial_t v(t) + \nabla_{v(t)} v(t), w(t) \rangle \mu = 0 \tag{6}$$

and (6) in turn implies that $\partial_t v + \nabla_v v$ must be the gradient of a function. Following convention we shall call it $-\nabla p$, so $\partial_t v + \nabla_v v = -\nabla p$. Alternatively we can write $P(\partial_t v + \nabla_v v) = 0$, and since v and therefore $\partial_t v$ are divergence free, we get

$$\partial_t v + P(\nabla_v v) = 0$$

or

$$\partial_t v + \nabla_v v = Q(\nabla_v v) \tag{7}$$

3 Function Spaces

We shall solve (7) by showing how it can be construed as an ordinary differential equation on an infinite dimensional manifold, so we now proceed to construct the manifold. First we note that the group of smooth diffeomorphisms of M can be given a manifold structure as follows: Given $\eta \in \mathscr{D}$ we consider the linear space of vector fields over η. It is

$$T_\eta \mathscr{D} = \{u : M \to TM \,|\, \pi \circ u = \eta\}$$

where $\pi : TM \to M$ is the tangent bundle of M. Then if ζ is sufficiently near η in $\mathscr{D}$ we get for each $x \in M$ a unique minimal geodesic γ_x from $\eta(x)$ to $\zeta(x)$. Letting $u(x)$ be the tangent vector to γ_x at $\eta(x)$ we get $u \in T_\eta \mathscr{D}$. Furthermore if $\exp : TM \to M$ is the exponential map of M, then $\exp \circ u = \zeta$. Thus composition with exp gives a bijection between a neighborhood of zero in $T_\eta \mathscr{D}$ and a neighborhood of η in $\mathscr{D}$. We take this bijection to be a chart about η in $\mathscr{D}$. If η_1 and η_2 are two

elements of $\mathscr{D}$, we get a smooth transition from one chart to another because exp is a smooth function. Also with these charts the tangent space of $\mathscr{D}$ at η is naturally identified with $T_\eta\mathscr{D}$.

We now have a manifold structure for $\mathscr{D}$, but the spaces $T_\eta\mathscr{D}$ have a C^∞ topology which comes from an infinite set of norms and thus is not a Banach space. Hence the basic theorems of differential analysis (i.e., the inverse function theorem or the convergence of Picard iteration for ordinary differential equations) do not hold. To surmount this difficulty, we enlarge our space by requiring only finitely many derivatives. We shall use the H^s topology requiring that derivatives up to order s be in L^2 and calling the resulting space $\mathscr{D}^s$. The H^s topology is given by an inner product on each $T_\eta\mathscr{D}^s$ as follows: For $\alpha, \beta \in T_\eta\mathscr{D}^s$ there exist $u, w \in T_{id}\mathscr{D}^s$ such that $\alpha = u \circ \eta$ and $\beta = w \circ \eta$. We define

$$(\alpha, \beta)_s := \sum_{k=0}^{s} \int_M \langle \nabla^k u, \nabla^k w \rangle \circ \eta \, \mu$$

where ∇^k is the kth order covariant derivative.

The Sobolev imbedding theorem tells us that the H^s topology is stronger that the C^k topology if $s > n/2 + k$ where n is the dimension of the manifold. We shall require that s be greater than $n/2+1$ so that the topology is stronger than C^1. In this case $\mathscr{D}^s$ is included in the group of all C^1 diffeomorphisms and it is a group as well (see [2] for details). We proceed to look at volume preserving diffeomorphisms.

Let $\mathscr{D}_\mu = \{\eta \in \mathscr{D} | \eta^*(\mu) = \mu\}$ and let $\mathscr{D}^s_\mu$ be its H^s extension. Consider the map

$$\psi : \mathscr{D}^s \to H^{s-1}(\Lambda^n)$$

defined by $\psi(\eta) = \eta^*(\mu)$. which takes a diffeomorphism into an n-form.

$$\int_M \psi(\eta) = \int_M \eta^*(\mu) = \int_{\eta(M)} \mu = \int_M \mu$$

so the range of ψ is included in

$$H^{s-1}_\mu(\Lambda^n) = \{\nu \in H^{s-1}(\Lambda^n) | \int_M \nu = \int_M \mu\}.$$

This is clearly an affine subspace of $H^{s-1}(\Lambda^n)$ of codimension one.

The derivative of ψ at the identity of $\mathscr{D}^s$ is $T_{id}\psi : T_{id}\mathscr{D}^s \to H^{s-1}(\Lambda^n)$, given by $T_{id}\psi(u) = \mathscr{L}_u(\mu) = \mathrm{div}(u)\mu$. The tangent space to $H^{s-1}_\mu(\Lambda^n)$ is

$$H^{s-1}_0(\Lambda^n) = \{\lambda \in H^{s-1}(\Lambda^n) | \int_M \lambda = 0\}$$

Given a λ in this tangent space we can solve

$$\Delta f = \lambda/\mu$$

for an H^{s+1} function f. Then $T_{id}\psi(\nabla f) = \Delta f\mu = \lambda$. Hence $T_{id}\psi$ is surjective. Similarly for any $\eta \in \mathscr{D}^s$, we can write an element of $T_\eta\mathscr{D}^s$ as $u\circ\eta$ where $u \in T_{id}\mathscr{D}^s$. Then a direct calculation shows that

$$T_\eta\psi(u\circ\eta) = \eta^*(\mathscr{L}_u(\mu)) = \mathrm{div}(u)\circ\eta\,\eta^*(\mu).$$

In this case given λ as above, we find $u \in T_{id}\mathscr{D}^s$ such that $\mathrm{div}\,u = (\lambda/\eta^*(\mu))\circ\eta^{-1}$. Then $T_\eta\psi(u\circ\eta) = \lambda$ as before.

Thus we have shown that for any $\eta \in \mathscr{D}^s_\mu$ and any $\lambda \in H^{s-1}_0(\Lambda^n)$, there exists $\alpha \in T_\eta\mathscr{D}^s$ such that $T_\eta\psi(\alpha) = \lambda$. It follows that $\psi : \mathscr{D}^s \to H^{s-1}_\mu(\Lambda^n)$ is a submersion so $\psi^{-1}(\mu) = \mathscr{D}^s_\mu$ is a submanifold of $\mathscr{D}^s$. Furthermore the tangent space to $\mathscr{D}^s_\mu$ at each η is the null-space of $T_\eta\psi : T_\eta\mathscr{D}^s \to H^s(\Lambda^n)$. Thus $T_\eta\mathscr{D}^s_\mu = \{u\circ\eta|\,\mathrm{div}(u) = 0\}$.

4 Proof of Well-Posedness

We shall show that (7) can be construed as a second order o.d.e. on $\mathscr{D}^s_\mu$. We can write (7) as an equation in $\eta(t)$ if $v(t)$ is defined by $\dot\eta = v\circ\eta \in T_\eta\mathscr{D}^s_\mu$. Then $\ddot\eta = (\partial_t v + \nabla_v v)\circ\eta$ so (7) becomes $\ddot\eta = Q(\nabla_v v)\circ\eta$, which is:

$$\ddot\eta = (Q(\nabla_{\dot\eta\circ\eta^{-1}}\dot\eta\circ\eta^{-1}))\circ\eta \tag{8}$$

We write this as:

$$\ddot\eta = Z(\eta,\dot\eta) \tag{9}$$

a second order o.d.e. on $\mathscr{D}^s_\mu$.

If we can show that Z is a smooth function, well-posedness will follow automatically from the fundamental theorem of o.d.e.'s.

To study (9) we will find it useful to introduce additional notation. Given any differential (or pseudo-differential) operator L on sections of a vector bundle over M and given $\eta \in \mathscr{D}^s$ we define L_η by

$$L_\eta f = L(f\circ\eta^{-1})\circ\eta$$

L_η is easily seen to be smooth in η. In fact if $\eta(s)$ is a curve in $\mathscr{D}^s$ and $\frac{d}{ds}\eta = w\circ\eta$ then

$$\frac{d}{ds}(L_\eta) = [\nabla_w, L]_\eta$$

where $[\ ,\ ]$ denotes the commutator. Thus $\frac{d}{ds}(L_\eta)$ has the same order as L.

We introduce the projection operator $Q_\eta : T_\eta \mathscr{D}^s \to T_\eta \mathscr{D}^s$ defined by $Q_\eta(\alpha) = (Q(\alpha \circ \eta^{-1})) \circ \eta$. Taking the union of Q_η over all $\eta \in \mathscr{D}^s$, we get $\tilde{Q} : T\mathscr{D}^s \to T\mathscr{D}^s$; that is, $\tilde{Q}$ is defined on the whole tangent bundle of $\mathscr{D}^s$.

We recall that at $\eta = id$, $Q(u)$ is just the gradient part of u, so $Q(u) = \nabla \Delta^{-1} \operatorname{div} u$. Since the null-space of Δ is the constant functions, Δ^{-1} is defined only up to an additive constant. However ∇ kills constant functions so $\nabla \Delta^{-1}$ is uniquely defined. Clearly $Q_\eta = (\nabla \Delta^{-1})_\eta \operatorname{div}_\eta$. Thus with our new notation we get:

$$Z(\eta, \dot{\eta}) = (\nabla \Delta^{-1})_\eta (\operatorname{div}(\nabla_v v) \circ \eta)$$

where $v = \dot{\eta} \circ \eta^{-1}$.

But since $\dot{\eta} \in T_\eta \mathscr{D}^s_\mu$, we get $\operatorname{div} v = 0$. Hence $(\operatorname{div} \nabla_v)v = [\operatorname{div}, \nabla_v]v$. Thus we get:

$$Z(\eta, \dot{\eta}) = (\nabla \Delta^{-1})_\eta [\operatorname{div}, \nabla_v]_\eta \dot{\eta} \tag{10}$$

The"sub-η" operators are smooth in η as we have seen. $[\operatorname{div}, \nabla_v]$, being a commutator of first order operators is also first order and $\nabla \Delta^{-1}$ has order minus one. Thus the composition is of order zero, so it is a bounded operator from H^s to H^s. We see in (10) that it is linear and therefore smooth in $\dot{\eta}$. However v also depends on $\dot{\eta}$ and η, since it is defined as $\dot{\eta} \circ \eta^{-1}$. We must check that this dependence is also smooth. To do this we introduce a new variable z to isolate the v dependence. We compute $[\operatorname{div}, \nabla_v]_\eta z$ for some H^s vector field z. using local coordinates we get:

$$[\operatorname{div}, \nabla_v]_\eta z = \partial_i (\dot{\eta}^j \circ \eta^{-1}) \partial_j (z^i \circ \eta^{-1}) \circ \eta + \partial_k (\Gamma^k_{ij} \circ \eta^{-1} \dot{\eta}^i \circ \eta^{-1} z^j \circ \eta^{-1}) \circ \eta$$

for some smooth functions Γ^k_{ij} and with repeated indices summed. This expression is smooth in $(\eta, \dot{\eta})$ as a function from H^s to H^{s-1} since it involves first derivatives.[1] Following it by $(\nabla \Delta^{-1})_\eta$ makes it smooth from H^s to H^s. Thus $Z(\eta, \dot{\eta})$ is smooth so (8) is a smooth o.d.e. on $\mathscr{D}^s_\mu$.

Therefore given $\eta(0) = id$ and $\dot{\eta}(0) \in T_{id} \mathscr{D}^s_\mu$ we get an interval $(-T_b, T_e)$ (with T_b and T_e positive or infinite) and a unique smooth curve $\eta : (-T_b, T_e) \to \mathscr{D}^s_\mu$ which satisfies (8). Furthermore the curve depends smoothly on $\dot{\eta}(0)$.

5 Further Remarks

1. The same analysis holds in the case that M is a manifold with smooth boundary, including the important case of a bounded domain in $\mathbf{R^n}$. Since each $\eta(t)$ is a diffeomorphism, it leaves the boundary set-wise invariant and one gets the condition:

$$\langle \dot{\eta}(t)(x), \nu(\eta(t)(x)) \rangle = 0$$

[1] Alternatively we could avoid detailed calculation by noting that $[\operatorname{div}_\eta, \nabla_v]_\eta z = -\frac{d}{dt}(\operatorname{div}_{\eta(t)})z$ which is smooth since div_η is smooth in η.

on the boundary, where ν is the normal to the boundary. We also need a boundary condition for $-\nabla p = Q(\nabla_v v)$. But $\langle \partial_t v, \nu\rangle = \langle P(\nabla_v v), \nu\rangle$, so we must have $\langle -\nabla p, \nu\rangle = \langle \nabla_v v, \nu\rangle$. Thus $-\Delta p = \operatorname{div}(\nabla_v v)$ as before and p also has a Neumann boundary condition. Note that $\langle \nabla_v v, \nu\rangle = -\langle v, \nabla_v \nu\rangle$ so the boundary condition does not involve derivatives of v.

2. The same technique of solving an o.d.e. on an H^s function space can be used to solve for geodesics on groups of diffeomorphisms which preserve a symplectic form [3] or a contact form [6]. Ebin and Preston [6] also contains physical applications, namely geostrophic and quasigeostrophic flows, and the Vlasov or Vlasov-Maxwell equations provide an application for the symplectic case. See [8].
3. The system of equations:

$$\partial_t v + \nabla_v v = -\nabla p \quad \operatorname{div} v = 0$$

involves derivatives in both time and space, so it was not thought to be amenable to o.d.e. methods. The general feeling was that if one wrote it in the form $\partial_t u = L(u)$, then L would have to involve spatial derivatives and therefore could not take H^s into H^s. Using the variables $(\eta, \dot{\eta})$ we got a system of order zero so an o.d.e. approach was possible. Because of this the appearance of [4] was met with a good deal of surprise and even some suspicion.

References

1. Arnol'd, V.I.: Sur la géométrie différentielle des groupes de Lie de dimension infinie et ses applications a l'hydrodynamique des fluides parfaits. Ann. Inst. Fourier **16**, 319–361 (1966)
2. Ebin, D.G.: The manifold of Riemannian metrics. In: Proceedings of Symposia in Pure Mathematics, vol. 15, pp. 11–40. AMS, Providence (1970)
3. Ebin, D.G.: Geodesics on the symplectomorphism group. Geom. Funct. Anal. **22**(1), 202–212 (2012)
4. Ebin, D.G., Marsden, J.: Groups of diffeomorphisms and the motion of an incompressible fluid. Ann. Math. **92**(1), 102–163 (1970)
5. Russian translation of Ebin, D.G., Marsden, J.: Groups of diffeomorphisms and the motion of an incompressible fluid. Ann. Math. **92**(1), 102–163 (1970). Matematika **17**(6), 111–146 (1973)
6. Ebin, D.G., Preston, S.C.: Riemannian geometry on the quantomorphism group. Arnold Math Journal, DOI 10.1007/540598-014-0002-2 (2014)
7. Marsden, J., Abraham, R.: Hamiltonian mechanics on Lie groups and hydrodynamics. In: Proceedings of Symposia Pure Mathematics, vol. 16, pp. 237–244 (1970)
8. Marsden, J.E., Weinstein, A.: The hamiltonian structure of the Vlasov equations. Physica D **4**, 394–406 (1982)

Dual Pairs for Non-Abelian Fluids

François Gay-Balmaz and Cornelia Vizman

Abstract This paper is a rigorous study of two dual pairs of momentum maps arising in the context of fluid equations whose configuration Lie group is the group of automorphisms of a trivial principal bundle, generically called here non-abelian fluids. It is shown that the actions involved are mutually completely orthogonal, which directly implies the dual pair property.

1 Introduction

It is well-known that the flow of the Euler equations of a perfect fluid can be formally interpreted as a geodesic on the group of volume preserving diffeomorphisms of the fluid domain, relative to an L^2 Riemannian metric, [1]. This result has been at the origin of many developments of the methods of symmetry and reduction for the study of incompressible fluids, their Clebsch variables and vortices, as initiated in [33]. For instance, in [33] Marsden and Weinstein discovered a pair of momentum maps associated to the Euler equations that geometrically justifies the existence of Clebsch canonical variables for ideal fluid motion and explains the Hamiltonian structure of point vortex solutions in terms of the (Lie-Poisson) Hamiltonian structure of the Euler equations. As claimed in [33], and rigorously shown in [11], this pair of momentum maps forms a *dual pair* in the sense that the Lie group associated to each of the momentum maps acts transitively on the level set of the other momentum map. In order to obtain such a result, it has been necessary to restrict each of the acting Lie groups to its commutator subgroup and to centrally extend these subgroups. This gives rise to the quantomorphism group as a central extension of the group of Hamiltonian diffeomorphisms, and to the Ismagilov central extension of the group of exact volume preserving diffeomorphisms.

F. Gay-Balmaz (✉)
CNRS, LMD, École Normale Supérieure de Paris, Paris, France
e-mail: francois.gay-balmaz@lmd.ens.fr

C. Vizman
Department of Mathematics, West University of Timişoara, 300223 Timişoara, Romania
e-mail: vizman@math.uvt.ro

D.E. Chang et al. (eds.), *Geometry, Mechanics, and Dynamics*, Fields Institute Communications 73, DOI 10.1007/978-1-4939-2441-7_7

A pair of momentum maps has also been described for PDEs associated to geodesics on the group of (non necessarily volume preserving) diffeomorphisms, the so-called EPDiff equations, by Holm and Marsden in [22]. One of the momentum maps provides singular solutions of the PDE (e.g. for the H^1 metric, as it does for the peakon solutions of the Camassa-Holm equations [4]), whereas the other momentum map provides a constant of motion for the collective dynamics of these singular solutions, by the Noether Theorem. It has been shown in [11] that these momentum maps also form a dual pair.

Since the seminal result of Arnold, the geometric formulation via diffeomorphism groups and the associated methods of symmetry and reduction have been developed in order to apply to a large class of equations arising in hydrodynamics, such as compressible fluid and magnetohydrodynamics in [34]. More recently, it has been observed [7–9] that several models of complex fluids and (possibly non-abelian Yang-Mills) charged fluids require the use of the group of automorphisms of a principal bundle as configuration Lie group (or its volume preserving version), instead of a group of diffeomorphisms. In this case, the base of the principal bundle is the fluid domain, whereas its structure group is given by the order parameter group in the case of complex fluids, or by the symmetry Lie group of the underlying Yang-Mills theory in the case of charged fluids. We refer to Theorem 3.3 in [9] for a summary of the geometric formulation of several models of non-abelian fluids. We refer to [2, 3, 27] and reference therein, for further information about the physics literature on non-abelian fluids.

The simplest situation, which is also the case of interest for this paper, corresponds to geodesic equations on the automorphism group of a principal bundle (referred to as EPAut equations) or on its volume preserving subgroup (referred to as $\mathrm{EPAut}_{\mathrm{vol}}$ equations). Examples are provided by the equations of motion of a non-abelian charged perfect fluid moving under the influence of a fixed external Yang-Mills field, which describe the geodesic flow of the Kaluza-Klein L^2 metric on the group of volume preserving automorphisms [7]. As explained in [14], other examples treated in the literature can be seen as geodesic equations on the automorphism group of a trivial principal bundle. These are the two-component Camassa-Holm equations [5, 29], its modified version considered in [24] and its higher dimensional and anisotropic versions studied in [23]. In [23, 24], the modified versions were also shown to admit singular solutions given by a momentum map.

A pair of momentum maps explaining geometrically the above singular solutions has been considered in [14] in the general context of the EPAut equations on arbitrary principal bundles. In particular, it was found that these momentum maps are associated to the actions of two groups of automorphisms on a manifold of equivariant embeddings, thereby extending, from the EPDiff to the EPAut case, the momentum map setting developed in [22].

Concerning the volume preserving situation (i.e. the $\mathrm{EPAut}_{\mathrm{vol}}$ case), a pair of momentum maps has been found in [14] that extends the dual pair for the ideal fluid found in [33]. Interestingly, the proper definition of one of the momentum maps needs the introduction of new infinite-dimensional Lie groups, such as the group of special Hamiltonian automorphisms and the group of Vlasov chromomorphisms,

defined in [14]. In this case, one of the momentum maps yields a Clebsch representation that extends the classical Clebsch representation for ideal fluid to the non-abelian case, whereas the other momentum map recovers, as a particular case, the expression of the Klimontovich particle solution of the Yang-Mills Vlasov equations.

Dual Pairs of Momentum Maps

Let us briefly recall the definition of a dual pair in the finite dimensional context, as formalized in [38]. Let (M, ω) be a finite dimensional symplectic manifold and let P_1, P_2 be two finite dimensional Poisson manifolds. A pair of Poisson mappings

$$P_1 \xleftarrow{\mathbf{J}_L} (M, \omega) \xrightarrow{\mathbf{J}_R} P_2$$

is called a dual pair if $\ker T\mathbf{J}_L$ and $\ker T\mathbf{J}_R$ are symplectic orthogonal complements of one another, i.e. $(\ker T\mathbf{J}_L)^\omega = \ker T\mathbf{J}_R$. In infinite dimensions, due to the weakness of the symplectic form, one has to impose both identities [11]

$$(\ker T\mathbf{J}_L)^\omega = \ker T\mathbf{J}_R \quad \text{and} \quad (\ker T\mathbf{J}_R)^\omega = \ker T\mathbf{J}_L. \tag{1}$$

In many cases of interest, and this will be the case in the present paper too, the Poisson maps $\mathbf{J}_1$ and $\mathbf{J}_2$ are momentum mappings arising from the commuting Hamiltonian actions of two Lie groups H and G on M. We assume that both momentum maps are equivariant, so that they are Poisson maps with respect to the Lie-Poisson structure on the dual Lie algebras $\mathfrak{h}^*$ and $\mathfrak{g}^*$:

$$\mathfrak{h}^* \xleftarrow{\mathbf{J}_L} (M, \omega) \xrightarrow{\mathbf{J}_R} \mathfrak{g}^*. \tag{2}$$

In this case the dual pair conditions (1) become $\mathfrak{g}_M^\omega = \mathfrak{h}_M^{\omega\omega}$ and $\mathfrak{h}_M^\omega = \mathfrak{g}_M^{\omega\omega}$, because $\ker T\mathbf{J}_R = \mathfrak{g}_M^\omega$ and $\ker T\mathbf{J}_L = \mathfrak{h}_M^\omega$.

The actions are said to be *mutually completely orthogonal* [30] if the G-orbits and the H-orbits are symplectic orthogonal to each other. In infinite dimensions we need again two identities

$$\mathfrak{g}_M = \mathfrak{h}_M^\omega \quad \text{and} \quad \mathfrak{h}_M = \mathfrak{g}_M^\omega. \tag{3}$$

These can be rewritten as $\mathfrak{g}_M = \ker T\mathbf{J}_L$ and $\mathfrak{h}_M = \ker T\mathbf{J}_R$, which means that the infinitesimal actions of $\mathfrak{g}$ resp. $\mathfrak{h}$ on level sets of momentum maps $\mathbf{J}_L$ resp. $\mathbf{J}_R$ are transitive.

In finite dimensions the mutually completely orthogonality identities (3) are equivalent to the fact that (2) is a dual pair. In the infinite dimensional case, the mutually complete orthogonality property (3) implies the dual pair property, but

the converse is not true. A counterexample is provided by the dual pair associated to perfect free boundary fluids, as shown in [13]. In fact, both dual pair conditions (1) follow from just one of the conditions (3).

Dual pair structures arise naturally in classical mechanics. For example, in [31] (see also [6, 16] and [26]) it was shown that the concept of dual pair of momentum maps can be useful for the study of bifurcations in Hamiltonian systems with symmetry. More recently, it was shown in [12] how the rigorous dual pair property of the ideal fluid momentum maps can be used to describe a new class of infinite dimensional coadjoint orbits of the Hamiltonian group.

Plan of the Paper

The goal of the present paper is to show that the pairs of momentum maps found in [14] in the context of the EPAut and $\text{EPAut}_{\text{vol}}$ equations, form two *dual pairs*. In the infinite dimensional situation, this means that both the equalities $(\ker T\mathbf{J}_1)^\omega = \ker T\mathbf{J}_2$ and $(\ker T\mathbf{J}_2)^\omega = \ker T\mathbf{J}_1$ are true [11], since the equivalence between these equalities no longer holds in the infinite dimensional situation. In fact, we will show the stronger result that the actions are mutually completely orthogonal, in the sense that the orbits of one action are symplectic orthogonal to the orbits of the other action, *and vice versa*.

The plan of the paper is the following. In Section 2, we recall the expression of the Euler-Poincaré equations on the automorphism group of a principal bundle (the EPAut equations) in the case when the principal bundle is trivial. Then after reviewing the pair of momentum maps associated to the EPDiff equations [22], we will recall some facts concerning the pair of momentum maps associated to the EPAut equations [14]. These momentum maps will be shown in Section 3 to arise from mutually completely orthogonal actions and, therefore, to form a dual pair. In Section 4, we recall the expression of the Euler-Poincaré equations on the group of volume preserving automorphisms of a trivial principal bundle (the $\text{EPAut}_{\text{vol}}$ equations) and review from [14] some facts about the associated pair of momentum maps. We will then focus on a particular case relevant for the Yang-Mills Vlasov equations, arising when the total space of one of the principal bundles is a cotangent bundle. Finally, in Section 5 we show, still in this particular case and when the bundles are trivial, that the pair of momentum maps associated to the $\text{EPAut}_{\text{vol}}$ arise from mutually completely orthogonal actions and is therefore a dual pair.

2 The EPAut Equations and Momentum Maps

In this section we recall the expression of the Euler-Poincaré equations on the automorphism group of a principal bundle (the EPAut equations) in the case when the principal bundle is trivial, and we review some facts concerning the associated pair of momentum maps.

2.1 The Automorphism Group and Euler-Poincaré Equations

The automorphism group $\mathscr{A}ut(P)$ of a right principal bundle $\pi : P \to M$, with structure group $\mathscr{O}$, consists of all $\mathscr{O}$-equivariant smooth diffeomorphisms of P. Any automorphism $\tilde{\varphi} \in \mathscr{A}ut(P)$ induces a smooth diffeomorphism φ of the base M, by the condition $\pi \circ \tilde{\varphi} = \varphi \circ \pi$. The diffeomorphisms of M that can be obtained this way form the subgroup $\mathrm{Diff}(M)_{[P]} \subset \mathrm{Diff}(M)$ of diffeomorphisms preserving the isomorphism class of P. It is a subgroup which contains the identity component of $\mathrm{Diff}(M)$, so it consists of connected components of $\mathrm{Diff}(M)$. We will denote by $\mathfrak{aut}(P)$ the Lie algebra of $\mathscr{A}ut(P)$. It consists of all $\mathscr{O}$-equivariant smooth vector fields on P.

When the bundle P is trivial, i.e. $P \simeq M \times \mathscr{O} \to M$, the group of all automorphisms of P is isomorphic to the semidirect product group

$$\mathscr{A}ut(P) \simeq \mathrm{Diff}(M) \circledS \mathscr{F}(M, \mathscr{O}),$$

where $\mathscr{F}(M, \mathscr{O})$ denotes the group of smooth $\mathscr{O}$-valued functions defined on M. Let us recall that the group structure of the semidirect product reads

$$(\varphi_1, a_1)(\varphi_2, a_2) = (\varphi_1 \circ \varphi_2, (a_1 \circ \varphi_2)a_2).$$

To a couple $(\varphi, a) \in \mathrm{Diff}(M) \circledS \mathscr{F}(M, \mathscr{O})$, is associated the automorphism

$$(x, g) \in M \times \mathscr{O} \mapsto (\varphi(x), a(x)g) \in M \times \mathscr{O}. \tag{4}$$

The Lie algebra of the automorphism group is isomorphic to the semidirect product Lie algebra $\mathfrak{aut}(P) \simeq \mathfrak{X}(M) \circledS \mathscr{F}(M, \mathfrak{o})$, where $\mathfrak{o}$ is the Lie algebra of the structure group $\mathscr{O}$, $\mathfrak{X}(M)$ denotes the space of smooth vector fields on M, and $\mathscr{F}(M, \mathfrak{o})$ denotes the Lie algebra of smooth $\mathfrak{o}$-valued functions defined on M.

Euler-Poincaré Equations, EPDiff, and EPAut

Let G be a Lie group with Lie algebra $\mathfrak{g}$ and consider a right G-invariant Lagrangian $L : TG \to \mathbb{R}$ defined on the tangent bundle TG of G. Let $\ell : \mathfrak{g} \to \mathbb{R}$ be the reduced Lagrangian associated to L, that is $\ell(\xi) = L(g, \dot{g})$, with $\xi = \dot{g}g^{-1}$. By applying the process of Lagrangian reduction, the Euler-Lagrange equations for L are equivalent to the Euler-Poincaré equations for ℓ,

$$\partial_t \frac{\delta \ell}{\delta \xi} + \mathrm{ad}^*_\xi \frac{\delta \ell}{\delta \xi} = 0,$$

see e.g. [32] for a detailed exposition. When $G = \mathrm{Diff}(M)$, these equations are called the EPDiff equations, see [22]. Similarly, when $G = \mathscr{A}ut(P)$, these

equations will be called the *EPAut equations*. In the following Proposition we give the EPAut equations in the case when P is a trivial principal bundle. We refer to [36, 37], for the geodesic case and to [14] for the general case.

Proposition 1 (The EPAut Equations on a Trivial Bundle [14]). *Consider a reduced Lagrangian* $\ell : \mathfrak{X}(M) \circledS \mathscr{F}(M, \mathfrak{o}) \to \mathbb{R}$ *and identify the dual Lie algebra with the space* $\Omega^1(M) \otimes \mathrm{Den}(M) \times \mathscr{F}(M, \mathfrak{o}^*) \otimes \mathrm{Den}(M)$ *by using the* L^2 *pairing, where* $\mathrm{Den}(M)$ *denotes the space of densities on* M*. Then the EPAut equations are*

$$\begin{cases} \dfrac{\partial}{\partial t}\dfrac{\delta \ell}{\delta \mathbf{u}} + \pounds_{\mathbf{u}} \dfrac{\delta \ell}{\delta \mathbf{u}} + \dfrac{\delta \ell}{\delta \nu} \cdot \mathbf{d}\nu = 0 \\ \dfrac{\partial}{\partial t}\dfrac{\delta \ell}{\delta \nu} + \pounds_{\mathbf{u}} \dfrac{\delta \ell}{\delta \nu} + \mathrm{ad}^*_{\nu} \dfrac{\delta \ell}{\delta \nu} = 0, \end{cases} \tag{5}$$

where $(\mathbf{u}, \nu) \in \mathfrak{X}(M) \circledS \mathscr{F}(M, \mathfrak{o})$ *and the operator* $\pounds_{\mathbf{u}}$ *denotes the Lie derivative acting on tensor densities.*

In the special case $M = S^1$ and $G = S^1$, for suitable Lagrangians, we obtain the two component Camassa-Holm equation [5] and the modified two-component Camassa-Holm equation [24]. Equations for complex and nonabelian fluids are obtained from the Euler-Poincaré equations (5) by extending them to include advected quantities or/and coupling them with the Euler-Lagrange equations for the Yang-Mills fields. We refer to [15, 19–21] for the description of the noncanonical Hamiltonian structures and to [7–9] for the Lagrangian and Hamiltonian reductions approaches.

Remark 1 (Manifold Structures). In this paper, all the (finite dimensional) manifolds involved are smooth, Hausdorff, and paracompact (to admit partition of unity). All the maps considered are smooth (i.e. C^∞). All the manifolds are assumed to have no boundary.

The space of smooth functions defined on a compact manifold is a Fréchet manifold in a natural way. The space of embeddings is an open subset of this Fréchet manifold, hence a Fréchet manifold itself [28].

2.2 A Pair of Momentum Maps for the EPAut Equations

Review of the EPDiff Case

Let S and M be two manifolds with $\dim S \leq \dim M$. Suppose that S is compact and carries a volume form μ_S. As explained in Remark 1, the space $\mathrm{Emb}(S, M)$ of embeddings of S into M is a Fréchet manifold. Recall from [22] that the pair of momentum maps associated to the EPDiff equation is obtained by considering the cotangent lifted action of the groups $\mathrm{Diff}(S)$ and $\mathrm{Diff}(M)$ on the manifold $\mathrm{Emb}(S, M)$:

$$\mathfrak{X}(M)^* \xleftarrow{\mathbf{J}_L} T^* \mathrm{Emb}(S, M) \xrightarrow{\mathbf{J}_R} \mathfrak{X}(S)^*. \tag{6}$$

Note that the tangent space $T_{\mathbf{Q}}\,\mathrm{Emb}(S,M)$ consists of vector fields $\mathbf{V_Q}: S \to TM$ covering the embedding $\mathbf{Q}$. Since a volume form μ_S has been fixed, the cotangent space $T^*_{\mathbf{Q}}\,\mathrm{Emb}(S,M)$ can be identified with the space of 1-forms $\mathbf{P_Q}: S \to T^*M$ covering $\mathbf{Q}$.

The left momentum map

$$\mathbf{J}_L(\mathbf{P_Q}) = \int_S \mathbf{P_Q}(x)\delta(m - \mathbf{Q}(x))\mu_S$$

provides the formula for singular solutions of the EPDiff equations, whereas the right momentum map

$$\mathbf{J}_R(\mathbf{P_Q}) = \mathbf{P_Q} \cdot T\mathbf{Q}$$

provides a Noether conserved quantity for the (collective) Hamiltonian dynamics of these singular solutions in terms of the canonical variable $\mathbf{P_Q} \in T^*\,\mathrm{Emb}(S,M)$. Here $T\mathbf{Q}: TS \to TM$ denotes the tangent map to the embedding $\mathbf{Q}$.

These expressions of the momentum maps are obtained from the following general formula. Let G be a Lie group acting on a manifold Q, and consider the cotangent lifted action of G on T^*Q. Then this action admits the equivariant momentum map $\mathbb{J}: T^*Q \to \mathfrak{g}^*$ given by

$$\langle \mathbb{J}(\alpha_q), \xi \rangle = \langle \alpha_q, \xi_Q(q) \rangle, \quad \alpha_q \in T^*Q, \quad \xi \in \mathfrak{g}, \tag{7}$$

where ξ_Q is the infinitesimal generator of the action of G on Q associated to the Lie algebra element ξ. Recall that the momentum map $\mathbb{J}$ verifies the condition $\mathbf{d}\mathbb{J}_\xi = \mathbf{i}_{\xi_{T^*Q}}\Omega_{can}$, where Ω_{can} is the canonical symplectic form, ξ_{T^*Q} is the infinitesimal generator of the G-action on T^*Q, and $\mathbb{J}_\xi: T^*Q \to \mathbb{R}$ is the function defined by $\mathbb{J}_\xi(\alpha_q) := \langle \mathbb{J}(\alpha_q), \xi \rangle$. By equivariance, $\mathbb{J}$ is a Poisson map relative to the canonical symplectic form on T^*Q and the Lie-Poisson structure on $\mathfrak{g}^*$.

Momentum Maps for the EPAut Equations

In [14], a pair of momentum maps analogue to (6) has been constructed for the EPAut equations. It is obtained by considering two principal $\mathscr{O}$-bundles $\pi_S: P_S \to S$ and $\pi_M: P_M \to M$, and the cotangent lifted action of the automorphism groups $\mathscr{A}ut(P_S)$ and $\mathscr{A}ut(P_M)$ on the manifold $Q_{KK} := \mathrm{Emb}_{\mathscr{O}}(P_S, P_M)$ of all smooth $\mathscr{O}$-equivariant embeddings of P_S into P_M:

$$\mathfrak{aut}(P_M)^* \xleftarrow{\mathbf{J}_L} T^*\,\mathrm{Emb}_{\mathscr{O}}(P_S, P_M) \xrightarrow{\mathbf{J}_R} \mathfrak{aut}(P_S)^*. \tag{8}$$

We assume that both S and $\mathscr{O}$ are compact, so P_S is compact too and Q_{KK} is a Fréchet manifold (see Remark 1).

When both P_S and P_M are trivial principal bundles, we have the identification

$$Q_{KK} \simeq \mathrm{Emb}(S, M) \times \mathscr{F}(S, \mathscr{O}), \tag{9}$$

see Lemma 3.7 in [14]. In a similar way with (4), the equivariant embedding associated to a pair $(\mathbf{Q}, \gamma) \in \mathrm{Emb}(S, M) \times \mathscr{F}(S, \mathscr{O})$ is the map $(x, g) \in S \times \mathscr{O} \mapsto (\mathbf{Q}(x), \gamma(x)g) \in M \times \mathscr{O}$. The tangent space $T_\gamma \mathscr{F}(S, \mathscr{O})$ consists of functions $v_\gamma : S \to T\mathscr{O}$ covering γ and the cotangent space $T^*_\gamma \mathscr{F}(S, \mathscr{O})$ consists of functions $\kappa_\gamma : S \to T^*\mathscr{O}$ covering γ.

We now recall from [14] the expression of the cotangent momentum maps in the case of trivial bundles.

2.2.1 Left Action Momentum Map

The left action of $\mathscr{A}ut(M \times \mathscr{O}) \simeq \mathrm{Diff}(M) \circledS \mathscr{F}(M, \mathscr{O}) \ni (\varphi, a)$ on $Q_{KK} \ni (\mathbf{Q}, \gamma)$ is defined by

$$(\varphi, a)(\mathbf{Q}, \gamma) := (\varphi \circ \mathbf{Q}, (a \circ \mathbf{Q})\gamma). \tag{10}$$

Given a Lie algebra element $(\mathbf{u}, \nu) \in \mathfrak{X}(M) \circledS \mathscr{F}(M, \mathfrak{o})$, the infinitesimal generator associated to the left action (10) reads $(\mathbf{u}, \nu)_{Q_{KK}}(\mathbf{Q}, \gamma) = (\mathbf{u} \circ \mathbf{Q}, (\nu \circ \mathbf{Q})\gamma)$. By applying formula (7) with $\mathfrak{g} = \mathfrak{X}(M) \circledS \mathscr{F}(M, \mathfrak{o})$, we get the expression

$$\langle \mathbf{J}_L(\mathbf{P}_\mathbf{Q}, \kappa_\gamma), (\mathbf{u}, \nu) \rangle = \langle \mathbf{P}_\mathbf{Q}, \mathbf{u} \circ \mathbf{Q} \rangle + \langle \kappa_\gamma, (\nu \circ \mathbf{Q})\gamma \rangle,$$

so that the momentum map $\mathbf{J}_L : T^*Q_{KK} \to \mathfrak{X}(M)^* \times \mathscr{F}(M, \mathfrak{o})^*$ reads

$$\mathbf{J}_L \left(\mathbf{P}_\mathbf{Q}, \kappa_\gamma \right) = \left(\int_S \mathbf{P}_\mathbf{Q} \delta(x - \mathbf{Q}) \mu_S, \int_S \kappa_\gamma \gamma^{-1} \delta(x - \mathbf{Q}) \mu_S \right), \tag{11}$$

where $\mathfrak{X}(M)^*$ and $\mathscr{F}(M, \mathfrak{o})^*$ denote the distributional dual spaces.

2.2.2 Right Action Momentum Map

The right action of $\mathscr{A}ut(S \times \mathscr{O}) = \mathrm{Diff}(S) \circledS \mathscr{F}(S, \mathscr{O}) \ni (\psi, b)$ on $Q_{KK} \ni (\mathbf{Q}, \gamma)$ is defined by

$$(\mathbf{Q}, \gamma)(\psi, b) := (\mathbf{Q} \circ \psi, (\gamma \circ \psi)b). \tag{12}$$

Given a Lie algebra element $(\mathbf{v}, \zeta) \in \mathfrak{X}(S) \circledS \mathscr{F}(S, \mathfrak{o})$, the infinitesimal generator reads $(\mathbf{v}, \zeta)_{Q_{KK}}(\mathbf{Q}, \gamma) = (T\mathbf{Q} \cdot \mathbf{v}, T\gamma \cdot \mathbf{v} + \gamma\zeta)$, where $\gamma\zeta \in T_\gamma \mathscr{F}(S, \mathscr{O})$ denotes the left translation of ζ by γ. By applying the cotangent momentum map formula (7) to $\mathfrak{g} = \mathfrak{X}(S) \circledS \mathscr{F}(S, \mathfrak{o})$, we get

$$\langle \mathbf{J}_R(\mathbf{P_Q}, \kappa_\gamma), (\mathbf{v}, \zeta)\rangle = \langle \mathbf{P_Q}, T\mathbf{Q}\cdot\mathbf{v}\rangle + \langle \kappa_\gamma, T\gamma\cdot\mathbf{v} + \gamma\zeta\rangle,$$

so that the momentum map $\mathbf{J}_R : T^*Q_{KK} \to \mathfrak{X}(S)^* \times \mathscr{F}(S, \mathfrak{o})^*$ reads

$$\mathbf{J}_R\left(\mathbf{P_Q}, \kappa_\gamma\right) = \left(\mathbf{P_Q}\cdot T\mathbf{Q} + \kappa_\gamma\cdot T\gamma, \gamma^{-1}\kappa_\gamma\right), \tag{13}$$

where we note that, as opposed to $\mathbf{J}_L$ in (11), $\mathbf{J}_R$ takes values in the regular dual.

Remark 2. Both momentum maps are equivariant, since they are momentum maps for cotangent lifted actions. In particular they are formally Poisson maps for the Lie-Poisson bracket on Lie algebra duals. Note that the definition of Poisson brackets leads to several difficulties in the infinite dimensional case, this is why the above property only holds at a formal level. In the next section we will show that these momentum maps form a dual pair. Even if the Poisson properties only hold at a formal level, the dual pair property can be rigorously verified, as in [11].

3 The Dual Pair Property of the EPAut Momentum Maps

As shown in [11], the EPDiff momentum maps (6) introduced in [22] form a dual pair when restricted to the open subset $T^*\operatorname{Emb}(S, M)^\times$ of $T^*\operatorname{Emb}(S, M)$, consisting of one-forms on M along S which are everywhere non-zero on S, i.e. $\mathbf{P_Q}(x) \neq 0$ for all $x \in S$. Note that $T^*\operatorname{Emb}(S, M)^\times$ is invariant under the actions of both $\operatorname{Diff}(S)$ and $\operatorname{Diff}(M)$.

The pair of EPAut momentum maps (8) was introduced in [14]. We shall now show the dual pair property for these EPAut momentum maps in the case of trivial bundles, that is, with momentum maps given by (11) and (13).

3.1 Cotangent Lifted Actions

Let $T^*Q^\times_{KK}$ denote the open subset of T^*Q_{KK} consisting of pairs $(\mathbf{P_Q}, \kappa_\gamma)$ with the property that for any $x \in S$, the pair $(\mathbf{P_Q}(x), \kappa_\gamma(x)) \in T^*_{\mathbf{Q}(x)}M \times T^*_{\gamma(x)}\mathscr{O}$ is non-zero. Note again that $T^*Q^\times_{KK}$ is invariant under the actions of both $\mathscr{A}ut(S \times \mathscr{O})$ and $\mathscr{A}ut(M \times \mathscr{O})$.

We compute below the explicit form of the cotangent lifted actions of the automorphism groups on $T^*Q^\times_{KK}$, that we will need in order to prove the dual pair property.

3.1.1 Left Cotangent Action

The formula for the cotangent lifted action of $\mathscr{A}ut(M\times\mathscr{O}) = \mathrm{Diff}(M) \circledS \mathscr{F}(M,\mathscr{O})$ on T^*Q_{KK} is

$$(\varphi, a)\cdot(\mathbf{P_Q}, \kappa_\gamma) = \left(T^*\varphi^{-1}\cdot\left(\mathbf{P_Q} - \langle \kappa_\gamma\gamma^{-1}, \delta^l a\circ\mathbf{Q}\rangle\right), (a\circ\mathbf{Q})\kappa_\gamma\right), \tag{14}$$

where $\delta^l a = a^{-1}\mathbf{d}a \in \Omega^1(M,\mathfrak{o})$ denotes the left logarithmic derivative of $a \in \mathscr{F}(M,\mathscr{O})$, and therefore $\delta^l a\circ\mathbf{Q}$ is a section of the vector bundle $\mathbf{Q}^*(T^*M)\otimes\mathfrak{o}\to S$. Indeed, using the expression of the tangent lift of the action (10) given by

$$(\varphi, a)\cdot(\mathbf{V_Q}, v_\gamma) = \left(T\varphi\cdot\mathbf{V_Q}, (a\circ\mathbf{Q})v_\gamma + (Ta\cdot\mathbf{V_Q})\gamma\right),$$

one computes the cotangent lifted action (14) as follows. Using the expression of the inverse in the semidirect product $(\varphi, a)^{-1} = (\varphi^{-1}, a^{-1}\circ\varphi^{-1})$, we have

$$\begin{aligned}
\langle(\varphi,a)\cdot(\mathbf{P_Q},\kappa_\gamma),(V_{\varphi\circ\mathbf{Q}}, v_{(a\circ\mathbf{Q})\gamma})\rangle &= \left\langle(\mathbf{P_Q},\kappa_\gamma),(\varphi^{-1}, a^{-1}\circ\varphi^{-1})\cdot(V_{\varphi\circ\mathbf{Q}}, v_{(a\circ\mathbf{Q})\gamma})\right\rangle\\
&= \left\langle\mathbf{P_Q}, T\varphi^{-1}\cdot V_{\varphi\circ\mathbf{Q}}\right\rangle\\
&\quad + \left\langle\kappa_\gamma, (a^{-1}\circ\mathbf{Q})v_{(a\circ\mathbf{Q})\gamma} + (T(a^{-1}\circ\varphi^{-1})\cdot V_{\varphi\circ\mathbf{Q}})(a\circ\mathbf{Q})\gamma\right\rangle\\
&= \left\langle\mathbf{P_Q}, T\varphi^{-1}\cdot V_{\varphi\circ\mathbf{Q}}\right\rangle + \left\langle\kappa_\gamma\gamma^{-1}, (Ta^{-1}(T\varphi^{-1}\cdot V_{\varphi\circ\mathbf{Q}}))(a\circ\mathbf{Q}),\right\rangle\\
&\quad + \left\langle(a\circ\mathbf{Q})\kappa_\gamma, v_{(a\circ\mathbf{Q})\gamma}\right\rangle\\
&= \left\langle T^*\varphi^{-1}\cdot\left(\mathbf{P_Q} + \langle\kappa_\gamma\gamma^{-1}, \delta^r(a^{-1})\circ\mathbf{Q}\rangle\right), V_{\varphi\circ\mathbf{Q}}\right\rangle + \left\langle(a\circ\mathbf{Q})\kappa_\gamma, v_{(a\circ\mathbf{Q})\gamma}\right\rangle\\
&= \left\langle T^*\varphi^{-1}\cdot\left(\mathbf{P_Q} - \langle\kappa_\gamma\gamma^{-1}, \delta^l a\circ\mathbf{Q}\rangle\right), V_{\varphi\circ\mathbf{Q}}\right\rangle + \left\langle(a\circ\mathbf{Q})\kappa_\gamma, v_{(a\circ\mathbf{Q})\gamma}\right\rangle,
\end{aligned}$$

which shows (14). We used in the last step the relation $\delta^r(a^{-1}) = -\delta^l a$ between left and right logarithmic derivatives, where the right logarithmic derivative is defined by $\delta^r a = (\mathbf{d}a)a^{-1}\in\Omega^1(M,\mathfrak{o})$.

3.1.2 Right Cotangent Action

The formula for the cotangent lifted action of $\mathscr{A}ut(S\times\mathscr{O}) = \mathrm{Diff}(S) \circledS \mathscr{F}(S,\mathscr{O})$ on T^*Q_{KK} reads

$$(\mathbf{P_Q}, \kappa_\gamma)\cdot(\psi, b) = \left((\mathbf{P_Q}\circ\psi)\,\mathrm{Jac}_\psi, (\kappa_\gamma\circ\psi)b\,\mathrm{Jac}_\psi\right), \tag{15}$$

where Jac_ψ denotes the Jacobian of ψ relative to the volume form μ_S, i.e. $\psi^*\mu_S = \mathrm{Jac}_\psi\,\mu_S$. Indeed, from the expression of the tangent lift of the action (12) given by

$$(V_\mathbf{Q}, v_\gamma)\cdot(\psi, b) = (V_\mathbf{Q}\circ\psi, (v_\gamma\circ\psi)b)$$

one computes the cotangent lifted action (15) as follows.

$$\begin{aligned}
&\langle (\mathbf{P}_\mathbf{Q}, \kappa_\gamma) \cdot (\psi, b), (V_{\mathbf{Q}\circ\psi}, v_{(\gamma\circ\psi)b}) \rangle \\
&\qquad = \langle (\mathbf{P}_\mathbf{Q}, \kappa_\gamma), (V_{\mathbf{Q}\circ\psi}, v_{(\gamma\circ\psi)b}) \cdot (\psi^{-1}, b^{-1} \circ \psi^{-1}) \rangle \\
&\qquad = \langle \mathbf{P}_\mathbf{Q}, V_{\mathbf{Q}\circ\psi} \circ \psi^{-1} \rangle + \langle \kappa_\gamma, (v_{(\gamma\circ\psi)b} b^{-1}) \circ \psi^{-1}) \rangle \\
&\qquad = \langle (\mathbf{P}_\mathbf{Q} \circ \psi) \operatorname{Jac}_\psi, V_{\mathbf{Q}\circ\psi} \rangle + \langle (\kappa_\gamma \circ \psi) b \operatorname{Jac}_\psi, v_{(\gamma\circ\psi)b} \rangle,
\end{aligned}$$

which shows (15).

3.2 Transitivity Results

In order to prove the dual pair property, we shall show the stronger result that the actions of $\mathscr{A}ut(M \times \mathscr{O})$ and $\mathscr{A}ut(S \times \mathscr{O})$ on $T^*Q^\times_{KK}$ are mutually completely orthogonal.

We will use the following lemma (Lemma 4.2 in [11]), detached from the proof of Proposition 3 in [17].

Lemma 1. *Let (M, g) be a Riemannian manifold and $N \subset M$ a submanifold. Let E be the normal bundle $TN^\perp$ viewed as a tubular neighborhood of N in M, with the identification done by the Riemannian exponential map. Then any section $\lambda \in \Gamma(T^*M|_N)$ vanishing on TN, when restricted to $TN^\perp$, defines a smooth function $h \in \mathscr{F}(E)$, linear on each fiber, whose differential along N satisfies $(\mathbf{d}h)|_N = \lambda$ (as sections of $T^*M|_N$).*

The first transitivity result is shown in the following proposition.

Proposition 2. *The group $\mathscr{A}ut(M \times \mathscr{O})$ acts infinitesimally transitively on the level sets of the momentum map $\mathbf{J}_R$ given in (13) restricted to $T^*Q^\times_{KK}$.*

Proof. The left action $(\varphi, a)(\mathbf{Q}, \gamma) = (\varphi \circ \mathbf{Q}, (a \circ \mathbf{Q})\gamma)$ of $\mathscr{A}ut(M \times \mathscr{O})$ on Q_{KK} is transitive on connected components. This can be seen as follows. Given $(\mathbf{Q}_1, \gamma_1)$ and $(\mathbf{Q}_2, \gamma_2)$ in the same connected component of Q_{KK}, by the transitivity of the action of $\mathrm{Diff}(M)$ on connected components of $\mathrm{Emb}(S, M)$ [18], we find a diffeomorphism φ such that $\mathbf{Q}_2 = \varphi \circ \mathbf{Q}_1$. By a standard argument using a partition of unity, it is possible to extend $\gamma_2 \circ \gamma_1^{-1} \in \mathscr{F}(S, \mathscr{O})$ in a smooth way to a smooth function $a \in \mathscr{F}(M, \mathscr{O})$ along the embedding $\mathbf{Q}_1$.

Consider two pairs $(\mathbf{P}_\mathbf{Q}, \kappa_\gamma)$ and $(\mathbf{P}'_{\mathbf{Q}'}, \kappa'_{\gamma'})$ in the same level set of $\mathbf{J}_R$, so that

$$\mathbf{P}_\mathbf{Q} \cdot T\mathbf{Q} + \kappa_\gamma \cdot T\gamma = \mathbf{P}'_{\mathbf{Q}'} \cdot T\mathbf{Q}' + \kappa'_{\gamma'} \cdot T\gamma' \quad \text{and} \quad \gamma^{-1}\kappa_\gamma = (\gamma')^{-1}\kappa'_{\gamma'}. \tag{16}$$

The left action of $\mathscr{A}ut(M \times \mathscr{O})$ being transitive on connected components of Q_{KK}, we can focus on the action of the isotropy group of $(\mathbf{Q}, \gamma)$ on the cotangent fiber over $(\mathbf{Q}, \gamma)$. Hence we assume that both pairs have the same foot point $(\mathbf{Q}, \gamma)$, so that the identities above become

$$\mathbf{P}_\mathbf{Q} \cdot T\mathbf{Q} = \mathbf{P}'_\mathbf{Q} \cdot T\mathbf{Q} \quad \text{and} \quad \kappa'_\gamma = \kappa_\gamma.$$

The two objects that characterize the $\mathbf{J}_R$ level set of $(\mathbf{P}_\mathbf{Q}, \kappa_\gamma)$ over $(\mathbf{Q}, \gamma)$ are

$$\alpha := \mathbf{P}_\mathbf{Q} \cdot T\mathbf{Q} \in \Omega^1(S) \quad \text{and} \quad \sigma := \kappa_\gamma \gamma^{-1} \in \mathscr{F}(S, \mathfrak{o}^*).$$

Because the embedding $\mathbf{Q}$ is fixed, we can move the objects to the submanifold $N = \mathbf{Q}(S)$ of M. We will denote by the same letters their push-forward by the diffeomorphism $\mathbf{Q} : S \to N$, namely $\alpha \in \Omega^1(N)$ and $\sigma \in \mathscr{F}(N, \mathfrak{o}^*)$. We also identify $T^*_\mathbf{Q} \mathrm{Emb}(S, M) = \Gamma(\mathbf{Q}^* T^* M)$ with $\Gamma(T^*M|_N)$, via the diffeomorphism $\mathbf{Q}$. We consider the affine subspace

$$\Gamma_\alpha(T^*M|_N) := \{\mathbf{P} \in \Gamma(T^*M|_N) : \mathbf{P}|_{TN} = \alpha\} \subset \Gamma(T^*M|_N),$$

whose directing linear subspace is given by the space of sections of the conormal bundle to the submanifold N of M

$$\Gamma_0(T^*M|_N) = \{\mathbf{P} \in \Gamma(T^*M|_N) : \mathbf{P}|_{TN} = 0\}.$$

We define an open subset of $\Gamma_\alpha(T^*M|_N)$ by

$$\Gamma_\alpha(T^*M|_N)^\sigma := \{\mathbf{P} \in \Gamma(T^*M|_N) \,:\, \mathbf{P}|_{TN} = \alpha \text{ and } \mathbf{P}(x) \neq 0, \forall\, x \in \sigma^{-1}(0)\}.$$

The isotropy group of $(\mathbf{Q}, \gamma)$ is a semidirect product group,

$$\mathscr{A}ut(M \times \mathscr{O})_{(\mathbf{Q},\gamma)} = \mathrm{Diff}_N(M) \circledS \mathscr{F}_N(M, \mathscr{O}), \tag{17}$$

where $\mathrm{Diff}_N(M)$ denotes the subgroup of diffeomorphisms of M that fix the submanifold $N = \mathbf{Q}(S)$ of M pointwise and $\mathscr{F}_N(M, \mathscr{O}) := \{a : M \to \mathscr{O} \,|\, a(x) = e, \forall x \in N\}$. Its isotropy Lie algebra of $(\mathbf{Q}, \gamma)$ is the semidirect product $\mathfrak{X}_N(M) \circledS \mathscr{F}_N(M, \mathfrak{o})$, where $\mathfrak{X}_N(M)$ denotes the Lie algebra of vector fields on M that vanish on N, the Lie algebra of $\mathrm{Diff}_N(M)$, and $\mathscr{F}_N(M, \mathfrak{o}) := \{\nu : M \to \mathfrak{o} \mid \nu(x) = 0, \forall\, x \in N\}$, the Lie algebra of $\mathscr{F}_N(M, \mathscr{O})$.

The isotropy group acts by (14) on the cotangent fiber over $(\mathbf{Q}, \gamma)$, so it preserves the second component

$$(\varphi, a) \cdot (\mathbf{P}_\mathbf{Q}, \kappa_\gamma) = \left(T^*\varphi^{-1} \cdot \left(\mathbf{P}_\mathbf{Q} - \langle \kappa_\gamma \gamma^{-1}, \delta^l a \circ \mathbf{Q} \rangle\right) . \kappa_\gamma\right). \tag{18}$$

Its restriction to the level sets of $\mathbf{J}_R$ can be seen an action on $\Gamma_\alpha(T^*M|_N)^\sigma$:

$$(\varphi, a) \cdot \mathbf{P} = \left(\mathbf{P} - \langle \sigma, (\delta^l a)|_N \rangle\right) \circ (T\varphi^{-1})|_N. \tag{19}$$

We notice that $(\delta^l a)|_{TN} = \delta^l(a|_N) = \delta^l e = 0$ for all $a \in \mathscr{F}_N(M, \mathscr{O})$ and $T\varphi^{-1}|_{TN} = \mathrm{id}_{TN}$ for all $\varphi \in \mathrm{Diff}_N(M)$, so we have indeed an action on $\Gamma_\alpha(T^*M|_N)^\sigma$.

The infinitesimal action of the isotropy Lie algebra $\mathfrak{X}_N(M) \circledS \mathscr{F}_N(M, \mathfrak{o})$ on $\Gamma_\alpha(T^*M|_N)^\sigma$ is obtained by differentiating the action (19):

$$(\mathbf{u}, \nu)_{\Gamma_\alpha(T^*M|_N)^\sigma}(\mathbf{P}) = -\mathbf{P} \circ (\nabla \mathbf{u})|_N - \langle \sigma, (\mathbf{d}\nu)|_N \rangle, \tag{20}$$

where we used the fact that the differential at the identity of the logarithmic derivative map $\delta^l : \mathscr{F}(M, \mathscr{O}) \to \Omega^1(M, \mathfrak{o})$ is $\mathbf{d} : \mathscr{F}(M, \mathfrak{o}) \to \Omega^1(M, \mathfrak{o})$.

The transitivity result we have to prove can now be rephrased as infinitesimal transitivity of the action (20). This means to show that, given $\mathbf{P} \in \Gamma_\alpha(T^*M|_N)^\sigma$, for every $P' \in \Gamma_0(T^*M|_N)$ there exists $(\mathbf{u}, \nu) \in \mathfrak{X}_N(M) \circledS \mathscr{F}_N(M, \mathfrak{o})$ such that

$$P' = -\mathbf{P} \circ (\nabla \mathbf{u})|_N - \langle \sigma, (\mathbf{d}\nu)|_N \rangle. \tag{21}$$

For this we proceed as in [11]. We fix a Riemannian metric on M and denote by ∇, $\sharp$, and $\| \ \|$ the Levi-Civita covariant derivative, the sharp operator, and the norm associated to the Riemannian metric, respectively. We also fix an inner product on the (finite dimensional) Lie algebra $\mathfrak{o}$ with induced norm $\| \ \|$ (both on $\mathfrak{o}$ and on $\mathfrak{o}^*$) and induced isomorphism $\sharp : \mathfrak{o}^* \to \mathfrak{o}$.

Since $\mathbf{P}$ and σ cannot vanish simultaneously, the function $\|\mathbf{P}\|^2 + \|\sigma\|^2$ is non-zero everywhere on N, so we can consider the section

$$\lambda := \frac{P'}{\|\mathbf{P}\|^2 + \|\sigma\|^2} \in \Gamma_0(T^*M|_N).$$

Lemma 1 can be applied to the restriction of λ to the normal bundle over the submanifold $N \subset M$ (viewed as a tubular neighborhood of N) because the restriction of λ to TN vanishes. We thus obtain from λ a function f on the normal bundle, linear on each fiber, with the property that the differential of f along N is λ, i.e. $(\mathbf{d}f)|_N = \lambda$ as sections of $T^*M|_N$. Using the tubular neighborhood of N we build a smooth function on M, identical to f on a neighborhood of N, also denoted by f. In particular f vanishes on N since λ clearly vanishes on the zero section of $T^*M|_N$.

From this function f we define the pair $(\mathbf{u}, \nu) \in \mathfrak{X}_N(M) \times \mathscr{F}_N(M, \mathfrak{o})$ by $\mathbf{u} := -f\widetilde{\mathbf{P}^\sharp}$ and $\nu := -f\widetilde{\sigma^\sharp}$, where $\widetilde{\mathbf{P}^\sharp} \in \mathfrak{X}(M)$ is an arbitrary smooth extension of $\mathbf{P}^\sharp : N \to TM$ and $\widetilde{\sigma^\sharp} \in \mathscr{F}(M, \mathfrak{o})$ is an arbitrary smooth extension of $\sigma^\sharp : N \to \mathfrak{o}$, both obtained by a standard argument using a partition of unity.

The computation $-(\nabla \mathbf{u})|_N = (f\nabla\widetilde{\mathbf{P}^\sharp})|_N + ((\mathbf{d}f)\widetilde{\mathbf{P}^\sharp})|_N = (\mathbf{d}f)|_N\mathbf{P}^\sharp = \lambda\mathbf{P}^\sharp$ implies that

$$-\mathbf{P} \circ (\nabla \mathbf{u})|_N = \mathbf{P} \circ (\lambda \mathbf{P}^\sharp) = \frac{\|\mathbf{P}\|^2}{\|\mathbf{P}\|^2 + \|\sigma\|^2} P'.$$

On the other hand $-(\mathbf{d}\nu)|_N = (f\mathbf{d}\widetilde{\sigma^\sharp})|_N + ((\mathbf{d}f)\widetilde{\sigma^\sharp})|_N = (\mathbf{d}f)|_N\sigma^\sharp = \lambda\sigma^\sharp$ implies that

$$-\langle\sigma, (\mathbf{d}\nu)|_N\rangle = \langle\sigma, \lambda\sigma^\sharp\rangle = \frac{\|\sigma\|^2}{\|\mathbf{P}\|^2 + \|\sigma\|^2}P'.$$

By adding them we get (21), which ensures the infinitesimal transitivity of the action (20) of $\mathfrak{X}_N(M) \circledS \mathscr{F}_N(M, \mathfrak{o})$ on $\Gamma_\alpha(T^*M|_N)^\sigma$.

The next Proposition is the analogue of Proposition 2 but for the right action and the left momentum map.

Proposition 3. *The group $\mathscr{A}ut(S \times \mathscr{O})$ acts transitively on level sets of the momentum map $\mathbf{J}_L$ given in (11) restricted to $T^*Q^\times_{KK}$.*

Proof. Suppose that $(\mathbf{P}_\mathbf{Q}, \kappa_\gamma)$ and $(\mathbf{P}'_{\mathbf{Q}'}, \kappa'_{\gamma'})$ lie in the same level set of $\mathbf{J}_L$, i.e. $\mathbf{J}_L(\mathbf{P}_\mathbf{Q}, \kappa_\gamma) = \mathbf{J}_L(\mathbf{P}'_{\mathbf{Q}'}, \kappa'_{\gamma'})$. We thus have

$$\int_S \mathbf{P}_\mathbf{Q} \cdot (X \circ \mathbf{Q})\mu_S = \int_S \mathbf{P}'_{\mathbf{Q}'} \cdot (X \circ \mathbf{Q}')\mu_S$$

and

$$\int_S \kappa_\gamma\gamma^{-1}(f \circ \mathbf{Q})\mu_S = \int_S \kappa'_{\gamma'}(\gamma')^{-1}(f \circ \mathbf{Q}')\mu_S,$$

] for all $X \in \mathfrak{X}(M)$ and all $f \in \mathscr{F}(M, \mathfrak{o})$.

These identities ensure that the embeddings $\mathbf{Q}$ and $\mathbf{Q}'$ have the same image: $\mathbf{Q}(S) = \mathbf{Q}'(S)$. In order to prove this, we fix $x_0 \in S$. If $\mathbf{P}_\mathbf{Q}(x_0) \neq 0$, then from the first equality we obtain that $\mathbf{Q}(x_0) \in \mathbf{Q}'(S)$. Indeed, if this is not the case, then we can find X with compact support $K = \operatorname{supp} X$ such that $K \ni \mathbf{Q}(x_0)$ and $K \cap \mathbf{Q}'(S) = \varnothing$. Such an X can also be chosen such that $\int_S \mathbf{P}_\mathbf{Q} \cdot (X \circ \mathbf{Q})\mu_S \neq 0$, whereas we always have $\int_S \mathbf{P}'_{\mathbf{Q}'} \cdot (X \circ \mathbf{Q}')\mu_S = 0$. This is in contradiction with the hypothesis. If $\mathbf{P}_\mathbf{Q}(x_0) = 0$, then, by the definition of $T^*Q^\times_{KK}$, $\kappa_\gamma(x_0) \neq 0$. Then also $\kappa_\gamma(x_0)\gamma(x_0)^{-1} \neq 0$ and we use the second identity with the same argument as above, to get $\mathbf{Q}(x_0) \in \mathbf{Q}'(S)$. Doing this for all $x_0 \in S$ proves that $\mathbf{Q}(S) \subset \mathbf{Q}'(S)$ and, similarly, that $\mathbf{Q}'(S) \subset \mathbf{Q}(S)$.

Since $\mathbf{Q}(S) = \mathbf{Q}'(S)$, there exists $\psi \in \mathrm{Diff}(S)$ such that $\mathbf{Q}' = \mathbf{Q} \circ \psi$. Plugging this into the first identity above and using a change of variables, we get

$$\int_S \mathbf{P}_\mathbf{Q} \cdot (X \circ \mathbf{Q})\mu_S = \int_S (\mathbf{P}'_{\mathbf{Q}'} \circ \psi^{-1}) \cdot (X \circ \mathbf{Q}) \operatorname{Jac}_{\psi^{-1}} \mu_S,$$

for all $X \in \mathfrak{X}(M)$. We know that $\operatorname{Jac}_{\psi^{-1}} = \operatorname{Jac}_\psi^{-1} \circ \psi^{-1}$, so $\mathbf{P}'_{\mathbf{Q}'} = (\mathbf{P}_\mathbf{Q} \circ \psi) \operatorname{Jac}_\psi$, the first component of (15).

Let $b = (\gamma^{-1} \circ \psi)\gamma' \in \mathscr{F}(S, \mathscr{O})$, so $\gamma' = (\gamma \circ \psi)b$, which we plug into the second identity above to get

$$\int_S \kappa_\gamma \gamma^{-1}(f \circ \mathbf{Q})\mu_S = \int_S \kappa'_{\gamma'} b^{-1}(\gamma^{-1} \circ \psi)(f \circ \mathbf{Q} \circ \psi)\mu_S$$
$$= \int_S \left((\kappa'_{\gamma'} b^{-1}) \circ \psi^{-1}\right) \gamma^{-1}(f \circ \mathbf{Q}) \operatorname{Jac}_{\psi^{-1}} \mu_S.$$

Since $f \circ \mathbf{Q}$ is arbitrary in $\mathscr{F}(S, \mathfrak{o})$, we get $\kappa_\gamma = \left((\kappa'_{\gamma'} b^{-1}) \circ \psi^{-1}\right) \operatorname{Jac}_{\psi^{-1}}$. This means that $\kappa'_{\gamma'} = (\kappa_\gamma \circ \psi) b \operatorname{Jac}_\psi$, the second component of (15).

From the preceding propositions we obtain that the commuting actions of $\mathscr{A}ut(M \times \mathscr{O})$ and $\mathscr{A}ut(S \times \mathscr{O})$ are mutually completely orthogonal. We thus get the following result.

Theorem 1. *The momentum maps* (11) *and* (13) *associated to the EPAut equations, form a dual pair:*

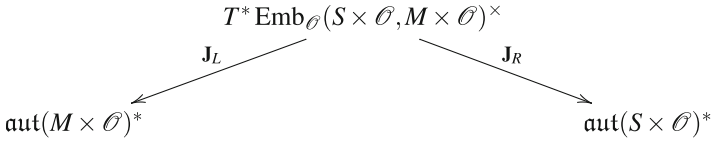

Recall that the momentum map $\mathbf{J}_L$ provides the formula for possible singular solutions of the EPAut equations on M [14]. Being equivariant, $\mathbf{J}_L$ is a formally Poisson map relative to the canonical symplectic form on $T^*\operatorname{Emb}_{\mathscr{O}}(S \times \mathscr{O}, M \times \mathscr{O})^\times$ and the Lie-Poisson structure on $\mathfrak{aut}(M \times \mathscr{O})^*$. This ensures that the parameterization of the singular solutions in terms of $\mathbf{P}_\mathbf{Q}$ and κ_γ are Clebsch variables in the sense of [33]. The dual pair property tells us that $\mathscr{A}ut(S \times \mathscr{O})$ is the gauge group of that Clebsch representation. Since $\mathbf{J}_R$ is $\mathscr{A}ut(S \times \mathscr{O})$-invariant, it follows that $\mathbf{J}_R$ is a Noether conserved quantity for the canonical dynamics of these singular solutions.

Whereas the map $\mathbf{J}_L$ is a geometric object that is always well-defined, it is not always true that the corresponding EPAut equations admit these singular solutions. This happens only for a certain class of Hamiltonians h for which the expression $h \circ \mathbf{J}_L$ is well-defined. Such a class includes the modified Camassa-Holm equation [24] together with its higher dimensional and anisotropic versions studied in [23]. It is interesting to mention that while it is well known that the strong solutions of these EPAut equations are described by geodesics of a right-invariant metric on $\mathscr{A}ut(M \times \mathscr{O})$, the singular solutions also admit a geodesic interpretation. Indeed, this follows from a general result in [10] (see Theorem 2.5), that the singular solutions given by $\mathbf{J}_L$ are described by geodesics $t \mapsto (\mathbf{Q}(t), \gamma(t))$ on a $\mathscr{A}ut(M \times \mathscr{O})$-orbit in $\operatorname{Emb}_{\mathscr{O}}(S \times \mathscr{O}, M \times \mathscr{O})^\times$, relative to the normal metric associated to the right-invariant metric on $\mathscr{A}ut(M \times \mathscr{O})$.

Being equivariant, the momentum map $\mathbf{J}_R$ also yields Clebsch variables for the EPAut equation on S. The dual pair property again ensures that $\mathscr{A}ut(M \times \mathscr{O})$ is the gauge group the Clebsch representation.

4 The Incompressible EPAut Equation and Momentum Maps

In this section we recall the expression of the Euler-Poincaré equations on the group of volume preserving automorphisms of a trivial principal bundle (the $\mathrm{EPAut}_{\mathrm{vol}}$ equations) and review from [14] some facts about the associated pair of momentum maps. We will then focus on a particular case relevant for the Yang-Mills Vlasov equations, arising when the total space of one of the principal bundles is a cotangent bundle (the so called Yang-Mills phase space).

4.1 The Group of Volume Preserving Automorphisms

Let $\pi : P \to M$ be a principal $\mathscr{O}$-bundle and suppose that M is orientable, endowed with a Riemannian metric g. Let μ_M be the volume form induced by g.

The group $\mathscr{A}ut_{\mathrm{vol}}(P)$ consists, by definition, of the automorphisms of the principal bundle P which descend to volume preserving diffeomorphisms of the base manifold M with respect to the volume form μ_M. Its Lie algebra, denoted by $\mathfrak{aut}_{\mathrm{vol}}(P)$ consists of equivariant vector fields such that their projection to M is divergence free.

Remark 3 (Kaluza-Klein Metric and Induced Volume). Given a principal connection $\mathscr{A} \in \Omega^1(P, \mathfrak{o})$ on P and an inner product τ on $\mathfrak{o}$, one defines the Kaluza-Klein Riemannian metric on P as

$$\kappa(U_p, V_p) = g(T\pi(U_p), T\pi(V_p)) + \tau(\mathscr{A}(U_p), \mathscr{A}(V_p)), \quad U_p, V_p \in T_pP.$$

The induced volume form μ_P on P is given by

$$\mu_P = \pi^* \mu_M \wedge \mathscr{A}^* \det_\tau,$$

where $\mathscr{A}^* \det_\tau$ denotes the pullback by the connection $\mathscr{A} : TP \to \mathfrak{o}$ of the canonical determinant form induced by τ on $\mathfrak{o}$. Supposing that τ is Ad-invariant, the Kaluza-Klein metric κ and the volume form μ_P induced by κ are $\mathscr{O}$-invariant. Given $\varphi \in \mathscr{A}ut(P)$, we have the equivalence

$$\varphi \in \mathscr{A}ut_{\mathrm{vol}}(P) \Leftrightarrow \varphi^* \mu_P = \mu_P,$$

see Lemma 4.1 in [14]. As a consequence, the Lie algebra $\mathfrak{aut}_{\mathrm{vol}}(P)$ coincides with the Lie algebra of equivariant divergence free vector fields with respect to μ_P.

When the principal bundle is trivial, i.e. $\pi : P \simeq M \times \mathscr{O} \to M$, the group $\mathscr{A}ut_{\mathrm{vol}}(P)$ is isomorphic to the semidirect product group

$$\mathscr{A}ut_{\mathrm{vol}}(P) \simeq \mathrm{Diff}_{\mathrm{vol}}(M) \circledS \mathscr{F}(M, \mathscr{O}),$$

where $\mathrm{Diff}_{\mathrm{vol}}(M)$ acts on $\mathscr{F}(M, \mathscr{O})$ by composition on the right. Its Lie algebra is the semidirect product Lie algebra $\mathfrak{aut}_{\mathrm{vol}}(P) \simeq \mathfrak{X}_{\mathrm{vol}}(M) \circledS \mathscr{F}(M, \mathfrak{o})$. Using the L^2 pairing associated to the volume form μ_M, we identify the dual as

$$\mathfrak{aut}_{\mathrm{vol}}(P)^* \simeq \mathfrak{X}_{\mathrm{vol}}(M)^* \times \mathscr{F}(M, \mathfrak{o})^* = \Omega^1(M)/\mathbf{d}\mathscr{F}(M) \times \mathscr{F}(M, \mathfrak{o}^*).$$

The Euler-Poincaré equations on the automorphism group $\mathscr{A}ut_{\mathrm{vol}}(P)$ (the EPAut$_{\mathrm{vol}}$ equations) take the following form when P is a trivial principal bundle.

Proposition 4 (The EPAut$_{\mathrm{vol}}$ Equations on a Trivial Principal Bundle [14]). *Consider a reduced Lagrangian $\ell : \mathfrak{X}_{\mathrm{vol}}(M) \circledS \mathscr{F}(M, \mathfrak{o}) \to \mathbb{R}$. Then the associated EPAut$_{\mathrm{vol}}$ equations are*

$$\begin{cases} \dfrac{\partial}{\partial t}\dfrac{\delta \ell}{\delta \mathbf{u}} + \pounds_{\mathbf{u}} \dfrac{\delta \ell}{\delta \mathbf{u}} + \dfrac{\delta \ell}{\delta v} \cdot \mathbf{d} v = -\mathbf{d} p \\ \dfrac{\partial}{\partial t}\dfrac{\delta \ell}{\delta v} + \mathrm{ad}^*_v \dfrac{\delta \ell}{\delta v} + \mathbf{d}\left(\dfrac{\delta \ell}{\delta v}\right) \cdot \mathbf{u} = 0, \end{cases} \tag{22}$$

where $(\mathbf{u}, v) \in \mathfrak{X}_{\mathrm{vol}}(M) \circledS \mathscr{F}(M, \mathfrak{o})$ and the operator $\pounds_{\mathbf{u}}$ denotes the Lie derivative acting on one-forms. The first equation is written in $\Omega^1(M)$ and $p \in \mathscr{F}(M)$ denotes the pressure, determined from the incompressibility condition $\mathrm{div}\, \mathbf{u} = 0$.

We refer to [14] for the description of the EPAut$_{\mathrm{vol}}$ equations on an arbitrary principal bundle.

4.2 Review of the Ideal Fluid Case

The pair of momentum maps associated to the Euler equations discovered in [33] justifies geometrically the existence of Clebsch canonical variables for ideal fluid motion and explains the Hamiltonian structure of point vortex solutions in terms of the Hamiltonian structure of the Euler equations. As claimed in [33], and rigorously shown in [11], this pair of momentum maps forms a dual pair.

Given a compact volume manifold (S, μ) and a symplectic manifold (M, ω), the pair of momentum maps arise from the commuting symplectic actions of the groups $\mathrm{Diff}_{\mathrm{symp}}(M)$ and $\mathrm{Diff}_{\mathrm{vol}}(S)$ on the Fréchet manifold $\mathrm{Emb}(S, M)$ endowed with the symplectic form

$$\bar{\omega}(f)(u_f, v_f) := \int_S \omega(f(x))(u_f(x), v_f(x))\mu_S.$$

In order to get Hamiltonian actions it is needed to replace these groups by the subgroups $\mathrm{Diff}_{\mathrm{ham}}(M)$ and $\mathrm{Diff}_{\mathrm{ex}}(S)$ of Hamiltonian and exact volume preserving diffeomorphisms, respectively. Furthermore, in order to have equivariance, required from the dual pair properties, it is needed to consider central extensions of these groups, given by the group of quantomorphisms (central extension of $\mathrm{Diff}_{ham}(M)$) and the Ismagilov central extension of $\mathrm{Diff}_{\mathrm{ex}}(S)$, respectively [11].

In the particular case when the symplectic form is exact, $\omega = -\mathbf{d}\theta$, one can stay with the whole group $\mathrm{Diff}_{\mathrm{vol}}(S)$ (instead of $\mathrm{Diff}_{\mathrm{ex}}(S)$) and the central extension is not needed. Another simplification arises in this case, since the quantomorphism group can be written as a topologically trivial extension of $\mathrm{Diff}_{\mathrm{ham}}(M)$, with the help of a group 2-cocycle B [25],

$$B(\varphi_1, \varphi_2) := \int_{m_0}^{\varphi_2(m_0)} \left(\theta - \varphi_1^*\theta\right), \quad \varphi_1, \varphi_2 \in \mathrm{Diff}_{\mathrm{ham}}(M),$$

extension denoted by $\mathrm{Diff}_{\mathrm{ham}}(M) \times_B \mathbb{R}$.

4.2.1 The Right Action Momentum Map

The natural action of the group $\mathrm{Diff}_{\mathrm{vol}}(S)$ on $\mathrm{Emb}(S, M)$ is Hamiltonian with equivariant momentum map $\mathbf{J}_R(f) = [f^*\theta]$, where $\omega = -\mathbf{d}\theta$. Here the dual of $\mathfrak{X}_{\mathrm{vol}}(S)$ is identified with the quotient space $\Omega^1(S)/\mathbf{d}\Omega^0(S)$. If in addition $H^1(S) = 0$, then this dual can be identified with the space $\mathbf{d}\Omega^1(S)$ of vorticities, and the right momentum map becomes $\mathbf{J}_R(f) = -f^*\omega$, [33].

Lemma 2. $\mathrm{Diff}_{\mathrm{ham}}(M)$ *acts transitively on connected components of level sets of the right leg momentum map* $\mathbf{J}_R : \mathrm{Emb}(S, M) \to \Omega^1(S)/\mathbf{d}\Omega^0(S)$, $\mathbf{J}_R(f) = [f^*\theta]$.

Proof. The transitivity of the action of $\mathrm{Diff}_{\mathrm{ham}}(M)$ on connected components of level sets of $\mathbf{J}_R$ follows from the transitivity of the action of $\mathfrak{X}_{\mathrm{ham}}(M)$ on level sets of $\mathbf{J}_R$, since the constructions can be performed smoothly depending on a parameter. We start again with an arbitrary vector field v_f on M along f such that $T_f\mathbf{J}_R \cdot v_f = [f^*\pounds_{v_f}\theta] = 0$. There exists a function $\bar{h} \in C^\infty(S)$ whose differential is $\mathbf{d}\bar{h} = -f^*\mathbf{i}_{v_f}\mathbf{d}\theta$. We extend it to a function $h_1 \in C^\infty(M)$ such that $\bar{h} = h_1 \circ f$. Now the 1-form β on M along S defined by

$$\beta = \mathbf{d}h_1 \circ f + \mathbf{i}_{v_f}(\mathbf{d}\theta \circ f) \in \Gamma(f^*T^*M)$$

vanishes on vectors tangent to $f(S) \subset M$. By Lemma 4.2 from [11] we find $h_2 \in C^\infty(M)$ such that $\beta = \mathbf{d}h_2 \circ f$. It follows that $\mathbf{d}(h_1 - h_2) \circ f = -\mathbf{i}_{v_f}d\theta = \mathbf{i}_{v_f}\omega$, so $v_f = X_{h_1-h_2} \circ f \in \mathfrak{X}_{\mathrm{ham}}(M)_{\mathrm{Emb}}(f)$.

4.2.2 The Left Action Momentum Map

The Lie algebra of the quantomorphism group is the central extension $C^\infty(M)$ of the Lie algebra of Hamiltonian vector fields

$$h \in C^\infty(M) \longmapsto X_h \in \mathfrak{X}_{\text{ham}}(M), \quad \mathbf{i}_{X_h}\omega = \mathbf{d}h.$$

Its dual can be identified with the space of compactly supported densities $\text{Den}_c(M)$, so the infinitesimally equivariant left leg momentum map is $\mathbf{J}_L(f) = f_*\mu$, [33].

Lemma 3 ([11]). $\text{Diff}_{\text{vol}}(S)$ *acts transitively on level sets of the left leg momentum map* $\mathbf{J}_L : \text{Emb}(S, M) \to \text{Den}_c(M)$.

Proof. Let $f_1, f_2 \in \text{Emb}(S, M)$ such that $\mathbf{J}_L(f_1) = \mathbf{J}_L(f_2)$. Then we have

$$\int_S (h \circ f_1)\mu = \int_S (h \circ f_2)\mu, \quad h \in C^\infty(M). \tag{23}$$

A first consequence is that the two embeddings have the same image in M, so there exists $\psi \in \text{Diff}(S)$ such that $f_2 = f_2 \circ \psi$. We rewrite the identity (23) as $\int_S (h \circ f_2)\psi^*\mu = \int_S (h \circ f_2)\mu$ for all $h \circ f_2 \in C^\infty(S)$, and we deduce $\psi^*\mu = \mu$. We found $\psi \in \text{Diff}_{\text{vol}}(S)$ such that $f_2 = f_1 \circ \psi$.

The group of volume preserving diffeomorphisms $\text{Diff}_{\text{vol}}(S)$ and the quantomorphism group $\text{Diff}_{\text{ham}}(M) \times_B \mathbb{R}$ have mutually completely orthogonal actions on the manifold of embeddings $\text{Emb}(S, M)$, so

$$\begin{array}{ccc} & \text{Emb}(S,M) & \\ {\scriptstyle \mathbf{J}_L}\swarrow & & \searrow{\scriptstyle \mathbf{J}_R} \\ \text{Den}_c(M) = C^\infty(M)^* & & \mathfrak{X}_{\text{vol}}(S)^* = \Omega^1(S)/\mathbf{d}\Omega^0(M) \end{array}$$

is a dual pair.

4.3 A Pair of Momentum Maps for the $\text{EPAut}_{\text{vol}}$ Equations

The above setting for the ideal fluid equations has been developed in [14] for the $\text{EPAut}_{\text{vol}}$ equations as follows.

Let $\pi_S : P_S \to S$ be a principal $\mathscr{O}$-bundle and consider another principal $\mathscr{O}$-bundle $\pi_M : P_M \to M$ such that P_M carries an exact symplectic form $\omega = -\mathbf{d}\theta$, where $\theta \in \Omega^1(P_M)$ is $\mathscr{O}$-invariant. Assume that both S and $\mathscr{O}$ are compact, hence P_S is compact too. As above, we endow P_S with the $\mathscr{O}$-invariant volume form $\mu_{P_S} = \pi^*\mu_S \wedge \mathscr{A}^* \det_\tau$, where τ is an Ad-invariant inner product on $\mathfrak{o}$ and $\mathscr{A}$ a principal connection on P_S.

The space of $\mathscr{O}$-equivariant embeddings from P_S into P_M, denoted by $Q_{KK} = \mathrm{Emb}_{\mathscr{O}}(P_S, P)$, is a Fréchet manifold because P_S is compact (see Remark 1). We endow the manifold Q_{KK} with the symplectic form $\bar{\omega}$ given by

$$\bar{\omega}(f)(u_f, v_f) := \int_{P_S} \omega(f(p))(u_f(p), v_f(p))\mu_{P_S}.$$

The function under the integral is $\mathscr{O}$-invariant, so the right hand side can be written as an integral over S. The local triviality of the bundle $P_S \to S$ ensures the non-degeneracy of $\bar{\omega}$.

We describe below the momentum maps associated to the $\mathrm{EPAut}_{\mathrm{vol}}$ equations. In this context, the manifold $\mathrm{Emb}(S, M)$ and the groups $\mathrm{Diff}_{\mathrm{vol}}(S, \mu)$ and $\mathrm{Diff}_{\mathrm{ham}}(M) \times_B \mathbb{R}$ of the ideal fluid case will be replaced by the manifold $\mathrm{Emb}_{\mathscr{O}}(P_S, P_M)$, the group $\mathscr{A}ut_{\mathrm{vol}}(P_S)$ of volume preserving automorphisms, and the group $\mathscr{V}\mathscr{C}hrom(P_M)$ of Vlasov chromomorphisms, respectively.

4.3.1 Left Action Momentum Map

Let us denote by $\mathscr{A}ut_{\mathrm{ham}}(P_M) := \mathscr{A}ut(P_M) \cap \mathrm{Diff}_{\mathrm{ham}}(P_M)$ the group of Hamiltonian automorphisms of P_M whose Lie algebra $\mathfrak{aut}_{\mathrm{ham}}(P_M)$ consists of $\mathscr{O}$-equivariant Hamiltonian vector fields on P_M. This group acts symplectically by composition on the left on $\mathrm{Emb}_{\mathscr{O}}(P_S, P_M)$ and admits a momentum which is not equivariant and hence not Poisson. As in [11], in order to obtain an equivariant momentum map, we have to consider the central extension of $\mathscr{A}ut_{\mathrm{ham}}(P_M)$ by the cocycle

$$B(\varphi_1, \varphi_2) := \int_{p_0}^{\varphi_2(p_0)} \left(\theta - \varphi_1^*\theta\right), \quad \varphi_1, \varphi_2 \in \mathscr{A}ut_{\mathrm{ham}}(P_M), \tag{24}$$

where the integral is taken along a smooth curve connecting the point p_0 with the point $\varphi_2(p_0)$. The cohomology class of B is independent of the choice of the point p_0 and the one-form θ such that $-\mathbf{d}\theta = \omega$, see Theorem 3.1 in [25]. As shown in [14], in order to obtain an equivariant momentum map, one needs to consider the subgroup $\overline{\mathscr{A}ut}_{\mathrm{ham}}(P_M)$ of $\mathscr{A}ut_{\mathrm{ham}}(P_M)$, whose Lie algebra consists of Hamiltonian vector fields associated to $\mathscr{O}$-invariant Hamiltonian functions on (P_M, ω).

This group is referred to as the group of *special Hamiltonian automorphisms*. Its central extension $\mathscr{V}\mathscr{C}hrom(P_M) := \overline{\mathscr{A}ut}_{\mathrm{ham}}(P_M) \times_B \mathbb{R}$ is called the *Vlasov chromomorphism group* since it is the configuration Lie group for Yang-Mills Vlasov plasmas in chromohydrodynamics. The Lie algebra of $\mathscr{V}\mathscr{C}hrom(P_M)$ is isomorphic to the space of functions on M whose Lie bracket is given by the reduced Poisson bracket on $M = P_M/\mathscr{O}$ obtained by reduction of the symplectic Poisson bracket on (P_M, ω). We refer to [14] for more details regarding the definition of these groups.

The group $\mathscr{V}\mathscr{C}hrom(P_M)$ acts symplectically on the left on the symplectic manifold $(\mathrm{Emb}_{\mathscr{O}}(P_S, P), \bar{\omega})$ and admits the momentum map

$$\mathbf{J}_L : \mathrm{Emb}_{\mathscr{O}}(P_S, P_M) \to \mathscr{F}(M)^* = \mathscr{F}_{\mathscr{O}}(P_M)^*, \quad \langle \mathbf{J}_L(f), h\rangle = \int_{P_S} \tilde{h}(f(p))\mu_{P_S}, \tag{25}$$

where $h \in \mathscr{F}(M)$ and $\tilde{h} = h \circ \pi_M \in \mathscr{F}_{\mathscr{O}}(P_M)$. Since the function $p \mapsto \tilde{h}(f(p))$ on P_S is $\mathscr{O}$-invariant, it defines a function on S, and we have in fact an integral over S. By abuse of notation, we can write

$$\mathbf{J}_L(f) = \int_S \delta(n - f(p))\mu_S \in \mathscr{F}(M)^*.$$

Remark 4 (Special Hamiltonian Automorphisms). It is interesting to recall here that the group $\mathrm{Diff}_{\mathrm{ham}}(M, \omega)$ is of central importance in Hamiltonian mechanics, since it contains the flows of Hamiltonian systems on the symplectic manifold (M, ω). In the same way, the group $\overline{\mathscr{A}ut}_{\mathrm{ham}}(P_M, \omega)$ of special Hamiltonian automorphisms, where $P_M \to M$ is a $\mathscr{O}$-principal bundle and the symplectic form ω is $\mathscr{O}$-invariant, is the corresponding group in the case of Hamiltonian systems with symmetries. It contains the flows of Hamiltonian systems with $\mathscr{O}$-symmetries.

An important example in this context are Wong's equations for a nonabelian charged particle in a fixed Yang-Mills field. They arise as a Hamiltonian system on $(P_M, \omega) = (T^*P, \Omega_{\mathrm{can}})$, where $P \to Q$ is a $\mathscr{O}$-principal bundle over the physical space Q of the particle, see [35].

4.3.2 Right Action Momentum Map

The group $\mathscr{A}ut_{\mathrm{vol}}(P_S)$ acts symplectically on the right on the symplectic manifold $(\mathrm{Emb}_{\mathscr{O}}(P_S, P), \bar{\omega})$ and admits the momentum map

$$\mathbf{J}_R : \mathrm{Emb}_{\mathscr{O}}(P_S, P_M) \to \mathfrak{aut}_{\mathrm{vol}}(P_S)^* = \Omega^1_{\mathscr{O}}(P_S)/\mathbf{d}\mathscr{F}_{\mathscr{O}}(P_S), \quad \mathbf{J}_R(f) = [f^*\theta]. \tag{26}$$

The identification $\mathfrak{aut}_{\mathrm{vol}}(P_S)^* = \Omega^1_{\mathscr{O}}(P_S)/\mathbf{d}\mathscr{F}_{\mathscr{O}}(P_S)$ is made by using the duality pairing induced by the duality pairing

$$\langle \alpha, X\rangle := \int_{P_S} \alpha(X)\mu_{P_S} \tag{27}$$

between $\mathfrak{aut}(P_S)$ and $\mathfrak{aut}(P_S)^* = \Omega^1(P_S)$. Note that in (27) the function $\alpha(X)$ is $\mathscr{O}$-invariant since both X and α are equivariant, so it induces a function on S so that the duality pairing can be rewritten as an integral over S with respect to μ_S.

4.3.3 The Pair of Momentum Maps

In summary, we have the following pair of momentum maps associated to the $\mathrm{EPAut}_{\mathrm{vol}}$ equation

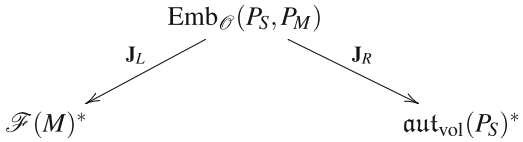

Being equivariant, the momentum maps $\mathbf{J}_L$ and $\mathbf{J}_R$ are Poisson maps and hence yield Clebsch variables for the Lie-Poisson systems on $\mathscr{F}(M)^*$ and the $\mathrm{EPAut}_{\mathrm{vol}}$ equations on P_S, respectively. Note that the Lie-Poisson system on $\mathscr{F}(M)^*$ is a Vlasov system whose Poisson bracket is not symplectic but is the reduced Poisson bracket on $M = P_M/\mathscr{O}$. The momentum map $\mathbf{J}_L$ provides the expression of singular solutions for this Lie-Poisson system.

When $P_M = T^*\bar{P}$, where $\bar{P}$ is itself a $\mathscr{O}$-principal bundle, this system is related to Yang-Mills Vlasov equation and in this case $\mathbf{J}_L$ can be identified with the single particle solution, which is of central importance for the theory of Yang-Mills charged fluids, [15]. This particular setting will be considered in the following section.

Note also that, since both momentum maps are invariant under the action of the group associated to their partner momentum map, they also provide Noether conserved quantities for these Clebsch variables. The dual pair property that will be shown below will allow us to identify the gauge groups of these Clebsch representations.

4.4 *Yang-Mills Phase Space*

We now consider the special case when the total space of the principal bundle $\pi_M : P_M \to M$ is the cotangent bundle of another principal bundle $\bar{\pi} : \bar{P} \to \bar{M}$. We endow $P_M = T^*\bar{P}$ with the canonical symplectic form $\Omega_{\bar{P}} = -\mathbf{d}\Theta_{\bar{P}}$ and we let $\mathscr{O}$ act on $T^*\bar{P}$ by cotangent lift. Thus we have $P_M = T^*\bar{P} \to M = T^*\bar{P}/\mathscr{O}$. This particular choice is motivated by the example of the Yang-Mills Vlasov equation, as mentioned in [14], in which case $\bar{\pi} : \bar{P} \to \bar{M}$ is the principal bundle of the Yang-Mills theory involved. If moreover $\bar{\pi} : \bar{P} \simeq \bar{M} \times \mathscr{O} \to M$ is a trivial $\mathscr{O}$-bundle, then we have $P_M = T^*\bar{M} \times T^*\mathscr{O}$ and $M = T^*\bar{M} \times \mathfrak{o}^*$, so that the left momentum map (25) takes value in the space $\mathscr{F}(T^*\bar{M} \times \mathfrak{o}^*)^*$ of Yang-Mills Vlasov distributions. Note that in this case $\pi_M : P_M \to M$ is also a trivial principal $\mathscr{O}$-bundle, since we have the equivariant diffeomorphism

$$\rho : T^*\bar{M} \times T^*\mathscr{O} \to \left(T^*\bar{M} \times \mathfrak{o}^*\right) \times \mathscr{O}, \quad \rho(\alpha_q, \alpha_g) = \left((\alpha_q, \alpha_g g^{-1}), g\right). \tag{28}$$

If the bundle $\pi_S : P_S \simeq S \times \mathscr{O} \to S$ is also trivial, then we have the identification

$$Q_{KK} = \mathrm{Emb}_{\mathscr{O}}(P_S, T^*\bar{P}) \simeq \mathrm{Emb}(S, T^*\bar{M} \times \mathfrak{o}^*) \times \mathscr{F}(S, \mathscr{O}) \tag{29}$$

(see Lemma 3.8 in [14]). More precisely, to the equivariant embedding $f : S \times \mathscr{O} \to T^*\bar{M} \times T^*\mathscr{O}$, $f(x, g) = \big(\mathbf{P_Q}(x), \kappa_\gamma(x)g\big)$, where $\mathbf{P_Q} : S \to T^*\bar{M}$ and $\kappa_\gamma : S \to T^*\mathscr{O}$, we associate the pair $((\mathbf{P_Q}, \sigma), \gamma) \in \mathrm{Emb}(S, T^*\bar{M} \times \mathfrak{o}^*) \times \mathscr{F}(S, \mathscr{O})$, where $\sigma := \kappa_\gamma \gamma^{-1} : S \to \mathfrak{o}^*$. Note also that, since the bundle P_S is trivial, we have $\mu_{P_S} = \mu_S \wedge \det_\tau$. Choosing the Ad-invariant inner product τ such that $\mathrm{Vol}(\mathscr{O}) = 1$, we have $\mu_{P_S} = \mu_S \wedge \mu_{\mathscr{O}}$, where $\mu_{\mathscr{O}}$ is the Haar measure on the compact group $\mathscr{O}$.

The pair of momentum maps (26) and (25) becomes

$$\begin{array}{ccc} & \mathrm{Emb}_{\mathscr{O}}(S \times \mathscr{O}, T^*\bar{M} \times T^*\mathscr{O}) & \\ {\scriptstyle \mathbf{J}_L} \swarrow & & \searrow {\scriptstyle \mathbf{J}_R} \\ \mathscr{F}(T^*\bar{M} \times \mathfrak{o}^*)^* & & \mathfrak{aut}_{\mathrm{vol}}(S \times \mathscr{O})^* \end{array}$$

Notice that the Lie bracket on $\mathscr{F}(T^*\bar{M} \times \mathfrak{o}^*)$ is the reduced Poisson bracket given here by

$$\{f, g\}_M = \{f, g\}_{T^*\bar{M}} + \{f, g\}_+, \quad f, g \in \mathscr{F}(T^*\bar{M} \times \mathfrak{o}^*),$$

where the first term denotes the canonical Poisson bracket on $T^*\bar{M}$ and the second term is the Lie-Poisson bracket on $\mathfrak{o}^*$,

$$\{f, g\}_+(\sigma) = \left\langle \sigma, \left[\frac{\delta f}{\delta \sigma}, \frac{\delta g}{\delta \sigma}\right] \right\rangle, \quad f, g \in C^\infty(\mathfrak{o}^*).$$

It is obtained by Poisson reduction of the canonical Poisson bracket on $T^*(\bar{M} \times \mathscr{O})$.

The expression of these momentum maps were obtained in [14]. For later use, we provide below some details concerning their derivation.

4.4.1 Left Action Momentum Map

By specifying formula (25) to our case, we can write the left momentum map as

$$\mathbf{J}_L : \mathrm{Emb}_{\mathscr{O}}(S \times \mathscr{O}, T^*\bar{M} \times T^*\mathscr{O}) \to \mathscr{F}_{\mathscr{O}}(T^*\bar{M} \times T^*\mathscr{O})^* = \mathscr{F}(T^*\bar{M} \times \mathfrak{o}^*)^*,$$

where, for $h \in \mathscr{F}(T^*\bar{M} \times \mathfrak{o}^*)$, $\tilde{h} = h \circ \pi_M \in \mathscr{F}(T^*\bar{M} \times T^*\mathscr{O})$ and $f(x, g) = ((\mathbf{P_Q}(x), \kappa_\gamma(x)g)$,

$$\langle \mathbf{J}_L(f), h \rangle = \int_{S \times \mathscr{O}} \tilde{h}(\mathbf{P_Q}(x), \kappa_\gamma(x)g)\mu_{P_S} = \int_S h\left(\mathbf{P_Q}(x), \kappa_\gamma(x)\gamma(x)^{-1}\right)\mu_S.$$

Formally, using the identification $f = ((\mathbf{P_Q}, \sigma), \gamma)$ given in (29), this can be written as

$$\mathbf{J}_L(\mathbf{P_Q}, \sigma, \gamma) = (\mathbf{P_Q}, \sigma)_* \mu_S. \tag{30}$$

4.4.2 Right Action Momentum Map

By specifying formula (26) to our case, we can write the momentum map of the right action as

$$\mathbf{J}_R : \mathrm{Emb}_{\mathscr{O}}(S \times \mathscr{O}, T^*\bar{M} \times T^*\mathscr{O}) \to \mathfrak{aut}_{\mathrm{vol}}(S \times \mathscr{O})^* = \Omega^1_{\mathscr{O}}(S \times \mathscr{O})/\mathbf{d}\mathscr{F}(S)$$
$$\mathbf{J}_R(f) = [f^*\Theta_{\bar{P}}] = [f^*(\Theta_{\bar{M}} + \Theta_{\mathscr{O}})],$$

where $\Theta_{\bar{P}}$, $\Theta_{\bar{M}}$, $\Theta_{\mathscr{O}}$ are the canonical one-forms on $T^*\bar{P}$, $T^*\bar{M}$, $T^*\mathscr{O}$, respectively.

The identification of $\mathfrak{X}_{\mathrm{vol}}(S) \circledS \mathscr{F}(S, \mathfrak{o})$ with the Lie algebra $\mathfrak{aut}_{\mathrm{vol}}(S \times \mathscr{O})$ of invariant divergence free vector fields on $S \times \mathscr{O}$, namely $(u, \xi)(x, g) = (u(x), \xi(x)g)$, provides an identification of their duals: $(\mathfrak{X}_{\mathrm{vol}}(S) \circledS \mathscr{F}(S, \mathscr{O}))^* = \big(\Omega^1(S)/\mathbf{d}\mathscr{F}(S)\big) \times \mathscr{F}(S, \mathfrak{o}^*)$ with $\mathfrak{aut}_{\mathrm{vol}}(S \times \mathscr{O})^* = \Omega^1_{\mathscr{O}}(S \times \mathscr{O})/\mathbf{d}\mathscr{F}(S)$, via the map $([\alpha], \nu) \mapsto [(\alpha, \nu)]$, where $(\alpha, \nu)(v_x, \xi_g) = \alpha(v_x) + \nu(x)(\xi_g g^{-1})$.

We now show that in terms of the identification $f = ((\mathbf{P_Q}, \sigma), \gamma)$ in (29), the right momentum map has the expression

$$\mathbf{J}_R((\mathbf{P_Q}, \sigma), \gamma) = \Big(\big[\mathbf{P}_{\mathbf{Q}}^* \Theta_{\bar{M}} + \langle \sigma, \delta^r \gamma \rangle\big], \mathrm{Ad}^*_\gamma \sigma\Big) \in \big(\Omega^1(S)/\mathbf{d}\mathscr{F}(S)\big) \times \mathscr{F}(S, \mathfrak{o}^*). \tag{31}$$

Knowing that $\kappa_\gamma = \sigma\gamma$, the first component $\alpha \in \Omega^1(S)$ of $f^*\Theta_{\bar{P}}$ reads

$$\alpha(v_x) = (f^*(\Theta_{\bar{M}} + \Theta_{\mathscr{O}}))(v_x, 0_e) = \mathbf{P}_{\mathbf{Q}}^* \Theta_{\bar{M}}(v_x) + \kappa_\gamma^* \Theta_{\mathscr{O}}(v_x),$$

for all $v_x \in T_x S$. Using the definition of the canonical one-form $\Theta_{\mathscr{O}}$, we have

$$(\kappa_\gamma^* \Theta_{\mathscr{O}})(v_x) = \big\langle \kappa_\gamma(x), T_x(\pi \circ \kappa_\gamma) \cdot v_x \big\rangle = \langle \sigma(x)\gamma(x), T_x\gamma \cdot v_x \rangle = \langle \sigma, \delta^r \gamma \rangle (v_x),$$

where $\pi : T^*\mathscr{O} \to \mathscr{O}$.

Given $\beta \in T^*\mathscr{O}$, we denote by $\ell_\beta : \mathscr{O} \to T^*\mathscr{O}$ the orbit map defined by $\ell_\beta(g) = \beta g$. For the second component $\nu \in \mathscr{F}(S, \mathfrak{o}^*)$ of $f^*\Theta_{\bar{P}}$ we compute for all $\xi \in \mathfrak{o}$:

$$\begin{aligned}\langle \nu(x), \xi \rangle &= (f^*\Theta_{\bar{P}})(0_x, \xi) = \Theta_{\mathscr{O}}(T\ell_{\kappa_\gamma(x)}(\xi)) = \big\langle \kappa_\gamma(x), (T\pi \circ T\ell_{\kappa_\gamma(x)})(\xi) \big\rangle \\ &= \big\langle \kappa_\gamma(x), \gamma(x)\xi \big\rangle = \langle \gamma(x)^{-1}\kappa_\gamma(x), \xi \rangle,\end{aligned}$$

where we used the identity $(T\pi \circ T\ell_\beta)(\xi) = \pi(\beta)\xi$, valid for all $\beta \in T^*\mathscr{O}$. Hence we obtain $\nu = \gamma^{-1}\kappa_\gamma = \gamma^{-1}\sigma\gamma = \mathrm{Ad}^*_\gamma \sigma$. By combining the above formulas we get the desired expression (31).

Note that when $H^1(S) = 0$, then the dual space $\left(\Omega^1(S)/\mathbf{d}\mathscr{F}(S)\right) \times \mathscr{F}(S, \mathfrak{o}^*)$ is isomorphic to the space $\mathbf{d}\Omega^1(S) \times \mathscr{F}(S, \mathfrak{o}^*)$ and we can write the first component of the momentum map as a vorticity as follows

$$\mathbf{J}_R((\mathbf{P_Q}, \sigma), \gamma) = \left(-\mathbf{P}^*_{\mathbf{Q}}\Omega_{\bar{M}} - (\sigma\gamma)^*\Omega_{\mathscr{O}}, \mathrm{Ad}^*_\gamma \sigma\right),$$

where $\Omega_{\bar{M}} = -\mathbf{d}\Theta_{\bar{M}}$ and $\Omega_{\mathscr{O}} = -\mathbf{d}\Theta_{\mathscr{O}}$ are the canonical symplectic forms on $T^*\bar{M}$ and $T^*\mathscr{O}$, respectively.

5 The Dual Pair Property of the $\mathrm{EPAut}_{\mathrm{vol}}$ Momentum Maps

In this section we will focus on the particular case of the Yang-Mills phase space described in Section 4.4. We assume that the principal bundles are trivial, i.e. $P_M = T^*\bar{P}$, $\bar{P} \simeq \bar{M} \times \mathscr{O}$, $P_S \simeq S \times \mathscr{O}$, so the commuting actions of the groups $\mathscr{A}ut_{\mathrm{vol}}(S \times \mathscr{O})$ and $\overline{\mathscr{A}ut}_{\mathrm{ham}}(T^*\bar{M} \times T^*\mathscr{O})$ on the symplectic manifold Q_{KK} become

$$(\eta, \gamma) \cdot (\psi, b) = (\eta \circ \psi, (\gamma \circ \psi)b), \quad \psi \in \mathrm{Diff}(S), \quad b \in \mathscr{F}(S, \mathscr{O})$$

$$(\varphi, a) \cdot (\eta, \gamma) = (\varphi \circ \eta, (a \circ \eta)\gamma), \quad \varphi \in \mathrm{Diff}(T^*\bar{M} \times \mathfrak{o}^*), a \in \mathscr{F}(T^*\bar{M} \times \mathfrak{o}^*, \mathscr{O}),$$

for $(\eta, \gamma) \in Q_{KK} \simeq \mathrm{Emb}(S, T^*\bar{M} \times \mathfrak{o}^*) \times \mathscr{F}(S, \mathscr{O})$ (see (29)). The associated momentum maps have been described in (30) and (31).

In the next two propositions, we shall show the transitivity results needed to obtain the dual pair property of these momentum maps. We will use the following Lemma, a direct generalization of the corresponding formula on Lie groups, i.e. when the manifold $\bar{M}$ is absent, see e.g. Proposition 13.4.3. in [32].

Lemma 4. *Let $\tilde{h} \in \mathscr{F}(T^*\bar{M} \times T^*\mathscr{O})^{\mathscr{O}}$ and let $h \in \mathscr{F}(T^*\bar{M} \times \mathfrak{o}^*)$ be the function defined by $\tilde{h}(\alpha_m, \alpha_g) := h(\alpha_m, \alpha_g g^{-1})$. Then the Hamiltonian vector field $X_{\tilde{h}}$ on $T^*\bar{M} \times T^*\mathscr{O}$, pushed forward to $(T^*\bar{M} \times \mathfrak{o}^*) \times \mathscr{O}$ by the right trivialization ρ from (28), reads*

$$\left(\rho_* X_{\tilde{h}}\right)(\alpha_m, \sigma, g) = \left(\left(X_{h_\sigma}(\alpha_m), -\mathrm{ad}^*_{\frac{\delta h_{\alpha_m}}{\delta \sigma}} \sigma\right), \frac{\delta h_{\alpha_m}}{\delta \sigma} g\right),$$

where $h_\sigma : T^*M \to \mathbb{R}$ is defined by $h_\sigma(\alpha_m) := h(\alpha_m, \sigma)$, $h_{\alpha_m} : \mathfrak{o}^* \to \mathbb{R}$ is defined by $h_{\alpha_m}(\sigma) := h(\alpha_m, \sigma)$, and X_{h_σ} denotes the Hamiltonian vector field associated to h_σ on $T^*\bar{M}$.

Proposition 5. *The group $\overline{\mathscr{A}ut}_{\mathrm{ham}}(T^*\bar{M} \times T^*\mathscr{O})$ acts infinitesimally transitively on the level sets of the momentum map $\mathbf{J}_R$ given in (31).*

Proof. Recall that the Lie algebra of $\overline{\mathscr{A}ut}_{\mathrm{ham}}(T^*\bar{M}\times T^*\mathscr{O})$ consists of Hamiltonian vector fields $X_{\tilde{h}}$ associated to $\mathscr{O}$-invariant Hamiltonian functions $\tilde{h}\in\mathscr{F}(T^*\bar{M}\times T^*\mathscr{O})^{\mathscr{O}}$. Given $f=(\eta,\gamma)=((\mathbf{P_Q},\sigma),\gamma)\in Q_{KK}$, and using Lemma 4 above, the infinitesimal action reads

$$(X_{\tilde{h}})_{Q_{KK}}(\eta,\gamma)=\left(\left(X_{h_\sigma}\circ\mathbf{P_Q},-\operatorname{ad}^*_{\frac{\delta h}{\delta\sigma}\circ\eta}\sigma\right),\left(\frac{\delta h}{\delta\sigma}\circ\eta\right)\gamma\right). \tag{32}$$

We shall now write the derivative of the momentum map $\mathbf{J}_R$ (31) at $(\eta,\gamma)\in Q_{KK}$ in direction $(v_\eta,u_\gamma)\in T_{(\eta,\gamma)}Q_{KK}$. Note that we have $v_\eta=(v_{\mathbf{P_Q}},v_\sigma)$, where $v_{\mathbf{P_Q}}:S\to T(T^*\bar{M})$ is a smooth map covering $\mathbf{P_Q}:S\to T^*\bar{M}$ and $v_\sigma:S\to\mathfrak{o}^*$ is a smooth map, and $u_\gamma:S\to T\mathscr{O}$ is a smooth map covering $\gamma:S\to\mathscr{O}$. In particular $u_\gamma\gamma^{-1}\in\mathscr{F}(S,\mathfrak{o})$. Using the expression (34) of the differential of the right logarithmic derivative map $\delta^r:\mathscr{F}(S,\mathscr{O})\mapsto\Omega^1(S,\mathfrak{o})$ shown in Lemma 5 below, we obtain the expression

$$\begin{aligned}&T_{(\eta,\gamma)}\mathbf{J}_R\cdot(v_\eta,u_\gamma)\\&=\left([\mathbf{P}_\mathbf{Q}^*\pounds_{v_{\mathbf{P_Q}}}\Theta_{\bar{M}}+\langle\operatorname{ad}^*_{u_\gamma\gamma^{-1}}\sigma+v_\sigma,\delta^r\gamma\rangle+\langle\sigma,\mathbf{d}(u_\gamma\gamma^{-1})\rangle],\operatorname{Ad}^*_\gamma(\operatorname{ad}^*_{u_\gamma\gamma^{-1}}\sigma+v_\sigma)\right)\\&\qquad\in\Omega^1(S)/\mathbf{d}\mathscr{F}(S)\times\mathscr{F}(S,\mathfrak{o}^*)=\mathfrak{aut}_{\mathrm{vol}}(S\times\mathscr{O})^*.\end{aligned}$$

In order to obtain the transitivity result, we have to show that any vector (v_η,u_γ) in the kernel of $T_{(\eta,\gamma)}\mathbf{J}_R$ can be obtained from an infinitesimal generator of the left $\overline{\mathscr{A}ut}_{\mathrm{ham}}(T^*\bar{S}\times T^*\mathscr{O})$-action. More precisely, for any vector $(v_\eta,u_\gamma)\in T_{(\eta,\gamma)}Q_{KK}$ with $\operatorname{ad}^*_{u_\gamma\gamma^{-1}}\sigma+v_\sigma=0$ and such that $\mathbf{P}_\mathbf{Q}^*\pounds_{v_{\mathbf{P_Q}}}\Theta_{\bar{M}}+\langle\sigma,\mathbf{d}(u_\gamma\gamma^{-1})\rangle$ is an exact 1-form on S, there exists $h\in\mathscr{F}(T^*\bar{M}\times\mathfrak{o}^*)$ such that

$$v_{\mathbf{P_Q}}=X_{h_\sigma}\circ\mathbf{P_Q},\quad v_\sigma=-\operatorname{ad}^*_{\frac{\delta h}{\delta\sigma}\circ\eta}\sigma,\quad u_\gamma=\left(\frac{\delta h}{\delta\sigma}\circ\eta\right)\gamma.$$

Define $j:=u_\gamma\gamma^{-1}\in\mathscr{F}(S,\mathfrak{o})$, so that we have $u_\gamma=j\gamma$ and $v_\sigma=-\operatorname{ad}^*_j\sigma$. We will show that there exists $h\in\mathscr{F}(T^*\bar{M}\times\mathfrak{o}^*)$ such that

$$j=\frac{\delta h}{\delta\sigma}\circ\eta. \tag{33}$$

To achieve this we use the fact that $\mathbf{P}_\mathbf{Q}^*\pounds_{v_{\mathbf{P_Q}}}\Theta_{\bar{M}}+\langle\sigma,\mathbf{d}j\rangle$ is exact, hence there exists $h_0\in\mathscr{F}(S)$ such that $\mathbf{P}_\mathbf{Q}^*\mathbf{i}_{v_{\mathbf{P_Q}}}\mathbf{d}\Theta_{\bar{M}}+\langle\mathbf{d}\sigma,j\rangle=\mathbf{d}h_0$. By a standard argument using a partition of unity, we extend in a smooth way the function h_0 to a function $h_1\in\mathscr{F}(T^*\bar{M}\times\mathfrak{o}^*)$ via the embedding $\eta:S\to T^*\bar{M}\times\mathfrak{o}^*$, i.e. such that $h_0=h_1\circ\eta$. Then we consider the 1-form

$$\lambda:=(\mathbf{d}h_1)\circ\eta-\mathbf{i}_{v_{\mathbf{P_Q}}}(\mathbf{d}\Theta_{\bar{M}}\circ\mathbf{P_Q})-j_\eta$$

on $T^*\bar{M} \times \mathfrak{o}^*$ along S, where j_η is the 1-form on $T^*\bar{M} \times \mathfrak{o}^*$ along η with first component zero and second component given by $j : S \to \mathfrak{o} = \mathfrak{o}^{**}$.

The form λ vanishes on $T(\eta(S))$, the tangent space to the submanifold $\eta(S)$ of $T^*\bar{M} \times \mathfrak{o}^*$. From Lemma 1, there exists a function $h_2 \in \mathscr{F}(T^*\bar{M} \times \mathfrak{o}^*)$ such that $\lambda = (\mathbf{d}h_2) \circ \eta$. The function $h := h_1 - h_2$ satisfies $(\mathbf{d}h) \circ \eta = \mathbf{i}_{v_{\mathbf{P_Q}}}(\mathbf{d}\Theta_{\bar{M}} \circ \mathbf{P_Q}) + j_\eta$, therefore it verifies (33) as desired.

From (33) we obtain $u_\gamma = (\frac{\delta h}{\delta \sigma} \circ \eta)\gamma$ and $v_\sigma = -\operatorname{ad}^*_{\frac{\delta h}{\delta \sigma} \circ \eta} \sigma$. Moreover, $(\mathbf{d}h_\sigma) \circ \mathbf{P_Q} = \mathbf{i}_{v_{\mathbf{P_Q}}}(\mathbf{d}\Theta_{\bar{M}} \circ \mathbf{P_Q})$, hence $v_{\mathbf{P_Q}} = X_{h_\sigma} \circ \mathbf{P_Q}$. Thus we have shown that any (v_η, u_γ) in the kernel of $T_{(\eta,\gamma)}\mathbf{J}_R$ can be written as (32) for some $h : T^*\bar{M} \times \mathfrak{o}^* \to \mathbb{R}$.

Lemma 5. *The differential of the right logarithmic derivative*

$$\delta^r : \mathscr{F}(M, \mathscr{O}) \to \Omega^1(M, \mathfrak{o}), \quad \delta^r\gamma = (\mathbf{d}\gamma)\gamma^{-1},$$

at the point $\gamma \in \mathscr{F}(M, \mathscr{O})$ in direction $u_\gamma \in \Gamma(\gamma^* T\mathscr{O})$ is

$$\mathbf{d}_\gamma \delta^r(u_\gamma) = \mathbf{d}(u_\gamma \gamma^{-1}) + \operatorname{ad}_{u_\gamma \gamma^{-1}} \delta^r\gamma. \tag{34}$$

Proof. By taking the derivative of the identity $\delta^r(\gamma'\gamma) = \delta^r\gamma' + \operatorname{Ad}_{\gamma'} \delta^r\gamma$, relative to γ' at $\gamma' = e$ in direction $v = u_\gamma\gamma^{-1}$, one obtains

$$\mathbf{d}_\gamma \delta^r(u_\gamma) = \mathbf{d}_e \delta^r(u_\gamma \gamma^{-1}) + \operatorname{ad}_{u_\gamma \gamma^{-1}} \delta^r\gamma.$$

The lemma follows now from the formula $\mathbf{d}_e \delta^r(v) = \mathbf{d}v$ for all $v \in \mathscr{F}(M, \mathfrak{o})$.

Proposition 6. *The group $\mathscr{A}ut_{\mathrm{vol}}(S \times \mathscr{O})$ acts transitively on the level sets of the momentum map $\mathbf{J}_L$ given in* (30).

Proof. We need to show that given two embeddings $(\eta_1, \gamma_1), (\eta_2, \gamma_2) \in \mathrm{Emb}_{\mathscr{O}}(S \times \mathscr{O}, T^*\bar{M} \times T^*\mathscr{O})$ in the same level set of $\mathbf{J}_L$, there exists a volume preserving automorphism $(\psi, b) \in \mathscr{A}ut_{\mathrm{vol}}(S \times \mathscr{O})$, such that $(\eta_2, \gamma_2) = (\eta_1 \circ \psi, (\gamma_1 \circ \psi)b)$.

The equality $\mathbf{J}_L(\eta_1, \gamma_1) = \mathbf{J}_L(\eta_2, \gamma_2)$ reads $\int_S (h \circ \eta_1)\mu_S = \int_S (h \circ \eta_2)\mu_S$, for all functions $h \in \mathscr{F}(T^*\bar{S} \times \mathfrak{o}^*)$, so the embeddings η_1 and η_2 have the same image in $T^*\bar{M} \times \mathfrak{o}^*$. Therefore, there exists a unique diffeomorphism ψ of S such that $\eta_2 = \eta_1 \circ \psi$.

It follows that the volume form $\nu_S := (\psi^{-1})^*\mu_S$ satisfies $(\eta_2)_*\mu_S = (\eta_1)_*\nu_S$, i.e. $\int_S (h \circ \eta_1)\mu_S = \int_S (h \circ \eta_2)\mu_S = \int_S (h \circ \eta_1)\nu_S$ for all $h \in \mathscr{F}(T^*\bar{S} \times \mathfrak{o}^*)$. Because η_1 and η_2 are embeddings, we conclude that $\mu_S = \nu_S$, so $\psi^*\mu_S = \mu_S$ and ψ is a volume preserving diffeomorphism of S.

By defining the map $b := (\gamma_1^{-1} \circ \psi)\gamma_2 \in \mathscr{F}(S, \mathscr{O})$, we obtain that the automorphism $(\psi, b) \in \mathscr{A}ut_{\mathrm{vol}}(S \times \mathscr{O})$ satisfies $(\eta_2, \gamma_2) = (\eta_1 \circ \psi, (\gamma_1 \circ \psi)b) = (\eta_1, \gamma_1) \cdot (\psi, b)$, as required.

From the two transitivity results above, we obtain that the actions are mutually completely orthogonal and hence we get the following result.

Theorem 2. *The momentum maps* (30) *and* (31) *associated to the actions of the groups* $\overline{\mathscr{A}ut}_{\mathrm{ham}}(T^*\bar{M}\times T^*\mathscr{O})\times_B \mathbb{R}$ *and* $\mathscr{A}ut_{\mathrm{vol}}(S\times\mathscr{O})$ *on* $\mathrm{Emb}_{\mathscr{O}}(S\times\mathscr{O}, T^*\bar{M}\times T^*\mathscr{O})$*, form a dual pair for the EPAut*$_{vol}$ *equations*

$$\begin{array}{ccc} & \mathrm{Emb}_{\mathscr{O}}(S\times\mathscr{O}, T^*\bar{M}\times T^*\mathscr{O}) & \\ {\scriptstyle \mathbf{J}_L}\swarrow & & \searrow{\scriptstyle \mathbf{J}_R} \\ \mathscr{F}(T^*\bar{M}\times\mathfrak{o}^*)^* & & \mathfrak{aut}_{\mathrm{vol}}(S\times\mathscr{O})^* \end{array}$$

6 Conclusion and Future Works

In this paper, we have shown that the pairs of momentum maps associated to the EPAut equations and its incompressible version arise from mutually completely orthogonal actions and are therefore dual pairs. We have obtained this result for the case of trivial principal bundles. For the incompressible situation we have restricted our study to the physical relevant case of the Yang-Mills phase space. Further studies will be necessary in order to show the same results without these restrictions.

References

1. Arnold, V.I.: Sur la géométrie différentielle des groupes de Lie de dimension infinie et ses applications à l'hydrodynamique des fluides parfaits. Ann. Inst. Fourier, Grenoble **16**, 319–361 (1966)
2. Bambah, B.A., Mahajan, S.M., Mukku, C.: Yang–Mills magnetofluid unification. Phys. Rev. Lett. **97**, 072301 (2006)
3. Bistrovic, B., Jackiw, R., H. Li, Nair, V.P., Pi, S.-Y.: Non-abelian fluid dynamics in Lagrangian formulation. Phys. Rev. D **67**(2), 025013 (2003)
4. Camassa, R., Holm, D.D.: An integrable shallow water equation with peaked solitons. Phys. Rev. Lett. **71**, 1661–1664 (1993)
5. Chen, M., Liu, S., Zhang, Y.: A two-component generalization of the Camassa–Holm equation and its solutions. Lett. Math. Phys. **75**, 1–15 (2005)
6. Cushman, R., Rod, D.: Reduction of the semisimple 1:1 resonance. Physica D **6**, 105–112 (1982)
7. Gay-Balmaz, F., Ratiu, T.S.: Reduced Lagrangian and Hamiltonian formulations of Euler-Yang-Mills fluids. J. Symplectic Geom. **6**, 189–237 (2008)
8. Gay-Balmaz, F., Ratiu, T.S.: The geometric structure of complex fluids. Adv. Appl. Math. **42**, 176–275 (2009)
9. Gay-Balmaz, F., Ratiu, T.S.: Geometry of nonabelian charged fluids. Dyn. PDEs **8**(1), 5–19 (2011a)
10. Gay-Balmaz, F., Ratiu, T.S.: Clebsch optimal control formulation in mechanics. J. Geom. Mech. **3**(1), 47–79 (2011b)
11. Gay-Balmaz, F., Vizman, C.: Dual pairs in fluid dynamics. Ann. Glob. Anal. Geom. **41**(1), 1–24 (2012)

12. Gay-Balmaz, F., Vizman, C.: Isotropic submanifolds and coadjoint orbits of the Hamiltonian group, Preprint (2014)
13. Gay-Balmaz, F., Vizman, C.: A dual pair for free boundary fluids, to appear in International Journal of Geometric Methods in Modern Physics
14. Gay-Balmaz, F., Tronci, C., Vizman, C.: Geometric dynamics on the automorphism group of principal bundles: geodesic flows, dual pairs and chromomorphism groups. J. Geom. Mech. **5**(1), 39–84 (2013)
15. Gibbons, J., Holm, D.D., Kupershmidt, B.A.: The Hamiltonian structure of classical chromohydrodynamics. Physica D **6**, 179–194 (1983)
16. Golubitsky, M., Stewart, I.: Generic bifurcation of Hamiltonian systems with symmetry. Physica D **24**, 391–405 (1987)
17. Haller, S., Vizman, C: Non–linear Grassmannians as coadjoint orbits. Math. Ann. **329**, 771–785 (2004)
18. Hirsch, M.W.: Differential Topology. Graduate Texts in Mathematics, vol. 33. Springer, New York (1976)
19. Holm, D.D.: Hamiltonian dynamics of a charged fluid, including electro- and magnetohydrodynamics. Phys. Lett. A **114**, 137–141 (1986)
20. Holm, D.D.: Euler-Poincaré dynamics of perfect complex fluids. In: Holmes, P., Newton, P., Weinstein, A. (eds.) Geometry, Mechanics, and Dynamics: 60th Birthday Volume for J. E. Marsden. Springer, New York (2002)
21. Holm, D.D., Kupershmidt, B.A.: The analogy between spin glasses and Yang-Mills fluids. J. Math. Phys. **29**, 21–30 (1988)
22. Holm, D.D., Marsden, J.E.: Momentum maps and measure-valued solutions (peakons, filaments and sheets) for the EPDiff equation. Prog. Math. **232**, 203–235 (2004)
23. Holm, D.D., Tronci, C.: Geodesic flows on semidirect-product Lie groups: geometry of singular measure-valued solutions. Proc. R. Soc. A **465**, 457–476 (2008)
24. Holm, D.D., Ó Náraigh, L., Tronci, C.: Singular solutions of a modified two-component Camassa-Holm equation. Phys. Rev. E **79**, 016601 (2009)
25. Ismagilov, R.S., Losik, M., Michor, P.W.: A 2-cocycle on a group of symplectomorphisms. Moscow Math. J. **6** (2006), 307–315 (2006)
26. Iwai, T.: On reduction of two degree of freedom Hamiltonian systems by an S^1 action, and $SO_0(1,2)$ as a dynamical group. J. Math. Phys. **26**, 885–893 (1985)
27. Jackiw, R., Nair, V.P., Pi, S.-Y., Polychronakos, A.P.: Perfect fluid theory and its extensions. J. Phys. A **37**(42, 2004), R327–R432 (2004)
28. Kriegl, A., Michor, P.W.: The Convenient Setting of Global Analysis. Mathematical Surveys and Monographs, vol. 53, American Mathematical Society, Providence, RI (1997)
29. Kuz'min, P.A.: Two-component generalizations of the Camassa–Holm equation. Math. Notes **81**, 130–134 (2007)
30. Libermann, P., Marle, C.-M.: Symplectic Geometry and Analytical Mechanics. D. Reidel Publishing Company, Dordrecht (1987)
31. Marsden, J.E.: Generic bifurcation of Hamiltonian systems with symmetry. Appendix to Golubitsky and Stewart. Physica D **24**, 391–405 (1987)
32. Marsden, J.E., Ratiu, T.S.: Introduction to Mechanics and Symmetry, 2nd edn. Springer, New York (1999)
33. Marsden, J.E., Weinstein, A.: Coadjoint orbits, vortices, and Clebsch variables for incompressible fluids. Physica D **7**, 305–323 (1983)
34. Marsden, J.E., Ratiu, T.S., Weinstein, A.: Semidirect product and reduction in mechanics. Trans. Am. Math. Soc. **281**, 147–177 (1984)
35. Montgomery, R.: Canonical formulations of a classical particle in a Yang-Mills field and Wong's equations. Lett. Math. Phys. **8**, 59–67 (1984)
36. Vizman, C.: Geodesics on extensions of Lie groups and stability: the superconductivity equation. Phys. Lett. A **284**, 23–30 (2001)
37. Vizman, C.: Geodesic equations on diffeomorphism groups. SIGMA Symmetry Integrability Geom. Methods Appl. **4**, 22–30 (2008)
38. Weinstein, A.: The local structure of Poisson manifolds. J. Diff. Geom. **18**, 523–557 (1983)

The Role of SE(d)-Reduction for Swimming in Stokes and Navier-Stokes Fluids

Henry O. Jacobs

Abstract Steady swimming appears both periodic and stable. These characteristics are the very definition of limit cycles, and so we ask "Can we view swimming as a limit cycle?" In this paper we will not be able to answer this question in full. However, we shall find that reduction by SE(d)-symmetry brings us closer. Upon performing reduction by symmetry, we will find a stable fixed point which corresponds to a motionless body in stagnant water. We will then speculate on the existence of periodic orbits which are "approximately" limit cycles in the reduced system. When we lift these periodic orbits from the reduced phase space, we obtain dynamically robust relatively periodic orbits wherein each period is related to the previous by an SE(d) phase. Clearly, an SE(d) phase consisting of nonzero translation and identity rotation means directional swimming, while non-trivial rotations correspond to turning with a constant turning radius.

1 Introduction

Many engineers have a justifiable predilection for coordinate-based descriptions of the world. However, the use of coordinate-free descriptions is consistently leveraged in Jerry Marsden's work to gain insights which would otherwise have been clouded by the complexities which coordinates bring with them. For example, proving anything non-trivial about the inviscid fluid equations

$$\partial_t u^i + u^j \partial_j u_i + \partial_i p = 0, \qquad \partial_i u^i = 0, \qquad u \in \mathfrak{X}(\mathbb{R}^d) \tag{1}$$

is notoriously difficult. However, with the publication of [3] differential geometers were permitted to substitute (1) with a right-trivialized geodesic equation on a Lie group (i.e. an Euler-Poincaré equation). In particular, if one was willing to use

H.O. Jacobs (✉)
Department of Mathematics, Imperial College London, Huxley Building, 180 Queen's Gate Road, London SW7 2AZ, UK
e-mail: hoj201@gmail.com

D.E. Chang et al. (eds.), *Geometry, Mechanics, and Dynamics*, Fields Institute Communications 73, DOI 10.1007/978-1-4939-2441-7_8

geometry, one could study inviscid fluids *without the need to invoke* (1) *directly!* Only three years later, the proof of local existence-uniqueness was realized by David Ebin and Jerry Marsden using these coordinate-free notions [11].

In studying swimming in the mid-Reynolds regime, one is confronted with coupling a solid body to a Navier-Stokes fluid. It is just as true today as it was in 1966 that the Navier-Stokes equations are difficult to work with. A very modest extension of [3] allows us to view fluid-structure problems as forced Lagrangian systems on principal bundles [22]. In this paper, we will use this geometric characterization of fluid-structure interaction to study swimming in viscous flows. We will use these geometric tools to explore the question: *Can we reasonably interpret swimming as a limit cycle?* Unfortunately, we will not be able answer this question in full. However, we will be able to clarify the crucial role which SE(d)-symmetry will play in the final answer. *A limit-cycle interpretation of swimming is valuable because it would conform with an existing body of knowledge derived from laboratory and computer experiments. Moreover, this simple characterization of swimming could be of interest to control engineers who desire to use passive mechanisms to achieve robust behavior with simple open-loop control algorithms.*

1.1 Main Contributions

We will understand the system consisting of a body immersed in a fluid as a dissipative system evolving on a phase space P. One observes that the system is invariant with respect to the group of isometries of $\mathbb{R}^d$, i.e. the special Euclidean group SE(d). This observation suggests that one can describe the system evolving on the quotient manifold $[P] = \frac{P}{\mathrm{SE}(d)}$. Given this reduction, the main contributions of this paper are:

- Under reasonable assumptions on the Lagrangian and the viscous frictions, we will prove the existence of an asymptotically stable point for the dynamics in $[P]$.
- We will illustrate how relative limit cycles are produced by exponentially stable equilibria in finite-dimensional dynamical systems under sufficiently small time-periodic perturbations.
- For sufficiently small time-periodic internal body forces, we will speculate on the existence of loops in $[P]$ which approximately satisfy the dynamics.
- We illustrate how loops in $[P]$ are lifted to paths in P, where each period is related to the previous by a rigid rotation and translation.

1.2 Background

There exists a substantial body of knowledge in the form of computational and biological experiments which are consistent with the hypothesis that swimming could be interpreted as a limit cycle. For example, experiments involving tethered

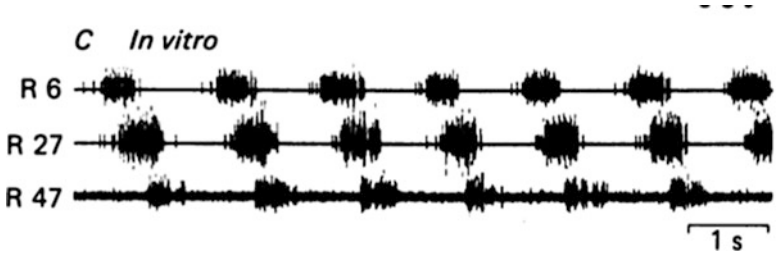

Fig. 1 An in-vitro EMG recording of a lamprey spinal chord in "fictive swimming" [46]

dead fish immersed in a flow behind a bluff body suggest an ability to passively harvest energy from the surrounding vorticity of the flow. The same studies also provide a relevant example of oscillatory behavior as a stable state for an unactuated system [6]. Moreover, in living fish, periodic motor neuron actuation has been recorded directly and periodic internal elastic forces have been approximated via linear elasticity models [40]. Finally, the notion of central pattern generators,[1] has become widely accepted among biologists studying locomotion [10, 15, 18]. In particular, a central pattern generator for lamprey swimming has been identified and EMG readings have been recorded in-vitro to verify that the swimming mechanism does not rely solely on feedback [46] (see Figure 1). These experiments and observations from biology suggest that passive mechanisms might play a significant role in understanding swimming.

Additionally, numerical experiments involving rigid bodies with oscillating forces suggest that uniform motion (i.e. flapping flight) is an attracting state for certain pairs of frequencies and Reynolds numbers [2, 48]. Closer to what will be demonstrated here, numerical simulations of a 2-dimensional model of a lamprey at high (but not infinite) Reynolds numbers illustrate swimming as an emergent phenomenon arising asymptotically from time-periodic internal body forces. Trajectories of this system converge to cyclic behavior after very few oscillations when starting from rest [44] see (Figure 2). A similar study was carried out to understand the difference between periodic control forces and prescribed kinematics in [47]. Here, regular periodic behavior was observed for both. Moreover, the prescribed kinematic swimmers were unable to swim in the inviscid regime due to time-reversibility, while coherent locomotion was consistently observed for both the forced and prescribed kinematic swimmers at $Re = 70, 140, 350, 560, 700$. Finally, after the initial submission of this article, a series of numerical experiments to test this "limit-cycle hypothesis" were performed for n-linked swimmers. Here, the authors viewed swimming as analogous to the emergence of limit cycles in a forced-damped harmonic oscillator in what they refer to as the "forced-damped-oscillation framework." The numerical experiments consisted of placing an n-linked chain with

[1] Central patter generators (CPGs) are neural networks which produce time-periodic signals.

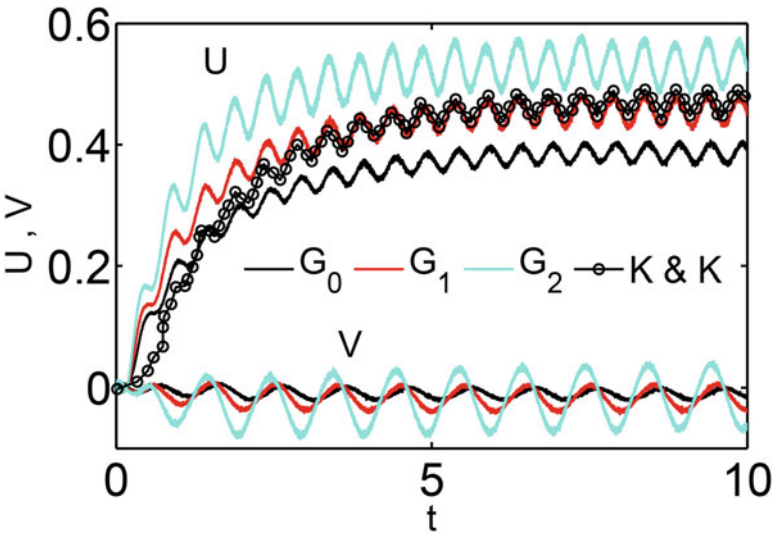

Fig. 2 A plot taken from [44] of the horizontal velocity, U, and vertical velocity, V, of n-linked swimmers with time-periodic internal body forces

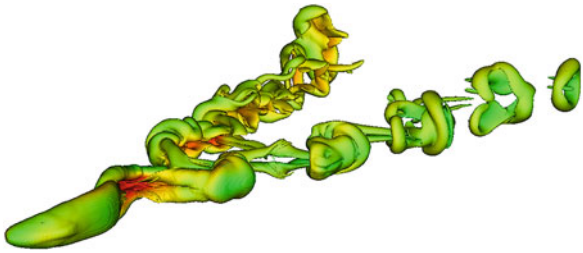

Fig. 3 A vorticity isosurface of an n-linked swimmer courtesy of [7]

an elastic restoring force on the joint angles into a Navier-Stokes fluid using the immersed body method. The results consistently suggested that the dynamics admit a stable relative limit cycle [7] (Figure 3).

In this paper we will approach the problem of fluid-structure interaction in Navier-Stokes fluids as an instance of Lagrangian reduction by symmetry [9]. Recent work based upon a modest generalization of [3] has accomplished this reduction by viewing the configuration space of fluid-structure interaction as a $\mathrm{Diff}_{\mathrm{vol}}(\approx\!\!\approx_{b_0})$-principal bundle, where $\mathrm{Diff}_{\mathrm{vol}}(\approx\!\!\approx_{b_0})$ is the diffeomorphism group for the reference-domain of the fluid [22]. In particular, the standard equations of motion for a passive body immersed in a Navier-Stokes fluid can be seen as dissipative Lagrange-Poincaré equations. Following Professor Marsden's tradition of giving credit to Jean le Rond d'Alembert for his formulation of the Lagrange-d'Alembert principle, it would be fair to label the equations of motion for a body immersed in a Navier-Stokes fluid as an instance of *Lagrange-Poincaré-d'Alembert equations*. Just as [3] allowed geometers to replace the coordinate-based description

of an Euler fluid with an Euler-Poincaré equation, [22] will serve as a sanity check for us, and allow us to replace the equations for a Navier-Stokes fluid coupled to an elastic solid with a Lagrange-Poincaré-d'Alembert equation.

It is worth noting that the constructions to be presented in this paper are different from those typically employed in applications of differential geometry to fluid-structure interaction. In the low Reynolds regime, one frequently encounters geometric constructions initially articulated in [41]. Similarly, in the potential flow regime, a similar set of constructions was described in [28]. Both of these constructions lead to a number of insights in aquatic locomotion at extreme Reynolds numbers [12, 24–27, 38]. Principal connections are crucial for these constructions, but interpolating between these extreme Reynolds regimes has proven difficult. In particular, *there will be absolutely no principal connections in this paper*. Moreover, in the inviscid regime vorticity shedding does not occur. Yet, vorticity shedding plays a fundamental role for biolocomotion in the middle and high Reynolds swimming [45]. An expansion of geometric mechanics to the Navier-Stokes regime is one goal of this paper.

1.3 Conventions and Notation

All objects and morphisms will be assumed to be sufficiently smooth. Moreover, we will not address the existence or uniqueness of solutions for fluid-structure systems and all algebraic manipulations will be interpreted formally. If M is a smooth manifold then we will denote the tangent bundle by $\tau_M : TM \to M$, and the tangent lift of a map $f : M \to N$ will be denoted $Tf : TM \to TN$. The set of vector fields on M will be denoted $\mathfrak{X}(M)$ and the set of time-periodic vector fields on M will be denoted $\mathfrak{X}(M)^{S^1}$. A deformation of a vector field $X \in \mathfrak{X}(M)$ is a continuous[2] sequence of vector fields $X_\varepsilon \in \mathfrak{X}(M)$ parametrized by a real parameter $\varepsilon \in \mathbb{R}$ which takes values in a neighborhood of $0 \in \mathbb{R}$ and is such that $X_0 = X$. Given that $\mathfrak{X}(M)$ is contained in $\mathfrak{X}(M)^{S^1}$, we can consider time-periodic deformations of vector fields as well. The flow of a vector-field, X, (perhaps time-dependent) will be denoted by Φ_t^X. Lastly, given any map $f : M \to N$, the map $f^{-1} : f(M) \subset N \to \mathrm{Set}(M)$ is the set-valued map defined by $f^{-1}(n) = \{m \in M \,|\, f(m) = n\}$.

2 Limit Cycles

Let M be a finite-dimensional Riemannian manifold with norm $\|\cdot\| : TM \to \mathbb{R}$. We can use the norm to define the notion of exponential stability. Informally, an exponentially stable equilibrium is an equilibrium for which nearby trajectories are

[2] We view $\mathfrak{X}(M)$ as a Fréchet vector space.

attracted to at an exponential rate. Formally, we say an equilibrium is *exponentially stable* if the spectrum of the linearized system lies *strictly* in the left half of the complex plane. However, the following (and equivalent) definition will be of greater use.

Definition 1. Let $x^* \in M$ be an equilibrium of the vector field $X \in \mathfrak{X}(M)$. Let $TX \in \mathfrak{X}(TM)$ be the tangent lift of X. We call x^* an *exponentially stable equilibrium* if there exists a $\lambda < 0$ such that

$$\frac{d}{dt}\|v(t)\| < \lambda\|v(0)\|, \quad \forall t > 0$$

where $v(t)$ is a solution curve of TX.

If one prefers to view exponential stability in terms of flows, we can use the Riemannian distance metric $d : M \times M \to \mathbb{R}$. Then, an exponentially stable equilibrium $x^* \in M$ of a vector field $X \in \mathfrak{X}(M)$ is an equilibrium where there exists a neighborhood $U \subset M$ containing x^* such that for any integral curve $x(t)$ with $x(0) \in U$ the equation

$$d(x(t), x^*) < e^{\lambda t} d(x(0), x^*), \quad \forall t > 0$$

holds for some $\lambda < 0$.

A special property of exponentially stable equilibria is what some control theorists call *robustness* [49] and what some dynamical systems theorists call *persistence* [13, 14, 19]. Let $X_\varepsilon \in \mathfrak{X}(M)$ be a deformation of the vector field $X \in \mathfrak{X}(M)$. Given an exponentially stable point $x^* \in M$ of X, we can assert the existence of exponentially stable equilibria of X_ε for sufficiently small ε. This robustness of behavior can be vastly generalized by considering normally hyperbolic invariant manifolds.

Definition 2 (Normally Hyperbolic Invariant Manifold[3]). Let $N \subset M$ be a compact invariant submanifold of the vector field $X \in \mathfrak{X}(M)$, and let Φ_t^X be the flow of X. We call N a *normally hyperbolically invariant manifold* if there exists a $T\Phi_t$-invariant splitting $T_N M \equiv TN \oplus E^s \oplus E^u$ and rates $\rho^s < -\rho < 0 < \rho < \rho^u$ such that

$$\|T\Phi_t^X(v)\| \leq C \cdot e^{\rho|t|}\|v\|, \quad \forall v \in TN, t \in \mathbb{R} \tag{2}$$

$$\|T\Phi_t^X(v)\| \leq C_u \cdot e^{\rho_u t}\|v\|, \quad \forall v \in E^u, t \leq 0 \tag{3}$$

$$\|T\Phi_t^X(v)\| \leq C_s \cdot e^{\rho_s t}\|v\|, \quad \forall v \in E^s, t \geq 0 \tag{4}$$

for some constants $C, C_u, C_s > 0$. If E^u has trivial fibers, then we call N an *exponentially stable invariant manifold*.

[3]This definition was taken from the introduction of [13] and is equivalent to the definition used in [19].

Now that we are equipped with the definition of a normally hyperbolic invariant manifold, we can state the persistence theorem (a.k.a. Fenichel's theorem).

Theorem 1 (See Theorem 1 of [14] or Section 4 of [19]). *Let $X_\varepsilon \in \mathfrak{X}(M)$ be a deformation of $X \in \mathfrak{X}(M)$ and let $N \subset M$ be a compact normally hyperbolic invariant manifold of X. Then for sufficiently small $\varepsilon > 0$ there exists a normally hyperbolic invariant manifold, $N_\varepsilon \subset M$ of X_ε which is diffeomorphic to N and contained in a neighborhood of N.*

We will not need Theorem 1 in its full generality because we will only be concerned with a special instance of normally hyperbolic invariant manifolds. In particular, we will be concerned with exponentially stable limit cycles.

Definition 3 (Exponentially Stable Limit Cycle). An exponentially stable invariant manifold which is homeomorphic to S^1 is called an *exponentially stable limit cycle*.

We can alternatively define an exponentially stable limit cycle using the distance metric $d : M \times M \to \mathbb{R}$. Given a periodic trajectory $x^*(t)$, the orbit Γ is an exponentially stable limit cycle if there exists a neighborhood U of Γ and a contraction rate $\lambda < 0$ such that

$$d(x(t), \Gamma) \leq e^{\lambda t} d(x(0), \Gamma) \quad \forall t > 0$$

for all solution curves $x(t)$ with $x(0) \in U$. In any case, a direct corollary of Theorem 1 is the persistence of exponentially stable limit cycles. That is to say:

Corollary 1. *Let Γ be an exponentially stable limit cycle of $X \in \mathfrak{X}(M)$ and let $X_\varepsilon \in \mathfrak{X}(M)$ be a deformation of X. Then for sufficiently small $\varepsilon > 0$ there exists an exponentially stable limit cycle Γ_ε of X_ε which is in a neighborhood of Γ.*

Given a time-periodic vector field $Y \in \mathfrak{X}(M)^{S^1}$, we can consider the *autonomous* vector field on the time-augmented phase space $M \times S^1$ given by $Y \times \partial_\theta \in \mathfrak{X}(M \times S^1)$. In particular, the vector field $Y \times \partial_\theta$ corresponds to the autonomous dynamical system

$$\dot{\theta} = 1, \qquad \dot{x} = Y(x, \theta).$$

If the vector field $Y \times \partial_\theta$ admits an exponentially stable limit cycle $(x(t), \theta(t)) \in M \times S^1$, then $\theta(t) := t \mod 2\pi$ and $x(t)$ is 2π-periodic. This observation justifies the following definition.

Definition 4. Let $Y \in \mathfrak{X}(M)^{S^1}$. Given a periodic solution curve $x(t) \in M$, we call the orbit $\Gamma := x(S^1)$ a *non-autonomous exponentially stable limit cycle* if $\Gamma \times S^1$ is an exponentially stable limit cycle for $Y \times \partial_\theta$.

Given the definition of a non-autonomous exponentially stable limit cycle, we can specialize Corollary 1 to the case of time-periodic dynamical systems. In particular, we arrive at:

Proposition 1. *Let $x^* \in M$ be an exponentially stable equilibrium of $X \in \mathfrak{X}(M)$ and let $X_\varepsilon \in \mathfrak{X}(M)^{S^1}$ be a time-periodic deformation of X. Then for sufficiently small $\varepsilon > 0$ the vector field X_ε admits a non-autonomous exponentially stable limit cycle in a neighborhood of x^*.*

Proof. Because x^* is an exponentially stable equilibrium of X, we can see that (x^*, θ) for $\theta \in S^1$ is a solution curve of $X \times \partial_\theta$ with orbit $\{x^*\} \times S^1$. In particular, $\{x^*\} \times S^1$ is an exponentially stable limit cycle with a contraction rate ρ_s equal to the contraction rate of x^* in the dynamical system defined by $\dot{x} = X(x)$. By Corollary 1, the vector field $X_\varepsilon \times \partial_\theta \in \mathfrak{X}(M \times S^1)$ also exhibits a limit cycle, $(x_\varepsilon(\theta), \theta)$, in a neighborhood of $\{x^*\} \times S^1$. This means that $x_\varepsilon(\theta)$ is a non-autonomous exponentially stable limit cycle for X_ε in a neighborhood of x^*. □

The significance of Proposition 1 is that we can time-periodically deform systems with exponentially stable equilibria to produce non-autonomous exponentially stable limit cycles.

Example 1. Consider the equations of motion for a perturbed linear damped mass-spring system,

$$\frac{d}{dt}\begin{bmatrix} x \\ y \end{bmatrix} = \begin{bmatrix} y \\ -x - y \end{bmatrix} + \varepsilon \begin{bmatrix} 0 \\ \sin(t) \end{bmatrix}. \tag{5}$$

We see that for $\varepsilon = 0$, the system admits an exponentially stable point $(x, \dot{x}) = (0, 0)$. When $\varepsilon > 0$, the non-autonomous limit cycle of Proposition 1 emerges. Typical trajectories of the system for $\varepsilon = 0, 1$ are shown in Figures 4 and 5.

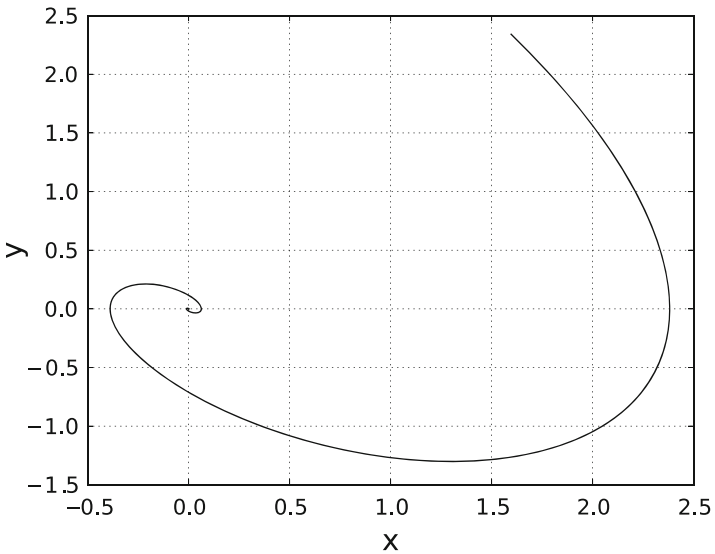

Fig. 4 A trajectory of (5) with $\varepsilon = 0$

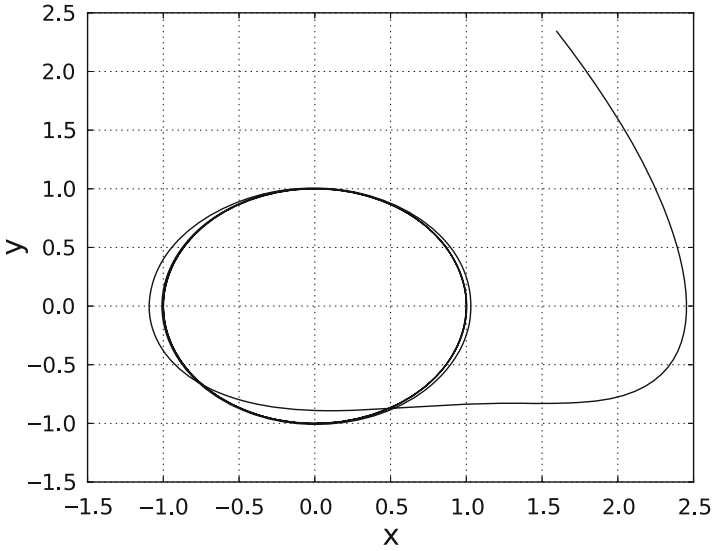

Fig. 5 A trajectory of (5) with $\varepsilon = 1$

3 Relative Limit Cycles

In this section we will consider dynamical systems with Lie group symmetries. Let G be a Lie group which acts on M by a left action. The G-orbit of a point $x \in M$ is the set $[x] := \{g \cdot x | g \in G\} \equiv G \cdot x$. We denote the quotient space by $[M] := \{[x] : x \in M\}$ and we call the map $\pi : x \in M \mapsto G \cdot x \in [M]$ the quotient projection. If the action of G is free and proper, then the quotient projection is a smooth surjection and the triple $(M, [M], \pi)$ is a fiber bundle known as a *principal G-bundle* [1, Proposition 4.1.23].

We now present the natural notions of G-invariance for function on M. Note that for any $[f] \in C^\infty([M])$, we can define the smooth function $[f] \circ \pi \in C^\infty(M)$. Moreover, $[f] \circ \pi$ is G-invariant because

$$[f] \circ \pi(g \cdot x) = [f](G \cdot (g \cdot x)) = [f](G \cdot x) = [f] \circ \pi(x).$$

Conversely, for a G-invariant function $f \in C^\infty(M)$, we see that $f(G \cdot x) = f(x)$. Noting that the left-hand side of this equation involves the application of f to a G-orbit, we have apparently found a function $[f] \in C^\infty([M])$ such that $[f] \circ \pi = f$. In other words, the set of G-invariant functions on M is identifiable with the set of smooth function on $[M]$.

This G-invariance for functions on M extends to G-invariant vector fields. We do this by extending the action on M to an action on TM by the tangent lift. In particular, the action of g on a point $v = \frac{dx}{dt} \in TM$ is given by

$$g \cdot v := \left.\frac{d}{dt}\right|_{t=0} (g \cdot x(t)).$$

In this case, we call $X \in \mathfrak{X}(M)$ a G-invariant vector field if

$$g \cdot X(x) = X(g \cdot x) \quad \forall g \in G, x \in M. \tag{6}$$

Moreover, the flow Φ_t^X is G-invariant as well. For if X is G-invariant and $x(t) \in M$ is a solution curve, then

$$\frac{d}{dt}(g \cdot x(t)) = g \cdot \dot{x}(t) = g \cdot X(x(t)) = X(g \cdot x(t)).$$

Thus, $g \cdot x(t)$ is a solution and so $g \circ \Phi_t^X = \Phi_t^X \circ g$.

Proposition 2. *If $X \in \mathfrak{X}(M)$ is G-invariant then there exists a unique vector field $[X] \in \mathfrak{X}([M])$ such that $T\pi \cdot X = [X] \circ \pi$. Moreover, the flow of $[X]$ is π-related to the flow of X. In other words, the diagrams*

$$\begin{array}{ccc} M & \xrightarrow{X} & TM \\ \downarrow{\scriptstyle \pi} & & \downarrow{\scriptstyle T\pi} \\ [M] & \xrightarrow{[X]} & T[M] \end{array} \qquad , \qquad \begin{array}{ccc} M & \xrightarrow{\Phi_t^X} & M \\ \downarrow{\scriptstyle \pi} & & \downarrow{\scriptstyle \pi} \\ [M] & \xrightarrow{\Phi_t^{[X]}} & [M] \end{array}$$

are commutative.

Given a pair $X \in \mathfrak{X}(M)$ and $[X] \in \mathfrak{X}([M])$ which satisfies (6), we call $[X]$ the reduced vector field and X the unreduced vector field. This correspondence between X and $[X]$ allows us to discuss relative periodicity.

Definition 5 (Relative Periodicity). Let $X \in \mathfrak{X}(M)$ be a G-invariant vector field on the G-principal bundle $\pi : M \to [M]$. Let $[X] \in \mathfrak{X}([M])$ be the reduced vector field. The orbit of a solution curve $x(t)$ of X is called a *relatively periodic orbit* if $\pi(x(t))$ is a periodic orbit of $[X]$.

A remarkable characteristic of relative periodic orbits is the following.

Proposition 3. *Let $X \in \mathfrak{X}(M)$ be a G-invariant vector field. If $x(t)$ is a relative periodic orbit of period T, then there exists some $g \in G$ such that $x(T) = g \cdot x(0)$. Moreover, $x(kT) = g^k \cdot x(0)$ for each $k \in \mathbb{Z}$.*

We call the element $g \in G$ of Proposition 3 the *phase shift* of the periodic orbit $\pi(x(t))$. To hint at the relevance of this concept to locomotion, we should mention that if $G = \mathrm{SE}(d)$, the phase shift implies that the system undergoes regular and periodic changes in position and orientation. We now seek to study exponentially stable manifestations of relative periodicity. This brings us to the notion of a relative limit cycle.

Definition 6. An orbit $x(t) \in M$ of a G-invariant vector field $X \in \mathfrak{X}(M)$ is called a *relative exponentially stable limit cycle* if $\pi(x(t))$ is an exponentially stable limit cycle for the reduced vector field $[X]$. Finally, if $Y \in \mathfrak{X}(M)^{S^1}$ is G-invariant with reduced vector field $[Y] \in \mathfrak{X}_{S^1}([M])$, then we call the orbit of a trajectory $x(t) \in M$ a *non-autonomous exponentially stable relative limit cycle* if $\pi(x(t)) \in [M]$ is a non-autonomous exponentially stable limit cycle.

Proposition 4. *Let $X \in \mathfrak{X}(M)$ be G-invariant, and let $[X] \in \mathfrak{X}([M])$ be the reduced vector field of X. Let $\Gamma \subset [M]$ be a limit cycle of $[X]$. Then there exists an open neighborhood U of $\pi^{-1}(\Gamma) \subset M$ wherein each point is attracted towards a relative limit cycle contained in $\pi^{-1}(\Gamma)$.*

Before we provide the proof of this proposition, it is useful to illustrate the following lemma which relates the distance metric on M with the natural distance metric on $[M]$.

Lemma 1. *If the Riemannian metric on M is G-invariant, then the distance metric $d : M \times M \to \mathbb{R}$ is G-invariant as well. The function on $[M] \times [M]$ given by $[d]([x],[y]) := d(G \cdot x, G \cdot y)$ is a metric and satisfies the equality $d(x, G \cdot y) = [d]([x],[y])$.*

Equipped with Lemma 1, we are now ready to prove Proposition 4.

Proof (Proof of Proposition 4). Let $[U]$ be a neighborhood of Γ. Then $U = \pi^{-1}([U]) \subset M$ is an open set as well, since π is continuous. Therefore, given an arbitrary $x \in U$, we see by Lemma 1 that $\frac{d}{dt}(d(x, \pi^{-1}(\Gamma))) = \frac{d}{dt}(d(\pi(x), \Gamma)) < \lambda d(\pi(x), \Gamma) = \lambda d(x, \pi^{-1}(\Gamma))$. Thus, the solution is attracted towards $\pi^{-1}(\Gamma)$. However, $\pi^{-1}(\Gamma)$ is foliated by relative limit cycles. □

Later we will want to see how time-periodic perturbations generate stable and relatively periodic behavior. This motivates us to state the following proposition.

Proposition 5. *Let $X \in \mathfrak{X}(M)$ be G-invariant and let $[X] \in \mathfrak{X}([M])$ be the reduced vector field of X. Let q^* be an exponentially stable equilibria of $[X]$. If $X_\varepsilon \in \mathfrak{X}(M)^{S^1}$ is a time-periodic G-invariant deformation of X, then for sufficiently small $\varepsilon > 0$ the vector field X_ε admits a non-autonomous exponentially stable relative limit cycle.*

Proof. Let $[X_\varepsilon] \in \mathfrak{X}([M])^{S^1}$ be the reduced vector field corresponding to X_ε for each ε. We can then verify that $[X_\varepsilon]$ is a deformation of $[X]$. By Proposition 1, the vector field $[X_\varepsilon]$ admits a non-autonomous exponentially stable limit cycle for sufficiently small ε. It follows that X_ε must admit non-autonomous exponentially stable relative limit cycles. □

Example 2. Consider the system on $\mathbb{R}^3$ given by

$$\frac{d}{dt}\begin{bmatrix} x \\ y \\ z \end{bmatrix} = \begin{bmatrix} y \\ -x - y \\ y - x^2 - xy \end{bmatrix} + \varepsilon \begin{bmatrix} 0 \\ \sin(t) \\ \cos(t) \end{bmatrix}. \tag{7}$$

We see that this system is invariant under translations in the z-coordinate. This is a $(\mathbb{R}, +)$-symmetry and the quotient projection is given by $\pi(x, y, z) = (x, y)$. The reduced vector field is given by equation (5). By Proposition 5, (7) must admit relative limit cycles for sufficiently small $\varepsilon > 0$. Moreover, as the symmetry of the system is along the z-axis, by Proposition 3 each period of the relative limit cycle should be related to the previous period by a constant vertical shift. Typical trajectories for $\varepsilon = 0, 1$ are depicted in Figures 6 and 7

Example 2 illustrates how a $(\mathbb{R}, +)$-symmetry lead to a system with a stable non-autonomous relative limit cycle wherein each period was related to the previous by a constant translation along the z-axis. The goal of this article is to characterize swimming as a stable non-autonomous relative limit cycle with respect to an $\mathrm{SE}(d)$-symmetry wherein each period is related to the previous by a constant translation and rotation of space. In order to do this, we must express fluid-structure problems in a geometric formalism. In particular, we will follow the constructions of [22] to do this, using the Lagrange-d'Alembert formalism.

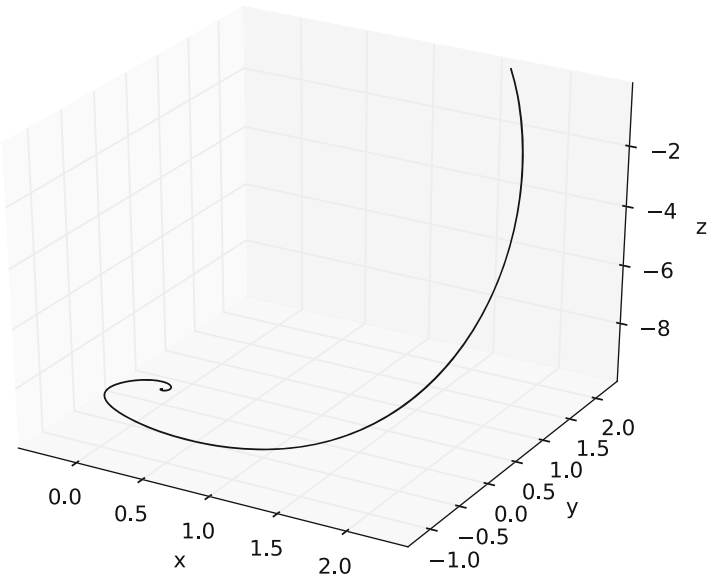

Fig. 6 A trajectory of (7) with $\varepsilon = 0$

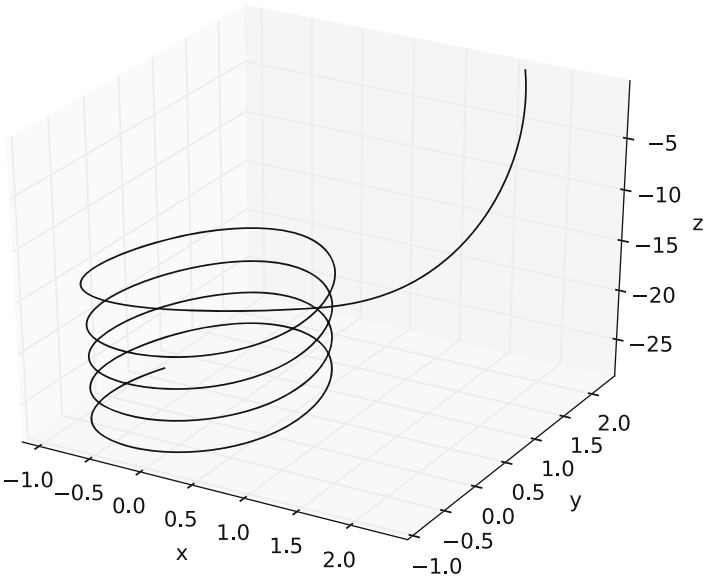

Fig. 7 A trajectory of (7) with $\varepsilon = 1$

4 Lagrange-d'Alembert Formalism

In this section, we review the Lagrange-d'Alembert formalism for simple mechanical systems. If Q is equipped with a Riemanian metric, $\langle \cdot, \cdot \rangle_Q : TQ \oplus TQ \to \mathbb{R}$, then it is customary to consider Lagrangians of the form

$$L(q, \dot{q}) = \frac{1}{2}\langle \dot{q}, \dot{q} \rangle_Q - U(q), \tag{8}$$

where $U : Q \to \mathbb{R}$. We call a Lagrangian of this form a *simple mechanical Lagrangian*. For simple mechanical Lagrangians, and external force fields $F : TQ \to T^*Q$, the Lagrange-D'Alembert equations take the form

$$\frac{D\dot{q}}{Dt} = \nabla U(q) + \sharp\left(F(q, \dot{q})\right), \tag{9}$$

where $\frac{D}{Dt}$ is the Levi-Cevita covariant derivative, ∇U is the gradient of U, and $\sharp : T^*Q \to TQ$ is the sharp operator induced by the Riemannian metric [1, Proposition 3.7.4]. It is notable that (9) is equivalent to the Lagrange-d'Alembert variational principle

$$\delta \int_0^T L(q, \dot{q}) dt = \int_0^T \langle F(q, \dot{q}), \delta q \rangle dt$$

with respect to variations δq with fixed end points [35, Chapter 7]. We denote the vector field associated to (9) by $X_{TQ} \in \mathfrak{X}(TQ)$, and its flow is given by Φ_t^{TQ}.

5 Fluid-Structure Interaction

In this section, we will place fluid structure-interactions in the Lagrange-d'Alembert formalism. Specifically, we will understand a body immersed in a fluid as a simple mechanical Lagrangian system with a dissipative force field, in the sense of (9). This is commonly referred to as the "material description" in fluid mechanics. Moreover, we will reduce the system by a particle relabeling symmetry, so that the fluid is described in the "spatial description" via the Navier-Stokes equations. Finally, we will identify 'frame-invariance' (a.k.a objectivity) as a left $\mathrm{SE}(d)$-symmetry.

5.1 Navier Stokes Fluids in the Lagrange-d'Alembert Formalism

In this paper, we seek to understand swimming in the mid-Reynolds regime. Specifically this entails invoking the Navier-Stokes equations with non-zero viscosity. It was discovered in [3] that the Navier-Stokes equations with zero viscosity could be handled in the Euler-Poincaré formalism. Moreover, it is mentioned in [4, Chapter 1, section 12] that the Navier-Stokes equations can be viewed in this framework with the simple addition of a dissipative force. In this section, we will describe this formulation of the Navier-Stokes equations.

Consider the manifold $\mathbb{R}^d$ with the standard flat metric and volume form $dx = dx^1 \wedge \cdots \wedge dx^d$. One can consider the infinite-dimensional Lie group of volume-preserving diffeomorphisms, $\mathrm{Diff}_{\mathrm{vol}}(\mathbb{R}^d)$, where the group multiplication is simply the composition of diffeomorphisms.[4] The configuration of a fluid flowing on $\mathbb{R}^d$ relative to some reference configuration is described by an element $\varphi \in \mathrm{Diff}_{\mathrm{vol}}(\mathbb{R}^d)$. Given a curve $\varphi_t \in \mathrm{Diff}_{\mathrm{vol}}(\mathbb{R}^d)$, one can differentiate it to obtain a tangent vector $\dot{\varphi}_t = \frac{d}{dt}\varphi_t \in T\,\mathrm{Diff}_{\mathrm{vol}}(\mathbb{R}^3)$. One can interpret $\dot{\varphi}$ as a map from $\mathbb{R}^d$ to $T\mathbb{R}^d$ by the natural definition $\dot{\varphi}(x) = \frac{d}{dt}\varphi_t(x)$. Therefore, a tangent vector, $\dot{\varphi} \in T\,\mathrm{Diff}_{\mathrm{vol}}(\mathbb{R}^d)$, over a diffeomorphism $\varphi \in \mathrm{Diff}_{\mathrm{vol}}(\mathbb{R}^d)$ is simply the smooth map $\dot{\varphi} : \mathbb{R}^d \to T\mathbb{R}^d$, such that $\tau_{\mathbb{R}^d} \circ \dot{\varphi} = \varphi$ where $\tau_{\mathbb{R}^d} : T\mathbb{R}^d \to \mathbb{R}^d$ is the tangent bundle projection. Moreover, $\dot{\varphi} \circ \varphi^{-1}$ is a smooth divergence-free vector field on $\mathbb{R}^d$. We call $\dot{\varphi}$ the *material* representation of the velocity, while $\dot{\varphi} \circ \varphi^{-1} \in \mathfrak{X}_{\mathrm{vol}}(\mathbb{R}^d)$ is the spatial representation. The Lagrangian, $L : T(\mathrm{Diff}_{\mathrm{vol}}(\mathbb{R}^d)) \to \mathbb{R}$, is the kinetic energy of the fluid,

$$L(\varphi, \dot{\varphi}) := \frac{1}{2} \int_{\mathbb{R}^d} \|\dot{\varphi}(x)\|^2 dx.$$

[4] This is a pseudo Lie group. We will assume that all diffeomorphisms approach the identity as $\|x\| \to \infty$ sufficiently rapidly for all computations to make sense. In particular, the existence of a Hodge-decomposition for our space is important. Sufficient conditions for our purposes are provided in [8] and [43].

One can derive the Euler-Lagrange equations on $\mathrm{Diff}_{\mathrm{vol}}(\mathbb{R}^d)$ with respect to the Lagrangian L to obtain the equations of motion for an ideal fluid. However, this Lagrangian exhibits a symmetry.

Proposition 6 ([3]). *The Lagrangian L is symmetric with respect to the right action* $\mathrm{Diff}_{\mathrm{vol}}(\mathbb{R}^d)$ *on* $T\,\mathrm{Diff}_{\mathrm{vol}}(\mathbb{R}^d)$.

Moreover, it is simple to verify the proposition:

Proposition 7. *The action of* $\mathrm{Diff}_{\mathrm{vol}}(\mathbb{R}^d)$ *on* $T\,\mathrm{Diff}_{\mathrm{vol}}(\mathbb{R}^d)$ *is free and proper. The quotient space* $T\,\mathrm{Diff}_{\mathrm{vol}}(\mathbb{R}^d)/\,\mathrm{Diff}_{\mathrm{vol}}(\mathbb{R}^d) = \mathfrak{X}_{\mathrm{div}}(\mathbb{R}^d)$ *and the quotient projection is the right Maurer-Cartan form,*

$$\rho : (\varphi, \dot{\varphi}) \in T\,\mathrm{Diff}(\mathbb{R}^d) \mapsto u = \dot{\varphi} \circ \varphi^{-1} \in \mathfrak{X}_{\mathrm{div}}(\mathbb{R}^d).$$

This symmetry is referred to as the *particle relabeling symmetry*. As a result of this symmetry, Proposition 2 suggests that we can write equations of motion on $\mathfrak{X}_{\mathrm{div}}(\mathbb{R}^d)$. It was the discovery of [3] that these equations could be written as

$$\partial_t u + u \cdot \nabla u = -\nabla p, \quad \mathrm{div}(u) = 0,$$

which one will recognize as the inviscid fluid equations. Moreover, if we define the linear map, $f_\mu : \mathfrak{X}_{\mathrm{vol}}(\mathbb{R}^d) \to \mathfrak{X}^*_{\mathrm{vol}}(\mathbb{R}^d)$ given by

$$\langle f_\mu(u), w \rangle = \mu \int_{\mathbb{R}^d} \Delta u(x) \cdot w(x) dx,$$

then we derive the Lagrange-D'Alembert equations by lifting f_μ (via the right Maurer-Cartan form) to obtain a force field $F : T(\mathrm{Diff}_{\mathrm{vol}}(\mathbb{R}^3)) \to T^*(\mathrm{Diff}_{\mathrm{vol}}(\mathbb{R}^3))$. If we do this, then reduction by $\mathrm{Diff}_{\mathrm{vol}}(\mathbb{R}^3)$ yields a spatial velocity field, $u(t)$, which satisfies the Navier-Stokes equations

$$\partial_t u + u \cdot \nabla u = -\nabla p - \mu \Delta u, \quad \mathrm{div}(u) = 0.$$

5.2 Solids

Let $\mathscr{B}$ be a compact manifold with boundary $\partial\mathscr{B}$ and volume form $d\,\mathrm{vol}_{\mathscr{B}}$. Let $\mathrm{Emb}(\mathscr{B})$ denote the set of embeddings of $\mathscr{B}$ into $\mathbb{R}^d$. Finally, let $\mathrm{SE}(d)$ denote the set of isometries of $\mathbb{R}^d$.

We view each $b \in \mathrm{Emb}(\mathscr{B})$ as a map $b : \mathscr{B} \hookrightarrow \mathbb{R}^d$, while viewing $z \in \mathrm{SE}(d)$ as a map $z : \mathbb{R}^d \to \mathbb{R}^d$. We can compose these maps to obtain a new map $z \circ b : \mathscr{B} \hookrightarrow \mathbb{R}^d$, which itself embeds $\mathscr{B}$ into $\mathbb{R}^d$. That is to say, the assignment $b \mapsto z \circ b$ is a left action of $\mathrm{SE}(d)$ on $\mathrm{Emb}(\mathscr{B})$. It is elementary to observe that this action is free and proper, and makes $\mathrm{Emb}(\mathscr{B})$ into an $\mathrm{SE}(d)$-principal bundle. The configuration

manifold for the body is given by a $\mathrm{SE}(d)$-invariant submanifold $B \subset \mathrm{Emb}(\mathscr{B})$ (possibly finite-dimensional). Therefore, the quotient space $[B] = \frac{B}{\mathrm{SE}(d)}$ is a smooth manifold and $\pi^B_{[B]} : B \to [B]$ is a $\mathrm{SE}(d)$-principal bundle as well. We call $[B]$ the *shape-space*, following [36].

The Lagrangian for the body, $L_B : TB \to \mathbb{R}$, will be that of a simple mechanical system. The reduced-potential energy will be given by a function $[U] : [B] \to \mathbb{R}$, and the potential energy is defined as $U := [U] \circ \pi^B_{[B]}$. Equivalently, we may define $U : B \to \mathbb{R}$ first, with the assumption that we choose something which is $\mathrm{SE}(d)$-invariant.

To define the kinetic energy, we must first understand the tangent bundle $TB \subset T\,\mathrm{Emb}(\mathscr{B})$. By applying the dynamic definition of tangent vectors, we can derive that a $(b, \dot{b}) \in T\,\mathrm{Emb}(\mathscr{B})$ must be a pair of maps, $b \in \mathrm{Emb}(\mathscr{B})$ and $\dot{b} : \mathscr{B} \hookrightarrow T\mathbb{R}^d$, such that $\dot{b}(x)$ is a vector over $b(x)$ for all $x \in \mathscr{B}$. Moreover, a $(b, \dot{b}) \in TB$ is an element of $T\,\mathrm{Emb}(\mathscr{B})$ tangential to $B \subset \mathrm{Emb}(\mathscr{B})$. We see that for each $z \in \mathrm{SE}(d)$, we can consider the map $Tz : T\mathbb{R}^d \to T\mathbb{R}^d$, and we define the action of z on TB by the assignment $(b, \dot{b}) \in TB \mapsto (z \circ b, Tz \circ \dot{b}) \in TB$. This defines a free and proper left $\mathrm{SE}(d)$ action on TB so that TB is an $\mathrm{SE}(d)$-principal bundle. We will assume the existence of an $\mathrm{SE}(d)$-invariant Riemannian metric $\langle \cdot, \cdot \rangle_{\mathscr{B}} : TB \oplus TB \to \mathbb{R}$, and that the kinetic energy is $K(b, \dot{b}) = \frac{1}{2}\langle (b, \dot{b}), (b, \dot{b}) \rangle_B$.

Finally, without any dissipation, our solid body could "jiggle" forever due to conservation of energy. To amend this, we will include a dissipative force given by a fiber-bundle map, $F_{\mathscr{B}} : T[B] \to T^*[B]$, such that the storage function

$$\langle F_{\mathscr{B}}(v_{[b]}), v_{[b]} \rangle : T[B] \to \mathbb{R} \tag{10}$$

is convex on each fiber of $T[B]$ and reaches a maximum at zero where it vanishes. For example, a negative definite quadratic form would be admissible. Such a force has the effect of dampening the rate of change in the shape of the body, but it will not dampen motions induced by the action of $\mathrm{SE}(d)$. In other words, we assume that a jiggling body eventually comes to rest with some shape $s_{\min} \in [B]$ by the dissipation of energy.

Example 3. Consider a two-link body in $\mathbb{R}^2$. The configuration manifold B consists of rigid embeddings of the two links into $\mathbb{R}^2$ such that the embeddings respect the constraint that the links are joined at the hinge (see Figure 8). In particular, B is isomorphic to a subset of $S^1 \times S^1 \times \mathbb{R}^2$ if we let the tuple $(\phi_1, \phi_2, x, y) \in S^1 \times S^1 \times \mathbb{R}^2$ denote a configuration where $\phi_1, \phi_2 \in S^1$ are the angles between the links and the x-axis, while $(x, y) \in \mathbb{R}^2$ is the location of the hinge. Under this identification, the action of an element $(\theta, X, Y) \in \mathrm{SE}(2)$ on $(\phi_1, \phi_2, x, y) \in B$ is given by

$$(\theta, X, Y) \cdot \begin{pmatrix} \phi_1 \\ \phi_2 \\ x \\ y \end{pmatrix} = \begin{pmatrix} \theta + \phi_1 \\ \theta + \phi_2 \\ \cos(\theta)x - \sin(\theta)y + X \\ \sin(\theta)x + \cos(\theta)y + Y \end{pmatrix}.$$

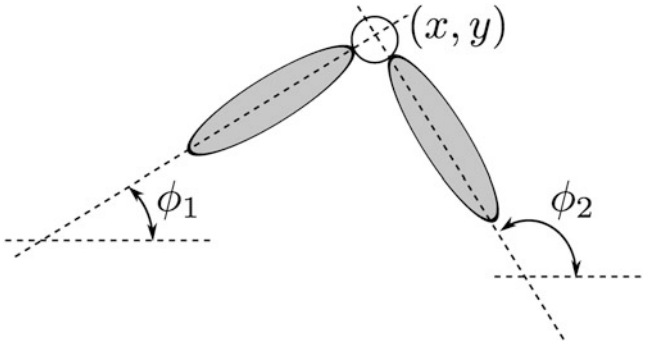

Fig. 8 A diagram of the swimmer from Example 3

Under this action, we find that the shape space is $[B] = S^1$ and that the quotient projection from B to $[B]$ is given by $\pi^B_{[B]}(\phi_1, \phi_2, x, y) = \phi_1 - \phi_2$. In other words, the shape of the body is described by the interior angle of the hinge. Finally, we may consider a potential energy derived from a linear spring between the hinges given by $U(\phi_1, \phi_2, x, y) = \frac{k}{2}(\phi_1 - \phi_2 - \bar{\theta})^2$ for some constant equilibrium interior angle $\bar{\theta} \in S^1$. It should be evident that this potential energy is SE(2)-invariant. The kinetic energy of the i^{th} body is

$$K_i = \frac{I_i}{2}\dot{\phi}_i^2 + \frac{M_i}{2}\left([\dot{x} - \sin(\phi_i)\dot{\phi}_i]^2 + [\dot{y} + \cos(\phi_i)\dot{\phi}_i]^2\right),$$

where M_i and I_i are the mass and rotational inertial of the i^{th} body, respectively. The Lagrangian is therefore $L_B = K_1 + K_2 - U$. Lastly, the force $F_B = \dot{\phi}_2 d\phi_2 - \dot{\phi}_1 d\phi_1$ provides an SE(2)-invariant elastic friction force. The effect of F_B is to dampen changes in the interior angle $\theta = \phi_2 - \phi_1$. In particular, θ parametrizes the shape space of this body, and so F_B can be said to dampen changes in shape.

Example 4. The theory of linear elasticity assumes $\mathscr{B}$ to be a Riemannian manifold with a mass density $\rho \in \bigwedge^n(\mathscr{B})$ and metric $\langle \cdot, \cdot \rangle_{\mathscr{B}} : T\mathscr{B} \oplus T\mathscr{B} \to \mathbb{R}$. Here, the configuration manifold is $B = \text{Emb}(\mathscr{B})$ and the potential energy is

$$U(b) = \frac{1}{2}\int_{b(\mathscr{B})} \text{trace}\left([I - C_b]^T \cdot [I - C_b]\right) b_* d\,\text{vol}_{\mathscr{B}},$$

where C_b is the push-forward of the metric $\langle \cdot, \cdot \rangle_{\mathscr{B}}$ by $b : \mathscr{B} \hookrightarrow \mathbb{R}^d$, a.k.a. the *right Cauchy-Green strain tensor*. The SE(d)-invariant kinetic energy, $K : TB \to \mathbb{R}$, is given by

$$K(b, \dot{b}) = \frac{1}{2}\int_{\mathscr{B}} \|\dot{b}(x)\|^2 \rho(x) dx.$$

This Lagrangian yields the standard model of linear elasticity and is known to be SE(d)-invariant, a.k.a. *objective* [34]. As we can not easily coordinate B in this example, we cannot expect to easily obtain a concrete description of the shape space, $[B]$. Nonetheless, by the SE(d)-invariance of U, there must exist a function $[U] : [B] \to \mathbb{R}$ such that $U = [U] \circ \pi^B_{[B]}$.

The above examples are merely instances of possible models we may choose for the body. Identifying a physical model of the solid body is a necessary precondition for understanding the effect of internal body forces on the system. In particular, this is the approach taken in [44] and [7]. To quote [44], "the motion of the body emerges as a balance between internal muscular force and external fluid forces." The emphasis on the importance of the internal mechanics of the swimming body can become fairly sophisticated. These sophisticated solid-mechanical concerns can be important for understanding the role of passive mechanisms in biomechanics. For example, fibered structures can exhibit a "counter-bend phenomena" in which an increased curvature in one region of a structure yields a decrease elsewhere in ways which aide swimming [16]. These advanced topics will not be addressed here, but we recall them only to put this work in a proper context.

5.3 Fluid-Solid Interaction

Let $\mathscr{B}$, B, $L_{\mathscr{B}}$, $F_{\mathscr{B}}$ be as described in the previous section. Given an embedding $b \in B$, let $\approx_b$ denote the set

$$\approx_b = \text{closure}\left\{\mathbb{R}^d \setminus b\left(\mathscr{B}\right)\right\}.$$

The set $\approx_b$ is the region which will be occupied by the fluid given the embedding of the body b. If the body configuration is given by $b_0 \in B$ at time 0 and $b \in B$ at time t, then the configuration of the fluid is given by a volume-preserving diffeomorphism from $\approx_{b_0}$ to $\approx_b$, i.e. an element of $\text{Diff}_{\text{vol}}(\approx_{b_0}, \approx_b)$. Given a reference configuration $b_0 \in B$ for the body, we define the configuration manifold as

$$Q := \{(b, \varphi) \quad | \quad b \in B, \varphi \in \text{Diff}_{\text{vol}}(\approx_{b_0}, \approx_b)\}.$$

One should note that the manifold Q has some extra structure. In particular, the Lie group $G := \text{Diff}_{\text{vol}}(\approx_{b_0})$ represents the symmetry group for the set of particle labels, and acts on Q on the right by sending

$$(b, \varphi) \in Q \mapsto (b, \varphi \circ \psi) \in Q$$

for each $\psi \in G$ and $(b, \varphi) \in Q$. Given this action, the following proposition is self-evident.

Proposition 8. *The projection $\pi_B^Q : Q \to B$ defined by $\pi_B^Q(b, \varphi) = b$ makes Q into a principal G-bundle over B.*

Now we must define the Lagrangian. To do this, it is useful to note that the system should be invariant with respect to particle relabelings of the fluid, and so the Lagrangian should be invariant with respect to the right action of G on TQ given by

$$(b, \dot{b}, \varphi, \dot{\varphi}) \in TQ \mapsto (b, \dot{b}, \varphi \circ \psi, \dot{\varphi} \circ \psi) \in TQ$$

for each $\psi \in G$. As a result, we can define a Lagrangian on the quotient space TQ/G. Incidentally, this quotient space is much closer to the space typically encountered in fluid-structure interaction.

Proposition 9 (Proposition 2 of [22]). *The quotient space TQ/G can be identified with the set*

$$\begin{aligned} P := \{(b, \dot{b}, u) \quad | \quad & (b, \dot{b}) \in TB, \\ & u \in \mathfrak{X}_{\mathrm{div}}(\approx_b), \\ & u(b(x)) = \dot{b}(x), \forall x \in \partial\mathscr{B}\}. \end{aligned} \tag{11}$$

Under this identification, the quotient map $\pi_{/G}^{TQ} : TQ \to P$ is given by $\pi_{/G}^{TQ}(b, \dot{b}, \varphi, \dot{\varphi}) = (b, \dot{b}, \dot{\varphi} \circ \varphi^{-1})$. Moreover, P is naturally equipped with the bundle projection $\tau(b, \dot{b}, u) = b$ and the vector bundle structure $(b, \dot{b}_1, u_1) + (b, \dot{b}_2, u_2) = (b, \dot{b}_1 + \dot{b}_2, u_1 + u_2)$, for all $(b, \dot{b}_1, u_1), (b, \dot{b}_2, u_2) \in \tau^{-1}(b)$ and all $b \in B$.

Proof. Observe that $\pi_{/G}^{TQ}(v \circ \psi) = \pi_{/G}^{TQ}(v)$ for all $\psi \in G$ and $v \in TQ$. Therefore, $\pi_{/G}^{TQ}$ maps the coset $v \cdot G$ to a single element of P. Conversely, given an element $(b, \dot{b}, u) \in P$, we see that $(\pi_{/G}^{TQ})^{-1}(b, \dot{b}, u)$ is the set of element in $(b, \dot{b}, \varphi, \dot{\varphi}) \in TQ$ such that $u = \dot{\varphi} \circ \varphi^{-1}$. However, this set of elements is just the coset $v \cdot G$, where v is any element such that $\pi_{/G}^{TQ}(v) = (b, \dot{b}, u)$. Thus, $\pi_{/G}^{TQ}$ induces an isomorphism between TQ/G and P. Additionally, we can check that $\pi_{/G}^{TQ}(v + w) = \pi_{/G}^{TQ}(v) + \pi_{/G}^{TQ}(w)$ and $\tau(\pi_{/G}(v)) = \tau_Q(v) \cdot G$. Therefore, the desired vector bundle structure is inherited by P as well, and $\pi_{/G}$ becomes a vector bundle morphism. Finally, the map $\rho(b, \dot{b}, u) = (b, \dot{b})$ is merely the map $T\pi_B^Q : TQ \to TB$ modulo the action of G. That is to say, $\rho \circ \pi_{/G}^{TQ} = T\pi_B^Q$. This equation makes ρ well-defined because π_G^Q is G-invariant. □

As a guide for the reader, we provide the following commutative diagram.

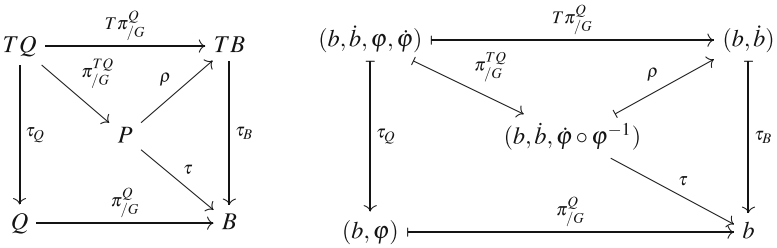

Note that the fluid velocity component $u \in \mathfrak{X}_{\text{div}}(\approx_b)$ for a $(b, \dot{b}, u) \in P$ may point in directions transverse to the boundary of the fluid domain $\approx_b$. This reflects the fact that the boundary is time-dependent. The condition $\dot{b}(x) = u(b(x))$ on the boundary states that the boundary of the body moves with the fluid, and is the mathematical description of the no-slip condition.

We now define the reduced Lagrangian $\ell : P \to \mathbb{R}$ by

$$\ell(b, \dot{b}, u) = L_{\mathscr{B}}(b, \dot{b}) + \frac{1}{2} \int_{\approx_b} \|u(x)\|^2 dx.$$

This induces the standard Lagrangian

$$L := l \circ \pi^{TQ}_{/G} : TQ \to \mathbb{R}, \tag{12}$$

which is a simple mechanical Lagrangian consisting of the kinetic energy of the fluid and body minus the potential energy of the body described in Section 5.2. Moreover, L is G-invariant by construction.

Additionally, we wish to add a viscous force on the fluid, $F_\mu : TQ \to T^*Q$. Given a coefficient of viscosity, μ, we can define the reduced viscous friction force field $f_\mu : P \to P^*$ by

$$\langle f_\mu(b, v_b, u), (b, w_b, w) \rangle = \mu \int_{\approx_b} \Delta u(x) \cdot w(x) dx,$$

and define the unreduced force $F_\mu : TQ \to T^*Q$ by

$$\langle F_\mu(v), w \rangle = \langle f_\mu(\pi_{/G}(v)), \pi_{/G}(w) \rangle.$$

We finally define the total force on our system to be

$$F = F_\mu + (F_{\mathscr{B}} \circ T\pi^Q_B), \tag{13}$$

where $F_{\mathscr{B}}$ is the dissipative force on the shape of the body mentioned in §5.2. This total force F descends via $\pi_{/G}$ to a reduced force $F_{/G} : P \to P^*$ where P^* is the

dual vector bundle to P. The reduced force is given explicitly in terms of f_μ and $F_{\mathscr{B}}$ by $F_{/G} = f_\mu + (F_{\mathscr{B}} \circ \rho)$. One can verify directly from this expression that $\langle F(v), w\rangle = \langle F_{/G}(\pi_{/G}(v)), \pi_{/G}(w)\rangle$.

We now introduce a consequence which follows from the G-invariance of F and L.

Proposition 10. *Let $X_{TQ} \in \mathfrak{X}(TQ)$ denote the Lagrange-d'Alembert vector field, and let $\Phi_t^{X_{TQ}} : TQ \to TQ$ denote the flow map associated with the Lagrangian $L : TQ \to \mathbb{R}$ and the force $F : TQ \to T^*Q$. Then there exists a vector field $X_P \in \mathfrak{X}(P)$ and a flow map $\Phi_t^{X_P} : P \to P$ which are $\pi_{/G}^{TQ}$-related to X_{TQ} and $\Phi_t^{X_{TQ}}$.*

Proof. Let $q : [0, t] \to Q$ be a curve such that the time derivative $(q, \dot{q}) : [0, t] \to TQ$ is an integral curve of the Lagrange-d'Alembert equations with initial condition $(q, \dot{q})(0)$ and final condition $(q, \dot{q})(t)$. Then the Lagrange-d'Alembert variational principle states that

$$\delta \int_0^t L((q, \dot{q})(\tau))d\tau = \int_0^t \langle F((q, \dot{q})(\tau), \delta q(\tau)\rangle d\tau$$

for all variations of the curve $q(\cdot)$ with fixed endpoints. Note that for each $\psi \in G$, the action satisfies $\int_0^t L((q, \dot{q})(\tau)d\tau = \int_0^t L((q, \dot{q})(\tau) \circ \psi)d\tau$, and the variation on the right hand side of the Lagrange-d'Alembert principle is

$$\begin{aligned}\int_0^t \langle F((q, \dot{q})(\tau)), \delta q(\tau)\rangle d\tau &= \int_0^t \langle F_{/G}(\pi_{/G}((q, \dot{q})(\tau), \pi_{/G}(\delta q(\tau))\rangle d\tau \\ &= \int_0^t \langle F((q, \dot{q})(\tau) \circ \psi), \delta q(\tau) \circ \psi\rangle d\tau.\end{aligned}$$

Therefore, we observe that

$$\delta \int_0^t L((q, \dot{q})(\tau) \circ \psi)d\tau = \int_0^t \langle F((q, \dot{q})(\tau) \circ \psi), \delta q(\tau) \circ \psi\rangle d\tau$$

for arbitrary variations of the curve $q(\cdot)$ with fixed end points. However, the variation $\delta q \circ \psi$ is merely a variation of the curve $q \circ \psi(\cdot)$ because

$$\delta q(\tau) \circ \psi = \left.\frac{\partial}{\partial \epsilon}\right|_{\epsilon=0} (q(\tau, \epsilon) \circ \psi),$$

and if $q(\tau, \epsilon)$ is a deformation of $q(\tau)$, then $q(\tau, \epsilon) \circ \psi$ is a deformation of $q(\tau) \circ \psi$ by construction. Therefore,

$$\delta \int_0^t L((q, \dot{q})(\tau) \circ \psi)d\tau = \int_0^t \langle F((q, \dot{q})(\tau) \circ \psi), \delta(q \circ \psi)\rangle d\tau$$

for arbitrary variations of the curve $q \circ \psi$ with fixed end points. This last equation states that the curve $(q, \dot{q}) \circ \psi$ satisfies the Lagrange-d'Alembert principle. Thus, the flow $\Phi_t^{X_{TQ}}$ is G-invariant, as is the vector field X_{TQ}. By Proposition 2, there exists a $\pi_{/G}^{TQ}$-related flow and vector field on TQ/G. By Proposition 9, we obtained the desired vector field $X_P \in \mathfrak{X}(P)$, and its flow $\Phi_t^{X_P} : P \to P$. □

Now that we know there exists a flow on P, one can ask for the equations of motion.

Proposition 11. *The flow map of P mentioned in Proposition 10 for the Lagrangian L and force F is identical to the flow of the Lagrange-Poincaré-d'Alembert equation:*

$$u_t + u \cdot \nabla u = -\nabla p - \nu \Delta u$$
$$\frac{D\dot{q}}{Dt} + \nabla U(q) = \sharp(F(q, \dot{q}) + F_{\partial \mathscr{B}}),$$

where $F_{\partial \mathscr{B}} : P \to T^*B$ is the force that the fluid exerts on the body in order to satisfy the no-slip boundary condition.

Proof. This is Theorem 4.2 of [22] paired with (9). Roughly speaking, one can obtain these equations of motion by performing Lagrange-Poincaré-d'Alembert reduction following [9]. This involves choosing a principal connection $A : TQ \to \mathfrak{g}$. The spatial velocity field is reconstructed by $u = h^{\uparrow}(b, \dot{b}, \varphi) + \varphi_* A(b, \dot{b}, \varphi, \dot{\varphi})$, where $h^{\uparrow}$ is the horizontal lift. □

5.4 Reduction by Frame Invariance

Consider the group of isometries of $\mathbb{R}^d$ denoted $\mathrm{SE}(d)$. Each $z \in \mathrm{SE}(d)$ sends $(b, \dot{b}, u) \in TQ/G$ to $(z(b, \dot{b}), z_* u) \in P$, where $z_* u \in \mathfrak{X}_{\mathrm{div}}(\approx_{z \circ b})$ is the push-forward of the fluid velocity field $u \in \mathfrak{X}(\approx_b)$. This action is free and proper on P so that the projection $\pi_{[P]}^P : P \to [P]$, where $[P] := \frac{P}{\mathrm{SE}(d)}$ is a principal bundle [1, Prop 4.1.23]. Additionally, $\mathrm{SE}(d)$ acts by vector-bundle morphisms, which are isomorphisms on each fiber. Therefore, $[P]$ inherits a vector-bundle structure from P.

Proposition 12. *There exists a unique vector-bundle projection $[\tau] : [P] \to [B]$ and a map $[\rho] : [P] \to T[B]$ such that $[\tau] \circ \pi_{[P]}^P = \tau$ and $[\rho] \circ \pi_{[P]}^P = \rho$.*

Proof. We see that $\tau(z \cdot \xi) = z \cdot \tau(\xi)$ for any $z \in \mathrm{SE}(d)$ and $\xi \in P$. Applying the above formula to an $\mathrm{SE}(d)$-orbit of P, i.e. a member of $[P]$, maps to an $\mathrm{SE}(d)$-orbit of B, i.e. a member of $[B]$. Thus the map $[\tau] : [P] \to [B]$ is well-defined by the condition $\tau = [\tau] \circ [\cdot]$. The same argument makes the map $[\rho] : [P] \to T[B]$. The vector-bundle structure on $[P]$ can be observed directly. □

As everything in sight is SE(d)-invariant, it is not surprising that we can express reduced equations of motion on $[P]$.

Proposition 13. *There exists a vector field $X_{[P]} \in \mathfrak{X}([P])$ and a flow-map $\Phi_t^{[P]} : [P] \to [P]$ which is $\pi^P_{[P]}$-related to X_P and $\Phi_t^{X_P}$.*

Proof. Let $q : [0,T] \to Q$ be a curve such that the time derivative $(q,\dot{q}) : [0,T] \to TQ$ is an integral curve of the Lagrange-d'Alembert equations with initial condition $(q,\dot{q})_0$ and final condition $(q,\dot{q})_T$. Then the Lagrange-d'Alembert variational principle states that

$$\delta \int_0^T L(q,\dot{q})dt = \int_0^T \langle F(q,\dot{q}), \delta q\rangle dt$$

for all variations of the curve $q(\cdot)$ with fixed endpoints. Note that for each $\psi \in G$ and $z \in \mathrm{SE}(d)$, the action satisfies $\int_0^T L(q,\dot{q})dt = \int_0^T L(z\cdot(q,\dot{q})\circ\psi)dt$ and the virtual-work is

$$\begin{aligned}\int_0^T \langle F(q,\dot{q}), \delta q\rangle dt &= \int_0^T \langle F_{/G}(z\cdot\pi_{/G}(q,\dot{q}), z\cdot\pi_{/G}(\delta q)\rangle dt \\ &= \int_0^T \langle F(z\cdot(q,\dot{q})\circ\psi), z\cdot\delta q\circ\psi\rangle dt.\end{aligned}$$

Therefore we observe that

$$\delta \int_0^T L(z\cdot(q,\dot{q})\circ\psi)dt = \int_0^T \langle F(z\cdot(q,\dot{q})\circ\psi), z\cdot\delta q\circ\psi\rangle dt$$

for arbitrary variations of the curve $q(\cdot)$ with fixed end points. However, the variation $z\cdot\delta q\circ\psi$ is merely a variation of the curve $z\cdot q\circ\psi(\cdot)$. Therefore,

$$\delta \int_0^T L(z\cdot(q,\dot{q})\circ\psi)dt = \int_0^T \langle F(z\cdot(q,\dot{q})\circ\psi), \delta(z\cdot q\circ\psi)\rangle dt$$

for arbitrary variations of the curve $z\cdot q\circ\psi$ with fixed end points. This last equation states that the curve $z\cdot(q,\dot{q})\circ\psi$ satisfies the Lagrange-d'Alembert principle. Thus, $\Phi_T^{TQ}(z\cdot(q,\dot{q})_0\circ\psi) = z\cdot\Phi_T^{TQ}(q,\dot{q})\circ\psi$. Since $\psi \in G$ was arbitrary, we may apply Φ_T^{TQ} to the entire coset $z\cdot(q,\dot{q})\cdot G$ to find $\Phi_T^{TQ}(z\cdot(q,\dot{q})\cdot G) = z\cdot\Phi_T^{TQ}(q,\dot{q})\cdot G$. This map from G-cosets to G-cosets is the defining condition for Φ_T^P. Therefore, the last equation states that $\Phi_T^P(z\cdot\xi) = z\cdot\Phi_T^P(\xi)$, where $\xi = \pi^{TQ}_{/G}((q,\dot{q})_0)$. In other words, Φ_T^P is SE(d)-invariant. Therefore, by Proposition 2 the theorem follows. □

6 Asymptotic Behavior

It is commonplace to assume that the asymptotic behavior of a simple mechanical system with dissipation approaches a state of minimum energy. In this section, we will verify that the asymptotic behavior of the Lagrangian system described in the previous section tends towards the minimizers of the elastic potential energy, U.

Proposition 14. *Assume the Lagrangian L of (12) and the external force F of (13). Let $q : [0, \infty) \to Q$ be a curve such that the time derivative $(q, \dot{q}) : [0, \infty) \to TQ$ is an integral curve of the Lagrange-d'Alembert equations for the Lagrangian L and the force F. Then the ω-limit set of $(q, \dot{q})(\cdot)$ is contained in the set $dU^{-1}(0) := \{(q, 0) \in TQ \quad | \quad dU(q) = 0\}$.*

Proof. The energy is the function $E : TQ \to \mathbb{R}$ given by

$$E(q, \dot{q}) := \langle \mathbb{F}L(q, \dot{q}), \dot{q} \rangle - L(q, \dot{q}).$$

Given any Lagrangian system on a Riemannian manifold where the Lagrangian is the kinetic energy minus the potential energy, the time derivative of the generalized energy under the evolution of the Lagrange-d'Alembert equations is given by $\dot{E} = \langle F(\dot{q}), \dot{q} \rangle$. In this case, we find

$$\dot{E}(q, \dot{q}) = \langle F_{\mathscr{B}}(\dot{b}), \dot{b} \rangle + \langle F_{\mu}(q, \dot{q}), (q, \dot{q}) \rangle.$$

However, by (10), this is a convex function on each fiber of TQ in a neighborhood of the zero-section. Therefore the ω-limit of $(q, \dot{q})(\cdot)$, denoted M^{ω}, must be a subset of the zero section of TQ. Moreover, the Lagrange-D'Alembert equations state

$$\frac{D\dot{q}}{Dt} = -\nabla U(b) + \sharp(F(q, \dot{q})),$$

where $\sharp : T^*Q \to TQ$ is the sharp map associated the metric on Q. However, $F(q, \dot{q}) = 0$ when $\dot{q} = 0$, which is the case for points in M^{ω}. Thus, the vector field on M^{ω} must satisfy

$$\frac{D\dot{q}}{Dt} = -\nabla U(b).$$

However, M^{ω} is an invariant set. Therefore, the Lagrange-d'Alembert vector field must be tangential to M^{ω}. As M^{ω} is contained in the zero-section of TQ, the second derivative of $q(t)$ must vanish in order to remain in the zero section. Thus, we find $\frac{D\dot{q}}{Dt} = 0$ on M^{ω} which implies $\nabla U = 0$ on M^{ω}. That is to say, $M^{\omega} \subset dU^{-1}(0)$. □

Corollary 2. *Let $[U] : [B] \to \mathbb{R}$ be the unique function on the shape-space of the body such that $[U]([b]) = U(b)$ for all $b \in B$. Assume that $[U]$ has a unique*

minimizer $s_{\min} \in [B]$*, and let* $(s_{\min})^0_\uparrow \in [P]$ *denote the element of the zero section of* $[\tau] : [P] \to [B]$ *above* $s_{\min} \in [B]$*. If* $(q, \dot{q}) : [0, \infty) \to TQ$ *is an integral curve of the Lagrange-d'Alembert equations, then* $[\xi](t) = [\pi_{/G}(q, \dot{q}(t))]$ *must approach* $(s_{\min})^0_\uparrow \in [P]$*. If the flow of the Lagrange-d'Alembert equations is complete, this means that* $(s_{\min})^0_\uparrow$ *is a global (weakly) hyperbolically stable fixed point for the vector field* $X_{[P]}$*.*

Proof. In Proposition 14, we showed that solutions approach points within the set $dU^{-1}(0)$ asymptotically. This implies that the dynamics on $[P]$ must approach $d[U]^{-1}(0)$ asymptotically. However, there is only one such point. □

In the next section, we will periodically perturb this stable equilibria to obtain a loop in $[P]$.

Example 5. Consider the swimmer of Example 3 and Figure 8. Corollary 2 asserts that the state where the swimmer and the water is stationary and $\phi_1 - \phi_2 = \bar{\theta}$ is asymptotically stable.

7 Swimming

In order to understand swimming, let us consider a time-periodic internal body force, $F_{\text{swim}} : T[B] \times S^1 \to T^*[B]$. Such a force should be designed to model the time-periodic activation of muscles in a fish, or control forces for an underwater vehicle. This force can be lifted via the map $\pi^B_{[B]} \circ \pi^Q_B : Q \to [B]$ to obtain a $G, \text{SE}(d)$-invariant invariant force on Q. *The addition of this time periodic force on* Q *alters the Lagrange-d'Alembert equations linearly by the addition of a* $G, \text{SE}(d)$*-invariant time-periodic vector field* X_{swim}. To consider small perturbations, we can consider scaling this time-periodic force by a real parameter $\varepsilon \in \mathbb{R}^+$, so that the Lagrange-d'Alembert vector field is now given by the time-periodic vector field $X_{TQ,\varepsilon} = X_{TQ} + \varepsilon X_{\text{swim}} \in \mathfrak{X}(TQ)^{S^1}$. This deformed vector-field is also $G, \text{SE}(d)$-invariant; thus, there exists a reduced vector fields $X_{P,\varepsilon} \in \mathfrak{X}(P)^{S^1}$ which is π^Q_P-related to $X_{TQ,\epsilon}$, and a vector field $X_{[P],\varepsilon} \in \mathfrak{X}([P])^{S^1}$ which is $\pi^P_{[P]}$-related to $X_{P,\varepsilon}$. The vector field $X_{[P],\varepsilon}$ is a time-periodic deformation of $X_{[P]}$. As $X_{[P]}$ admits an asymptotically stable point by Corollary 2, we are reasonably close to being able to prove the existence of a SE(d)-relative limit cycle for $X_{P,\varepsilon}$ for small $\varepsilon > 0$.

Desideratum: *For sufficiently small* $\varepsilon > 0$*, the vector-field* $X_{[P],\varepsilon}$ *admits a non-autonomous exponentially stable limit cycle. Moreover,* $X_{P,\varepsilon}$ *admits stable relative limit cycle.*

If we were to assume Proposition 5 held for infinite-dimensional dynamical systems, then as $X_{[P],\varepsilon}$ is a deformation of $X_{[P]}$ we could deduce that $X_{P,\varepsilon}$ admits a non-autonomous exponentially stable limit cycle for sufficiently small $\varepsilon > 0$. As a result, this would imply $X_{P,\epsilon}$ admits SE(d)-relative limit cycles which are $\pi^P_{[P]}$-related to the limit cycle in $[P]$.

Unfortunately, we are unable to do this because Proposition 5 is limited to finite-dimensional manifolds and vector fields with exponentially stable points. The vector-field $X_{[P]}$ is on an infinite-dimensional space where we have only proven asymptotic stability. We will not overcome this difficulty; however, we are at least able to speculate on how to deal with this. For example, there does exist extensions of normal hyperbolicity and persistence to infinite-dimensional dynamical systems on a Hilbert manifold [5, 23]. Alternatively, we could consider finite-dimensional models for fluid-structure interaction, such as the immersed boundary method [39]. In the next section, we will informally speculate on this latter approach.

7.1 Analytic Concerns and Approximate Relative Limit Cycles

Up until now, the paper has been fairly rigorous and complete. This start of this section marks the end of this theorem-proof formalism. Instead, we provide a more speculative discussion on how one can overcome the challenges to obtaining relative limit cycles in P.

There are two issues of concern. The first is the lack of a "spectral gap" with respect to the equilibrium associated to $s_{\min} \in [B]$. That is to say, it is not immediately obvious if there exists a convergence bound $\rho > 0$ with respect to $s_{\min}$, as is required in order to use Theorem 1 and its offspring, Proposition 5. It is possible that there does not exist any such ρ. For simple mechanical systems, ρ is related to the spectrum of the Rayleigh dissipation function. In our case, this spectrum includes the spectrum of the Laplace-operator on a non-compact domain, which *does not contain a spectral gap!*

The second issue is the non-completeness of $[P]$. As Q is an infinite-dimensional Fréchet manifold, so is $[P]$. This is a concern because both Theorem 1 and Proposition 5 require completeness in order to provide an existence-uniqueness result. There do exist generalizations of Theorem 1 to infinite-dimensional Banach manifolds, but not Fréchet manifolds [5, 23].

Therefore, using the persistence theorem directly will not allow us to assert the existence of a relative limit cycle on P. Perhaps other methods besides normal hyperbolicity theory could be employed, but this would be an exploration for another paper.

However, we can consider an option which is morally the converse of an idea illustrated in [23], wherein discrete approximations are invoked. There exists a number of finite-dimensional models for the space P used by engineers to study fluid-structure interaction. It is fairly common to approximate the fluid velocity field on a finite-dimensional space and model the solid using a finite element method (e.g. [39]). Let us call this finite-dimensional space P_{discrete}. Moreover, one can usually act on P_{discrete} by $\text{SE}(d)$ by simply rotating and translating the finite elements and the grid. If the model on P_{discrete} converges as the time step and spatial resolution go to zero, then we could reasonably restrict ourselves to methods which dissipate energy at a rate which is quadratic and positive definite in the state velocity.

This is not too much to expect, as a good method ought to converge.[5] By the same arguments as before, the dynamics will exhibit hyperbolically stable equilibria on the quotient space $[P_{\text{discrete}}] = \frac{P_{\text{discrete}}}{\text{SE}(d)}$. Upon adding a periodic perturbation to the dynamics on $[P_{\text{discrete}}]$, one could apply Proposition 5 directly to assert the existence of a non-autonomous exponentially stable relative limit cycle $\gamma_{\text{discrete}}(t) \in P_{\text{discrete}}$. In particular, by Proposition 3, $\gamma_{\text{discrete}}(t)$ must satisfy

$$\gamma_{\text{discrete}}(t) = z^{\lfloor t \rfloor} \cdot \gamma_{\text{discrete}}(t - \lfloor t \rfloor)$$

for some $z \in \text{SE}(d)$, where $\lfloor t \rfloor = \sup\{k \in \mathbb{Z} : k \leq t\}$. If the model on P_{discrete} converges, then there exists a trajectory in $\gamma(s) \in P$ which is well-approximated by $\gamma_{\text{discrete}}(t)$, over a single time period, by the definition of "convergence." Then, the equation $\gamma(t) = z^{\lfloor t \rfloor} \cdot \gamma(t - \lfloor t \rfloor)$ would hold up to numerical error. In other words, the immersed body would move in an *approximately* relatively periodic fashion, reminiscent of swimming.

8 Conclusion and Future Work

It is widely observed that steady swimming is periodic, and this observation inspired the question, "Is it possible to interpret swimming as a limit cycle?" In this paper, we have illustrated the crucial role played by SE(d)-reduction in answering this question. Moreover, we have posed a possible answer, accurate up to the spatial discretization error of a numerical method. The existence of these hypothetical relative limit cycles would provide robustness to mechanisms of locomotion, and conform with behavior observed in real systems [2, 7, 29, 30, 44, 47]. *Given the complexity of fluid-structure interaction, it is not immediately clear that one could expect such orderly behavior.* This potential orderliness could be exploited in a number of applications.

1. **Robotics and Optimal Control** The interpretation of swimming as a limit cycle may permit a non-traditional framework for controller design. For example, if our control forces are parametrized by a space C, then we may consider the set of loops, loop(C). The limit cycle hypothesis would imply the existence of a subset $W \subset \text{loop}(C)$ and a map $\Gamma : W \to \text{loop}([P])$ which outputs the periodic limit cycle in $[P]$, resulting asymptotically from the time-periodic control signals in W. Given Γ, we may define a control cost functional on W based upon a reward function on loop($[P]$). As such a cost functional would only respond to the asymptotic behavior of the system, one could surmise that it would not overreact to transient dynamics.

[5] The immersed boundary method [39] and smooth-particle hydrodynamics [17, 32] are both candidates.

2. **Transient Dynamics** Although trajectories may approach a limit cycle, the transient dynamics are still important. The transient dynamics would re-orient and translate the body before orderly periodic behavior takes effect. Therefore, if one desires to create locomotion through periodic control inputs, one should try to get onto a limit cycle quickly in order to minimize the duration where transient dynamics dominate.
3. **Pumping** In the current setup, one could consider a reference frame attached to the body. In this reference frame, "swimming" manifests as fluid moving around the body in a regular fashion. This change in our frame of reference describes pumping.
4. **Passive Dynamics** This paper does *not* address the dual problem. By the dual problem, we mean: "Given a constant fluid velocity at infinity, what periodic motion (if any) will a tethered body approach as time goes to infinity?" In this dual problem, the motion of the body is given first, and parameters such as the period of the limit cycle are emergent phenomena. In particular, the dual problem of a flapping flag immersed in a fluid with a constant velocity at infinity has received much attention in the applied mathematics community (see [42] and references therein). Here, it is generally not the case that a limit cycle will emerge, and the system is capable of admitting chaos.
5. **Other types of locomotion** The notion that walking may be viewed as a limit cycle is fairly common [20, 33, 37]. Moreover, it is conceivable that flapping flight is a limit cycle as well [31]. However, for both of these systems, SE(3) symmetry is broken by the direction of gravity. Because of this, it is not immediately clear that one can import the methods used here to understand flapping flight and terrestrial locomotion. However, perhaps this is merely a challenge to be overcome. In particular, these systems still exhibit SE(2) symmetry. For the case of 2D bipedal walkers, we have an $\mathbb{R}$-symmetry and the stability problems due to falling will not manifest. Here, one can find limit cycles using regularized models of the ground [21].

Acknowledgements The notion of swimming as a limit cycle was initially introduced to me by Erica J. Kim while she was studying hummingbirds. Additionally, Sam Burden, Ram Vasudevan, and Humberto Gonzales provided much insight into how to frame this work for engineers. I would also like to thank Professor Shankar Sastry for allowing me to stay in his lab for a year and meet people who are outside of my normal research circle. I would like to thank Eric Tytell for suggesting relevant articles in neurobiology, Amneet Pal Singh Bhalla for allowing me to reproduce figures from [7], and Peter Wallen for allowing me to reproduce figures from [46]. An early version of this paper was written in the context of Lie groupoid theory, where the guidance of Alan Weinstein was invaluable. Jaap Eldering and Joris Vankerschaver have given me more patience than I may deserve by reading my papers and checking my claims. Major contributions to the bibliography and the overall presentation of the paper were provided by Jair Koiller. Finally, the writing of this paper was solidified with the help of Darryl Holm. This research has been supported by the European Research Council Advanced Grant 267382 FCCA and NSF grant CCF-1011944.

References

1. Abraham, R., Marsden, J.E.: Foundations of Mechanics, Benjamin/Cummings Publishing Co. Inc. Advanced Book Program, Reading, MA (1978). Second edition, revised and enlarged, with the assistance of Tudor Ratiu and Richard Cushman. Reprinted by AMS Chelsea (2008)
2. Alben, S., Shelley, M.J.: Coherent locomotion as an attracting state for a free flapping body. Proc. Natl. Acad. Sci. USA **102**(32), 11163–11166 (2005)
3. Arnold, V.I.: Sur la géométrie différentielle des groupes de lie de dimenision infinie et ses applications à l'hydrodynamique des fluides parfaits. Annales de l'Institute Fourier **16**, 316–361 (1966)
4. Arnold, V.I., Khesin, B.A.: Topological Methods in Hydrodynamics. Applied Mathematical Sciences, vol. 24. Springer, New York (1992)
5. Bates, P.W., Lu, K., Zeng, C.: Existence and persistence of invariant manifolds for semiflows in Banach space. Mem. Am. Math. Soc. **135**(645), viii+129 (1998)
6. Beal, D.N., Hover, F.S., Triantafyllou, M.S., Liao, J.C., Lauder, G.V.: Passive propulsion in vortex wakes. J. Fluid Mech. **549**, 385–402 (2006)
7. Bhalla, A.P.S., Griffith, B.E., Patankar, N.A.: A forced damped oscillation framework for undulatory swimming provides new insights into how propultion arises in active and passive swimming. PLOS Comput. Biol. **9**(6), e1003097 (2013)
8. Cantor, M.: Perfect fluid flows over $\mathbf{R}^n$ with asymptotic conditions. J. Funct. Anal. **18** (1975), 73–84.
9. Cendra, H., Marsden, J.E., Ratiu, T.S.: Lagrangian reduction by stages. Memoirs of the American Mathematical Society, vol. 152. American Mathematical Society, Providence, RI (2001)
10. Delcomyn, F.: Neural basis of rhythmic behavior in animals. Science **210**(4469), 492–498 (1980)
11. Ebin, D.G., Marsden, J.E.: Groups of diffeomorphisms and the motion of an incompressible fluid. Ann. Math. **92**, 102–163 (1970)
12. Ehlers, K.M., Koiller, J.: Micro-swimming without flagella: propulsion by internal structures. Regul. Chaotic Dynam. **16**(6), 623–652 (2011)
13. Eldering, J.: Normally Hyperbolic Invariant Manifolds: The Noncompact Case. Atlantis Series in Dynamical Systems. Atlantis Press, Paris, France (2013)
14. Fenichel, N.: Persistence and smoothness of invariant manifolds for flows. Indiana Univ. Math. J. **21**, 193–226 (1971)
15. Friesen, W.O.: Reciprocal inhibition: a mechanism underlying oscillatory animal movements. Neurosci. Biobehav. Rev. **18**(4), 547–553 (1994)
16. Gadelha, H., Gaffney, E.A., Goriely, A.: The counterbend phenomena in flagellar axonemes and cross-linked filament bundles. Proc. Natl. Acad. Sci. **110**(30), 12180–12185 (2013)
17. Gingold, R.A., Monaghan, J.J.: Smoothed particle hydrodynamics: theory and application to non-spherical stars. Mon. Not. R. Astron. Soc. **181**, 375–389 (1977)
18. Grillner, S., Wallen, P.: Central pattern generators for locomotion, with special reference to vertebrates. Annu. Rev. Neurosci. **8**, 233–261 (1985)
19. Hirsch, M.W., Pugh, C.C., Shub, M.: Invariant Manifolds. Lecture Notes in Mathematics, vol. 583. Springer, New York (1977)
20. Hobbelen, D.G.E., Wisse, M.: Limit-cycle walking. In: Humanoid Robots: Human-Like Machines, pp. 277–294. Itech, Vienna (2007)
21. Jacobs, H.O., Eldering, J.: Limit cycle walking on a regularized ground. Preprint. March 2013. arXiv:1212.1978[math.DS]
22. Jacobs, H., Vankerschaver, J.: Fluid-structure interaction in the Lagrange-Poincaré formalism: the Navier-Stokes and inviscid regimes. J. Geom. Mech. **6**(1), 39–66 (2014)
23. Jones D.A., Shkoller, S.: Persistence of invariant manifolds for nonlinear PDEs. Stud. Appl. Math. **102**(1), 27–67 (1999)

24. Kanso, E., Marsden, J.E., Rowley, C.W., Melli-Huber, J.B.: Locomotion of articulated bodies in a perfect fluid. J. Nonlinear Sci. **15**(4), 255–289 (2005)
25. Kelly, S.D., Murray, R.M.: The geometry and control of dissipative systems. In: Proceedings of the 35th Conference on Decisions and Control, December (1996)
26. Kelly, S.D., Murray, R.M.: Modelling efficient pisciform swimming for control. Int. J. Robust Nonlinear Control **10**(4), 217–241 (2000)
27. Koiller, J., Ehlers, K., Montgomery, R.: Problems and progress in microswimming. J. Nonlinear Sci. **6**(6), 507–541 (1996)
28. Lewis, D., Marsden, J., Montgomery, R., Ratiu, T.: The Hamiltonian structure for dynamic free boundary problems. Physica D (Nonlinear Phenomena) **18**(1–3), 391–404 (1986)
29. Liao, J.C., Beal, D.N., Lauder, G.V., Triantafyllou, M.S..: Fish exploiting vortices decrease muscle activity. Science **302**, 1566–1569 (2003)
30. Liao, J.C., Beal, D.N., Lauder, G.V., Triantafyllou, M.S.: The Karman gait: novel body kinematics of rainbow trout swimming in a vortex street. J. Exp. Biol. **206**(6), 1059–1073 (2003)
31. Liu, B., Ristroph, L., Weathers, A., Childress, S., Zhang, J.: Intrinsic stability of a body hovering in an oscillating airflow. Phys. Rev. Lett. **108**, 068103 (2012)
32. Lucy, B.L.: A numerical approach to testing the fission hypothesis. Astron. J. **82**, 1013–1924 (1977)
33. Mariano, G., Chatterjee, A., Ruina, A., Coleman, M.: The simplest walking model: stability, complexity, and scaling. J. Biomech. Eng. **120**(2), 281–288 (1998)
34. Marsden, J.E., Hughes, T.J.R.: Mathematical Foundations of Elasticity. Dover, Columbia (1983)
35. Marsden, J.E., Ratiu, T.S.: Introduction to Mechanics and Symmetry. Texts in Applied Mathematics, vol. 17, 2nd edn. Springer, New York (1999)
36. Marsden, J.E., Montgomery, R., Ratiu, T.S.: Reduction, Symmetry, and Phases in Mechanics. Memoirs of the American Mathematical Society, no. 436, vol. 88. American Mathematical Society, Providence, RI (1990)
37. McGreer, T.: Passive dynamic walking. Int. J. Robot. **9**(2), 62–82 (1990)
38. Munnier, A.: Passive and self-propelled locomotion for an elastic swimmer in a perfect fluid. SIAM J. Appl. Dyn. Syst. **10**(4), 1363–1403 (2011)
39. Peskin, C.: The immersed boundary method. Acta Numerica **11**, 479–513 (2002)
40. Shadwick, R.E.: Muscle dynamics in fish during steady swimming. Am. Zool. **38**, 755–70 (1998)
41. Shapere, A., Wilczek, F.: Geometry of self-propulsion at low Reynolds number. J. Fluid Mech. **198**, 557–585 (1989)
42. Shelley, M. J., Vandenberghe, N., Zhang, J.: Heavy flags undergo spontaneous oscillations in flowing water. Phys. Rev. Lett. **94**, 094302 (2005)
43. Troyanov, M.: On the Hodge decomposition in $\mathbb{R}^n$. Mosc. Math. J. **9**(4), 899–926, 936 (2009)
44. Tytell, E.D., Hsu, C., Williams, T.L., Cohen, A.H., Fauci, L.J.: Interactions between internal forces, body stiffness, and fluid environment in a neuromechanical model of lamprey swimming. Proc. Natl. Acad. Sci. **107**(46), 19832–19837 (2010)
45. Vogel, S.: Comparative Biomechanics. Princeton University Press, Princeton (2003)
46. Wallen, P., Williams, T.L.: Fictive locomotion in the lamprey spinal chord in vitro compared with swimming in the intact and spinal animal. J. Physiol. **347**, 225–239 (1984)
47. Wilson, M.W., Eldredge, J.D.: Performance improvement through passive mechanics in jellyfish-inspired swimming. Int. J. Non-Linear Mech. **46**(4), 557–567 (2011)
48. Zhang, J., Liu, N., Lu, X.: Locomotion of a passively flapping flat plate. J. Fluid Mech. **659**, 43–68 (2010)
49. Zhou, K., Doyle, J.C.: Essentials of Robust Control, 1st edn. Prentice Hall, New Jersey (1997)

Lagrangian Mechanics on Centered Semi-direct Products

Leonardo Colombo and Henry O. Jacobs

Abstract There exist two types of semi-direct products between a Lie group G and a vector space V. The left semi-direct product, $G \ltimes V$, can be constructed when G is equipped with a left action on V. Similarly, the right semi-direct product, $G \rtimes V$, can be constructed when G is equipped with a right action on V. In this paper, we will construct a new type of semi-direct product, $G \bowtie V$, which can be seen as the 'sum' of a right and left semi-direct product. We then parallel existing semi-direct product Euler-Poincaré theory. We find that the group multiplication, the Lie bracket, and the diamond operator can each be seen as a sum of the associated concepts in right and left semi-direct product theory. Finally, we conclude with a toy example and the group of 2-jets of diffeomorphisms above a fixed point. This final example has potential use in the creation of particle methods for problems on diffeomorphism groups.

1 Introduction

It is no secret that the use of symmetry and a preference for algebraic simplicity pervaded much (if not all) of Jerry's intellectual endeavours. Certainly one of these algebraic structures would be semi-direct products, which pepper his research in the form of rigid bodies, complex fluids, plasmas [12, 13], the KdV equation [14], and the heavy top [8].

In this paper we will investigate a new semi-direct product which is inspired by a careful analysis of the second order jet groupoid. To begin, let G be a Lie group and V be a vector space on which G acts by a left action. Given these ingredients, we may form the Lie group $G \ltimes V$, which is isomorphic to $G \times V$ as a set, but equipped with the composition

L. Colombo
ICMAT Nicolás Cabrera, No 13-15, Campus de Cantoblanco, UAM, 28049 Madrid, Spain
e-mail: leo.colombo@icmat.es

H.O. Jacobs (✉)
Department of Mathematics, Imperial College London, Huxley Building,
180 Queen's Gate Road, London SW7 2AZ, UK
e-mail: hoj201@gmail.com

D.E. Chang et al. (eds.), *Geometry, Mechanics, and Dynamics*, Fields Institute Communications 73, DOI 10.1007/978-1-4939-2441-7_9

$$(g, v) \cdot_{\ltimes} (h, w) = (g \cdot h, g \cdot w + v), \quad \forall (g, v), (h, w) \in G \ltimes V.$$

A standard example of a system which evolves on a left semi-direct product is the heavy top, where $G = \mathrm{SO}(3)$ and $V = \mathbb{R}^3$. In contrast, if G acts on V by a right action, we may form the right semi-direct product $G \rtimes V$ defined by the composition

$$(g, v) \cdot_{\rtimes} (h, w) = (g \cdot h, w + v \cdot h).$$

A standard example of a system whose configurations describe a right semi-direct product is a fluid with a vector-valued advected parameter [8]. In any case, it seems natural to surmise that the composition law

$$(g, v) \cdot_{\bowtie} (h, w) = (g \cdot h, g \cdot w + v \cdot h) \tag{1}$$

yields a new type of semi-direct product. The first result of this article is that (1) is a valid composition law in some circumstances, and we call the corresponding Lie group a *centered semi-direct product*. This group is not completely novel in the sense that it is isomorphic to a left semi-direct product with respect to the left action $v \mapsto g \cdot v \cdot g^{-1}$ through the group homomorphism $(g, v) \mapsto (g, v \cdot g^{-1})$. Simultaneously, this group is isomorphic to a right semi-direct product as well.[1] Nonetheless, it is still fascinating to observe the consequence of this symmetric formulation of the group structure.

The second result is that the second order Taylor expansions (or second order jets) of diffeomorphisms over a fixed point form a centered semi-direct product. The main motivation behind understanding this example is to allow us to develop particle-based methods for complex fluid simulation and image registration algorithms.

1.1 Background

The semi-direct product is a standard tool used in the construction of new Lie groups and plays an interesting role in geometric mechanics when the normal subgroup is interpreted as an advected parameter. A standard example is the modeling of the 'heavy-top', wherein the axis of rotation is described by $\mathbb{R}^3$ and is advected by the action of SO(3). In other words, the configuration space for the heavy top can be described as the left semi-direct product $\mathrm{SO}(3) \ltimes \mathbb{R}^3$ [8]. Another standard example is the modeling of liquid crystals, in which we consider the right semi-direct product $\mathrm{SDiff}(M) \rtimes V$. In this case, $\mathrm{SDiff}(M)$ is the set of volume-preserving diffeomorphisms of a volume manifold M, and V is a vector space of maps from M into some Lie algebra and $\mathrm{SDiff}(M)$ acts on V by pullback [5, 6]. Of course, the tangent bundle of a Lie group, TG, is isomorphic to a left semi-direct product $G \ltimes \mathfrak{g}$ by left-trivializing the group structure of TG. Additionally, TG is isomorphic to a

[1] This observation was pointed out to us by Peter Michor.

right semi-direct product $G \rtimes \mathfrak{g}$ when the group structure of TG is right trivialized [1, section 5.3]. Thus, we see that this method of constructing groups can be found in a number of instances. In this article, we introduce a new type of semi-direct product which extends the existing semi-direct product theory.

A motivating example will be a desire to understand the second order jet-groupoid of a manifold M [10, section 12]. As will be illustrated in Section 1.3, an isotropy group of the second order jet groupoid exhibits a group structure which can be written as a centered semi-direct product. A thorough understanding of the jet groupoid can be useful for the creation of new particle-based methods wherein the particles carry jet data in addition to position and velocity data. One advantage of such a particle method is the possibility for a discrete form of Kelvin's circulation theorem [9]. Building such particle methods can be useful in scenarios in which one desires to work with the material representation of a fluid. For example, the free energy of liquid crystal is a function of the gradient of a director field advected by the fluid. Computing this advection requires the use of second order jet data and therefore a small portion of the material representation of the fluid is invoked [5, 6]. Additionally, the use of jet data can be useful in the realm of image registration algorithms in the field of medical imaging. In particular, it is common to use the material representation of the EPDiff equations to implement the Large Deformation Diffeomorphic Metric Mapping (LDDMM) framework [2, 4]. In particular, "Landmark LDDMM" discretizes the EPDiff equation using particle methods [15]. A version of Landmark LDDMM wherein the particles can carry higher order jet data is described in [16]. Thus, keeping track of jet data may play a significant role in the construction of particle-based integrators for fluid modeling and medical imaging algorithms.

1.2 Main Contributions

In this paper, we accomplish a sequence of goals, each building upon the previous. In particular:

1. In Section 2, we define a new type of semi-direct product that we dub a *centered semi-direct product*.
2. In Proposition 4, we derive the Lie algebra of a centered semi-direct product and its associated structures.
3. In Section 3, we develop the Euler-Poincaré theory of centered semi-direct products in parallel with the existing theory of semi-direct product reduction [8].
4. In Section 4, we describe the centered semi-direct product Euler-Poincaré equations for a few examples. We present one toy example before presenting the theory for an isotropy group of the second order jet groupoid.

Combined, these items allow for a computationally tractable algebraic understanding of second order jets and perhaps open the door to applications which were previously overlooked by geometric mechanicians.

1.3 A Motivating Example

Let $\mathrm{Diff}(M)$ denote the diffeomorphisms group of a manifold M. For a fixed $x \in M$ we may define the isotropy subgroup

$$\mathrm{Iso}(x) = \{\varphi \in \mathrm{Diff}(M) \quad | \quad \varphi(x) = x\}.$$

Let $\varphi \in \mathrm{Iso}(x)$ and note that $T_x\varphi$ is a linear automorphism of the vector-space T_xM. In particular:

Proposition 1. *The functor "T_x" is a group homomorphism from* $\mathrm{Iso}(x)$ *to* $\mathrm{GL}(T_xM)$.

Proof. Clearly $\mathrm{Iso}(x)$ and $\mathrm{GL}(T_xM)$ are both Lie groups. Let $\varphi, \psi \in \mathrm{Iso}(x)$. Then $T_x\varphi \circ T_x\psi = T_x(\varphi \circ \psi)$. □

This observation has implications for computation for the following reason: By definition, $T_x\varphi$ approximates φ in a neighborhood of $x \in M$. Thus, if one desired to model a continuum with activity at x, then $T_x\varphi$ carries some of the crucial data to do this task. In particular, this is computationally tractable as the dimension of $\mathrm{GL}(T_xM)$ is equal to $(\dim M)^2$.

However, the group $\mathrm{GL}(n)$ only captures the linearization of a diffeomorphism. If we desire to capture some of the nonlinearity then we might consider looking into the second jet of these diffeomorphisms (see Figure 1). We can do so by considering the functor TT_x. Let $\varphi \in \mathrm{Iso}(x)$ so that $TT_x\varphi$ is a map from $T(T_xM)$ to $T(T_xM)$. However, T_xM is a vector-space so that $T(T_xM) \approx T_xM \times T_xM$. The second component represents the vertical component and the isomorphism between TT_xM and $T_xM \times T_xM$ is given by the vertical lift

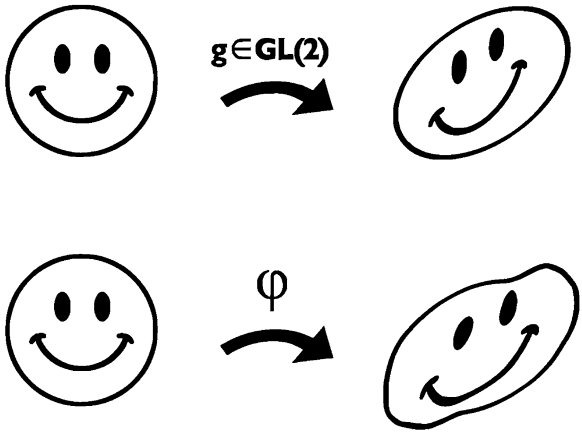

Fig. 1 Depicted is a diffeomorphism with a trivial second order jet (i.e. a linear transformation) and diffeomorphism with a nontrivial second order jet

$$v^{\uparrow}(v_1, v_2) = \left.\frac{d}{d\epsilon}\right|_{\epsilon=0} (v_1 + \epsilon v_2).$$

We can therefore represent $TT_x\varphi$ as $(T_x\varphi, A_\varphi)$ where $A_\varphi : T_xM \times T_xM \to T_xM$ is the symmetric $(1,2)$ tensor

$$A^k_{ij} = \frac{\partial^2 \varphi^k}{\partial x_i \partial x_j}(x) \tag{2}$$

where φ^k is the kth component of φ. In other words, upon choosing a Riemannian metric to induce an coordinate system at x we obtain the 1–1 correspondence

$$TT_x\varphi \leftrightarrow (A_1, A_2)$$

where $A_1 = \frac{\partial \varphi^i}{\partial x^j}$ and A_2 is given by (2). If we denote the set of rank $(1,2)$-tensors on T_xM which are symmetric in the covariant indices by $\mathscr{S}^1_2(x)$, then this correspondence is given by a map

$$\Psi : \mathscr{J}^2\big|^x_x(\mathrm{Diff}(M)) \to \mathrm{GL}(T_xM) \times \mathscr{S}^1_2(x)$$

where $\mathscr{J}^2\big|^x_x(\mathrm{Diff}(M))$ is the group of second order Taylor expansions about x of diffeomorphisms which send x to itself (these are called second order jets). This allows us to write the Lie group structure of $\mathscr{J}^2\big|^x_x(\mathrm{Diff}(M))$ as a type of semi-direct product. In particular:

Proposition 2. *If we represent $TT_x\varphi$ and $TT_x\psi$ as (A_1, A_2) and (B_1, B_2) where $A_1 = T_x\varphi$, $B_2 = T_x\psi$, $A_2 = \frac{\partial^2 \varphi^k}{\partial x^i \partial x^j}$, and $B_2 = \frac{\partial^2 \psi^k}{\partial x^i \partial x^j}$, then $TT_x\varphi \circ TT_x\psi \equiv TT_x(\varphi \circ \psi)$ is given by the composition*

$$(A_1, A_2) \circ (B_1, B_2) = (A_1 \circ B_1, A_1 \circ B_2 + A_2 \circ (B_1 \times B_1)).$$

Proof. We find that

$$\frac{\partial}{\partial x_i}(\varphi^k \circ \psi) = \frac{\partial \varphi^k}{\partial x_l} \cdot \frac{\partial \psi^l}{\partial x_i} \circ \psi$$

and the second derivative is

$$\begin{aligned}\frac{\partial}{\partial x_j}\frac{\partial}{\partial x_i}(\varphi^k \circ \psi) &= \frac{\partial}{\partial x_j}\left(\frac{\partial \varphi^k}{\partial x_l} \cdot \frac{\partial \psi^l}{\partial x_i} \circ \psi\right) \\ &= \left(\frac{\partial^2 \varphi^k}{\partial x_l \partial x_m}\frac{\partial \psi^l}{\partial x_i}\frac{\partial \psi^m}{\partial x_j} + \frac{\partial \varphi^k}{\partial x_l}\frac{\partial^2 \psi^l}{\partial x_i \partial x_j}\right) \circ \psi.\end{aligned}$$

Noting that $\psi(x) = x$ we can set

$$A_1 = \left.\frac{\partial \varphi^k}{\partial x_l}\right|_x, \quad A_2 = \left.\frac{\partial^2 \varphi^k}{\partial x_i \partial x_j}\right|_x$$
$$B_1 = \left.\frac{\partial \psi^k}{\partial x_l}\right|_x, \quad B_2 = \left.\frac{\partial^2 \psi^k}{\partial x_i \partial x_j}\right|_x$$

and rewrite the equations in the form

$$\frac{\partial}{\partial x_i}(\varphi^k \circ \psi) = A_1 \cdot B_1$$
$$\frac{\partial}{\partial x_j}\frac{\partial}{\partial x_i}(\varphi^k \circ \psi) = A_1 \cdot B_2 + A_2 \circ (B_1 \times B_1).$$

Therefore, if we define the composition

$$(A_1, A_2) \cdot (B_1, B_2) := (A_1 \cdot B_1, A_1 \cdot B_2 + A_2 \circ (B_1 \times B_1))$$

on the manifold $\mathrm{GL}(T_x M) \times \mathscr{S}^1_2$, then $\Psi : \mathscr{J}^2|^x_x(\mathrm{Diff}(M)) \to \mathrm{GL}(T_x M) \times \mathscr{S}^1_2$ is a Lie group isomorphism by construction. □

We see that the composition law of Proposition 2 is of the form described in equation (1). In this paper, we will condense the composition law for second order jets to the algebraic level and study (1) in the abstract Lie group setting. Of course, one would naturally like to consider diffeomorphisms which are not contained in $\mathrm{Iso}(x)$. However, this extension brings us into the realm of Lie groupoid theory and will need to be addressed in future work.

2 A Centered Semi-direct Product Theory

In this section, we will discover a new type of semi-direct product. We will outline the necessary ingredients for the construction of such a Lie group and we will derive the corresponding structures on the Lie algebra.

2.1 Preliminary Material on Lie Groups

Let G be a Lie group with identity $e \in G$ and Lie algebra $\mathfrak{g}$. In this section we will establish notation and recall relevant notions related to Lie groups and Lie algebras.

2.1.1 Group Actions

Let V be a vector space. A *left action* of G on V is a smooth map $\rho_L : G \times V \to V$ for which:

$$\rho_L(e, v) = v \text{ and } \rho_L(g, \rho_L(h, v)) = \rho_L(gh, v), \quad \forall g, h \in G, \forall v \in V.$$

As using the symbol 'ρ_L' can become cumbersome and since we will only need a one left Lie group action in a given context, we will opt to use the notation $g \cdot v := \rho_L(g, v)$. Finally, the *induced infinitesimal left action* of $\mathfrak{g}$ on V is

$$\xi \cdot v := \frac{d}{d\epsilon}\Big|_{\epsilon=0} \exp(\epsilon \cdot \xi) \cdot v, \quad \forall \xi \in \mathfrak{g}, v \in V.$$

Similarly, a *right action* of G on V is the smooth map $\rho_R : V \times G \to V$ for which:

$$\rho_R(v, e) = v \text{ and } \rho_L(\rho_L(v, g), h) = \rho_L(v, gh), \quad \forall g, h \in G, \forall v \in V.$$

Again, we will primarily use the notation $v \cdot g := \rho_R(v, g)$ for right actions. The *induced infinitesimal right action* of $\mathfrak{g}$ on V is given by

$$v \cdot \xi = \frac{d}{d\epsilon}\Big|_{\epsilon=0} v \cdot \exp(\epsilon \cdot \xi) \quad , \quad \forall \xi \in \mathfrak{g}, v \in V$$

Lastly, we say that the left action and the right action *commute* if

$$(g \cdot v) \cdot h = g \cdot (v \cdot h)$$

for any $g, h \in G$ and $v \in V$.

2.1.2 Adjoint and Coadjoint Operators

In this section we will recall the "AD, Ad, ad"-notation used in [7]. For $g \in G$ we define the *inner automorphism* $\mathrm{AD} : G \times G \to G$ as $\mathrm{AD}(g, h) \equiv \mathrm{AD}_g(h) = ghg^{-1}$. Differentiating AD with respect to the second argument along curves through the identity produces the *Adjoint representation* of G on $\mathfrak{g}$ denoted $\mathrm{Ad} : G \times \mathfrak{g} \to \mathfrak{g}$ and given by

$$\mathrm{Ad}_g(\eta) = \frac{d}{d\epsilon}\Big|_{\epsilon=0} \left(\mathrm{AD}_g(\exp(\epsilon\eta))\right) = g \cdot \eta \cdot g^{-1},$$

for $g \in G$ and $\xi \in \mathfrak{g}$. Differentiating Ad with respect to the first argument along curves through the identity produces the *adjoint* operator $\mathrm{ad} : \mathfrak{g} \times \mathfrak{g} \to \mathfrak{g}$ given by

$$\mathrm{ad}_\xi(\eta) = \left.\frac{d}{d\epsilon}\right|_{\epsilon=0} (\mathrm{Ad}_{\exp(\epsilon\xi)}(\eta)) = \xi \cdot \eta - \eta \cdot \xi.$$

The ad-map is an alternative notation for the Lie bracket of $\mathfrak{g}$ in the sense that

$$\mathrm{ad}(\xi, \eta) \equiv \mathrm{ad}_\xi(\eta) \equiv [\xi, \eta].$$

For each $\xi \in \mathfrak{g}$ the map $\mathrm{ad}_\xi : \mathfrak{g} \to \mathfrak{g}$ is linear and therefore has a formal dual $\mathrm{ad}^*_\xi : \mathfrak{g}^* \to \mathfrak{g}^*$ which we call the *coadjoint operator*. Explicitly, ad^*_ξ is defined by the relation

$$\langle \mathrm{ad}^*_\xi(\mu), \eta \rangle = \langle \mu, \mathrm{ad}_\xi(\eta) \rangle \tag{3}$$

for each $\eta \in \mathfrak{g}$ and $\mu \in \mathfrak{g}^*$.

2.2 Centered Semi-direct Products

In this section, we will construct a semi-direct product which can be thought of as a 'sum' of a right semi-direct product and a left semi-direct product.

Proposition 3. *Let G be a Lie group which acts on a vector-space V via left and right group actions. Then, the product $G \times V$ with the composition law*

$$(g_1, v_1) \cdot (g_2, v_2) := (g_1 g_2, g_1 \cdot v_2 + v_1 \cdot g_2) \tag{4}$$

is a Lie group if and only if the left and right actions of G commute.

Proof. It is clear that $G \times V$ is a smooth manifold and that the composition law (4) is a smooth map. We must prove that this composition makes $G \times V$ a group.

- That the composition map (4) produces another element of $G \times V$ can be observed directly. Thus 'closure' is satisfied.
- The identity element is given by $(e, 0) \in G \times V$ where $e \in G$ is the identity of G.
- The inverse element of an arbitrary $(g, v) \in G \times V$ is $(g^{-1}, -g^{-1} v g^{-1})$ where g^{-1} is the inverse of $g \in G$.
- Given three elements of $G \times V$ we find

$$\begin{aligned}(g_1, v_1) \cdot ((g_2, v_2) \cdot (g_3, v_3)) &= (g_1, v_1) \cdot (g_2 g_3, g_2 \cdot v_3 + v_2 \cdot g_3) \\ &= (g_1 g_2 g_3, g_1 \cdot (g_2 \cdot v_3 + v_2 \cdot g_3) + v_1 \cdot (g_2 g_3)) \\ &= ((g_1 g_2) g_3, (g_1 g_2) \cdot v_3 + g_1 \cdot (v_2 \cdot g_3) + (v_1 \cdot g_2) \cdot g_3)\,.\end{aligned}$$

By the commutativity of the group actions we may equate the above line with:

$$\begin{aligned}
&= ((g_1g_2)g_3, (g_1g_2)\cdot v_3 + (g_1\cdot v_2)\cdot g_3 + (v_1\cdot g_2)\cdot g_3)\\
&= ((g_1g_2)g_3, (g_1g_2)\cdot v_3 + (g_1\cdot v_2 + v_1\cdot g_2)\cdot g_3)\\
&= ((g_1g_2), g_1\cdot v_2 + v_1\cdot g_2)\cdot (g_3, v_3)\\
&= ((g_1, v_1)\cdot (g_2, v_2))\cdot (g_3, v_3).
\end{aligned}$$

Thus, the associative property is satisfied.

Moreover, all maps in sight including the inverse map are smooth. In conclusion we see that $G \times V$ with the composition (4) defines a Lie group. Moreover, if the left and right actions of G on V do *not* commute, then we can observe that associativity is violated. □

Definition 1. Given commuting left and right representations of a group G on a vector space V, the Lie group $G \times V$ with the composition (4) is denoted $G \bowtie V$ and called the *centered semi-direct product* of G and V.

It customary to denote the left semi-direct product using the symbol $\ltimes$ and the right semi-direct product via the symbol $\rtimes$. We justify our use of the symbol $\bowtie$ in that the concept of centered semi-direct product is merely a 'sum' of a left and a right semi-direct product. The formula $\bowtie = \rtimes + \ltimes$ can be used as a heuristic throughout the paper. In particular, this heuristic applies to the Lie algebra.

Proposition 4. *Let $G \bowtie V$ be a centered-semi direct product Lie group. The Lie algebra $\mathfrak{g} \bowtie V$ is given by the set $\mathfrak{g} \times V$ with the Lie bracket*

$$[(\xi_1, v_1), (\xi_2, v_2)]_{\bowtie} = \left([\xi_1, \xi_2]_{\mathfrak{g}}, (\xi_1\cdot v_2 + v_1\cdot \xi_2) - (\xi_2\cdot v_1 + v_2\cdot \xi_1)\right), \tag{5}$$

for $\xi_1, \xi_2 \in \mathfrak{g}$, $v_1, v_2 \in V$.

Proof. Firstly, it is simple to verify that the tangent space at the identity, $(e, 0) \in G \times V$, is $\mathfrak{g} \times V$. To derive the Lie bracket, we will derive the ad-map via the Ad and AD-maps. For $(g, v), (h, w) \in G \bowtie V$ we find

$$\begin{aligned}
\mathrm{AD}_{(g,h)}(h, w) &= (gh, v\cdot h + g\cdot w)\cdot (g^{-1}, -g^{-1}\cdot v\cdot g^{-1})\\
&= (\mathrm{AD}_g(h), v\cdot hg^{-1} + g\cdot w\cdot g^{-1} - \mathrm{AD}_g(h)\cdot v\cdot g^{-1}).
\end{aligned}$$

If we substitute (h, w) with the ϵ-dependent curve $(\exp(\epsilon \cdot \xi_2), \epsilon \cdot v_1)$ we can calculate the *adjoint operator*, $\mathrm{Ad} : (G \rtimes V) \times (\mathfrak{g} \rtimes V) \to \mathfrak{g} \rtimes V$. Given by

$$\begin{aligned}\mathrm{Ad}_{(g,v)}(\xi_2, v_2) &= \frac{d}{d\epsilon}\bigg|_{\epsilon=0} \mathrm{AD}_{(g,v)}(\exp(\epsilon \cdot \xi_1), \epsilon \cdot v_1) \\ &= (\mathrm{Ad}_g(\xi_2); v \cdot \xi_2 g^{-1} + g \cdot v_2 \cdot g^{-1} - \mathrm{Ad}_g(\xi_2) \cdot v \cdot g^{-1}).\end{aligned}$$

If we substitute (g, v) with the t-dependent curve $(\exp(t\xi_1), tv_2)$ we can differentiate with respect to t to produce the adjoint operator $\mathrm{ad} : (\mathfrak{g} \rtimes V) \times (\mathfrak{g} \rtimes V) \to \mathfrak{g} \rtimes V$. Specifically, the adjoint operator is given by

$$\begin{aligned}\mathrm{ad}_{(\xi_1,v_1)}(\xi_2, v_2) &= \frac{d}{dt}\bigg|_{t=0} (\mathrm{Ad}_{(\exp(t\cdot\xi_1), t\cdot v_1)}(\xi_2, v_2)) \\ &= \frac{d}{dt}\bigg|_{t=0} (g\xi_2 g^{-1}, v \cdot \xi_2 g^{-1} - g\xi_2 g^{-1} \cdot v \cdot g^{-1} + g \cdot v_2 \cdot g^{-1}) \\ &= (\mathrm{ad}_{\xi_1}(\xi_2), \xi_1 \cdot v_2 + v_1 \cdot \xi_2 - \xi_2 \cdot v_1 - v_2 \cdot \xi_1) \\ &= ([\xi_1, \xi_2]_{\mathfrak{g}}, (\xi_1 \cdot v_2 + v_1 \cdot \xi_2) - (\xi_2 \cdot v_1 + v_2 \cdot \xi_1)).\end{aligned}$$

Noting that the ad-map is merely an alternative notation for the Lie bracket completes the proof. □

We complete this section by defining operations designed to express interaction terms between momenta in V and momenta in G in mechanical systems.

Definition 2. The *heart operator* $\heartsuit : \mathfrak{g} \times V^* \to V^*$ is defined by

$$\langle \xi \heartsuit \alpha, v \rangle_V := \langle \alpha, \xi \cdot v - v \cdot \xi \rangle_V. \tag{6}$$

The *diamond operator*, $\diamond : V \times V^* \to \mathfrak{g}^*$, is defined as

$$\langle v \diamond \alpha, \xi \rangle_{\mathfrak{g}} := \langle \alpha, v \cdot \xi - \xi \cdot v \rangle_V. \tag{7}$$

The diamond operator can be seen as the sum of a diamond operator of a left semi-direct product and that of a right semi-direct product [8]. If we view $G \rtimes V$ as a Lie group and take the corresponding Line variations then the heart operator and diamond operator comes into play. However, if we restrict the variations so that V acts as an advected parameter, only the diamond operator is present. We will elaborate on both these options in the next section.

3 Euler-Poincaré Theory

The Euler-Lagrange equations on a Lie group, $\tilde{G}$, can be expressed by a vector field over $T\tilde{G}$. If the Lagrangian is $\tilde{G}$-invariant then the equations of motion are $\tilde{G}$-invariant as well and the evolution equations can be reduced. While the unreduced system evolves by the *Euler-Lagrange* equations on $T\tilde{G}$, the reduced dynamics evolve on the quotient $T\tilde{G}/\tilde{G}$. However, $T\tilde{G}/\tilde{G}$ is just an alternative description of the Lie algebra $\tilde{\mathfrak{g}}$ and so the reduced equations of motion can be described on $\tilde{\mathfrak{g}}$ where we call them the *Euler–Poincaré equations.* This reduction procedure is summarized by the commutative diagram:

$$\begin{array}{ccc} T\tilde{G} & \xrightarrow{\text{flow by 'EL'}} & T\tilde{G} \\ \Big\downarrow{\scriptstyle /\tilde{G}} & & \Big\downarrow{\scriptstyle /\tilde{G}} \\ \tilde{\mathfrak{g}} & \xrightarrow[\text{flow by 'EP'}]{} & \tilde{\mathfrak{g}} \end{array}$$

To be even more specific. A Lagrangian $L : T\tilde{G} \to \mathbb{R}$ is said to be *(right) $\tilde{G}$-invariant* if

$$L((\tilde{g}, \dot{\tilde{g}}) \cdot h) = L(\tilde{g}, \dot{\tilde{g}})$$

for all $h \in \tilde{G}$. If L is $\tilde{G}$-invariant, then L is uniquely specified by its restriction $\ell = L|_{\tilde{\mathfrak{g}}} : \tilde{\mathfrak{g}} \to \mathbb{R}$. The Euler-Poincaré theorem states that the Euler-Lagrange equations

$$\frac{d}{dt}\left(\frac{\delta L}{\delta \dot{\tilde{g}}}\right) - \frac{\delta L}{\delta \tilde{g}} = 0$$

on $T\tilde{G}$ are equivalent to the Euler-Poincaré equations and reconstruction formula

$$\frac{d}{dt}\left(\frac{\delta \ell}{\delta \tilde{\xi}}\right) = -\operatorname{ad}^*_{\tilde{\xi}}\left(\frac{\delta \ell}{\delta \tilde{\xi}}\right), \quad \tilde{\xi} := \dot{\tilde{g}} \cdot \tilde{g}^{-1}.$$

A review of Euler-Poincaré reduction is given in [11, Ch 13] while a specialization to the case of semidirect products with advected parameters is described in [8]. In this section we will specialize the Euler-Poincaré theorem to the case of centered semi-direct products by setting $\tilde{G} = G \bowtie V$.

To begin let us compute how variations of curves in the group induce variations on the trivializations of the velocities to the Lie algebra. Studying such variations will allow us to transfer the variational principles on the group to variational principles on the Lie algebra.

Proposition 5. *Let $G \rtimes V$ be a centered semi-direct product and consider a curve $(g, v)(t) \in G \rtimes V$. Let $(\xi_g(t), \xi_v(t)) := (\dot{g}(t), \dot{v}(t)) \cdot (g(t), v(t))^{-1} \in \mathfrak{g} \rtimes V$ be the right trivialization of $(\dot{g}, \dot{v})(t)$. An arbitrary variation of $(g, v)(t)$ is given by*

$$(\delta g, \delta v)(t) = (\eta_g, \eta_v)(t) \cdot (g, v)(t) \in T_{(g,v)(t)}(G \rtimes V),$$

where $(\eta_g, \eta_v)(t) \in \mathfrak{g} \rtimes V$. Given such a variation, the induced variation on (ξ_g, ξ_v) is given by

$$\begin{aligned}(\delta\xi_g, \delta\xi_v) &= (\dot{\eta}_g - \mathrm{ad}_{\xi_g}\eta_g, \dot{\eta}_v + (\eta_g\xi_v + \eta_v\xi_g) - (\xi_g\eta_v + \xi_v\eta_g)) \\ &= \frac{d}{dt}(\eta_v, \eta_v) - [(\xi_g, \xi_v), (\eta_g, \eta_v)]_{\rtimes}.\end{aligned} \tag{8}$$

Proof. For any Lie group, $\tilde{G}$, and any curve $\tilde{g}(t) \in \tilde{G}$, the variation of $\tilde{\xi}(t) := \dot{\tilde{g}}(t) \cdot \tilde{g}^{-1}(t)$ induced by the variation $\delta\tilde{g}(t) = \tilde{\eta}(t) \cdot \tilde{g}(t)$ is $\delta\tilde{\xi} = \dot{\tilde{\eta}} - [\tilde{\xi}, \tilde{\eta}]$. For matrix groups see [11, Theorem 13.5.3] and [3] for the general case. If we set $\tilde{G} = G \rtimes V$ and use the bracket derived in Proposition 4 then the theorem follows. □

Now that we understand the relationship between variations of curves in $G \rtimes V$ and the induced variations in $\mathfrak{g} \rtimes V$ we can state the Euler-Poincaré theorem for centered semi-direct products.

Theorem 1. *Let $L : T(G \rtimes V) \to \mathbb{R}$ be (right) $G \rtimes V$-invariant, and let $\ell : \mathfrak{g} \rtimes V \to \mathbb{R}$ be its reduced Lagrangian. Let $(g, v)(t) \in G \rtimes V$ and denote the right trivialized velocity by $(\xi_g, \xi_v)(t) := (\dot{g}, \dot{v})(t) \cdot (g, v)(t)^{-1}$. Then the following statements are equivalent:*

(i) Hamilton's principle holds. That is,

$$\delta \int_{t_0}^{t_1} L(g(t), \dot{g}(t), v(t))dt = 0 \tag{9}$$

for variations of $(g, v)(t)$ with fixed endpoints.

(ii) $(g, v)(t)$ satisfies the Euler-Lagrange equations for L.

(iii) The constrained variational principle

$$\delta \int_{t_0}^{t_1} \ell(\xi_g(t), \xi_v(t))dt = 0 \tag{10}$$

holds on $\mathfrak{g} \times V$ for variations of the form

$$(\delta\xi_g, \delta\xi_v) = (\dot{\eta}_g - \mathrm{ad}_{\xi_g}\eta_g, \dot{\eta}_v + \eta_g\xi_v - \xi_v\eta_g + \eta_v\xi_g - \xi_g\eta_v), \tag{11}$$

where $(\eta_g, \eta_v)(t)$ is an arbitrary curve in $\mathfrak{g} \rtimes V$ which vanishes at the endpoints.

(iv) The Euler-Poincaré equations

$$\frac{d}{dt}\left(\frac{\delta \ell}{\delta \xi_g}\right) + \mathrm{ad}^*_{\xi_g}\left(\frac{\delta \ell}{\delta \xi_g}\right) + \xi_v \diamond \frac{\delta \ell}{\delta \xi_v} = 0, \quad \frac{d}{dt}\left(\frac{\delta \ell}{\delta \xi_v}\right) + \xi_g \heartsuit \frac{\delta \ell}{\delta \xi_v} = 0$$

hold on $\mathfrak{g} \bowtie V$.

Proof. The equivalence *(i)* and *(ii)* holds for any configuration manifold and so, in particular it holds in this case.

Next we show the equivalence *(iii)* and *(iv)*. We compute the variations of the action integral to be

$$\begin{aligned}
\delta \int_{t_0}^{t_1} \ell(\xi_g(t), \xi_v(t))dt &= \int_{t_0}^{t_1} \left\langle \frac{\delta \ell}{\delta \xi_g}, \delta \xi_g \right\rangle + \left\langle \frac{\delta \ell}{\delta \xi_v}, \delta \xi_v \right\rangle dt \\
&= \int_{t_0}^{t_1} \left\langle \frac{\delta \ell}{\delta \xi_g}, \dot{\eta}_g - \mathrm{ad}_{\xi_g} \eta_g \right\rangle \\
&\quad + \left\langle \frac{\delta \ell}{\delta \xi_v}, \dot{\eta}_v + \eta_g \xi_v - \xi_v \eta_g + \eta_v \xi_g - \xi_g \eta_v \right\rangle dt
\end{aligned}$$

and applying integration by parts and equation (3) we find

$$\begin{aligned}
&= \int_{t_0}^{t_1} \left\langle -\frac{d}{dt}\left(\frac{\delta \ell}{\delta \xi_g}\right) - \mathrm{ad}^*_{\xi_g}\left(\frac{\delta \ell}{\delta \xi_g}\right), \eta_g \right\rangle + \left\langle -\frac{d}{dt}\frac{\delta \ell}{\delta \xi_v}, \eta_v \right\rangle \\
&\quad + \left\langle \frac{\delta \ell}{\delta \xi_v}, \eta_g \xi_v - \xi_v \eta_g \right\rangle + \left\langle \frac{\delta \ell}{\delta \xi_v}, \eta_v \xi_g - \xi_g \eta_v \right\rangle dt \\
&\quad + \left\langle \frac{\delta \ell}{\delta \xi_g}, \eta_g \right\rangle \Big|_{t_0}^{t_1} + \left\langle \frac{\delta \ell}{\delta \xi_v}, \eta_v \right\rangle \Big|_{t_0}^{t_1} \\
&= \int_{t_0}^{t_1} \left\langle -\frac{d}{dt}\left(\frac{\delta l}{\delta \xi_g}\right) - \mathrm{ad}^*_{\xi_g}\left(\frac{\delta \ell}{\delta \xi_g}\right) - \left(\xi_v \diamond \frac{\delta \ell}{\delta \xi_v}\right), \eta_g \right\rangle \\
&\quad + \left\langle -\frac{d}{dt}\left(\frac{\delta \ell}{\delta \xi_v}\right) - \xi_g \heartsuit \frac{\delta \ell}{\delta \xi_v}, \eta_v \right\rangle dt.
\end{aligned}$$

By noting that $(\eta_g, \eta_v)(t)$ is arbitrary on the interior of the integration domain, the result follows.

Finally, we show that *(i)* and *(iii)* are equivalent. The $G-$invariance of L implies that the integrands in (9) and (10) are equal. However, by Proposition 5 all the variations of $(g, v)(t)$ with fixed endpoints induce, and are induced by, variations $(\delta \xi_g, \delta \xi_v)(t) \in \mathfrak{g} \bowtie V$ of the form given in equation (11). Conversely if *(i)* holds with respect to arbitrary variations $(\delta g, \delta v)$, we define

$$(\eta_g, \eta_v)(t) = (\delta g, \delta v) \cdot (g, v)^{-1},$$

to produce the variation of (ξ_g, ξ_v) given in equation (11). □

Remark 1. There is a left invariant version of theorem (1) in which $(\xi_g, \xi_v) := (g, v)^{-1} \cdot (\dot{g}, \dot{v})$ and L is left $G \bowtie V$-invariant. In this case the Euler-Poincaré equations take the form

$$\frac{d}{dt}\left(\frac{\delta \ell}{\delta \xi_g}\right) - \mathrm{ad}^*_{\xi_g}\left(\frac{\delta \ell}{\delta \xi_g}\right) - \xi_v \diamondsuit \frac{\delta \ell}{\delta \xi_v} = 0,$$
$$\frac{d}{dt}\left(\frac{\delta \ell}{\delta \xi_v}\right) - \xi_g \heartsuit \frac{\delta \ell}{\delta \xi_v} = 0.$$

Remark 2. There is a version of semi-direct product mechanics wherein the vector-space V is a set of *advected parameters* as in [8]. In this case we impose the holonomic constraint

$$\dot{v} = \dot{g} \cdot v + v \cdot \dot{g}$$

and the set of admissible variations in $\mathfrak{g} \bowtie V$ become

$$\delta \xi_g = \dot{\eta}_g - [\xi_g, \eta_g], \quad \delta v = \eta_g \cdot v + v \cdot \eta_g.$$

If we do this, the $\heartsuit$-term is removed and $\frac{\delta \ell}{\delta v}$ equation is replaced with a holonomic constraint. In particular we find that

$$\frac{d}{dt}\left(\frac{\delta \ell}{\delta \xi_g}\right) \pm \mathrm{ad}^*_{\xi_g}\left(\frac{\delta \ell}{\delta \xi_g}\right) \pm \xi_v \diamondsuit \frac{\delta \ell}{\delta \xi_v} = 0 \tag{12}$$

$$\frac{dv}{dt} = \xi_g \cdot v + v \cdot \xi_g. \tag{13}$$

where we use a plus sign for right trivialization and a minus sign for left trivialization.

4 Examples

In this section we will present two examples of Euler-Poincaré equations on centered semidirect products. This first is a toy example designed to illustrate how computations of the diamond and heart operators can be done in practice. The second example is concerns second order jets as described in Section 1.3.

4.1 A Toy Example

Consider the group $\mathrm{GL}(n)$ and let $\mathrm{Mat}(n)$ denote the vector space of $n \times n$ real matrices. Noting that $\mathrm{GL}(n)$ acts on $\mathrm{Mat}(n)$ by left and right multiplication, we can define the composition law on the Lie group $GL(n) \ltimes \mathrm{Mat}(n)$ by:

$$(A, v) \cdot (B, w) = (AB, Aw + vB).$$

Moreover, we can identify $\mathfrak{gl}^*(n)$ with $\mathfrak{gl}(n)$ and $\mathrm{Mat}(n)^*$ with $\mathrm{Mat}(n)$ by the matrix trace pairing $\langle A, B\rangle = \mathrm{trace}(A^T B)$. This allows us to calculate the heart operator $\heartsuit : \mathfrak{gl}(n) \times \mathrm{Mat}(n)^* \to \mathrm{Mat}(n)$ as

$$\begin{aligned}
\langle A\heartsuit w, v\rangle &= \langle w, A \cdot v - v \cdot A\rangle \\
&= \mathrm{trace}\left(w^T (A \cdot v - v \cdot A)\right) \\
&= \mathrm{trace}\left(w^T \cdot (A \cdot v) - w^T (v \cdot A)\right) \\
&= \mathrm{trace}\left((w^T \cdot A)v - (A \cdot w^T) \cdot v\right) \\
&= \mathrm{trace}\left((w^T \cdot A - A \cdot w^T) \cdot v\right) \\
&= \mathrm{trace}\left((A^T w - w \cdot A^T)^T \cdot v\right) \\
&= \langle A^T w - w A^T, v\rangle
\end{aligned}$$

Therefore,

$$A\heartsuit w = A^T w - w A^T.$$

By a similar calculation, diamond operator is found to be

$$v\diamondsuit w = v^T w - w v^T,$$

and the coadjoint action on $\mathrm{GL}(n)$ is given by

$$\mathrm{ad}^*_A(\alpha_A) = A^T \cdot \alpha_A - \alpha_A \cdot A^T.$$

Now, we have all the ingredients to write the Euler-Poincaré equations. Given a reduced Lagrangian $\ell : \mathfrak{gl}(n) \ltimes \mathrm{Mat}(n) \to \mathbb{R}$ we may denote the reduced momenta by

$$\mu = \frac{\delta \ell}{\delta \xi}, \quad \gamma = \frac{\delta \ell}{\delta v}.$$

where $(\xi, v) \in \mathfrak{gl}(n) \ltimes \mathrm{Mat}(n)$. The Euler-Poincaré equations can be written as

$$\begin{aligned}
\dot{\mu} &= (\xi^T \mu - \mu \xi^T) + v^T \gamma - \gamma v^T \\
\dot{\gamma} &= \xi^T \gamma - \gamma \xi^T.
\end{aligned}$$

4.2 An Isotropy Group of a Second Order Jet Groupoid

In Proposition 1 we illustrated how the second order jets of diffeomorphisms of the stabilizer group of a point $x \in M$ is identifiable with a centered semidirect product. In particular, if $\dim(M) = n$ we can consider the group $\mathrm{GL}(n) \ltimes \mathscr{S}^1_2$, where $\mathscr{S}^1_2$ is the set of $(1,2)$-tensors which are symmetric in the covariant indices. For the moment we shall consider the larger space of all $(1,2)$-tensors denoted $\mathscr{T}^1_2$. If we let $\mathbf{e}_1, \ldots, \mathbf{e}_n \in \mathbb{R}^n$ be a basis with dual basis $\mathbf{e}^1, \ldots, \mathbf{e}^n \in (\mathbb{R}^n)^*$ we can write an arbitrary element of $\mathscr{T}^1_2$ as

$$T = T^i_{jk} \mathbf{e}_i \otimes \mathbf{e}^j \otimes \mathbf{e}^k.$$

The left action of $\mathrm{GL}(n)$ on $\mathscr{T}^1_2$ is

$$g \cdot T := T^i_{jk}(g \cdot \mathbf{e}_i) \otimes \mathbf{e}^j \otimes \mathbf{e}^k \equiv T^i_{jk} g^l_i \mathbf{e}_l \otimes \mathbf{e}^j \otimes \mathbf{e}^k$$

while the right action is

$$T \cdot g := T^i_{jk} \mathbf{e}_i \otimes (g^T \cdot \mathbf{e}^j) \otimes (g^T \cdot \mathbf{e}^k).$$

Clearly these actions commute, and so we may form the centered semidirect product Lie group $\mathrm{GL}(n) \ltimes \mathscr{T}^1_2$.

Let us now focus on the Lie algebra. The Lie algebra $\mathfrak{gl}(n)$ is equivalent to $\mathscr{T}^1_1$ and the Lie bracket is then given in the bases $\mathbf{e}_i \otimes \mathbf{e}^j$ by

$$[\xi, \eta] = (\xi^i_k \eta^k_j - \eta^i_k \xi^k_j) \mathbf{e}_i \otimes \mathbf{e}^j,$$

where $\xi = \xi^i_j \mathbf{e}_i \otimes \mathbf{e}^j$ and $\eta = \eta^i_j \mathbf{e}_i \otimes \mathbf{e}^j$. We can use the dual basis $\mathbf{e}^i \otimes \mathbf{e}_j$ to see that the coadjoint action of ξ on $\mu = \mu^j_i \mathbf{e}^i \otimes \mathbf{e}_j$ is given by

$$\mathrm{ad}^*_\xi \mu = (\mu^j_k \xi^k_i - \mu^k_i \xi^j_k) \mathbf{e}^i \otimes \mathbf{e}_j.$$

By differentiation we see that the infinitesimal left and right actions of $\mathfrak{gl}(n)$ on $\mathscr{T}^1_2$ are given by

$$\begin{aligned} \xi \cdot T &= T^i_{jk} \xi^l_i \mathbf{e}_l \otimes \mathbf{e}^j \otimes \mathbf{e}^k \\ T \cdot \xi &= T^i_{lk} \left[\mathbf{e}_i \otimes (\xi^j_l \cdot \mathbf{e}^l) \otimes \mathbf{e}^k + \mathbf{e}_i \otimes \mathbf{e}^j \otimes (\xi^k_l \cdot \mathbf{e}^l) \right] \\ &= (T^i_{lk} \xi^l_j + T^i_{jl} \xi^l_k) \mathbf{e}_i \otimes \mathbf{e}^j \otimes \mathbf{e}^k. \end{aligned}$$

If we choose an arbitrary element $\alpha \in (\mathscr{T}^1_2)^* \equiv \mathscr{T}^2_1$ given by

$$\alpha = \alpha^{jk}_i \mathbf{e}^i \otimes \mathbf{e}_j \otimes \mathbf{e}_k$$

we find that

$$\langle \alpha, \xi \cdot T \rangle = (\alpha_l^{jk} \xi_i^l) T_{jk}^i = (\alpha_i^{lk} T_{lk}^j) \xi_j^i$$
$$\langle \alpha, T \cdot \xi \rangle = (\alpha_i^{lk} \xi_l^j + \alpha_i^{jl} \xi_l^k) T_{jk}^i = (\alpha_l^{jk} T_{ik}^l + \alpha_l^{kj} T_{ki}^l) \xi_j^i.$$

Therefore the heart operator is given by

$$\xi \heartsuit \alpha = (\xi_i^l \alpha_l^{jk} - \alpha_i^{lk} \xi_l^j - \alpha_i^{jl} \xi_l^k) \mathbf{e}^i \otimes \mathbf{e}_j \otimes \mathbf{e}_k$$

and the diamond operator is

$$\alpha \diamond T = (\alpha_l^{jk} T_{ik}^l + \alpha_l^{kj} T_{ki}^l - \alpha_i^{lk} T_{lk}^j) \mathbf{e}^i \otimes \mathbf{e}_j.$$

Given a reduced Lagrangian $\ell : \mathfrak{gl}(n) \bowtie \mathscr{T}_2^1 \to \mathbb{R}$ we can denote $\mu = \frac{\delta \ell}{\delta \xi}$ and $\gamma = \frac{\delta \ell}{\delta T}$. In terms of the basis $\mathbf{e}^i \otimes \mathbf{e}_j$ and $\mathbf{e}_i \otimes \mathbf{e}^j \otimes \mathbf{e}^k$ we may write the (right) Euler-Poincaré equations as:

$$\dot{\mu}_i^j = \alpha_i^{lk} T_{lk}^j + \mu_k^j \xi_i^k - \mu_i^k \xi_k^j - \alpha_l^{jk} T_{ik}^l - \alpha_l^{kj} T_{ki}^l$$
$$\dot{T}_{jk}^i = \xi_i^l \alpha_l^{jk} - \alpha_i^{lk} \xi_l^j - \alpha_i^{jl} \xi_l^k.$$

By restricting $\mathscr{T}_2^1$ to the subspace $\mathscr{S}_2^1$, we can obtain a Lie group which models second order jets of diffeomorphisms as demonstrated in Proposition 2. This example provides a first step towards the creation of higher-order, spatially accurate particle methods [9, section 4]. Moreover, the data of second order jets is necessary for the advection of quantities seen in complex fluids in which the advected parameters depend on gradients of the flow [5, 6]. Therefore, the structures described here may prove useful in the construction of particle-based integrators for complex fluids as well.

5 Conclusion

In this paper, we have presented a variant of traditional semi-direct products, dubbed centered semi-direct products, and we have illustrated the associated Euler-Poincaré theory. The diamond operator, the group multiplication, and the Lie bracket can all be seen as sums of the associated concepts for left and right semi-direct products. As a result, the Euler-Poincaré theory associated with centered semi-direct products can also be seen as a sum of the left and right invariant Euler-Poincaré theories for semi-direct products. Presently, many of these constructions remain fairly theoretical. However, an isotropy group of the second order jet groupoid can be seen as a centered semi-direct product. This has potential applications in simulation of complex fluids. We hope this paper provides a stepping stone towards realizing this application.

Acknowledgements We would like to thank Darryl D. Holm for providing the initial stimulus for this project. The work of L. C has been supported by MICINN (Spain) Grant MTM2010-21186-C02-01, MTM 2011-15725-E, ICMAT Severo Ochoa Project SEV-2011-0087 and IRSES-project "Geomech-246981". L. C owes additional thanks to CSIC and the JAE program for a JAE-Pre grant. The work of H.O. J was supported by European Research Council Advanced Grant 267382 FCCA.

References

1. Abraham, R., Marsden, J.E., Ratiu, T.S.: Manifolds, tensor analysis, and applications. In: Applied Mathematical Sciences, vol. 75, 3rd edn. Springer, New York (2009)
2. Beg, M.F., Miller, M.I., Trouvé, A., Younes, L.: Computing large deformation metric mappings via geodesic flows of diffeomorphisms. Int. J. Comput. Vis. **61**(2), 139–157 (2005)
3. Bloch, A.M., Krishnaprasad, P.S., Marsden, J.E., Ratiu, T.S.: The Euler Poincaré equations and double bracket dissipation. Commun. Math. Phys. **175**, 1–42 (1996)
4. Bruveris, M., Gay-Balmaz, F., Holm, D.D., Ratiu, T.S.: The momentum map representation of images. J. Nonlinear Sci. **21**, 115–150 (2011)
5. Gay-Balmaz, F., Ratiu, T.S.: The geometric structure of complex fluids. Adv. Appl. Math. **42**(2), 176–275 (2009)
6. Holm, D.D.: Euler-Poincaré dynamics of perfect complex fluids. Geometry, mechanics, and dynamics, pp. 113–167. Springer, New York (2002). http://dx.doi.org/10.1007/b97525
7. Holm, D.D.: Geometric Mechanics: Parts I and II, 2nd edn. Imperial College Press, London (2008)
8. Holm, D.D., Marsden, J.E., Ratiu, T.S.: The Euler Poincaré equations and semidirect products with applications to continuum theories. Adv. Math. **137**, 1–81 (1998)
9. Jacobs, H.O., Ratiu, T.S., Desbrun, M.: On the coupling between an ideal fluid and immersed particles. Phys. D 265, 40–56 (2013). http://doi:10.1016/j.physd.2013.09.004
10. Kolar, I., Michor, P.W., Slovak, J.: Natural Operations in Differential Geometry. Springer, New York (1999)
11. Marsden, J.E., Ratiu, T.S.: Introduction to Mechanics and Symmetry. Texts in Applied Mathematics, vol. 17, 2nd edn. Springer, Berlin (1999)
12. Marsden, J.E., Ratiu, T.S., Weinstein, A.: Semidirect products and reduction in mechanics. Trans. Am. Math. Soc. **281**(1), 147–177 (1984)
13. Marsden, J.E., Ratiu, T., Weinstein, A.: Reduction and Hamiltonian structures on duals of semidirect product Lie algebras. In: Fluids and Plasmas: Geometry and Dynamics (Boulder, Colo., 1983). Contemporary Mathematics, vol. 28, pp. 55–100. American Mathematical Society, Providence (1984). MR 751975 (86a:58031)
14. Marsden, J.E., Misiolek, G., Perlmutter, M., Ratiu, T.S.: Symplectic reduction for semidirect products and central extensions. Differ. Geom. Appl. **9**(1–2), 173–212 (1998). Symplectic geometry. MR 1636304 (2000f:53113)
15. Mumford, D., Desolneux, A.: Pattern Theory: The Stochastic Analysis of Real-World Signals. A K Peters, Natick, MA (2010)
16. Sommer, S., Nielsen, M., Darkner, S., Pennec, X.: Higher-order momentum distributions and locally affine lddmm registration. SIAM J. Imag. Sci. **6**(1), 341–367 (2013)

Vortices on Closed Surfaces

Stefanella Boatto and Jair Koiller

Dedicated to the memory of Jerry Marsden

Abstract It was recognized, since the seminal papers of Arnold (Ann Inst Grenoble 16:319–361, 1966) and Ebin-Marsden (Ann Math Ser 2 92(1):102–163, 1970), that Euler's equations are the right reduction of the geodesic flow in the group of volume preserving diffeomorphisms. In 1983 Marsden and Weinstein (Physica D 7:305–323, 1983) went one step further, pointing out that vorticity evolves on a coadjoint orbit on the dual of the infinite dimensional Lie algebra consisting of divergence free vectorfields. Here we pursue a suggestion of that paper, namely, to present an intrinsic Hamiltonian formulation for a special coadjoint orbit, which contains the motion of N point vortices on a closed two dimensional surface S with Riemannian metric g. Our main results reformulate the problem on the plane, mainly C.C. Lin' s works (Lin, Proc Natl Acad Sci USA 27:570–575; Lin, Proc Natl Acad Sci USA 27:575–577, 1941) about vortex motion on multiply connected planar domains. Our main tool is the Green function $G_g(s, s_o)$ for the Laplace-Beltrami operator of (S, g), interpreted as the stream function produced by a unit point vortex at $s_o \in S$. Since the surface has no boundary, the vorticity distribution ω has to satisfy the global condition $\iint_S \omega\, \Omega = 0$, where Ω is the area form. Thus the Green function equation has to include a background of uniform counter-vorticity. As a consequence, vortex dynamics is affected by global geometry. Our formulation satisfies Kimura's requirement (Kimura, Proc R Soc Lond A 455:245–259, 1999) that a vortex dipole describes geodesic motion. A single vortex drifts on the surface, with Hamiltonian given by Robin's function, which in the case of topological spheres is related to the Gaussian curvature (Steiner, Duke Math J 129(1):63–86, 2005). Results on numerical simulations on flat tori, the catenoid and in the triaxial

S. Boatto
Departamento de Matemática Aplicada, Instituto de Matemática da UFRJ, C.P. 68530, Cidade Universitária, 21945-970 Rio de Janeiro, RJ, Brazil
e-mail: boatto.stefanella@gmail.com

J. Koiller (✉)
Instituto Nacional de Metrologia, Qualidade e Tecnologia (INMETRO), Av. Nossa Senhora das Graças 50, 25250-020 Duque de Caxias, RJ, Brazil
e-mail: jairkoiller@gmail.com

D.E. Chang et al. (eds.), *Geometry, Mechanics, and Dynamics*, Fields Institute Communications 73, DOI 10.1007/978-1-4939-2441-7_10

ellipsoid are depicted. We present a number of questions, intending to connect point vortex streams on surfaces with questions from the mathematical mainstream.

1 Introduction and Main Results

A natural motivation to study vortex flows on curved surfaces is the atmospheric circulation on Earth and the flow on the oceans [202], and, more generally, the planetary atmospheres epitomized by Jupiter's great red spot [125, 134]. In addition, since the mid 1990s there is a growing interest coming from condensed matter and atomic physics, specially liquid crystals, superfluids and Bose-Einstein condensates [66, 148, 201].

The aim of this paper is to describe, in coordinate free fashion, how N point vortices s_j of strengths κ_j move on a closed (compact, boundaryless, orientable) surface S with Riemannian metric g. The main results were announced in [17] and [109]. *Our main tool is the Green function of the Laplace-Beltrami operator*, $G(s, s_o)$, interpreted as the stream function produced by a unit point vortex at $s_o \in S$ with a background uniform counter vorticity field.

A *vortex core* is a small round disk (in the metric sense), with a very high value of vorticity on an ocean of low countervorticity. The problem of proving the long time stability of vortex cores on surfaces is of great importance. One possible complication, as indicated in (2) below, is that the core will tend to drift along the surface due not only to curvature but also due to nonlocal effects.

This problem is way beyond our powers, but we are optimistic that analysts can give a positive answer for surfaces in the same positive way that it was obtained in the planar case in the 1980s, see [206, 207].[1] Heuristically, we call the attention that what physicists call the "core energy desingularization method" ([71], 1997) should also work on surfaces, because of the nature of the singular behavior of Green's function near the diagonal:

$$G(s, s_o) \sim \frac{1}{2\pi} \log d(s, s_o), \quad \text{as } s \to s_o. \tag{1}$$

Here $d(s, s_o)$ is the distance function of the metric.

In particular, we argue that a single vortex s_o must move on a closed surface obeying the Hamiltonian system (Ω_g, R_g), governed by the desingularization R_g (called *Robin's function*)

$$R_g(s_o) = \lim_{s \to s_o} G_g(s, s_o) - \frac{1}{2\pi} \log d(s, s_o). \tag{2}$$

Ω_g is the area form of g.[2]

[1] There is an earlier preprint by Wan, Marsden, Ratiu and Weinstein, [208]

[2] Metrics such that the Robin function is constant may be called "hydrodynamically neutral". C. Ragazzo (personal communication) is characterizing this new type of canonical metrics.

We show that *pairs* of opposite point vortices satisfy Kimura's requirement [103]: two infinitesimally close ones follow geodesic motion. The study of long time stability of symmetric vortex structures in the plane has just recently attracted the analyst's interest (see e.g. [35]). This question on surfaces seems quite challenging.

1.1 Marsden and Weinstein: Vortices as Coadjoint Orbits

Instrumental for this essay is Marsden and Weinstein 1983 remarkable paper ("Coadjoint orbits, vortices, and Clebsch variables for incompressible fluids" [135]) interpreting a vorticity field as an element of the dual of $T_{Id}\mathrm{Diff}_{\mathrm{vol}}$, the Lie algebra of divergence free vector fields. In hindsight this Marsden-Weinstein paper is a natural continuation of Arnold's seminal paper [3]. They show that vorticity evolves on a coadjoint orbit by the usual rules of Geometric Mechanics. They exhibit the corresponding KAKS bracket and the reduced Hamiltonian. In Section 7 of [135] there is an observation outlining the construction of the symplectic structure for point vortices on a two-dimensional Riemannian manifold.

> "The usual Hamiltonian equation of N vortices in just the restriction of the standard Euler equation Lie-Poisson Hamiltonian description to a particular coadjoint orbit, with the (infinite) self-energy terms ignored. We did this in $\mathbf{R}^2$ but the description also works for bounded domains or curved surfaces."

Indeed, our symplectic form (11) in $S \times \cdots \times S$,

$$\Omega_{\mathrm{collective}}(s_1, \cdots, s_N) = \sum_{\ell=1}^{N} \kappa_\ell \Omega(s_\ell),$$

follows immediately from the general expression for the reduced symplectic form, as outlined in [135], p. 317 for the planar case. Our Hamiltonian (10)

$$H = \sum_{1 \le i < j \le N} \kappa_i \kappa_j G_g(s_i, s_j) + \sum_{\ell=1}^{N} \frac{1}{2} \kappa_\ell^2 R_g(s_\ell)$$

is also straightforward. The general expression for the reduced Hamiltonian in the coadjoint orbit appears in p. 311 of [135], namely equation ($H_{\mathrm{vorticity}}$)

$$H = \int (\omega, \Delta^{-1}\omega)\mathrm{dvol}. \tag{3}$$

where

$$(\Delta^{-1}\omega)(\bullet) = \int G(\bullet, a)\omega(a)\mathrm{dvol}(a),$$

G being the Green function of the Laplace-Beltrami operator on the manifold. The nonlocal nature of vortex equations on surfaces[3] comes from the inversion Δ^{-1}.

Taking for the vorticity ω a sum of generalized functions with delta singularities (necessarily containing a background countervorticity in the case of closed surfaces) our Hamiltonian follows naturally: the cross terms are given by the Green function at the pairs $\kappa_i \kappa_j G(s_i, s_j)$ while the self contribution, after the "infinite self energy' removed, is given by Robin's function (2) at the vortices.

1.2 Green Functions

Green functions for the Laplace Beltrami operators are at the core of our paper. In [135] the fundamental role of Green functions is implicit in the Δ^{-1} operator on equation ($H_{\text{vorticity}}$), and explicitly used on Section 8.

Green functions should be in the basic toolkit of Geometric Mechanicists. The Green function of the Laplace-Beltrami operator is the keystone of Geometric Analysis. In pure mathematics, they are at the heart of the spectral theory, with ramifications on Riemann surfaces (automorphic functions and analytic number theory).

In the applied side, Green functions are instrumental for computational geometry and manifold learning. Jerry Marsden has leaded the geometric mechanics approach to discrete exterior calculus (joint work with Desbrun, Hirani, and Leok). Green functions are of fundamental importance for singular solutions of EPDiff equations, and for the Lagrangian averaged Euler equations (works of Marsden with Holm, and Ratiu).

Uniformization theory provides for each closed Riemann surface S, a "concrete" realization having a metric of constant curvature. For constant curvature metrics, explicit expressions for the Green functions are known for genus 0 (the sphere) and genus 1 (torus of any modulus). Computing Green functions (and their associated Robin functions) on genus ≥ 2 surfaces for metrics with curvature $K \equiv -1$ is still in its infancy [5]. It is clear by $SO(3)$ symmetry that Robins's function is a constant in the case of a sphere (computed by J. Steiner, [191]). It may seem surprising at first sight, but it is also constant for any flat torus (of arbitrary modular parameter).

A beautiful theory about Robin's function and spectral invariants of conformal classes of metrics was started by K. Okikiolu [153–155]. In short, vortex equations on surfaces belong to mainstream mathematics!

[3] We thank Boris Khesin for this fundamental observation.

1.3 Contributions of Jerry Marsden to Vortex Systems

Marsden advocated that Geometric Mechanics must go hand and hand with Analysis since his Annals of Mathematics paper with Ebin [64]. Here's a short sample of his many collaborations with Ratiu, Montgomery, Lewis and Holm: [93, 94, 94, 122, 123, 136, 138, 139]. Joint work with Ratiu and Raugel in the 1990s about the passage from three to two dimensions is also notable.

In the last 15 years, among his diversified interests, the dynamics of point vortices scientific was a subject of collaboration with many authors of several generations, and we mention just a few, apologizing for the omissions[4]: with Pekarsky and Shkoller [137, 158], for stability of point vortices on a sphere and with Rowley [178] for symplectic integrators; with Shashikanth, Burdick, Kelly, Kanso and Vankerhaver for vortex-structure interactions [184, 185, 204].

1.4 Vortex History on a Capsule

Circa 340 B.D. Aristoteles described typhoons in his *Metereologica*. Vorticity is clearly recognized in Leonardo da Vinci drawings. Descartes envisaged vortices as a possible mechanism for planet's dynamics in the solar system [7]. W.Thomson (also known as Lord Kelvin) and J.J. Thomson used vortices as a possible atomic theory [199]. This theory persisted for over 40 years until it was discarded after Rutherford's 1912 experiments—but some say that string theory is a revival.

Helmholtz' "Wirbel" paper (short for *Über integrale der hydrodynamischen gleichungen welche den Wirbelbewegungen entsprechen*, [87], 1858) came out a century after Euler's *Principes généraux du mouvement des fluides* ([67, 68], 1757)[5] where vorticity first appeared in mathematical form.[6]

Eighteen years later Kirchhoff presented the equations for point vortices in the plane (*Vorlesungen*, [105], chapter XX, p. 259, eq. (14)):

$$m_j \frac{dx_1}{dt} = \frac{\partial P}{\partial y_j}, \; m_j \frac{\partial y_1}{\partial t} = -\frac{\partial P}{\partial x_j}, \quad P = \sum \frac{1}{\pi} m_i m_j \log \rho_{ij} \tag{4}$$

(nowadays instead of m, vortex strengths are denoted by κ or $\Gamma/2\pi$, $1/\pi$ is omitted, and H replaces P).

[4] Jerry was just starting an ambitious project with Shadden and Dabiri on the interplay of vorticity with Lagrangian coherent structures [182, 183], a theme that is now flourishing.

[5] See historical appraisals on the special issue Euler Equations: 250 Years On in Physica D, [69].

[6] See [30] and [150] for excellent treatises and [1, 2, 16, 140, 209] for recent reviews.

This is a Hamiltonian system (Ω, H), where the symplectic form is the combination of planar areas weighted by the vorticities,

$$\Omega_{system} = \sum_j \kappa_j dx_j \wedge dy_j . \tag{5}$$

For arbitrary multiply connected planar domains $D \subset \mathbf{C}$, only in 1941 the correct Hamiltonian was found by Chia-Chiao Lin [126, 127], extended version in [128]. These papers were based on his thesis under Theodore von Kármán.[7]

1.5 Point Vortices on Curved Surfaces: Current Status

The modern study of vortices on surfaces starts with Bogomolov ([24], 1977) and Kimura and Okamoto ([104], 1987) with papers on the (round) sphere. The latter explicitly advocates the role of Green's function of the Laplace-Beltrami operator (in 1999 Kimura also presented the equations on the hyperbolic plane [103]). Many years before, however, vortex equations on the sphere were derived independently by I. Gromeka, a mathematician in Kazan [77], and by Ernst Zermelo,[8] in Göttingen [219].

Point vortex dynamics on surfaces, specially on the sphere, is becoming an active field of research. Among others, see for example: Aref et al. [1, 2], Polvani and Dritschel [162], Kidambi and Newton [99, 100], Borisov and al. [27–29, 31], Newton et al. [151, 152], Sulière and Tokieda [188], Montaldi et al. [144], Tronin [200]. For perturbative analysis, see Castilho and Machado [39] and Hwang and Kim [96, 101, 102].

Regarding existence of configurations of relative equilibria, see for example Lim, Montaldi and Roberts [124]; the linear stability analysis in the plane has a long history, see Havelock [85], Dritschell [62]. More recently, Kurakin [115, 116] and Cabral and Schmidt [38] extended the study to linear and nonlinear stability of a ring with a central vortex. They show how the Dirichlet criterion (weak Lyapunov theorem) is fundamental in this study.

A new line of research on linear and non-linear stability of relative equilibria and rings of vortices on surfaces of revolution. Follows a very incomplete list (we apologize for many omissions) of recent work (other papers will be also referenced in the sequel): Pekarski and Marsden [158], G. Patrick [157], Boatto and Cabral [15], Cabral et al. [37, 38], Laurent-Polz [118, 119], Boatto [14], Boatto and Simó [18], G. Roberts [175], Lim et al [124].

[7] C.C. Lin became an important applied mathematician at MIT and was president of SIAM 1973–1974 (http://www.math.mit.edu/people/profile?pid=155).

[8] Zermelo started as an applied mathematician! His 1899 Habilitation thesis on hydrodynamics was praised by no less than by Hilbert [63]. We thank Alexey Borisov and Ivan Mamaev for this information.

In his thesis A, Regis [169], using our techniques, started a study on the vortex dynamics on the triaxial ellipsoid. Numerical simulations indicate that the vortex pair system is nonintegrable, in contrast with the geodesic flow.

Doubly periodic arrays of vortices (flat tori) have been already studied by Stremler and Aref [193] and more recentlyby Stremler [192]. The two vortex system is integrable on any flat tori (the vortex linear impulse, although not globally defined, can be thought of a second integral). The three vortex system is integrable in the special case of total zero vorticity.

In his thesis, H. Viglioni [205] studied the dependence of the dynamics of two vortices on flat tori on the modular parameter (the modular parameter is defined by the angle between the sides of a fundamental parallelogram, and the proportion between them, see Section 4.1). For two vortices, the relative dynamics follows the level sets of the Green function, which is quite sensitive to the modular parameter. The full bifurcation diagram of the system in terms of the modular parameter was determined, and some striking phenomena were found.

Vortex systems on closed surfaces with genus greater or equal than two, obtained from the Poincaré disk modulo a discrete Moebius group, are uncharted territory.

1.6 Bose-Einstein Condensates on Surfaces

An experimental physicist could describe a BEC as a kind of "molasses made of bosons". All the bosons in the system will occupy the ground state of the trap, near the zero temperature, forming a giant wave function.[9] Quantum mechanical effects on Bose-Einstein Condensates are described by the Gross-Pitaevskii equation [159], which is similar to the Ginzburg-Landau equation used earlier in superconductivity. Both lead to point vortex equations much the same way as Euler's.

In magneto-optical traps (MOT, a technique developed by W. Ketterle that gave him the Nobel prize), atoms coming on a beam are slowed down by a laser counter beam and captured on a cloud. After collecting a large number of atoms, the lasers are turned off and a large magnetic field is turned on to confine the atoms magnetically. As they cool down they form Bose-Einstein condensates. The experimental methods allow full control over vortex creation and manipulation and observation techniques can track their dynamics. The atomic cloud can be manipulated by various techniques. They can be strongly compressed in one direction, leading to a two-dimensional condensate. There also techniques to transport condensates over other surfaces.

In early experiments, vortex crystals were observed all with the same quantized vorticity. Recently vortex pairs have been produced by passing a laser beam on the condensate [66, 147, 148]. From our perspective, it is also exciting that 2d toroidal traps are available for BECs experiments. Hopefully experimental techniques will allow to produce any desired surface geometry (with any genus!).

[9] For a recent review of cosmological BECs, see [174].

Among other technological possibilities, BECs are one of the leading choices in attempts to materialize quantum computation [86].

Remark 1. If a BEC could factorize big numbers [36], one hopes that the Riemann zeta function could somehow be lurking behind and appear in the theory. As it is well known, the approach Hilbert and Polya suggest to Riemann hypothesis is to find a direct connection between the notrivial zeros of Riemann's zeta function with the spectrum of some quantum mechanical problem. It is well known that the distribution of the spectrum of the Laplacian for geodesics on negative curvature surfaces has similar features of the distribution of zeros of $\zeta(z)$ [12, 13, 33]. As we will show, the vortex pair system contains the geodesic problem as a limit.

1.7 Organization of the Paper

Our main results are presented in Section 2. They represent a geometrization of C.C. Lin's theorems. Proofs are outlined in Section 3. In Section 4 we review the available analytical and numerical tools for the computation of Green functions. Examples of vortex pair systems are given in Section 5. In Section 6 we present a heuristic discussion on the role of Green functions, with emphasis on Prandtl-Batchelor's theorem. In Section 7 we present suggestions for further research. In the concluding Section 8, we summarize what we believe is new here.

In the Appendix, we present, in an elementary way, the geometric jargon around Poisson's equation which allows to recover the velocity field from the vorticity distribution. Intended for the benefit of readers that are not in the field of Geometric Mechanics, it is just a "baby" version of the general setting presented in [135].

We present some examples of the application of our formalism. Vortex pairs systems on surfaces of revolution are integrable teo degrees of freedom Hamiltonian systems with a S^1 symmetry. We provide in Section 5 some examples for the S^1 reduction. A numerical simulation of a vortex pair in the catenoid is compared with the geodesic system. Numerical simulations of the vortex pair system on a triaxial ellipsoid were performed in A. Regis thesis [169]. We present here some of their Poincaré sections, that indicate that the vortex pair is a nonintegrable KAM perturbation of Jacobi's geodesic problem. Some figures from H. Viglioni's thesis about the vortex dynamics of the flat torus were also generously offered.

2 Main Theorems

Recall that the Laplace-Beltrami operator $\Delta_g = \text{div grad}$ on a Riemannian manifold (M, g) is self-adjoint, negative definite with respect to the inner product

$$\langle f, g \rangle = \int_M fg \, d\text{vol}.$$

Following Kate Okikiolu [153], in the case of a two dimensional surface S without boundary, the Green function $G = G_{(S,g)}$ of Δ_g is characterized by the following properties (see Flucher and Gustafsson [71] for multiply connected planar regions):

Definition 1.

$$\begin{aligned} &\Delta_g\, G(s, s_o) = -\frac{1}{\text{Area(S)}} + \delta(s, s_o), \\ &G(s, s_o) - \log d(s, s_o)/2\pi \ \text{ bounded}, \\ &\int_S G(p, q)\Omega(q) = 0, \ \ G(s, s_o) = G(s_o, s). \end{aligned} \tag{6}$$

Here $d(s, s_o)$ is the geodesic distance with respect to the metric g, and Ω is the area form. G is the kernel of the integral operator that solves Poisson's equation, i.e.,

$$\Delta^{-1}\omega(s) = \int_S G(s, r)\omega(r)\, \Omega(r). \tag{7}$$

Definition 2. Robin's function.

$$R(s_o) = \lim_{S \to s_o} G(s, s_o) - \log d(s, s_o)/2\pi \tag{8}$$

$G(s, s_o)$ is smooth outside the diagonal, where it diverges logarithmically. To make a duo with Robin, we propose to the following

Definition 3. Batman's function.

$$B(s_1, s_2) = \frac{1}{2}(R(s_1) + R(s_2)) - (G(s_1, s_2) - \log d(s_1, s_2)/2\pi)\,. \tag{9}$$

Note that B is $O(d(s_1, s_2)^2)$. It seems to be a yet unexplored object in geometric function theory.

Our main result is consistent with earlier works by C. C. Lin [126–128] and Flucher and Gustafsson [71]. It can be seen as a mere geometrization of them.

Theorem 1 (Boatto and Koiller [17], 2008). *The Hamiltonian in $S \times \ldots \times S$ for N vortices is*

$$H = \sum_{1 \le i < j \le N} \kappa_i \kappa_j\, G_g(s_i, s_j) + \sum_{\ell=1}^{N} \frac{1}{2}\, \kappa_\ell^2\, R_g(s_\ell) \tag{10}$$

with symplectic form given by the weighted combination of the area forms

$$\Omega_{\text{collective}}(s_1, \cdots, s_N) = \sum_{\ell=1}^{N} \kappa_\ell \Omega(s_\ell). \tag{11}$$

An insight for the collective motion could be as follows.

Each vortex moves on the global stream, but with its own term regularized. It carries a "personal clock", that ticks according to the area form, in its current location.

Corollary 1 (Vortex Drift). *A single vortex moves according to*

$$\dot{s}_o = \text{sgrad}\, R(s_o), \tag{12}$$

where sgrad *means the symplectic gradient, also denoted by* $J\nabla$, J *being the rotation by ninety degrees in the tangent plane.*

The intuition is that the "rest of the universe", $S - s_o$, conspires to impinge its collective reaction on s_o, forcing it to drift: *eppur si muove!*

Physicists derived heuristically an interpretation for the solution of Poisson's equation with right hand side equal to the curvature, see [201], but its usefulness seems to be limited to genus zero. The precise result is remarkable:

Theorem 2 (J. Steiner [191]). *For any metric* g *on* S^2, *with Gaussian curvature* K_g,

$$R_g(s) = \frac{1}{2\pi}\, \Delta_g^{-1}\left[K_g(s) - 4\pi\right] + \frac{1}{A_g(S)} \text{trace} \Delta_g^{-1} \tag{13}$$

Remark 2. Jean Steiner calls attention that for genus ≥ 1 the difference between Robin's function $R_g(s)$ and $\frac{1}{2\pi}\, \Delta_g^{-1}(K_g)(s)$ is no longer a constant. See eq. (8) in [191] for $g = 1$, and Theorem 5 there. The fluctuation terms do not have a simple geometric interpretation.

The case of a pair of opposite vortices is specially important.

Corollary 2 (Vortex Pair Equations). *For a vortex pair the phase space is* $S \times S$, *and the symplectic form is*

$$\Omega_{\text{pair}} = \kappa(\Omega(s_1) - \Omega(s_2)), \tag{14}$$

where Ω *is the area form on* S *and the difference is taken on the pullback to* $S \times S$ *of the projections. The Hamiltonian can be rewritten as*

$$H = \kappa^2 \left(-\log d(s_1, s_2)/2\pi + B(s_1, s_2)\right). \tag{15}$$

Remark 3. Near the diagonal the dominant term is $-\log d(s_1, s_2)/2\pi$. For points distant from the diagonal it is better to use the direct format

$$H = -\kappa^2 \left(-G(s_1, s_2) + \frac{R(s_1) + R(s_2)}{2} \right). \tag{16}$$

Vortex dipoles have been found in Bose-Einstein condensates, [66, 148].

Using Gauss coordinates, we will prove that the vortex pair dynamics satisfies the requirement (or, if one prefers, the conjecture) suggested by Kimura [103]:

Theorem 3. *Kimura's requirement. A vortex dipole (a pair of infinitesimally close opposite vortices) describes geodesic motion.*

As Kimura beautifully wrote, vortex pairs are "curvature checkers".

Theorem 4 (Conformal Metrics). *Consider two metrics in the conformal class of S, related by a conformal factor h, i.e., $\tilde{g} = h^2 g$ and $\Omega_{\tilde{g}} = h^2 \Omega_g$. The Hamiltonian for the vortex system in the metric $\tilde{g}$ can be obtained from the Hamiltonian in the metric g by adding two terms:*

$$\tilde{H} = H - \frac{1}{4\pi} \sum_{\ell=1}^{N} \kappa_\ell^2 \log(h(s_\ell)) - \frac{\kappa}{\tilde{A}(S)} \sum_{\ell=1}^{N} \kappa_\ell \, \Delta_g^{-1} h^2(s_\ell), \quad \kappa = \sum_{\ell=1}^{N} \kappa_\ell. \tag{17}$$

The last term in (17) vanishes when the sum of the vorticities is zero.

Remark 4. From the operational point of view, when considering a surface that is a conformal deformation, say, of the unit sphere $S^2 \subset \Re^3$ as a *reference surface*, the above identification is interpreted as follows (see M. do Carmo [60], Section 4.2). Let $F : S^2 \to \tilde{S} \subset \Re^3$ the conformal map, g and $\tilde{g}$ be respectively the metrics induced in S^2 and $\tilde{S}$ by the euclidian metric $\langle , \rangle$ in $\Re^3$. The conformal factor is defined by

$$\langle \tilde{v}_1, \tilde{v}_2 \rangle = h^2(s) \langle v_1, v_2 \rangle$$

where $\tilde{v}_i = dF(s) \cdot v_i$, $i = 1, 2$, where s is the representative point *in the reference sphere* S^2. This was done for the triaxial ellipsoid in A. Regis thesis [169].

We thank Waldecir Bianchini for Figure 1.

Remark 5. Vortices with mass. Introducing impurities in the fluid is relevant due specially to current interest in Bose-Einstein condensates [8]. Columns of electrons on a parallel magnetic field have analogous equation of motion. For mathematical background, see [32, 110, 166]). For small masses, these systems exhibit slow-fast Hamiltonian phenomena [149]. See [168] for these phenonema on particles on a strong magnetic field. Let each s_j have a mass m_j besides its vorticity κ_j, contributing with a kinetic energy $\frac{1}{2m_j} \langle p_{s_j}, p_{s_j} \rangle$, where the bracket denotes the induced inner product in T^*S via the Legendre transform of g.

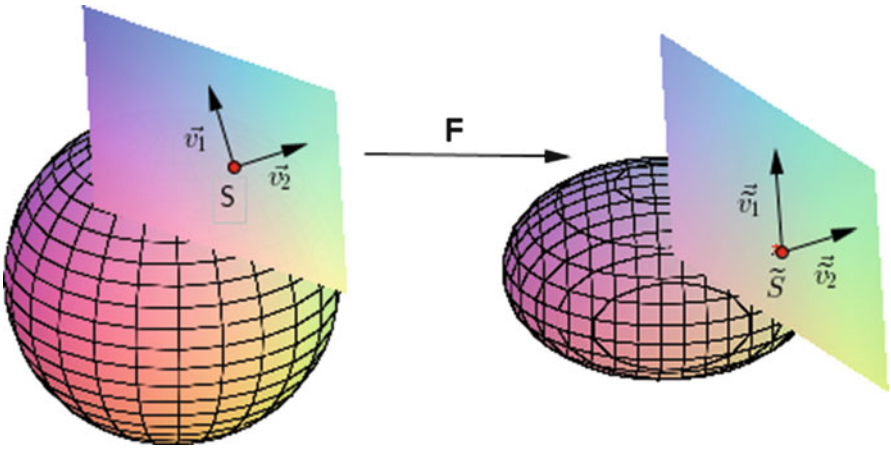

Fig. 1 The vortex dynamics in $\tilde{S}$ is pulled back to S via a conformal map F. *All the calculations for vortex systems in* $\tilde{S}$ *are made in the reference surface* S. The symplectic form pulls back to $\Omega_{\tilde{g}} = h^2(s)\,\Omega_g$. The new Hamiltonian is given by (17) where H is the Hamiltonian for the vortex dynamics on S with the original metric g and symplectic form Ω_g

Theorem 5. *Vortices with mass. The dynamics in* $T^*(S \times \ldots \times S)$ *is described by the Hamiltonian system*

$$H = \sum \frac{1}{2m_j} \langle p_{s_j}, p_{s_j} \rangle \; + \sum_{i<j} \kappa_i \kappa_j \, G(s_i, s_j) + \sum_{\ell=1}^{N} \frac{1}{2} \kappa_\ell^2 R_g(s_\ell) \tag{18}$$

$$\Omega_{\text{collective}} = \Omega_{can} + \sum_j \kappa_j \, \Omega(s_j) \tag{19}$$

where $\Omega_{can} = \text{''} \sum dp_j \wedge ds_j \text{''}$ *is the canonical 2-form of* $T^*(S \times \ldots \times S)$.

Remark 6. Due to the logarithmic singularity of the Green function the N-vortex system (10, 11) is not defined at the diagonals in $S \times \cdots \times S$. Blow up with time regularization studies are in need here.

3 Outline of the Proofs

3.1 Theorem 1 : Main Theorem

It it remarkable that the presence of $\Delta^{-1}\omega$ in (3) brings forward at the same time, the Green function in the cross terms and Robin's function for the self terms in the

Hamiltonian after removing the infinite self energy. Thus, from the point of view of glittering Geometric Mechanics, the argument presented in Section 1.1 should suffice. We *declare* Theorem 1 proved.

We must make a caveat, though. Even in the planar case, point vortex dynamics are considered by analysts as a "mathematical playground", and as such recognized by H. Aref [1]. Jerry Marsden analyst's side would propose to scrutinize at least some of the procedures to remove the infinite self energy in the plane, in order to see what could be used for surfaces. The *core energy method* is described by Flucher and Gustafsson as an "heuristic way of deriving a finite conserved quantity from an infinite energy. The guess obtained in this way can be verified a posteriori". They applied it for vortex problems on planar domains [71].

We assert that this procedure should work on surfaces as well. Consider a small Gauss system of normal coordinates around s_o. The gradient $\operatorname{grad} d(s, s_o)$ is a unit vector along the geodesic ray. The symplectic gradient $\operatorname{sgrad} d(s, s_o)$ is obtained by composition with J and is therefore tangent to the geodesic circles. Its flow leaves the geodesic disks invariant. The same is true for any function of the distance For $\log d(s, s_o)$ the vectors rotate with speed inversely proportional to $d(s, s_o)$. The kinetic energy confined in this blob diverges logarithmically.

The infinity can be removed (in physicists jargon, renormalized) provided only a small quantity of kinetic energy crosses the boundary of a geodesic disk in finite time. We invoke [71]: energy diffusion "can be neglected in the limit as the radius of the ball tends to zero", Section 5). This is true precisely due to the fact that $G(s, s_o) - d(s, s_o)/2\pi$ is bounded.

A related view is to ask for *how long* do regions of concentrated vorticity of Euler's PDE subsist. In the plane it was shown in the 1980s (by different methods) that small nearly circular vortex cores remains stable for a long time. Besides the works by Wan, Marsden, Ratiu and Weinstein and Wan and Pulvirenti mentioned before, see Tang, [197], and Constantin [42] and Iftimie et al. [97]; for recent work see Sideris [186]).

3.2 *Theorem 4: Conformal Transformations of the Domain*

Let $\tilde{g} = h^2 g$. How do the vortex problems on (S, g) and $(S, \tilde{g})$ relate? The symplectic form deforms as $\Omega \to h^2 \Omega$. In order to find the new Hamiltonian in terms of the old one, we need transformation formulas both for the Green and Robin functions.

Note that Green's function $G_{\tilde{g}}(s, s_o)$ for the Laplace-Beltrami operator on a closed surface is *not* conformally invariant. It *must* change, because the notion of background uniform vorticity is area dependent (except, obviously, when it is zero).

Fortunately, transformation formulas for Green and Robin functions are known:

Proposition 1 ([153]).

$$\tilde{G}(s,s_o) - G(s,s_o) = -\frac{1}{\tilde{A}}\left(\Delta_g^{-1}h^2(s) + \Delta_g^{-1}h^2(s_o)\right) + \frac{1}{\tilde{A}^2}\int_S h^2\Delta_g^{-1}h^2\,\Omega \tag{20}$$

$$\tilde{R}(s) = R(s) - \frac{1}{2\pi}h - \frac{2}{\tilde{A}}\Delta_g^{-1}h^2(s) + \frac{1}{\tilde{A}}\int_S h^2\Delta_g^{-1}h^2\Omega \tag{21}$$

Proof of Theorem 4. Recall that a map $F : (S,g) \to (\tilde{S},\tilde{S})$ between two Riemannian manifolds is conformal when

$$\tilde{g}(dF_s\cdot v_s,\ dF_s\cdot w_s) = h^2(s)g(v_s,w_s). \tag{22}$$

We identify $\tilde{S}$ with S via F, in other words, we use S to parametrize $\tilde{S}$. With this point of view, we are inducing a new metric $\tilde{g}_F(v_s,w_s)$ in S such that $\tilde{g}_F = h^2 g$. The new symplectic form in S is $\Omega \to h^2\Omega$.

We can get the Hamiltonian for the vortex system with the conformally changed metric after some simple algebra using (20) and (21). It is remarkable that the sum of the vorticities comes up in the last term.

$$\tilde{H} = H - \frac{1}{4\pi}\sum_{\ell=1}^{N}\kappa_\ell^2\,\log(h(s_\ell)) - \frac{\kappa}{\tilde{A}}\sum_{\ell=1}^{N}\kappa_\ell\Delta^{-1}h^2(s_\ell),\quad \kappa = \sum_{\ell=1}^{N}\kappa_\ell. \tag{23}$$

Proof of Proposition 1 (Following [154]). The trick is average over $\tilde{\Omega}$ twice using the "axioms" of Green's function. Consider the functions

$$G(s,s_o) - G(s,s_1) = E(s;s_o,s_1),\ \ \tilde{G}(s,s_o) - \tilde{G}(s,s_1) = \tilde{E}(s;s_o,s_1).$$

Both $\tilde{E}$ and E are harmonic up to $(+)$ and $(-)$ log singularities at s_o and s_1 so they differ by a constant c. To find this constant we do the $\Omega(s) = h^2(s)\Omega(s)$ average of

$$\tilde{E} - E = (\tilde{G}(s,s_o) - \tilde{G}(s,s_1)) - (G(s,s_o) - G(s,s_1)) = c.$$

The first two terms drop out while the last two give

$$\Delta^{-1}h^2(s_1) - \Delta^{-1}h^2(s_o) = c\,\tilde{A}.$$

Hence

$$(\tilde{G}(s,s_o) - \tilde{G}(s,s_1)) - (G(s,s_o) - G(s,s_1)) = \Delta^{-1}h^2(s_1)/\tilde{A} - \Delta^{-1}h^2(s_o)/\tilde{A}.$$

Again, average this expression, but now over $\Omega(s_1)$. We get

$$\tilde{G}(s,s_o)\tilde{A}-0-G(s,s_o)\tilde{A}+\Delta^{-1}h^2(s)=\int_S \Delta^{-1}h^2(s_1)h^2(s_1)\Omega(s_1)/\tilde{A}-\Delta^{-1}h^2(s_o).$$

This gives the transformation formulas $G \to \tilde{G}$. The transformation formula $R \to \tilde{R}$ follows by taking the limit $s \to s_o$ in

$$\tilde{G}(s,s_o)-\frac{\log(\tilde{d}(s,s_o))}{2\pi}=\left(\tilde{G}(s,s_o)-G(s,s_o)\right)+$$
$$+\left(G(s,s_o)-\frac{\log d(s,s_o)}{2\pi}\right)-\frac{\log(\tilde{d}(s,s_o)/d(s,s_o))}{2\pi}.$$

This completes the proof of Proposition 1.

3.3 *Proof of Kimura's Conjecture on Dipole Motion*

The Hamiltonian for a vortex pair (with opposite vorticities) writes as

$$H=-\kappa^2\frac{\log d(s_1,s_2)}{2\pi}+\kappa^2 B(s_1,s_2), \tag{24}$$

$$B(s_1,s_2)=\left[\frac{R(s_1)+R(s_2)}{2}-\left(G(s_1,s_2)-\frac{\log d(s_1,s_2)}{2\pi}\right)\right]. \tag{25}$$

Let $\kappa = O(\epsilon)$ and initial conditions $d(s_1(0),s_2(0)) = O(\epsilon)$. Kimura's conjectured that as $\epsilon \to 0$ the vorticity pair tends to move along a geodesic path.

Proof. Consider the truncated system where we take only the first term in (24). This yields a very simple system of ODEs,

$$\dot{s}_1=-\kappa\ \mathrm{sgrad}_{s_1}\ \log d(s_1,s_2),\ \ \dot{s}_2=\kappa\ \mathrm{sgrad}_{s_2}\ \log d(s_1,s_2). \tag{26}$$

Since initially $1/d(s_1,s_2) = O(\epsilon^{-1})$ and we took $\kappa = O(\epsilon)$, we expect this equation to represent the dominant $O(1)$ dynamics; in fact, the perturbation is at least $O(\epsilon^2)$. ($B(s_1,s_2) = O(\epsilon^2)$). In order to show that (26) leads to geodesic motion as $\epsilon \to 0$, we use Gauss coordinates [60, 194]

$$ds^2=du^2+G(u,v)dv^2,\ \ G(0,v)=1,\ \ \frac{\partial}{\partial u}_{|u=0}G(u,v)=0. \tag{27}$$

All the u-curves (making v = const.) are geodesics, but only the central v-curve (for $u = 0$) is guaranteed to be a geodesic. That is the curve we are focusing in. Take an s_o corresponding to an arbitrary v value on that central geodesic with $u \equiv 0$. In the (u,v) coordinates, $s_1(0) = (-\epsilon, v)$ and $s_2(0) = (\epsilon, v)$.

Invoking Gauss' lemma, we see that at $t = 0, \dot{s}_{1,2}$ will be tangent to v-curves. Indeed, is the Gauss coordinate system, we have

$$\dot{v}_1(0) = \kappa/2\epsilon \frac{1}{\sqrt{G(-\epsilon, v)}}, \quad \dot{v}_2(0) = \kappa/2\epsilon \frac{1}{\sqrt{G(\epsilon, v)}}, \quad \dot{u}_1(0) = \dot{u}_2(0) = O(\epsilon). \tag{28}$$

For the complete system (with the Batman contribution restored) in the limit as $\epsilon \to 0$ (27), with $\kappa = 2\epsilon$, we get

$$\dot{v}_1(0) = \dot{v}_2(0) = 1 + O(\epsilon), \quad \dot{u}_1(0), \dot{u}_2(0) = O(\epsilon). \tag{29}$$

For the latter we used that $\frac{\partial}{\partial u}_{|u=0} G(u, v) = 0$. Since v was arbitrary, this concludes the proof.

In Section 7 we present a more elaborate proof. The geodesic system will be viewed as a compactification of the vortex system along the diagonal of $S \times S$. For that purpose, a mapping will be constructed from a neighborhood of the diagonal to a neighborhood of the zero section of T^*S.

4 Are Green Functions Computable?

As a preliminary step for the next section on examples, we present a discussion about the computation of Green functions. Let $z = x + iy$ the complex parameter on the universal cover of S, the euclidian plane, the sphere or the hyperbolic plane. For the universal covers, the Green functions are (see Kimura [103] for details).

$$\text{i)} \quad G_E(z, z_o) = \frac{1}{2\pi} \log|z - z_o| \quad \text{(euclidian plane)} \tag{30}$$

$$\text{ii)} \quad G_H(z, z_o) = \frac{1}{2\pi} \log(\tanh d_H(z, z_o)/2) \quad \text{(hyperbolic plane)} \tag{31}$$

$$\text{iii)} \quad G_{Sph}(s, s_o) = \frac{1}{2\pi} \log(\sin d_S(s, s_o)/2) \quad \text{(sphere)} \tag{32}$$

where d_S and d_H are respectively, the spherical and hyperbolic distances

For an *open* Riemann surfaces such as the cylinder, the Green function can be easily computed (in closed form) by summing the $G_E(z, z_o)$ over all the replicas of z_o (one on every strip). The resulting Green function is [65]

$$G_{cyl} = \frac{1}{4\pi} \log(\cosh(x - x_o) - \cos(\phi - \phi_o)). \tag{33}$$

Thanks for Crowdy and Marshall, Green functions for multiply connected planar regions reached an algorithmic stage, see [50–56].

For deformed spheres (genus zero), the fact that there is just one conformal class, and J. Steiner's result (Theorem 2) makes their vortex dynamics amenable to theoretical and numerical experimentation.

4.1 Genus 1 Surfaces

The complex structure is defined by a fundamental polygon with generators $\omega_1 = (1,0)$ and $\omega_2 = \tau = (a,b),\ b > 0$. More precisely, $\mathbf{C}/G$ where G is a group of translations with generators ω_1, ω_2 with $\mathrm{Im}(\omega_2/\omega_1) > 0$. Given G' generated by ω_1', ω_2' the quotients are conformally equivalent if and only if the ratios $\tau = \omega_2/\omega_1$ and $\tau' = \omega_2'/\omega_1'$ are related by an unimodular transformation

$$\tau' = (a\tau + b)/(c\tau + d),\ a,b,c,d \in Z,\ ad - bc = 1.$$

The modular surface is therefore $\mathscr{M} = \{\mathrm{Im}\,\tau > 0\}/SL(2,Z)$. Green functions for the flat metrics, with τ as a parameter, can be constructed explicitly, using elliptic functions. See (34) below, and details in [130].

It is known that any given complex structure on genus 1 tori can be physically realized on $\mathbf{R}^3$ (a problem posed by Felix Klein[10]), see e.g. [73]. The transformation formulas between Green functions in the same conformal class (Proposition 1) pave the way for families of vortex problems on (genus 1) tori.

For all flat tori, due to the dependence of G on $z-w$, Robin's function is constant. Therefore, a single vortex s_o will not drift. In Figures 2, 3, 4, and 5, courtesy of Humberto Viglioni, level lines of Green functions of several flat tori are depicted. The level lines of $G(s, so)$ represent the path of a marker s.

Theorem 6. *Green function for the flat tori [129, 130].*

Consider a torus $T = \mathbf{C}/L$, where L is the lattice generated by 1 and $\tau = a + bi$, $b > 0$. Let $q = e^{\pi i \tau}$ so $|q| = e^{-\pi b} < 1$. Up to a constant $C(\tau)$, the Green function $G(z,w)$ for the Laplace operator on T is given by

$$G(z,w) = -\frac{1}{2\pi}\ln|\theta_1(z-w)| + \frac{1}{2b}(\mathrm{Im}(z-w))^2 + C(\tau). \tag{34}$$

where the theta function $\theta_1(z;\tau)$ is the exponentially convergent series

$$\theta_1(z;\tau) = 2\sum_{n=0}^{\infty}(-1)^n q^{(n+1/2)^2} sin((2n+1)\pi z),\ \ z = x + iy. \tag{35}$$

[10] We do not know if there is an algorithm to identify the complex structure and the conformal factor of a given embedded genus 1 surface.

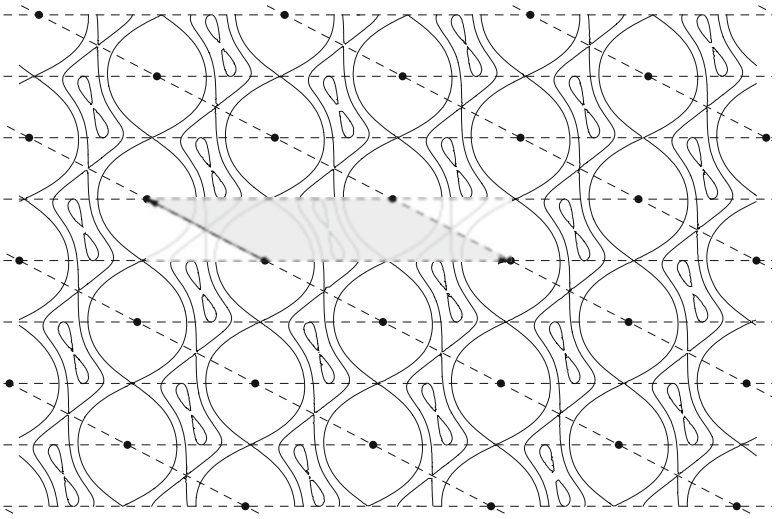

Fig. 2 Representation, at the complex plane, of the level curves for Green's function on a flat torus $T := \mathbf{C}/\Lambda(\omega_1, \omega_2)$, where $\Lambda(\omega_1, \omega_2)$ is the lattice generated by ω_1, represented by a dashed arrow, and ω_2, by a solid arrow. The black circles represent the vortex position. The singularities of Green's function are saddles and centers, in general 3 inside a fundamental domain. There are 5 singularities for exceptional values of the modular parameter $\tau = \omega_2/\omega_1$. These τ values form 1-parameter families, which are invariant under biholomorphisms. Courtesy of H. Viglioni

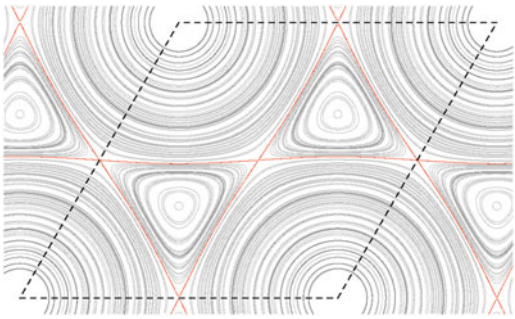

Fig. 3 Main exceptional case [130]: periods 1 and $\tau = e^{\pi i/3}$. Note the 5 critical points. The level lines of $G(s, so)$ represent the path of a marker s. Courtesy of H. Viglioni [205]

The Green functions have always three critical points (not counting the vortex): one of them corresponding to the vertices of the fundamental domain, and the other two are the half periods. In [130] it is shown that there are special 1-parameter families (parametrized by the modular parameter τ) with an extra pair of singular points. Viglioni [205] described the structure of these families inside the modular surface. The τ values where these 1-parameter families meet correspond to even very exceptional situations, namely, where the extra pair of singular points are born (or die). Subtle phenomena take place, yet to be fully explored.

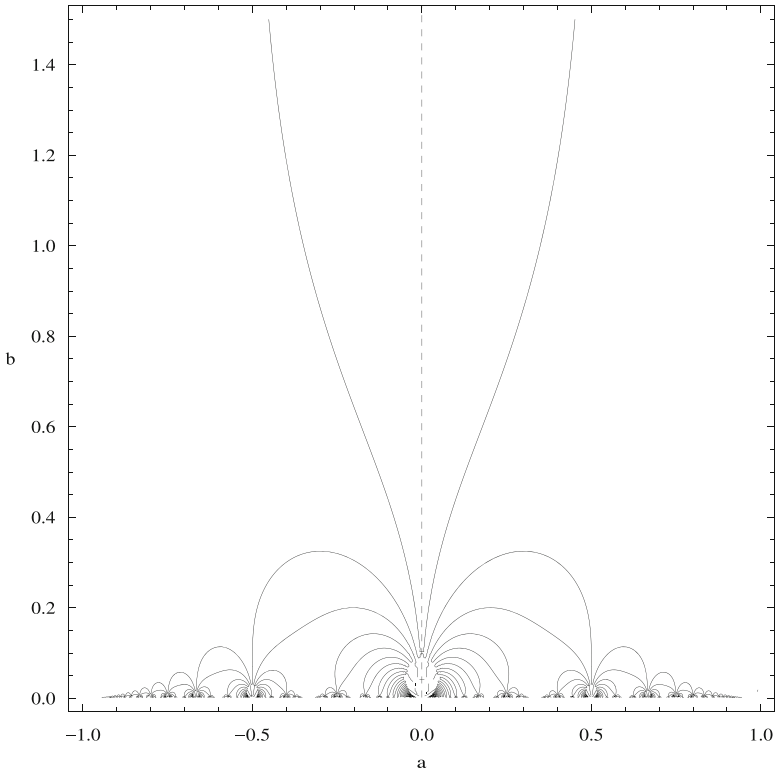

Fig. 4 Values of the modular parameter yielding degeneracies of Green's function at a half-period of the lattice. Two more centers emerge from a degenerated one which changes into a saddle. The infinite repetition is due to the invariance under the action of the modular group. Courtesy of H. Viglioni

4.2 Green's Function on Flat Tori; Constancy of Their Associated Robin's Function

We now explain why *for constant curvature metrics* the self drift to Robin's function occurs only if the genus of the surface is ≥ 2. For the round sphere it is obvious. A closed Riemann surface of genus ≥ 1 can be represented by a fundamental domain on the universal cover. Therefore, an n-vortex system on S can be represented by n vortices on the fundamental domain and their "clones" on every image domain. The Green function G_{S,g_o} of the constant curvature metric in S is formally given by a *Poincaré series*, where we also subtract, on every domain, the background countervorticity (with intensity equal to the inverse of the area).

The dependence of G on $z-w$ immediately brings as a consequence that Robin's function is a constant. It is interesting to see why this does not happen for higher genus. We now give a simple direct proof.

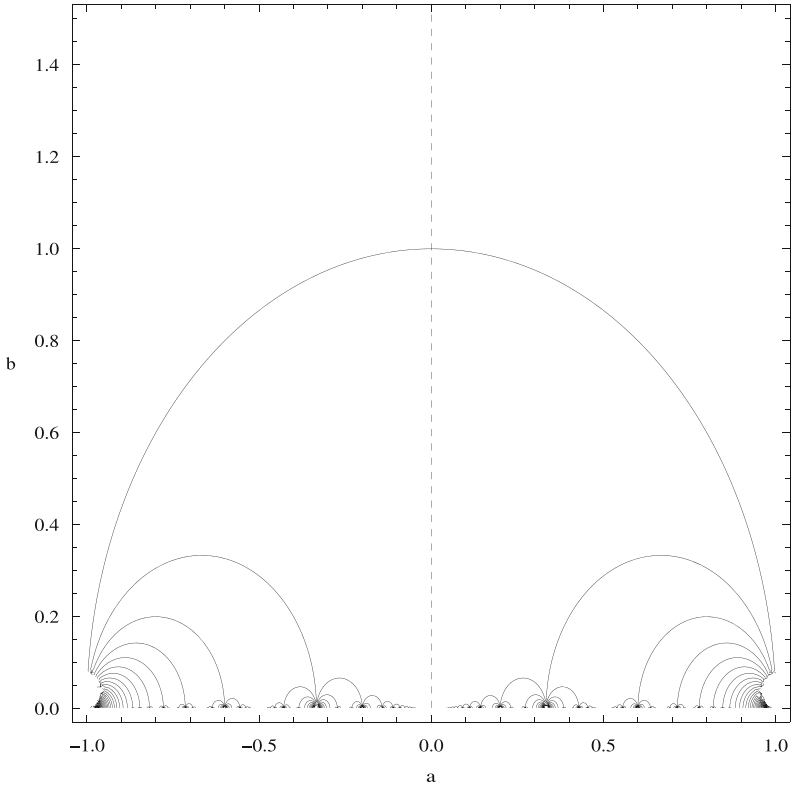

Fig. 5 Diagram in the parameter space $\tau = a + bi, \quad b > 0$, of homoclinic and heteroclinic connexions between half-periods in a normalized lattice $\Lambda(1, \tau)$. This diagram is invariant under the action of $SL(2, Z)$. Courtesy of H. Viglioni

Let $\mathcal{G}(z, w)$ the Green's function for the hyperbolic Laplacian on the Poincaré disk D or, equivalently, in the upper half plane, see (30) for the explicit expression. Let H a discrete Fuchsian subgroup of Moebius transformations, and $S = D/H$ the compact Riemann surface endowed with the canonical metric of curvature -1.

Let $\mathcal{F}$ a fundamental domain. The following formula for the *automorphic Green function* is attributed to Poincaré:

$$\mathcal{G}_S(z, w) = \sum_{g \in H} \left[\mathcal{G}(z, g \cdot w) - \frac{1}{\text{area}\mathcal{F}} \int_{\mathcal{F}} \mathcal{G}(z, g \cdot \xi)\, dA(\xi) \right] \tag{36}$$

Note that one needs to discount the background countervorticity to make the sum converge. Let now ϕ_t the flow of a Killing field for the hyperbolic metric *in the universal cover* D. We substitute

$$\mathcal{G}_S(\phi_t(z),\phi_t(w)) = \sum_{g\in H}\left[\mathcal{G}(\phi_t(z), g\phi_t(w)) - \frac{1}{\text{area}\mathcal{F}}\int_{\mathcal{F}}\mathcal{G}(\phi_t(z), g\cdot\xi)\,dA(\xi)\right].$$

The last term can be replaced by $\int_{\mathcal{F}}\mathcal{G}(z, g\cdot\xi)\,dA(\xi)$ but we are in trouble with the term in red. Since the Moebius transformation group is non commutative, in general

$$\mathcal{G}(\phi_t(z), g\phi_t(w)) \neq \mathcal{G}(\phi_t(z), \phi_t(gw))(\ = \mathcal{G}(z, gw)\ )$$

(In passing, this is a hand waving proof that there cannot exist Killing fields for genus ≥ 2. In MathOverflow one can find a much better argument by R. Bryant[11]).

4.3 Genus $\geq$ 2 Constant Curvature and Other Canonical Metrics

Helen Avelin obtained explicit expressions for the *resolvent* of the Laplace-Beltrami operator for surfaces of constant negative curvature obtained by tesselations of the Poincaré disk by certain Fuchsian groups, [5, 6]. However, as far as we know, there is no direct way to connect the resolvent (which contains a spectral parameter λ) to the Green function (6).

The subject is therefore in its infancy. Hopefully it will mature to the point that closed form expressions could be provided for the Green functions (6) associated to any element in Teichmüller space. The study of Green functions for other canonical metrics (Mandelstam, Arakelov, Bergman) is also in its infancy, but see recent work by Alexey Kokotov and collaborators for conical-flat metrics on polyhedral surfaces ([111, 112] and references therein).

4.4 Discrete Computational Geometry

This is a fast growing area. In his Ph.D. thesis Hirani [92] presents discrete analogues for the differential operators on surfaces. Discrete Green functions are studied in [196], discrete Riemann surfaces in [142].

Among other relevant references we mention work by Desbrun and collaborators, [59, 143] and Polthier's group [90, 160, 161]. See also [10, 19, 20, 61, 213, 214] For recent advances on numerical conformal mappings of surfaces, we refer specially to the work by S.-T. Yau and his collaborators in computer graphics, [41, 58, 80, 98, 131, 217, 218], and the recent book [81].

[11] http://www.mathoverflow.net/questions/122438/compact-surface-with-genus-geq-2-with-killing-field.

Green functions for the Laplace Beltrami operator are of interest not only in geometry, physics, probability and stochastic processes (including recent applications for finances). For instance, there is growing interest in machine learning community, see [10, 11, 181].

5 Examples

5.1 *Surfaces of Revolution: Momentum Map and Reduction*

In this section and the next, we summarize some results for vortex pairs presented in [109]. Let

$$X = (h(z)\cos(\phi), h(z)\sin(\phi), z)$$

a surface of revolution. The metric is

$$ds^2 = h^2(z)d\phi^2 + (1 + (dr/dz)^2)dz^2. \tag{37}$$

Gauss advocated changing to uniformizing coordinates (x, ϕ) where $x = x(z)$ is given by a quadrature

$$h^2(z) = (1 + (dh/dz)^2)(dh/dx)^2, \tag{38}$$

so that

$$ds^2 = h^2(z(x))(d\phi^2 + dx^2). \tag{39}$$

The momentum map corresponding to the ϕ-symmetry is given by

$$J = \int_{x_1}^{x_2} h^2(x)dx. \tag{40}$$

For Marsden-Weinstein's reduction [135], one needs to solve (40) for $x_2 = x_2(x_1, J)$, usually a transcendental equation (see below for examples).

The reduced symplectic form is obtained from $\Omega = h^2(x_1)d\phi_1 \wedge dx_1 - h^2(x_2)d\phi_2 \wedge dx_2$ simply by making $\phi_2 = 0$. In reduced coordinates (x_1, α), where $\alpha = \phi_1 - \phi_2$, the result is

$$\Omega_{\text{red}} = h^2(x_1)d\alpha \wedge dx_1. \tag{41}$$

The reduced 1-dof Hamiltonian is given by

$$H_{\text{red}} = -\kappa^2 G(x_1, x_2(x_1, J), \alpha) - \kappa^2 \frac{1}{4\pi}\left(\log h(x_1) + \log h(x_2(x_1, J))\right), \tag{42}$$

which allows us to draw directly the trajectories $H_{\text{red}} = h$ in the reduced plane (x_1, α). To get the time parametrization, one must solve

$$h^2(x_1)\dot{x}_1 = -\partial H_{\text{red}}/\partial\alpha, \quad h^2(x_1))\dot{\alpha} = \partial H_{\text{red}}/\partial x_1. \tag{43}$$

The final reconstruction is given by a quadrature. Since $x_2(t) = x_2(x_1(t), J)$, we get

$$\phi_2(t) = \phi_2(0) + \int_{t_o}^{t} \frac{1}{h^2(x_2(t))}\, \partial H/\partial x_{2|(x_1(t),\alpha(t),x_2(t))}, \quad \phi_1(t) = \phi_2(t) + \alpha(t). \tag{44}$$

5.1.1 Cone

Here $r(z) = az$. The uniformizing coordinates are (x, ϕ) with

$$z = \exp(bx), \quad b = a/\sqrt{1 + a^2}. \tag{45}$$

The momentum map is

$$J = \frac{a^2}{2b}\left(\exp(2bx_2) - \exp(2bx_1)\right). \tag{46}$$

In this case it is simple to solve for x_2 as a function of x_1 and J.

5.1.2 Torus

We consider the torus of revolution in $\Re^3$. The standard parametrization is given by

$$X(u, \phi) = ((R_2 + R_1 \cos u)\cos\phi, (R_2 + R_1 \cos u)\sin\phi, R_1 \sin u), \tag{47}$$

with metric

$$ds^2 = (R_2 + R_1 \cos u)^2 d\phi^2 + R_1 du^2. \tag{48}$$

We must find $u = u(x)$ such that $(R_2 + R_1 \cos u)^2 = R_1^2 (du/dx)^2$. One gets

$$x = \int^{u} \frac{1}{a + \cos(u')}\, du', \; a = R_2/R_1.$$

yielding

$$x = 2 \arctan\left(\frac{(a-1)\tan(1/2\,u)}{\sqrt{(a+1)(a-1)}}\right) \frac{1}{\sqrt{(a+1)(a-1)}}. \tag{49}$$

For $R_2 = R_1$ get a simpler expression

$$x = \tan(1/2\,u)\,.$$

The conformal factor is

$$h^2(x) = R_1^2(du/dx)^2 = \frac{4R_1^2}{1+x^2} \tag{50}$$

and the integral of motion is

$$J = 4R_1^2 \int_{\xi_1}^{\xi_2} \frac{1}{(1+\xi^2)^2} d\xi = R_1^2(P(x_2) - P(x_1)) \tag{51}$$

with

$$P = 2\,\frac{x}{1+x^2} + 2\,\arctan(x)\,. \tag{52}$$

No explicit solution seems to be directly available for the transcendental equation yielding x_2 as a function of x_1 and J.

5.1.3 Catenoid

The underlying Green function is (33). Its parametrization is given by

$$X(x,\phi) = (\cos(\phi)\cosh(x), \sin(\phi)\cosh(x), x), \quad ds^2 = \cosh^2(x)(d\phi^2 + dx^2). \tag{53}$$

Here

$$J = \frac{1}{2}\,[\,(\sinh(2x_2) + x_2) - (\sinh(2x_1) + x_1)] \tag{54}$$

The geodesic problem can be solved with elliptic functions [167]. But for the vortex systems, the transcendental equation

$$x + \sinh(2x) = a. \tag{55}$$

requires defining a new special function as a preliminary step towards analytically solving (43). Figs. 6 and 7 illustrate "Kimura's trinity" (shorthand for the trace of the pair of vortices and the geodesic in the middle).

The study of polygonal configurations of vortices in surfaces of revolution and their stability, in the lines of [120, 121] is in order.

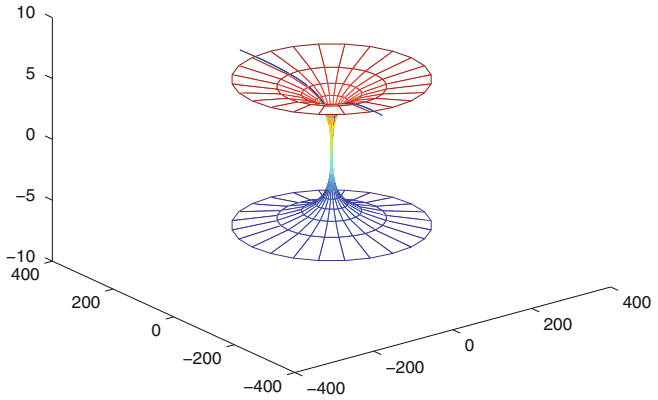

Fig. 6 Geodesic and vortex pairs on the catenoid, indistinguishable

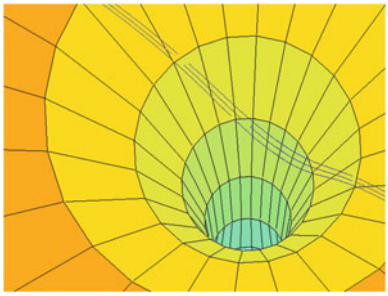

Fig. 7 Close up. The geodesic path between two close opposite vortices is revealed. We may call such structure a *Kimura trinity*

5.2 Vortex Pair Equations for Metrics g on S^2

Any metric g in the sphere S^2 is conformal to the standard constant curvature metric g_o, $g = h^2 g_o$. The symplectic form in $S^2 \times S^2$ is given by

$$\Omega_{\text{pair}} = \kappa \left(h^2(s_1)\Omega_o(s_1) - h^2(s_2)\Omega_o(s_2) \right) \tag{56}$$

where Ω_o is the area form of the sphere. The vortex pair Hamiltonian on a surface of genus zero is given by (omitting a 2π factor)

$$\begin{aligned} H &= -\frac{1}{2}\log\left(h(s_1)h(s_2)|s_1 - s_2|^2\right) = \\ &= -\left(\log|s_1 - s_2| + \frac{1}{2}\log h(s_1) + \frac{1}{2}\log h(s_2)\right) \end{aligned} \tag{57}$$

where $|\ |$ is the euclidian distance. The equations of motion are therefore

$$\dot{s_1} = \frac{1}{h^2(s_1)}\left(\frac{s_1 \times s_2}{|s_1 - s_2|^2} - \frac{1}{2} s_1 \times \mathrm{grad} h(s_1)\right) \tag{58}$$
$$\dot{s_2} = \frac{1}{h^2(s_2)}\left(\frac{s_1 \times s_2}{|s_1 - s_2|^2} + \frac{1}{2} s_2 \times \mathrm{grad} h(s_2)\right).$$

5.3 *Triaxial Ellipsoid*

Numerical simulations for a vortex pair in the triaxial ellipsoid were presented in the doctoral thesis of Adriano Regis [169]. As expected, nearby vortex pairs envelop geodesics. However, Poincaré sections suggest chaotic behavior for sufficiently distant initial positions. Near the diagonal of $S \times S$ the behavior seems a typical KAM type perturbation of the geodesic flow (see Figures 8, 9, and 10).

In order to obtain the equations of motion, in view of (58), one needs a conformal map from the standard sphere to the triaxial ellipsoid (with the induced euclidian metric). Such maps were constructed by Schering [180] in 1857, see also [46, 145]. Regis and Castilho opted to make a fresh start, following a suggestion in [109]. They take conformal quadric coordinates on the ellipsoid and sphero-conical coordinates on the sphere. The key point is to adjust the parameters in such a way that the images of octants on each surface cover the same rectangle in the plane.

The map is given in terms of two elliptic integrals and two inversions. The four ellipsoid umbilical points of the ellipsoid (see [194], Section 2.8) correspond to four special points in the sphere. The coordinate lines on both surfaces have similar distributions and reach the boundaries of an octants perpendicularly, so that can be continued to the contiguous ones.

Below a sample of A. Regis simulations.

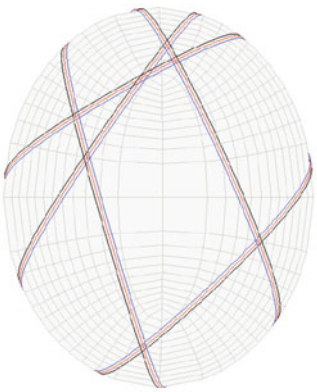

Fig. 8 Geodesic and nearby vortex pair on the 1-6-9 ellipsoid. Courtesy of Adriano Regis

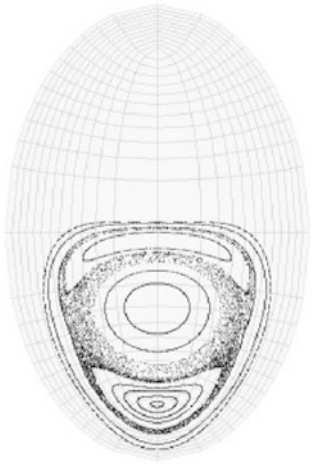

Fig. 9 Poincaré sections in the 1-4-9 ellipsoid. Courtesy of A. Regis. For details, see [169]

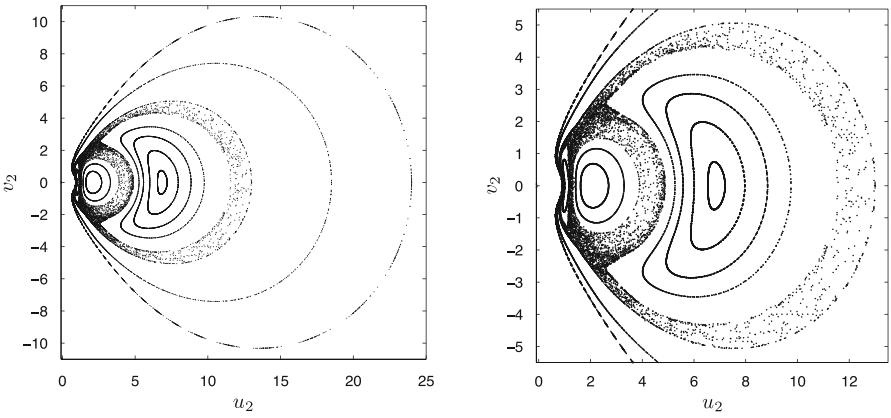

Fig. 10 Poincaré sections in the 1-4-9 ellipsoid. (u_2, v_2) representation. Courtesy of A. Regis

6 Heuristics for the Laplace Beltrami Green Function

Hydrodynamically, $G(s, s_o)$ is the stream function produced by a unit vortex at s_o. In the electrostatic interpretation, $G(s; s_o)$ is the potential at s created by a positive unit point charge at s_o, on a conductor with a uniformly distributed background negative charge. A test particle s with positive but negligible charge on the field generated by a unit charge will move according to

$$\dot{s} = \text{grad}G(s; s_o), \ \ s \neq s_o. \tag{59}$$

while a fluid particle (marker) s on the flow generated by an unit strength *bound* vortex s_o will move according to

$$\dot{s} = \text{sgrad}G(s; s_o), \ \ s \neq s_o. \tag{60}$$

We leave the following question for experimentalists. Can the Laplace Beltrami Green function be observed on surface fluid flows? More precisely, due to a small viscosity, vorticity is shed from the boundary. Will a steady state configuration eventually form, containing concentrated (opposite) vortices? Or will the counter-vorticity become homogeneously distributed?

In the spirit of Felix Klein's "Kaffeelöffel" [108] (reviewed in Saffman [179], chapter 6), we make the following *gedanken* experiment. A two dimensional fluid, initially at rest, occupies the whole area of a closed surface S. All of a sudden, a "turbine" (a geodesic disk whose boundary has some blades) is placed at a given point s_o and turned on.

Our *ansatz* is that, together the vortex at s_o, the counter vorticity will distributed homogeneously on the whole surface.[12]

6.1 Prandtl-Batchelor Theorem

Geophysical fluid dynamicists observe that in the presence of viscosity, vorticity tends to homogenize in atmospheric flows with closed streamlines [170].

This is the content of Prandtl-Batchelor theorem [9]. The proof, as presented e.g. in Childress ([40], Section 8.5), carries over *ipsis-literis* to curved surfaces. It is just a matter of introducing differential geometric invariant notation (see the Appendix), and was essentially already done in [215].

For historical information on Prandtl-Batchelor and some new results, see [203]. Batchelor's paper appeared in the inaugural volume of J. Fluid Mechanics. It seems that he was unaware of Prandtl's observation in ([163], 1905), the very paper that started boundary layer theory. Fig. 11 is taken from that famous paper.

Remark 7. We cannot sufficiently stress Jerry Marsden's enthusiasm in connecting himself and associates to real applications. He had a noble predecessor. As scientific leader in Göttingen, it was Klein that brought Prandtl over from Hannover [21]. The importance Felix Klein, as a promoter of applied mathematics, is perhaps not fully known by the mathematics community. With all due respect, the Klein project of the International Mathematical Union[13] could benefit from the outlook Klein had, as a "pure" mathematician, on Applied Mathematics. Klein himself divulged Geometric Mechanics in his two volumes on the Top, and of course, his Erlangen program *is* Geometric Mechanics!

[12] *Vorticity* is an *area* related concept. The area element of S will governs this homogenization. In geometric terminology, vorticity is a two-form. See the Appendix for details.

[13] http://www.mathunion.org/icmi/other-activities/klein-project/introduction/.

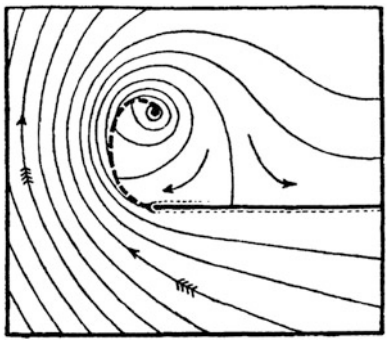

Fig. 11 Figure 4 of Prandtl [163], p. 488. The vortex sheet shed at the left tip of an edge moving down roll *clockwise*. If several of these edges are assembled as a watermill, then the shed vortices have *opposite* vorticity

6.2 Riemann Surfaces: Three Point Green Functions

The case where $\sum \kappa_j = 0$ has a special feature: *the stream function for a marker particle does not depend on the choice of metric in its conformal class*. Only the time parametrization does. This results from

$$\tilde{g} = h^2 g \quad \Rightarrow \Delta_{\tilde{g}} = h^{-2} \Delta_g .$$

which is a special property for two dimensions: Laplace-Beltrami operators in the same conformal class annihilate the same functions.

Denote by $G_S = G_S(s; s_o, s_1)$ be the *three points Green function* for S viewed just as a Riemann surface. It is the unique (up to a constant) real *harmonic* function for $s \in S$, that has a $(+)$ logarithmical singularity at s_o and a $(-)$ logarithmical singularity at s_1. The existence of such Green functions G_S can be taken as the starting point for closed Riemann surfaces theory (see e.g. Weyl [211], II.13, potential arising from a doublet source). Using fluid mechanics analogies to introduce the idea of a Riemann surface was the viewpoint of F. Klein [107] (see also [190]).

Definition 4. *A doublet, or dipole*, is the stream function of two infinitesimally close vortices of opposite circulation, the strength being suitably related to their distance so that the limit exists. In the plane, the stream function is proportional to $\cos(\theta)/r$.

On the other hand, by a *vortex pair* we have in mind two point vortices of opposite circulation at a finite distance.

Proposition 2. *The Green function G_s can be obtained form the Laplace-Beltrami Green function for any metric in the conformal class.*

$$G_S(s; s_o, s_1) = G_g(s; s_o) - G_g(s; s_1) \tag{61}$$

Conversely, if the three point Riemann surface Green function is known and an area form is chosen,

$$G_g(s;s_o) = \frac{1}{A(S)} \iint_S G_S(s;s_o,s_1)\,\Omega(s_1). \tag{62}$$

6.3 When the Total Vorticity Vanishes: Divisors

In Riemann surfaces theory, a 2-point divisor is a meromorphic function with two poles, each of order one. In Felix Klein's interpretation its complex integral represents a (complex) stream function for a perfect fluid on a Riemann surface. Taking real and complex parts one gets either a pair of source-sink ot a pair of opposite bound vortices. We fix a distinguished point s* and add a combination of N two point divisors where one of the poles is s*. Let the others be $\{s_1, \cdots, s_N\}$. We adjust the weights (vorticities) so that at s* the singularity disappears (this entails to have the sum of the vorticities equal to zero).[14]

If $\sum_{i=1}^{N} \kappa_i = 0$, then the following is the stream function governing the motion of a marker particle in the flow determined by *bound* vortices:

$$\psi(s) = \psi_{\text{conformal}}(s) = \sum_{j=1}^{N} \kappa_j\, G(s;s_j,s^*) \tag{63}$$

where s^* is an arbitrary chosen point in S (which turns out to be a regular point since the residue there vanishes). Irrespective of the metric in the class, the background vorticity in (63) is *zero* except at the poles s_j. The choice of s^* is irrelevant precisely because $\sum_{i=1}^{N} \kappa_i = 0$.

A key point in our paper is that, *even for zero total vorticity*, the Laplace-Beltrami Green functions must appear as soon as the primaries are set free to move (we then call the collection $\{s_1, \cdots, s_N\}$ a "moving divisor"). This is because the desingularization procedure requires using $G_g(s,s_o)$, even when the sum of the vorticities is zero. For one reason, the Riemann surface three point Green function is not symmetric with respect to its arguments. This already precludes using $G_S(s;s_j,s^*)$ for a Hamiltonian formulation.

It is striking is that all this is implicit in Marsden-Weinstein's Hamiltonian (3). At any rate, for any vortex problem in which the background vorticity vanishes, things simplify somewhat. The simple rule from [84] holds:

[14] *A priori* the flow of a marker has no intrinsic time. Time depends on choosing a metric in the conformal class of the complex structure. This is unavoidable, since we are doing incompressible hydrodynamics, so an area form must be present.

Proposition 3. *Let $\tilde{g} = h^2 g$. In a zero vorticity background, in order to find the $\tilde{g}$-metric regularized stream function for the motion of a vortex, subtract* $\log(h)/2\pi$ *from its g-regularized stream function.*

Proof. We have

$$\psi_{\text{reg}}(s_o) = \lim_{s \to s_o} \psi_{\text{conformal}}(s) - \log d(s, s_o)/2\pi.$$

Observe that, upon changing the metric, that

$$\log(\tilde{d}(s, s_o)) = \log\left(d(s, s_o) \frac{\tilde{d}(s, s_o)}{d(s, s_o)} \right) \sim \log(d(s, s_o)) + \log h(s_o) \quad \text{for } s \text{ near } s_o.$$

In particular, under a conformal transformation, C.C. Lin's additional term in the Hamiltonian [127] for Jordan domains is readily interpreted via Proposition 3. Let $f : (D, S, g) \to (\tilde{D}, \tilde{S}, \tilde{g})$ a conformal map between two Jordan domains,

$$\tilde{g}(df(s) \cdot u, df(s) \cdot v) = h^2(s)\, g(u, v). \tag{64}$$

Proposition 4. *Let $G_D(s; s_o)$ be the hydrodynamical Green function for a Jordan domain D . Then:*

$$\tilde{G}_{\tilde{D}}(\tilde{s}, \tilde{s}_o) = G_D(s; s_o) \tag{65}$$

The regularized Green function receives the correction

$$\tilde{g}(s_o) = g(s_o) - \frac{\log(h)}{2\pi}. \tag{66}$$

Note that the sign in equation (4.6) of [84] seem to need a correction from + to -.

7 Suggestions for Research

7.1 Numerical Experimentation and Visualizations

Theory and computation will come together to implement numerical methods for vortex dynamics on curved surfaces. While closed form expressions for Green function of the Laplace-Beltrami operator of constant curvature metrics will require further advances in automorphic function theory (specially for genus ≥ 2), in practice this step has already been achieved in computational geometry. We indicated some references in Section 4.4 and work on *discrete exterior calculus* started by Marsden and Desbrun.

Specialized *symplectic integrators* can be constructed on the reference sphere for conformal metrics. Families of tori embedded in $\mathbf{R}^3$ are also at hand for numerical experimentation. For instance, in the Clifford tori family, flat rectangular tori are embedded in $S^3 \subset \mathbf{R}^4$ in the standard way and then projected to $\mathbf{R}^3$ via stereographic projection. The conformal factor to the corresponding flat metric in their class can thus be explicitly obtained. More generally, one can attempt to do vortex dynamics in Clifford, Wilmore, Hopf and Lagrangian minimal tori.

7.2 Contour Dynamics

Starting with Zabusky and collaborators [164, 216], contour dynamics in the plane is an active subject, see e.g. [43, 57] for recent work. Choosing an appropriate class of vorticity functions is an important mathematical problem. Numerically, even if one starts with a smooth ω the time evolution of the system (82, 85) may reach a stand-off by the appearance of singularities, at least numerically. Starting with sharply defined islands of high (positive and negative) vorticity, in time, vortex patches blend or develop structures resembling filaments.

Can one develop theory and experimentation for contour dynamics on surfaces? Are there new stable structures besides the elliptical rotating spots in the sphere?

7.3 Physical Experiments

In Section 6.1 we asked if the Green function for the Laplace Beltrami Green function could be experimentally observed. One may consider a soap film over a sphere, and stir the flow by a small rotating grooved disk. Conceivably it will shed vortices of opposite circulations to the rotating disk. Will the shed vorticity be homogenized by viscosity? Or will turbulent behavior persist? Will contervorticity concentrate and vortices of opposite circulations appear?

7.4 Symplectomorphism Between $S \times S$ and T^*S and Kimura's Question

In two dimensions, "center-arrow coordinates" $(s_o, v) \in TS \mapsto (s_1, s_2) \in S \times S$ are defined via the exponential map,

$$s_1 = \exp(s_o, -Jv/2), \quad s_2 = \exp(s_o, Jv/2) \tag{67}$$

where J is the rotation in the tangent plane by $\pi/2$. Composed with the Legendre transformation between $(s_o, v) \in TS$ and $(s_o, p) \in T^*S$, we get a map between a neighborhood of the zero section of T^*S and a neighborhood of the diagonal on $S \times S$. The latter carries the symplectic form $\Omega_{S\times S} = \Omega_1 - \Omega_2$, while the former carries the canonical symplectic structure Ω_{T^*S}.

What is the relationship between them? Introduce a blow up parameter ϵ and make $v \to \epsilon v$. Using local coordinates, it is not hard to see that upon pullback, we get a deformation of the canonical symplectic structure,

$$\Omega_{S\times S} = \epsilon^2 \Omega_{T^*S} + O(\epsilon^4). \tag{68}$$

What is the $O(\epsilon^4)$ term?

7.5 Elaboration on Kimura's Conjecture

The relation between the canonical symplectic form Ω_{T^*S} in T^*S and the vortex symplectic form $\Omega_{S\times S}$ is a remarkable fact, and represents another proof of Kimura's conjecture, since the leading term of the Hamiltonian is the logarithm of the distance.

Finding the next term in the deformation expansion (in terms of local geometric quantities) is one of the steps to write the first correction term of vortex pair equations with respect to the geodesic problem.

The other required step (the expansion of the Hamiltonian in parameter ϵ) will be now described.

7.6 Expansions for Green and Batman Functions Near the Diagonal

The analysis of the Laplacian operator on manifolds is often undertaken with the help of the heat kernel [75, 78, 79, 177],

$$H(t, s_1, s_2) = \sum_{n\geq o} \exp(-\lambda t)\phi_n(s_o)\phi_n(s_1) \tag{69}$$

where $\{\phi_n\}$ is a normalized eigenbasis of the Laplace-Beltrami operator. The asymptotic behavior of the heat kernel near the diagonal can be studied both for short times and for long time using methods such as Hadamard parametrix.

The Green function for the Laplace-Beltrami can be expressed as

$$G(s_1, s_2) = \int_0^\infty H(t, s_1, s_2)\, dt = \sum_{n\geq o} \frac{1}{\lambda_n} \phi_n(s_o)\phi_n(s_1) \tag{70}$$

In terms of center-arrow coordinates, Batman's function (9) is an even on ϵ, starting with the quadratic term: $B(s_o, \epsilon v) = O(\epsilon^2)$. Is it possible obtain the "off-diagonal" expansion of G and B as a series in ϵ, whose coefficients are local, geometric quantities computed at s_o?

7.7 Integrability and Chaos: Vortex Dynamics in the Large

As we just discussed, in order to represent the vortex pair dynamics as an $O(\epsilon^2)$ perturbation of the geodesic system (see corollary 2), it suffices to find the first term of the Batman function expansion, and the first correction term to Ω_{T^*S}. It is known that the geodesic system is integrable on Liouville surfaces.

From the preceding, the vortex pair system seems to be in general a KAM perturbation. Apply Melnikov methods [95, 141, 176, 212] near homoclinic surfaces (degenerate invariant tori) of the geodesic system, for instance in the triaxial ellipsoid. Study "vortex billiards", the degenerate triaxial ellipsoid where the smaller axis vanishes.

Liouville metrics [25, 26] require genus 0 or 1. It is well known that geodesic systems are nonintegrable on all surfaces of negative curvature (genus $\geq$ 2). It should be not hard to show that vortex systems are also nonintegrable for genus $\geq$ 2. Are there metrics without S^1 symmetry on spheres or genus 1 tori for which the vortex pair system is integrable?

Suppose the initial conditions for the vortices are at such a finite distance so that the logarithmical term and the Batman term in the Hamiltonian are of the same order of magnitude. How close the vortex can come together? How far from each other can they get? How is the long time behavior of the vortex pair system? Have the conjugate and the cut locus (for the metric) a role in the vortex pair system?

7.8 Higher Dimensions

The statement of Theorem 1 makes sense for a compact Kahler manifold M^n. For instance, Calabi-Yau manifolds are important objects in mathematical physics. Is this generalization of (10) in line with ODEs representing singular solutions from established field theories? As to deformations of symplectic forms, the following is well known to grupoid experts. A deformation of Ω_{T^*S} can be constructed for S being any Poisson manifold using the theory of symplectic groupoids and of integration of Lie algebroids [45, 47, 48] and it has the property that the projection T*S to S yields a symplectic realization [49, 210]. In our case, S is already symplectic and the corresponding symplectic groupoid is $S \times S$ with the difference of the area forms.

7.9 Domains in a Riemann Surface: Schottky-Klein Prime Functions

Green functions for domains conformal to a multiply connected planar region are often classified into two types [71]. *First type* are motivated by electrostatics, where one takes $G = 0$ on all boundaries, possibly with different circulations around each of them. *Second kind*, or *modified* Green functions are more commonly used in hydrodynamics. One prescribes zero circulation around the boundaries, except at one of them; the values of $G_D = \text{const.}$ on the boundaries may differ, one of them being normalized to 0. As we mentioned in Section 4, Crowdy and Marshall brought to "implementational fruition" the task of obtaining Green functions in canonical planar domains, specially with the help of Schottky-Klein prime functions [53]. For recent work of prime functions on tori, see [76].

7.10 Schottky Doubles

In another tack, let $S_D = D + \overline{D}$ of a Jordan domain D, it is a *symmetric Riemann surface*. Consider metrics on S_D such that the reflection is an isometry. If at initial time each vortex on D corresponds to a symmetric one in $\overline{D}$, with opposite vorticity, then the configuration remains symmetric for all time. N-vortex motion on D is the restriction of the corresponding $2N$ vortex motion on S_D. This Schottky double construction is reminiscent of Thomson's image vortex method. The difference from planar regions is that here the domain may have "handles". In a similar vein, we may consider *involutions* on Riemann surfaces, [34, 44, 83, 156], both orientation preserving or reversing. The "naive rule" in Proposition 3 suffices in the case of a Jordan domains $D \subset S$, even if the sum of the vorticities in D is non zero. This is because the extended $2N$ vortex system on $S_D = D + \overline{D}$ (for which the vorticity sum is zero). The image structure is preserved under the dynamics.

Are there methods to obtain hydrodynamical Green functions on arbitrary Jordan domains D of Riemann surfaces S?

7.11 Blow Up and Regularization of Collisions

Unlike celestial mechanics, merging of vortex patches is not a catastrophic event. Thus it makes sense to implement blow up/regularization of point vortex collisions. See [88, 89, 91] for recent work on collisions of three and four vortex systems on the plane. Ernesto Lacomba [117] has also incorporated sources/sinks in the dynamics of point vortices in the plane. One should study these questions in the setting of curved surfaces.

7.12 Topological Methods: Compactifications

In the case of two opposite vortices, coordinates can be symmetrized, since interchanging them yields the same trajectory (time reversed). Together with a compactification of $S \times S -$ diagonal one obtains a field of directions in a quotient compact topological space. Some algebraic geometry and topology references are [22, 23, 72], for compactified, symmetrized products of N copies of a topological space minus the diagonals. See [74] for recent applications to robotics. The shape and orientation of the way the points approach each other is taken into account. This would pave the way for topological methods to study the dynamics (also in the presence of Lie group symmetries, see e.g. [106]).

7.13 Relation with Teichmuller Theory

For deforming surfaces, the complex structure changes in time (only for disks and topological spheres it does not, in view of the Riemann mapping theorem). How to account for this in the corresponding time dependent vortex equations?

7.14 Dynamics of Markers Around a Primary

A marker is governed by the 1 1/2 degrees of freedom system with Hamiltonian $G(s, s_o(t))$, where $s_o = s_o(t)$ is a solution of (12). Hence chaotic solutions for a marker are expected even for a flow determined by one vortex, since the latter in general has a drift motion on the surface.

7.15 Quantization of Vortex Systems

Is there a way to quantize the vortex pair system on the compactification of $S \times S -$ diagonal? Quantizing geodesic motion on (S, g) leads to the spectrum of the Laplace-Beltrami operator. As geodesics are limits of vortex pair systems one may wonder if is there a way to connect the latter to the Hilbert-Polya approach. Can a Bose Einstein condensate be realized on a two dimensional surface with prescribed, arbitrary geometry [187]?

7.16 Hard Analysis Questions

7.16.1 Thin Domains

How three dimensional flows squeezed between two nearby surfaces reduce to two dimensions? The case of a spherical shell was studied by Jerry Marsden in collaboration with Tudor Ratiu and Geneviève Raugel [136, 138]. As the transversal length goes to zero, are there extra terms due to the extrinsic curvatures of the surface, or due to non homogeneities (e.g. the container having nonuniform transversal length)?

7.16.2 Properties of Robin Functions

Electrostatics motivates finding the critical points of $G(s; s_o)$ (as a function of s with s_o fixed). Recently two interesting studies were published, [65, 130]. Revisit them for $R(s)$ instead of $G(s; s_o)$ on surfaces with variable curvature.

7.16.3 Core Energy Desingularization

Does the geometry of the surface entail novel effects in the long time behavior of vortex cores? As a single near circular vortex patch drifts on the surface, will the curvature change affect its stability? How about other relevant PDEs, such as Ginzburg-Landau and Gross-Pitaevskii,[15] that also lead to vortex type equations? A few additional references: [133] for Euler's equations, [165, 189] for the Ginzburg-Landau, [70] for Gross-Pitaevskii equations.

8 Final Remarks

Taking Marsden and Weinstein's 1983 seminal paper [135] as a guide, we showed how vortex equations can be written for all metrics on the conformal class of a Riemann surface. Our work geometrizes C.C. Lin's approach for planar domains using Green functions to construct the Hamiltonian. To justify using Robin's function to remove the infinite self energy at a vortex, we observed that Flucher and Gustaffson's core energy desingularization extends to curved surfaces, since the singularity involves $\log d(s_1, s_2)$. The transformation rules of Laplace-Beltrami Green functions (a lemma on J. Steiner thesis under K. Okikiolu) allowed us to extend, to closed surfaces, C.C. Lin's transformation formulas under conformal maps.

[15] See the appraisal by Terry Tao in http://www.terrytao.wordpress.com/2009/11/26/from-bose-einstein-condensates-to-the-nonlinear-schrodinger-equation/.

8.1 Comparison with Hally's Work [84]

Hally worked on (local) isothermal coordinates, under a simplifying hypothesis, that the surface is topologically equivalent to a Jordan domain (a multiply connected planar domain). Curiously, he proceeds in the end of the paper to apply the results to surfaces of revolution.

- Hally seems not to take advantage of the Green function for the Laplace Beltrami operator. In fact he states that "for surfaces topologically similar to the sphere . . . it is impossible to have a single point of isolated vorticity. Rather, there is a constraint that the sum of all vortex strengths must vanish."
- The starting point of Hally's derivation is equation (3.1), which is proposed on heuristic grounds. In (3.2), one of the terms of (3.2) is attributed to the (self) "velocity induced by the curvature of the surface of flow."

  However, that expression is not intrinsically defined and cannot be associated to curvature, as it depends only on first derivatives of the metric.
- In the derivation, Hally also introduces a regular complex potential ϕ^* (it is not clear how to find it) to take into account the external influences (e.g. other vortices). He says: "In the case of a closed surface with no boundaries these also include the effects of the vortex at infinity." Instead, we encoded everything in the (nonlocal nature of) the operator Δ_g^{-1}.

  Remarkably, as it often the case with physicists' derivations, for Jordan domains Hally's equations of motion are correct. We believe that our approach allows to explain his heuristics. The self contribution is encoded in Robin's function R. In our work, a key aspect is the transformation rules between Green functions.

8.2 What We Believe is New in This Paper

- We called the attention that the self term (Robin's function) has been slightly overlooked, since for the round sphere it is ia constant. For genus $g \geq 2$ or metrics with variable curvature, Theorem 1 posits a self contribution, governed by Robin's function.
- Somehow mystically for genus ≥ 2 the self term exists even when the curvature is constant ($K \equiv -1$). For a single vortex this phenomenon could be described as "motion due to topology" or a "relativity principle".
- The extra term in Theorem 4, which is present when there is a background vorticity:

$$\frac{\kappa}{\tilde{A}(S)} \sum_{\ell=1}^{N} \kappa_\ell \, \Delta_g^{-1} h^2(s_\ell), \quad \kappa = \sum_{\ell=1}^{N} \kappa_\ell .$$

It seems *not* to have been captured in previous studies.
- Conceptually, why the use of Green's function of the Laplace Beltrami for the vortex interaction is mandatory, even when the sum of the vorticities vanishes and there is no background vorticity.
- Practical: calling attention to advantages of the coordinate free approach. For instance, if one desires to study vortices around islands on a sphere, eg. [82, 195], it is enough to conformally map it to a planar region, and apply Theorem 4. When polygonal rings of vortices on a spheroid are considered, one can consider either a compensating constant background vorticity, or a concentrated compensating vortex at a pole. Results for the two cases are very different [14].

Acknowledgements We thank Jean Singer and Kate Okikiolu for informations about the Laplace-Beltrami Green functions; Milton Lopes Filho and Helena Nussenzveig Lopes for informations on hard analysis issues; Max Souza for calling the attention to the Prandtl-Batchelor theorem; Monica Caracanhas for informations about Bose-Einstein condensates. Most specially, we thank Adriano Regis and Humberto Viglioni for their permission to use some of the beautiful pictures from their thesis. We thank the many conversations with participants of the Geometric Mechanics seminars in Rio, We thank the Geometry, Mechanics and Control community, especially the colleagues in Spain (Madrid, Barcelona and the Canary Islands), and the colleagues in Russia, in Izhevsk and Moscow. For their everlasting encouragement (JK) wishes to thank Alan Weinstein, Tudor Ratiu and Darryl Holm, (SB) to Yoshifumi Kimura, Björn Gustafsson, David Dritschel, and Carles Simó. Both authors thank the referee for his(hers) very pertinent suggestions and criticisms.

This research project started around 2008. The authors were supported by the Brazilian agencies Faperj, Capes and CNPq for a number of research visits, specially the Science without Frontiers grant PVE 11/2012. We thank the agencies for the support to the workshop "N-vortex and N-body dynamics : common properties and approaches", held at UFRJ.[16] (JK) thanks specially the organizers of the "Focus Program on Geometry, Mechanics and Dynamics, the Legacy of Jerry Marsden at The Fields Institute, Toronto", the support of Fields institute and MITACS,[17] and the Institute of Computer Sciences at Izhevsk, Russia.[18] (JK) acknowledges specially an INMETRO-Pronametro fellowship during the final stage of the work.

Appendix: Complex, Metric and Symplectic Geometry of Two-Dimensional Hydrodynamics

This Appendix intends to present the differential geometry jargon for readers outside the field of Geometric Mechanics. This is a "baby" version of the differential geometric language of [135]. We denote by S a two dimensional *closed* (compact boundaryless) orientable manifold, endowed with a Riemannian metric g, and $D \subset S$ a Jordan domain (a region with compact closure whose boundary consists of a finite number of connected components each diffeomorphic to a circle).

[16] http://www.im.ufrj.br/lella/Nvortex.html.

[17] https://www.fields.utoronto.ca/programs/scientific/12-13/Marsden/.

[18] http://www.ics.org.ru/eng.

Perfect Flows in $\mathbf{R}^2$

Given a velocity field in the plane $\mathbf{u} = (u_1, u_2)$, its vorticity field, ω is

$$\omega\,\hat{z} = \nabla \times \mathbf{u} = \partial u_1/\partial y - \partial u_2/\partial x. \tag{71}$$

In *incompressible* flows, the velocity field verifies

$$\nabla \cdot \mathbf{u} = 0. \tag{72}$$

In the plane the incompressible condition entails that the velocity field $\mathbf{u} = (\dot{x}, \dot{y})$ can be written as a Hamiltonian system

$$u = -\frac{\partial \Psi}{\partial y}, \qquad v = \frac{\partial \Psi}{\partial x}, \tag{73}$$

where ψ is the stream function. If the flow is also *irrotational*, $\nabla \times \mathbf{u} = 0$ (except for singularities concentrated at points), then the stream function is *harmonic* up to these special points. The singularities are vortices, sinks or sources.

The vorticity field of an isolated unit point-vortex in the plane is given by $\omega(s; s_o) = \delta(\mathbf{z} - \mathbf{z}_o)$. It forces test-particles to move on circular orbits with velocities proportional to the inverse of the distance. The stream function is

$$G(z, z_o) = \frac{1}{2\pi} \log d(z, z_o),$$

where $z = (x, y)$, $z_o = (x_o, y_o)$ and $d(z, z_o) = \sqrt{(x - x_o)^2 + (y - y_o)^2}$.

It provides the kernel to solve Poisson's equation. Namely, when the vorticity field ω is given, one can recover the stream function via

$$\psi(z) = \Delta^{-1}\omega(z) = \iint G(z, z')\,\omega(z')\,\Omega(z') \tag{74}$$

where $\Omega = dA = dx \wedge dy$ is the area-form. See e.g. Malchioro and Pulvirenti [133], Majda and Bertozzi [132], for regularity assumptions.

Complex Geometry of Surfaces

The underlying *Riemann surface structure* of a surface S with a metric g is given by the atlas of Laplace-Beltrami isothermal coordinates. In two dimensions all metrics are automatically Kahler.

Complex geometry keeps the notion of angle between tangent vectors (thus the rotation operator J by 90 degrees of tangent vectors is well defined), but neglect lengths and areas. Teichmuller theory describes the possible complex structures on S.

Symplectic geometry, on the other hand, keeps the notion of area but neglects angles. Within a fixed complex geometry, varying the area forms produce the conformal class of Riemannian metrics compatible with that complex structure.

The *uniformization theorem* provides to each complex structure on S a *canonical metric of constant curvature*,[19] but there are other canonical metrics on a Riemann surface. In Mandelstam metrics the curvature is concentrated at isolated points, and can be used with triangulations of S. The Abel-Jacobi map embeds S on a complex torus with euclidian metric. This map induces in S the Arakelov metric and the related Bergman metric, see, e.g., [146].

Meromorphic Differentials and Direction Fields

Incompressible 2d hydrodynamics requires of an area form besides the complex structure. It is remarkable that only the complex structure is needed if one is interested just in the unparameterized trajectories of a marker particle, in the flow generated by a set of bound vortices with zero total vorticity. Changing a metric conformally, the speed of the marker will vary according to the conformal factor, but the physical path remains the same. Thus for the path of a marker on a flow determined by *bound* vortices, with zero total vorticity, one needs only the complex structure.[20]

Studying *primitives of Abelian differentials* is at the root of Riemann surface theory. In recent years pure mathematicians have started to explore the pair of oriented lines fields corresponding to meromorphic differentials.[21]

Representing the target Riemann sphere as the extended complex plane, it is more usual among fluid dynamicists to have the periods of the primitive in the real part ϕ. The complex part ψ is called the *stream function.* Combined they form the so-called *complex velocity potential*

$$F = \phi + i\,\psi \quad (dF = \text{a meromorphic differential}). \tag{75}$$

[19]Interestingly, in two dimensions the Ricci flow keeps the metric in its conformal class.

[20]The texts by Felix Klein's ([107], 1882) and Springer [190] use hydrodynamical analogies to motivate the concept of *meromorphic differentials* and divisors on Riemann surfaces. However, it seems that Riemann used only analogies from electrostatics, see [171–173, 198]).

[21]Their interest is in the interval exchange properties and ergodic properties associated to these two flows, see eg. [113].

Hodge Theory in 2 Dimensions

Given a metric $g = \langle\ ,\ \rangle$ compatible with the complex structure, consider the gradient and symplectic gradient operators grad (usually denoted ∇), sgrad $:=$ $J \circ$ grad (also denoted $\nabla^{\perp}$),

$$d\phi(\bullet) = \langle \text{grad}\,\phi, \bullet \rangle = \Omega(\text{sgrad}(\phi), \bullet). \tag{76}$$

There is a "baby Hodge theory" in two dimensions: identify functions with two-forms via $f \leftrightarrow f\Omega$ and vectorfields with 1-forms via $v \leftrightarrow \omega = \langle v, \bullet \rangle$.

With a metric we can view a meromorphic differential as a vectorfield. Let C be a closed curve enclosing a domain homeomorphic to a disk $D \subset S$. Orient C such that the frame n, t is positive, where t is the unit tangent vector and n points to the exterior of D. Let v be a vectorfield. The familiar formula in the plane

$$\oint_C \langle v, n \rangle\, ds = \iint_D \text{div}(v)\Omega \tag{77}$$

makes perfect sense on a surface. The coordinate free definition of the *divergence operator*, sending vectorfields to functions, can be given as follows (applying Stokes' theorem):

$$d\,\langle J(v), \bullet \rangle = \text{div}(v)\Omega. \tag{78}$$

Perfect Flows on Surfaces: Vorticity and Poisson's Equation

Incompressible hydrodynamics means: $\text{div}(v) = 0$ except for sources or sinks. On a compact surface S their divergences must add to zero. In *potential* flow $v = -\text{grad}\phi$ for a velocity potential ϕ, which in general is a multivalued function (in the Riemann surface sense).

The *circulation* $\oint_C \langle v, t \rangle ds$ of v around a closed curve $C = \partial D$ is of fundamental importance. The *vorticity distribution* forms the "sinews and muscles of fluid motion" (Küchemann [114]). Vortices are singularities that generate circulation. If the surface has nontrivial topology there exist perfect flows with nonzero circulations around the homology generators. The circulation on the boundary of a simply connected domain without internal singularities vanishes.

The Laplace operator is $\Delta = \text{div} \circ \text{grad}$. It is a negative definite self-adjoint operator with respect to $\langle f, g \rangle = \int_M fg\,\Omega$. The potential function of a perfect flow satisfies $\Delta\phi = 0$ (except on the singularities). As we mentioned above, its conjugate

harmonic function ψ is called the *stream* function. Combined they form the *velocity potential*.[22]

The velocity field v is tangent to the level lines of the stream function ψ, and can be described symplectically from ψ via

$$d\psi = \Omega(v, \bullet) \quad \Leftrightarrow \quad v = \text{sgrad}(\psi) = -\text{grad}(\phi). \tag{79}$$

Summarizing: velocity potentials and stream functions are harmonic up to singularities and/or multivaluedness; the complex function theory of S is in the background of 2d-hydrodynamics. A metric is not required for the path of a marker particle under the influence of bound singularities.

Using Stokes' theorem the line integral can be transformed into a double integral,

$$\oint_C \langle v, t\rangle ds = \oint_C \langle J(v), J(t)\rangle ds = \oint_C \langle J(v), -n\rangle ds = -\iint_D \text{div}(Jv)\, \Omega$$

But $J(v) = J(J\,\text{grad}\psi) = -\text{grad}\psi$. Hence

$$\oint_C \langle v, t\rangle ds = \iint_D \Delta\psi\ \Omega. \tag{80}$$

Hence the coordinate free definition of the surface rotational or vorticity distribution $\omega = \text{rot}v$ is

$$d\langle v, \bullet\rangle = \text{rot}(v)\Omega. \tag{81}$$

See [4] (definition 9.5 on p. 46 and (11.1–2) on p. 56) or [135] (Sections 4 and 6) for the corresponding definitions in higher dimensions. Two dimensional hydrodynamics is governed by Poisson's equation. If ψ is the stream function, it is easy to see from the definitions in the previous section that

$$\Delta\psi = \omega \quad \text{where} \quad \iint_S \omega\Omega = 0. \tag{82}$$

Lemma 1. *On a closed surface (of arbitrary genus) the source term must average to zero.*

$$\iint_S \omega\, \Omega = 0. \tag{83}$$

[22] Due to the historical influence of British fluid mechanicists, in planar domains with the euclidian metric flows due to complex potentials are defined as $-\overline{F'(z)}$.

Proof. $\iint_S \omega\Omega = \iint_S \Delta\psi dS = \iint_S \nabla\cdot\nabla\psi dS = \oint_{\partial S}\langle\nabla\psi, n\rangle ds = 0$, since there is no boundary. Alternatively, take a small curve C enclosing a disk D. The circulation of the velocity field can be computed as the double integral of the vorticity on D and minus that integral on $S - D$.

Lemma 2. *In two dimensions vorticity is a "material property"*

$$L_v\omega = \frac{\partial\omega}{\partial t} + \langle v, \mathrm{grad}\omega\rangle = 0. \tag{84}$$

Since $v = \mathrm{sgrad}\psi$*, this translates into*

$$\frac{\partial\omega}{\partial t} = \{\psi, \omega\} = \{\Delta^{-1}\omega, \omega\} \tag{85}$$

where $\{\ ,\ \}$ *is the Poisson tensor associated to the area form in* S.

References

1. (MR2337012)Aref, H.: Point vortex dynamics: a classical mathematics playground. J. Math. Phys. **48**(6), 065401 (2007)
2. Aref, H., Newton, P.K., Stremler, M.A., Tokieda, T., Vainchtein, D.: Vortex crystals. Adv. Appl. Math. **39**, 1–79 (2003)
3. (MR0202082) Arnold, V.I.: Sur la geométrie differentielle des groupes de Lie de dimension infinie et ses applications a l'hydrodynamique des fluids parfaits. Ann. Inst. Grenoble **16**, 319–361 (1966)
4. (MR1612569) Arnold, V.I., Khesin, B.A.: Topological Methods in Hydrodynamics. Applied Mathematical Sciences, vol. 125. Springer, New York (1998)
5. Avelin, H.: Computations of automorphic functions on fuchsian groups. Ph.D. thesis, Uppsala University, Department of Mathematics (2007). http://www.urn:nbn:se:uu:diva-8247
6. (MR2731548) Avelin, H.: Computations of Green's function and its Fourier coefficients on Fuchsian groups. Exp. Math. **19**(3), 317–534 (2010)
7. (MR0112798) Ball, W.W.R.: A Short Account of the History of Mathematics. Dover, New York (1940)
8. Bartosch, L.: Quantum dynamics of vortices in two-dimensional superfluids in the proximity to Mott insulators. Habilitationsschrift, Goethe Universität (2008). http://www.itp.uni-frankfurt.de/~lb/publicationsLB/BartoschHabilThesis.pdf
9. Batchelor, G.K.: On steady laminar flow with closed streamlines at large Reynolds number. J. Fluid Mech. **1**, 177–190 (1956)
10. (MR2460286) Belkin, M., Niyogi, P.: Towards a theoretical foundation for Laplacian-based manifold methods. J. Comput. Syst. Sci. **74**(8), 1289–1308 (2008)
11. (MR2504294) Belkin, M., Sun, J., Wang, Y.: Discrete Laplace operator on meshed surfaces. In: Computational Geometry (SCG'08), pp. 278–287. Association for Computing Machinery, New York (2008)
12. (MR2384544) Berry, M.: Three quantum obsessions. Nonlinearity **21**(2), T19–T26 (2008)
13. (MR1684543) Berry, M.V., Keating, J.P.: The Riemann zeros and eigenvalue asymptotics. SIAM Rev. **41**, 236–266 (1999)
14. (MR2425047) Boatto, S.: Curvature perturbations and stability of a ring of vortices. Discrete Continuous Dyn. Syst. Ser. B **10**(2–3), 349–375 (2008)

15. (MR2029132) Boatto, S., Cabral, H.: Nonlinear stability of a latitudinal ring of point-vortices on a nonrotating sphere. SIAM J. Appl. Math. **64**(1), 216–230 (2003)
16. Boatto, S., Crowdy, D.: Point-vortex dynamics. In: Françoise, J.-P., Naber, G.L., Tsun, T.S. (eds.) Encyclopedia of Mathematical Physics. Elsevier, Amsterdam (2006). ISBN:97800-12-51 26663-3
17. Boatto, S., Koiller, J.: Vortices on closed surfaces. arXiv: SG/0802.4313. Preprint
18. (MR2449799) Boatto, S., Simó, C.: Thomson's hexagon: a case of bifurcation at infinity. Physica D **237**, 2051–2057 (2008) (Proceedings of an International Conference. Euler Equations: 250 Years on (EE250), Aussois, 18–23 June 2007)
19. (MR1396732) Bobenko, A., Pinkall, U.: Discrete isothermic surfaces. J. Reine Angew. Math. **475**, 187–208 (1996)
20. (MR2365833) Bobenko, A., Springborn, B.: A discrete Laplace-Beltrami operator for simplicial surfaces. Discrete Comput. Geom. **38**(4), 740–756 (2007)
21. Bodenschatz, E., Eckert, : Prandtl and the Göttingen School. In: Davidson, P.A., Kaneda, Y., Moffatt, K., Sreenivasan, K.R. (eds.) A Voyage Through Turbulence. Cambridge University Press, Cambridge (2011)
22. (MR0991102) Bödigheimer, C., Cohen, F., Taylor, L.: On the homology of configuration spaces. Topology **28**(1), 111–123 (1989)
23. (MR1240884) Bödigheimer, C., Cohen, F., Milgram, R.: Truncated symmetric products and configuration spaces. Math. Z. **214**(2), 179–216 (1993)
24. (MR0475220) Bogomolov, V.A.: The dynamics of vorticity on a sphere (Russian). Izv. Akad. Nauk SSSR Ser. Meh. Zidk. Gaza **6**, 57–65 (1977)
25. (MR2036760) Bolsinov, A.V., Fomenko, A.T.: Integrable Hamiltonian Systems. Geometry, Topology, Classification. Chapman & Hall/CRC, Boca Raton (2004)
26. (MR2070866) Bolsinov, A., Jovanovic, B.: Integrable geodesic flows on Riemannian manifolds: construction and obstructions. In: Bokan, N., Djoric, M., Rakic, Z., Fomenko, A.T., Wess, J. (eds.) Contemporary Geometry and Related Topics, pp. 57–103. World Scientific Publishing, River Edge (2004)
27. (MR1780710) Borisov, A.V., Kilin, A.A.: Stability of Thomson's configurations of vortices on a sphere. Regul. Chaotic Dyn. **5**(2), 189–200 (2000)
28. (MR1693494) Borisov, A.V., Lebedev, V.G.: Dynamics of three vortices on a plane and a sphere. II. General compact case. Regul. Chaotic Dyn. **3**(2), 99–114 (1998)
29. (MR1704984) Borisov, A.V., Lebedev, V.G.: Dynamics of three vortices on a plane and a sphere. III. Noncompact case. Problems of collapse and scattering. J. Moser at 70 (Russian). Regul. Chaotic Dyn. **3**(4), 74–86 (1998)
30. Borisov, A.V., Mamaev, I.S.: Mathematical Methods in the Dynamics of Vortex Structures (in Russian). Institute of Computer Science, Moscow (2005)
31. (MR1652160) Borisov, A.V., Pavlov, A.E.: Dynamics and statics of vortices on a plane and a sphere - I. Regul. Chaotic Dyn. **3**(1), 28–38 (1998)
32. (MR2335746) Borisov, A.V., Mamaev, I.S., Ramodanov, S.M.: Dynamics of two interacting circular cylinders in perfect fluid. Discrete Contin. Dyn. Syst. **19**(2), 235–253 (2007)
33. Bourgade, P., Keating, J.P.: Quantum chaos, random matrix theory, and the Riemann ζ-function. Sèminaire Poincaré **XIV**, 115–153 (2010)
34. (MR1283011) Bujalance, E., Costa, A. Orientation reversing automorphisms of Riemann surfaces. Illinois J. Math. **38**(4), 616–623 (1994)
35. Burton, G., Lopes Filho, M., Nussenzveig Lopes, H.: Nonlinear Stability for steady vortex pairs. Comm. Math. Phys. **324**, 445-463 (2013)
36. Byrnes, T., Wen, K., Yamamoto, Y.: Macroscopic quantum computation using Bose–Einstein condensates. Phys. Rev. A **85**, 040306(R) (2012)
37. (MR1740937) Cabral, H., Schmidt, D.: Stability of relative equilibria in the problem of $N+1$ vortices. SIAM J. Math. Anal. **31**(2), 231–250 (2000)
38. (MR2020843) Cabral, H., Meyer, K., Schmidt, D.: Stability and bifurcations for the $N+1$ vortex motion on the sphere. Regul. Chaotic Dyn. **8**(3), 1–25 (2003)

39. (MR2392856) Castilho, C., Machado, H.: The N-vortex problem on a symmetric ellipsoid: a perturbation approach J. Math. Phys. **49**(2), 022703 (2008)
40. Childress, S.: An Introduction to Theoretical Fluid Mechanics. Courant Lecture Notes, vol. 19. AMS, Providence (2000)
41. (MR1779780) Chung, F., Yau, S.-T.: Discrete Green's functions. J. Combin. Theory Ser. A **91**(1–2), 191–214 (2000)
42. (MR0968694) Constantin, P., Titi, E.: On the evolution of nearly circular vortex patches. Commun. Math. Phys. **119**, 177–198 (1988)
43. (MR2141918) Córdoba, D., Fontelos, M., Mancho, A., Rodrigo, J.: Evidence of singularities for a family of contour dynamics equations. Proc. Natl. Acad. Sci. USA **102**(17), 5949–5952 (2005)
44. (MR2400392) Costa, A., Parlier, H.: A geometric characterization of orientation-reversing involutions. J. Lond. Math. Soc. (2) **77**(2), 287–298 (2008)
45. (MR0996653) Coste, A., Dazord, P., Weinstein, A.: Groupoides symplectiques. Publ. Dép. Math. Univ. Claude Bernard Lyon I Nouvelle Sér. A **2**, 1–62 (1987)
46. (MR1505251) Craig, T.: Orthomorphic projection of an ellipsoid upon a sphere. Am. J. Math. **3**(2), 114–127 (1880)
47. (MR1973056) Crainic, M., Fernandes, R.L.: Integrability of Lie brackets. Ann. Math. (2) **157**(2), 575–620 (2003)
48. (MR2128714) Crainic, M., Fernandes, R.L.: Integrability of Poisson brackets. J. Differ. Geom. **66**, 71–137 (2004)
49. Crainic, M., Marcut, I.: On the existence of symplectic realizations. arXiv:1009.2085v1 [math.DG] (2010)
50. (MR2222317) Crowdy, D.: Point vortex motion on the surface of a sphere with impenetrable boundaries. Phys. Fluids **18**, 036602 (2006)
51. (MR2147679) Crowdy, D., Marshall, J.: The motion of a point vortex around multiple circular islands. Phys. Fluids **17**(5), 056602 (2005)
52. (MR2156476) Crowdy, D., Marshall, J.: Analytical formulae for the Kirchhoff–Routh path function in multiply connected domains. Proc. R. Soc. A **461**, 2477–2501 (2005)
53. (MR2241034) Crowdy, D., Marshall, J.: Conformal mappings between canonical multiply connected domains. Comput. Methods Funct. Theory **6**(1), 59–76 (2006)
54. (MR2321816) Crowdy, D., Marshall, J.: Computing the Schottky-Klein prime function on the Schottky double of planar domains. Comput. Methods Funct. Theory **7**(1), 293–308 (2007)
55. (MR2334725) Crowdy, D., Marshall, J.: Green's functions for Laplace's equation in multiply connected domains. IMA J. Appl. Math. **72**(3), 278–301 (2007)
56. (MR2385119) Crowdy, D., Marshall, J.: Uniformizing the boundaries of multiply connected quadrature domains using Fuchsian groups. Physica D **235**(1–2), 82–89 (2007)
57. (MR2371154) Crowdy, D., Surana, A.: Contour dynamics in complex domains. J. Fluid Mech. **593**, 235–254 (2007)
58. (MR2339977) Dai, J., Luo, W., Jin, M., Zeng, W., He, Y., Yau, S.T., Gu, X.: Geometric accuracy analysis for discrete surface approximation. Comput. Aided Geom. Design **24**(6), 323–338 (2007)
59. (MR2405673) Desbrun, M., Kanso, E., Tong, Y.: Discrete differential forms for computational modeling. In: Bobenko, A.I., Schröder, P., Sullivan, J.M., Ziegler, G.M. (eds.) Discrete Differential Geometry. Oberwolfach Seminar, vol. 38, pp. 287–324. Birkhauser, Basel (2008)
60. (MR0394451) do Carmo, M.: Differential Geometry of Curves and Surfaces. Prentice-Hall, Englewood Cliffs (1976)
61. (MR2152094) Dong, S., Kircher, S., Garland, M.: Harmonic functions for quadrilateral remeshing of arbitrary manifolds. Comput. Aided Geom. Design **22**(5), 392–423 (2005)
62. Dritschel, D.G.: The stability and energetics of co-rotating uniform vortices. J. Fluid Mech. **157**, 95–134 (1985)
63. Ebbinghaus, H., Peckhaus, V.: Ernst Zermelo. An Approach to His Life and Work. Springer, Berlin (2007)

64. (MR0271984) Ebin, D.G., Marsden, J.: Groups of diffeomorphisms and the motion of an incompressible fluid. Ann. Math. Ser. 2 **92**(1), 102–163 (1970)
65. (MR2451285) Enciso, A., Peralta-Salas, D.: Geometrical and topological aspects of electrostatics on Riemannian manifolds. J. Geom. Phys. **57**, 1679–1696 (2007)
66. Engels, P.: Viewpoint: observing the dance of a vortex-antivortex pair, step by step. Physics (APS) **3**, 33 (2010)
67. (MR2449768) Euler, L.: General principles of the motion of fluids (adaptation by U. Frisch of an English translation by T. E. Burton). Physica D **237**(14–17), 1825–1839 (2008). Original article: Euler, L.: Principes généraux du mouvement des fluides. Mém. Acad. Sci. Berlin **11**, 274–315 (1757). http://www.math.dartmouth.edu/~euler/pages/E226.html
68. (MR2449769) Euler, L.: Principles of the motion of fluids (English adaptation by Walter Pauls). Physica D **237**(14–17), 1840–1854 (2008). http://www.math.dartmouth.edu/~euler/
69. (MR2449767) Eyink, G., Frisch, U., Moreau, R., Sobolevskii, A.: General Introduction (Proceedings of an International Conference. Euler Equations: 250 Years on (EE250), Aussois, 18–23 June 2007) Physica D **237**(14–17), 11–15 (2008)
70. (MR1500278) Farina, A., Saut, J.-C. (eds.): Stationary and time dependent Gross-Pitaevskii equations. In: Proceedings of Wolfgang Pauli Institute Thematic, Vienna, 2006. Contemporary Mathematics, vol. 473. American Mathematical Society, Providence (2008)
71. Flucher, M., Gustafsson, B.: Vortex motion in two-dimensional hydro/-mechanics. Preprint (TRITA-MAT-1997-MA-02) (Partly published as Ch. 15 in M. Flucher: Variational Problems with Concentration, Birkhäuser, 1999). http://www.math.kth.se/~gbjorn/flucher.pdf
72. (MR1259368) Fulton, W., MacPherson, R.: A compactification of configuration spaces. Ann. Math. (2) **139**(1), 183–225 (1994)
73. (MR0123709) Garsia, A.M., Rodemich, E.: An embedding of Riemann surfaces of genus one. Pac. J. Math. **11**, 193–204 (1961)
74. (MR2605308) Ghrist, R.: Configuration spaces, braids, and robotics. In: Berrick, A.J., Cohen, F.R., Hanbury, E., Wong, Y.-L., Wu, J. (eds.) Braids. Lecture Notes Series, Institute for Mathematical Sciences, National University of Singapore, vol. 19, pp. 263–304. World Scientific Publishing, Hackensack (2010)
75. (MR0458504) Gilkey, P.: The Index Theorem and the Heat Equation. (Notes by Jon Sacks) Mathematics Lecture Series, vol. 4. Publish or Perish Inc., Boston (1974)
76. (MR3001372) Green, C.C., Marshall, J.S.: Green's function for the Laplace-Beltrami operator on a toroidal surface. Proc. R. Soc. A **469**, 20120479 (2013)
77. (MR0056525) Gromeka, I.: Sobranie socinenii (Russian) (Collected works). Izdat. Akad. Nauk SSSR, Moscow (1952)
78. (MR1736868) Grigor´yan, A.: Estimates of heat kernels on Riemannian manifolds. In: Brian Davies, E., Safarov, Y. (eds.) Spectral Theory and Geometry (Edinburgh, 1998). London Mathematical Society Lecture Note Series, vol. 273, pp. 140–225. Cambridge University Press, Cambridge (1999)
79. (MR2569498) Grigor´yan, A.: Heat Kernel and Analysis on Manifolds. AMS/IP Studies in Advanced Mathematics, vol. 47, American Mathematical Society/International Press, Providence/Boston (2009)
80. (MR1958012) Gu, X., Yau, S.T.: Computing conformal structures of surfaces. Commun. Inform. Syst. **2**(2), 121–145 (2002)
81. (MR2439718) Gu, X., Yau, S.-T.: Computational Conformal Geometry. Advanced Lectures in Mathematics (ALM), vol. 3. International Press/Higher Education Press, Somerville/Beijing (2008)
82. (MR2106621) Gutkin, E., Newton, P.: The method of images and Green's function for spherical domains. J. Phys. A 37 **50**, 11989–12003 (2004)
83. (MR0930247) Haas, A., Susskind, P.: The geometry of the hyperelliptic involution in genus two. Proc. Am. Math. Soc. **105**(1), 159–165 (1989)
84. (MR0556289) Hally, D.: Stability of streets of vortices on surfaces of revolution with a reflection symmetry. J. Math. Phys. **21**(1), 211–217 (1980)

85. Havelock, H.: The stability of motion of rectilinear vortices in ring formation. Philos. Mag. **11**, 617–633 (1931)
86. Hecht, T.: Quantum computation with Bose-Einstein condensates. Thesis, Technische Universität München, Max- Planck-Institut für Quantenoptik (2004)
87. Helmholtz, H.: Über integrale der hydrodynamischen gleichungen welche den Wirbelbewegungen entsprechen. Crelles J. **55**, 25–55 (1858). http://www.dz-srv1.sub.uni-goettingen.de/sub/digbib/loader?did=D268537
88. (MR2305826) Hernández-Garduño, A., Lacomba, E.: Collisions and regularization for the 3-vortex problem. J. Math. Fluid Mech. **9**(1), 75–86 (2007)
89. Hernández-Garduño, A., Lacomba, E.: Collisions of four point vortices in the plane. arXiv:math-ph/0609016. Preprint
90. (MR2299728) Hildebrandt, K., Polthier, K., Wardetzky, M.: On the convergence of metric and geometric properties of polyhedral surfaces. Geom. Dedicata **123**, 89–112 (2006)
91. (MR2384554) Hiraoka, Y.: Topological regularizations of the triple collision singularity in the 3-vortex problem. Nonlinearity **21**, 361–379 (2008)
92. (MR2704508) Hirani, A.: Discrete exterior calculus. Ph.D. thesis, Calthech (2003). http://www.resolver.caltech.edu/CaltechETD:etd-05202003-095403
93. (MR0794110) Holm, D.D., Marsden, J.E., Ratiu, T., Weinstein, A.: Nonlinear stability of fluid and plasma equilibria. Phys. Rep. **123**(1–2), 1–116 (1985)
94. (MR1948165) Holm, D., Marsden, J., Ratiu, T.: The Euler-Poincaré equations in geophysical fluid dynamics. In: Norbury, J., Roulstone, I. (eds.) Large-Scale Atmosphere-Ocean Dynamics, vol. II, pp. 251–300. Cambridge University Press, Cambridge (2002)
95. (MR0641913) Holmes, P., Marsden, J.: Horseshoes in perturbations of Hamiltonian systems with two degrees of freedom. Commun. Math. Phys. **82**(4), 523–544 (1981/1982)
96. (MR2504469) Hwang, S., Kim, S.: Point vortices on hyperbolic sphere. J. Geom. Phys. **59**(4), 475–488 (2009)
97. (MR1984383) Iftimie, D., Lopes Filho, M.C., Nussenzveig Lopes, H.J.: On the large-time behavior of two-dimensional vortex dynamics. Physica D **179**(3–4), 153–160 (2003)
98. (MR2165683) Jin, M., Wang, Y., Gu, X., Yau, S.-T.: Optimal global conformal surface parameterization for visualization. Commun. Inform. Syst. **4**(2), 117–134 (2005)
99. (MR1621912) Kidambi, R., Newton, P.K.: Motion of three point vortices on a sphere. Physica D **116**, 143–175 (1998)
100. (MR1743082) Kidambi, R., Newton, P.K.: Point vortex motion on a sphere with solid boundaries. Phys. Fluids **12**(3), 581–588 (2000)
101. (MR2639049) Kim, S.: Latitudinal point vortex rings on the spheroid. Proc. R. Soc. Lond. Ser. A Math. Phys. Eng. Sci. **466**, 1749–1768 (2010)
102. (MR2604233) Kim, S.: The motion of point vortex dipole on the ellipsoid of revolution. Bull. Korean Math. Soc. **47**(1), 73–79 (2010)
103. (MR1700500) Kimura, Y.: Vortex motion on surfaces with constant curvature. Proc. R. Soc. Lond. A **455**, 245–259 (1999)
104. (MR0927662) Kimura, Y., Okamoto, H.: Vortex motion on a sphere. J. Phys. Soc. Jpn. **56**, 4203–4206 (1987)
105. Kirchhoff, G.: Vorlesungen über mathematische Physik, Mechanik, ch. XX. Teubner, Leipzig (1876). http://www.gallica.bnf.fr/ark:/12148/bpt6k99608d
106. (MR939269) Kirwan, F.: The topology of reduced phase spaces of the motion of vortices on a sphere. Physica D **30**(1–2), 99–123 (1988)
107. Klein, F.: Über Riemann's Theorie der Algebraischen Functionen (1882). http://www.gutenberg.org (E-book 20313, 2007)
108. Klein, F.: Über die Bildung von Wirbeln in reibungslosen Fl-ssigkeiten. In: Fricke, R., Ostrowski, A. (eds.) Gesammelte Mathematische Abhandlungen, vol. 3, pp. 710–713. Springer, Berlin (1923)
109. Koiller, J., Boatto, S.: Vortex pairs on surfaces. In: Etayo, F., Fioravanti, M., Santamara, R. (eds.) XVII International Fall Workshop on Geometry and Physics. AIP Conference Proceedings, vol. 1130, pp. 77–88 (2009)

110. (MR1291115) Koiller, J., Ragazzo, C., Oliva, W.: On the motion of two-dimensional vortices with mass. J. Nonlinear Sci. **4**(5), 375–418 (1994)
111. (MR2920506) Kokotov, A.: On the spectral theory of the Laplacian on compact polyhedral surfaces of arbitrary genus. In: Bobenko, A.I., Klein, C. (eds.) Computational Approach to Riemann Surfaces. Lecture Notes in Mathematics, vol. 2013, pp. 227–253. Springer, New York (2011)
112. Kokotov, A.: Compact polyhedral surfaces of an arbitrary genus and determinants of Laplacians. arXiv: 0906.0717v1. Preprint
113. (MR1490861) Kontsevich, M.: Lyapunov exponents and Hodge theory. In: Drouffe, J.M., Zuber, J.B. (eds.) The Mathematical Beauty of Physics (Saclay, 1996). Advanced Series in Mathematical Physics, vol. 24, pp. 318–332. World Scientific Publishing, River Edge (1997)
114. Küchemann, D.: Report on the I.U.T.A.M. symposium on concentrated vortex motions in fluids. J. Fluid Mech. **21**, 1–20 (1965)
115. Kurakin, L.G.: On the stability of the regular n-sided polygon of vortices. Dokl. Phys. **39**, 284–286 (1994)
116. (MR2683100) Kurakin, L.G., Ostrovskaya, I.V.: Stability of the Thomson vortex polygon with evenly many vortices ourside a circular domain. Sib. Math. J. **51**, 463–474 (2010)
117. (MR2640113) Lacomba, E.: Interaction of point sources and vortices for incompressible planar fluids. Qual. Theory Dyn. Syst. **8**(2), 371–379 (2009)
118. (MR1877972) Laurent-Polz, F.: Point vortices on a sphere: a case with opposite vorticities. Nonlinearity **115**, 143–171 (2002)
119. (MR2136829) Laurent-Polz, F.: Point vortices on a rotating sphere. Regul. Chaotic Dyn. **10**(1), 39–58 (2005)
120. (MR1411341) Lewis, D., Ratiu, T.: Rotating n-gon/$k\,n$-gon vortex configurations. J. Nonlinear Sci. **6**(5), 385–414 (1996)
121. (MR1753020) Lewis, D., Ratiu, T.: Polygonal vortex configurations. In: Lacomba, E., Llibre, J. (eds.) New Trends for Hamiltonian Systems and Celestial Mechanics (Cocoyoc, 1994). Advanced Series in Nonlinear Dynamics, vol. 8, pp. 249–262. World Scientific Publishing, River Edge (1996)
122. (MR0838352) Lewis, D., Marsden, J., Montgomery, R., Ratiu, T.: The Hamiltonian structure for dynamic free boundary problems. Physica D **18**(1–3), 391–404 (1986)
123. (MR0908023) Lewis, D., Marsden, J., Ratiu, T.: Stability and bifurcation of a rotating planar liquid drop. J. Math. Phys. **28**(10), 2508–2515 (1987)
124. (MR1811389) Lim, C., Montaldi, J., Roberts, M.: Relative equilibria of point vortices on the sphere. Physica D **148**(1–2), 97–135 (2001)
125. (MR2512175) Lim, C., Ding, X., Nebus, J.: Vortex Dynamics, Statistical Mechanics, and Planetary Atmospheres. World Scientific Publishing, Hackensack (2009)
126. (MR0006281) Lin, C.C.: On the motion of vortices in two dimensions. I. Existence of the Kirchhoff-Routh function. Proc. Natl. Acad. Sci. USA **27**, 570–575 (1941)
127. (MR0006282) Lin, C.C.: On the motion of vortices in two dimensions. II. Some further investigations on the Kirchhoff-Routh function. Proc. Natl. Acad. Sci. USA **27**, 575–577 (1941)
128. (MR0008204) Lin, C.C.: On the Motion of Vortices in Two Dimensions. Applied Mathematics Series, vol. 5. University of Toronto Studies, University of Toronto Press, Toronto (1943)
129. Lin, C.-S., Wang, C.L.: A function theoretic view of the mean field equations on tori. In: Proceeding of the International Conference on Geometric Analysis (TIMS, Taipei 2007). International Press, Cambridge (2008)
130. (MR2680484) Lin, C.S., Wang, C.L.: Elliptic functions, Green functions and the mean field equations on tori. Ann. Math. **172**(2), 911–954 (2010)
131. (MR2550076) Lui, L., Gu, X., Chan, T., Yau, S.-T.: Variational method on Riemann surfaces using conformal parameterization and its applications to image processing. Methods Appl. Anal. **15**(4), 513–538 (2008)

132. (MR1867882) Majda, A.J., Bertozzi, A.L.: Vorticity and Incompressible Flow. Cambridge Texts in Applied Mathematics, vol. 27. Cambridge University Press, Cambridge (2002)
133. (MR1245492) Marchioro, C., Pulvirenti, M.: Mathematical Theory of Incompressible Nonviscous Fluids. Applied Mathematical Sciences, vol. 96. Springer, New York (1994)
134. Marcus, P.S.: Jupiter's great red spot and other vortices. Annu. Rev. Astron. Astrophys. **31**, 523–569 (1993)
135. (MR0719058) Marsden, J.E., Weinstein, A.: Coadjoint orbits, vortices, and Clebsch variables for incompressible fluids. Physica D **7**, 305–323 (1983)
136. (MR1360783) Marsden, J.E., Ratiu, T., Raugel, G.: Équations d'Euler dans une coque sphérique mince. C. R. Acad. Sci. Paris Ser. I Math. **321**(0), 1201–1206 (1995)
137. Marsden, J.E., Pekarsky, S., Shkoller, S.: Stability of relative equilibria of point vortices on a sphere and symplectic integrators. Il Nuovo Cimento **22**(6), 793–802 (1999)
138. (MR1870305) Marsden, J.E., Ratiu, T., Raugel, G.: The Euler equations on thin domains. In: Fiedler, B., Gröoger, K., Sprekels, J. (eds.) International Conference on Differential Equations, Berlin, 1999, pp. 1198–1203. World Scientific Publishing, River Edge (2000)
139. (MR1779614) Marsden, J.E., Ratiu, T., Shkoller, S.: The geometry and analysis of the averaged Euler equations and a new diffeomorphism group. Geom. Funct. Anal. **10**(3), 582–599 (2000)
140. Meleshko, V., Aref, H.: A bibliography of vortex dynamics 1858–1956. Adv. Appl. Mech. **41**, 197–292 (2007)
141. (MR0156048) Melnikov, V.K.: On the stability of a center for time-periodic perturbations (Russian). Trudy Moskov. Mat. **12**, 3–52 (1963)
142. (MR2349680) Mercat, C.: Discrete Riemann surfaces. In: Papadopoulos, A. (ed.) Handbook of Teichmüller Theory, Volume I. IRMA Lectures in Mathematics and Theoretical Physics, vol. 11, pp. 541–575. European Mathematical Society, Zürich (2007)
143. (MR2047000) Meyer, M., Desbrun, M., Schröder, P., Barr, A.: Discrete differential-geometry operators for triangulated 2-manifolds. In: Hege, H., Polthier, K. (eds.) Visualization and Mathematics III. Mathematics and Visualization, pp. 35–57. Springer, Berlin (2003)
144. (MR2031280) Montaldi, J., Soulière, A., Tokieda, T.: Vortex dynamics on a cylinder. SIAM J. Appl. Dyn. Syst. **2**(3), 417–430 (2003)
145. Muller, B.: Kartenprojektionen des dreiachsigen ellipsoids. Diplomarbeit, Geodatisches Institut, University of Stuttgart (1991)
146. (MR1252997) Nag, S.: Riemann surfaces and their Jacobians: a toolkit. Indian J. Pure Appl. Math. **24**(12), 729–745 (1993)
147. Neely, T.: Formation, dynamics and decay of quantized vortices in Bose-Einstein condensates: elements of quantum turbulence. Ph.D. thesis, University of Arizona (2010)
148. Neely, T., Samson, E., Bradley, A., Davis, M., Anderson, B.: Observation of vortex dipoles in an oblate Bose-Einstein condensate. Phys. Rev. Lett. **104**, 160401 (2010)
149. (MR2446249) Neishtadt, A.I.: Averaging method and adiabatic invariants. In: Craig, W. (ed.) Hamiltonian Dynamical Systems and Applications. NATO Science for Peace and Security Series B. Physics and Biophysics, pp. 53–66. Springer, Dordrecht (2008)
150. (MR1831715) Newton, P.: The N-Vortex Problem: Analytical Techniques. Applied Mathematical Sciences, vol. 145. Springer, New York (2001)
151. (MR2471767) Newton, P., Sakajo, T.: Point vortex equilibria on the sphere via Brownian ratchets. Proc. R. Soc. Lond. Ser. A Math. Phys. Eng. Sci. **465**(2102), 437–455 (2009)
152. (MR2395512) Newton, P., Shokraneh, H.: Interacting dipole pairs on a rotating sphere. Proc. R. Soc. Lond. Ser. A Math. Phys. Eng. Sci. **464**(2094), 1525–1541 (2008)
153. (MR2452594) Okikiolu, K.: A negative mass theorem for the 2-torus. Commun. Math. Phys. **284**(3), 775–802 (2008)
154. (MR2377499) Okikiolu, K.: Extremals for logarithmic Hardy-Littlewood-Sobolev inequalities on compact manifold. Geom. Funct. Anal. **17**(5), 1655–1684 (2008)
155. (MR2525649) Okikiolu, K.: A negative mass theorem for surfaces of positive genus. Commun. Math. Phys. **290**(3), 1025–1031 (2009)

156. (MR2430437) Parlier, H.: Fixed point free involutions on Riemann surfaces. Israel J. Math. **166**, 297–311 (2008)
157. (MR1752604) Patrick, G.W.: Dynamics of perturbed relative equilibria of point vortices on the sphere or plane. J. Nonlinear Sci. **10**, 401–415 (2000)
158. (MR1653104) Pekarsky, S., Marsden, J.E.: Point vortices on a sphere: stability of relative equilibria. J. Math. Phys. **39**, 5894–5907 (1998)
159. Pitaevskii, L.P., Stringari, S.: Bose-Einstein Condensation. Clarendon Press, Oxford (2003)
160. (MR2047004) Polthier, K., Preuss, E.: Identifying vector fields singularities using a discrete hodge decomposition. In: Hege, H.C., Polthier, K. (eds.) Visualization and Mathematics III. Springer, New York (2002)
161. (MR1677691) Polthier, K., Schmies, M.: Straightest geodesics on polyhedral surfaces. In: Hege, H., Polthier, K. (eds.) Mathematical Visualization (Berlin, 1997), pp. 135–150. Springer, Berlin (1998)
162. Polvani, L.M., Dritschel, D.G.: Wave and vortex dynamics on the surface of a sphere. J. Fluid Mech. **255**, 35–64 (1993)
163. Prandtl, L.: Über Flüssigkeitsbewegung Bei Sehr Kleiner Reibung. Verhandlungen des dritten Internationalen mathematikerkongresses in Heidelberg (International Mathematical Congress, Heidelberg), pp. 484–491 (1904); Gesammelte Abhandlungen II, pp. 575–584 (1961) (English translation available from http://www.digital.library.unt.edu/ark:/67531/metadc65275/)
164. Pullin, D.: Contour dynamics methods. Annu. Rev. Fluid Mech. **24**, 89–115 (1992)
165. (MR1756634) Qing, J. : Ginzburg-Landau vortices and Mandelstam diagrams. Pac. J. Math. **194**(1), 189–197 (2000)
166. (MR2433412) Ramodanov, S.M.: On the motion of two mass vortices in perfect fluid. In: Borisov, A.V., et al. (eds.) IUTAM Symposium on Hamiltonian Dynamics, Vortex Structures, Turbulence. IUTAM Book Series, vol. 6, pp. 459–468. Springer, Dordrecht (2008)
167. (MR1502395) Rasor, S.E.: The geodesic lines on the helicoid. Ann. Math. **11**(2), 77–85 (1910)
168. (arXiv:1306.5054) Raymond, N., Ngoc, S.V.: Geometry and Spectrum in 2D Magnetic Wells (to appear in Annales de l'Institut Fourier)
169. Regis, A.: Dinâmica de vórtices pontuais sobre um elipsóide triaxial (portuguese) (Dynamics of point vortices on the triaxial ellipsoid). Ph.D. thesis, Departamento de Matemática da Universidade Federal de Pernambuco (2011)
170. Rhines, P.B., Young, W.R.: Homogenization of potential vorticity in planetary gyres. J. Fluid Mech. **122**, 347–367 (1982)
171. Riemann, B.: Theorie der Abel'schen Functionen. J. Reine Angew. Math. **54**, 101–155 (1857)
172. (MR1922078) Riemann, B.: Riemanniana Selecta (Spanish; Edited and with an introductory study by José Ferreirós). Clásicos del Pensamiento. CSIC, Madrid (2000)
173. (MR2121437) Riemann, B.: Collected papers (Translated from the 1892 German edition by R. Baker, C. Christenson, H. Orde). Kendrick Press, Heber City (2004)
174. Rindler-Daller, T., Shapiro, P.R.: Angular momentum and vortex formation in Bose-Einstein-condensed cold dark matter haloes. Mon. Not. R. Astron. Soc. **422**, 135–161 (2012)
175. (MR3071150) Roberts, G.E.: Stability of relative equilibria in the planar N-vortex problem. SIAM J. Appl. Dyn. Syst. **12**(2), 1114–1134 (2013)
176. (MR1409153) Robinson, C.: Melnikov method for autonomous Hamiltonians. In: Saari, D., Xia, Z. (eds.) Hamiltonian Dynamics and Celestial Mechanics (Seattle, WA, 1995). Contemporary Mathematics, vol. 198, pp. 45–53. American Mathematical Society, Providence (1996)
177. (MR1462892) Rosenberg, S.: The Laplacian on a Riemannian Manifold. Cambridge University Press, Cambridge (1997)
178. Rowley, C.W., Marsden, J.E.: Variational integrators for degenerate Lagrangians, with application to point vortices. In: Proceedings of the 41st IEEE Conference on Decision and Control. Proceedings IEEE Conference on Decision and Control, pp. 1521–1527 (2002)
179. (MR1217252) Saffman, P.G.: Vortex Dynamics. Cambridge Monograph on Mechanics and Applied Mathematics. Cambridge University Press, Cambridge (1992)

180. Schering, E.: Über die conforme abbildung des ellipsoids auf der ebene, ch. III. In: Gesammelte Mathematische Werke. Mayer and Muller, Berlin (1902)
181. Seo, S., Chung, M.K., Vorperian, H.K.: Heat kernel smoothing using laplace-beltrami eigenfunctions. In: Jiang, T., Navab, N., Pluim, J., Viergever, M. (eds.) Medical Image Computing and Computer-Assisted Intervention - MICCAI 2010. Lecture Notes in Computer Science, Springer-Verlag, Heidelberg, Germany, vol. 6363, pp. 505–512 (2010)
182. (MR2259296) Shadden, S.C., Dabiri, J.O., Marsden, J.E.: Lagrangian analysis of fluid transport in empirical vortex ring flows. Phys. Fluids **18**(4), 047105 (2006)
183. Shadden, S.C., Katija, K., Rosenfeld, M., Marsden, J.E., Dabiri, J.O.: Transport and stirring induced by vortex formation. J. Fluid Mech. **593**, 315–332 (2007)
184. (MR1886996) Shashikanth, B.N., Marsden, J.E., Burdick, J.W., Kelly, S.D.: The Hamiltonian structure of a two-dimensional rigid circular cylinder interacting dynamically with N point vortices. Phys. Fluids **14**(3), 1214–1227 (2002)
185. Shashikanth, B.N., Sheshmani, A., Kelly, S.D., Marsden, J.E.: Hamiltonian structure for a neutrally buoyant rigid body interacting with N vortex rings of arbitrary shape: the case of arbitrary smooth body shape. Theor. Comput. Fluid Dyn. **22**(1), 37–64 (2008)
186. (MR2538580) Sideris, T., Vega, L.: Stability in L^1 of circular vortex patches. Proc. Am. Math. Soc. **137**, 4199–4202 (2009)
187. (MR2278409) Smets, D., Bethuel, F., Orlandi, G.: Quantization and motion law for Ginzburg-Landau vortices. Arch. Ration. Mech. Anal. **183**(2), 315–370 (2007)
188. (MR1910864) Soulière, A., Tokieda, T.: Periodic motions of vortices on surfaces with symmetry. J. Fluid Mech. **460**, 83–92 (2002)
189. (MR2000979) Spirn, D.: Vortex motion law for the Schr-dinger-Ginzburg-Landau equations. SIAM J. Math. Anal. **34**(6), 1435–1476 (2003)
190. (MR0092855) Springer, G.: Introduction to Riemann Surfaces. Addison-Wesley Publishing Company, Reading (1957)
191. (MR2153456) Steiner, J.: A geometrical mass and its extremal properties for metrics on S^2. Duke Math. J. **129**(1), 63–86 (2005)
192. Stremler, M.A.: On relative equilibria and integrable dynamics of point vortices in periodic domains. Theor. Comput. Fluid Dyn. **24**, 25–37 (2010)
193. Stremler, M.A., Aref, H.: Motion of three point vortices in a periodic parallelogram. J. Fluid Mech. **392**, 101–128 (1999)
194. (MR0939369) Struik, D.J.: Lectures on Classical Differential Geometry (reprint of the second edition). Dover Publications, New York (1988)
195. (MR2418353) Surana, A., Crowdy, D.: Vortex dynamics in complex domains on a spherical surface. J. Comput. Phys. **227**(12), 6058–6070 (2008)
196. (MR2431284) Sushch, V.: Green function for a two-dimensional discrete Laplace-Beltrami operator. Cubo **10**(2), 47–59 (2008)
197. (MR0911087) Tang, Y.: Nonlinear stability of vortex patches. Trans. Am. Math. Soc. **304**(2), 617–638 (1987)
198. Tazzioli, R.: Riemann: Le géométre de la Nature. Les gènies de la Science. Pour la Science, Paris (2002)
199. Thomson, J.J.: Electricity and Matter. Westmister Archibald Conatable, Westminster (1904)
200. (MR2222436) Tronin, K.G.: Absolute choreographies of point vortices on a sphere. Regul. Chaotic Dyn. **11**(1), 123–130 (2006)
201. Turner, A.M., Vitelli, V., Nelson, D.R.: Vortices on curved surfaces. Rev. Mod. Phys. **82**, 1301–1348 (2010)
202. Vallis, G.K.: Atmospheric and Oceanic Fluid Dynamics. Cambridge University Press, Cambridge (2006)
203. van Wijngaarden, L.: Prandtl–Batchelor flows revisited. Fluid Dyn. Res. **39**, 267–278 (2007)
204. (MR2525759) Vankerschaver, J., Kanso, E., Marsden, J.E.: The geometry and dynamics of interacting rigid bodies and point vortices. J. Geom. Mech. **1**(2), 223–266 (2009)

205. Viglioni, H.: Dinâmica de Vórtices em Superfícies com Aplicações ao Problema de dois Vórtices no Toro Plano (Portuguese) (Dynamics of vortices on surfaces with aplications to the flat tori). Ph.D. thesis, Departamento de Matemática Aplicada da Universidade de São Paulo (2013)
206. (MR0751985) Wan, Y.H.: On the nonlinear stability of circular vortex patches. In Marsden, J.E. (ed.) Fluids and Plasmas: Geometry and Dynamics. Contemporary Mathematics, vol. 28, 3rd edn., pp. 215–220. American Mathematical Society, Providence (1984)
207. (MR0795112) Wan, Y.H., Pulvirenti, M.: Nonlinear stability of circular vortex patches. Commun. Math. Phys. **99**(3), 435–450 (1985)
208. Wan, Y.H., Marsden, J.E., Ratiu, T.S., Weinstein, A.: Nonlinear Stability of Circular Vortex Patches. Center for Pure and Applied Mathematics, vol. 162. University of California, Berkeley (1983)
209. (MR2777588) Wayne, C.E.: Vortices and two dimensional fluid motion. Notices AMS **58**(1), 10–19 (2011)
210. (MR0834280) Weinstein, A.: The local structure of Poisson manifolds. J. Differ. Geom. **18**, 523–557 (1983)
211. (MR0166351) Weyl, H.: The Concept of a Riemann Surface. Addison-Wesley, Reading (1964)
212. (MR0956468) Wiggins, S.: Global Bifurcations and Chaos: Analytical Methods. Applied Mathematical Sciences, vol. 73. Springer, New York (1988)
213. (MR2091201) Xu, G.: Convergence of discrete Laplace-Beltrami operators over surfaces. Comput. Math. Appl. **48**(3–4), 347–360 (2004)
214. (MR2091142) Xu, G.: Discrete Laplace-Beltrami operators and their convergence. Comput. Aided Geom. Design **21**(8), 767–784 (2004)
215. Yamagata, T., Matsuura, T.: A generalization of Prandtl-Batchelor theorem for planetary fluid flows in a closed geostrophic contour. Meteorol. Soc. Jpn. J. **59**, 615–619 (1981)
216. (MR1486273) Zabusky, N., Norman, J., Hughes, M., Roberts, K.: Contour dynamics for the Euler equations in two dimensions. J. Comput. Phys. **135**(2), 217–226 (1997)
217. (MR2516244) Zeng, W., Li, X., Yau, S.T., Gu, X.: Conformal spherical parametrization for high genus surfaces. Commun. Inform. Syst. **7**(3), 273–286 (2007)
218. (MR2550077) Zeng, W., Lui, L.M., Gu, X., Yau, S.-T.: Shape analysis by conformal modules. Methods Appl. Anal. **15**(4), 539–555 (2008)
219. Zermelo, E.: Hydrodynamische Untersuchungen über die Wirbelbewegungen in einer Kugelfläche. Z. Math. Phys. **47** 201–237 (1902)

The Geometry of Radiative Transfer

Christian Lessig and Alex L. Castro

Abstract We present the geometry and symmetries of radiative transfer theory. Our geometrization exploits recent work in the literature that enables to obtain the Hamiltonian formulation of radiative transfer as the semiclassical limit of a phase space representation of electromagnetic theory. Cosphere bundle reduction yields the traditional description over the space of positions and directions, and geometrical optics arises as a limit case when the amount of energy that is transported is disregarded. It is also shown that, in idealized environments, radiative transfer is a Lie-Poisson system with the group of canonical transformations as configuration space and symmetry group.

1 Introduction

Radiative transfer describes the transport of electromagnetic energy in macroscopic environments, classically when polarization effects are neglected [37]. The theory originates in work by Bouguer [6, 7] and Lambert [22] in the 18th century where light intensity and its measurement were first studied systematically, cf. Fig. 1. In the 19th and early 20th century the theory was then extended to include transport and scattering effects [9, 26, 42, 43]. To this day, however, radiative transfer is a phenomenological theory with a mathematical formulation that still employs the concepts introduced by Lambert in the 18th century—and this despite

C. Lessig (✉)
Computer Graphics Group, TU Berlin, Berlin, Germany

Now with the University of Toronto, Toronto, ON, Canada and Technische Universität Berlin, Berlin, Germany
e-mail: christian.lessig@tu-berlin.de

A.L. Castro
Imperial College, 180 Queen's gate, SW7 2AZ, London, UK
e-mail: alex.castro@mat.puc-rio.br

D.E. Chang et al. (eds.), *Geometry, Mechanics, and Dynamics*, Fields Institute Communications 73, DOI 10.1007/978-1-4939-2441-7_11

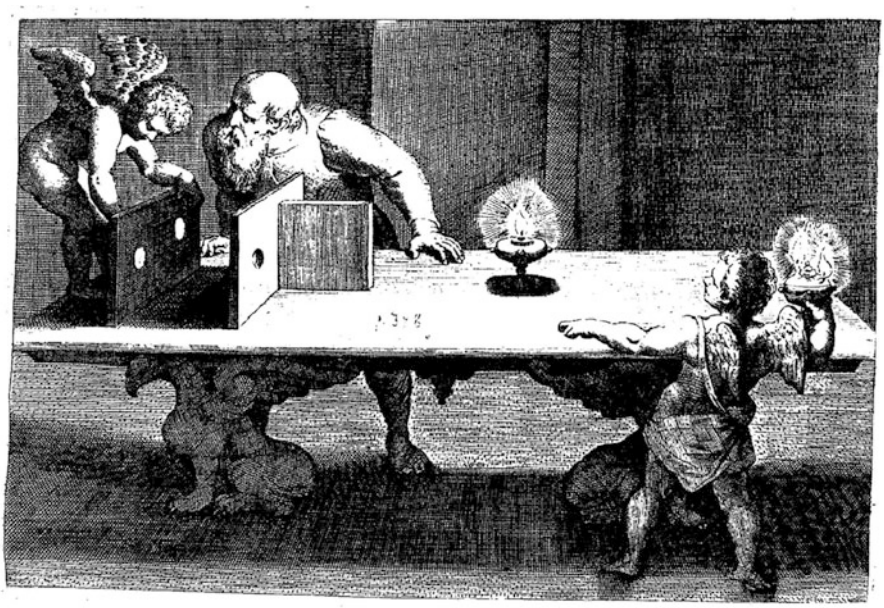

Fig. 1 Early research in radiometry as illustrated by Rubens (from [22])

the importance of the theory in a multitude of fields, such as medical imaging, remote sensing, computer graphics, atmospheric science, climate modelling, and astrophysics.

In the following, we will explain the physical foundations of radiative transfer in media with varying refractive index and we study the geometry of the theory and its symmetries; an overview is provided in Fig. 2. Following recent advances in applied mathematics, semi-classical analysis is employed to lift classical electromagnetic theory from configuration space $Q \subseteq \mathbb{R}^3$ to phase space T^*Q. By restricting the dynamics on T^*Q to a non-zero energy level and considering the short wavelength limit one obtains a transport equation for polarized light, and further only considering the energy that is transported and neglecting polarization leads to radiative transfer theory in a Hamiltonian formulation. Our derivation shows that the central quantity of radiative transfer theory is the phase space light energy density $\ell \in \mathrm{Den}(T^*Q)$ and that radiance, which plays this role in the classical formulation, is meaningful only in the context of measurements, the setting Lambert considered when he introduced the concept [22]. With the Hamiltonian formulation of radiative transfer on 6-dimensional phase space $T^*Q \cong \mathbb{R}^3 \times U$, the classical 5-dimensional description over the space of positions and directions is obtained when the conservation of frequency is exploited. The associated symmetry enables the reduction of the dynamics from the cotangent bundle T^*Q to the cosphere bundle $S^*Q = (T^*Q \setminus \{0\})/\mathbb{R}^+$ and time evolution is then described by contact dynamics. Fermat's principle, the Lagrangian formulation of geometrical optics,

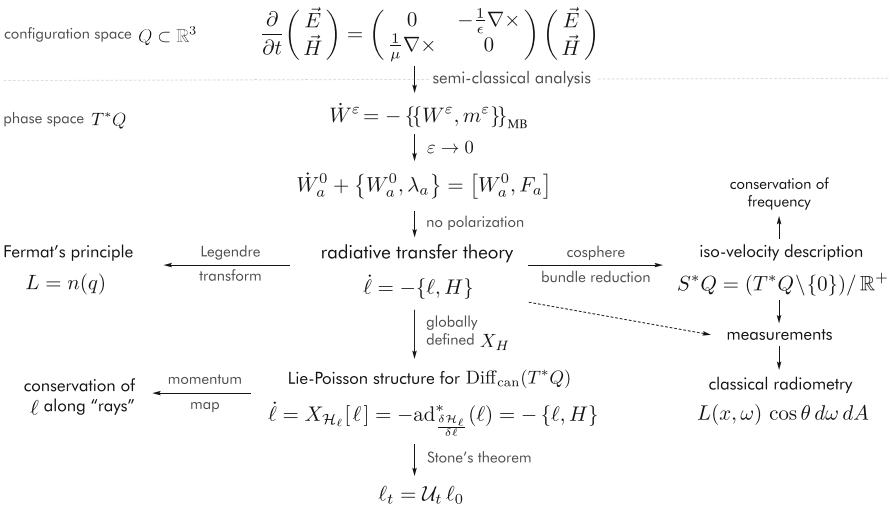

Fig. 2 Overview of the physical foundations and the geometric structure of radiative transfer theory. Semi-classical analysis yields a description of Maxwell's equations on phase space T^*Q where the electromagnetic field $\mathbf{F} = (\mathbf{E}, \mathbf{H})^T$ is represented by the Wigner transform W^ε and dynamics are governed by a matrix-valued analogue of the Moyal bracket $\{\{\,,\}\}_{\mathrm{MB}}$. When the short wavelength limit is considered, this leads to a transport equation for polarized light with the 2×2 matrix density W^0_a being formed by the classical Stokes parameters. When polarization is also neglected, W^0_a becomes the scalar light energy density $\ell \in \mathrm{Den}(T^*Q)$ whose dynamics are governed by the Poisson bracket. The classical five dimensional formulation of radiative transfer is obtained using cosphere bundle reduction with the light frequency being the associated conserved quantity. When radiative transfer is considered globally and the light energy density ℓ_t at time t forms a configuration of the system, radiative transfer becomes a Lie-Poisson system for the group $\mathrm{Diff}_{\mathrm{can}}(T^*Q)$ of canonical transformations

is obtained from the Hamiltonian formulation of radiative transfer through a non-canonical Legendre transform when energy transport is neglected. From our point of view, geometric optics is thus a special case of radiative transfer theory. When radiative transfer is considered from a global perspective with the light energy density $\ell_t \in \mathrm{Den}(T^*Q)$ at time t as a configuration of the system, the configuration space of the theory becomes the group $\mathrm{Diff}_{\mathrm{can}}(T^*Q)$ of canonical transformation. Radiative transfer has then a Lie-Poisson structure and the associated symmetry is the conservation of light energy density along trajectories in phase space. This provides a modern rationale for the classical law of "conservation of radiance along a ray" [36]. It also reveals a surprising similarity to Kelvin's circulation theorem in ideal fluid dynamics.

2 A Modern Formulation of Radiative Transfer Theory

Following recent work in the literature, in this section we will describe how the Hamiltonian formulation of radiative transfer arises as the asymptotic limit of Maxwell's equations and we will also study the geometry and symmetries of the system.

2.1 Derivation

From the scale hierarchy of electromagnetic radiation in physics it is apparent that radiative transfer has to arise at the short wavelength limit of Maxwell's equations, Hamilton's equations for electromagnetic field theory [29, p. 24]. Nonetheless, the exact correspondence was open for more than 200 years and still in the 1990s Mandel and Wolf [27] lamented that "in spite of the extensive use of the theory of radiative energy transfer, no satisfactory derivation of its basic equation from electromagnetic theory has been obtained up to now".[1] Recent work in applied mathematics [15, 16, 41, 47, 48] fills this gap and in the following we will summarize a rigorous derivation of radiative transfer theory from Maxwell's equations.

In a source free region $Q \subset \mathbb{R}^3$, Maxwell's equations are given by [5]

$$\frac{\partial}{\partial t}\begin{pmatrix}\mathbf{E}\\ \mathbf{H}\end{pmatrix} = \begin{pmatrix}0 & -\frac{1}{\varepsilon}\nabla\times\\ \frac{1}{\mu}\nabla\times & 0\end{pmatrix}\begin{pmatrix}\mathbf{E}\\ \mathbf{H}\end{pmatrix} \tag{1a}$$

$$\operatorname{div}(\mathbf{E}) = 0 \qquad \operatorname{div}(\mathbf{H}) = 0 \tag{1b}$$

where $\varepsilon : Q \to \mathbb{R}$ and $\mu : Q \to \mathbb{R}$ are the electric permittivity and magnetic permeability, respectively, and $\mathbf{E}$ and $\mathbf{H}$ represent the electric and magnetic fields; in the following it will be understood that these fields are divergence free. By introducing $\mathbf{F} = (\mathbf{E}, \mathbf{H})^T$, Eq. 1 can be written as

$$\dot{\mathbf{F}} = \mathbf{M}\,\mathbf{F} \tag{2}$$

and we will denote $\mathbf{M}$ as the Maxwell operator.[2] The classical observable of electromagnetic theory is the energy density $\mathscr{E}(q,t)$, given by

$$\mathscr{E}(q,t) = \|\mathbf{F}\|^2_{\varepsilon,\mu} = \frac{\varepsilon}{2}\|\mathbf{E}\|^2 + \frac{\mu}{2}\|\mathbf{H}\|^2. \tag{3}$$

[1] The first derivation of geometric optics from Maxwell's equations goes back to Sommerfeld and Runge [44], cf. [5, Chapter III] for historical details. Derivations of geometrical optics do not provide long time transport equations for the light energy density, cf. also [49].

[2] Eq. 2 is closely related to the spacetime formulation of electromagnetic theory with $\mathbf{F}$ being the components of the Faraday 2-form $F = E \wedge dt + B$, cf. [14, Sec. 3].

We are interested in the transport of the energy density $\mathscr{E}(q,t)$ in macroscopic environments. To describe this regime mathematically we introduce the scale parameter

$$\varepsilon = \lambda / d_n. \tag{4}$$

In Eq. 4, λ is the wavelength of light and d_n the average distance over which the refractive index $n = \sqrt{\varepsilon\,\mu} : Q \to \mathbb{R}$ varies, cf. [34, Chapter 22.5]. In macroscopic environments one has $\lambda \ll d_n$ and asymptotically these can thus be studied by letting $\varepsilon \to 0$. In the following, we will often write $\mathbf{F}^\varepsilon$, $\mathscr{E}^\varepsilon$ etc. to make the dependence of variables on the scale parameter explicit.

The classical approach to study short wavelength asymptotics is the Wenzel-Kramers-Brillouin (WKB) approximation.[3] However, this ansatz is limited in that solutions are only well defined until caustics form, at which point the approximation becomes multi-valued, and that the initial conditions must satisfy the WKB form $u^\varepsilon(q,t) = a(q,t)\, e^{iS(q,t)/\varepsilon}$. Additionally, Maxwell's equations describe the time evolution of the field $\mathbf{F}$, while we are interested in the limit $\varepsilon \to 0$ of the energy density $\mathscr{E}^\varepsilon(q,t)$ that depends quadratically on the field. This provides a serious obstruction for any approach to determine the transport of the limit energy density $\mathscr{E}^0(q,t)$ [45].

The limitations of classical approaches to describe the transport of the limit energy density $\mathscr{E}^0(q,t)$ can be circumvented by lifting electromagnetic theory to phase space T^*Q and studying the short wavelength limit there [16, 41]. The electromagnetic field $\mathbf{F}$ can be lifted to T^*Q using the Wigner transform [16, 52], yielding a 6×6 matrix density $W^\varepsilon[\mathbf{F}]$ whose components are given by

$$W^\varepsilon[\mathbf{F}]^\varepsilon_{ij}(q,p) = \frac{1}{(2\pi)^3} \int_Q e^{ip\cdot r}\, \mathbf{F}^\varepsilon_i(q - \frac{\varepsilon}{2} r)\, \mathbf{F}^\varepsilon_j(q + \frac{\varepsilon}{2} r)\, dr. \tag{5}$$

The lift of the Maxwell operator $\mathbf{M}^\varepsilon$ to phase space is provided by its matrix-valued symbol $m^\varepsilon(q,p)$ which can formally be expanded as $m^\varepsilon(q,p) = m^0(q,p) + \varepsilon m^1(q,p) + \varepsilon^2 m^2(q,p) + \cdots$. Time evolution on phase space is described by

$$\dot{W}^\varepsilon = -\{\!\{W^\varepsilon, m^\varepsilon\}\!\}_{\mathrm{MB}} \tag{6}$$

where $W^\varepsilon \equiv W^\varepsilon[\mathbf{F}]$ and $\{\!\{\,,\,\}\!\}_{\mathrm{MB}}$ is a matrix-valued "Moyal bracket" [16, Eq. 6.12]. Expanding this bracket one obtains

$$\dot{W}^\varepsilon = \frac{1}{\varepsilon}[W^\varepsilon, m^\varepsilon] - \frac{1}{2i}\left(\{W^\varepsilon, m^\varepsilon\} - \{m^\varepsilon, W^\varepsilon\}\right) + \mathscr{O}(\varepsilon) \tag{7}$$

[3] It is by now well known that the WKB approximation goes back to work by Liouville and Green in the first half of the 19th century.

where $\{\,,\}$ is commonly denoted as a matrix-valued "Poisson bracket"[4]; it is not a Poisson bracket in the formal sense and we will return to this point in Sec. 4. In contrast to the scalar Moyal bracket where the commutator in the first term vanishes by the commutativity of multiplication in the algebra $\mathscr{F}(T^*Q)$, in the matrix-valued case care is needed that the first term does not diverge as $\varepsilon \to 0$. This divergence can be circumvented by restricting dynamics to the eigenspaces of the Maxwell symbol m^ε. The diagonally identical symbol matrix is then in the ideal of the matrix algebra and the appropriately restricted commutator $[W^\varepsilon, m^\varepsilon]$ hence vanishes; this is the matrix-valued analogue of the Bohr-Sommerfeld quantization condition [25]. The eigenvalues of the Maxwell symbol are given by [41]

$$\lambda_0 = 0 \qquad \lambda_1 = \frac{c}{n(q)}\|p\| \qquad \lambda_2 = -\frac{c}{n(q)}\|p\|, \tag{8}$$

each having multiplicity two. Only λ_1 and λ_2 have physical significance, corresponding to forward and backward propagation in time. We will denote the projection onto the eigenspace associated with λ_a by Π_a, with $a \in \{1, 2\}$. Projecting the Wigner distribution W^ε onto the a^{th} eigenspace and taking the limit $\varepsilon \to 0$ yields

$$W_a^0 = \Pi_a W^0 \Pi_a = \frac{1}{2}\begin{bmatrix} I+Q & U+iV \\ U-iV & I-Q \end{bmatrix} dq\, dp. \tag{9}$$

The parameters I, Q, U, V in Eq. 9 are the Stokes parameters for polarized light. This provides much physical intuition for the projected limit Wigner distribution W_a^0. From Eq. 7 one obtains for the time evolution of W_a^0 that [16]

$$\dot{W}_a^0 = \Pi_a \left\{W_a^0, \lambda_a\right\} \Pi_a + \left[W_a^0, \Pi_a m^1 \Pi_a\right] = \left\{W_a^0, \lambda_a\right\} + \left[W_a^0, F_a^0\right] \tag{10}$$

where $F_a^0 = [\Pi_a, \{\lambda_a, \Pi_a\}] + \Pi_a m^1 \Pi_a$ and, as before, m^1 is the first order term in the formal expansion of the symbol m^ε in the order parameter ε. Intuitively, the "Poisson bracket" $\left\{W_a^0, \lambda_a\right\}$ describes the transport of the polarized radiation W_a^0 on phase space while the commutator $\left[W_a^0, F_a^0\right]$ is responsible for the change in polarization during transport, we will again come back to this in Sec. 4. Classical radiative transfer is a scalar theory and does not consider polarization. For unpolarized light the Stokes parameters satisfy $Q, U, V = 0$. The matrix density W_a^0 is then completely described by its trace, representing the intensity I of the radiation. We thus define the *light energy density* as

$$\ell = \operatorname{tr}(W_i^0) = \mathscr{L}(q, p)\, dq\, dp \in \operatorname{Den}(T^*Q). \tag{11}$$

It follows from Eq. 10 that the transport of $\ell \in \operatorname{Den}(T^*Q)$ is described by

$$\dot{\ell} = -\{\ell, H\} \tag{12}$$

[4]The matrix-valued "Poisson bracket" is computed by performing matrix multiplication with scalar multiplication replaced by the usual Poisson bracket, see for example [50, Appendix A].

with the Hamiltonian $H \in \mathscr{F}(T^*Q)$ being the eigenvalue λ_a, that is

$$H(q,p) = \pm \frac{c}{n(q)} \|p\|. \tag{13}$$

The light energy density $\ell \in \mathrm{Den}(T^*Q)$ is related to the limit electromagnetic energy density $\mathscr{E}(q) \in \mathrm{Den}(Q)$ by the fiber integral

$$\lim_{\varepsilon \to 0} \mathscr{E}^{\varepsilon}(q,t) = \int_{T_q^*Q} \ell = \int_{T_q^*Q} \mathscr{L}(q,p,t)\, dp \tag{14}$$

and $\ell \in \mathrm{Den}(T^*Q)$ can be understood as an angularly resolved form of the electromagnetic energy density. Hence, the light energy density $\ell \in \mathrm{Den}(T^*Q)$ together with Eq. 12 provide the sought after system to describe the transport of the limit energy density $\mathscr{E}^0(q,t)$. Eq. 12 describes the transport of electromagnetic energy in macroscopic environments to good approximation, as is evidenced by the success of radiative transfer in a wide range of fields.

2.2 Cosphere Bundle Reduction for Radiative Transfer

Eq. 12 describes radiative transfer theory as a Hamiltonian system on 6-dimensional phase space $T^*Q \cong \mathbb{R}^3 \times Q$. In the literature, however, the theory is usually defined over the 5-dimensional space of "positions and directions". The two descriptions are related through the symmetry associated with the well known conservation of frequency during transport. The Hamiltonian in Eq. 13 is homogeneous of degree one in the momentum, $H(q, \alpha p) = \alpha H(q,p)$, for $\alpha \in \mathbb{R}^+$, and, moreover, momentum and light frequency are proportional. This suggests that the symmetry group associated with the conservation of frequency is $(\mathbb{R}^+, \cdot)$ acting on the fibers T_q^*Q by $m_\alpha(q,p) = (q, \alpha\, p)$. As is well known [2, Appendix 4], the quotient space for this action is given by the cosphere bundle

$$S^*Q = \left(T^*Q \setminus \{0\}\right)/\mathbb{R}^+ \tag{15}$$

and for a Hamiltonian of degree one dynamics on T^*Q drop to a contact Hamiltonian flow along the Reeb vector field on S^*Q [39]. The cosphere bundle S^*Q, identified with the sphere bundle S^2Q using the standard metric in $\mathbb{R}^3$, provides a modern interpretation for the classical space of "positions and directions", and the homogeneity of the Hamiltonian explains why such a description on S^*Q is possible, despite the Hamiltonian character of the system that seemingly requires a description on an even dimensional space.

2.3 *Radiative Transfer as a Lie-Poisson System*

A central result in classical radiative transfer theory is the "conservation of radiance along a ray" [18]. The symmetry associated with this conservation law becomes apparent when the light energy density ℓ_t at time t, globally over all T^*Q, is considered as one configuration of the system. Time evolution can then be described by the pullback $\ell_t = \eta_t^* \ell_0$ along the map $\eta_t : T^*Q \to T^*Q$ that is generated by the flow of the Hamiltonian vector field X_H defined by Eq. 13, and when X_H is defined globally the set of all such maps η_t forms the infinite dimensional Lie group $\mathrm{Diff}_{\mathrm{can}}(T^*Q)$ of canonical transformations [11]. With respect to the initial light energy density ℓ_0 all physically valid configurations ℓ_t can then be described by an element η_t in $\mathrm{Diff}_{\mathrm{can}}(T^*Q)$ and the group becomes the configuration space of radiative transfer. We thus have that radiative transfer is a Lie-Poisson system for $\mathrm{Diff}_{\mathrm{can}}(T^*Q)$, cf. Fig. 3.

The Lie-Poisson structure for the group $\mathrm{Diff}_{\mathrm{can}}(T^*Q)$ was first studied by Marsden and coworkers in the context of plasma physics [30]. The Lie algebra $\mathfrak{g}$ of $\mathrm{Diff}_{\mathrm{can}}(T^*Q)$ are infinitesimal canonical transformations, that is $\mathfrak{g} \cong \mathfrak{X}_{\mathrm{Ham}}(T^*Q)$, and by identifying the Hamiltonian vector fields with the generating Hamiltonian functions, $\mathfrak{g} \cong \mathscr{F}(T^*Q)$, the dual Lie algebra $\mathfrak{g}^*$ becomes $\mathrm{Den}(T^*Q)$.[5] With $\mathfrak{g}^* \cong \mathrm{Den}(T^*Q)$, it is natural to consider the light energy density ℓ as an element in $\mathfrak{g}^*$. The time evolution of ℓ is then described by coadjoint action $\mathrm{Diff}_{\mathrm{can}}(T^*Q) \times \mathfrak{g}_+^* \to \mathfrak{g}_+^*$ in the Eulerian representation and infinitesimally this is given by [24, Sec. 3.3]

$$\dot{\ell} = \mathrm{ad}^*_{\frac{\delta \mathscr{H}}{\delta \ell}} \ell = \mathrm{ad}^*_H \ell = -\{\ell, H\}; \tag{16}$$

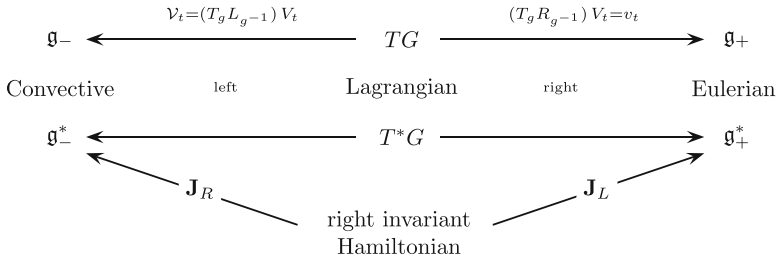

Fig. 3 The structure of Lie-Poisson systems. Classical examples of such systems are the rigid body, where the Lie group is SO(3) with a *left* invariant Hamiltonian, and the ideal Euler fluid, where the Lie-group is the group $\mathrm{Diff}_\mu(Q)$ of volume preserving diffeomorphisms with a *right* invariant Hamiltonian [1, 11]

[5] We disregard here some technical details in the construction of the dual Lie algebra. See for example [24, Chapter 2.3.5.3].

Table 1 Correspondence between ideal fluid dynamics and ideal radiative transfer. The fluid velocity is denoted by $v \in \mathfrak{X}_{\text{div}}(Q)$ and $\omega \in \Omega^2(Q)$ is the fluid vorticity

	Fluid dynamics	Radiative transfer
Lie group	$\text{Diff}_\mu(Q)$	$\text{Diff}_{\text{can}}(T^*Q)$
Lie algebra	$\mathfrak{X}_{\text{div}}(Q)$	$\mathfrak{X}_{\text{Ham}}(T^*Q)$
Dual Lie algebra	$\omega \in \Omega^2(Q)$	$\ell \in \text{Den}(T^*Q)$
Coadjoint action	$\dot{\omega} = -\pounds_v \omega$	$\dot{\ell} = -\pounds_{X_H} \ell$
Classical conservation law	Kelvin's theorem	Conservation of radiance

indeed, that the Poisson bracket describes infinitesimal coadjoint action $\text{ad}^* : \mathfrak{g} \times \mathfrak{g}^* \to \mathfrak{g}^*$ for $\text{Diff}_{\text{can}}(T^*Q)$ is an a posterior justification for considering the group as the configuration space for ideal radiative transfer [30, Sec. 6]. In Eq. 16, $\mathscr{H} \equiv \mathscr{H}[\ell]$ is the field Hamiltonian

$$\mathscr{H}[\ell] = \int_{T^*Q} \ell(q, p)\, H(q, p)\, dq\, dp \tag{17}$$

which is the density weighted integral of the "single particle" Hamiltonian $H(q, p)$ in Eq. 13. With the light energy density as an element in the dual Lie algebra, it follows immediately from the general theory of Lie-Poisson systems that the momentum map $\mathbf{J}_R$ is the convective light energy density and that this quantity is conserved [29, Theorem 11.4.1], cf. Fig. 3.[6] By the change of variables theorem, this can be interpreted as conservation of light energy density along trajectories in phase space and it provides a modern formulation and justification for "conservation of radiance along a ray" in the classical literature. Interestingly, with the Lie-Poisson structure a close formal analogy between ideal radiative transfer and ideal fluid dynamics exists, cf. Table 1.

Next to the transport on T^*Q, the time evolution of radiative transfer can also be understood as a functional analytic flow on the space of light energy densities. By identifying the Hamiltonian vector field X_H with an anti-self-adjoint operator, Stone's theorem [28, Theorem 6.2.18.3] enables us to describe radiative transfer as

$$\ell_t = \eta_t^* \ell_0 = U_t\, \ell_0 \tag{18}$$

where U_t is a unitary operator. Such a functional analytic representation of the action of an infinite dimensional diffeomorphism group is often referred to as Koopmanism [21], cf. also [32, Chapter 8.4]. An interesting aspect of Eq. 18 is that it provides a rigorous basis for the operator formulation of radiative transfer that can be found in the classical literature, see for example [10]. Eq. 18 also provides a natural starting point to include scattering effects, for example at surfaces, that do not have a geometric but a well known functional analytic description.

[6] A direct proof can be found in [24, Chapter 3.3].

3 Some Connections to the Classical Formulations

In this section, we will relate our geometric formulation of radiative transfer to classical radiometry and geometrical optics.

3.1 Classical Radiometry

To relate the phase space light energy density $\ell \in \mathrm{Den}(T^*Q)$ to radiance, the central quantity in the classical formulation of radiative transfer, we have to consider measurements, the question Lambert was studying when he introduced the concept [22]. Measurements determine the flux of light energy density, for example through the sensor of a camera. Mathematically, this flux can be determined using the transport theorem of tensor calculus [32, Theorem 8.1.12]. One then obtains that the energy E flowing through a 2-dimensional surface M in a time interval $[t_1, t_2]$ is given by

$$E = \int_{t_1}^{t_2} \int_{T^-M} i_{X_H} \ell = \int_{t_1}^{t_2} \int_M \frac{c}{n(q)} \int_{T_q^- M} \mathscr{L}(q, p)\, (\bar{p} \cdot \mathbf{n}(q))\, dA\, d\bar{p}\, dt \tag{19}$$

where $\bar{p}$ is a unit vector, $\mathbf{n}(q)$ the surface normal of M at q, and $T_q^- M$ the positive half-space of $T_q^* Q$ as defined by $\mathbf{n}(q)$ [24, Chapter 3.2.6]. When the light energy density is parameterized in spherical coordinates, an infinitesimal measurement can be written as

$$\mathscr{L}(q, \bar{p}, \nu)\, (\bar{p} \cdot \mathbf{n})\, dA\, d\bar{p} = \mathbf{n} \cdot (\mathscr{L}(q, \bar{p}, \nu)\, \bar{p}\, dA\, d\bar{p}\, d\nu) \tag{20}$$

and when no measurement surface, and hence no normal $\mathbf{n}$, is fixed one thus has for an infinitesimal measurement that

$$\Lambda = \mathscr{L}(q, \bar{p}, \nu)\, dA_\perp\, d\bar{p}\, d\nu \tag{21}$$

where $dA_\perp(\bar{p}) = \bar{p}\, dA$ is the standard area form for a surface orthogonal to the flow direction $\bar{p}$. The differential 2-form $\Lambda \in \Omega^2(Q)$ provides a modern interpretation of classical radiance. The cosine term $(p \cdot \mathbf{n})$, which is prevalent in the classical literature but usually only justified heuristically [36], can then be obtained rigorously through the pullback of Λ onto a surface with normal $\mathbf{n}$. We refer to [24] for the derivation of other concepts of classical radiometry such as vector irradiance.

Remark 1. In the past, it has often been overlooked that radiance is meaningful only in the context of measurements while the quantity that genuinely is transported in radiative transfer is the phase space light energy density $\ell \in \mathrm{Den}(T^*Q)$. This has led to considerable confusion even in recent literature [3].

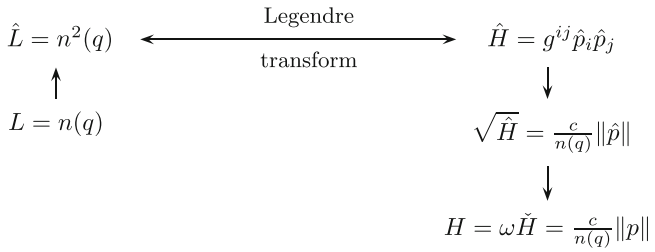

Fig. 4 Non-canonical Legendre transform relating radiative transfer to geometrical optics given by Fermat's principle

3.2 Radiative Transfer and Geometrical Optics

A question rarely considered in the classical literature on radiative transfer is the relationship of the theory to geometrical optics. The connection can be established by considering the Legendre transform of Fermat's principle. As is well known, directly performing the transform for the Lagrangian $L = n(q)$ leads to a vanishing Hamiltonian [20]. Following Arnold [2],[7] instead of length, given by $L = n(q)$, we shall hence consider the geometrical energy of a light path, given by $\hat{L} = n^2(q)$. This Lagrangian can be interpreted as corresponding to a diagonal metric $g_{ij} = n^2(q)/c^2\,\delta_{ij}$ and the associated geodesic flow is equivalently described by the Hamiltonian $\hat{H} = g^{ij}\,\hat{p}_i\,\hat{p}_j$ [19, p. 51] where $\hat{p}$ is the canonical momentum which is related to the kinetic momentum by $p = \omega\,\hat{p}$. Reverting the transition from path length to path energy, and including the factor of ω corresponding to energy we obtain for the Hamiltonian again Eq. 13. If we trace the diagram in Fig. 4 backwards, we see that, from the point of view of radiative transfer, geometrical optics is a limiting case when the amount of energy that is transported is disregarded.

4 Discussion and Open Questions

Our geometric formulation of radiative transfer and the identification of the Lie group structures that underlie the known conservation laws clarifies and unifies earlier work in the literature. Additionally, the use of tensor calculus overcomes the limitations of the current formulation, for example when measurements are considered, and it improves over earlier attempts that employed vector calculus [17] and measure theory [38] to obtain a modern mathematical foundation for radiative transfer.[8] The derivation of radiative transfer from electromagnetic theory that was presented in Sec. 2 largely follows recent work in applied mathematics [16, 41],

[7] We were told this idea goes back at least to Riemann.

[8] The status and shortcomings of many classical derivations of radiative transfer theory were recently summarized by Mishchenko [33].

which can be seen as a refinement of earlier but little known results in plasma physics.[9] Our presentation emphasized geometric aspects of the argument and it completed the connection to the classical formulations in the literature [3, 16, 41]. Nonetheless, the structures that underlie many aspects of the derivation remain currently unclear. In the following, we will collect some preliminary results on how to fill these gaps.

Additional insight into the derivation in Sec. 2 can be obtained by considering a density matrix formulation of electromagnetic theory before the phase space lift. In quantum mechanics, the density matrix for a pure state ψ is defined by $\rho = \psi\rangle\langle\psi$ and it represents the projection operator onto the one dimensional subspace spanned by ψ.[10] One of the advantages of this formulation is that it provides a faithful representation of the projective Hilbert space $\mathbb{CP}^n$ that serves as the configuration space of quantum mechanics, cf. [29, Chapter 5.4.3].[11] The density matrix for the electromagnetic field is known as the mutual coherence matrix [27, 54] and there typically defined as[12]

$$P_{ij}(q,t,\bar{q},\bar{t}) = F_i(q,t)\, F_j^*(\bar{q},\bar{t}). \tag{22}$$

Analogous to the situation in quantum mechanics, the trace $\mathrm{tr}(P)$ of the density matrix, for $(q,t) = (\bar{q},t)$, is proportional to the quadratic observable, the electromagnetic energy density $\mathscr{E}(q,t)$ [40]. Neither Eq. 22 nor the trace have an apparent geometric interpretation. However, we know from Eq. 3 that the energy density is given by $\mathscr{E} = \|\mathbf{F}\|^2_{\varepsilon,\mu}$. Using the Faraday 2-form $F = E \wedge dt + B$ this can be written as

$$\mathscr{E}(q,t) = \langle\langle F, F\rangle\rangle_{\varepsilon,\mu} = F \wedge \star_{\varepsilon,\mu} F \tag{23}$$

where $\star_{\varepsilon,\mu}$ is the Hodge dual induced by considering the electric permittivity and magnetic permeability as part of the metric. By definition of the wedge product, this is equivalent to

$$\mathscr{E}(q,t) = \mathrm{A}(F \otimes \star_{\varepsilon,\mu} F) \tag{24}$$

[9] See [37] and references therein and [53]. In theoretical optics, various alternative names are employed for the Wigner transform, cf. [4].

[10] The density matrix was introduced in a famous paper by von Neumann [35] to study statistical ensembles of states, an aspect we will not consider here but which is closely related to the questions considered in statistical optics, cf. [27].

[11] This representation of $\mathbb{CP}^n$ is the prototypical example of a C^*- or von Neumann algebra.

[12] In the statistical optics literature one typically considers statistical averages of the field components, which we omit here. This is the analogue of the probabilistic superposition of pure states in quantum mechanics.

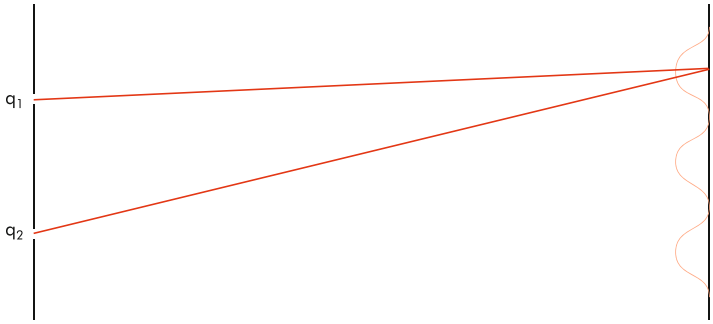

Fig. 5 Young's experiment: coherent electromagnetic radiation passes through the double slit formed by q_1 and q_2 and through interference forms the intensity pattern on the screen on the right

where A is the anti-symmetrization map [32, Defnition 7.1.3]. As can be shown by a straightforward computation, the anti-symmetrization in Eq. 24 is, in flat spacetime, equivalent to taking the trace of $\mathbf{F} \otimes \mathbf{F}$. We hence indeed have

$$\mathscr{E}(q,t) = \mathrm{A}(F \otimes \star_{\varepsilon,\mu} F) = \mathrm{tr}\,(\mathbf{F} \otimes \mathbf{F}). \tag{25}$$

It appears that $F \otimes \star_{\varepsilon,\mu} F$ provides a mathematically and physically more natural definition of the density matrix. The non-locality in the definition in Eq. 22 can be understood by considering interference phenomena such as those arising in the classical Young's interference experiment, cf. Fig. 5. There, interference arises from the superposition of the fields at the pinholes, and the interference fringes, and hence the intensity of the electromagnetic field, can be described through the nonlocal coherence matrix $P(q,t,\bar{q},t)$, see [54]. It needs to be studied if this idea can be made rigorous by considering the time dependence for F in Eq. 25 and exploiting that $F_t = U_t F_0$ where U_t is a unitary operator.

As in the case of the Schrödinger equation, differentiating the definition of the local density matrix with respect to time using the Leibniz rule and inserting Eq. 2 in the resulting expression yields $\dot{P} = -[P, M]$ where $[,]$ denotes the matrix commutator. As is well known [13, 55], under the semiclassical symbol calculus the commutator becomes the Moyal bracket on phase space, and, at least formally, it can be shown that the Wigner transform is the symbol of the density operator. Using the density matrix and its time evolution equation provides thus a more natural transition from Maxwell's equations on configuration space to Moyal bracket dynamics on phase space.

For the Schrödinger equation, the model problem in semiclassical analysis, the representation theory of the Heisenberg group plays a central role, as is evident from the Stone-von Neumann theorem, which, roughly speaking, states that all formulations of quantum mechanics are essentially unitarily equivalent. From the point of view of the Heisenberg group, the short wavelength limit is the group

contraction that yields the symplectic group. A question of interest to us is to understand which role the Heisenberg group plays for the asymptotic limit discussed in this paper. Interesting work in this context is for example those by Landsman [23] who discusses connections between Lie-Poisson reduction and quantization using the Heisenberg group.

Quite curious in the derivation in Sec. 2 are the matrix-valued "Moyal" and "Poisson" brackets that arise for example in Eq. 7 and Eq. 10. These brackets are known in the physics literature, e.g. [46, Chapter 16.3] [50, Appendix A], and they also appear in the microlocal and semiclassical analysis literature, cf. [16]. However, to our knowledge they have not been studied from a geometric point of view. One approach to generalize the Poisson bracket to the matrix-valued case is to consider

$$\dot{f} = -\{f, H\} = -\pounds_{X_H} f \tag{26}$$

in which case the right hand side has a natural extension for arbitrary tensors. For a matrix A, that is a $(1, 1)$ tensor, one then obtains

$$\dot{A} = -\pounds_{X_H} A = -\{A, H\} + [A, \bar{H}] \tag{27}$$

where the "Poisson bracket" for the matrix A is defined as before, as a component wise bracket, and $\bar{H}$ is the Hessian "matrix" of the Hamiltonian, that is the matrix of second partial derivatives. Eq. 27 has the same form as Eq. 10 although it is currently not clear to us under which conditions $\bar{H}$ coincides with the first order term m^1 of the symbol. For the situation where also the generator of the dynamics is matrix-valued, the connection between the symbol of an operator and the dispersion matrix, which is well understood from a physical point of view, seems to play a key role, cf. [41]. Preliminary work in the literature that considers matrix-valued quantization from a geometric perspective is [8, 12, 25], although to our knowledge no complete picture exists at the moment.

An interesting open question is also the transition from Maxwell's equations to radiative transfer in spacetime, the natural setting of electromagnetic theory. Although no general theory of covariant Poisson brackets in spacetime exists, for the special case of Maxwell's equations a bracket is known [31]. Moreover, the Faraday 2-form plays from the outset an important role in our derivation and semiclassical analysis naturally considers spacetime operators, cf. [55]. A derivation in this setting might also help to understand how the structure of electromagnetic theory manifests itself at the short wavelength limit and how the symmetries of radiative transfer theory arise.

Despite many connections, microlocal and semiclassical analysis are currently rarely considered in geometric mechanics. We believe this is an area ripe for further investigations. For example, in many situations microlocal analysis also allows the description of a Hamiltonian system on phase space T^*Q through an equivalent partial differential equation on configuration space Q. We believe that this provides additional insight into the plasma-to-fluid map [30] and might allow to generalize the result. It would also be interesting to explore how existing results, for example

for the Maxwell-Vlasov system [30] or Euler-Yang-Mills fluids, cf. [14], can be reformulated when electromagnetic theory is describes on phase space.

Although the Hamiltonian formulation of radiative transfer has been known in plasma physics for a long time [37], it has so far not been appreciated in other communities. We belief that the 5-dimensional formulation of radiative transfer that is prevalent in the literature, and which is incompatible with a Hamiltonian description that necessitates an even dimensional phase space, led to much confusion on the subject. Our reduction of the 6-dimensional Hamiltonian system to a contact Hamiltonian system on the cosphere bundle S^*Q clarifies this relationship. The Lie-Poisson structure of radiative transfer mirrors those of other systems in statistical mechanics whose time evolution is describes by the Vlasov equation [30], [51]. Nonetheless, since radiative transfer is rarely written in the form of Eq. 12 it was surprising to us that the classical law of conservation of radiance arises from a Lie-Poisson structure. Similarly, the structural similarities between ideal fluid dynamics and ideal light transport in Table 1 seem, from the point of view of the classical literature, quite remarkable.

5 Conclusion

This work owes much to Jerry Marsden, to his encouragement, and to his writings. Jerry told us that if there is a geometric formulation of radiative transfer then it is worth developing it. We always reminded ourselves of this when nothing seemed to fit together. Jerry's writings also repeatedly provided us a life line and they made geometric mechanics accessible to us.

Acknowledgements We thank Eugene Fiume, Mathieu Desbrun, Tudor Ratiu, Boris Khesin, and Jerry Marsden for discussions. C.L acknowledges support by the National Science and Engineering Council of Canada, as well as MITACS and GRAND National Centres of Excellence. C.L. was also supported by NSF grant CCF-1011944. A.C. thanks the University of Toronto and the Fields Institute for their hospitality and a postdoctoral fellowship during which this work was initiated.

References

1. Arnold, V.I.: Sur la géométrie différentielle des groupes de Lie de dimension infinie et ses applications à l'hydrodynamique des fluides parfaits. Annales de l'institut Fourier **16**, 319–361 (1966)
2. Arnold, V.I.: Mathematical Methods of Classical Mechanics. Graduate Texts in Mathematics, 2nd edn. Springer, New York (1989)
3. Bal, G.: Radiative transfer equations with varying refractive index: a mathematical perspective. J. Opt. Soc. Am. A **23**(7), 1639 (2006)
4. Bastiaans, M.J.: Application of the Wigner distribution function to partially coherent light. J. Opt. Soc. Am. A **3**(8), 1227 (1986)

5. Born, M., Wolf, E.: Principles of Optics: Electromagnetic Theory of Propagation, Interference and Diffraction of Light, 6th edn. Cambridge University Press, Cambridge (1985)
6. Bouguer, P.: Essai d'optique sur la gradation de la lumiere. Claude Jombert, Paris (1729)
7. Bouguer, P.: Traité d'Optique sur la gradation de la lumière. Translated by W. E. K. Middleton. H. L. Guerin et L. F. Delatour, Paris (1760)
8. Bursztyn, H., Waldmann, S.: Deformation quantization of hermitian vector bundles. Lett. Math. Phys. **53**(4), 349–365 (2000)
9. Chwolson, O.D.: Grundzüge einer mathematischen Theorie der inneren Diffusion des Lichtes. Bull. l'Acad. Imperiale Sci. St. Pétersbourg **33**, 221–256 (1889)
10. Duderstadt, J.J., Martin, W.R.: Transport Theory. Wiley, New York (1979)
11. Ebin, D.G., Marsden, J.E.: Groups of diffeomorphisms and the motion of an incompressible fluid. Ann. Math. **92**(1), 102–163 (1970)
12. Emmrich, C., Weinstein, A.: Geometry of the transport equation in multicomponent WKB approximations. Commun. Math. Phys. **176**(3), 701–711 (1996)
13. Evans, L.C., Zworski, M.: Semiclassical Analysis. Lecture Notes. University of California, Berkeley, CA (2011)
14. Gay-Balmaz, F., Ratiu, T.S.: Reduced Lagrangian and Hamiltonian formulations of Euler-Yang-Mills fluids. EN. J. Symplectic Geom. **6**(2), 189–237 (2008)
15. Gérard, P.: Microlocal defect measures. Commun. Partial Differ. Equat. **16**(11), 1761–1794 (1991)
16. Gérard, P., Markowich, P.A., Mauser, N.J., Poupaud, F.: Homogenization limits and wigner transforms. Commun. Pure Appl. Math. **50**(4), 323–379 (1997)
17. Gershun, A.: The Light Field. Translated by P. Moon, G. Timoshenko, and (Originally published in Russian (Moscow, 1936)). J. Math. Phys. **18**, 51–151 (1939)
18. Goodman, D.S.: General principles of geometrical optics. In: Bass, M. (ed.) Handbook of Optics, 3rd edn., pp. 1.3–1.92, Chap. 1. McGraw-Hill Companies (2010)
19. Jost, J.: Riemannian Geometry and Geometric Analysis. Universitext. Springer, New York (2008)
20. Kline, M., Kay, I.W.: Electromagnetic Theory and Geometrical Optics. Wiley, New York (1965)
21. Koopman, B.O.: Hamiltonian systems and transformations in hilbert space. Proc. Natl. Acad. Sci. **17**(5), 315–318 (1931)
22. Lambert, J.H., DiLaura, D.L.: Photometry or on the Measure and Gradation of Light, Colors, and Shade. Illuminating Engineering Society of North America, New York City (2001)
23. Landsman, N.P.: Mathematical Topics Between Classical and Quantum Mechanics. Springer Monographs in Mathematics. Springer, New York (1998)
24. Lessig, C.: Modern foundations of light transport simulation. Ph.D. thesis. University of Toronto, Toronto (2012)
25. Littlejohn, R., Flynn, W.: Geometric phases in the asymptotic theory of coupled wave equations. Phys. Rev. A **44**(8), 5239–5256 (1991)
26. Lommel, E.: Die Photometrie der diffusen Zurückwerfung. Ann. Phys. **272**(2), 473–502 (1889)
27. Mandel, L., Wolf, E.: Optical Coherence and Quantum Optics. Cambridge University Press, Cambridge, UK (1995)
28. Marsden, J.E., Hughes, T.J.R.: Mathematical Foundations of Elasticity. Dover Publications, New York (1983)
29. Marsden, J.E., Ratiu, T.S.: Introduction to Mechanics and Symmetry: A Basic Exposition of Classical Mechanical Systems. Texts in Applied Mathematics, 3rd edn. Springer, New York, 2009 (1999) [updated and revised, online]
30. Marsden, J.E., Weinstein, A., Ratiu, T.S., Schmid, R., Spencer, R. G.: Hamiltonian systems with symmetry coadjoint orbits and plasma physics. Atti Acad. Sci. Torino Cl. Sci. Fis. Math. Natur. **117**, 289–340 (1983)
31. Marsden, J.E., Montgomery, R., Morrison, P.J., Thompson, W.B.: Covariant poisson brackets for classical fields. Ann. Phys. **169**, 29–47 (1986)

32. Marsden, J.E., Ratiu, T.S., Abraham, R.: Manifolds, Tensor Analysis, and Applications. Applied Mathematical Sciences, 3rd edn. Springer, New York (2004)
33. Mishchenko, M.I.: Directional radiometry and radiative transfer: A new paradigm. J. Quant. Spectros. Radiat. Transf. **112**(13), 2079–2094 (2011)
34. Misner, C.W., Thorne, K.S., Wheeler, J.A.: Gravitation. W. H. Freeman, San Francisco (1973)
35. Neumann, J.V.: Wahrscheinlichkeitstheoretischer Aufbau der Quantenmechanik. Nachr. Kgl. Ges. d. Wiss. zu Gött. Math. Phys. Klasse, 245–272 (1927). https://eudml.org/doc/59230
36. Nicodemus, F.E.: Radiance. Am. J. Phys. **31**, 368–377 (1963)
37. Pomraning, G.C.: The Equations of Radiation Hydrodynamics. International Series of Monographs in Natural Philosophy. Pergamon Press, New York (1973)
38. Preisendorfer, R.W.: Radiative Transfer on Discrete Spaces. Pergamon Press, New York (1965)
39. Ratiu, T.S., Schmid, R.: The differentiable structure of three remarkable diffeomorphism groups. Math. Z. **177**(1), 81–100 (1981)
40. Roychowdhury, H., Wolf, E.: Determination of the electric cross-spectral density matrix of a random electromagnetic beam. Opt. Commun. **226**(1–6), 57–60 (2003)
41. Ryzhik, L., Papanicolaou, G., Keller, J.B.: Transport equations for elastic and other waves in random media. Wave Motion **24**(4), 43 (1996)
42. Schuster, A.: Radiation through a foggy atmosphere. Astrophys. J. **21**, 1–22 (1905)
43. Schwarzschild, K.: Über das Gleichgewicht der Sonnenatmosphäre. Nachr. Kgl. Ges. d. Wiss. zu Gött. Math. Phys. Klasse **195**, 41–53 (1906)
44. Sommerfeld, A., Runge, J.: Anwendung der Vektorrechnung auf die Grundlagen der geometrischen Optik. Ann. Phys. **340**(7), 277–298 (1911)
45. Sparber, C., Markowich, P.A., Mauser, N.J.: Wigner functions versus WKB-methods in multivalued geometrical optics. Asymptot. Anal. **33**(2), 153–187 (2003)
46. Spohn, H.: Dynamics of Charged Particles and Their Radiation Field. Cambridge University Press, Cambridge (2004)
47. Tartar, L.: H-measures, a new approach for studying homogenization, oscillations and concentration effects in partial differential equations. Proc. R. Soc. Edinb. **115A**, 193–230 (1990)
48. Tartar, L.: H-measures and applications. In: International Congress of Mathematics, pp. 1215–1223. Springer, Kyoto (1990)
49. Tartar, L.: The General Theory of Homogenization: A Personalized Introduction. Lecture notes of the Unione Matematica Italiana. Springer, New York (2010)
50. S. Teufel, S.: Adiabatic Perturbation Theory in Quantum Dynamics. Lecture Notes in Mathematics. Springer, New York (2003)
51. Tronci, C.: Geometric dynamics of Vlasov kinetic theory and its moments. Ph.D. thesis. Imperial College London (2008)
52. Wigner, E.: On the quantum correction for thermodynamic equilibrium. Phys. Rev. **40**(5), 749–759 (1932)
53. Wolf, E.: New theory of radiative energy transfer in free electromagnetic fields. Phys. Rev. D **13**, 869–886 (1976)
54. Wolf, E.: Introduction to the Theory of Coherence and Polarization of Light. Cambridge University Press, Cambridge (2007)
55. Wunsch, J.: Microlocal Analysis and Evolution Equations. Lecture Notes from 2008 CMI/ETH Summer School on Evolution Equations (2008). arXiv:0812.3181

A Soothing Invisible Hand: Moderation Potentials in Optimal Control

Debra Lewis

Abstract A moderation incentive is a continuously differentiable control-dependent cost term that is identically zero on the boundary of the admissible control region, and is subtracted from the 'do or die' cost function to reward sub-maximal control utilization in optimal control systems. A moderation potential is a function on the cotangent bundle of the state space determining Hamiltonian boundary value problems with solutions satisfying the control-parametrized Hamiltonian dynamics determined by an associated moderation incentive in accordance with Pontryagin's Maximum Principle. A multi-parameter family of moderation incentives for control-affine systems with quadratic control constraints possesses simple, readily calculated moderation potentials. An elementary planar projectile problem with controlled velocity illustrates the influence of the moderation incentive on the optimal trajectory.

1 Introduction

When modeling a conscious agent, the constant cost function of a traditional time minimization problem can be interpreted as representing a uniform stress or risk throughout the task, while more general cost functions model varying stresses and risks that depend on the current state and control values. Implementation of agent limitations via cost terms may be more natural—particularly for biological systems—than a possible/impossible dichotomy, in which constraints are explicitly incorporated in the state space. For example, consider the classic 'falling cat' problem, in which a cat is suspended upside down and then released. (See, e.g., [7, 12, 14].) Marey [12] gave a qualitative description of the self-righting maneuver, supported by high-speed photographs: the cat rotates the front and back halves of its body, altering the positions of its head and limbs to adjust its moments of inertia, causing the narrowed half to rotate significantly faster than the thickened half, with zero net angular velocity. Kane and Scher [7] introduced a simple mathematical model of a cat, consisting of a pair of coupled rigid bodies, and showed that

D. Lewis (✉)
Mathematics Department, University of California, Santa Cruz, Santa Cruz, CA 95064, USA
e-mail: lewis@ucsc.edu

D.E. Chang et al. (eds.), *Geometry, Mechanics, and Dynamics*, Fields Institute Communications 73, DOI 10.1007/978-1-4939-2441-7_12

self-righting with zero angular momentum is possible without alteration of the moments of inertia of the two halves of the body. To rule out the mechanically efficient but fatal solution in which the front and back halves simply counter-rotate, resulting in a 360° twist in the 'cat', Kane and Scher imposed a no-twist condition in their model. The resulting dynamical system has a natural and elegant formulation as an optimal control system [14]. However, actual cats can and do significantly twist their bodies, and splay or tuck their limbs; the images in [7] generated using the mathematical model and superposed on photographs of an actual cat significantly underestimate the relative motion between the front and back halves of the body.[1] Replacing the no-twist condition with a deformation-dependent term in the cost function that discourages excessively large relative motions allows more realistic motions.

The optimal control values for a purely state-dependent cost function lie on the boundary, if any, of the admissible control regions. In some situations, the optimization problem can be restricted to the boundary of the admissible region and solved using geometric optimization and integration methods (see, e.g., [8, 10, 11, 19]). If geometric methods are not available or desirable, penalty functions can be used to construct algorithms on an ambient vector space that respect the boundary due to the prohibitive (possibly infinite) expense of crossing the boundary; see, e.g., [3, 5], and references therein. For some state- and control-dependent cost functions, trajectories approaching the boundary of the admissible control region are so extravagant that the boundary can safely be left out of the mathematical model. However, a close approach to the boundary of the admissible region may be appropriate when making the best of a bad situation. Consider again the situation of the dropped cat: the cat is presumably eager to change its orientation before striking the ground—a typical cat can right itself when dropped from heights of approximately 1 m. Selection of an appropriate cost function is essential; a very high price for near-maximal control values may yield excessively leisurely solutions, while very low costs may result in near-crisis responses in almost all situations. Modeling a system using a family of cost functions parametrized by moderation or urgency can reveal qualitative features of optimal solutions that are not readily seen using a single cost function.

In time minimization problems, the time required to complete the maneuver is obviously *not* specified a priori. In more general situations, in which the cost function is a non-constant function of state and/or control values, the duration is still allowed to vary unless specified as fixed.[2] When applying Pontryagin's Maximum Principle, a necessary condition for optimality is that either the Hamiltonian equal

[1] It should be noted that the ultimate goal of Kane and Scher's investigation was the development of maneuvers that would allow astronauts to alter their orientation without grasping fixed objects while in zero gravity [6]. The no-twist condition is very reasonable for a spacesuit-clad human—the collarbone (not present in cats or many other quadrupeds) limits rotation of the shoulders relative to the hips, facilitating bipedal motion, and the bulky suit further limits bending and twisting.

[2] Problems in which the duration is to be determined are given pride of place in Pontryagin et al. [16]: "Let us note that (for fixed x_0 and x_1) the upper and lower limits, t_0 and $t_1 \ldots$ are not fixed numbers, but depend on the choice of control $u(t)$ which transfers the phase point from x_0 to x_1

zero or the control lie on the admissible control region boundary, unless the time for execution of the task is fixed [16]. Shifting the Hamiltonian by a constant leaves the evolution equations unchanged, but can significantly influence the optimal trajectories via the initial conditions; hence careful selection of the constant term in a non-constant cost function is crucial in the analysis of optimal control problems. In [9] we considered cost functions combining a purely state-dependent term modeling a do-or-die, 'whatever it takes' approach and a control- (and possibly state-) dependent term equaling zero on the boundary of the admissible control region; the resulting decreased cost on the interior of the control region resulting from the control-dependent term can be interpreted as an incentive rewarding sub-maximal control efforts. We introduced two families of control cost terms. One family was modeled on a quadratic control cost (see, e.g., [2, 4, 13], and references therein), shifted so as to equal zero on the boundaries of the admissible regions; the other, the elliptical moderation incentives, yields optimal controls that can be constructed using a combination of lifts and projections (see Figure 4 and the remark at the end of Section 3).

Optimal control on nonlinear manifolds has received significant attention in recent years, particularly situations in which the controls can be modeled as elements of a distribution within the tangent bundle of the state manifold, corresponding to (partially) controlled velocities. See, e.g. [4, 15, 17, 18], and references therein. Pontryagin's Maximum Principle on manifolds involves Hamiltonian dynamics with respect to the canonical symplectic structure on the cotangent bundle $T^*\mathscr{S}$ of the state space $\mathscr{S}$. We extend the notion of a moderation incentive to control systems on manifolds and develop general conditions under which moderation incentives determine a unique optimal control value for each point in the cotangent bundle of the state space.

One of the advantages of a quadratic 'kinetic energy' control cost for systems with admissible control regions is that the optimal control value is straightforward to compute—it can be computed directly as a non-parametrized Hamiltonian system on $T^*\mathscr{S}$. However, if the admissible control regions are bounded, a quadratic cost term can lead to non-differentiable controls. We construct a multi-parameter family of moderation incentives for affine nonlinear control systems with admissible control regions determined by quadratic forms, and determine the optimal control values for the associated cost functions. For all but one value of one of the parameters, this family yields differentiable optimal controls on the interior of the admissible control region. The upper limit of one of the parameter ranges determines generalizations of the shifted quadratic cost, with continuous controls that fail to be differentiable on the boundary of the admissible control regions. The lower limit, which is not attained, yields controls equal to those determined by a traditional logarithmic penalty function.

(these limits are determined by the relations $x(t_0) = x_0$ and $x(t_1) = x_1$)." appears on page 13; the treatment of fixed time problems is deferred to page 66.

Using the optimal controls for the incentives described above, we can construct functions, which we call moderation potentials, on the cotangent bundle of the state space such that solutions of Pontryagin's synthesis problem obey the associated Hamiltonian dynamics. Thus, rather than work with a family of parametrized Hamiltonians, we can find feedback laws generating trajectories determined by a traditional canonical Hamiltonian system. The moderation potentials for the multi-parameter family of moderation incentives constructed here have a relatively simple form. Some members of the family have particularly simple, geometrically meaningful, expressions.

We illustrate some of the key features of the moderated control problems using a simple two-dimensional controlled velocity problem: a vertically launched projectile is guided towards a fixed target; the speed is bounded by a function r of the horizontal component of the position. The optimal velocity and launch point are to be determined. The cost function is a combination of a term depending only on the horizontal component of the projectile's position models risk from ground-based defense of the target and a 'moderating' function of the control. We explore the behavior of the solutions of the synthesis problem as the parameters in the cost function determining the defense strength and level of moderation are varied.

2 Constants Matter: Moderation Incentives

We first establish notation and context: We assume that the set $\mathscr{S}$ of possible states is a smooth manifold (possibly with boundary), and consider control problems with state variable $z \in \mathscr{S}$ and control u in the state-dependent admissible control region $\mathscr{A}_z$ for z. The set

$$\mathscr{A} := \{(z, u) : z \in \mathscr{S} \text{ and } u \in \mathscr{A}_z\}$$

of admissible state/control pairs is assumed to be a topological manifold (typically with boundary). The evolution of the state variable is determined by a controlled vector field X. Specifically, $\dot{z} = X(z, u)$ for some continuous map $X : \mathscr{A} \to T\mathscr{S}$ satisfying $X(z, u) \in T_z\mathscr{S}$ for all $(z, u) \in \mathscr{A}$. (Here $T\mathscr{S}$ denotes the tangent bundle of the state space $\mathscr{S}$, and $T_z\mathscr{S}$ denotes the fiber of over z in $T\mathscr{S}$. See, e.g. [1, 4].) The control problem is to find a duration t_f and piecewise continuous curve $(z, u) : [0, t_f] \to \mathscr{A}$ satisfying the boundary conditions $z(0) = z_0$ and $z(t_f) = z_f$, with piecewise continuously differentiable state component z. The optimal control problem with instantaneous cost function $C : \mathscr{A} \to \mathbb{R}$ is to find all solutions minimizing the total cost

$$\int_0^{t_f} C(z(t), u(t))dt$$

over the set of all solutions of the control problem. The fixed time problem is defined analogously, but t_f is specified.

Given a purely state-dependent cost function $\hat{C} : \mathscr{S} \to \mathbb{R}$, we construct the cost function $C : \mathscr{A} \to \mathbb{R}$ by subtracting a control-dependent term $\tilde{C}(z, u)$ from the unmoderated cost $\hat{C}(z)$. Altering the cost by a constant influences the solutions of the optimization problem via the condition that the Hamiltonian equal zero along a solution of the synthesis problem if the optimal control lies in the interior of the admissible control region. To guide the selection of the control-dependent function $\tilde{C}$, we regard that term as an incentive for sub-maximal control investment, rather than a penalty. This motivates the condition that $\tilde{C}(z, u) = 0$ if $u \in \partial\mathscr{A}_z$.

Definition 1. Given an admissible space $\mathscr{A}$, $\tilde{C} \in \mathscr{C}^1(\mathscr{A}, [0, \infty))$ is a *moderation incentive* for $\mathscr{A}$ if for all $z \in \mathscr{S}$, $u \in \partial\mathscr{A}_z$ implies $\tilde{C}(z, u) = 0$.

If there are continuous functions $q : \mathscr{A} \to [0, 1]$ and $\Phi : \mathscr{S} \times [0, 1] \to \mathbb{R}$ with $\Phi^{-1}(0) = \mathscr{S} \times \{1\}$ such that for every $z \in \mathscr{S}$, $\partial\mathscr{A}_z = \{u \in \mathscr{A}_z : q(z, u) = 1\}$ and $s \mapsto \Phi(z, s)$ is a decreasing function, then $\tilde{C}(z, u) := \Phi(z, q(z, u))$ is a *monotonic moderation incentive* for $\mathscr{A}$ and q.

The following example illustrates the influence of shifting the cost function of an optimal control system for which the final time is not fixed. We consider a two dimensional system with controlled velocities. Starting from the horizontal axis, with vertical initial velocity, the goal is to hit a target (x_f, y_f). We assume that the projectile starts to the right of the target and consider a non-increasing unmoderated position-dependent cost term $\hat{C} : [x_f, \infty) \to \mathbb{R}^+$ depending only on the horizontal component of the position, modeling risk due to ground-based defense of the target, combined with a control- (and possibly position-) dependent moderation term. Given the final height y_f, we seek smooth trajectories $(x, y) : [0, t_f] \to \mathbb{R}^2$ satisfying $y(0) = \dot{x}(0) = 0$, $x(t_f) = x_f$, and $y(t_f) = y_f$. Neither the launch point $(x_0, 0)$ nor final time t_f are given. We have direct control over the velocity, with the constraint that the speed of the projectile never exceeds one.

We consider a pair of two-parameter families of cost functions, differing only by a constant. One parameter, c, scales a purely position-dependent term; the second, μ, scales a control-dependent term. One family yields inflexible solutions—the solution path is entirely determined by the boundary conditions, while the speed is simply rescaled by the ratio of the two parameters. The other family, in which the parameter μ scales a moderation incentive, has solutions for which the optimal path and speed both depend nontrivially on the parameters c and μ. A generalization of this problem is analyzed in Section 5. Here we simply summarize some of the key features of this system—our intent is only to remind the reader that analogous choices can have a profound influence on the solutions of optimal control systems if the final time t_f is not specified *a priori*, and hence should be systematically selected.

The cost functions

$$C_{\mathrm{ke}}(x, y, \dot{x}, \dot{y}; \mu) := \frac{\mu}{2} \|(\dot{x}, \dot{y})\|^2 + \frac{c}{2x^2} \quad \text{and} \quad C_{\mathrm{mi}}(\,\cdot\,; \mu) := C_{\mathrm{ke}}(\,\cdot\,; \mu) + 1 - \frac{\mu}{2} \tag{1}$$

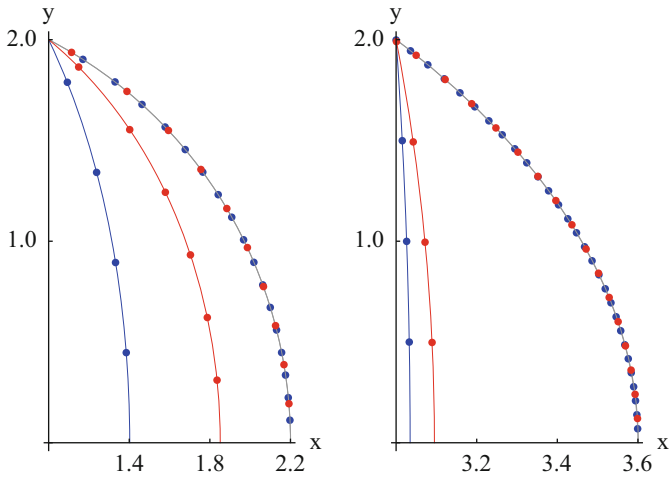

Fig. 1 Solutions of the vertical take-off targeting problem for sample target positions $(x_f, 2)$, cost function C_{mi}, and defense strengths c. Blue: $c = \frac{1}{2}$, red: $c = \frac{3}{2}$; left: $x_f = 1$, right: $x_f = 3$. Dots indicate projectile position at times $t = \frac{j}{2}$, $j \in \mathbb{N}$; colored lines indicate the traces of solutions for $\mu = 1 + \frac{c}{2x_f^2}$, the minimum value of μ determining smooth solutions; solid grey lines indicate those for $\mu = 2$, the maximum value of μ yielding an everywhere non-negative cost function. All solutions for the cost function C_{ke} lie on the grey curves

differ only by a constant, and the solutions for both cost functions trace out segment of ellipses with principal axes $\sqrt{1-(x_f/x_0)^2}$ and y_f/x_0, but there are important differences in the behavior of the solutions (See Figure 1).

The Hamiltonian associated to C_{ke} in the application of Pontryagin's Maximum Principle equals that of a point mass with mass μ and potential energy $-\frac{c}{2x^2}$; the constant difference between C_{ke} and C_{mi} influences the initial position and velocity through the condition that the Hamiltonian equal zero on an optimal trajectory unless the control lies on the boundary of the admissible control region.

- An optimal solution for C_{ke} traces an arc of a circle centered at the origin. The parameters c and μ influence the solution only through the rescaling of the speed by $\sqrt{c/\mu}$.
- The starting point x_0 for an optimal solution for C_{mi} depends nontrivially on both c and μ; specifically,

$$x_0^2 = \tfrac{b}{2} + \sqrt{\left(\tfrac{b}{2}\right)^2 + a\,d} \qquad \text{where} \qquad a = x_f^2 + y_f^2, \quad d = \tfrac{c}{2-\mu}, \quad b = x_f^2 - d.$$

x_0 and t_f are increasing functions of μ. The cost is non-negative on $\mathbb{R}^+$ iff $\mu \le 2$. Since smooth solutions satisfying the control constraint $1 \ge \dot{x}^2 + \dot{y}^2$ exist only if $1 + \frac{c}{2x_f^2} \le \mu \le 2$, we must have $x_f^2 \ge \frac{c}{2}$. The projectile follows a circular arc for the maximum moderation value $\mu = 2$.

3 Affine Nonlinear Control Systems and Ellipsoidal Admissible Control Regions

In [9] we introduced the notion of a moderation incentive for control systems in which both the state space and control regions were subsets of $\mathbb{R}^n$ and $\mathbb{R}^k$, and focused on the situation $n = k$. We now extend that strategy to nonlinear manifolds and introduce a family of moderation incentives for systems in which the admissible control regions $\mathscr{A}_z$ are the unit balls with respect to state-dependent norms. The optimal controls for these incentives are rescalings of the image of the auxiliary variable (now an element of the cotangent bundle of the state manifold) under a mapping determined by the norms.

Definition 2. Given a family of positive-definite quadratic forms Q_z on $\mathbb{R}^k$ such that $z \mapsto Q_z$ is $\mathscr{C}^1$, we will say that a control problem with admissible region

$$\mathscr{A} := \left\{(z, u) \in \mathscr{S} \times \mathbb{R}^k : Q_z(u) \leq 1\right\}$$

has *ellipsoidal control regions*.

If there are continuous vector fields f and g_j, $j = 0, \ldots, k$, on $\mathscr{S}$ such that

$$\dot{z} = X(z, u) = f(z) + \Sigma_{j=1}^{k} u_j g_j(z),$$

the system is said to be *affine nonlinearly controlled*, or *control-affine*; f is the *drift* vector field. (See, e.g., [4, 18].)

Given a control-affine system with ellipsoidal control regions, for each $z \in \mathscr{S}$, let L_z and $\langle\!\langle\ ,\ \rangle\!\rangle_z$ denote respectively the invertible symmetric linear map and inner product on $\mathbb{R}^k$ satisfying

$$Q_z(u) = \left\langle u, L_z^{-1} u \right\rangle \qquad \text{and} \qquad \langle\!\langle u, v \rangle\!\rangle_z = \left\langle u, L_z^{-1} v \right\rangle$$

for all $u \in \mathbb{R}^k$. Define the maps $M_z : \mathbb{R}^k \to T\mathscr{S}$, $\lambda : T^*\mathscr{S} \to \mathbb{R}^k$, and $\ell : T^*\mathscr{S} \to [0, \infty)$ by

$$M_z u := \Sigma_{j=1}^{k} u_j g_j(z), \qquad \lambda(\psi_z) := L_z(M_z^* \psi_z),$$

and

$$\ell(\psi_z)^2 := Q_z(\lambda(\psi_z)) = \psi_z \cdot (X(z, \lambda(\psi_z)) - f(z)).$$

Here $T^*\mathscr{S}$ denotes the cotangent bundle of $\mathscr{S}$; see, e.g., [1, 4]. Finally, define the map
$\nu : \ell^{-1}(\mathbb{R}^+) \to \mathbb{R}^k$ by

$$\nu(\psi_z) := \tfrac{1}{\ell(\psi_z)} \lambda(\psi_z) \in \partial \mathscr{A}_z.$$

Proposition 1. *Consider a control-affine system with ellipsoidal control regions. Let* $F \in \mathscr{C}^0(\mathscr{S}\times[0,1],[0,\infty))$ *be a function satisfying* $F^{-1}(0) = \mathscr{S}\times\{0\}$ *and such that* $x \mapsto F(z,x)$ *is increasing and differentiable on* $(0,1)$*, with* $\lim_{x\to 1}\frac{\partial F}{\partial x}(z,x) < \infty$*, for every* $z \in \mathscr{S}$*. Given* $p \geq 1$*, define* $x : \mathscr{S}\times\mathbb{R}^+\times[0,1]\to\mathbb{R}$ *by*

$$x(z,\ell,s) := \ell\, s + F(z, 1-s^p)\,. \tag{2}$$

If there is a function σ *on* $\mathscr{S}\times\mathbb{R}^+$ *such that for every* $(z,\ell)\in\mathscr{S}\times\mathbb{R}^+$*,* $s\mapsto x(z,\ell,s)$ *achieves its maximum exactly at* $\sigma(z,\ell)$*, then the moderation incentive*

$$\tilde{C}(z,u) := F\left(z, 1-Q_z(u)^{\frac{p}{2}}\right) \tag{3}$$

has optimal control value

$$\upsilon(\psi_z) := \begin{cases} \sigma(\psi_z)\,\nu(\psi_z) & \text{if} \quad \ell(\psi_z)\neq 0 \\ 0 & \text{if} \quad \ell(\psi_z) = 0 \end{cases} \tag{4}$$

at $\psi_z \in T^*\mathscr{S}$.

Proof. Fix $\psi_z \in T^*\mathscr{S}$. Define $\tilde{F}_{\psi_z} : \mathscr{A}_z \to \mathbb{R}$ by

$$\tilde{F}_{\psi_z}(u) := \psi_z\cdot(X(z,u) - f(z)) + F\left(z, 1-Q_z(u)^{\frac{p}{2}}\right),$$

and $x_{\psi_z} : [0,1]\to\mathbb{R}$ by $x_{\psi_z}(s) := x(z,\ell(\psi_z),s)$.

If $\lambda(\psi_z) = 0$, $\tilde{F}_{\psi_z}(u) = F\left(z, 1-Q_z(u)^{\frac{p}{2}}\right)$, which achieves its maximum at $u = 0$.

We now show that if $\lambda(\psi_z)\neq 0$, then $\tilde{F}_{\psi_z}$ takes its maximum on the line segment

$$\{s\,\nu(\psi_z) : 0\leq s\leq 1\},$$

and hence, since $\tilde{F}_{\psi_z}(s\,\nu(\psi_z)) = x_{\psi_z}(s)$, the maximum of $\tilde{F}_{\psi_z}$ coincides with the maximum of x_{ψ_z}. The restriction of $\tilde{F}_{\psi_z}$ to the interior of $\mathscr{A}$ is differentiable, with gradient

$$\nabla\tilde{F}_{\psi_z}(u) = \lambda(\psi_z) - p\,\frac{\partial F}{\partial x}\left(z, 1-Q_z(u)^{\frac{p}{2}}\right) Q_z(u)^{\frac{p}{2}-1}.$$

Hence if $\lambda(\psi_z)\neq 0$, any critical point of $\tilde{F}_{\psi_z}$ in the interior of $\mathscr{A}$ has the form $u = s\,\nu(\psi_z)$ for $s\in(0,1)$ satisfying

$$\frac{\ell(\psi_z)}{p} = s^{p-1}\,\frac{\partial F}{\partial x}\left(z, 1-Q_z(s\,\nu(\psi_z))^{\frac{p}{2}}\right) = s^{p-1}\,\frac{\partial F}{\partial x}(z, 1-s^p)\,. \tag{5}$$

Note that if $\lambda(\psi_z) \neq 0$, and hence $\ell(\psi_z) \neq 0$, then s satisfies (5) iff s is a critical point of x_{ψ_z}.

Since $F(z,0) = 0$ implies that $F\left(z, 1 - Q_z(u)^{\frac{p}{2}}\right) = 0$ for $u \in \partial\mathscr{A}_z$,

$$\max_{u \in \partial\mathscr{A}_z} \tilde{F}_{\psi_z}(u) = \max_{Q_z(u)=1} \langle\langle \lambda(\psi_z), u \rangle\rangle_z .$$

Hence a standard Lagrange multiplier argument shows that the restriction of $\tilde{F}_{\psi_z}$ to $\partial\mathscr{A}_z$ achieves its maximum, $\ell(\psi_z) = x_{\psi_z}(1)$, at $\nu(\psi_z)$.

Finally, $\tilde{F}_{\psi_z}(0) = F(z,1) = x_{\psi_z}(0)$.

Remark 1. If (4) is the optimal control for a moderation incentive of the form (3), with scaling factor σ, and $\mu \in \mathscr{C}^0(\mathscr{S}, \mathbb{R}^+)$, then

$$\tilde{C}_\mu(z,u) := \mu(z)\, F\left(z, 1 - Q_z(u)^{\frac{p}{2}}\right)$$

is a moderation incentive with scaling factor obtained by replacing $\ell(\psi_z)$ with $\ell_\mu(\psi_z) := \frac{\ell(\psi_z)}{\mu(z)}$ in (4).

A moderation incentive is required to take the value zero on the boundary of the admissible control regions, but is not required to have a finite derivative there. If the derivative of the incentive is unbounded as the control u approaches $\partial\mathscr{A}_z$, the optimal control lies in the interior of $\mathscr{A}_z$.

Lemma 1. *If $F : \mathscr{S} \times [0,1] \to [0,\infty)$ satisfies $F^{-1}(0) = \mathscr{S} \times \{0\}$, and for every $z \in \mathscr{S}$ the function $x \mapsto F(z,x)$ is $\mathscr{C}^2$ on $(0,1)$, with decreasing positive derivative satisfying*

$$\lim_{x \to 0} \frac{\partial F}{\partial x}(z,x) = \infty,$$

then $s \mapsto x(z,\ell,s)$ given by (2) achieves its maximum at a unique point $s_*(z,\ell) \in (0,1)$ if $p > 1$, or if $p = 1$ and F_z is strictly decreasing.

The associated map $\sigma : \ell^{-1}(\mathbb{R}^+) \to (0,1)$ given by $\sigma(\psi_z) := s_*(z, \ell(\psi_z))$ is $\mathscr{C}^1$.

Proof. Setting $y = 1 - s^p$ and $c = \frac{\ell(\psi_z)}{p} > 0$, (5) takes the form $c(1-y)^{\frac{1}{p}-1} = \frac{\partial F}{\partial x}(z,y)$, with unique solution $y(c) \in (0,1)$. The map $s \mapsto s^{p-1} \frac{\partial F}{\partial x}(z, 1-s^p)$ has a $\mathscr{C}^1$ strictly positive derivative on $(0,1)$. Hence the Implicit Function Theorem implies that the map σ determined by (5) is $\mathscr{C}^1$ on $\ell^{-1}(\mathbb{R}^+)$.

We now define a family of monotonic moderation incentives for control-affine systems with ellipsoidal control regions. These incentives generalize the moderation incentives introduced in [9]. The dogleg parameters $\alpha \in (0,1]$ and $p \geq 1$ can be interpreted as tuning the overall shape of the control response curve, while the state-dependent moderation strength function $\mu \in \mathscr{C}^0(\mathscr{S}, \mathbb{R}^+)$ scales the instantaneous

control cost. (Use of the term 'dogleg' is motivated by the shape of the response curve for values of α near 1; varying these parameters alters the abruptness of the dogleg bend. See Figures 2 and 3.)

Theorem 1. *Given* $0 < \alpha \leq 1 \leq p$, *excluding* $\alpha = 1 = p$, *and* $\mu \in \mathscr{C}^0(\mathscr{S}, \mathbb{R}^+)$,

$$\tilde{C}_{\alpha,p}(z, u; \mu) = \tfrac{\mu(z)}{p\,\alpha} \left(1 - Q_z(u)^{\frac{p}{2}}\right)^{\alpha} \tag{6}$$

is a monotonic moderation incentive for $\mathscr{A}$.

If $0 < \alpha < 1$, *the unique optimal control parameter (4) for* $\tilde{C}_{\alpha,p}$ *has the scaling*

$$\sigma_{\alpha,p}(\psi_z; \mu) = \rho^{-1}_{\alpha,p}(\ell_\mu(\psi_z)), \tag{7}$$

where $\rho_{\alpha,p} : [0, 1] \to [0, \infty)$ *and* $\ell_\mu : T^*\mathscr{S} \to [0, \infty)$ *are given by*

$$\rho_{\alpha,p}(s) := s^{p-1}\,(1 - s^p)^{\alpha-1} \qquad \textit{and} \qquad \ell_\mu(\psi_z) := \frac{\ell(\psi_z)}{\mu(z)}.$$

If $\alpha = 1 < p$, *then*

$$\sigma_{1,p}(\psi_z; \mu) := \min\left\{\ell_\mu(z)^{\frac{1}{p-1}}, 1\right\} \tag{8}$$

is the optimal scaling.

Proof. For $0 < \alpha \leq 1$, $F_\alpha(x) := \frac{1}{\alpha}x^\alpha$ is differentiable, with decreasing positive derivative, on $(0, 1]$. For $0 < \alpha < 1$, $\lim_{x\to 0} F'_\alpha(x) = \infty$, so the rescaling of F_α by $\frac{\mu(z)}{p}$ satisfies the conditions of Lemma 1.

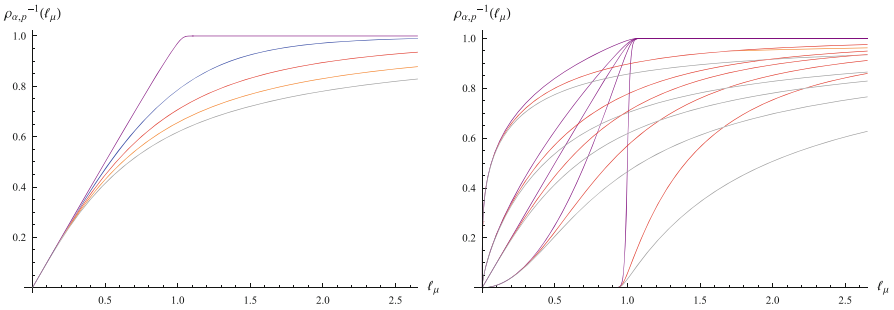

Fig. 2 Plots of $\rho^{-1}_{\alpha,p}\left(\ell_\mu\right)$ for different values of the dogleg parameters α and p. Purple: $\alpha = \frac{99}{100}$; blue: $\alpha = \frac{3}{4}$; red: $\alpha = \frac{1}{2}$; orange: $\alpha = \frac{1}{4}$; gray: limiting case $\alpha \to 0$. Left: $p = 2$. Right: $p = 1.01, 1.5, 2, 2.5, 5$; convexity for small values of s increases with p (the approximate step function in the right hand graph is associated to $\alpha = \frac{99}{100}$, $p = 1.01$)

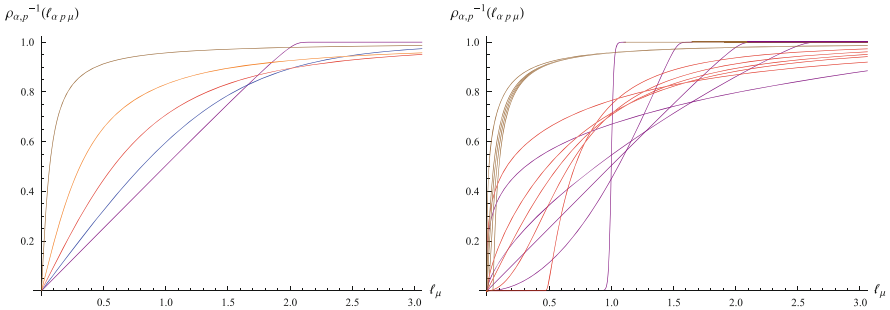

Fig. 3 Plots of $\rho_{\alpha,p}^{-1}\left(\frac{\ell_\mu}{\alpha\, p}\right)$ for different values of the dogleg parameters α and p. Purple: $\alpha = \frac{99}{100}$; blue: $\alpha = \frac{3}{4}$; red: $\alpha = \frac{1}{2}$; orange: $\alpha = \frac{1}{4}$; brown: $\alpha = \frac{1}{20}$. Left: $p = 2$. Right: $p = 1.01, 1.5, 2, 2.5, 5$

The case $\alpha = 1 < p$ requires a direct application of Proposition 1, since $F_1' \equiv 1$. In this case,

$$\frac{x_{\psi_z}(s)}{\mu(z)} = \ell_\mu(\psi_z)\, s + \tfrac{1}{p}\,(1 - s^p)$$

is the restriction of a polynomial to $[0, 1]$. If $\ell_\mu(\psi_z) \leq 1$, the maximum of x_{ψ_z} coincides with that of the polynomial, which occurs at $s = \ell_\mu(\psi_z)$. If $\ell_\mu(\psi_z) \geq 1$, the maximum occurs at one of the endpoints; since

$$x_{\psi_z}(0) = \frac{\mu(z)}{p} < \ell(\psi_z) = x_{\psi_z}(1),$$

x_{ψ_z} achieves its maximum of $\ell(\psi_z)$ at 1 in this case.

3.1 *Special Cases:* $\alpha = 1$, $\alpha \to 0$, *and* $\frac{1}{\alpha} = p$

For some special values of the parameters α and p, simple closed form expressions for the optimal scaling $\sigma_{\alpha,p}$ exist (Figure 3).

The dogleg parameter values $\alpha = 1$, $p = 2$ correspond to the quadratic control cost used in the projectile problem in Sect. 2. Note that when $\alpha = 1$, the optimal scaling is not differentiable at $\partial\mathscr{A}_z$.

The limit $\lim_{\alpha\to 0} \tilde{C}_{\alpha,p}$ is not well-defined, but

$$\rho_{0,p}(s) := \lim_{\alpha\to 0} \rho_{\alpha,p}(s) = \frac{s^{p-1}}{1 - s^p} = -\tfrac{d}{ds} \ln\left((1 - s^p)^{\frac{1}{p}}\right)$$

is well-defined and invertible on $[0, 1)$. In particular, the optimal scaling associated to the logarithmic control cost

$$C(z, u) = -\tfrac{1}{2} \ln(1 - Q_z(u))$$

is $\rho_{0,2}^{-1}(\ell_\mu(\psi_z))$. Thus the controls determined by the family $\tilde{C}_{\alpha,2}$ determine a homotopy between optimal controls determined by a 'kinetic energy' control cost and a logarithmic control cost. (Logarithmic penalty functions are widely used in the engineering literature to enforce inequality constraints.)

In the case $\alpha = \frac{1}{p} < 1$, we can explicitly invert $\rho_{\frac{1}{p},p}$:

$$\sigma_{\frac{1}{p},p}(\psi_z; \mu) = \left(1 + \ell_\mu(\psi_z)^{-q}\right)^{-\frac{1}{p}} \qquad \text{for} \qquad \frac{1}{p} + \frac{1}{q} = 1, \tag{9}$$

and hence the optimal control is

$$\upsilon_{\frac{1}{p},p}(\psi_z; \mu) = \frac{\ell(\psi_z)^{q-2}}{(\mu(z)^q + \ell(\psi_z)^q)^{\frac{1}{p}}} \lambda(\psi_z)$$

if $\lambda(\psi_z) \neq 0$.

Remark 2. When the drift field is trivial, the optimal control for $\frac{1}{\alpha} = p = 2$ has the following geometric interpretation:

$$\upsilon_{\frac{1}{2},2}(\psi_z) = \frac{\lambda(\psi_z)}{\|(\lambda(\psi_z), \mu(z))\|_{Q_z}},$$

where $\|(u, t)\|_Q^2 = Q(u) + t^2$ is the norm on $\mathbb{R}^{k+1}$ induced by a quadratic form Q on $\mathbb{R}^k$. Thus $\upsilon_{\frac{1}{2},2}(\psi_z)$ is the control component of the projection of $(\lambda(\psi_z), \mu(z))$ onto the $\| \ \|_{Q_z}$ unit ball in $\mathbb{R}^{k+1}$. (See Figure 4.) We will further investigate the moderated controls for $\alpha\ p = 1$, particularly that for $p = 2$, in future work.

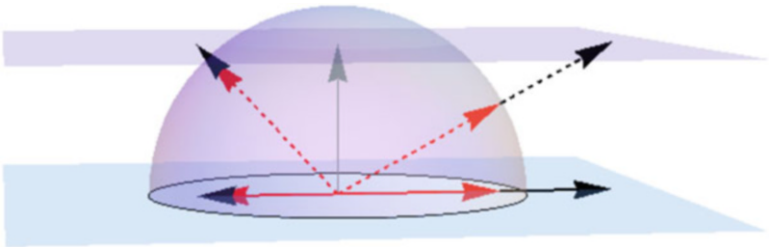

Fig. 4 The optimal control for $\frac{1}{\alpha} = p = 2$ implemented as lift into control–moderation space, followed by projection onto the unit sphere, then projection back into control space. Black solid arrows: $\lambda(\psi_z)$; black dashed: $(\lambda(\psi_z), \mu(z))$; red dashed: $\frac{(\lambda(\psi_z),\mu(z))}{\|(\lambda(\psi_z),\mu(z))\|_{Q_z}}$; red solid: $\frac{\lambda(\psi_z)}{\|(\lambda(\psi_z),\mu(z))\|_{Q_z}}$

4 Moderation Potentials and the Synthesis Problem

Pontryagin's Maximum Principle relates optimal control to Hamiltonian dynamics: if the state space $\mathscr{S}$ is an n-dimensional subset of $\mathbb{R}^n$, then a solution $(z, u) : [0, t_f] \to \mathscr{A} \subseteq \mathbb{R}^n \times \mathbb{R}^k$ of the control problem minimizing the total cost has an associated curve $\lambda : [0, t_f] \to \mathbb{R}^n$ such that (z, λ) satisfies Hamilton's equations for the time-dependent Hamiltonian

$$H_t(\tilde{z}, \lambda) := \lambda^T X(\tilde{z}, u(t)) - C(\tilde{z}, u(t)),$$

and

$$H_t(z(t), \lambda(t)) = \max_{u \in \mathscr{A}_{z(t)}} \left(\lambda(t)^T X(z(t), u) - C(z(t), u)\right).$$

(See [16] for the precise statement and proof of the Maximum Principle.) Pontryagin's optimality conditions are necessary, but not sufficient. Their appeal lies in their constructive nature—well-known results and techniques for boundary value problems and Hamiltonian dynamics can be used to construct the pool of possibly optimal trajectories. This construction is referred to as the synthesis problem in [16]; we will use that terminology here.

The generalization of Hamilton's equations to a nonlinear state manifold $\mathscr{S}$ utilizes the canonical symplectic structure on the cotangent bundle $T^*\mathscr{S}$ of the state manifold. (See, e.g., [4] for additional background and discussion.) We now introduce the formulation of the synthesis problem that will be used here. Given our focus on systems with state-dependent admissible control regions, we impose the condition that the parametrized Hamiltonians be extensible to neighborhoods of possibly optimal values, so as to guarantee that the time-dependent Hamiltonian vector field is defined on a neighborhood of the current state z even when the control is on the boundary $\partial\mathscr{A}_z$ of that state's admissible control region.

Given that the admissible control regions can vary with the state variable, we explicitly require that the vector field X and cost term C with fixed control value be extensible to neighborhoods of the points of interest. Let $\pi : T^*\mathscr{S} \to \mathscr{S}$ denote the canonical projection, with $\pi^{-1}(z) = T^*_z\mathscr{S}$,

$$\mathscr{P} := \{(\psi_z, u) : (\pi(\psi_z), u) \in \mathscr{A}\},$$

and $\mathbb{P}_1 : \mathscr{A} \to \mathscr{S}$ denote projection onto the first factor. Given $H \in \mathscr{C}^1(T^*\mathscr{S}, \mathbb{R})$, let X_H denote the Hamiltonian vector field determined by H and the canonical symplectic structure on $T^*\mathscr{S}$. Define the Hamiltonian $H : \mathscr{P} \to \mathbb{R}$ and $\chi : T^*\mathscr{S} \to \mathbb{R}$ by

$$H(\psi_z, u) := \psi_z \cdot X(z, u) - C(z, u) \qquad \text{and} \qquad \chi(\psi_z) := \max_{u \in \mathscr{A}_z} H(\psi_z, u). \tag{10}$$

Definition 3. If for every $(\psi_z, u_*) \in \mathscr{P}$ satisfying $H(\psi_z, u_*) = \chi(\psi_z)$ there is a neighborhood $\mathscr{V}$ of z such that the restrictions of $X(\,\cdot\,, u_*)$ and $C(\,\cdot\,, u_*)$ to $\mathscr{V}$ are restrictions to $\mathscr{V} \cap \mathbb{P}_1(\mathscr{A})$ of $\mathscr{C}^1$ maps on $\mathscr{V}$, then X and C are *synthesizable*.

A curve $(\Psi, \upsilon) : [0, t_f] \to \mathscr{P}$ satisfying

$$\dot{\Psi}(t) = X_{H_t}(\Psi(t)) \qquad \text{and} \qquad H_t(\Psi(t)) = \chi(\Psi(t))$$

for the local time-dependent Hamiltonians $H_t(\psi_z) := H(\psi_z, \upsilon(t))$ determined by synthesizable X and C is a solution of the *synthesis problem* determined by X, C and the boundary data $z_0 = \pi(\Psi(0))$ and $z_f = \pi(\Psi(t_f))$ if $H_0(\Psi(0)) = 0$.

If (Ψ, υ) satisfies the all of the above conditions except the condition that $H_0(\Psi(0)) = 0$, then (Ψ, υ) is a solution of the *fixed time synthesis problem* of duration t_f.

We will focus on finding solutions of the synthesis problem, and will not formulate general conditions under which such solutions are in fact global optimizers.

One of the advantages of the quadratic 'kinetic energy' control cost terms frequently used in geometric optimal control for systems with controlled velocities and unbounded admissible control regions is that the optimal control value is straightforward to compute—it is simply the inverse Legendre transform of ψ_z—and hence the synthesis problem can be approached directly as a non-parametrized Hamiltonian system on $T^*\mathscr{S}$. However, if the admissible control regions are bounded, a 'kinetic energy' cost term can lead to non-differentiable controls. (See, e.g. [9].) We now identify conditions under which a control-dependent cost function determines solutions of the synthesis problem corresponding to solutions of a traditional Hamiltonian system on $T^*\mathscr{S}$.

Nondegeneracy of the symplectic structure guarantees that two Hamiltonian vector fields agree at ψ_z iff ψ_z is a critical point of the difference of the corresponding Hamiltonians. For fixed $\psi_z \in T^*\mathscr{S}$, we can define $h_{\psi_z} \in \mathscr{C}^1(\mathscr{A}_z, \mathbb{R})$ by $h_{\psi_z}(u) := H(\psi_z, u)$. If H is $\mathscr{C}^1$ and h_{ψ_z} achieves its maximum at a point u_* in the interior $\mathscr{A}_z^o$ of the admissible control region $\mathscr{A}_z$ at z, then u_* is a critical point of h_{ψ_z}. It follows that if H is $\mathscr{C}^1$ and there is a $\mathscr{C}^1$ map υ such that $H(\,\cdot\,, \upsilon(\,\cdot\,)) = \chi$ and $\upsilon(\psi_z) \in \mathscr{A}_z^o$ for every $\psi_z \in T^*\mathscr{S}$, then

$$\mathrm{d}(\chi - H(\,\cdot\,, u_*))(\psi_z)(w_{\psi_z}) = dH(\psi_z, u_*)(0, d_{\psi_z}\upsilon(w_{\psi_z})) = \mathrm{d}h_{\psi_z}(u_*)(d_{\psi_z}\upsilon(w_{\psi_z})) = 0$$

for $u_* = \upsilon(\psi_z)$ and all $w_{\psi_z} \in T_{\psi_z}T^*\mathscr{S}$.

If there is a $\mathscr{C}^0$ map υ such that $H(\,\cdot\,, \upsilon(\,\cdot\,)) = \chi$, but υ is not everywhere differentiable, or can take values on the boundaries of the admissible control region, then the above argument is not applicable, but we may still be able to replace the parametrized Hamiltonians $H(\,\cdot\,, u_*)$ with the function χ.

The solution of the synthesis problem can be simplified given a feedback law that allows replacement of the control-parametrized Hamiltonian with a conventional autonomous Hamiltonian on the cotangent bundle $T^*\mathscr{S}$. We now show that the moderation incentives $\tilde{C}_{\alpha,p}$ have such control laws. The key concerns are

formulation of relatively simple expressions for the Hamiltonians and verification of the differentiability of the Hamiltonian on the boundaries of the admissible control regions.

Proposition 2. *If*

1. *X and C are synthesizable,*
2. *χ given by (10) is $\mathscr{C}^1$,*
3. *$\Psi : [0, t_f] \to T^*\mathscr{S}$ is a solution of the canonical Hamiltonian system with Hamiltonian χ, and*
4. *there is a curve $u : [0, t_f] \to \mathscr{P}$ such that $(\Psi(t), u(t)) \in \mathscr{P}$ and*

$$H(\Psi(t), u(t)) = \chi(\Psi(t)) \qquad \text{and} \qquad \mathrm{d}(H(\,\cdot\,, u(t)) - \chi)(\Psi(t)) = 0$$

for $0 \le t \le t_f$,

then (Ψ, u) is a solution of the fixed time synthesis problem of duration t_f determined by X, C, and the boundary data $z_0 = \pi(\Psi(0))$ and $z_f = \pi(\Psi(t_f))$.

If, in addition, $H(\Psi(0)) = 0$, then Ψ determines a solution of the synthesis problem.

Proof. For each $t \in [0, t_f]$, synthesizability of X and C implies that there is a neighborhood $\mathscr{V}_t$ of $\pi(\Psi(t))$ such that $H_t := H(\,\cdot\,, \upsilon(t)) \in \mathscr{C}^1(\pi^{-1}(\mathscr{V}_t))$. $0 = d(\chi - H_t)(\Psi(t))$ implies

$$\dot{\Psi}(t) = X_\chi(\Psi(t)) = X_{H_t}(\Psi(t))$$

and

$$H_t(\Psi(t)) = H(\Psi(t), \upsilon(t)) = \chi(\Psi(t))$$

for $0 \le t \le t_f$. Hence (Ψ, υ) is a solution of the fixed time synthesis problem. If the Hamiltonian is identically zero along the trajectory, then (Ψ, υ) is a solution of the synthesis problem.

Definition 4. If

1. $\tilde{C}$ is a moderation incentive,
2. the pair X and $-\tilde{C}$ is synthesizable,
3. χ given by (10) for $C = -\tilde{C}$ is $\mathscr{C}^1$
4. there is a unique map $\upsilon \in \mathscr{C}^0(T^*\mathscr{S})$ such that
   a. $graph(\upsilon) \subseteq \mathscr{P}$,
   b. $H(\,\cdot\,, \upsilon(\,\cdot\,)) = \chi$, and
   c. for every $\psi_z \in T^*\mathscr{S}$, ψ_z is a critical point of $\chi - H(\,\cdot\,, \upsilon(\psi_z))$,

then we will say that χ is a *moderation potential* for $\tilde{C}$ and X.

It follows immediately from Proposition 2 and Definition 4 that if χ is a moderation potential for synthesizable X and $\tilde{C}, \hat{C} \in \mathscr{C}^1(\mathscr{S})$, and $\Psi : [0, t_f] \to T^*\mathscr{S}$ is a solution of Hamilton's equations for the Hamiltonian $\chi - \hat{C} \circ \pi$, then $(\Psi, \upsilon \circ \Psi)$ is a solution of the synthesis problem determined by $X, C = \hat{C} \circ \mathbb{P}_1 - \tilde{C}$, and the boundary data $z_0 = \pi(\Psi(0))$ and $z_f = \pi(\Psi(t_f))$. If, in addition, $H(\Psi(0)) = \hat{C}(\pi(\Psi(0)))$, then Ψ determines a solution of the synthesis problem.

We now show that moderation potentials exist for the family of moderation incentives constructed in Theorem 1. For some subfamilies, the moderation potentials have particularly simple expressions.

Theorem 2. *The moderation incentives (6) have moderation potentials*

$$\chi_{\alpha,p}(\psi_z; \mu) := a_0(\psi_z) + \mu(z)\, \hat{\chi}_{\alpha,p}(\ell_\mu(\psi_z)), \tag{11}$$

where $a_0(\psi_z) := \psi_z \cdot f(z)$ *is the contribution of the drift field,*

$$\hat{\chi}_{\alpha,p}(r) := r\, s \left(1 + \tfrac{1}{\alpha\, p} \left(r\, s^{1-\alpha\, p}\right)^{\frac{1}{\alpha-1}}\right)\Big|_{s=\rho^{-1}_{\alpha,p}(r)} \tag{12}$$

if $0 < \alpha < 1$, *and*

$$\hat{\chi}_{1,p}(r) := \begin{cases} \frac{1}{p} + \frac{1}{q} & r^q \quad r < 1 \\ r & \quad\ r \geq 1 \end{cases}, \qquad \textit{where} \quad \tfrac{1}{p} + \tfrac{1}{q} = 1. \tag{13}$$

Proof. Setting $r = \ell_\mu(\psi_z)$ for notational simplicity, Theorem 1 implies that

$$\frac{\chi_{\alpha,p}(\psi_z) - a_0(\psi_z)}{\mu(z)} = s\, r + \frac{1}{\alpha\, p}\,(1 - s^p)^\alpha \Big|_{s=\rho^{-1}_{\alpha,p}(r)}. \tag{14}$$

For $0 < \alpha < 1$, we can simplify this expression as follows:

$$r = \rho_{\alpha,p}(s) = s^{p-1}\,(1 - s^p)^{\alpha-1}$$

implies that

$$(1 - s^p)^\alpha = \left(r\, s^{p-1}\right)^{\frac{\alpha}{\alpha-1}}.$$

Substituting this into (14) and regrouping terms yields (12).

In the case $\alpha = 1$,

$$s \mapsto r\, s + \tfrac{1}{p}\,(1 - s^p) \tag{15}$$

is the restriction of a polynomial to $[0, 1]$. The maximum of the polynomial (15) occurs at $r^{\frac{1}{p-1}}$; hence if $r < 1$, the maximum is

$$r^{1+\frac{1}{p-1}} + \tfrac{1}{p}\left(1 - r^{\frac{p}{p-1}}\right) = \tfrac{1}{p} + \left(1 - \tfrac{1}{p}\right) r^{\frac{p}{p-1}}.$$

If $1 \leq r$, the maximum occurs at one of the endpoints; since $\frac{1}{p} < 1$, in this case (15) achieves its maximum of r at 1.

Direct utilization of conservation of the Hamiltonian H can simplify the analysis of the synthesis problem in many situations. However, when numerically approximating solutions of Hamiltonian systems, discretion must be used when combining conservation laws with discretization to avoid artificial accelerations and related errors. We now focus on explicit use of the conservation law, not to endorse it as a general purpose strategy, but to emphasize the role of the specific value of the Hamiltonian in determining solutions satisfying given boundary conditions. The following results play a pivotal role in our analysis of the projectile problem in Section 5.

We can express the optimal scalings for the moderation incentives $\tilde{C}_{\alpha,p}$ as functions $\hat{\sigma}_{\alpha,p}$ of

$$\phi(z; h) := \frac{\hat{C}(z) + h}{\mu(z)}, \tag{16}$$

where h denotes the difference of the Hamiltonian and the drift potential a_0 at ψ_z.

Proposition 3. *The optimal scaling for the moderation incentive $\tilde{C}_{\alpha,p}$ and associated Hamiltonian (21) satisfies*

$$\sigma_{\alpha,p}(\psi_z; \mu) = \hat{\sigma}_{\alpha,p}(\phi(z; H(\psi_z) - a_0(\psi_z))),$$

where $\hat{\sigma}_{\alpha,p} : \mathbb{R} \to (0, 1)$ and $\tau_{\alpha,p} : (0, 1) \to \mathbb{R}$ are given by

$$\hat{\sigma}_{\alpha,p}(\phi) = \left(1 - \tau_{\alpha,p}^{-1}(\phi)\right)^{\frac{1}{p}} \qquad \text{and} \qquad \tau_{\alpha,p}(w) := w^{\alpha-1}\left(1 + \left(\tfrac{1}{\alpha p} - 1\right) w\right) \tag{17}$$

if $0 < \alpha < 1 \leq p$, and

$$\hat{\sigma}_{1,p}(\phi) = \begin{cases} \left(\dfrac{p\phi - 1}{p - 1}\right)^{\frac{1}{p}} & \frac{1}{p} \leq \phi < 1 \\ 1 & \phi \geq 1 \end{cases} \tag{18}$$

if $p > 1$.

Proof. If $0 < \alpha < 1$ and $\lambda(\psi_z) \neq 0$, (7) and (16) imply that

$$\hat{\chi}_{\alpha,p}(\rho_{\alpha,p}(\sigma_{\alpha,p}(\psi_z;\mu))) = \phi(z,h). \tag{19}$$

The composition $\hat{\chi}_{\alpha,p} \circ \rho_{\alpha,p}$ can be simplified as follows. Substituting

$$\rho_{\alpha,p}(s)s^{1-\alpha\, p} = s^{(1-\alpha)p}\,(1-s^p)^{\alpha-1} = (s^{-p}-1)^{\alpha-1}$$

into (12) and regrouping terms yields

$$\begin{aligned}
\hat{\chi}_{\alpha,p}(\rho_{\alpha,p}(s)) &= \rho_{\alpha,p}(s)\, s\left(1+\tfrac{1}{\alpha\, p}\,(s^{-p}-1)\right)\\
&= (1-s^p)^{\alpha-1}\, s^p\left(1+\tfrac{1}{\alpha\, p}\,(s^{-p}-1)\right)\\
&= (1-s^p)^{\alpha-1}\left(\tfrac{1}{\alpha\, p}+\left(1-\tfrac{1}{\alpha\, p}\right)s^p\right)\\
&= \tau_{\alpha,p}\,(1-s^p)\,.
\end{aligned}$$

$\tau_{\alpha,p}$ is strictly decreasing for $0 < \alpha \leq 1$, and hence is invertible. Solving (19) for $\sigma_{\alpha,p}(\psi_z;\mu)$ yields (17).

If $\alpha = 1 < p$, then (13) implies

$$\hat{\chi}^{-1}_{1,p}(\phi) = \begin{cases} \left(q\left(\phi-\frac{1}{p}\right)\right)^{\frac{1}{q}} & \text{if} \quad \phi < 1 \\ \phi & \text{if} \quad \phi \geq 1 \end{cases}, \qquad \text{where} \quad \tfrac{1}{p}+\tfrac{1}{q} = 1.$$

Substituting $\ell_\mu(\psi_z) = \hat{\chi}^{-1}_{1,p}(\phi)$ in (8) and simplifying yields (18).

In the case $\alpha = \frac{1}{p}$, the moderation potential and optimal scaling are particularly simple. We will make use of the following expressions in Section 5 when analyzing generalizations of the projectile example from Section 1.

Corollary 1. *If* $\alpha = \frac{1}{p} < 1$, *then*

$$\chi_{\frac{1}{p},p}(\psi_z;\mu) - a_0(\psi_z) = \|(\ell(\psi_z),\mu(z))\|_q = (\ell(\psi_z)^q + \mu(z)^q)^{\frac{1}{q}}\,,$$

where $\frac{1}{p}+\frac{1}{q} = 1$, *and*

$$\hat{\sigma}_{\frac{1}{p},p}(\phi) = (1-\phi^{-q})^{\frac{1}{p}}\,. \tag{20}$$

Proof. Setting $q = \frac{p}{p-1}$ and substituting $\alpha = \frac{1}{p}$ and (9) into (12) yields

$$\hat{\chi}_{\frac{1}{p},p}(r) = r\, s\, (1 + r^{-q})|_{s=(1+r^{-q})^{-\frac{1}{p}}} = r\, (1 + r^{-q})^{\frac{1}{q}} = (r^q + 1)^{\frac{1}{q}}\,.$$

Hence

$$\chi_{\frac{1}{p},p}(\psi_z) - a_0(\psi_z) = \mu(z)\, \hat{\chi}_{\frac{1}{p},p}(\ell_\mu(\psi_z)) = \mu(z)\, \left(\ell_\mu(\psi_z)^q + 1\right)^{\frac{1}{q}} = (\ell(\psi_z)^q + \mu(z)^q)^{\frac{1}{q}}\,.$$

(20) follows immediately from (17).

5 Vertical Take-Off Projectile with Controlled Velocity

To illustrate some features of moderation potentials, we return to the two dimensional projectile system with controlled velocities briefly considered in Section 2, generalizing the cost functions and admissible control regions. This system's features were chosen so that application of Pontryagin's Maximum Principle yields an integrable Hamiltonian system—we can express the height of the projectile and the elapsed time as definite integrals of functions of the horizontal position. Further specialization yields situations in which these definite integrals have closed form expressions in terms of elliptic integrals or logarithms, facilitating comparison of solutions with different moderation incentives, admissible control regions, and targets. In particular, we shall see that the solutions change in a highly nontrivial way as the level set of the Hamiltonian containing the solution changes; this illustrates the essential difference between the synthesis problem, for which solutions must lie in the zero level set, from the fixed time synthesis problem, for which the appropriate level set is determined in part by the time constraint.

We first briefly review the projectile problem from Section 2 and describe the generalizations considered here. The task is to hit a target (x_f, y_f), starting from an unspecified position $(x_0, 0)$ on the horizontal axis to the right of the target, with vertical initial velocity; the state space is $\mathscr{S} = I \times \mathbb{R}$ for a closed interval $I \subset \mathbb{R}^+$ of the form $[x_f, \infty)$ or $[x_f, x_{\max}]$. The velocity is the control, i.e. $(\dot{x}, \dot{y}) = u$.

The admissible control region $\mathscr{A}_{(x,y)}$ associated to $(x, y) \in \mathscr{S}$ is the closed ball of radius $r(x)$ centered at the origin for a given function $r \in \mathscr{C}^0(I, \mathbb{R}^+)$. The unmoderated position-dependent cost term $\hat{C} \in \mathscr{C}^1(I, \mathbb{R}^+)$ is a function of the horizontal component of the position. The moderation incentives have the form $\mu(x)\tilde{C}_{\alpha,p}$ for $\mu \in \mathscr{C}^0(I, \mathbb{R}^+)$ satisfying $\mu(x) < p\,\alpha\,\hat{C}(x)$ for all $x \in I, \alpha$ and p as in Section 4.

We identify $T^*\mathscr{S}$ with $\mathscr{S} \times \mathbb{R}^2$, and write $\psi_z = ((x, y), \psi)$. We abuse notation, in the interest of reminding the reader of the invariance of key constructs, denoting quantities depending on the state variables as depending on x, rather than the pair

(x, y), and dropping the base point from ψ_z. The quadratic form determining the admissible control regions takes the form

$$Q_x(u) = r(x)^{-2} \|u\|^2 ;$$

hence $L_x\psi = r(x)\psi$, and $\lambda(\psi) = r(x)\psi$ is simply a rescaling of ψ. In particular, the vertical take-off condition is equivalent to the requirement that $\psi_z(0)$ be vertical.

Our hypotheses were chosen so as to yield an integrable system: a pair of scalar conservation laws allow us to express ψ as a function of x and thus reduce the synthesis problem to a first order ODE solvable by quadrature. In Proposition 3 we showed how conservation of the Hamiltonian can be used to express the optimal scaling as a function of the state variables and the value of the Hamiltonian. The Hamiltonian

$$H(x, \psi) = \chi_{\alpha,p}((x, \psi); \mu) - \hat{C}(x), \tag{21}$$

for the projectile system is independent of y (the moderation potential $\chi_{\alpha,p}$ is given by (11)); hence it follows from Noether's Theorem that the second component of ψ is a constant of the motion for the canonical Hamiltonian system determined by H. (See, e.g. [1, 4].) We now show that the additional conserved quantity of this system can be used to determine the optimal control in terms of x and the value h of the Hamiltonian. The resulting evolution equation can be solved explicitly only in special situations, but implicit solutions expressing y and t as definite integrals depending on x can be formulated as follows.

Proposition 4. *Let $x_0 \in I$ and $h \in \mathbb{R}$ satisfy $\phi(x_0; h) \in \hat{\chi}_{\alpha,p}(\mathbb{R}^+)$ for $0 < \alpha < 1 \leq p$ or $\alpha = 1 < p$. Define $n_{\alpha,p}(\,\cdot\,; h) : [x_f, x_0] \to \mathbb{R}^+$ and $w_{\alpha,p}(\,\cdot\,; h) : [x_f, x_0]^2 \to \mathbb{R}^+$ by*

$$n_{\alpha,p}(x; h) := \frac{\mu(x)\hat{\chi}^{-1}_{\alpha,p}(\phi(x; h))}{r(x)} \qquad \text{and} \qquad w_{\alpha,p}(x, x_0; h) := \left(\frac{n_{\alpha,p}(x_0; h)}{n_{\alpha,p}(x, h)}\right)^2 .$$

If $n_{\alpha,p}(\,\cdot\,; h)$ has a strict minimum at x_0, then

$$y_{\alpha,p}(x; x_0, h) := \int_x^{x_0} \frac{d\xi}{\sqrt{w_{\alpha,p}(x_0, \xi; h) - 1}} \tag{22}$$

and

$$t_{\alpha,p}(x; x_0, h) := \int_x^{x_0} \frac{d\xi}{r(\xi)\hat{\sigma}_{\alpha,p}(\xi; h)\sqrt{1 - w_{\alpha,p}(\xi, x_0; h)}} \tag{23}$$

for $x_f \leq x < x_0$ implicitly determine the state variables of a solution in the level set $H^{-1}(h)$ of the Hamiltonian system determined by (21).

Proof. Invertibility of $\hat{\chi}_{\alpha,p}$ follows from the identity

$$\hat{\chi}_{\alpha,p}(\rho_{\alpha,p}(s)) = \tau_{\alpha,p}\,(1 - s^p)$$

and the invertibility of $\rho_{\alpha,p}$ and $\tau_{\alpha,p}$. Thus $\ell_\mu(\psi_z) = \hat{\chi}^{-1}_{\alpha,p}(\phi(z;h))$ and hence

$$\|\psi\| = \frac{\ell(\psi)}{r(x)} = \frac{\mu(x)\ell_\mu(\psi)}{r(x)} = n_{\alpha,p}(x;h)$$

along a solution $((x,y),\psi)$ lying in $H^{-1}(h)$ of the canonical Hamiltonian system determined by H.

The initial condition $\dot{x}(0) = 0$ implies that $\psi(0) = (0,\psi_2)$; since $\psi_2 \neq 0$ is constant and $n_{\alpha,p}(x;h)$ has a strict minimum at x_0, it follows that ψ is always nonzero and that ψ_1 equals zero only when $t = 0$. Hence

$$\frac{\psi}{\|\psi\|} = \frac{1}{\|\psi\|}\left(-\sqrt{\|\psi\|^2 - \psi_2^2}, \psi_2\right) = \left(-\sqrt{1 - \frac{\|\psi(0)\|^2}{\|\psi\|^2}}, \frac{\|\psi(0)\|}{\|\psi\|}\right). \tag{24}$$

(The signs are determined by the conditions $x_f < x_0$ and $y_f > 0$, which imply that $\dot{x}$ is negative and $\dot{y}$ is positive.)

It follows that there are functions $y_{\alpha,p}(x;x_0,h)$ and $t_{\alpha,p}(x;x_0,h)$ such that if $X_{\alpha,p}(x;x_0,h)$ denotes the value of the Hamiltonian vector field determined by (21) at the point $(x, y_{\alpha,p}(x;x_0,h))$, then

$$y'_{\alpha,p}(x;x_0,h) = \frac{X_{\alpha,p}(x;x_0,h)_2}{X_{\alpha,p}(x;x_0,h)_1} = -\sqrt{\frac{w_{\alpha,p}(x,x_0;h)}{1 - w_{\alpha,p}(x,x_0;h)}} = -\frac{1}{\sqrt{w_{\alpha,p}(x_0,x;h) - 1}},$$

and hence (22) holds. Analogously,

$$t'_{\alpha,p}(x;x_0,h) = \frac{1}{X_{\alpha,p}(x;x_0,h)_1}$$

implies (23).

Remark 3. If we introduce the angle $\theta_{\alpha,p}(x;x_0,h) := \sin^{-1}\sqrt{w_{\alpha,p}(x;x_0,h)}$, with $\theta_{\alpha,p}(x;x_0,h) \in \left(\frac{\pi}{2},\pi\right)$, then (24) implies that ψ has polar coordinates

$$(n_{\alpha,p}(x;x_0,h), \theta_{\alpha,p}(x;x_0,h))$$

at (x,y) and

$$y'_{\alpha,p}(x;x_0,h) = \tan\theta_{\alpha,p}(x;x_0,h).$$

However, we have found it more convenient in specific calculations to work with $w_{\alpha,p}$.

Proposition 4 provides implicit equations for solutions of the Hamiltonian system with Hamiltonian (21). Such trajectories qualify as solutions of the synthesis problem only if additional conditions on the parameters x_0 and h are satisfied.

Synthesis problem. The projectile must strike the target and the solution curve must lie in the zero level set of the Hamiltonian. Hence the initial position x_0 determines a solution of the synthesis problem $\iff$ $y_{\alpha,p}(x_f; x_0, 0) = y_f$.

Fixed time synthesis problem. The projectile must strike the target at the specified time t_f. Hence the initial position x_0 and Hamiltonian value h determine a solution of the time t_f synthesis problem $\iff$ $y_{\alpha,p}(x_f; x_0, h) = y_f$ and $t_{\alpha,p}(x_f; x_0, h) = t_f$.

Remark 4. Given x_0 and h such that $y_{\alpha,p}(\,\cdot\,; x_0, h)$ and $t_{\alpha,p}(\,\cdot\,; x_0, h)$ are well-defined on $[x_f, x_0]$ and $y_{\alpha,p}(x_f; x_0, h) = y_f$, one can, of course, *a posteriori* specify $t_{\alpha,p}(x_f; x_0, h)$ as the desired duration, thereby obtaining a solution of the corresponding fixed time optimal control problem. However, if there is a family of pairs (x_0, h) determining solutions of different durations that all strike the target and only one of these solutions will be implemented, some criterion for selecting that solution must be established.

5.1 $\alpha = \frac{1}{2}$, $p = 2$, and Constant $\frac{\mu}{r}$

The expressions for $y_{\alpha,p}$ and $t_{\alpha,p}$ as functions of x take a particularly simple form if $\alpha = \frac{1}{2}$, $p = 2$, and μ is proportional to the function r specifying the radii of the admissible control regions.

Corollary 2. *If $\frac{\mu}{r}$ is constant on I and $\phi(x; h) < 1$ for $x_f \le x < x_0$, define*

$$v(x_0, h) := \sqrt{1 - \phi(x_0; h)^{-2}}$$

and

$$\tilde{y}(x; x_0, h) := \int_x^{x_0} \frac{d\xi}{\sqrt{\left(\frac{\phi(\xi;h)}{\phi(x_0;h)}\right)^2 - 1}} \tag{25}$$

for $x_f \le x < x_0$. Then

$$y_{\frac{1}{2},2}(x; x_0, h) = v(x_0, h)\, \tilde{y}(x; x_0, h) \tag{26}$$

and

$$t_{\frac{1}{2},2}(x;x_0,h)=\int_x^{x_0}\frac{d\xi}{r(u)\sqrt{1-\left(\frac{\phi(x_0;h)}{\phi(\xi;h)}\right)^2}}.$$

Proof. $\hat{\chi}^{-1}_{\frac{1}{2},2}(\phi)=\sqrt{1-\phi^2}$ and $\frac{\mu}{r}=$ constant imply that

$$w_{\frac{1}{2},2}(x_0,x;h)=\left(\frac{\hat{\chi}^{-1}_{\frac{1}{2},2}(\phi(x;h))}{\hat{\chi}^{-1}_{\frac{1}{2},2}(\phi(x_0;h))}\right)^2=\frac{1-\phi(x;h)^2}{1-\phi(x_0;h)^2}=\frac{\left(\frac{\phi(x;h)}{\phi(x_0;h)}\right)^2-1}{1-\phi(x_0;h)^{-2}}+1.$$

Analogously,

$$1-w_{\frac{1}{2},2}(x,x_0;h)=\frac{1-\left(\frac{\phi(x_0;h)}{\phi(x;h)}\right)^2}{1-\phi(x;h)^{-2}}=\frac{1-\left(\frac{\phi(x_0;h)}{\phi(x;h)}\right)^2}{\hat{\sigma}_{\frac{1}{2},2}(x;h)^2}.$$

Substituting these expressions and $p=q=2$ into (22) and (23) yields (26).

The vertical component of the velocity at position $(x,y(x))$ is given by

$$\frac{y'_{\frac{1}{2},2}(x)}{t'_{\frac{1}{2},2}(x)}=v(x_0,h)r(x)\sqrt{\frac{1-\left(\frac{\phi(x_0;h)}{\phi(x;h)}\right)^2}{\left(\frac{\phi(x;h)}{\phi(x_0;h)}\right)^2-1}}=v(x_0,h)r(x)\frac{\phi(x_0;h)}{\phi(x;h)}.$$

Corollary 2 reveals several distinctive features of this special situation.

- The relationship between t and x does not depend on the value of the constant ratio $\frac{\mu}{r}$.
- The function $\tilde{y}$ determines the optimal solution of the unmoderated problem, corresponding to $\mu\equiv 0$, with initial velocity on the boundary of the admissible control region.
- The relationship between y and x depends on the ratio $\frac{\mu}{r}$ only via the scaling factor $v(x_0,h)$.
- x_0 determines a trajectory with energy h passing through the point (x_f,y_f) iff $(1,y_f)$ lies on the positive quadrant of the ellipsoid with principal axes $\phi(x_0;h)$ and $\tilde{y}(x_f;x_0,h)$.

If $\phi(x_0;0)$ and $\tilde{y}(x_f;x_0,0)$ determine a family of non-intersecting ellipsoids parametrized by x_0, then the synthesis problem with target (x_f,y_f) has a unique solution for each admissible value of the ratio $\frac{\mu}{r}$, with initial position $(x_0,0)$ and

initial velocity $(0, v(x_0, 0)\rho(x_0))$, for the unique value of x_0 such that the ellipse with principal axes $\phi(x_0; 0)$ and $\tilde{y}(x_f; x_0, 0)$ passes through $(1, y_f)$.

We now further specialize, considering the position-dependent cost term $\hat{C}(x) = \frac{c}{2x^2} + 1$ and admissible control region radius functions $r(x) = \frac{1}{x}$ or $r(x) = 1$. In these cases we can explicitly express $\tilde{y}$ and t as functions of x in terms of logarithms (for $\rho(x) = \frac{1}{x}$) or elliptic integrals (for $\rho(x) \equiv 1$). We present the solutions only for $h = 0$, corresponding to solutions of the synthesis problem; the expressions for nonzero h are similar, but involve somewhat messier coefficients.

If we set $\eta(x, x_0) := \sqrt{\left(\frac{c}{2x_0}\right)^2 - x^2}$, then

$$\tilde{y}(x; x_0, 0) = \left(\frac{c}{2x_0} + x_0\right)\left(\ln\left(\eta(x, x_0) + \sqrt{x_0^2 - x^2}\right) - \ln \eta(x_0, x_0)\right)$$

and

$$2t_{\frac{1}{2},2}(x; x_0, 0) = \left(\frac{c}{2x_0} + x_0\right)\tilde{y}(x; x_0, 0) - \eta(x, x_0)\sqrt{x_0^2 - x^2}$$

if $r(x) = \frac{1}{x}$.

Trajectories for some representative values of c, $\frac{\mu}{r}$, x_f, and x_0, with $r(x) = \frac{1}{x}$ and $y_f = 1$, are shown in Figure 5. Note that the more moderate the strategy, the further x_0 is from the target and the slower the initial ascent. Trajectories with moderation factor near the maximum allowable value show a slow, nearly vertical early phase, executed in relatively 'safe' territory (i.e. a subinterval of I on which $\hat{C}$ takes relatively small values) followed by a rapid, nearly horizontal late phase; those with low moderation factor launch closer to the target and rapidly pursue a more rounded path. Note that for this system, changes in the moderation factor $\frac{\mu}{r}$ result in relatively small changes in the optimal trajectory until $\frac{\mu}{r}$ is close to the maximum value.

The moderation factor does not correspond simply to increased or reduced sensitivity to risk, but influences the approach to reducing risk—a more moderate solution takes more time and travels a longer path overall, but in doing so, is able to devote most of its (constrained) speed to nearly horizontal motion when moving through the high-risk zone near the target. The differences as the moderation factor is changed are smaller if the risk is lower, either due to a smaller value of the risk factor c or to relatively large x_f, resulting in relatively small variation in risk from x_0 to x_f.

If we let $\mathscr{E}_E$ and $\mathscr{E}_F$ denote the incomplete elliptic integrals of the first and second kind, and define

$$\tilde{\gamma}_{\pm}(u; k) := \mathscr{E}_F(\sin^{-1} u; k) \pm \mathscr{E}_E(\sin^{-1} u; k), \qquad k(x_0) := -\left(1 + \frac{4x_0^2}{c}\right),$$

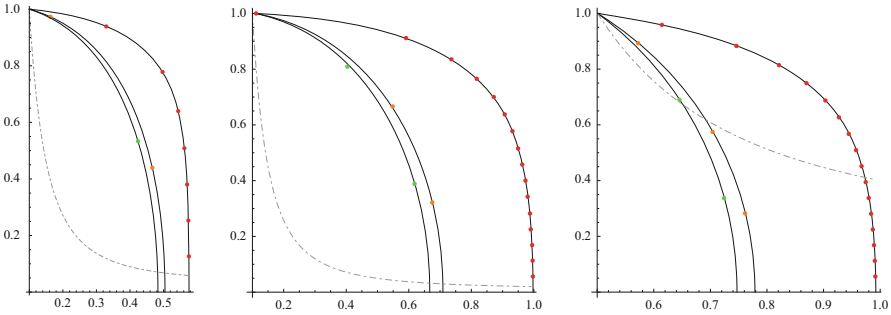

Fig. 5 Sample trajectories for $\alpha = \frac{1}{2}$, $p = 2$, and $r(x) = \frac{1}{x}$. Colored dots indicate positions at $t_j := \frac{j}{4}$. Left: $c = \frac{2}{3}$; green: $\frac{\mu}{r} = .05$, gold: $\frac{\mu}{r} = \frac{1}{\sqrt{3}}$, red: $\frac{\mu}{r} = \frac{2}{\sqrt{3}} - .05$; $x_f = \frac{1}{10}$. Center and right: $c = 2$; green: $\frac{\mu}{r} = .05$; gold: $\frac{\mu}{r} = 1$; red: $\frac{\mu}{r} = 1.95$; $x_f = \frac{1}{10}$ (center) or $\frac{1}{2}$ (right). The gray dashed lines indicate the normalized unmoderated cost $\frac{\hat{C}(x)}{\hat{C}(x_f)}$

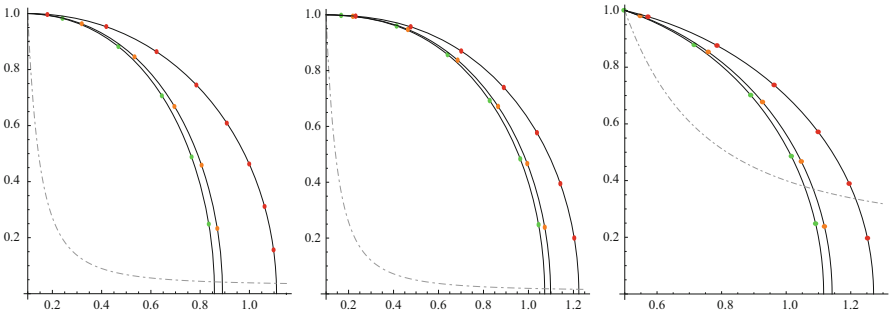

Fig. 6 Sample trajectories for $\alpha = \frac{1}{2}$, $p = 2$, and $r \equiv 1$. Colored dots indicate positions at $t_j := \frac{j}{4}$. Left: $c = \frac{2}{3}$; green: $\frac{\mu}{r} = .05$, gold: $\frac{\mu}{r} = \frac{1}{\sqrt{3}}$, red: $\frac{\mu}{r} = \frac{2}{\sqrt{3}} - .05$; $x_f = \frac{1}{10}$. Center and right: $c = 2$; green: $\frac{\mu}{r} = .05$; gold: $\frac{\mu}{r} = 1$; red: $\frac{\mu}{r} = 1.95$; $x_f = \frac{1}{10}$ (center) or $\frac{1}{2}$ (right). The gray dashed line indicates the normalized unmoderated cost $\frac{\hat{C}(x)}{\hat{C}(x_f)}$

and

$$\gamma_{\pm}(x; x_0) := x_0 \left(\tilde{\gamma}_{\pm} \left(\tfrac{x}{x_0}; k(x_0) \right) - \tilde{\gamma}_{\pm}(1; k(x_0)) \right),$$

then

$$\tilde{y}(x; x_0, 0) = \frac{\gamma_-(x; x_0)}{1 + \frac{1}{\hat{C}(x_0)}} \qquad \text{and} \qquad 2\, t_{\frac{1}{2},2}(x; x_0, 0) = \gamma_+(x; x_0) + \tfrac{1}{k(x_0)} \gamma_-(x; x_0)$$

if $r \equiv 1$.

Trajectories for some representative values of c, $\frac{\mu}{r}$, x_f, and x_0, with $r(x) \equiv 1$ and $y_f = 1$, are shown in Figure 6. As before, the more moderate the strategy, the further

x_0 is from the target and the slower the ascent. However, since the admissible control region is the unit ball for all values of x, there is less variation in the speed along any given solution and in the paths of the different solutions. All of the trajectories trace follow paths that are nearly, but not exactly, elliptical.

5.2 $\alpha = 1$, $p = 2$, and Constant $\frac{\mu}{r}$

We now consider the parameters values and cost functions (1) used in Section 2: $C_{\text{mi}} = \tilde{C}_{1,2}(\,\cdot\,, \mu) - \hat{C}$ for $\hat{C}$ as above and constant μ, and $C_{\text{ke}} = C_{\text{mi}} - 1 + \frac{\mu}{2}$. Thus solutions of the synthesis problem for C_{ke} correspond to solutions of an appropriate fixed time synthesis problem for C_{mi}. We derive the solutions of the synthesis problem for a general $\hat{C}$ (depending only on x) and Hamiltonian value h, before specializing to C_{mi}.

When $\alpha = 1$ and $p = 2$, the condition that the instantaneous cost be positive everywhere imposes the inequality $\phi(x; 0) > \frac{1}{2}$, and (18) takes the form

$$\hat{\chi}_{1,2}^{-1}(\phi) = \begin{cases} \sqrt{2\phi - 1} & \text{if} \quad \frac{1}{2} \le \phi < 1 \\ \phi & \text{if} \quad \phi \ge 1 \end{cases} \tag{27}$$

and

$$\hat{\sigma}_{1,2}(x; h) = \min\left\{\sqrt{2\,\phi(x; h) - 1}, 1\right\}.$$

For simplicity, we consider only trajectories such that either $\frac{1}{2} \le \phi(x; h) \le 1$ for $x_f \le x \le x_0$ or $1 \le \phi(x; h)$ for $x_f \le x \le x_0$; determining more general solutions involves patching together solutions of these kinds. Equation (27) implies that

$$w_{1,2}(x; x_0, h) = \begin{cases} \dfrac{2\,\phi(x_0; h) - 1}{2\,\phi(x; h) - 1} & \text{if} \quad \frac{1}{2} \le \phi(x_0; h) < \phi(x; h) \le 1 \\ \left(\dfrac{\phi(x_0; h)}{\phi(x; h)}\right)^2 & \text{if} \quad 1 \le \phi(x_0; h) \end{cases}$$

for constant $\frac{\mu}{r}$.

If $1 \le \phi(x_0; h)$, comparing (22) to (25) and (23) to (26) shows that in this situation

$$y_{1,2}(x; x_0, h) = \tilde{y}(x; x_0, h) = \frac{y_{\frac{1}{2},2}(x; x_0, h)}{v(x_0; h)} \qquad \text{and} \qquad t_{1,2}(x; x_0, h) = t_{\frac{1}{2},2}(x; x_0, h).$$

If $\frac{1}{2} \le \phi(x;h) \le 1$ for $x_f \le x \le x_0$, then

$$\frac{y_{1,2}(x;x_0,h)}{\hat{\sigma}_{1,2}(x_0;h)} = t_{1,2}(x;x_0,h) = \int_x^{x_0} \frac{d\xi}{\sqrt{2(\phi(\xi;h) - \phi(x_0;h))}}.$$

If we further specialize to the case $\hat{C}(x) = 1 + \frac{c}{2x^2}$, $r \equiv 1$, then

$$t_{1,2}(x;x_0,h) = \sqrt{\frac{x_0^2 - x^2}{\zeta(x_0)}} \qquad \text{and} \qquad \hat{\sigma}_{1,2}(x_0;h) = \zeta(x_0) + \tfrac{2(1+h)}{\mu} - 1$$

$$\text{for} \qquad \zeta(x_0) := \frac{c}{\mu\, x_0^2},$$

where μ denotes the constant value of the moderation factor. It follows that the projectile paths are segments of ellipses centered at the origin. We can easily express $z = (x, y)$ explicitly as a function of t in this case:

$$z_{1,2}(t;h) = \left(\sqrt{x_0^2 - \zeta(x_0)t^2}, \hat{\sigma}_{1,2}(x_0;h)t \right).$$

Setting $h = 0$ yields the state information of the synthesis problem for C_{mi}, while setting $h = \frac{\mu}{2} - 1$ gives the corresponding information for C_{ke}.

Remark 5. The graphs of $y_{1,2}(\,\cdot\,;x_0,h)$ are very nearly elliptical if $1 \le \phi(x_0;h)$, but do not exactly coincide with segments of ellipses.

References

1. Abraham, R., Marsden, J.E.: Foundations of Mechanics. Benjamin/Cummings Publishing Company, Reading, MA (1978)
2. Baillieul, J., Willems, J.C.: Mathematical Control Theory. Springer, New York (1999)
3. Bertolazzi, E., Biral, F., Da Lio, M.: Real-time motion planning for multibody systems: real life application examples. Multibody Syst. Dyn. **17**, 119–139 (2007)
4. Bloch, A.: Nonholonomic Mechanics and Control. Springer, New York (2003)
5. Bonnans, J.F., Guilbaud, Th.: Using logarithmic penalties in the shooting algorithm for optimal control problems. Optim. Control Appl. Methods **24**, 257–278 (2003)
6. Crane, R.: A copycat astronaut. LIFE **16**, 77–78 (1968)
7. Kane, T.R., Scher, M.P.: A dynamical explanation of the falling cat phenomenon. Int. J. Solids Struct. **5**, 663–670 (1969)
8. Leimkuhler, B., Reich, S.: Simulating Hamiltonian Dynamics. Cambridge University Press, Cambridge (2005)
9. Lewis, D.: Optimal control with moderation incentives (2010, preprint). arXiv:1001.0211v1 [math.OC]
10. Lewis, D., Olver, P.: Geometric integration algorithms on homogeneous manifolds. Found. Comput. Math. **2**, 363–392 (2002)

11. Lewis, D., Simo, J.C.: Conserving algorithms for the dynamics of Hamiltonian systems on Lie groups. J. Nonlinear Sci. **4**, 253–299 (1994)
12. Marey, E.-J.: Méchanique animale. La Nature **1119**, 569–570 (1894)
13. Montgomery, R.: Optimal control of deformable bodies and its relation to gauge theory. Math. Sci. Res. Inst. Publ. **22**, 403–438 (1991)
14. Montgomery, R.: Gauge theory of the falling cat. Fields Inst. Commun. **1**, 193–218 (1993)
15. Nijmeijer, H., van der Schaft, A.J.: Nonlinear Dynamical Control Systems. Springer, New York (1990)
16. Pontryagin, L.S., Boltyanskii, V.G., Gamkrelidze, R.V., Mishchenko, E.F.: The Mathematical Theory of Optimal Processes. Interscience Publishers, New York (1962)
17. Sontag, E.D.: Integrability of certain distributions associated with actions on manifolds and applications to control problems. In: Nonlinear Controlability and Optimal Control, pp. 81–131. Dekker, New York (1990)
18. Sontag, E.D.: Mathematical Control Theory: Deterministic Finite Dimensional Systems. Springer, New York (1998)
19. SYNODE Publication Database: http://www.math.ntnu.no/num/synode/bibliography.php (2003)

The Local Description of Discrete Mechanics

Juan C. Marrero, David Martín de Diego, and Eduardo Martínez

Dedicated to the memory of J.E. Marsden

Abstract In this paper, we introduce local expressions for discrete Mechanics. To apply our results simultaneously to several interesting cases, we derive these local expressions in the framework of Lie groupoids, following the program proposed by Alan Weinstein (Fields Inst Commun 7:207–231, 1996). To do this, we will need some results on the geometry of Lie groupoids, as, for instance, the construction of symmetric neighborhoods or the existence of local bisections. These local descriptions will be particularly useful for the explicit construction of geometric integrators for mechanical systems (reduced or not), in particular, discrete Euler-Lagrange equations, discrete Euler-Poincaré equations, discrete Lagrange-Poincaré equations... These topics are closely related with a part of Marsden's work. In addition, the results contained in this paper can be considered as a local version of the study that we have started in Marrero et al. (Nonlinearity 19(6):1313–1348, 2006), on the geometry of discrete Mechanics on Lie groupoids.

J.C. Marrero
Sección de Matemáticas, Unidad Asociada ULL-CSIC Geometría Diferencial y Mecánica Geométrica, Departamento de Matemáticas, Estadística e Investigación Operativa, Universidad de La Laguna, Tenerife, Canary Islands, Spain
e-mail: jcmarrer@ull.edu.es

D. Martín de Diego (✉)
Instituto de Ciencias Matemáticas, CSIC-UAM-UC3M-UCM, Campus de Cantoblanco, UAM, C/Nicolás Cabrera, 15 28049 Madrid, Spain
e-mail: david.martin@icmat.es

E. Martínez
IUMA - Departamento de Matemática Aplicada, Facultad de Ciencias, Universidad de Zaragoza, 50009 Zaragoza, Spain
e-mail: emf@unizar.es

D.E. Chang et al. (eds.), *Geometry, Mechanics, and Dynamics*, Fields Institute Communications 73, DOI 10.1007/978-1-4939-2441-7_13

1 Introduction

The use of geometrical methods in the study of dynamical systems (discrete or continuous) starts by searching for geometrical structures invariant with respect to the given dynamics (see [1]). It turns out the various such structures emerge naturally for classical mechanical systems, as for instance, symplectic or Poisson structures, together with various bundle structures. Another geometrical feature that is common to all such systems is the presence of symmetries either because there is a redundant or extra information in the description of the system or because the system possesses an intrinsic invariance. To actually solve them, it is necessary in most occasions to use numerical methods. Recently, a new breed of ideas in numerical analysis have come that incorporates the geometry of the systems into the analysis and that allows accurate and robust algorithms with lower spurious effects than the traditional ones (see [12] and references therein). Our approach employs the theory of discrete Mechanics and variational integrators [22, 30] to derive an integrator for the dynamics preserving some of the geometry of the original system. All this theory of discrete mechanics and their corresponding integrators have been quickly developed in the last twenty years mainly by Jerrold Marsden in Caltech, with the collaboration of students, postdocts and collaborators. Marsden and coworkers not only have studied from a geometrical perspective these new family of methods, but they have also explored concrete applications as, for instance, robotic simulation, spacecraft mission design, computer vision, fluid simulations, animation, between many others (see [7–11, 15, 16]).

One of the reasons for this formidable range of applications of variational integrators comes from their easy adaptability to different classes of mechanical systems: forced or dissipative systems, holonomically constrained systems, explicitly time-dependent systems, systems with frictional contact, nonholonomic dynamics, multisymplectic field theories among others (see [13, 14, 17, 18, 22, 23, 27, 28]).

From Jerrold Marsden we have learn to appreciate the importance of symmetry in the study of dynamical systems and, also of course, in discrete dynamics. In this sense, with our contribution in honor to J.E. Marsden we will follow his program, trying to emphasize the role of symmetry in discrete variational integrators using the unifying point of view given by the Lie groupoid theory. The study of discrete Mechanics on Lie groupoids was proposed by A. Weinstein in [29]. This setting is general enough to include discrete counterparts of several types of fundamental equations in Mechanics as for instance, standard Euler-Lagrange equations for Lagrangians defined on tangent bundles [1], Euler-Poincaré equations for Lagrangians defined on Lie algebras [24, 25], Lagrange-Poincaré equations for Lagrangians defined on Atiyah bundles, etc. Such discrete counterpart is obtained by discretizing the continuous Lagrangian to the corresponding Lie groupoid and then applying a discrete variational derivation of the discrete equations of motion. As simple examples, for a given differentiable manifold Q, the discrete version of

the tangent bundle TQ is the product manifold $Q \times Q$, equipped with the pair Lie groupoid structure; for a given Lie group G, the discrete version of its Lie algebra $\mathfrak{g}$ is the Lie group G.

A Lie groupoid G is a natural generalization of the concept of a Lie group, where now not all elements are composable. The product $g_1 g_2$ of two elements is only defined on the set of composable pairs $G_2 = \{(g, h) \in G \times G \,|\, \beta(g) = \alpha(h)\}$ where $\alpha : G \longrightarrow M$ and $\beta : G \longrightarrow M$ are the source and target maps over a base manifold M. Moreover, in a Lie groupoid we have a set of identities playing a similar role that the identity element in group theory. The infinitesimal counterpart of the notion of a Lie groupoid is the notion of a Lie algebroid $\tau_{AG} : AG \to M$, in the same way as the infinitesimal counterpart of the notion of a Lie group is the notion of a Lie algebra, or in other words, the discrete version of a Lie algebroid is a Lie groupoid.

In [21] we have elucidated the geometrical framework for discrete Mechanics on Lie groupoids. In that paper, we found intrinsic expressions for the discrete Euler-Lagrange equations, and we have introduced the Poincaré-Cartan sections, the discrete Legendre transformations and the discrete evolution operator in both the Lagrangian and the Hamiltonian formalism. The notion of regularity has been completely characterized and we have proven the symplecticity of the discrete evolution operators. The applicability of these developments has been stated in several interesting examples, in particular for the case of discrete Lagrange-Poincaré equations. In fact, the general theory of discrete symmetry reduction directly follows from our results.

The main objective of this paper is to obtain local expressions for the different objects appearing in discrete Mechanics on Lie groupoids. For this proposal, it is necessary to introduce symmetric neighborhoods of a Lie groupoid. A symmetric neighborhood is an open neighborhood of one point in the manifold of the identities which is "natural" with respect to the structure maps of the Lie groupoid, in the sense of Proposition 1. Using the coordinates associated to a symmetric neighborhood we may write the local expressions of left and right invariant vector fields, $\overleftarrow{X}$ and $\overrightarrow{X}$ associated to a section $X \in \Gamma(\tau_{AG})$ of the associated Lie algebroid. Now, as we have deduced in [6], the discrete Euler-Lagrange equations for a discrete Lagrangian $L_d : G \to \mathbb{R}$ are

$$\overleftarrow{X}(g_k)(L_d) - \overrightarrow{X}(g_{k+1})(L_d) = 0 \,, \quad (g_k, g_{k+1}) \in G_2 \,.$$

Therefore, from this expression, we easily obtain the local expression of the discrete Euler-Lagrange equations associated to a discrete Lagrangian $L_d : G \to \mathbb{R}$, the discrete Legendre transformations and we locally characterize the regularity of the discrete problem.

An interesting point is that when using symmetric neighborhoods we are implicitly assuming that the discrete flow is well defined on this neighborhood. However, this is not the more general situation since, in principle, the point g_k and its image g_{k+1} under the discrete flow may be far enough in such a way both are not

included in the same symmetric neighborhood. In order to tackle this problem we will use bisections of the Lie groupoid which permits to translate neighborhoods of two composable elements g_k and g_{k+1} to a symmetric neighborhood at the identity point $\beta(g_k) = \alpha(g_{k+1})$.

The organization of the paper is as follows. In Section 2 we recall some constructions and results on discrete Mechanics on Lie groupoids which will be used in the next sections. In Section 3, we will obtain a local expression of the discrete Euler-Lagrange equation for a discrete Lagrangian function on a symmetric neighborhood in the Lie groupoid where it is defined. In addition we will discuss the existence of local discrete Euler-Lagrange evolution operators in such a symmetric neighborhood. Moreover, several interesting examples are considered. The existence of general local discrete Euler-Lagrange evolution operators is studied in Section 4. For this purpose, we will use bisections on the Lie groupoid. The paper ends with our conclusions and a description of future research directions.

2 Groupoids and Discrete Mechanics

2.1 Lie Groupoids

In this Section, we will recall the definition of a Lie groupoid and some generalities about them are explained (for more details, see [4, 20]).

A ***groupoid*** over a set M is a set G together with the following structural maps:

- A pair of maps $\alpha : G \to M$, the ***source***, and $\beta : G \to M$, the ***target***. Thus, an element $g \in G$ is thought as an arrow from $x = \alpha(g)$ to $y = \beta(g)$ in M

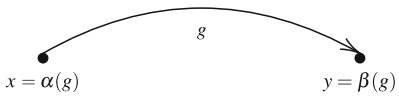

  The maps α and β define the set of composable pairs

$$G_2 = \{(g, h) \in G \times G / \beta(g) = \alpha(h)\}.$$

- A ***multiplication*** $m : G_2 \to G$, to be denoted simply by $m(g, h) = gh$, such that
  - $\alpha(gh) = \alpha(g)$ and $\beta(gh) = \beta(h)$.
  - $g(hk) = (gh)k$.

If g is an arrow from $x = \alpha(g)$ to $y = \beta(g) = \alpha(h)$ and h is an arrow from y to $z = \beta(h)$ then gh is the composite arrow from x to z

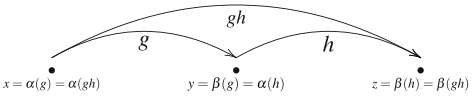

- An ***identity map*** $\varepsilon : M \to G$, a section of α and β, such that
  - $\varepsilon(\alpha(g))g = g$ and $g\varepsilon(\beta(g)) = g$.
- An ***inversion map*** $i : G \to G$, to be denoted simply by $i(g) = g^{-1}$, such that
  - $g^{-1}g = \varepsilon(\beta(g))$ and $gg^{-1} = \varepsilon(\alpha(g))$.

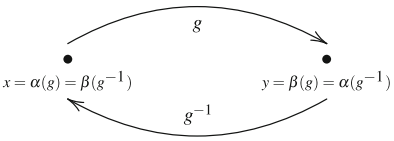

A groupoid G over a set M will be denoted simply by the symbol $G \rightrightarrows M$.

The groupoid $G \rightrightarrows M$ is said to be a ***Lie groupoid*** if G and M are manifolds and all the structural maps are differentiable with α and β differentiable submersions. If $G \rightrightarrows M$ is a Lie groupoid then m is a submersion, ε is an immersion and i is a diffeomorphism. Moreover, if $x \in M$, $\alpha^{-1}(x)$ (resp., $\beta^{-1}(x)$) will be said the ***α-fiber*** (resp., the ***β-fiber***) of x.

On the other hand, if $g \in G$ then the ***left-translation by*** $g \in G$ and the ***right-translation by*** g are the diffeomorphisms

$$l_g : \alpha^{-1}(\beta(g)) \longrightarrow \alpha^{-1}(\alpha(g)) \ ; \ h \longrightarrow l_g(h) = gh,$$
$$r_g : \beta^{-1}(\alpha(g)) \longrightarrow \beta^{-1}(\beta(g)) \ ; \ h \longrightarrow r_g(h) = hg.$$

Note that $l_g^{-1} = l_{g^{-1}}$ and $r_g^{-1} = r_{g^{-1}}$.

A vector field $\tilde{X}$ on G is said to be ***left-invariant*** (resp., ***right-invariant***) if it is tangent to the fibers of α (resp., β) and $\tilde{X}(gh) = (T_h l_g)(\tilde{X}_h)$ (resp., $\tilde{X}(gh) = (T_g r_h)(\tilde{X}(g))$), for $(g, h) \in G_2$.

Now, we will recall the definition of the ***Lie algebroid associated with*** G.

We consider the vector bundle $\tau : AG \to M$, whose fiber at a point $x \in M$ is $A_x G = V_{\varepsilon(x)}\alpha = Ker(T_{\varepsilon(x)}\alpha)$. It is easy to prove that there exists a bijection between the space $\Gamma(\tau)$ and the set of left-invariant (resp., right-invariant) vector

fields on G. If X is a section of $\tau : AG \to M$, the corresponding left-invariant (resp., right-invariant) vector field on G will be denoted $\overleftarrow{X}$ (resp., $\overrightarrow{X}$), where

$$\overleftarrow{X}(g) = (T_{\varepsilon(\beta(g))} l_g)(X(\beta(g))), \tag{1}$$

$$\overrightarrow{X}(g) = -(T_{\varepsilon(\alpha(g))} r_g)((T_{\varepsilon(\alpha(g))} i)(X(\alpha(g)))), \tag{2}$$

for $g \in G$. Using the above facts, we may introduce a Lie algebroid structure $([\![\cdot, \cdot]\!], \rho)$ on AG, which is defined by

$$\overleftarrow{[\![X, Y]\!]} = [\overleftarrow{X}, \overleftarrow{Y}], \quad \rho(X)(x) = (T_{\varepsilon(x)}\beta)(X(x)), \tag{3}$$

for $X, Y \in \Gamma(\tau)$ and $x \in M$. Note that

$$\overrightarrow{[\![X, Y]\!]} = -[\overrightarrow{X}, \overrightarrow{Y}], \quad [\overrightarrow{X}, \overleftarrow{Y}] = 0, \tag{4}$$

$$Ti \circ \overrightarrow{X} = -\overleftarrow{X} \circ i, \quad Ti \circ \overleftarrow{X} = -\overrightarrow{X} \circ i, \tag{5}$$

(for more details, see [5, 20]).

2.2 Discrete Euler-Lagrange Equations

Let G be a Lie groupoid with structural maps

$$\alpha, \beta : G \to M, \quad \varepsilon : M \to G, \quad i : G \to G, \quad m : G_2 \to G.$$

Denote by $\tau : AG \to M$ the Lie algebroid of G.

A ***discrete Lagrangian*** is a function $L_d : G \to \mathbb{R}$. Fixed $g \in G$, we define the set of admissible sequences with values in G:

$$\mathscr{C}_g^N = \{(g_1, \ldots, g_N) \in G^N \ / \ (g_k, g_{k+1}) \in G_2 \text{ for } k = 1, \ldots, N-1 \text{ and } g_1 \ldots g_N = g\}.$$

An admissible sequence $(g_1, \ldots, g_N) \in \mathscr{C}_g^N$ is a solution of ***the discrete Euler-Lagrange equations*** if

$$0 = \sum_{k=1}^{N-1} \left[\overleftarrow{X}_k(g_k)(L_d) - \overrightarrow{X}_k(g_{k+1})(L_d) \right], \quad \text{for } X_1, \ldots, X_{N-1} \in \Gamma(\tau).$$

For $N = 2$ we obtain that $(g, h) \in G_2$ is a solution if

$$\overleftarrow{X}(g)(L_d) - \overrightarrow{X}(h)(L_d) = 0$$

for every section X of AG.

2.3 Discrete Poincaré-Cartan Sections

Given a Lagrangian function $L_d : G \to \mathbb{R}$, we will study the geometrical properties of the discrete Euler-Lagrange equations.

Consider the vector bundle

$$\pi^\tau : P^\tau G = V\beta \oplus V\alpha \to G$$

where $V\alpha$ (respectively, $V\beta$) is the vertical bundle of the source map $\alpha : G \to M$ (respectively, the target map $\beta : G \to M$). Then, one may introduce a Lie algebroid structure on $\pi^\tau : P^\tau G = V\beta \oplus V\alpha \to G$. The anchor map $\rho^{P^\tau G} : P^\tau G = V\beta \oplus V\alpha \to TG$ is given by

$$\rho^{P^\tau G}(X_g, Y_g) = X_g + Y_g, \quad \text{for } (X_g, Y_g) \in V_g\beta \oplus V_g\alpha$$

and the Lie bracket $[\![\cdot, \cdot]\!]^{P^\tau G}$ on the space $\Gamma(\pi^\tau)$ is characterized by the following relation

$$[\![(\overrightarrow{X}, \overleftarrow{Y}), (\overrightarrow{X'}, \overleftarrow{Y'})]\!]^{P^\tau G} = (-\overrightarrow{[\![X, X']\!]}, \overleftarrow{[\![Y, Y']\!]}), \tag{6}$$

for $X, Y, X', Y' \in \Gamma(\tau)$ (see [21]).

Now, define the ***Poincaré-Cartan 1-sections*** $\Theta^-_{L_d}, \Theta^+_{L_d} \in \Gamma((\pi^\tau)^*)$ as follows

$$\Theta^-_{L_d}(g)(X_g, Y_g) = -X_g(L_d), \qquad \Theta^+_{L_d}(g)(X_g, Y_g) = Y_g(L_d), \tag{7}$$

for each $g \in G$ and $(X_g, Y_g) \in V_g\beta \oplus V_g\alpha$.

If d is the differential of the Lie algebroid $\pi^\tau : P^\tau G = V\beta \oplus V\alpha \to G$ we have that $dL_d = \Theta^+_{L_d} - \Theta^-_{L_d}$ and so, using $d^2 = 0$, it follows that $d\Theta^+_{L_d} = d\Theta^-_{L_d}$. This means that there exists a unique 2-section $\Omega_{L_d} = -d\Theta^+_{L_d} = -d\Theta^-_{L_d}$, that will be called the ***Poincaré-Cartan*** 2-section. This 2-section will be important for studying symplecticity of the discrete Euler-Lagrange equations.

Let X be a section of the Lie algebroid $\tau : AG \to M$. Then, one may consider the sections $X^{(1,0)}$ and $X^{(0,1)}$ of the vector bundle $\pi^\tau : P^\tau G = V\beta \oplus V\alpha \to G$ given by

$$X^{(1,0)}(g) = (\overrightarrow{X}(g), 0_g), \quad X^{(0,1)}(g) = (0_g, \overleftarrow{X}(g)), \quad \text{for } g \in G.$$

Moreover, if $g \in G$, $\{X_\gamma\}$ (respectively, $\{Y_\mu\}$) is a local basis of $\Gamma(\tau)$ in an open subset U (respectively, V) of M such that $\alpha(g) \in U$ (respectively, $\beta(g) \in V$) then $\{X_\gamma^{(1,0)}, Y_\mu^{(0,1)}\}$ is a local basis of $\Gamma(\pi^\tau)$ in $\alpha^{-1}(U) \cap \beta^{-1}(V)$ and

$$\Omega_{L_d}(X_\gamma^{(1,0)}, Y_\mu^{(1,0)}) = \Omega_{L_d}(X_\gamma^{(0,1)}, Y_\mu^{(0,1)}) = 0, \tag{8}$$

and

$$\Omega_{L_d}(X_\gamma^{(1,0)}, Y_\mu^{(0,1)}) = \overleftarrow{Y_\mu}(\overrightarrow{X_\gamma}(L_d)) = \overrightarrow{X_\gamma}(\overleftarrow{Y_\mu}(L_d)). \tag{9}$$

(for more details, see [21]).

2.4 Discrete Lagrangian Evolution Operator

We say that a differentiable mapping $\Psi : G \longrightarrow G$ is a ***discrete flow*** or a ***discrete Lagrangian evolution operator for*** L_d if it verifies the following properties:

- graph$(\Psi) \subseteq G_2$, that is, $(g, \Psi(g)) \in G_2$, $\forall g \in G$.
- $(g, \Psi(g))$ is a solution of the discrete Euler-Lagrange equations, for all $g \in G$, that is,

$$\overleftarrow{X}(g)(L_d) - \overrightarrow{X}(\Psi(g))(L_d) = 0 \tag{10}$$

for every section X of AG and every $g \in G$.

2.5 Discrete Legendre Transformations

Given a discrete Lagrangian $L_d : G \to \mathbb{R}$ we define two ***discrete Legendre transformations*** $\mathbb{F}^- L_d : G \longrightarrow A^*G$ and $\mathbb{F}^+ L_d : G \longrightarrow A^*G$ as follows (see [21])

$$(\mathbb{F}^- L_d)(h)(v_{\varepsilon(\alpha(h))}) = -v_{\varepsilon(\alpha(h))}(L_d \circ r_h \circ i), \text{ for } v_{\varepsilon(\alpha(h))} \in A_{\alpha(h)}G, \tag{11}$$

$$(\mathbb{F}^+ L_d)(g)(v_{\varepsilon(\beta(g))}) = v_{\varepsilon(\beta(g))}(L_d \circ l_g), \text{ for } v_{\varepsilon(\beta(g))} \in A_{\beta(g)}G. \tag{12}$$

Remark 1. Note that $(\mathbb{F}^+ L_d)(g) \in A^*_{\beta(g)}G$ and $(\mathbb{F}^- L_d)(h) \in A^*_{\alpha(h)}G$. Furthermore, if $\{X_\gamma\}$ (respectively, $\{Y_\mu\}$) is a local basis of $\Gamma(\tau)$ in an open subset U such that $\alpha(h) \in U$ (respectively, $\beta(g) \in V$) and $\{X^\gamma\}$ (respectively, $\{Y^\mu\}$) is the dual basis of $\Gamma(\tau^*)$, it follows that

$$\mathbb{F}^- L_d(h) = \overrightarrow{X}_\gamma(h)(L_d)X^\gamma(\alpha(h)), \quad \mathbb{F}^+ L_d(g) = \overleftarrow{Y}_\mu(g)(L_d)Y^\mu(\beta(g)).$$

2.6 Discrete Regular Lagrangians

A Lagrangian $L_d : G \to \mathbb{R}$ on a Lie groupoid G is said to be ***regular*** if the Poincaré-Cartan 2-section Ω_{L_d} is symplectic on the Lie algebroid $\pi^\tau : P^\tau G \equiv V\beta \oplus_G V\alpha \to G$, that is, Ω_{L_d} is nondegenerate (see [21]).

Using (9), we deduce that the Lagrangian L_d is regular if and only if for every $g \in G$ and every local basis $\{X_\gamma\}$ (respectively, $\{Y_\mu\}$) of $\Gamma(\tau)$ on an open subset U (respectively, V) of M such that $\alpha(g) \in U$ (respectively, $\beta(g) \in V$) we have that the matrix $\overrightarrow{X_\gamma}(\overleftarrow{Y_\mu}(L_d))$ is regular on $\alpha^{-1}(U) \cap \beta^{-1}(V)$.

In [21], we have proved that the following conditions are equivalent:

- $L_d : G \to \mathbb{R}$ is a regular discrete Lagrangian function.
- The Legendre transformation $\mathbb{F}^- L_d$ is a local diffeomorphism.
- The Legendre transformation $\mathbb{F}^+ L_d$ is a local diffeomorphism.

Moreover, if $L_d : G \to \mathbb{R}$ is regular and $(g_0, h_0) \in G_2$ is a solution of the discrete Euler-Lagrange equations for L_d then there exist two open subsets U_0 and V_0 of G, with $g_0 \in U_0$ and $h_0 \in V_0$, and there exists a (local) discrete Lagrangian evolution operator $\Psi_{L_d} : U_0 \to V_0$ such that:

- $\Psi_{L_d}(g_0) = h_0$,
- Ψ_{L_d} is a diffeomorphism and
- Ψ_{L_d} is unique, that is, if U_0' is an open subset of G, with $g_0 \in U_0'$ and $\Psi'_{L_d} : U_0' \to G$ is a (local) discrete Lagrangian evolution operator then $\Psi'_{L_d}|U_0 \cap U_0' = \Psi_{L_d}|U_0 \cap U_0'$.

3 Discrete Euler-Lagrange Equations: Symmetric Neighborhoods

3.1 Symmetric Neighborhoods

First, we prove the following result

Proposition 1. *Let $\mathscr{U}$ be an open subset of G and $x_0 \in M$ be a point such that $\varepsilon(x_0) \in \mathscr{U}$. There exists an open subset $\mathscr{W} \subset \mathscr{U}$ of G with $\varepsilon(x_0) \in \mathscr{W}$ and such that*

1. *$\varepsilon(\alpha(\mathscr{W})) \subset \mathscr{W}$ and $\varepsilon(\beta(\mathscr{W})) \subset \mathscr{W}$,*
2. *$i(\mathscr{W}) = \mathscr{W}$, and*
3. *$m((\mathscr{W} \times \mathscr{W}) \cap G_2) \subset \mathscr{U}$.*

*The open subset $\mathscr{W}$ is said to be a **symmetric neighborhood** associated to $\mathscr{U}$ and x_0.*

Proof. The multiplication map $m\colon G_2 \to G$ is continuous, so that we may choose an open subset $\mathscr{W}_1$ of G such that $\varepsilon(x_0) \in \mathscr{W}_1$ and $m((\mathscr{W}_1 \times \mathscr{W}_1) \cap G_2) \subset \mathscr{U}$. Since the identity map $\varepsilon\colon M \to G$ is also continuous, we deduce that there exists an open subset $\mathscr{V}'$ of M such that $x_0 \in \mathscr{V}'$ and $\varepsilon(\mathscr{V}') \subset \mathscr{W}_1$. Thus, if we consider the open $\mathscr{W}_2$ of G given by $\mathscr{W}_2 = \mathscr{W}_1 \cap \alpha^{-1}(\mathscr{V}') \cap \beta^{-1}(\mathscr{V}')$, then it is clear that $\varepsilon(x_0) \in \mathscr{W}_2$ and moreover it is easy to prove that $\varepsilon(\alpha(\mathscr{W}_2)) \subset \mathscr{W}_2$ and $\varepsilon(\beta(\mathscr{W}_2)) \subset \mathscr{W}_2$, and also $m((\mathscr{W}_2 \times \mathscr{W}_2) \cap G_2) \subset \mathscr{U}$. Finally, if we take $\mathscr{W} = \mathscr{W}_2 \cap i(\mathscr{W}_2)$ it follows that $\mathscr{W}$ satisfies the three above mentioned conditions.

3.2 Local Coordinate Expressions of Structural Maps

On a symmetric neighborhood of a point it is easy to get local coordinate expressions for the structure maps of the Lie groupoid G. We consider a point $x_0 \in M$ and a local coordinate system (x, u), defined in a neighborhood $\mathscr{U} \subset G$ of $\varepsilon(x_0)$, adapted to the fibration $\alpha\colon G \to M$, i.e. if the coordinates of $g \in \mathscr{U}$ are (x^i, u^γ) then the coordinates of $\alpha(g) \in M$ are (x^i). We can moreover assume that the identities correspond to elements with coordinates $(x, 0)$. The target map β defines a local function b as follows: if the coordinates of g are (x, u), then the coordinates of $\beta(g)$ are $\mathsf{b}(x, u)$. Note that $\mathsf{b}(x, 0) = x$. Two elements g and h with coordinates (x, u) and (y, v) are composable if and only if $y = \mathsf{b}(x, u)$. Hence local coordinates for G_2 are given by (x, u, v).

To obtain a local description for the product, we consider a symmetric neighborhood $\mathscr{W}$ associated to x_0 and $\mathscr{U}$. If two elements $g, h \in \mathscr{W}$ with coordinates (x, u) and (y, v) respectively, are composable then $y = \mathsf{b}(x, u)$, and the product gh has coordinates $(x, \mathsf{p}(x, u, v))$ for some smooth function p. We will write

$$(x, u) \cdot (y, v) = (x, \mathsf{p}(x, u, v)). \tag{13}$$

The relation $\beta(gh) = \beta(h)$, for $(g, h) \in G_2$, imposes the restriction $\mathsf{b}(y, v) = \mathsf{b}(x, \mathsf{p}(x, u, v))$, i.e.

$$\mathsf{b}(\mathsf{b}(x, u), v) = \mathsf{b}(x, \mathsf{p}(x, u, v)). \tag{14}$$

The property $g\varepsilon(\beta(g)) = g$, for $g \in \mathscr{W}$, is locally equivalent to the equation $\mathsf{p}(x, u, 0) = u$; while the property $\varepsilon(\alpha(g))g = g$ is locally equivalent to the equation $\mathsf{p}(x, 0, v) = v$. Therefore

$$\mathsf{p}(x, u, 0) = u, \qquad \mathsf{p}(x, 0, v) = v. \tag{15}$$

Associativity $(gh)k = g(hk)$ imposes the further relation

$$\mathsf{p}(x, \mathsf{p}(x, u, v), w) = \mathsf{p}(x, u, \mathsf{p}(y, v, w)) \qquad \text{with } y = \mathsf{b}(x, u). \tag{16}$$

In what follows we will use the following functions defined in terms of $\mathsf{b}(x, u)$ and $\mathsf{p}(x, u, v)$,

$$\begin{aligned} \rho^i_\gamma(x) &= \frac{\partial \mathsf{b}^i}{\partial u^\gamma}(x, 0) \\ L^\gamma_\mu(x, u) &= \frac{\partial \mathsf{p}^\gamma}{\partial v^\mu}(x, u, 0) \\ R^\gamma_\mu(x, v) &= \frac{\partial \mathsf{p}^\gamma}{\partial u^\mu}(x, 0, v). \end{aligned} \tag{17}$$

We will also take into account that

$$\begin{aligned} &\frac{\partial \mathsf{p}^\gamma}{\partial u^\mu}(x, u, 0) = \delta^\gamma_\mu && \frac{\partial^2 \mathsf{p}^\gamma}{\partial u^\mu \partial u^\nu}(x, u, 0) = 0 \\ &\frac{\partial \mathsf{p}^\gamma}{\partial v^\mu}(x, 0, v) = \delta^\gamma_\mu && \frac{\partial^2 \mathsf{p}^\gamma}{\partial v^\mu \partial v^\nu}(x, 0, v) = 0, \end{aligned} \tag{18}$$

which follow from (15). The only relevant second order derivatives are given by

$$C^\gamma_{\mu\nu}(x) \equiv \frac{\partial^2 \mathsf{p}^\gamma}{\partial u^\mu \partial v^\nu}(x, 0, 0) - \frac{\partial^2 \mathsf{p}^\gamma}{\partial v^\mu \partial u^\nu}(x, 0, 0). \tag{19}$$

From the definition of L^γ_μ and R^γ_μ it follows that

$$\begin{aligned} C^\gamma_{\mu\nu}(x) &= \frac{\partial L^\gamma_\nu}{\partial u^\mu}(x, 0) - \frac{\partial L^\gamma_\mu}{\partial u^\nu}(x, 0) \\ &= \frac{\partial R^\gamma_\mu}{\partial v^\nu}(x, 0) - \frac{\partial R^\gamma_\nu}{\partial v^\mu}(x, 0). \end{aligned} \tag{20}$$

On the other hand, if $i : G \to G$ is the inversion we have that

$$i(x, u) = (\mathsf{b}(x, u), \iota(x, u))$$

and the condition $i(\varepsilon(x)) = \varepsilon(x)$, for all $x \in M$, implies that

$$\iota(x, 0) = 0.$$

Moreover, using that $\mathsf{p}(x,u,\iota(x,u))=0$, we deduce that

$$\frac{\partial \mathsf{p}^\gamma}{\partial u^\mu}(x,u,\iota(x,u))+\frac{\partial \iota^\nu}{\partial u^\mu}(x,u)\frac{\partial \mathsf{p}^\gamma}{\partial v^\nu}(x,u,\iota(x,u))=0.$$

Thus, from (18), we obtain that

$$\frac{\partial \iota^\gamma}{\partial u^\mu}(x,0)=-\delta^\gamma_\mu. \tag{21}$$

3.3 Invariant Vector Fields

The local expression for left- and right-translations are easy to obtain. For $g_0 \in \mathscr{W} \subset G$ the left translation l_{g_0} is the map $l_{g_0}\colon \alpha^{-1}(\beta(g_0)) \to \alpha^{-1}(\alpha(g_0))$, given by $l_{g_0}g = g_0 g$. If g_0 has coordinates (x_0,u_0), then the elements on the α-fiber $\alpha^{-1}(\beta(g_0))$ have coordinates of the form $(\mathsf{b}(x_0,u_0),v)$, and the coordinates of $l_{g_0}g$ are $(x_0,\mathsf{p}(x_0,u_0,v))$. We will write

$$l_{(x_0,u_0)}(\mathsf{b}(x_0,u_0),v)=(x_0,\mathsf{p}(x_0,u_0,v)). \tag{22}$$

Similarly, for $h_0 \in \mathscr{W} \subset G$ the right translation map $r_{h_0}\colon \beta^{-1}(\alpha(h_0)) \to \beta^{-1}(\beta(h_0))$, is defined by $r_{h_0}g = gh_0$. If h_0 has coordinates (x_0,u_0), then the elements on the β-fiber $\beta^{-1}(\alpha(h_0))$ have coordinates of the form (x,u) with the restriction $\mathsf{b}(x,u)=x_0$, and the coordinates of $r_{h_0}g$ are $(x,\mathsf{p}(x,u,u_0))$. We will write

$$r_{(x_0,u_0)}(x,u)=(x,\mathsf{p}(x,u,u_0)). \tag{23}$$

A left-invariant vector field is of the form $\overleftarrow{X}(g) = T_{\varepsilon(\beta(g))}l_g(v)$ for $v \in \ker T_{\varepsilon(\beta(g))}\alpha$. To obtain a local basis of left-invariant vector fields we can take the local coordinate basis $e_\gamma = \frac{\partial}{\partial u^\gamma}|_{\varepsilon(\beta(g))}$ of $\ker T_{\varepsilon(\beta(g))}\alpha$. Thus, for $g \in G$ with coordinates (x,u), we have

$$\overleftarrow{e_\gamma}(g)=T_{\varepsilon(\beta(g))}l_g\left(\frac{\partial}{\partial u^\gamma}\Big|_{\varepsilon(\beta(g))}\right)=\frac{\partial \mathsf{p}^\mu}{\partial v^\gamma}(x,u,0)\frac{\partial}{\partial u^\mu}\Big|_g=L^\mu_\gamma(x,u)\frac{\partial}{\partial u^\mu}\Big|_{(x,u)}. \tag{24}$$

Similarly, a right-invariant vector field can be written in the form $\overrightarrow{X}(g) = T_{\varepsilon(\alpha(g))}r_g(v)$ for $v \in \ker T_{\varepsilon(\alpha(g))}\beta$. To obtain a local basis of right-invariant vector fields we first have to look for a basis of the vector space $\ker T_{\varepsilon(\alpha(g))}\beta$. From the definition of the functions ρ^i_γ, it follows easily that the vectors $f_\gamma = \rho^i_\gamma \frac{\partial}{\partial x^i} - \frac{\partial}{\partial u^\gamma}$ are in $\ker T_{\varepsilon(\alpha(g))}\beta$, and moreover they are related to the vectors e_γ by the inversion

map, that is $Ti(e_\gamma) = f_\gamma$. It follows that a basis of right invariant vector fields is given by

$$\begin{aligned}\overrightarrow{e_\gamma}(g) &= T_{\varepsilon(\alpha(g))}r_g\left(-\rho^i_\gamma \frac{\partial}{\partial x^i}\Big|_{\varepsilon(\alpha(g))} + \frac{\partial}{\partial u^\gamma}\Big|_{\varepsilon(\alpha(g))}\right)\\ &= -\rho^i_\gamma(x)\frac{\partial}{\partial x^i}\Big|_g + \left(-\rho^i_\gamma(x)\frac{\partial \mathsf{p}^\mu}{\partial x^i}(x,0,u) + \frac{\partial \mathsf{p}^\mu}{\partial u^\gamma}(x,0,u)\right)\frac{\partial}{\partial u^\mu}\Big|_g \qquad (25)\\ &= -\rho^i_\gamma(x)\frac{\partial}{\partial x^i}\Big|_g + R^\mu_\gamma(x,u)\frac{\partial}{\partial u^\mu}\Big|_g,\end{aligned}$$

where as before (x, u) are the coordinates for $g \in G$. Note that, from (15), we deduce that $\dfrac{\partial \mathsf{p}^\mu}{\partial x^i}(x, 0, u) = 0$.

3.4 The Lie Algebroid of G

The Lie algebroid of G is defined on the vector bundle $\tau\colon E \to M$ with fiber at the point $x \in M$ given by $E_x = \ker T_{\varepsilon(x)}\alpha$. A local basis of sections of E is given by the coordinate vector fields $e_\gamma(x) = \frac{\partial}{\partial u^\gamma}|_{\varepsilon(x)}$. The anchor is the map $\rho\colon E \to TM$ defined by $\rho(a) = T_{\varepsilon(x)}\beta(a)$, where $x = \tau(a)$. In local coordinates, if $a = y^\gamma e_\gamma(x)$ then $\rho(a) = \rho^i_\gamma(x)y^\gamma \frac{\partial}{\partial x^i}\Big|_x$. The bracket is defined in terms of the bracket of left-invariant vector fields. A simple calculation shows that $[\overleftarrow{e_\gamma}, \overleftarrow{e_\mu}] = C^\nu_{\gamma\mu}\overleftarrow{e}_\nu$, with $C^\nu_{\gamma\mu}$ given by (19), from where we get $[\![e_\gamma, e_\mu]\!] = C^\nu_{\gamma\mu}e_\nu$.

3.5 Discrete Euler-Lagrange Equations

Consider now a discrete Lagrangian function L_d. A composable pair $(g, h) \in G_2$ satisfies the Euler-Lagrange equations for L_d if

$$\overleftarrow{X}(g)(L_d) = \overrightarrow{X}(h)(L_d) \qquad \text{for every section } X \text{ of } E. \qquad (26)$$

If both g and h are on the same symmetric neighborhood $\mathscr{W}$, with coordinates (x, u) for g and (y, v) for h, we can apply the local results above and we readily get the coordinate expression of the Euler-Lagrange equations

$$L^\mu_\gamma(x,u)\frac{\partial L_d}{\partial u^\mu}(x,u) + \rho^i_\gamma(y)\frac{\partial L_d}{\partial x^i}(y,v) - R^\mu_\gamma(y,v)\frac{\partial L_d}{\partial u^\mu}(y,v) = 0 \qquad (27)$$

$$y = \mathsf{b}(x,u), \qquad (28)$$

where the second equation takes into account that $\beta(g) = \alpha(h)$.

Assume that we have a solution $(g_0, h_0) \in G_2$ of the Euler-Lagrange equations. To analyze the existence of solution of the Euler-Lagrange equations for elements $(g, h) \in G_2$ near (g_0, h_0), we can apply the implicit function theorem. In the application of such a theorem, the relevant matrix $[(\mathbb{F}L_d)^\gamma_\mu]_{\gamma,\mu=1,\dots,m}$ is the following

$$(\mathbb{F}L_d)^\gamma_\mu(x,u) = \rho^i_\mu(x)\frac{\partial^2 L_d}{\partial x^i \partial u^\gamma}(x,u) - \frac{\partial R^\nu_\mu}{\partial u^\gamma}(x,u)\frac{\partial L_d}{\partial u^\nu}(x,u) + \\ - R^\nu_\mu(x,u)\frac{\partial^2 L_d}{\partial u^\nu \partial u^\gamma}(x,u). \tag{29}$$

Proposition 2. *Let (y_0, v_0) be the coordinates of the point h_0. The following statements are equivalent.*

- *The matrix $(\mathbb{F}L_d)^\alpha_\beta(y_0, v_0)$ is regular.*
- *The Poincare-Cartan 2-section Ω_{L_d} is non-degenerate at the point h_0.*
- *The map $\mathbb{F}^- L_d$ is a local diffeomorphism at h_0.*

Any of them implies the following: There exist open neighborhoods $\mathscr{X}_0 \subseteq \mathscr{W}$ and $\mathscr{Y}_0 \subseteq \mathscr{W}$ of g_0 and h_0 such that if $g \in \mathscr{X}_0$ then there is a unique $\Psi(g) = h \in \mathscr{Y}_0$ satisfying that the pair (g, h) is a solution of the Euler-Lagrange equations for L_d. In fact, the map $\Psi : \mathscr{X}_0 \to \mathscr{Y}_0$ is a local discrete Euler-Lagrange evolution operator.

Proof. We first notice that the local expression of the map $\mathbb{F}^-_{L_d}$ is

$$(\mathbb{F}^-_{L_d})(x,u) = \left(x, -\rho^i_\gamma(x)\frac{\partial L_d}{\partial x^i}(x,u) + R^\mu_\gamma(x,u)\frac{\partial L_d}{\partial u^\mu}(x,u)\right).$$

The differential of this local function at the point $h \equiv (y_0, v_0)$ is of the form

$$\begin{bmatrix} I_n & 0 \\ * & -\mathbb{F}L_d(y_0, v_0) \end{bmatrix}$$

from where the equivalence of the first and the third assertions immediately follows.

For the second we just take a local basis of sections $\{e_\gamma\}$ of E, defined in a neighborhood of x_0 and associated to the α-vertical vector fields $\frac{\partial}{\partial u^\gamma}$, and we compute the value of Ω_{L_d} on the associated basis $\{e^{(1,0)}_\gamma, e^{(0,1)}_\gamma\}$. From (8) and (9) it follows that $\Omega_{L_d}(h_0)$ is regular if and only if the matrix

$$\Omega_{\gamma\mu}(y_0, v_0) = \Omega_{L_d}(e^{(1,0)}_\gamma, e^{(0,1)}_\mu)(h_0) = \overleftarrow{e_\mu}(\overrightarrow{e_\gamma}(L_d))(h_0)$$

is regular. From the expressions (24) and (25) this matrix is

$$\begin{aligned}\Omega_{\gamma\mu}(y_0,v_0) &= -L_\mu^\theta \frac{\partial}{\partial u^\theta}\left(\rho_\gamma^i \frac{\partial L_d}{\partial x^i} - R_\gamma^\nu \frac{\partial L_d}{\partial u^\nu}\right)(y_0,v_0)\\ &= -L_\mu^\theta \left(\rho_\gamma^i \frac{\partial^2 L_d}{\partial x^i \partial u^\theta} - \frac{\partial R_\gamma^\sigma}{\partial u^\theta}\frac{\partial L_d}{\partial u^\sigma} - R_\gamma^\sigma \frac{\partial^2 L_d}{\partial u^\sigma \partial u^\theta}\right)(y_0,v_0)\\ &= -L_\mu^\theta(y_0,v_0)(\mathbb{F}L_d)_\gamma^\theta(y_0,v_0).\end{aligned}$$

It follows from (24) that the matrix $L_\mu^\theta(y_0,v_0)$ is regular. Thus, we get that the regularity of the matrix $(\mathbb{F}L_d)_\gamma^\theta(y_0,v_0)$ is equivalent to the regularity of $\Omega_{L_d}(h_0)$.

Finally, let λ_μ be the left-hand side of the discrete Euler-Lagrange equations (27) once the equation (28) has been used

$$\begin{aligned}\lambda_\mu(x,u,v) = L_\mu^\gamma(x,u)\frac{\partial L_d}{\partial u^\gamma}(x,u) + \rho_\mu^i(\mathsf{b}(x,u))\frac{\partial L_d}{\partial x^i}(\mathsf{b}(x,u),v) +\\ - R_\mu^\gamma(\mathsf{b}(x,u),v)\frac{\partial L_d}{\partial u^\gamma}(\mathsf{b}(x,u),v). \qquad (30)\end{aligned}$$

We want to study the existence of solution of the discrete Euler-Lagrange equations $\lambda_\mu(x,u,v) = 0$ in a neighborhood of the point (x_0,u_0,v_0), where (x,u) are the data and v is the unknown. Applying the implicit function theorem we have to study the regularity of the matrix $\frac{\partial \lambda_\mu}{\partial v^\gamma}(x_0,u_0,v_0)$. A straightforward calculation shows that this matrix is just

$$\frac{\partial \lambda_\mu}{\partial v^\gamma}(x_0,u_0,v_0) = (\mathbb{F}L_d)_\mu^\gamma(y_0,v_0) \qquad \text{with } y_0 = \mathsf{b}(x_0,u_0),$$

from where our last assertion readily follows.

Remark 2. Suppose that $h_0 \in \varepsilon(M)$. Then, h_0 has local coordinates $(y_0,0)$. Moreover, from (17) and (18), it follows that the matrix $L_\mu^\gamma(y_0,0)$ is the identity matrix. Therefore, we deduce that the matrix $\Omega_{\gamma\mu}(y_0,0)$ is, up to the sign, the matrix $(\mathbb{F}L_d)_\gamma^\mu(y_0,0)$ (see the proof of Theorem 2 in Section 4.2).

In general the Euler-Lagrange equations are understood as the equations determining $h \equiv (y,v)$ from the already known data $g \equiv (x,u)$, as we did in the proof of the above theorem. However, we can also try to solve these equations backwards to obtain (x,u) from (y,v). Instead of applying again the implicit function theorem to the system of equations (27) and (28) we can rewrite the equations in a different coordinate system, adapted to the fibration β, as follows. On the open subset $\bar{\mathscr{U}} = i(\mathscr{U})$ we consider the local coordinates $(\bar{x},\bar{u})$ defined as $(\bar{x},\bar{u}) = (x,u)\circ i$, where i is the inversion map in the groupoid. Since $\beta \circ i = \alpha$, we have that these new coordinates are adapted to the submersion β and we can proceed as in the

previous case. In these coordinates, a basis of the left-invariant and right-invariant vector fields is

$$\overleftarrow{e_\gamma}(\bar{x},\bar{u}) = -\rho_\gamma^i(\bar{x})\frac{\partial}{\partial \bar{x}^i}\Big|_{(\bar{x},\bar{u})} + R_\gamma^\mu(\bar{x},\bar{u})\frac{\partial}{\partial \bar{u}^\mu}\Big|_{(\bar{x},\bar{u})}\,, \tag{31}$$

$$\overrightarrow{e_\gamma}(\bar{x},\bar{u}) = L_\gamma^\mu(\bar{x},\bar{u})\frac{\partial}{\partial \bar{u}^\mu}\Big|_{(\bar{x},\bar{u})}\,. \tag{32}$$

3.6 Examples

We present here some illustrative examples.

3.6.1 Pair or Banal Groupoid

We consider as a first example the pair (banal) groupoid $G = M \times M$, where the structural maps are

$$\alpha(x,y) = x,\quad \beta(x,y) = y,\quad \varepsilon(x) = (x,x),\quad i(x,y) = (y,x),$$
$$m((x,y),(y,z)) = (x,z).$$

The Lie algebroid of G is isomorphic to the standard Lie algebroid $\tau_M : TM \to M$, therefore the pair groupoid is considered as the discrete phase space for discretization of Lagrangian functions $L : TM \to \mathbb{R}$.

Let $x_0 \in M$ and a local coordinate system (x^i) defined on a neighborhood $\mathscr{V}'$ of x_0. Then $\mathscr{U} = \mathscr{V}' \times \mathscr{V}'$ is obviously a symmetric neighborhood. For a fixed $h > 0$, an associated coordinate system adapted to the α-projection is

$$x^i(x_1,x_2) = x^i(x_1) \qquad \text{and} \qquad u^i(x_1,x_2) = \frac{x^i(x_2) - x^i(x_1)}{h}.$$

Obviously the identities correspond to the elements $(x^i, 0)$ in this coordinate system and $\alpha(x,u) = x$ and $\beta(x,u) = x + hu$. On the other hand, the composition of two elements (x,u) and $(x + hu, v)$ is $(x, u + v)$. Therefore $\mathsf{p}(x,u,v) = u + v$. The inversion map is now $i(x,u) = (x + hu, -u)$.

If we take the natural local coordinate basis $\left\{\frac{\partial}{\partial u^i}|_{\varepsilon(x_1)}\right\}$ of $\ker T_{\varepsilon(x_1)}\alpha$ then

$$\frac{\overleftarrow{\partial}}{\partial u^i} = \frac{\partial}{\partial u^i}$$
$$\frac{\overrightarrow{\partial}}{\partial u^i} = -h\frac{\partial}{\partial x^i} + \frac{\partial}{\partial u^i}.$$

Therefore, the discrete Euler-Lagrange equations are

$$\frac{\partial L_d}{\partial u^i}(x,u) + h\frac{\partial L_d}{\partial x^i}(y,v) - \frac{\partial L_d}{\partial u^i}(y,v) = 0$$
$$y = x + hu.$$

The discrete Lagrangian is regular if the matrix

$$h\frac{\partial^2 L_d}{\partial x^i \partial u^j}(x,u) - \frac{\partial^2 L_d}{\partial u^i \partial u^j}(x,u)$$

is non singular.

Example 1. As a concrete simple example, consider the continuous Lagrangian $L: \mathbb{R}^{2n} \to \mathbb{R}$:

$$L(x,\dot{x}) = \frac{1}{2}\dot{x}^T M \dot{x} - V(x)$$

(with M a constant symmetric invertible matrix). A typical discretization for the lagrangian is, for instance,

$$L_d(x,u) = \frac{h}{2}u^T M u - hV(x + \frac{h}{2}u).$$

Then, the discrete Euler-Lagrange equations are:

$$M\frac{v-u}{h} = -\frac{1}{2}\left(\frac{\partial V}{\partial x}(x + \frac{h}{2}u) + \frac{\partial V}{\partial x}(y + \frac{h}{2}v)\right)$$
$$y = x + hu,$$

which leads us the classical implicit midpoint rule.

If on the other hand, we take the discretization

$$\begin{aligned} L_d(x,u) &= \frac{h}{2}\left(L(x,u) + L(x+hu,u)\right) \\ &= \frac{h}{2}u^T M u - \frac{h}{2}\left(V(x) + V(x+hu)\right), \end{aligned}$$

then the corresponding discrete Euler-Lagrange equations are:

$$M\frac{v-u}{h} = -\frac{\partial V}{\partial x}(y)$$
$$y = x + hu,$$

which is a representation of the Störmer-Verlet method.

Remark 3. The previous description corresponds to the choice of a symmetric neighborhood adapted to the fibration $\alpha : M \times M \to M$. In previous literature (see for instance [2, 18]) the authors introduce retraction maps, that is, a smooth mapping R from the tangent bundle TM onto M with the following properties $R_x(0_x) = x$ and, $T_{0_x} R_x = \mathrm{id}_{T_x M}$, with the canonical identification $T_{0_x} T_x M \equiv T_x M$. In our setting we can think in these retraction maps as local identifications of the α-fiber near of the identity with the tangent space to the base manifold. In the next subsection, we will use the retractions maps to locally identify the Lie groupoid with its associated Lie algebroid.

3.6.2 Lie Groups

Another interesting example corresponds to the case of Lie groups. In this case, we consider a Lie group G as a groupoid over one point $M = \{\mathfrak{e}\}$, the identity element of G. The structural maps are

$$\alpha(g) = \mathfrak{e}, \quad \beta(g) = \mathfrak{e}, \quad \varepsilon(\mathfrak{e}) = \mathfrak{e}, \quad i(g) = g^{-1}, \quad m(g,h) = gh, \quad \text{for } g, h \in G.$$

The Lie algebroid associated with G is just the Lie algebra $\mathfrak{g} = T_{\mathfrak{e}} G$ of G.

Near the identity, it is interesting to regard the elements $g \in G$ as small displacements on the Lie group. Thus, it is possible to express each term through a Lie algebra element that can be regarded as the averaged velocity of this displacement. This is typically accomplished using a retraction map $\tau : \mathfrak{g} \to G$ which is an analytic local diffeomorphism around the identity such that $\tau(\xi)\tau(-\xi) = \mathfrak{e}$, where $\xi \in \mathfrak{g}$ (see [3]). Thereby τ provides a local chart on the Lie group.

Given a retraction map τ its right trivialized tangent $\mathrm{d}\tau_\xi : \mathfrak{g} \to \mathfrak{g}$ and is inverse $\mathrm{d}\tau_\xi^{-1} : \mathfrak{g} \to \mathfrak{g}$ are defined for all $\eta \in \mathfrak{g}$ as follows

$$T_\xi \tau(\eta) = T_{\mathfrak{e}} r_{\tau(\xi)} \left(\mathrm{d}\tau_\xi(\eta)\right) \equiv \mathrm{d}\tau_\xi(\eta)\, \tau(\xi),$$
$$T_{\tau(\xi)} \tau^{-1}((T_{\mathfrak{e}} r_{\tau(\xi)})\eta) = \mathrm{d}\tau_\xi^{-1}(\eta).$$

The retraction map allows us to transport locally the Lie group structure on an open symmetric neighborhood of G to a local τ-dependent Lie group structure on the Lie algebra $\mathfrak{g}$ defined on a local neighborhood V of $0 \in \mathfrak{g}$. We will write $\tau(h\xi) = g$ for an enough small time step $h > 0$ such that $h\xi \in V \subseteq \mathfrak{g}$.

Now, on the Lie algebra it is easy to consider local coordinates because it is a vector space. In consequence, fixing a basis $\{e_\gamma\}$ of $\mathfrak{g}$, we induce coordinates (u^γ) on $\mathfrak{g}$.

In these coordinates, a basis of left- and right-invariant vector fields is

$$\overleftarrow{e_\gamma}(\eta) = T_{\tau(h\eta)} \tau^{-1}(\tau(h\eta) e_\gamma) = \mathrm{d}\tau_{h\eta}^{-1}(\mathrm{Ad}_{\tau(h\eta)} e_\gamma)$$
$$\overrightarrow{e_\gamma}(\eta) = T_{\tau(h\eta)} \tau^{-1}(e_\gamma \tau(h\eta)) = \mathrm{d}\tau_{h\eta}^{-1}(e_\gamma),$$

where $\eta \in \mathfrak{g}$. Given a Lagrangian $l : \mathfrak{g} \to \mathbb{R}$, we deduce that the discrete Euler-Poincaré equations are:

$$\overleftarrow{e_\gamma}(\eta_k)(l) - \overrightarrow{e_\gamma}(\eta_{k+1})(l) = 0,$$

or, alternatively, as discrete Lie-Poisson equations [24, 25]:

$$Ad^*_{\tau(h\eta_k)}\mu_k - \mu_{k+1} = 0,$$

where

$$\mu_k = (\mathrm{d}\tau^{-1}_{h\eta_k})^* \frac{\partial l}{\partial \xi}(\eta_k) \ .$$

Example 2. As an example of retraction map we will consider the Cayley transform which is one of the most computationally efficient parametrizations of a Lie group. The Cayley map $\mathrm{cay} : \mathfrak{g} \to G$ is defined by $\mathrm{cay}(\xi) = (\mathfrak{e} - \frac{\xi}{2})^{-1}(\mathfrak{e} + \frac{\xi}{2})$ and is valid for a general class of quadratic groups as for instance $SO(n)$, $SE(n)$ or $Sp(n)$ (see [12]). Its right trivialized derivative and inverse are given by

$$\mathrm{dcay}_\xi \, \eta = (\mathfrak{e} - \frac{\xi}{2})^{-1} \, \eta \, (\mathfrak{e} + \frac{\xi}{2})^{-1}$$
$$\mathrm{dcay}^{-1}_\xi \, \eta = (\mathfrak{e} - \frac{\xi}{2}) \, \eta \, (\mathfrak{e} + \frac{\xi}{2}).$$

In this case it is possible to write more explicitly the Lie-Poincaré equations. In fact, we have that

$$\overleftarrow{e_\gamma}(\eta) = (\mathfrak{e} + \frac{h\eta}{2}) \, e_\gamma \, (\mathfrak{e} - \frac{h\eta}{2})$$
$$\overrightarrow{e_\gamma}(\eta) = (\mathfrak{e} - \frac{h\eta}{2}) \, e_\gamma \, (\mathfrak{e} + \frac{h\eta}{2}),$$

with $\eta \in \mathfrak{so}(3)$. Therefore, the discrete Euler-Poincaré equations are:

$$\begin{aligned} 0 = & \langle (\mathfrak{e} + \frac{h\eta_k}{2}) \, e_\gamma \, (\mathfrak{e} - \frac{h\eta_k}{2}), \frac{\partial l}{\partial \xi}(\eta_k) \rangle \\ & - \langle (\mathfrak{e} - \frac{h\eta_{k+1}}{2}) \, e_\gamma \, (\mathfrak{e} + \frac{h\eta_{k+1}}{2}), \frac{\partial l}{\partial \xi}(\eta_{k+1}) \rangle \\ = & \langle e_\gamma - \frac{h}{2}[e_\gamma, \eta_k] - \frac{h^2}{4}\eta_k e_\gamma \eta_k, \frac{\partial l}{\partial \xi}(\eta_k) \rangle \\ & - \langle e_\gamma + \frac{h}{2}[e_\gamma, \eta_{k+1}] - \frac{h^2}{4}\eta_{k+1} e_\gamma \eta_{k+1}, \frac{\partial l}{\partial \xi}(\eta_{k+1}) \rangle. \end{aligned}$$

As a concrete example, we consider the case of the group $SO(3)$, using the Cayley transformation and fixing the standard basis of its Lie algebra $\mathfrak{so}(3)$:

$$e_1 = \begin{pmatrix} 0 & 0 & 0 \\ 0 & 0 & -1 \\ 0 & 1 & 0 \end{pmatrix}, \quad e_2 = \begin{pmatrix} 0 & 0 & 1 \\ 0 & 0 & 0 \\ -1 & 0 & 0 \end{pmatrix}, \quad e_3 = \begin{pmatrix} 0 & -1 & 0 \\ 1 & 0 & 0 \\ 0 & 0 & 0 \end{pmatrix}.$$

Thus, the elements η_k, η_{k+1} in $\mathfrak{g}$ will have coordinates (x_k, y_k, z_k) and $(x_{k+1}, y_{k+1}, z_{k+1})$, respectively, in this fixed basis. This allows us to write the previous discrete Euler-Poincaré equations as follows:

$$\begin{aligned}
0 = {} & \left(1 + \frac{h^2 x_k^2}{4}\right) \left.\frac{\partial L}{\partial x}\right|_k + \left(\frac{h^2 x_k y_k}{4} + \frac{h z_k}{2}\right) \left.\frac{\partial L}{\partial y}\right|_k \\
& - \left(\frac{h y_k}{2} - \frac{h^2 x_k z_k}{4}\right) \left.\frac{\partial L}{\partial z}\right|_k - \left(1 + \frac{h^2 x_{k+1}^2}{4}\right) \left.\frac{\partial L}{\partial x}\right|_{k+1} \\
& + \left(\frac{h z_{k+1}}{2} - \frac{h^2 x_{k+1} y_{k+1}}{4}\right) \left.\frac{\partial L}{\partial y}\right|_{k+1} - \left(\frac{h y_{k+1}}{2} + \frac{h^2 x_{k+1} z_{k+1}}{4}\right) \left.\frac{\partial L}{\partial z}\right|_{k+1} \\
0 = {} & \left(\frac{h^2 x_k y_k}{4} - \frac{h z_k}{2} +\right) \left.\frac{\partial L}{\partial x}\right|_k + \left(1 + \frac{h^2 y_k^2}{4}\right) \left.\frac{\partial L}{\partial y}\right|_k \\
& + \left(\frac{h x_k}{2} + \frac{h^2 y_k z_k}{4}\right) \left.\frac{\partial L}{\partial z}\right|_k - \left(\frac{h z_{k+1}}{2} + \frac{h^2 x_{k+1} y_{k+1}}{4}\right) \left.\frac{\partial L}{\partial x}\right|_{k+1} \\
& - \left(1 + \frac{h^2 y_{k+1}^2}{4}\right) \left.\frac{\partial L}{\partial y}\right|_{k+1} + \left(\frac{h x_{k+1}}{2} - \frac{h^2 y_{k+1} z_{k+1}}{4}\right) \left.\frac{\partial L}{\partial z}\right|_{k+1} \\
0 = {} & \left(\frac{h y_k}{2} + \frac{h^2 x_k z_k}{4}\right) \left.\frac{\partial L}{\partial x}\right|_k - \left(\frac{h x_k}{2} - \frac{h^2 y_k z_k}{4}\right) \left.\frac{\partial L}{\partial y}\right|_k \\
& + \left(1 + \frac{h^2 z_k}{4}\right) \left.\frac{\partial L}{\partial z}\right|_k + \left(\frac{h y_{k+1}}{2} - \frac{h^2 x_{k+1} z_{k+1}}{4}\right) \left.\frac{\partial L}{\partial x}\right|_{k+1} \\
& - \left(\frac{h x_{k+1}}{2} + \frac{h^2 y_{k+1} z_{k+1}}{4}\right) \left.\frac{\partial L}{\partial y}\right|_{k+1} - \left(1 + \frac{h^2 z_{k+1}}{4}\right) \left.\frac{\partial L}{\partial z}\right|_{k+1},
\end{aligned}$$

where $L : \mathbb{R}^3 \to \mathbb{R}$ is defined by $L(x, y, z) = l(xe_1 + ye_2 + ze_3)$.

3.7 Transformation or Action Lie Groupoid

The theory of Lie groupoids covers other interesting examples that are useful for the construction of variational integrators for different mechanical systems. This is the case of transformation or action Lie groupoids. Let $\tilde{G}$ be a Lie group and $\cdot : M \times \tilde{G} \to M$, $(x, \tilde{g}) \in M \times \tilde{G} \mapsto x\tilde{g}$, a right action of $\tilde{G}$ on M. Consider the Lie groupoid $G = M \times \tilde{G}$ over M with structural maps given by

$$\begin{array}{l} \alpha(x, \tilde{g}) = x, \quad \beta(x, \tilde{g}) = x\tilde{g}, \quad \varepsilon(x) = (x, \tilde{\mathfrak{e}}), \\ m((x, \tilde{g}), (x\tilde{g}, \tilde{g}')) = (x, \tilde{g}\tilde{g}'), \quad \text{and} \quad i(x, \tilde{g}) = (x\tilde{g}, \tilde{g}^{-1}). \end{array} \tag{33}$$

where $\tilde{\mathfrak{e}}$ is the identity on $\tilde{G}$. The Lie groupoid G is called the action or transformation Lie groupoid. Its associated Lie algebroid is the action algebroid $pr_1 : M \times \tilde{\mathfrak{g}} \to M$ where $\tilde{\mathfrak{g}}$ is the Lie algebra of Lie group $\tilde{G}$ (see [21] for details about the Lie algebroid structure). We have that $\Gamma(pr_1) \cong \{\bar{\eta} : M \to \tilde{\mathfrak{g}} \mid \bar{\eta} \text{ is a smooth mapping}\}$. In particular, if $\eta \in \tilde{\mathfrak{g}}$ then η defines a constant section $C_\eta : M \to \tilde{\mathfrak{g}}$ of $pr_1 : M \times \tilde{\mathfrak{g}} \to M$: $C_\eta(x) = (x, \eta)$ for all $x \in M$. It is possible to check that the corresponding left- and right-invariant vector fields on G are (see [21]):

$$\overleftarrow{C}_\eta(x, \tilde{g}) = (0_x, \overleftarrow{\eta}(\tilde{g})), \quad \overrightarrow{C}_\eta(x, \tilde{g}) = (-\eta_M(x), \overrightarrow{\eta}(\tilde{g})), \tag{34}$$

for $(x, \tilde{g}) \in G = M \times \tilde{G}$ and where η_M is the infinitesimal generator of the right action $\cdot : M \times \tilde{G} \to M$ associated with η.

Let $L_d : G = M \times \tilde{G} \to \mathbb{R}$ be a discrete Lagrangian. Then, a composable pair $((x_k, \tilde{g}_k), (x_k\tilde{g}_k, \tilde{g}_{k+1})) \in G_2$ is a solution of the discrete Euler-Lagrange equations for L_d if

$$\overleftarrow{C}_\eta(x_k, \tilde{g}_k)(L_d) - \overrightarrow{C}_\eta(x_k\tilde{g}_k, \tilde{g}_{k+1})(L_d) = 0, \text{ for all } \eta \in \mathfrak{g}.$$

Given a retraction map $\tau : \tilde{\mathfrak{g}} \to \tilde{G}$, we can transport the Lie group structure on an open symmetric neighborhood of $\tilde{\mathfrak{e}}$ in $\tilde{G}$ to an open neighborhood of 0 in $\tilde{\mathfrak{g}}$ as in Subsection 3.6.2. Moreover, if $x_0 \in M$, we may assume, without loss of generality, that this neighborhood acts on an open neighborhood U of the point $x_0 \in M$. Thus if $\tilde{\xi} \in \tilde{\mathfrak{g}}$ the flow $\Phi_{\tilde{\xi}_M}$ of the fundamental vector field $\tilde{\xi}_M$ associated with this local action is given by

$$\Phi_{\tilde{\xi}_M}(t, x) = x \exp_{\tilde{G}}(t(h\tilde{\xi}))$$

for $t \in \mathbb{R}$ and $x \in U$. Therefore, as in the previous section, fixed a basis $\{e_\gamma\}$ of $\tilde{\mathfrak{g}}$, we induce a basis of left- and right-invariant vector fields

$$\overleftarrow{C_{e_\gamma}}(x, \tilde{\eta}) = (0, \mathrm{d}\tau^{-1}_{h\tilde{\eta}}(\mathrm{Ad}_{\tau(h\tilde{\eta})}e_\gamma))$$
$$\overrightarrow{C_{e_\gamma}}(x, \tilde{\eta}) = (-h(e_\gamma)_M(x), \mathrm{d}\tau^{-1}_{h\tilde{\eta}}(e_\gamma)),$$

where $\tilde{\eta} \in \tilde{\mathfrak{g}}$ and $x \in U$. Given a Lagrangian $l : M \times \tilde{\mathfrak{g}} \to \mathbb{R}$, we deduce that the discrete Euler-Lagrange equations are:

$$0 = \mathrm{d}\tau^{-1}_{h\tilde{\eta}_k}(\mathrm{Ad}_{\tau(h\tilde{\eta}_k)}e_\gamma)(l_{x_k}) - \mathrm{d}\tau^{-1}_{h\tilde{\eta}_{k+1}}(e_\gamma)(l_{x_{k+1}}) + h(e_\gamma)_M(x_{k+1})(l_{\tilde{\eta}_{k+1}}),$$
$$x_{k+1} = x_k\tau(h\tilde{\eta}_k)\ ,$$

where for every $\tilde{\eta} \in \tilde{\mathfrak{g}}$ (resp., $x \in M$) we denote by $l_{\tilde{\eta}}$ (resp., l_x) the real function on M (resp., on $\tilde{\mathfrak{g}}$) given by $l_{\tilde{\eta}}(y) = l(y, \tilde{\eta})$ (resp., $l_x(\tilde{\eta}') = l(x, \tilde{\eta}')$).

Example 3. As a typical example of a discrete system defined on a transformation Lie groupoid consider a discretization of the heavy top [19, 21, 26]. This system is modelled on the transformation Lie algebroid $\tau : S^2 \times \mathfrak{so}(3) \to S^2$ with Lagrangian

$$L_c(\Gamma, \Omega) = \frac{1}{2}\Omega \cdot \mathbb{I}\Omega - mgd\ \Gamma \cdot \mathrm{e},$$

where $\Omega \in \mathbb{R}^3 \simeq \mathfrak{so}(3)$ is the angular velocity, Γ is the direction opposite to the gravity and e is a unit vector in the direction from the fixed point to the center of mass, all them expressed in a frame fixed to the body. The constants m, g and d are respectively the mass of the body, the strength of the gravitational acceleration and the distance from the fixed point to the center of mass. The matrix $\mathbb{I}$ is the inertia tensor of the body.

We will also use the Cayley transformation on $SO(3)$ to describe the discrete Euler-Lagrange equations for the heavy top. We have that

$$\overleftarrow{C_{e_\gamma}}(\Gamma, \eta) = \left(0, (\mathfrak{e} + \frac{h\eta}{2})\, e_\gamma\, (\mathfrak{e} - \frac{h\eta}{2})\right)$$
$$\overrightarrow{C_{e_\gamma}}(\Gamma, \eta) = \left(h\Gamma e_\gamma, (\mathfrak{e} - \frac{h\eta}{2})\, e_\gamma\, (\mathfrak{e} + \frac{h\eta}{2})\right),$$

with

$$\eta = \begin{pmatrix} 0 & -\Omega_3 & \Omega_2 \\ \Omega_3 & 0 & -\Omega_1 \\ -\Omega_2 & \Omega_1 & 0 \end{pmatrix},$$

$\{e_\gamma\}$ the standard basis on $SO(3)$ and $\Gamma \in S^2$.

Therefore, the discrete Euler-Lagrange equations are:

$$\begin{aligned}
0 = &\langle (\mathfrak{e} + \frac{h\eta_k}{2})\, e_\gamma\, (\mathfrak{e} - \frac{h\eta_k}{2}), \frac{\partial (L_c)_{\Gamma_k}}{\partial \xi}(\eta_k)\rangle \\
&-\langle (\mathfrak{e} - \frac{h\eta_{k+1}}{2})\, e_\gamma\, (\mathfrak{e} + \frac{h\eta_{k+1}}{2}), \frac{\partial (L_c)_{\Gamma_{k+1}}}{\partial \xi}(\eta_{k+1})\rangle \\
&+h\Gamma_{k+1} e_\gamma \cdot \frac{\partial (L_c)_{\eta_{k+1}}}{\partial \Gamma}(\Gamma_{k+1}) \\
\Gamma_{k+1} = &\ \Gamma_k \text{ cay } (h\eta_k),
\end{aligned}$$

or, in other terms

$$\begin{aligned}
0 = &\ I_1(\Omega_1)_k \left(1 + \frac{h^2(\Omega_1)_k^2}{4}\right) + I_2(\Omega_2)_k \left(\frac{h^2(\Omega_1)_k(\Omega_2)_k}{4} + \frac{h(\Omega_3)_k}{2}\right) \\
&-I_3(\Omega_3)_k \left(\frac{h(\Omega_2)_k}{2} - \frac{h^2(\Omega_1)_k(\Omega_3)_k}{4}\right) - I_1(\Omega_1)_{k+1} \left(1 + \frac{h^2(\Omega_1)_{k+1}^2}{4}\right) \\
&+I_2(\Omega_2)_{k+1} \left(\frac{h(\Omega_3)_{k+1}}{2} - \frac{h^2(\Omega_1)_{k+1}(\Omega_2)_{k+1}}{4}\right) \\
&-I_3(\Omega_3)_{k+1} \left(\frac{h(\Omega_2)_{k+1}}{2} + \frac{h^2(\Omega_1)_{k+1}(\Omega_3)_{k+1}}{4}\right) \\
&+hmgd(Z_{k+1}\mathrm{e}_2 - Y_{k+1}\mathrm{e}_3)
\end{aligned}$$

$$\begin{aligned}
0 = &\ I_1(\Omega_1)_k \left(\frac{h^2(\Omega_1)_k(\Omega_2)_k}{4} - \frac{h(\Omega_3)_k}{2} +\right) + I_2(\Omega_2)_k \left(1 + \frac{h^2(\Omega_2)_k^2}{4}\right) \\
&+I_3(\Omega_3)_k \left(\frac{h(\Omega_1)_k}{2} + \frac{h^2(\Omega_2)_k(\Omega_3)_k}{4}\right) - I_1(\Omega_1)_{k+1} \left(\frac{h(\Omega_3)_{k+1}}{2} + \frac{h^2(\Omega_1)_{k+1}(\Omega_2)_{k+1}}{4}\right) \\
&-I_2(\Omega_2)_{k+1} \left(1 + \frac{h^2(\Omega_2)_{k+1}^2}{4}\right) + I_3(\Omega_3)_{k+1} \left(\frac{h(\Omega_1)_{k+1}}{2} - \frac{h^2(\Omega_2)_{k+1}(\Omega_3)_{k+1}}{4}\right) \\
&+hmgd(X_{k+1}\mathrm{e}_3 - Z_{k+1}\mathrm{e}_1) \\
0 = &\ I_1(\Omega_1)_k \left(\frac{h(\Omega_2)_k}{2} + \frac{h^2(\Omega_1)_k(\Omega_3)_k}{4}\right) - I_2(\Omega_2)_k \left(\frac{h(\Omega_1)_k}{2} - \frac{h^2(\Omega_2)_k(\Omega_3)_k}{4}\right) \\
&+I_3(\Omega_3)_k \left(1 + \frac{h^2(\Omega_3)_k}{4}\right) + I_1(\Omega_1)_{k+1} \left(\frac{h(\Omega_2)_{k+1}}{2} - \frac{h^2(\Omega_1)_{k+1}(\Omega_3)_{k+1}}{4}\right) \\
&-I_2(\Omega_2)_{k+1} \left(\frac{h(\Omega_1)_{k+1}}{2} + \frac{h^2(\Omega_2)_{k+1}(\Omega_3)_{k+1}}{4}\right) - I_3(\Omega_3)_{k+1} \left(1 + \frac{h^2(\Omega_3)_{k+1}}{4}\right) \\
&-hmgd(X_{k+1}\mathrm{e}_2 - Y_{k+1}\mathrm{e}_1) \\
0 = &\ (X_{k+1}, Y_{k+1}, Z_{k+1}) - (X_k, Y_k, Z_k)(\mathfrak{e} - \frac{h\eta_k}{2})^{-1}(\mathfrak{e} + \frac{h\eta_k}{2})
\end{aligned}$$

where $\Gamma_k = (X_k, Y_k, Z_k) \in \mathbb{R}^3$ with $X_k^2 + Y_k^2 + Z_k^2 = 1$, $\mathrm{e} = (\mathrm{e}_1, \mathrm{e}_2, \mathrm{e}_3)$ and

$$\eta_k = \begin{pmatrix} 0 & -(\Omega_3)_k & (\Omega_2)_k \\ (\Omega_3)_k & 0 & -(\Omega_1)_k \\ -(\Omega_2)_k & (\Omega_1)_k & 0 \end{pmatrix},$$

Remark 4. Our approach also admits other interesting examples. For instance, assume that we have a discrete system modeled by a discrete Lagrangian $L_d : M \times M \times G \to \mathbb{R}$ which is an approximation of a continuous Lagrangian $L : TM \times \mathfrak{g} \to \mathbb{R}$. This Lagrangian typically appears as reduction of a G-invariant Lagrangian function $\tilde{L} : T(M \times G) \to \mathbb{R}$ (see [21], for the general case). Of course we can combine the techniques exposed in Subsections 3.6.1 and 3.6.2 to obtain a local description of the corresponding discrete Euler-Lagrange equations in terms of the continuous Lagrangian L.

4 Bisections and Discrete Euler-Lagrange Evolution Operators

One of the main limitations of the techniques exposed in Section 3 is that we need to work in a neighborhood of the identities of the Lie groupoid G. Using an enough small time stepping we can guarantee that the evolution of the evolution operator for a discrete Lagrangian takes values on the chosen symmetric neighborhood, even it is possible to adapt the time stepping to make it happen. Another possibility is to use the notion of bisections on Lie groupoids. As we will see it will allow us to consider points far from the identities completing our local description of discrete Mechanics.

We consider now the general case of a solution $(g_0, h_0) \in G_2$ of the Euler-Lagrange equations where the points g_0 and $h_0 \in G$ are not necessarily close enough to be contained in a common symmetric neighborhood. If we want to obtain a local expression of the discrete Euler-Lagrange operator which connects the above points, we must choose suitable neighborhoods of g_0 and h_0. For this purpose, we will consider a symmetric neighborhood $\mathscr{W}$, a local bisection through the point g_0 and a local bisection through h_0. By left-translation and right-translation (induced by these sections) of $\mathscr{W}$ we will get such neighborhoods.

4.1 Bisections of a Lie Groupoid

The results contained in this section are well-known in the literature (see, for instance, [4, 20]). However, to make the paper more self-contained, we will include the proofs of them.

Let $G \rightrightarrows M$ be a Lie groupoid with source $\alpha : G \to M$ and target $\beta : G \to M$.

Definition 1. A ***bisection*** of G is a closed embedded submanifold Σ of G such that the restrictions of both α and β to Σ are diffeomorphisms.

A bisection defines both a section Σ_α of α and a section Σ_β of β as follows.

Proposition 3. *Given a bisection Σ the map $\Sigma_\alpha = (\alpha|_\Sigma)^{-1}$ is a smooth section of α such that $\mathrm{Im}(\Sigma_\alpha) = \Sigma$ and $\beta \circ \Sigma_\alpha$ is a diffeomorphism. Alternatively, the map $\Sigma_\beta = (\beta|_\Sigma)^{-1}$ is a smooth section of β such that $\mathrm{Im}(\Sigma_\beta) = \Sigma$ and $\alpha \circ \Sigma_\beta$ is a diffeomorphism.*

Proof. Indeed, since $\alpha|_\Sigma \colon \Sigma \to M$ is a diffeomorphism, the map Σ_α is well defined and satisfies $\alpha \circ \Sigma_\alpha = \mathrm{id}_M$. Moreover $\mathrm{Im}\, \Sigma_\alpha = \mathrm{Im}((\alpha_\Sigma)^{-1}) = \Sigma$ and $\beta \circ \Sigma_\alpha = (\beta|_\Sigma) \circ (\alpha|_\Sigma)^{-1}$ is a diffeomorphism because it is a composition of diffeomorphisms. The proof of the second statement is similar.

Notice that the diffeomorphisms $\beta \circ \Sigma_\alpha$ and $\alpha \circ \Sigma_\beta$ are each one the inverse of the other

$$(\beta \circ \Sigma_\alpha)^{-1} = \alpha \circ \Sigma_\beta \qquad \text{and} \qquad (\alpha \circ \Sigma_\beta)^{-1} = \beta \circ \Sigma_\alpha.$$

Definition 2. A ***local bisection*** of G is a closed embedded submanifold $\mathscr{W}$ of G such that there exist open subsets $\mathscr{U}, \mathscr{V} \subset M$ for which both $\alpha|_{\mathscr{W}} \colon \mathscr{W} \to \mathscr{U}$ and $\beta|_{\mathscr{W}} \colon \mathscr{W} \to \mathscr{V}$ are diffeomorphisms.

Proposition 4. *Given a local bisection $\mathscr{W}$ the map $\mathscr{W}_\alpha = (\alpha|_{\mathscr{W}})^{-1}$ is a smooth local section of α defined on the open set $\mathscr{U}$ such that $(\mathscr{W}_\alpha)(\mathscr{U}) = \mathscr{W}$ and $\beta \circ \mathscr{W}_\alpha \colon \mathscr{U} \to \mathscr{V}$ is a diffeomorphism. Alternatively, the map $\mathscr{W}_\beta = (\beta|_{\mathscr{W}})^{-1}$ is a smooth local section of β defined on the open set $\mathscr{V}$ such that $(\mathscr{W}_\beta)(\mathscr{V}) = \mathscr{W}$ and $\alpha \circ \mathscr{W}_\beta \colon \mathscr{V} \to \mathscr{U}$ is a diffeomorphism.*

Proof. The proof is a straightforward modification of the proof for global bisections.

We will need the following straightforward result.

Lemma 1. *Let A and B be linear subspaces of a finite dimensional vector space V, with $\dim(A) = \dim(B)$. There exists a linear subspace $C \subset V$ such that $A \oplus C = V$ and $B \oplus C = V$.*

Proof. Let $\{c_i\}$ be a basis of $A \cap B$. We complete to a basis $\{c_i, a_\alpha\}$ of A, and we also complete to a basis $\{c_i, b_\alpha\}$ of B. Then $\{c_i, a_\alpha, b_\alpha\}$ is a basis of $A + B$, which can be completed to a basis $\{c_i, a_\alpha, b_\alpha, d_J\}$ of V. Then, the subspace $C = \mathrm{span}\{a_\alpha + b_\alpha, d_J\}$ is such that $A \oplus C = V$ and $B \oplus C = V$.

Proposition 5 (Existence of Local Bisections). *Given $g \in G$ there exists a local bisection $\mathscr{W}$ such that $g \in \mathscr{W}$.*

Proof. Since the dimensions of $\ker(T_g\alpha)$ and $\ker(T_g\beta)$ are equal, there exists a subspace $I \subset T_gG$ such that $T_gG = \ker(T_g\alpha) \oplus I$ and $T_gG = \ker(T_g\beta) \oplus I$. Notice that, since α and β are submersions, we have that $T_g\alpha(I) = T_{\alpha(g)}M$ and $T_g\beta(I) = T_{\beta(g)}M$.

Let $\Sigma \subset G$ be any submanifold such that $g \in \Sigma$ and $T_g\Sigma = I$. The maps $T_g\alpha|_\Sigma$ and $T_g\beta|_\Sigma$ are linear isomorphisms at the point g. Indeed $\mathrm{Im}(T_g\alpha|_\Sigma) = T_g\alpha(I) = T_{\alpha(g)}M$, and similarly $\mathrm{Im}(T_g\beta|_\Sigma) = T_g\beta(I) = T_{\beta(g)}M$, and $\dim(M) = \dim(I)$. By the inverse function theorem, it follows that there exist open subsets $\mathscr{W}^\alpha$ and $\mathscr{W}^\beta$ in Σ and $\mathscr{U}^\alpha$ and $\mathscr{V}^\beta$ in M such that $g \in \mathscr{W}^\alpha \cap \mathscr{W}^\beta$ and $\alpha|_{\mathscr{W}^\alpha}: \mathscr{W}^\alpha \to \mathscr{U}^\alpha$ and $\beta|_{\mathscr{W}^\beta}: \mathscr{W}^\beta \to \mathscr{V}^\beta$ are diffeomorphisms. By taking $\mathscr{W} = \mathscr{W}^\alpha \cap \mathscr{W}^\beta$, $\mathscr{U} = \alpha(\mathscr{W})$ and $\mathscr{V} = \beta(\mathscr{W})$ we have that $\mathscr{W}$ is a local bisection and $g \in \mathscr{W}$.

In what follows we do not distinguish, in the notation, global and local bisections; all then will be denoted by Σ.

Definition 3. Given a local bisection Σ defined on the open sets $\mathscr{U}$ and $\mathscr{V}$, the local ***left translation*** by Σ is the map $L_\Sigma: \alpha^{-1}(\mathscr{V}) \to \alpha^{-1}(\mathscr{U})$ defined by

$$L_\Sigma(g) = hg, \qquad \text{where } h = \Sigma_\beta(\alpha(g)),$$

and the local ***right translation*** by Σ is the map $R_\Sigma: \beta^{-1}(\mathscr{U}) \to \beta^{-1}(\mathscr{V})$ defined by

$$R_\Sigma(g) = gh, \qquad \text{where } h = \Sigma_\alpha(\beta(g)).$$

Alternatively, the left action is $\Sigma \cdot g = hg$, where $h \in \Sigma$ is the uniquely defined element such that $\beta(h) = \alpha(g)$. Similarly the right action is $g \cdot \Sigma = gh$, where $h \in \Sigma$ is the uniquely defined element such that $\alpha(h) = \beta(g)$. Observe that both L_Σ and R_Σ are diffeomorphisms.

It is easy to see that, for a bisection Σ, the left action L_Σ preserves the β-fibers and maps α-fibers to α-fibers. Similarly, the right action R_Σ preserves the α-fibers and maps β-fibers to β-fibers.

The left action L_Σ by a bisection Σ extends the natural left action in the groupoid and we have $(\Sigma \cdot g)h = \Sigma \cdot (gh)$, or in other words $L_\Sigma \circ l_g = l_{\Sigma \cdot g}$. Moreover, since it preserves the α-fibers, it maps left-invariant vector fields to left invariant vector fields

$$TL_\Sigma(\overleftarrow{X}(g)) = \overleftarrow{X}(L_\Sigma\, g) \qquad \text{for every } X \in \Gamma(\tau). \tag{35}$$

Similarly, we have $(hg) \cdot \Sigma = h(g \cdot \Sigma)$ or $R_\Sigma \circ r_g = R_{g \cdot \Sigma}$, from where

$$TR_\Sigma(\overrightarrow{X}(g)) = \overrightarrow{X}(R_\Sigma\, g) \qquad \text{for every } X \in \Gamma(\tau). \tag{36}$$

4.2 General Discrete Euler-Lagrange Evolution Operators

Let $L_d : G \to \mathbb{R}$ be a discrete Lagrangian function and consider a solution $(g_0, h_0) \in G_2$ of the discrete Euler-Lagrange equations, that is,

$$\overleftarrow{X}(g_0)(L_d) - \overrightarrow{X}(h_0)(L_d) = 0, \quad \text{for all } X \in \Gamma(\tau).$$

We denote by $x_0 \in M$ the point

$$x_0 = \beta(g_0) = \alpha(h_0).$$

Then, we consider the following objects:

- A symmetric neighborhood $\mathscr{W}$ associated with x_0 and some open subset U of G, with local coordinates (x, u) as in Section 3.2. We will denote by V the corresponding open subset of M and by (y) the local coordinates on V.
- A local bisection Σ_0 of G such that $g_0 \in \Sigma_0$.
- A local bisection Υ_0 of G such that $h_0 \in \Upsilon_0$.

We will assume, without the loss of generality, that the section $(\Sigma_0)_\beta$ (respectively, $(\Upsilon_0)_\alpha$) is defined on the open subset V of M.

It is clear that $\mathscr{W}_{\Sigma_0} = L_{\Sigma_0}(\mathscr{W})$ is an open neighborhood of g_0 in G diffeomorphic to $\mathscr{W}$. On $\mathscr{W}_{\Sigma_0}$ we may consider a local coordinate system (x, u) defined as follows: if $g \in \mathscr{W}_{\Sigma_0}$ then there exists a unique $g_{\mathscr{W}} \in \mathscr{W}$ such that $L_{\Sigma_0}(g_{\mathscr{W}}) = g$; the coordinates of the point g are the coordinates in the symmetric neighborhood $\mathscr{W}$ of the point $g_{\mathscr{W}}$.

Similarly, $\mathscr{W}_{\Upsilon_0} = R_{\Upsilon_0}(\mathscr{W})$ is an open neighborhood of h_0 in G diffeomorphic to $\mathscr{W}$. On $\mathscr{W}_{\Upsilon_0}$ we consider local coordinates (y, v) defined as follows: for $h \in \mathscr{W}_{\Upsilon_0}$ we consider the unique point $h_{\mathscr{W}} \in \mathscr{W}$ such that $R_{\Upsilon_0}(h_{\mathscr{W}}) = h$, and we assign to h the coordinates (y, v) of $h_{\mathscr{W}}$ in the symmetric neighborhood $\mathscr{W}$.

Moreover, using the same notation as in Section 3.2, the pair of elements $(g, h) = (L_{\Sigma_0}(g_{\mathscr{W}}), R_{\Upsilon_0}(h_{\mathscr{W}})) \in \mathscr{W}_{\Sigma_0} \times \mathscr{W}_{\Upsilon_0}$ is composable if and only if $y = \mathsf{b}(x, u)$.

To find the local equations satisfied by the coordinates of a solution (g, h) of the discrete Euler-Lagrange equations for L_d

$$\overleftarrow{e_\gamma}(g)(L_d) - \overrightarrow{e_\gamma}(h)(L_d) = 0, \quad \text{for all } \gamma, \tag{37}$$

we take into account equations (35) and (36), from where we get that equations (37) hold if and only if

$$(T_{g_{\mathscr{W}}} L_{\Sigma_0})(\overleftarrow{e_\gamma}(g_{\mathscr{W}}))(L_d) - (T_{h_{\mathscr{W}}} R_{\Upsilon_0})(\overrightarrow{e_\gamma}(h_{\mathscr{W}}))(L_d) = 0, \quad \text{for all } \gamma$$

or, equivalently,

$$\overleftarrow{e_\gamma}(g_{\mathscr{W}})(L_d \circ L_{\Sigma_0}) - \overrightarrow{e_\gamma}(h_{\mathscr{W}})(L_d \circ R_{\Upsilon_0}) = 0, \quad \text{for all } \gamma.$$

In conclusion, using (24) and (25), we have proved

Theorem 1. *The pair $(g, h) = (L_{\Sigma_0}(g_{\mathscr{W}}), R_{\Upsilon_0}(h_{\mathscr{W}})) \in \mathscr{W}_{\Sigma_0} \times \mathscr{W}_{\Upsilon_0}$ is a solution of the discrete Euler-Lagrange equations for L_d if and only if the local coordinates of g and h*

$$g \cong (x, u) \cong g_{\mathscr{W}}, \quad h \cong (y, v) = (\mathsf{b}(x, u), v) \cong h_{\mathscr{W}}$$

satisfy the equations

$$L^{\gamma}_{\mu}(x,u)\frac{\partial(L_d\circ L_{\Sigma_0})}{\partial u^{\gamma}}(x,u)+\rho^{i}_{\mu}(y)\frac{\partial(L_d\circ R_{\Upsilon_0})}{\partial x^{i}}(y,v)+ - R^{\gamma}_{\mu}(y,v)\frac{\partial(L_d\circ R_{\Upsilon_0})}{\partial u^{\gamma}}(y,v)=0. \tag{38}$$

Note that the coordinates of g_0 and h_0 in $\mathscr{W}_{\Sigma_0}$ and $\mathscr{W}_{\Upsilon_0}$, respectively, are $(x_0,0)$. Next, as in Section 3.5, we will consider the matrix $(\mathbb{F}L_d)^{\gamma}_{\mu}(x,u)$, where

$$\begin{aligned}(\mathbb{F}L_d)^{\gamma}_{\mu}(x,u) =&\rho^{i}_{\mu}(x)\frac{\partial^2(L_d\circ R_{\Upsilon_0})}{\partial x^{i}\partial u^{\gamma}}(x,u)+\\ &-\frac{\partial R^{\nu}_{\mu}}{\partial u^{\gamma}}(x,u)\frac{\partial(L_d\circ R_{\Upsilon_0})}{\partial u^{\nu}}(x,u)+\\ &-R^{\nu}_{\mu}(x,u)\frac{\partial^2(L_d\circ R_{\Upsilon_0})}{\partial u^{\nu}\partial u^{\gamma}}(x,u).\end{aligned}$$

Then, we have the following result:

Theorem 2. *The following statements are equivalent.*

- *The matrix* $(\mathbb{F}L_d)^{\gamma}_{\mu}(x_0,0)$ *is regular.*
- *The Poincare-Cartan 2-section* Ω_{L_d} *is non-degenerate at the point* h_0.
- *The map* $\mathbb{F}^{-}L_d$ *is a local diffeomorphism at* h_0.

Any of them implies the following: there exist open neighborhoods $\tilde{\mathscr{W}}_{\Sigma_0}\subseteq\mathscr{W}_{\Sigma_0}$ *and* $\tilde{\mathscr{W}}_{\Upsilon_0}\subseteq\mathscr{W}_{\Upsilon_0}$ *of* g_0 *and* h_0 *such that if* $g\in\tilde{\mathscr{W}}_{\Sigma_0}$ *then there is a unique* $\Psi(g)=h\in\tilde{\mathscr{W}}_{\Upsilon_0}$ *satisfying that the pair* (g,h) *is a solution of the Euler-Lagrange equations for* L_d. *In fact, the map* $\Psi:\tilde{\mathscr{W}}_{\Sigma_0}\to\tilde{\mathscr{W}}_{\Upsilon_0}$ *is a local discrete Euler-Lagrange evolution operator.*

Proof. If the matrix $(\mathbb{F}L_d)^{\gamma}_{\mu}(x_0,0)$ is regular then, using Theorem 1 and the implicit function theorem, we deduce the result about the existence of the local discrete Euler-Lagrange evolution operator $\Psi:\tilde{\mathscr{W}}_{\Sigma_0}\to\tilde{\mathscr{W}}_{\Upsilon_0}$.

On the other hand, the map R_{Υ_0} is a diffeomorphism from an open neighborhood of $\varepsilon(x_0)$ in the α-fiber $\alpha^{-1}(x_0)$ to an open neighborhood of h_0 in the α-fiber $\alpha^{-1}(x_0)$. Indeed, (a) it is well defined: if $h\in\alpha^{-1}(x_0)$ then

$$\alpha(R_{\Upsilon_0}(h))=\alpha(h\cdot\Upsilon_0)=\alpha(h)=x_0,$$

so that $R_{\Upsilon_0}(h)\in\alpha^{-1}(x_0)$; (b) it is injective: it is the restriction of a local diffeomorphism to an α-fiber; and (c) it is surjective: $\beta\circ(\Upsilon_0)_{\alpha}$ is a diffeomorphism, so that if $h'\in\alpha^{-1}(x_0)$ there exists $x\in M$ such that $(\beta\circ(\Upsilon_0)_{\alpha})(x)=\beta(h')$, from where $h=h'[(\Upsilon_0)_{\alpha}(x)]^{-1}\in\alpha^{-1}(x_0)$ and hence $R_{\Upsilon_0}(h)=h'$.

Consequently, if

$$w^{\gamma}(h_0) = (T_{\varepsilon(x_0)} R_{\Upsilon_0})(\frac{\partial}{\partial u^{\gamma}}_{|\varepsilon(x_0)}), \text{ for all } \gamma,$$

then $\{w^{\gamma}(h_0)\}$ is a basis of the vertical bundle to α at the point h_0.

Moreover, if $\overrightarrow{e_{\mu}}$ is the right-invariant vector field on $\mathscr{W}_{\Upsilon_0}$ given by

$$\overrightarrow{e_{\mu}}(h) = (T_{h_{\mathscr{W}}} R_{\Upsilon_0})(\overrightarrow{e_{\mu}}(h_{\mathscr{W}})), \quad \text{for } h = R_{\Upsilon_0}(h_{\mathscr{W}}) \in \mathscr{W}_{\Upsilon_0}$$

then, using (25), it follows that

$$\overrightarrow{e}_{\mu}(L_d) \circ R_{\Upsilon_0} = -\rho^i_{\mu} \frac{\partial (L_d \circ R_{\Upsilon_0})}{\partial x^i} + R^{\nu}_{\mu} \frac{\partial (L_d \circ R_{\Upsilon_0})}{\partial u^{\nu}}$$

which implies that the matrix $(w^{\gamma}(h_0)(\overrightarrow{e_{\mu}}(L_d)))$ is, up to the sign, $(\mathbb{F}L_d)^{\gamma}_{\mu}(x_0, 0)$.

In addition, from (11) and (36), we deduce that the local expression of the restriction of $\mathbb{F}^- L_d$ to $\mathscr{W}_{\Upsilon_0}$ is

$$(\mathbb{F}^- L_d)(x,u) = (x, -\rho^i_{\gamma}(x) \frac{\partial (L_d \circ R_{\Upsilon_0})}{\partial x^i}(x,u) + R^{\mu}_{\gamma}(x,u) \frac{\partial (L_d \circ R_{\Upsilon_0})}{\partial u^{\mu}}(x,u)).$$

These facts prove the result.

Now, as in Section 3.5, we consider local coordinates $(\bar{x}, \bar{u})$ on $i(\mathscr{U}) = \bar{\mathscr{U}}$ given by $(\bar{x}, \bar{u}) = (x,u) \circ i$. Note that $\mathscr{W} \subseteq \bar{\mathscr{U}}$ and, thus, we have local coordinates on $\mathscr{W}_{\Sigma_0}$ and $\mathscr{W}_{\Upsilon_0}$ which we also denote by $(\bar{x}, \bar{u})$.

As above, using equations (31) and (32), we may prove that a pair $(g,h) = (L_{\Sigma_0}(g_{\mathscr{W}}), R_{\Upsilon_0}(h_{\mathscr{W}})) \in \mathscr{W}_{\Sigma_0} \times \mathscr{W}_{\Upsilon_0}$ is a solution of the discrete Euler-Lagrange equations for L_d if and only if the local coordinates of g and h

$$g \cong (\bar{y}, \bar{v}) = (\mathsf{b}(\bar{x}, \bar{u}), \bar{v}) \cong g_{\mathscr{W}}, \quad h \cong (\bar{x}, \bar{u}) \cong h_{\mathscr{W}}$$

satisfy the equations

$$\begin{aligned} 0 = & -\rho^i_{\mu}(\mathsf{b}(\bar{x}, \bar{u})) \frac{\partial (L_d \circ L_{\Sigma_0})}{\partial \bar{x}^i}(\mathsf{b}(\bar{x}, \bar{u}), \bar{v}) + \\ & + R^{\gamma}_{\mu}(\mathsf{b}(\bar{x}, \bar{u}), \bar{v}) \frac{\partial (L_d \circ L_{\Sigma_0})}{\partial \bar{u}^{\gamma}}(\mathsf{b}(\bar{x}, \bar{u}), \bar{v}) + \\ & - L^{\gamma}_{\mu}(\bar{x}, \bar{u}) \frac{\partial (L_d \circ R_{\Upsilon_0})}{\partial \bar{u}^{\gamma}}(\bar{x}, \bar{u}). \end{aligned} \tag{39}$$

In order to apply the implicit function theorem (using (39), we want to obtain $\bar{v}$ in terms of $\bar{x}$ and $\bar{u}$ in a neighborhood of (x_0, u_0, v_0)), we consider the matrix $\overline{(\mathbb{F}L)}^{\gamma}_{\mu}(\bar{x}, \bar{u})$, where

$$\begin{aligned}\overline{(\mathbb{F}L)}^{\gamma}_{\mu}(\bar{x}, \bar{u}) =& \rho^{i}_{\mu}(\bar{x}) \frac{\partial^2 (L_d \circ R_{\Upsilon_0})}{\partial \bar{x}^i \partial \bar{u}^{\gamma}}(\bar{x}, \bar{u}) + \\ &- \frac{\partial R^{\nu}_{\mu}}{\partial \bar{u}^{\gamma}}(\bar{x}, \bar{u}) \frac{\partial (L_d \circ R_{\Upsilon_0})}{\partial \bar{u}^{\nu}}(\bar{x}, \bar{u}) + \\ &- L^{\nu}_{\mu}(\bar{x}, \bar{u}) \frac{\partial^2 (L_d \circ R_{\Upsilon_0})}{\partial \bar{u}^{\nu} \partial \bar{u}^{\gamma}}(\bar{x}, \bar{u}). \end{aligned} \tag{40}$$

Then, one may prove the following result.

Theorem 3. *The following statements are equivalent.*

- *The matrices* $(\mathbb{F}L_d)^{\gamma}_{\mu}(x_0, 0)$ *and* $\overline{(\mathbb{F}L)}^{\gamma}_{\mu}(x_0, 0)$ *are regular.*
- *The Poincare-Cartan 2-section* Ω_{L_d} *is non-degenerate at the points* g_0 *and* h_0.
- *The maps* $\mathbb{F}^+ L_d$ *and* $\mathbb{F}^- L_d$ *are local diffeomorphisms at* g_0 *and* h_0.

Any of them implies the following: there exist open neighborhoods $\tilde{\mathscr{W}}_{\Sigma_0} \subseteq \mathscr{W}_{\Sigma_0}$ *and* $\tilde{\mathscr{W}}_{\Upsilon_0} \subseteq \mathscr{W}_{\Upsilon_0}$ *of* g_0 *and* h_0 *and a unique (local) discrete Euler-Lagrange evolution operator* $\Psi : \tilde{\mathscr{W}}_{\Sigma_0} \to \tilde{\mathscr{W}}_{\Upsilon_0}$ *such that* $\Psi(g_0) = h_0$. *In addition,* Ψ *is a diffeomorphism.*

Proof. Suppose that the matrices $(\mathbb{F}L)^{\gamma}_{\mu}(x_0, 0)$ and $\overline{(\mathbb{F}L)}^{\gamma}_{\mu}(x_0, 0)$ are regular. Then, the existence of the local discrete Euler-Lagrange evolution operator $\Psi : \tilde{\mathscr{W}}_{\Sigma_0} \to \tilde{\mathscr{W}}_{\Upsilon_0}$ is guaranteed by Theorem 2. Moreover, using (39), (40) and the implicit function theorem, we deduce that there exist open neighborhoods of g_0 and h_0 which we will assume, without the loss of generality, that are $\tilde{\mathscr{W}}_{\Sigma_0}$ and $\tilde{\mathscr{W}}_{\Upsilon_0}$ and, in addition, there exists a smooth map

$$\Xi : \tilde{\mathscr{W}}_{\Upsilon_0} \to \tilde{\mathscr{W}}_{\Sigma_0}$$

such that, for each $h \in \tilde{\mathscr{W}}_{\Upsilon_0}$, the pair $(\Xi(h), h)$ is a solution of the discrete Euler-Lagrange equations for L_d.

Thus, from Theorem 2, we obtain that

$$\Psi \circ \Xi = id, \quad \Xi \circ \Psi = id, \tag{41}$$

which implies that Ψ is a diffeomorphism. Indeed, if $g \in \tilde{\mathscr{W}}_{\Sigma_0}$ then there is a unique element h in $\tilde{\mathscr{W}}_{\Upsilon_0}$, namely $h = \Psi(g)$, such that (g, h) is a solution of the discrete Euler-Lagrange equations for L_d. This proves (41) and thus Ψ is a diffeomorphism.

On the other hand, the map L_{Σ_0} is a diffeomorphism from an open neighborhood of $\varepsilon(x_0)$ in $\beta^{-1}(x_0)$ on an open neighborhood of g_0 in $\beta^{-1}(x_0)$. Using this fact, (12), (24), (35) and proceeding as in the proof of Theorem 2, we deduce the result.

4.3 Application

Let $L_d : G \to \mathbb{R}$ be a discrete regular Lagrangian. Starting with a symmetric neighborhood $\mathscr{W}$ of the Lie groupoid G, we have local expressions for the discrete Euler-Lagrange equations assuming that we can solve it on the symmetric neighborhood. If this is not the case, we are forced to use bisections.

To illustrate this, assume that G is a connected Lie group and $\mathscr{W}$ is a symmetric neighborhood of the identity $\mathfrak{e} \in G$. Assume that there exists a family of points of G: $\{g_i\}_{1\leq i\leq m}$ and $\{h_j\}_{1\leq j\leq n}$, with $g_1 = h_1 = \mathfrak{e}$ such that $G = \bigcup_{i=1}^{m} g_i \mathscr{W} = \bigcup_{j=1}^{n} \mathscr{W} h_j$ (for instance, if G is compact this property is verified).

Given an initial point g, then there exists at least an integer I, $1 \leq I \leq m$ such that $g \in g_I \mathscr{W}$ ($g_I \in G$ is the bisection using our notation). Now, we try to find an integer J, $1 \leq J \leq n$ such that there exists a solution $h \in \mathscr{W} h_J$ of the following equation defined on the symmetric neighborhood $\mathscr{W}$:

$$(T_{g_I^{-1}g} L_{g_I})(\overleftarrow{e_\gamma}(g_I^{-1}g))(L_d) - (T_{hh_J^{-1}} R_{h_J})(\overrightarrow{e_\gamma}(hh_J^{-1}))(L_d) = 0, \quad \text{for all } \gamma$$

where $\{e_\gamma\}$ is a basis of the Lie algebra $\mathfrak{g}$. If we find this J, $1 \leq J \leq n$, we will say that the pair $(g, h) \in G_2$ is a solution of the discrete Euler-Lagrange equations for L_d.

We will explore in a future paper these techniques working with points not included in symmetric neighborhoods or points not included in the neighborhoods where the retraction maps are local diffeomorphisms.

5 Conclusions and Future Work

In this paper we have studied the local description of discrete Mechanics. In Section 3, we have found a local description of the discrete Euler-Lagrange equations using the notion of symmetric neighborhood on Lie groupoids. In Section 4, we extend this construction for points outside of this type of neighborhoods using bisections. We expect that our results apply to a wide range of numerical methods using discrete variational calculus.

On the other hand, this paper will also open the possibility to easily adapt our construction to other families of geometric integrators derived from discrete Mechanics, as for instance, forced or dissipative systems, holonomic constraints, explicitly time-dependent systems [22], frictional contact [28] nonholonomic constraints [13], multisymplectic field theories [23] and discrete optimal control [14, 17, 27].

Acknowledgements This work has been partially supported by MEC (Spain) Grants MTM2009-13383, MTM2010-21186-C02-01, MTM2011-15725E, MTM2012-33575, MTM2012-34478,

MTM2013-42870-P Aragon government project DGA-E24/1, project of the Canary Government Prod ID20100210, the ICMAT Severo Ochoa project SEV-2011-0087 and the European project IRSES-project "Geomech-246981". JCM acknowledges the partial support from IUMA (University of Zaragoza). JCM and DMdD have benefited from attending the conference *Focus Program on Geometry, Mechanics and Dynamics, the legacy of Jerry Marsden*, held at the Fields Institute, so they thank the organizers for their invitation.

References

1. Abraham, R., Marsden, J.E.: Foundations of Mechanics, 2nd edn. Benjamin/Cummings, Reading (1978)
2. Absil, P.-A., Mahony, R., Sepulchre, R.: Optimization Algorithms on Matrix Manifolds. Princeton University Press, Princeton (2008)
3. Bou-Rabee, N., Marsden, J.E.: Hamilton-Pontryagin integrators on Lie groups: introduction and structure-preserving properties. Found. Comput. Math. **9**(2), 197–219 (2009)
4. Cannas da Silva, A., Weinstein, A.: Geometric Models for Noncommutative Algebras. Berkeley Mathematics Lecture Notes Series, vol. 10. American Mathematical Society/Berkeley Center for Pure and Applied Mathematics, Providence/Berkeley (1999)
5. Coste, A., Dazord, P., Weinstein, A.: Grupoïdes symplectiques Publ. Dép. Math. Lyon **2/A**, 1–62 (1987)
6. de León, M., Marrero, J.C., Martínez, E.: Lagrangian submanifolds and dynamics on Lie algebroids. J. Phys. A Math. Gen. **38**, R241–R308 (2005)
7. Desbrun, M., Hirani, A.N., Marsden, J.E.: Discrete exterior calculus for variational problems in computer vision and graphics. Proc. CDC **42**, 4902–4907 (2003)
8. Fetecau, R.C., Marsden, J.E., Ortiz, M., West, M.: Nonsmooth Lagrangian mechanics and variational collision integrators. SIAM J. Appl. Dyn. Syst. **2**(3), 381–416 (2003)
9. Fetecau, R.C., Marsden, J.E., West, M.: Variational multisymplectic formulations of nonsmooth continuum mechanics. In: Kaplan, E., Marsden, J.E., Sreenivasan, K.R. (eds.) Perspectives and Problems in Nonlinear Science: A Celebratory Volume in Honor of Larry Sirovich, pp. 229–262. Springer, New York (2003)
10. Gawlik, E.S., Marsden, J.E., Campagnola, S., Moore, A.: Invariant manifolds, discrete mechanics, and trajectory design for a mission to Titan. AAS **09-226**, 1887–1903 (2009)
11. Gawlik, E.S., Mullen, P., Pavlov, D., Marsden, J.E., Desbrun, M.: Geometric, variational discretization of continuum theories. Physica D **240**(21), 1724–1760 (2011)
12. Hairer, E., Lubich, Ch., Wanner, G.: Geometric Numerical Integration. Structure-Preserving Algorithms for Ordinary Differential Equations. Springer Series in Computational Mathematics, vol. 31. Springer, Heidelberg (2010)
13. Iglesias, D., Marrero, J.C., Martín de Diego, D., Martínez, E.: Discrete nonholonomic Lagrangian systems on Lie groupoids. J. Nonlinear Sci. **18**(3), 221–276 (2008)
14. Jiménez, F., Kobilarov, K., Martín de Diego, D.: Discrete variational optimal control. J. Nonlinear Sci. **23**(3), 393–426 (2013)
15. Kharevych, L., Weiwei, L. ,Tong, Y., Kanso, E., Marsden, J.E., Schröder, P., Desbrun, M.: Geometric, variational integrators for computer animation. In: Eurographics/ACM SIGGRAPH Symposium on Computer Animation, pp. 1–9 (2006)
16. Koon, W.S., Lo, M.W., Marsden, J.E., Ross, S.D.: Dynamical systems, the three-body problem and space mission design. In: International Conference on Differential Equations, Berlin, 1999, vols. 1, 2, pp. 1167–1181. World Scientific Publishing, River Edge (2000)
17. Leok, M.: Foundations of computational geometric mechanics. Control and dynamical systems. California Institute of Technology (2004)
18. Leok, M., Ohsawa, T.: Variational and geometric structures of discrete Dirac mechanics. Found. Comput. Math. **11**(5), 529–562 (2011)

19. Lewis, D., Ratiu, T., Simo, J.C., Marsden, J.E.: The heavy top: a geometric treatment. Nonlinearity **5**(1), 1–48 (1992)
20. Mackenzie, K.: General Theory of Lie Groupoids and Lie Algebroids. London Mathematical Society Lecture Note Series, vol. 213. Cambridge University Press, Cambridge (2005)
21. Marrero, J.C., Martín de Diego, D., Martínez, E.: Discrete Lagrangian and Hamiltonian mechanics on Lie groupoids. Nonlinearity **19**(6), 1313–1348 (2006); Corrigendum: Nonlinearity **19**(12), 3003–3004 (2006)
22. Marsden, J.E., West, M.: Discrete mechanics and variational integrators. Acta Numer. **10**, 357–514 (2001)
23. Marsden, J.E., Patrick, G.W., Shkoller, S.: Multisymplectic geometry, variational integrators, and nonlinear PDEs. Commun. Math. Phys. **199**(2), 351–395 (1998)
24. Marsden, J.E., Pekarsky, S., Shkoller, S.: Discrete Euler-Poincaré and Lie-Poisson equations. Nonlinearity **12**(6), 1647–1662 (1999)
25. Marsden, J.E., Pekarsky, S., Shkoller, S.: Symmetry reduction of discrete Lagrangian mechanics on Lie groups. J. Geom. Phys. **36**(1–2), 140–151 (2000)
26. Martínez, E.: Lagrangian mechanics on Lie algebroids. Acta Appl. Math. **67**, 295–320 (2001)
27. Ober-Blöbaum, S., Junge, O., Marsden, J.E.: Discrete mechanics and optimal control: an analysis. ESAIM Control Optim. Calc. Var. **17**(2), 322–352 (2011)
28. Pandolfi, A., Kane, C., Marsden, J.E., Ortiz, M.: Time-discretized variational formulation of non-smooth frictional contact. Int. J. Numer. Methods Eng. **53**(8), 1801–1829 (2002)
29. Weinstein, A: Lagrangian mechanics and groupoids. Fields Inst. Commun. **7**, 207–231 (1996)
30. Wendlandt, J.M., Marsden, J.E.: Mechanical integrators derived from a discrete variational principle. Physica D **106**(3–4), 223–246 (1997)

Keplerian Dynamics on the Heisenberg Group and Elsewhere

Richard Montgomery and Corey Shanbrom

For Jerry

Abstract Posing Kepler's problem of motion around a fixed "sun" requires the geometric mechanician to choose a metric and a Laplacian. The metric provides the kinetic energy. The fundamental solution to the Laplacian (with delta source at the "sun") provides the potential energy. Posing Kepler's three laws (with input from Galileo) requires symmetry conditions. The metric space must be homogeneous, isotropic, and admit dilations. Any Riemannian manifold enjoying these three symmetry properties is Euclidean. So if we want a semblance of Kepler's three laws to hold but also want to leave the Euclidean realm, we are forced out of the realm of Riemannian geometries. The Heisenberg group (a subRiemannian geometry) and lattices provide the simplest examples of metric spaces enjoying a semblance of all three of the Keplerian symmetries. We report success in posing, and solving, the Kepler problem on the Heisenberg group. We report failures in posing the Kepler problem on the rank two lattice and partial success in solving the problem on the integers. We pose a number of questions.

1 Introduction

Newton formulated and solved what we call today "Kepler's problem" – the problem whose negative energy solutions are Keplerian ellipses. The essential backdrop to the problem is Euclidean three-space and its group of isometries and scalings. Can we pose Kepler's problem on an arbitrary metric space? What properties must the space have if Kepler's three laws, or ghosts of these laws, are to hold?

R. Montgomery (✉)
Department of Mathematics, University of California, Santa Cruz, Santa Cruz, CA 95064, USA
e-mail: rmont@count.ucsc.edu

C. Shanbrom
Department of Mathematics and Statistics, California State University, Sacramento, Sacramento, CA 95819, USA
e-mail: corey.shanbrom@csus.edu

D.E. Chang et al. (eds.), *Geometry, Mechanics, and Dynamics*, Fields Institute Communications 73, DOI 10.1007/978-1-4939-2441-7_14

In 'Foundations of Mechanics' [1], Abraham and Marsden formulate classical mechanics as dynamical systems on the tangent or cotangent bundle of a Riemannian manifold, which they call "natural mechanical systems". The Riemannian metric defines the kinetic energy. One must choose a potential energy. In order to formulate Kepler's problem on our manifold, we take this potential to be the fundamental solution to the Laplacian. We choose a point on the manifold to be our "sun," which is the delta function source of the fundamental solution. Following Galileo we assume that the choice of location of the sun does not matter: that is, we will assume that our space is homogeneous.

The mildest Riemannian departures from Euclidean space are the spaces of constant curvature: the sphere and hyperbolic space. About a century and a half before 'Foundations,' Lobachevksy [14], one of the founders of hyperbolic geometry, posed the Kepler problem as a "natural mechanical system" on hyperbolic space. Later, Serret [17] posed the Kepler problem on the sphere. Additional history and references appear in [8] (the research content of [8] appeared in a refereed journal as [6] and [7], however [8] has a much more thorough history). Extensions of the Kepler problem to surfaces of non-constant curvature have also been studied; in particular, Darboux [10] attempted to extend Bertrand's theorem to surfaces of revolution. More recent work in this direction can be found in [16] and [20].

Kepler's 1st and 2nd laws hold in each of the three constant curvature geometries: hyperbolic space, the 3-sphere, and the original flat Euclidean space. But Kepler's 3rd law fails for these non-flat geometries for the simple reason that they admit no continuous scaling symmetries, or "dilations."

We argue that in order to even formulate Kepler's third law our metric space must admit dilations. But if a space admits dilations, and is not Euclidean, then it cannot even be Riemannian! (We sketch the proof of this fact below.) The non-Euclidean spaces which admit dilations are subRiemannian: they are the Carnot groups. The simplest Carnot group is the Heisenberg group.

This observation brings us to our main problem: pose and solve the Kepler problem on the Heisenberg group. We will pose it. We will not fully solve it. We will show that all periodic solutions to the Kepler problem on the Heisenberg group must lie on the zero energy surface, and that the problem is integrable *when restricted to this zero energy surface*. Such solutions are described in Figures 2 and 4. A modified version of Kepler's third law holds for the periodic solutions.

To write down the Kepler-Heisenberg problem we must have an explicit expression for the potential: it is the fundamental solution for the *sub*Laplacian on the Heisenberg group. Luckily, Folland [5] found such an expression in 1970.

We will also attempt to pose and solve Kepler's problem on some lattices. Lattices almost admit dilations: we can scale by positive integer scaling factors, but we cannot invert these scaling factors. The integers form the simplest lattice. We will pose and solve a Kepler problem on the integers. Our 'solutions' are of a high school nature. (We apologize in advance if our treatment here embarrasses readers with any skill in numerical methods and discretization.) These solutions are indicated in Figure 5.

We then try to pose and solve the Kepler problem on the integer lattice in the plane where we run into fundamental problems which lead us to believe that the

very definition of a discrete dynamical system is not yet well formulated. The heart of this problem is that the differences of values of the lattice potential – that being the fundamental solution of the lattice Laplacian – are irrational.

DEDICATION AND ACKNOWLEDGEMENTS. This article is dedicated to the memory of Jerry and in thanks for all his inspiration. We would also like to thank the GMC group, in particular, David Martín de Diego, Juan Carlos Marrero, and Edith Padron for inviting us to the summer school in 2011 outside of Madrid. The formulation of the Kepler-Heisenberg problem was inspired by talking with many of the participants at that summer school.

2 Kepler's 3 Laws in a Metric Space

Let's recall Kepler's three laws for the motion of planets around the sun.

K1. Planets travel on ellipses with one focus the sun.
K2. Equal areas are swept out in equal times. This law is equivalent to the conservation of the planet's angular momentum about the sun.
K3. Period-Size: The period T of an orbit and its size a (semi-major axis) are related by a universal monomial relation $a^3 = CT^2$.

The Keplerian planet moves in a Euclidean space. Do Kepler's laws even make sense on a general metric space? If not, what restrictions must we impose on the metric space in order to make sense of a particular law? We discuss what is required of our metric space in order to formulate the corresponding law.

K1. We can define an "ellipsoid" for any metric space X. Fix two foci $S, F \in X$ and a positive number $2a$. Consider the locus of points $x \in X$ for which $d(S, x) + d(x, F) = 2a$. If this locus is to be a curve then the metric space must be two-dimensional, for example, a smooth surface. K1 requires then that X is a two-dimensional, or that its Keplerian dynamics can be reduced to two-dimensions. Kepler's problem has been posed and solved satisfactorily on the two-sphere and on the hyperbolic plane as described in the introduction. Its solutions satisfy K1.

K2 is equivalent to conservation of angular momentum. Angular momentum is conserved if the kinetic and potential energies in Newton's formulation of the Kepler problem are invariant under rotations about the sun. This requires isotropicness: all directions in the metric space are the same, at least through the sun. The two-sphere and the hyperbolic plane enjoy rotational symmetry and hence K2.

K3 is a scaling law. It is an immediate consequence of the fact that the Newtonian potential $V(x) = c/|x|$ is homogeneous of degree -1. This homogeneity implies the space-time symmetry $x, t \mapsto \lambda x, \lambda^{3/2} t$, which is to say: if $x(t)$ solves Kepler's equation then so does $\lambda x(\lambda^{-3/2} t)$. From one periodic solution $x(t)$ we generate a one-parameter family x_λ. The energy-period relation in K3 for this family follows from the scaling symmetry.

2.1 Kepler's Third Law for Homogeneous Potentials in Euclidean Space

Any homogeneous potential V on a Euclidean space enjoys a version of K3. Homogeneity is a scaling symmetry: $x \mapsto \lambda x \implies V(x) \mapsto V(\lambda x) = \lambda^{-\alpha} V(x)$. We try to extend the symmetry to time and velocities by a power law ansatz: $(x, t, v) \mapsto (\lambda x, \lambda^{\beta} t, \lambda^{-\nu} v)$. Balancing the resulting scalings of potential and kinetic energies implies that $\nu = \alpha/2$. The requirement $v = dx/dt$ yields $\beta = 1 + (\alpha/2)$. We are led to the extended scalings

$$(x, t, v) \mapsto (\lambda x, \lambda^{1+\alpha/2} t, \lambda^{-\alpha/2} v).$$

In terms of curves $\gamma(t)$, which are maps from t to x-space, the scaling operation is

$$\gamma(t) \mapsto \gamma_\lambda(t) = \lambda \gamma(\lambda^{-(1+\alpha/2)} t).$$

One verifies that if γ satisfies Newton's equation $\ddot{\gamma} = -\nabla V(\gamma)$ then so does γ_λ. (Use that ∇V is homogeneous of degree $-\alpha - 1$.) The scaling symmetry thus takes solutions of energy H to solutions of energy $\lambda^{-\alpha} H$. Now if γ is periodic of period T and with typical size a, then γ_λ is periodic of period $\lambda^{\beta} T = \lambda^{1+\alpha/2} T$ and typical size λa. We thus arrive at our modified K3: $T^2 = C a^{2+\alpha}$.

2.2 Dilations

To have an analogue of K3, our metric space must, like Euclidean space, admit dilations.

Definition 1. A dilation of the metric space (X, d) with center $S \in X$ and dilation factor λ is a map $\delta_\lambda : X \to X$ which fixes S and satisfies $d(\delta_\lambda x, \delta_\lambda y) = \lambda d(x, y)$ for all $x, y \in X$. We say that the metric space X admits dilations if there is a dilation of X with dilation factor λ for each $\lambda > 0$.

Spherical and hyperbolic metrics admit no dilations. K3 fails for both.

2.3 Keplerian Symmetries

We will restrict ourselves to metric spaces X which

- are homogeneous (1)
- are isotropic (2)
- admit dilations. (3)

We will call these three properties the *Keplerian symmetry assumptions*.

Historical Motivation. Newton's biggest victory was probably his derivation of Kepler's laws K1, K2, K3, from more basic laws: Galilean invariance, his equation $F = ma$, and the specific choice of force F as '$1/r^2$.' From these laws he derived what we today call Kepler's differential equation $\ddot{q} = -q/|q|^3$ and thence K1–3. A subset of the Galilean group is the group of spatial isometries and this relates to homogeneity and isotropicness. Dilations, as discussed above, are included so as to get a version of Kepler's third law.

We recall the formal definition homogeneity and isotropicness. Let $Isom(X)$ denotes the group of isometries of X. Homogeneity asserts that $Isom(X)$ acts transitively on X. Isotropicness asserts that $Isom(X)$ acts transitively on the space of directions through any point $S \in X$. The sphere and the hyperbolic plane are homogeneous and isotropic, but they do not admit dilations.

Proposition 1. *If a Riemannian manifold is homogeneous and admits dilations then it is a Euclidean space.*

Proof (sketch). See Gromov [12], prop. 3.15. Gromov defines the metric tangent cone T_pX of any metric space at any point $p \in X$ as the pointed limit $(X, \lambda d)$ as $\lambda \to \infty$. This limit need not always exist, but it does exist for Riemannian manifolds and equals the usual tangent plane, with its induced Euclidean metric. If the metric d admits a dilation with scale factor λ then (X, d) is isometric to $(X, \lambda d)$. Letting $\lambda \to \infty$ we see that such an X is isometric to its metric tangent cone T_pX for all p. □

Consequently, if we insist on satisfying all three Keplerian symmetries (1)–(3) while also leaving the realm of Euclidean spaces, we must also leave the world of Riemannian manifolds! The simplest non-Euclidean metric space satisfying (1)–(3) is the Heisenberg group with its subRiemannian metric.

2.4 Kepler's Problem and the Laplacian

Before formulating the Kepler-Heisenberg problem, we look into how the standard Kepler problem fits within the framework of "natural mechanical systems" and thus how it generalizes to general Riemannian manifolds. This background will yield a straightforward way to place the Kepler problem in the Heisenberg context.

The Hamiltonian for the standard Kepler problem on $\mathbb{R}^3$ is

$$H = \frac{1}{2}(p_x^2 + p_y^2 + p_z^2) - \frac{\alpha}{r},$$

where $r = \sqrt{x^2 + y^2 + z^2}$ and $\alpha > 0$. Why the $1/r$ potential? Perhaps the best answer is that $U = \frac{1}{4\pi r}$ is the fundamental solution for the Laplacian Δ on (Euclidean!) $\mathbb{R}^3$, i.e. the solution to $\Delta U = -\delta_0$. (See [3] and references therein.) The choice of sign convention is due to the positivity of the operator $-\Delta$.

The kinetic term in H is the principal symbol of the Laplacian, so we can write

$$H(q,p) = \frac{1}{2}\sigma_\Delta - \alpha\Delta_q^{-1} \qquad (*)$$

where σ_L denotes the principal symbol of L, and $\Delta^{-1}(q) = K(q,0)$, where $K(x,y) = U(x-y)$ is the Green's function for the Laplacian (and where $\alpha = \frac{1}{4\pi}$). This reformulation suggests that we can pose the Kepler problem as a Hamiltonian system on any 'space' X with a 'Laplacian' Δ.

This prescription (*) for H leaves us with a number of puzzles.

2.5 Problems

What is the cotangent bundle of an arbitrary 'space' X? Assuming we make sense of H as a function on the cotangent bundle of X, then what are Hamilton's equations on T^*X? Can we ever compute the fundamental solution Δ_q^{-1} of our Laplacian?

All these questions have answers in the Riemannian case. The principal symbol has the coordinate expression

$$\sigma_\Delta(p) = \Sigma g^{ij}(q)\, p_i\, p_j$$

– it is the standard cometric of kinetic energy. The fundamental solution of the Laplacian has been explicitly computed for hyperbolic n-space, so we have a hyperbolic Kepler problem.

If X is a compact manifold without boundary, then the fundamental solution Δ_q^{-1} does not exist for topological reasons. For example, we cannot have a single gravitational source on the sphere. There must be an opposing sink elsewhere on the sphere. To formulate the Kepler problem on the sphere, one places the sink antipodally to the source. See [6, 7], or [17] for a precise formulation.

Remark. We have focused our study on generalizations of the Kepler problem which preserve the symmetry content of K1–K3. Others have tried to generalize Kepler so as to preserve one or more of the following properties, where $V = c/r$ denotes the gravitational potential.

1) V is a fundamental solution to the Laplace equation in $\mathbb{R}^3$.
2) Bertrand's theorem: excluding the harmonic oscillator potential, V is the only rotationally symmetric potential on Euclidean space all of whose bounded non-collision orbits are closed.
3) The Kepler problem is superintegrable: the common level sets of all its integrals have (typically) codimension 1 in phase space.

All three properties are retained by the Kepler problem in the sphere and hyperbolic plane. However, in our generalizations, we lose properties (2) and (3).

3 Kepler's Problem on the Heisenberg Group!

3.1 Heisenberg Geometry

Consider $\mathbb{R}^3$ with standard x, y, z coordinates, endowed with the two vector fields

$$X = \frac{\partial}{\partial x} - \frac{1}{2} y \frac{\partial}{\partial z} \qquad Y = \frac{\partial}{\partial y} + \frac{1}{2} x \frac{\partial}{\partial z}.$$

Then X, Y span the canonical contact distribution D on $\mathbb{R}^3$ with induced Lebesgue volume form. Curves are called horizontal if they are tangent to D. Declaring X, Y orthonormal defines the standard subRiemannian structure on the Heisenberg group and yields the Carnot-Carathéodory metric $ds^2_{\mathbb{H}} = dx^2 + dy^2$. Geodesics are qualitatively helices: lifts of circles and lines in the xy-plane. The horizontal constraint implies that the z-coordinate of a curve grows like the area traced out by the projection of the curve to the xy-plane. See Figure 1 and Chapter 1 of [15].

The Heisenberg (sub)Laplacian is

$$\Delta = X^2 + Y^2,$$

a second order subelliptic operator, and the only correct choice for 'Laplacian' on the Heisenberg group. We have

$$[X, Y] = \frac{\partial}{\partial z} =: Z$$

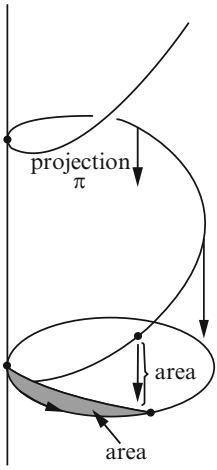

Fig. 1 A Heisenberg geodesic

and $[X, Z] = [Y, Z] = 0$. There are the commutation relations of the Heisenberg Lie algebra, hence the name. The Heisenberg group $\mathbb{H}$ is the simply connected Lie group with Lie algebra the Heisenberg algebra and is diffeomorphic to $\mathbb{R}^3$. In x, y, z coordinates the Heisenberg group law reads

$$(x_1, y_1, z_1) \cdot (x_2, y_2, z_2) = (x_1 + x_2, y_1 + y_2, z_1 + z_2 + \tfrac{1}{2}(x_1 y_2 - x_2 y_1)).$$

Left multiplication is an isometry and the vector fields X, Y are left invariant.

3.2 The Heisenberg Kepler Problem

Folland [5] has derived an explicit formula for the fundamental solution for the Heisenberg Laplacian! It is

$$U := \Delta_q^{-1} = \frac{\alpha}{\rho^2}, \qquad \rho = \{(x^2 + y^2)^2 + \tfrac{1}{16} z^2\}^{1/4}.$$

Here $\alpha = 2/\pi$. Let p_x, p_y, p_z be the dual momenta to x, y, z so that together x, y, z, p_x, p_y, p_z form canonical coordinates on $T^*\mathbb{H}$. Then

$$P_X = p_x - \tfrac{1}{2} y p_z, \quad P_Y = p_y + \tfrac{1}{2} x p_z$$

are dual momenta to X, Y, and

$$K = \tfrac{1}{2}(P_X^2 + P_Y^2) = \tfrac{1}{2}\sigma_\Delta$$

is the Heisenberg kinetic energy, given canonically by the cometric. (See Chapter 1 of [15].) K generates the subRiemannian geodesic flow on the Heisenberg group. We see that Keplerian dynamics on the Heisenberg group are the Hamiltonian dynamics for the canonical Hamiltonian

$$H = K - U.$$

There is *no* explicit formula for the Heisenberg subRiemannian distance function $||(x, y, z)||_{\mathbb{H}} := d_{sr}((x, y, z), (0, 0, 0))$, measuring the distance from a point to the origin . So the mix of K and U – of geodesic and subLaplacian – is quite interesting and it is rather remarkable that we can write down the Hamiltonian in closed form.

The dilation on the Heisenberg group is

$$\delta_\lambda(x, y, z) = (\lambda x, \lambda y, \lambda^2 z).$$

Like the subRiemannian distance, the function ρ is positive homogeneous of degree 1 with respect to this dilation. Since the Heisenberg sphere is homeomorphic to

the Euclidean sphere, the standard argument which shows that any two norms on $\mathbb{R}^n$ are Lipshitz equivalent shows that ρ and $||\cdot||_{\mathbb{H}}$ are Lipshitz equivalent: there exist positive constants c, C such that $c\rho(x, y, z) < ||(x, y, z)||_{\mathbb{H}} < C\rho(x, y, z)$ for $(x, y, z) \neq 0$.

Following the procedure described in Section 2.1, we find that if a curve γ solves Newton's equation $\ddot{\gamma}(t) = \nabla U(\gamma(t))$, where ∇ denotes the subRiemannian gradient, then so does

$$\gamma_\lambda(t) := \delta_\lambda(\gamma(\lambda^{-2}t)).$$

Then given a periodic orbit γ with period T (see Section 3.5), we get a family of periodic orbits γ_λ with periods $\lambda^2 T$. Choosing a suitable notion of the 'size' a of a periodic orbit yields the Heisenberg version of Kepler's third law:

$$T^2 = Ca^4.$$

The isometry group of the Heisenberg group is generated by translations and rotations. The translations denote the action of the Heisenberg group on itself by left multiplication. These project to translations of the xy-plane. The rotations form the circle group of rotations about the z axis. In addition we have the discrete 'reflection' $(x, y, z) \mapsto (x, -y, -z)$. Translations act transitively: the Heisenberg group is homogeneous. Rotations act transitively on (allowable) directions: the Heisenberg group is isotropic. Thus the Heisenberg group enjoys the three Keplerian symmetry properties.

3.3 Hamiltonian Dynamics

The dilation on phase space $T^*\mathbb{H}$ is

$$\delta_\lambda : (x, y, z, p_x, p_y, p_z) \mapsto (\lambda x, \lambda y, \lambda^2 z, \lambda^{-1} p_x, \lambda^{-1} p_y, \lambda^{-2} p_z).$$

This is generated by the function $J = xp_x + yp_y + 2zp_z$, which satisfies $\dot{J} = 2H$. When $H = 0$, J is a first integral. Note that $\delta_\lambda : H \mapsto \lambda^{-2} H$.

Now change to cylindrical coordinates (r, θ, z) on $\mathbb{H}$. We have the induced conjugate momenta $p_r = (xp_x + yp_y)/r$ and $p_\theta = xp_y - yp_x$. Our Hamiltonian is

$$H = \tfrac{1}{2} p_r^2 + \tfrac{1}{2}\left(\frac{p_\theta}{r} + \tfrac{1}{2} r p_z\right)^2 - \alpha\rho^{-2}.$$

Note that this does not depend on θ due to rotational symmetry, and the corresponding angular momentum p_θ is conserved.

On the smooth submanifold of phase space $\{H = 0\}$, we have three (independent) conserved quantities H, p_θ, and J, and a theorem of Arnold (see [2]) says

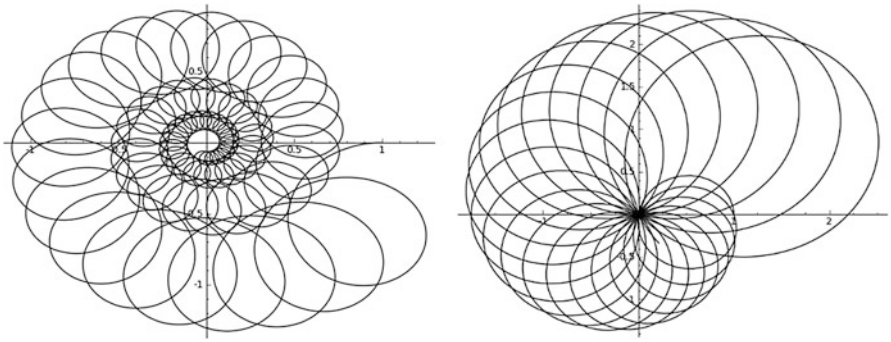

Fig. 2 Projections of zero-energy orbits to the xy-plane

that our system is integrable by quadratures here. See Figure 2 for approximations of orbits which exhibit this integrable behavior as well as the helical Heisenberg geometry. For this reason, we will mostly focus on the $H = 0$ case. This is especially justified in light of the following.

Lemma 1. *Periodic orbits must have zero energy.*

Proof. If $\gamma(t) = (x(t), y(t), z(t), p_x(t), p_y(t), p_z(t))$ satisfies $\gamma(0) = \gamma(T)$ for some $t = T$, then $J = xp_x + yp_y + 2zp_z$ is also periodic. But we know the time derivative of J is constant, given by $\dot{J} = 2H$. Since J cannot be monotonically increasing nor decreasing, we must have $\dot{J} = 2H = 0$, so $H = 0$. □

Periodic orbits exist and the existence proof forms part of C.S.'s thesis [18] – see Section 3.5 below. We will momentarily report progress with integration of the $H = 0$ system, but first we gather other dynamical results.

Proposition 2. *If $H < 0$ then any solution is bounded.*

Proof. Suppose $H = -h$ where h is positive. Then $K - U = -h$, so

$$U = K + h \geq h,$$

since K is always non-negative. Then a solution $(x(t), y(t), z(t))$ in configuration space must satisfy

$$0 \leq ((x^2 + y^2)^2 + \tfrac{1}{16}z)^{1/2} < \frac{\alpha}{h},$$

where α and h are positive constants. □

Proposition 3. *The only solutions in the plane $z = 0$ are lines through the origin.*

Proof. The equations for $\dot{z}$ and $\dot{\theta}$ satisfy the relation

$$\dot{z} = \tfrac{1}{2}r^2\dot{\theta}.$$

For a path lying in the plane $z = 0$, this implies either $r = 0$ or $\dot{\theta} = 0$. In the first case, the path is trivial. In the second, it lies on a line through the origin. Such a curve may be parametrized by

$$\gamma(t) = (c_1 t^{1/2}, c_2 t^{1/2}, 0, \tfrac{1}{2} c_1 t^{-1/2}, \tfrac{1}{2} c_2 t^{-1/2}, 0).$$

It is easy to verify that the desired equations are satisfied, and that $H = 0$. □

Proposition 4. *The only solutions constant in configuration space are*

$$\gamma(t) = (0, 0, k, 0, 0, -\tfrac{4\alpha}{k^2} t).$$

Proof. This is an easy calculation. Note that such solutions are unbounded in phase space, and satisfy $H < 0$. □

Next, we explicitly integrate the equations of motion on a codimension 3 submanifold, and recover conics reminiscent of the Euclidean Kepler problem. Consider the smooth submanifold $N = \{z = p_z = p_\theta = 0\}$. This submanifold is invariant under the dynamics, since $\dot{z} = \dot{p}_z = \dot{p}_\theta = 0$ on N. The Hamiltonian is

$$H|_N = \tfrac{1}{2} p_r^2 - \frac{\alpha}{r^2},$$

which has the form of a classical central force problem in the plane. Fix an energy level $H|_N = h$. Then since $p_r = \dot{r}$, we can explicitly solve for $r(t)$ as follows.

Proposition 5. *On N, $r(t)$ traces out a hyperbola if $h > 0$, an ellipse if $h < 0$, and a parabola if $h = 0$.*

Proof. The Hamiltonian may be rewritten as the simple ODE

$$\tfrac{1}{2}\left(\frac{dr}{dt}\right)^2 = \frac{\alpha}{r^2} + h.$$

Assume temporarily that $h \neq 0$. Integrating, we find

$$t = \int dt = \tfrac{1}{\sqrt{2}} \int \frac{r}{\sqrt{\alpha + r^2 h}} dr = \tfrac{1}{h\sqrt{2}} \sqrt{\alpha + r^2 h},$$

which may be rewritten $r^2 - 2ht^2 = -\frac{\alpha}{h}$. Since $\alpha > 0$, this curve in the t, r-plane is an ellipse for $h < 0$ and a hyperbola for $h > 0$.

If $h = 0$, we find that

$$t = \tfrac{1}{\sqrt{2\alpha}} \int r dr = \tfrac{1}{2\sqrt{2\alpha}} r^2,$$

and thus $r^2 = \sqrt{8\alpha}\, t$. □

We conclude this section with the following conjecture:

Conjecture 1. There is an open set of initial conditions whose orbits are asymptotic to helices.

This behavior is suggested by numerical experiment and by the fact that U and its derivatives tend to zero as orbits tend towards ∞.

3.4 Integration of the Case $H = 0$

We now focus on the $H = 0$ case and reduce the integrability of the equations of motion to the parametrization of a family of degree 6 algebraic plane curves.

Let $\tilde{H} = \frac{K}{U}$. Then integral curves for $\tilde{H}$ are the same as geodesics for the metric $U ds^2_{\mathbb{H}}$. When $H = 0$, this is the same as the metric $(H + U) ds^2_{\mathbb{H}}$, whose geodesics correspond to integral curves for H, according to the Jacobi-Maupertuis principle. Thus, the flow of H is the same as the flow of $\tilde{H}$ up to reparametrization on the hypersurface $\{H = 0\} = \{\tilde{H} = 1\}$.

A short calculation shows that both J and p_θ Poisson commute with $\tilde{H}$. (Recall $\{H, J\} = 2H$.) This demonstrates the scale invariance of $\tilde{H}$; $\delta_\lambda \colon \tilde{H} \mapsto \tilde{H}$. More importantly, we have three independent quantities conserved by the flow of $\tilde{H}$. Thus, we have an integrable system on $\{H = 0\} = \{\tilde{H} = 1\}$.

Change our third coordinate $z \mapsto v = z/r^2$. We have conjugate momenta $\tilde{p}_r, p_\theta, p_v$. In these coordinates, we have $J = r\tilde{p}_r$ (as in the Euclidean case) and $\tilde{H} = \tilde{H}(p_\theta, J, v, p_v)$. On the submanifold $\{H = 0\}$, we have $\tilde{H} = 1$. Also, the initial conditions determine the constants J and p_θ. Thus, given initial conditions, $\tilde{H}$ is a function of v and p_v only. We arrive at the following result.

Proposition 6. *When $\tilde{H} = 1$, any solution must project to an algebraic curve in the v, p_v-plane.*

These curves are naturally degree 10 but can be reduced to degree 6 by changing variables. Examples are shown in Figure 3. If we can parametrize these curves, we should be able to bootstrap up to find explicit solutions.

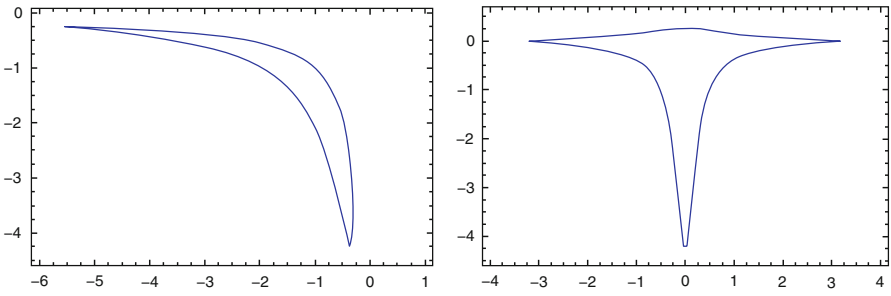

Fig. 3 Curves in the v, p_v-plane corresponding to $J = 3$, $p_\theta = 1$ (*left*) and $J = 0$, $p_\theta = 1$ (*right*)

3.5 Periodic Orbits

Despite the fact that the $H = 0$ case is integrable, we have not been able to explicitly solve the equations. However, we know that periodic orbits exist.

Take $L = K + U$ as our Lagrangian and impose the horizontal constraint $\dot{z} = \frac{1}{2}x\dot{y} - \frac{1}{2}y\dot{x}$. Then the tangent $(\gamma, \dot{\gamma})$ of any trajectory must lie on the zero set of the function

$$G = \tfrac{1}{2}x\dot{y} - \tfrac{1}{2}y\dot{x} - \dot{z}.$$

The calculus of variations tells us that if $\gamma\colon [0, T] \to \mathbb{H}$ is a minima of the action functional $\int_0^T L dt$ which also satisfies our constraint, then there exists a scalar function $\lambda = \lambda(t)$ such that γ is a minima of the modified action functional

$$A(\gamma) = \int_0^T L_\lambda(t, \gamma, \dot{\gamma}) dt,$$

where we have written $L_\lambda(t, \gamma, \dot{\gamma}) = L(\gamma, \dot{\gamma}) - \lambda(t)G(\gamma, \dot{\gamma})$. Setting the first variation of A equal to zero and integrating by parts yields the Euler-Lagrange equations:

$$\begin{aligned}
\ddot{x} &= -\lambda\dot{y} - \tfrac{1}{2}\dot{\lambda}y - 2\alpha x(x^2 + y^2)\rho^{-6} \\
\ddot{y} &= \lambda\dot{x} + \tfrac{1}{2}\dot{\lambda}x - 2\alpha y(x^2 + y^2)\rho^{-6} \\
\dot{\lambda} &= -\tfrac{\alpha}{16}z\rho^{-6}.
\end{aligned}$$

When $\lambda = p_z$ we find that these agree with Hamilton's equations.

Application of the direct method in the calculus of variations applied to $A(\gamma)$ yields a proof of the existence of periodic orbits. One works in the Hilbert space $H^1(S^1, \mathbb{H})$ and requires that admissible curves are horizontal and satisfy the symmetry conditions

$$\gamma(t + T/k) = R_{2\pi/k}\gamma(t) \tag{S1}$$

$$z(t + T/2) = -z(t) \tag{S2}$$

where

$$R_{2\pi/k} = \begin{bmatrix} \cos(2\pi/k) & -\sin(2\pi/k) & 0 \\ \sin(2\pi/k) & \cos(2\pi/k) & 0 \\ 0 & 0 & 1 \end{bmatrix}$$

and $k \geq 3$ is any odd positive integer. Any admissible curve is therefore necessarily periodic, with additional symmetry. A suggestive approximation of such a curve with $k = 3$ is shown in Figure 4.

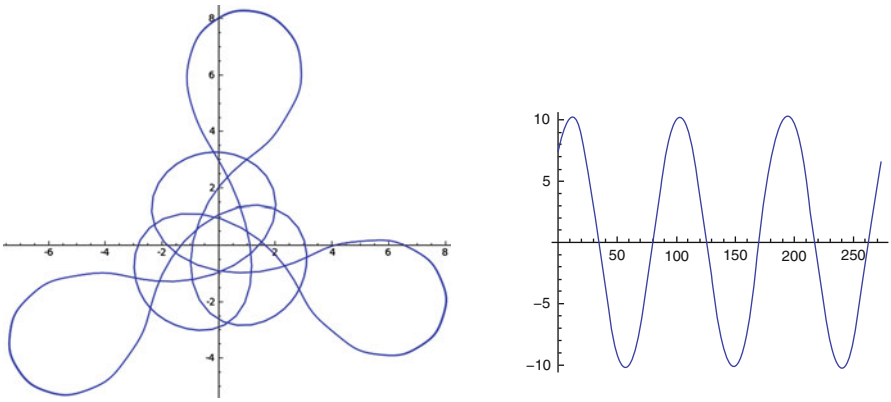

Fig. 4 Projection of an orbit to the xy-plane (*left*) and z-coordinate over time (*right*)

The idea is to choose a minimizing sequence γ_n of curves in this space, and show that they converge within the space to some γ_*. Applying elementary analysis and the principle of symmetric criticality shows that γ_* must minimize the action, thereby satisfying the Euler-Lagrange equations. A central difficulty lies in proving that γ_* does not pass through the singularity at the origin. A full existence proof appears in the thesis of C.S. [18].

3.6 A Failure of Reduction

Newton reduced his two-body problem to the Kepler problem in Euclidean space. There is no analogous reduction for the two-body problem on the Heisenberg group, nor is there for the two-body problem on the sphere or in hyperbolic space. We discuss the geometric roots of this failure.

We begin by writing down the Heisenberg two-body problem. Let $q_1, q_2 \in \mathbb{H} \cong \mathbb{R}^3$ denote the positions of two bodies moving in the Heisenberg group $\mathbb{H}$. Let their masses be m_1, m_2. Their individual kinetic energies are

$$K_i = \frac{1}{2m_i}((P_X^{(i)})^2 + (P_Y^{(i)})^2)$$

where P_X^i, P_Y^i are the horizontal momenta of each body, as in Section 3.2. The Heisenberg two-body problem is defined by the Hamiltonian

$$H = K_1 + K_2 - \kappa m_1 m_2 U(q_1^{-1} q_2),$$

where κ is the Gravitational constant and U is Folland's fundamental solution. H is a Hamiltonian on the cotangent bundle of $\mathbb{H} \times \mathbb{H}$, and is invariant under the (cotangent lift of the left) translation $(q_1, q_1) \mapsto (gq_1, gq_2)$, $g \in \mathbb{H}$.

We know of two derivations of Kepler's problem (on Euclidean space) from Newton's two-body problem. We will call these the 'algebraic' and the 'group-theoretic' derivations. The 'algebraic derivation' begins with the equation $F = ma$ for each body. Divide the equation for each body by its mass to get equation for the acceleration $\ddot{q}_i$ of each body's position vector q_i. Subtract one equation from the other to obtain the ODE of Kepler's problem, $\ddot{q} = -\alpha q/|q|^3$, for the difference vector $q = q_1 - q_2$. The 'group theoretic derivation' depends on the conservation of the total linear momentum, the invariance of Newton's mechanics with respect to Galilean boosts, and the abelian nature of the translation group. If P is the total linear momentum and M the total mass, we boost by the velocity $-P/M$ to get to a new representation of the same dynamics in which the total linear momentum is zero. Then we reduce by translation at the value 0 by placing the center of mass at the origin. Finally, we compute that each mass separately satisfies Kepler's equation with the origin – the center of mass – now playing the role of "sun".

The algebraic derivation fails on the Heisenberg group because the 'difference vector' $g_1(t)^{-1}g_2(t)$ of two Heisenberg geodesics is not a Heisenberg geodesic. Why is this lack of being a geodesic a problem? Set the Heisenberg Gravitational constant $\kappa = 0$ so the two-body problem reduces to two uncoupled Heisenberg geodesic problems. Play the algebraic game. Our 'difference vector' does not satisfy the Heisenberg geodesic equations or any other pretty Hamiltonian equation. But in the Newtonian-Euclidean case, the difference vector travels like a free particle, i.e., moves in a straight line – as it should with $\alpha = 0$ in Kepler's problem. Things will just get worse for $\kappa \neq 0$.

The failure of the group theoretic derivation goes a bit deeper and is perhaps more enlightening. What is a 'Galilean boost' for an arbitrary Lie group? We choose some 'translation velocity' ξ and multiply elements x_0 by $exp(t\xi)$. Euclidean space enjoys the wonderful property that $exp(t\xi)x_0 = x_0 + t\xi$ describes free motion; it is a geodesic. This assertion is false for the Heisenberg group: with the exception of the lines in the plane $z = 0$, the Heisenberg geodesics through the origin are not one-parameter subgroups. As a result, applying a boost to a solution $(q_1(t), q_2(t))$ to the Heisenberg two-body problem will not yield a solution. There is a conserved total 'linear momentum': the momentum map for the (left) translation action. But we cannot use it to 'Galilean boost' the 'center of mass velocity' down to zero. Even if this total linear momentum were initially zero, we still seem to be stuck. The non-Abelian nature of the group appears to block us from writing the reduced Hamiltonian at zero as a Kepler Hamiltonian on the 'diagonal group' of elements $q = q_1^{-1}q_2$.

In spherical and hyperbolic geometry, reduction of the two-body problem to the Kepler problem fails for similar reasons. See [9]. In the spherical case, Shchepetilov [19] used the Morales-Ramis theory to prove that the two-body problem in these two geometries is not meromorphically integrable.

Question. Is the two-body problem on the Heisenberg group non-integrable?

4 Kepler's Problem on a Lattice

Lattices admit one-sided dilations: we can scale a lattice $\mathbb{L}$ by a positive integer c and land back in the lattice, stretching all distances by c. They admit Laplacians. So we might be able to begin to investigate Kepler's 3rd law on $\mathbb{L}$.

What are Newton's equations on $\mathbb{L}$? Since we must hop from lattice site to lattice site, we must choose our time variable t to be discrete:

$$t = \ldots, -1, 0, 1, 2, \ldots.$$

A 'solution' to Newton's equations will then be a 'discrete curve'

$$\gamma : \mathbb{Z} \to \mathbb{L}, \qquad \mathbb{L} \text{ our lattice},$$

satisfying a difference equation which mimics Newton's equations. In 1st order Hamiltonian form these equations should resemble

$$\frac{d\gamma}{d[t]} = p$$

$$\frac{dp}{d[t]} = -\nabla V(\gamma(t)),$$

where the differential is the discrete difference operator

$$\frac{d\gamma}{d[t]} = \gamma(t+1) - \gamma(t),$$

and where $V : \mathbb{L} \to \mathbb{R}$ is our potential. The standard interpretation of ∇V is in terms of its differential

$$dV(\ell) : \mathbb{E}_\ell \to \mathbb{R}, \quad \ell \in \mathbb{L},$$

where $\mathbb{E} = \mathbb{E}_\ell$ is the set of edges (chosen lattice generator) leaving the lattice site ℓ, and where

$$dV(\ell)(e) = V(\ell') - V(\ell), \quad e = [\ell, \ell'] \text{ an edge.}$$

Then we can rewrite our Newton difference equations as

$$\gamma(t+1) = \gamma(t) + p(t) \tag{4}$$

$$p(t+1) = p(t) - dV(\gamma(t)). \tag{5}$$

What is the momentum, $p(t)$? We add to it $dV(\gamma(t))$, so it must lie in the same space as dV, which is

$$\mathbb{E}^* = \mathbb{E}_\ell^* = \text{ real valued functions on } \mathbb{E}_\ell.$$

This 'cotangent space at ℓ' is a vector space isomorphic to $\mathbb{R}^d$, where d is the degree of a vertex: the number of edges leaving ℓ. Good. Now, how do we add $p(t) \in \mathbb{E}^*$ to a lattice site $\ell = \gamma(t) \in \mathbb{L}$ in order to get a new lattice site $\gamma(t+1)$ as in the 1st Newton equation? *We seem to be missing the 'mass matrix' or 'cometric' of mechanics.*

Definition 2. A lattice cometric is a 'non-trivial' map

$$\mathbb{M} : \mathbb{E}^* \to \mathbb{L}.$$

With this tentative definition we can now try to write down 'Newton's equations'

$$\gamma(t+1) = \gamma(t) + \mathbb{M}(p(t)) \tag{6}$$

$$p(t+1) = p(t) - dV(\gamma(t)), \tag{7}$$

which define a discrete dynamics on the phase space $\mathbb{L} \times \mathbb{E}^*$. The resulting dynamics have some vague relation to the corresponding formal Hamiltonian

$$H(\ell, p) = \frac{1}{2} p\mathbb{M}p + V(\ell),$$

but we aren't sure how to interpret the term $p\mathbb{M}p$.

4.1 Kepler's Problem on $\mathbb{Z}$

The Laplacian Δ on $\mathbb{Z}$ is given by $\Delta f(n) = f(n+1) - 2f(n) + f(n-1)$.

EXERCISE. Show that $U(n) = -\frac{1}{2}|n|$ is a fundamental solution for the Laplacian on $\mathbb{Z}$ with source at $S = 0$.

Take the Kepler constant $\alpha = 2$ so that the 'Newtonian potential' $V = -\alpha U$ is $V = |n|$. The Hamiltonian is

$$H(n, p) = \frac{1}{2} p^2 + |n|.$$

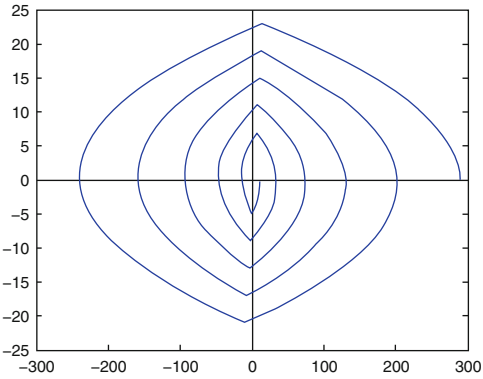

Fig. 5 A Kepler orbit in integer phase space: the (n, p)-plane

Since $\frac{d}{d[n]}|n| = sgn(n)$ is the sign of n, 1 if $n > 0$ and -1 if $n \leq 0$, we find that with this choice of α the discrete gradient is integer valued. We get a good discrete dynamical system. Newton's equations (in 1st order form) become

$$n(j+1) = n(j) + p(j)$$

$$p(j+1) = p(j) - sgn(n).$$

A solution is depicted in Figure 5.

At each iteration, the 'lattice momentum' p decreases by one as long as $n > 0$ and increases by 1 as long as $n < 0$. (We have to make a choice at $n = 0$; above we chose $sgn(0) = -1$.) Note that as long as the initial condition $p(0)$ is an integer, it remains an integer, and we stay on the lattice!

Because of this happy coincidence with p's evolution, we did not need to worry about where p lived. It is a real number that happens to evolve to stay integral. Our momentum space is not $\mathbb{E}^* \cong \mathbb{R}^2$. (There are two directions, right and left, on the lattice, hence the dimension 2.) We also did not need to choose a 'lattice cometric' $\mathbb{M}$. If any choice was made, it seems to have been '1' as written in the Hamiltonian. The happy coincidence does not happen when we go up to the rank 2 lattice.

4.2 Kepler on the Rank 2 Lattice

The rank 2 lattice is $\mathbb{Z}^2$ with elements written $\ell = (n, m)$. As a metric space, we use the distance

$$d((n, m), (n', m') = |n - n'| + |m - m'|.$$

The Laplacian is

$$\Delta f(\ell) = \sum_{\ell' :\, d(\ell,\ell')=1} (f(\ell') - f(\ell)).$$

Let U denote the fundamental solution, this being the 'most bounded' solution to $\Delta U = \delta_0$, where δ_0 is the lattice delta function corresponding to placing the sun at the origin. (There is a lattice Liouville theorem, so U can be made unique up to an additive constant.) There is no closed form expression for U. However, any particular value of U can be computed recursively. Indeed, the fundamental solution is a well studied object with applications to the theory of electrical circuits [4], solid state physics, and quantum mechanics. Some values of the lattice Green's function are reproduced in Figure 6 from [13]. (We thank the brothers Hollos for permission to reproduce their table.)

We write the formal Hamiltonian

$$H(\ell, p) = \frac{1}{2} p\mathbb{M}p - \alpha U(\ell)$$

and derive Hamilton's equations

$$\ell(t+1) = \ell(t) + \mathbb{M}p(t)$$

$$p(t+1) = p(t) + \alpha d\, U(\ell(t))$$

where

$$\mathbb{M} : \mathbb{R}^4 = \mathbb{E}^* \to \mathbb{Z}^2.$$

The vector p is a 4-vector with components $(p_{up}, p_{down}, p_{right}, p_{left})$ corresponding to the 4 edges, which are the 4 directions of motion, through each vertex. We have, for example $d\,U(\ell)_{up} = U(\ell + e_2) - U(\ell)$ where $e_2 = (0, 1)$ represents motion in the 'up' direction. The second Hamilton equation makes sense.

When we try to parse the first Hamilton equation we get stuck. What do we take for $\mathbb{M} : \mathbb{R}^4 \to \mathbb{Z}^2$? We require $\mathbb{M}$ to be non-constant. Certainly $\mathbb{M}$ will not be continuous! Ideally $\mathbb{M}$ is 'linear':

$$\mathbb{M}(kp) = k\mathbb{M}(p), \quad k \in \mathbb{Z},$$

but this is probably not possible in any reasonable sense. One possibility for $\mathbb{M}$ is to argue that there is a 'canonical' projection $\Pi : \mathbb{R}^4 \to \mathbb{R}^2$, for example, $\Pi(p_{up}, p_{down}, p_{right}, p_{left}) = \frac{1}{2}(p_{up} + p_{down}, p_{right} + p_{left})$, and a canonical embedding of our lattice as $\mathbb{Z}^2 \subset \mathbb{R}^2$. Then choose $\mathbb{M}(p)$ to be the lattice point closest to $\Pi(p)$. This leaves us to worry about what to do if $\Pi(p)$ is midway between lattice points. Flip a coin?

We are stuck and look forward to some of our readers unsticking us.

Fig. 6 Values of the Green's function g on $\mathbb{Z}^2$, taken from [13]

n	m	g(n,m)
0	0	0
1	0	$\frac{1}{4}$
1	1	$\frac{1}{\pi}$
2	0	$1-\frac{2}{\pi}$
2	1	$\frac{2}{\pi}-\frac{1}{4}$
2	2	$\frac{4}{3\pi}$
3	0	$\frac{17}{4}-\frac{12}{\pi}$
3	1	$\frac{23}{3\pi}-2$
3	2	$\frac{2}{3\pi}+\frac{1}{4}$
3	3	$\frac{23}{15\pi}$
4	0	$20-\frac{184}{3\pi}$
4	1	$\frac{40}{\pi}-\frac{49}{4}$
4	2	$3-\frac{118}{15\pi}$
4	3	$\frac{12}{5\pi}-\frac{1}{4}$
4	4	$\frac{176}{105\pi}$
5	0	$\frac{401}{4}-\frac{940}{3\pi}$
5	1	$\frac{3323}{15\pi}-70$
5	2	$\frac{97}{4}-\frac{1118}{15\pi}$
5	3	$\frac{499}{35\pi}-4$
5	4	$\frac{20}{21\pi}+\frac{1}{4}$
5	5	$\frac{563}{315\pi}$
6	0	$521-\frac{24526}{15\pi}$
6	1	$\frac{1234}{\pi}-\frac{1569}{4}$
6	2	$168-\frac{18412}{35\pi}$

4.3 Euler-Lagrange Formulation

We can make a bit more sense of the Euler Lagrange version of lattice dynamics. Fix a positive integer T, the 'time of flight,' and initial and final vertices, $v_0, v_1 \in \mathbb{Z}^2$. There will be two formulations. In both, we consider discrete paths $\gamma : \{0, 1, \ldots, T\} \to \mathbb{Z}^2$ which join v_0 to v_1 in time T, and we minimize an 'action functional' A among all such discrete paths.

Version 1: Minimize the action

$$A(\gamma) = \sum_{t=0}^{T} \{ \frac{1}{2} (|\frac{d}{d[t]} \gamma(t)|_1)^2 + \alpha U(\gamma(t)) \}$$

among all discrete paths γ joining v_0 to v_1 in discrete time T.

Here $|\frac{d}{d[t]}\gamma(t)|_1 = d(\gamma(t+1), \gamma(t))$, so half of its square represents kinetic energy.

Version 2: Call a discrete path 'continuous' if either $d(\gamma(t+1), \gamma(t)) = 1$ or $\gamma(t+1) = \gamma(t)$. Minimize the same action as Version 1, but now over all continuous paths. (In this case the kinetic term $\frac{1}{2}(|\frac{d}{d[t]}\gamma(t)|_1)^2$ is either $1/2$ or 0 at each time step.)

We are guaranteed a solution to Version 2 exists since there are only a finite number of 'continuous' paths joining v_0 to v_1. We suspect that if we move too fast the kinetic energy becomes too large, so that Version 1 is 'coercive' and one can argue that again there are only a finite number of paths that matter.

It seems doubtful that any decent Euler-Lagrange type difference equation 'dynamics' will result from either principle. Indeed, take the case $\alpha = 0$ of a 'free particle' on the lattice, and take $v_0 = (0,0)$, $v_1 = (n,m)$, $n > m \geq 0$. There are $(n+1)m$ shortest paths from v_0 to v_1. Just draw box-paths, always moving either right or up. Their lengths are all $n + m = d(v_0, v_1)$. If $T < d(v_0, v_1)$ then there are no paths connecting the two points. If $T = d(v_0, v_1)$ then their actions are all $\frac{1}{2}T$. If $T > d(v_0, v_1)$ the action remains the same; we just stay still for the requisite times $T - d(v_0, v_1)$. This means either (i) all points $v_1 = (n,m)$ with $nm \neq 0$ are conjugate to v_0, or (ii) that there is no good 'free' dynamical equation, so likely no good Euler-Lagrange equations in general.

4.4 *Quantum Mechanics to Classical Mechanics on Cayley Graphs?*

By a graph here we mean the usual combinatorial collection of vertices and edges. We write Γ for the set of vertices and view Γ as 'configuration space.' The graph Laplacian is the operator $\Delta : \ell_2(\Gamma) \to \ell_2(\Gamma)$ defined by

$$\Delta f(v) = \sum_{v' : [v,v'] \text{ an edge}} (f(v') - f(v)).$$

If Γ is finite there will be no fundamental solution; that is, there is no solution to $\Delta U_S = \delta_S$ where δ_S is the discrete δ function centered at the sun: $\delta_S(S) = 1, \delta_S(v) = 0, v \neq S$. If Γ is finite, a necessary condition for the solvability of $\Delta V = f$ is $\Sigma f(v) = 0$, which will fail for $f = \delta_S$.

Regardless of whether or not Γ has a Green's function, it has plenty of potentials, meaning functions $V \in \ell_2(\Gamma)$. Consequently for each choice of Planck's constant $\hbar$ we have a Schrodinger operator:

$$\hbar^2\Delta + V : \ell_2(\Gamma) \to \ell_2(\Gamma).$$

There is a large active field of graph Laplacians and quantum mechanics on graphs. There is undoubtedly a theory of quantum mechanics on Γ.

4.4.1 Challenge

Don't you think this quantum mechanics ought to have a classical limit? If 'yes' then please answer: what are the correct Newton's equations for an arbitrary potential, on an arbitrary graph?

4.4.2 Cayley Graph of a Group

Let Γ be a finitely generated group and $e_1, \ldots, e_d \in \Gamma$ be a fixed set of generators for Γ (so every element of Γ is a product of the e_i's or their inverses). Form the graph whose vertices are the elements $x \in \Gamma$ and for which two vertices $x, y \in \Gamma$ are joined by an edge if and only if either $y = xe_i$ or $x = ye_i$ for some generator e_i. Count each edge as having length 1. Define the distance between points x and y in Γ to be the minimum of the lengths of the paths joining x to y. This distance is always an integer, since the length of a path is just the number of edges it contains.

In this representation, the 'Lie algebra' of the Cayley graph will be the tangent space at the identity: the disjoint union of d copies of $\mathbb{Z}$. Alternatively, it is the subset of $\mathbb{Z}^d$ consisting of vectors for which all but one component is zero.

4.4.3 Example: Lattices

Take $\Gamma = \mathbb{Z}^2$ to be the lattice of integers in the plane, with standard generators $e_1 = (1, 0), e_2 = (0, 1)$. Then the Cayley graph of $\mathbb{Z}^2$ realized as above has the vertices of a standard infinite sheet of graph paper in $\mathbb{R}^2$. Its Lie algebra consists of integer points on the x-axis unioned with the collection of integer points on the y-axis.

4.4.4 Kepler Symmetries of Cayley Graphs

Every Cayley graph satisfies Keplerian symmetry property (1) of being homogeneous since Γ acts on itself on the right by isometries. View the generators as the 'directions.' Then if the automorphism group of the group Γ acts transitively on its generating set $e_1, \ldots, e_d$, the metric is isotropic; it satisfies Keplerian symmetry property (2). Finally we can send e_i to e_i^k. In some instances this defines a group

homomorphism of Γ *into* itself. Then the Cayley graph admits one-sided dilations and so satisfies (3). The examples we know of groups whose Cayley graphs satisfy (1), (2) and (3) are the lattices $\mathbb{Z}^d$, the lattices in nilpotent groups, and the free group on d generators. In the continuous case, we know how to derive a Kepler's third law from the Keplerian symmetry (3). Is there an analogous construction in the discrete case?

4.5 Full Disclosure: R.M.

I have little interest in any kind of graph for its own sake. I am not a combinatorist, nor a discrete group theorist!

In contrast to the dozens of books that Jerry wrote in his life, I have mustered the courage and stamina to write a single book in this life. (Jerry continues to amaze.) In that book I devoted a chapter to trying to understand one of the big ideas of Gromov in his paper 'On Groups of Polynomial Growth ...' [11] in which he used subRiemannian ideas to solve a problem in discrete group theory. Consider a discrete finitely generated group Γ. Select some generators and form the group's Cayley graph. We say the group is 'of polynomial growth' if the number of vertices of the Cayley graph lying inside a ball of radius R is bounded by a polynomial in R as $R \to \infty$. (If Γ is of polynomial growth with respect to one set of generators, it is of polynomial growth with respect to any other set of generators.) The lattices, and the integer lattice in the Heisenberg group are examples of groups of polynomial growth. More generally, the lattices in any Carnot group are of polynomial growth. The free group on 2 generators in not of polynomial growth: its balls have exponential growth, roughly 3^R. There is a notion of a group being 'virtually nilpotent,' and it was known that virtually nilpotent implies polynomial growth. Gromov proved the converse: polynomial growth implies virtually nilpotent.

Gromov's paper is mind-blowing – the most astounding application of subRiemannian geometry that I know of made by a human. (Cats and micro-organisms have made their own astounding applications.) Gromov scales the edges of the Cayley graph by ϵ, then takes the limit as $\epsilon \to 0$. He proves, in essence, that the result converges to a Carnot group – a metric of subRiemannian type on a nilpotent Lie group – and from this the theorem easily follows. (I am stretching the truth here, but that is the spirit of Gromov's paper. There are many technicalities.) What I find so compelling about Gromov's paper is the going back and forth between the wonderful world of smooth metric spaces – Lie groups even – which I know and love, and the chopped up world of discrete objects that I find so frightening at times. Can we similarly go back and forth in dynamics? That is what I would like to see in some 'Kepler problem on a lattice.'

References

1. Abraham, R., Marsden, J.E.: Foundations of Mechanics. Benjamin-Cummings, Reading (1978)
2. Arnold, V.I., Kozlov, V.V., Neishtadt, A.I.: Mathematical Aspects of Classical and Celestial Mechanics, 3rd edn. Springer, Berlin (2010)
3. Albouy, A.: Projective dynamics and classical gravitation. arXiv:math-ph/0501026v2 (2005)
4. Cserti, J.: Application of the lattice Green's function for calculating the resistance of infinite networks of resistors. Am. J. Phys. **68**, 896–906. arXiv:cond-mat/9909120v4 (2000).
5. Folland, G.: A fundamental solution for a subelliptic operator. Bull. Am. Math. Soc. **79**, 373–376 (1973)
6. Diacu, F., Perez-Chavela, E., Santoprete, M.: The n-body problem in spaces of constant curvature. Part I: relative equilibria. J. Nonlinear Sci. **22**, 247–266 (2012)
7. Diacu, F., Perez-Chavela, E., Santoprete, M.: The n-body problem in spaces of constant curvature. Part II: singularities. J. Nonlinear Sci. **22**, 267–275 (2012)
8. Diacu, F., Perez-Chavela, E., Santoprete, M.: The n-body problem in spaces of constant curvature. arXiv:0807.1747v6 [math.DS] (2008)
9. Diacu, F.: The non-existence of centre-of-mass and linear-momentum integrals in the curved N-body problem. arXiv:1202.4739v1 [math.DS] (2012)
10. Darboux, G.: Étude d'une question relative au mouvement d'un point sur une surface de révolution. Bull. Soc. Math. Franc. **5**, 100–113 (1887)
11. Gromov, M.: Groups of polynomial growth and expanding maps. Publ. Math. IHES **53**, 53–73 (1981)
12. Gromov, M.: Metric Structures for Riemannian and Non-riemannian Spaces, 3rd printing. Birkhauser, Boston (2007)
13. Hollos, S., Hollos, R.: The lattice Green function for the Poisson equation on an infinite square lattice. arXiv:cond-mat/0509002v1 [cond-mat.other] (2005)
14. Lobachevsky, N.I.: The new foundations of geometry with full theory of parallels [in Russian], 1835–1838. In: Collected Works, V. 2, GITTL, Moscow, p. 159 (1949)
15. Montgomery, R.: A tour of subRiemannian geometries. In: Mathematical Surveys and Monographs, vol. 91. American Mathematical Society, Providence (2002). http://www.ams.org/books/surv/091/ and http://www.ams.org/books/surv/091/surv091-endmatter.pdf
16. Santoprete, M.: Gravitational and harmonic oscillator potentials on surfaces of revolution. J. Math. Phys. **49**, 042903, 16 pp (2008)
17. Serret, P.J.: Théorie nouvelle géométrique et mécanique des lignes a double courbure. Librave de Mallet-Bachelier, Paris (1860)
18. Shanbrom, C.: Two problems in sub-Riemannian geometry. Ph.D. Thesis, UC Santa Cruz (2013)
19. Shchepetilov, A.: Nonintegrability of the two-body problem in constant curvature spaces. J. Phys. A **39**, 5787–5806 (2006)
20. Zagryadskii, O.A., Kudryavtseva, E.A., Fedoseev, D.A.: A generalization of Bertrand's theorem to surfaces of revolution. Sbornik **203**, 39–78 (2012)

On the Completeness of Trajectories for Some Mechanical Systems

Miguel Sánchez

Abstract The classical tools which ensure the completeness of both, vector fields and second order differential equations for mechanical systems, are revisited. Possible extensions in three directions are discussed: infinite dimensional Banach (and Hilbert) manifolds, Finsler metrics and pseudo-Riemannian spaces, the latter including links with some relativistic spacetimes. Special emphasis is taken in the cleaning up of known techniques, the statement of open questions and the exploration of prospective frameworks.

1 Introduction

As explained in the classical Abraham and Marsden book [1, p. 71], the completeness of vector fields *is often stressed in the literature since it corresponds to well-defined dynamics persisting eternally*. However, in many circumstances one has to live with incompleteness and, in this case, incompleteness may mean the failure of our model. Remarkably, this happens in General Relativity, where singularities have become so common (Schwarzschild spacetime, Raychauduri equation, theorems by Penrose and Hawking. . .) that one expects to find incompleteness under physically reasonable general assumptions—and one hopes that the quantum viewpoint will be able to explain the physical meaning of singularities. In any case, the possible completeness or incompleteness becomes a fundamental property of the model.

In his early works at the beginning of the seventies, Marsden gave two remarkable results on completeness. The first, in collaboration with Weinstein [68], extends previous works on the completeness of Hamiltonian vector fields by Gordon [33], Ebin [23] and others. The second, about the geodesic completeness of compact homogeneous pseudo-Riemannian manifolds [47], was one of the few results ensuring completeness instead of incompleteness in the Lorentzian setting of that time. The results on the side of geodesics in the Lorentzian setting have increased notably since then (see the review [14]). Moreover, some connections with the

M. Sánchez (✉)
Facultad de Ciencias, Departamento de Geometría y Topología, Universidad de Granada, Campus Fuentenueva s/n, E18071 Granada, Spain
e-mail: sanchezm@ugr.es

D.E. Chang et al. (eds.), *Geometry, Mechanics, and Dynamics*, Fields Institute Communications 73, DOI 10.1007/978-1-4939-2441-7_15

original Riemannian results for Hamiltonian systems have appeared. This has been a stimulus for the recent update and extension of such Riemannian results carried out by the author and his coworkers in [17].

The aim of this paper is to revisit these results, formulating them in a general framework, and pointing out new open questions as well as new lines of study. The paper is organized into three parts. In the first (Section 2), some preliminaries on infinite-dimensional Banach manifolds endowed with Finsler metrics are introduced. From our viewpoint, this is the natural framework for the completeness of first order systems (vector fields), and some second order ones can be reduced to this setting.

In Section 3 we study completeness for both, first and second order systems. For first order, we review some old results [1, 2, 23, 33, 68] formulating them in the general Banach Finsler case, and also allowing the time-dependence of the vector fields. We introduce *primary bounds* (Definition 1) here, which allow the purification of previous techniques (Theorem 1). For second order, i.e., trajectories accelerated by potentials and other time-dependent forces, we give a general result on completeness in Riemannian Hilbert manifolds (Theorem 2), which summarizes and extends those in [17, 23, 33, 68]. The latter are also simplified technically because, even though our proof uses comparison criteria between differential equations as in previous references, here such criteria are reduced essentially to the elementary Lemma 1—and the bounds through *positively complete* functions introduced in [68] reduce to primary bounds as well. We suggest the possibility of going further in two directions: the time-dependence of the potentials and the Finsler Banach framework.

Section 4 deals with (finite-dimensional) pseudo-Riemannian manifolds. Here there is a great diversity of results and techniques (see [14]), and we focus on two topics. Firstly, results regarding manifolds with a high degree of symmetry. In particular, the extension of Marsden's Theorem 5 to conformally related metrics (Theorem 6), is explained by using the techniques in the previous section. Secondly, the geometry of wave type spacetimes. This provides a simple link between Riemannian and Lorentzian results (Theorem 9) with new exciting open questions—some of them collected together at the end.

2 Preliminaries on Infinite-Dimensional Manifolds

Some preliminaries on Banach manifolds are introduced here. Results on the elements which will be relevant for the posterior results will be gathered together, and a framework for tentative generalizations will be provided. Special emphasis is focused on the role of paracompactness for the ambient manifold, as this condition will be equivalent to the existence of a C^0-Finsler metric such that its associated distance metrizes the manifold topology. The role of smoothability for Finsler

metrics is also emphasized. Essentially, C^0 smoothability is sufficient for distance estimates in first order problems (Section 3.1), but further smoothability may be required for the development of second order ones (Section 3.2).

We will follow conventions on Banach and Hilbert manifolds as in the original papers by Palais [51–53], as well as books such as Abraham et al. [2], Lang [44], Deimling [20], Kriegl and Michor [42] or Moore's notes [49].

2.1 Banach Manifolds and Finsler Metrics

2.1.1 Topological Conventions

Any Banach manifold M will be always assumed C^k with $k \geq 1$, as well as *connected, Hausdorff and paracompact* and, thus, normal.[1] A *n-manifold* will be a finite dimensional Banach manifold with dimension $n \in \mathbb{N}$. When the infinite dimension is allowed, we will remark explicitly that M is Banach (say, modelled on some Banach space B with norm $\| \cdot \|$) or, when applicable, that it is Hilbert (modelled on some real Hilbert space H with inner product $\langle \cdot, \cdot \rangle$). When indefinite metrics are considered, as in Section 4, M will be typically a n-manifold.

2.1.2 Finsler Banach Manifolds

F will denote a (reversible) Finsler metric on the Banach manifold M, and (M, F) will be called a Finsler Banach manifold. This notion is taken in the sense of Palais [52], that is, F yields a norm at each tangent space:

$$F_p : T_pM \to \mathbb{R} \tag{1}$$

which admits a C^k chart (U, φ), $p \in U, \varphi : U \subset M \to B$ such that the induced norms

$$\| u \|_q := F_q(d(\varphi^{-1})_{\varphi(q)}(u)) \qquad \forall u \in B, \tag{2}$$

(here d denotes the differential or tangent map) satisfy: (a) they are equivalent to the natural norm $\| \cdot \|$ of B (i.e., $\epsilon_q \| \cdot \|_q \leq \| \cdot \| \leq \epsilon_q^{-1} \| \cdot \|_q$ for some $0 < \epsilon_q < 1$

[1] In particular, our Banach manifolds will be always regular and, so, some difficulties pointed out by Palais in [53] (see Sect. 2 including the Appendix therein), will not apply. The central role of paracompactness from the topological viewpoint is stressed in Figure 1. Notice that, as a difference with the finite dimensional case, second countability does not imply paracompactness (see for example [46], [42, Sect. 27.6] or [53]).

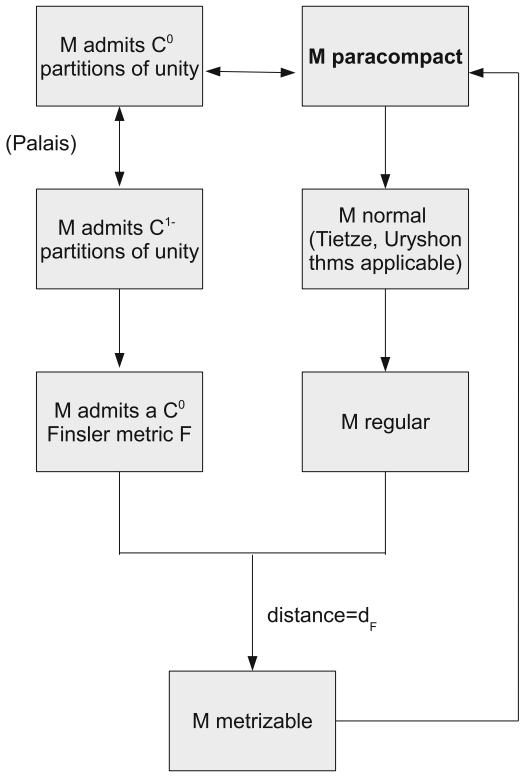

Fig. 1 Topological properties related to the paracompactness of a (connected, Hausdorff) Banach manifold

and all $q \in U$) , and (b) they vary continuously at p (i.e., for each $0 < \epsilon < 1$ there exists a neighborhood $U_\epsilon \subset U$ of p such that $\epsilon \parallel \cdot \parallel_q \leq \parallel \cdot \parallel_p \leq \epsilon^{-1} \parallel \cdot \parallel_q$ for all $q \in U_\epsilon$).

As norms cannot be differentiable at[2] 0, the $C^{k'}$ differentiability of the norm $\parallel \cdot \parallel$ means always away from 0. The Finsler metric is called $C^{k'}$ (for $0 \leq k' \leq k-1$) if F_p is $C^{k'}$ and varies smoothly with p in a $C^{k'}$ way (i.e., for any chart (U, ϕ) as above the map $U \times (B \setminus \{0\}) \to \mathbb{R}, (q, u) \mapsto \parallel u \parallel_q$ is $C^{k'}$).

2.1.3 Existence of Finsler Metrics

The question of the existence of a C^0 Finsler metric depends only on topological grounds, but the existence of a $C^{k'}$ one with $k' > 0$ is much subtler. Namely, on the one hand the hypothesis of paracompactness on M becomes equivalent to the

[2]By the same reason that neither is the absolute value function on $\mathbb{R}$. Moreover, at least in the finite-dimensional case, the square of a norm is smooth at 0 if and only if the norm comes from a scalar product [67, Prop. 4.1].

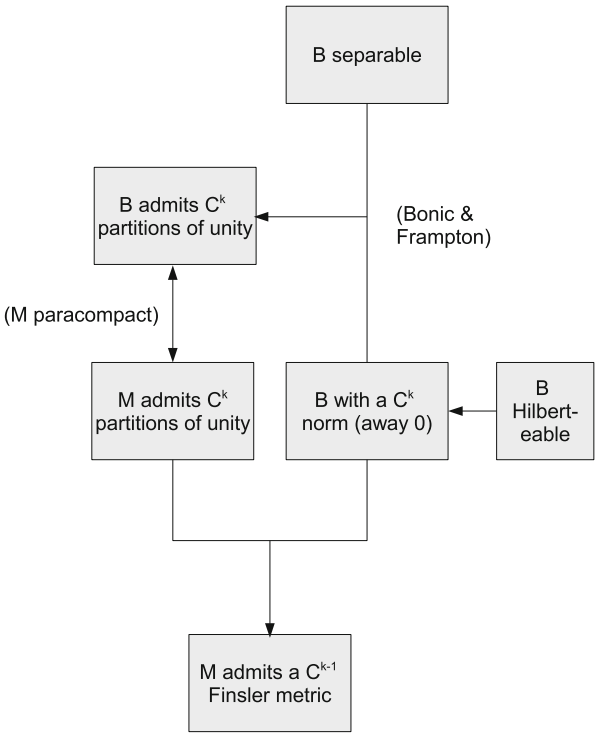

Fig. 2 Existence of smooth Finsler metrics on a manifold M modelled on the Banach space B

existence of C^0-partitions of the unity subordinated to any open covering. By a result of Palais [52, Th. 1.6], [53, Sect. 3], it is also equivalent to the existence of locally Lipschitz partitions of the unity, and this allows ensuring the existence of C^0 Finsler metrics in any Banach manifold [52, Th. 2.11]. On the other hand, when the model Banach space B admits C^k partitions of the unity subordinate to any open covering (which happens, in particular, when B is separable and admits a C^k norm away from 0, see [9], [2, Prop. 5.5.18, 5.5.19]), then the Banach manifold M also admits C^k partitions of the unity [2, Th. 5.5.12] and, in this case, M admits C^{k-1}-Finsler metrics too (Figure 2).

Remark 1. It is worth pointing out that, even though the differentiability of F may be useful for some issues (see Section 3.2.2 below), it will not be especially relevant for the estimates which involve length or distances in the first order problems to be studied in Section 3.1. This fact is used implicitly in time-dependent problems. In fact, this case is commonly handled by transforming it into a non time-dependent one, defined on the product manifold $M \times \mathbb{R}$ which is endowed with a natural direct sum of Finsler metrics (namely, the addition of the Finsler metrics of the factors), see Remark 3. Nevertheless, this direct sum is non-differentiable away from 0 even if differentiability is assumed for the metric on each factor (notice that it is not guaranteed the differentiability on a vector tangent to the product whenever one of its two components is equal to zero).

2.1.4 Distance Associated to a Finsler Metric

Remember that our definition of a Finsler metric F includes its *reversibility* (i.e., $F(v) = F(-v)$ for all tangent vector $v \in TM$). So, F defines a natural distance by taking the infimum of the lengths of the curves connecting each pair of points. This distance will be denoted d_F or, simply, d if there is no possibility of confusion. One can prove that the topology generated by d agrees with the manifold topology by using the regularity of the manifold. Palais [53, p. 202] and, so, that all Finsler Banach manifolds are metrizable.[3]

We will speak about the completeness of (M, F) in the sense of metric completeness, i.e., the convergence of Cauchy sequences for (M, d). One can also consider geodesics for (M, F) (for example, in the sense of locally length-minimizing curves of constant speed, with other characterizations under further smoothability, see Section 3.2.2) and we will say that (M, F) is *geodesically complete* when its inextensible geodesics are defined on all $\mathbb{R}$. In the infinite-dimensional case, the completeness of (M, F) implies geodesic completeness but, as stressed by Atkin [3], neither geodesic completeness implies metric completeness nor other consequences of Hopf–Rinow theorem hold.

In order to make estimates with the distances, we fix a *base* point $p_0 \in M$ and denote

$$|p| = d(p, p_0) \qquad \forall p \in M. \tag{3}$$

(This notation will be used when the properties under study are independent of the chosen point p_0.)

2.2 Pseudo-Riemannian Metrics and Hilbert Manifolds

2.2.1 Pseudo-Riemannian Metrics on Banach Manifolds

When the model space B of the Banach manifold M is reflexive, it is natural to define a $C^{k'}(k' \leq k-1)$ pseudo-Riemannian metric g as a $C^{k'}$ choice of a continuous symmetric bilinear form g_p at each tangent space T_pM such that the associated "flat" map (to lower indexes in finite dimension) into the dual space given by

$$\flat_p : T_pM \to T_pM^*, \quad v_p \mapsto g_p(v_p, \cdot) \tag{4}$$

[3] Consistently, paracompactness can be deduced from the hypothesis of metrizability (or even just from pseudo-metrizability, see [2, Lemma 5.515]).

is a homeomorphism (if this condition on $\flat_b$ were not imposed, one would speak of a *weak* pseudo-Riemannian metric, and the reflexivity of B would not be required). The set of all such bilinear forms g_p can be identified via a chart around p with an open subset of the set $\mathrm{BL}_{sym}(B)$ of all the continuous symmetric bilinear forms on B. As $\mathrm{BL}_{sym}(B)$ is naturally a Banach space too, the pseudo-Riemannian metric g can be regarded as a section of a fiber bundle on M with fiber $\mathrm{BL}_{sym}(B)$ (see [44, Ch VII.1]).

2.2.2 Riemannian Metrics on Hilbert Manifolds

When the pseudo-Riemannian metric g is positive definite then we say that it is Riemannian. As we are assuming that $\flat_p$ is a homeomorphism, the model space B is then Hilberteable. So, it will be denoted H, and we will consider only Riemannian metrics on Hilbert manifolds. Notice that, for any Riemannian metric g, one has an associated Finsler metric given by $F(v) = \sqrt{g(v,v)}$ for all $v \in TM$. So, the bounds required in the definition of continuity for F in the Finslerian case (see (a) and (b) below formula (2)), hold here in terms of the norm associated to the inner product $\langle \cdot, \cdot \rangle$ of H. Moreover, this norm is always C^∞ away from 0. Thus, any C^k Hilbert manifold modelled on a separable space H admits C^k partitions of the unity and, then, a C^{k-1} Riemannian metric. Riemannian metrics on Hilbert manifolds, as well as their geodesics, are extensively studied in the literature, see for example [44] or, for the separable case, [40]. A type of Hopf–Rinow theorem for separable Riemann Hilbert manifolds can be found in [40, Th. 2.1.3] (including the "Notes" therein; recall also [3]); some related remarkable properties can be seen in [25].

2.3 Concluding Remarks and Conventions

For the convenience of the reader, a summary on the topological and smooth-related results commented above is provided in Figures 1 and 2. Basic detailed background can be found in [52, 53] and [2]. In what follows, all the objects will be *smooth* i.e. as differentiable as possible according to the discussion above. In the case of first order problems (Section 3.1), this will mean at least C^2 for any Banach manifold M and C^1 for any vector field X on M. As emphasized in Remarks 1 and 3, Finsler metrics are required only C^0 at this stage. Further requirements of smoothability will be needed for the second order case (Section 3.2). In the (indefinite) finite-dimensional case (Section 4), the issues on smoothability are not especially relevant and, so, the reader may either track them or just assume C^∞ smoothability.

3 Completeness of Trajectories in a Positive-Definite Infinite-Dimensional Setting

This section is divided into two subsections. The first one is devoted to the problem of the completeness of a vector field. We start by reviewing some results. These have essentially been known from the seventies [23, 33, 68] and explained in [1, 2]. They are extended here to the (C^0) Finsler setting when possible (Propositions 1, and 2). Then, the notion of *primarily complete* function is introduced (Definition 1). Primary bounds for a vector field allows us to give an optimal result on completeness in the Finsler Banach case, Theorem 1. The time-dependent case is specially discussed in Remark 3 and the last part of the subsection.

In the second subsection, our Theorem 2 (plus Remark 6) summarizes and extends the results on second order differential equations in [17, 23, 33, 68]. The proof is carried out in three conceptually independent steps. The first one is just a standard reduction to the first order case. The second one deals with technical bounds. This is carried out here just by using systematically the simple Lemma 1. In the third step, the subtleties of the infinite dimensional case (first studied by Ebin [23]), are stressed.

Further discussions are also provided in this second subsection. Firstly, the relation between the previous notion of *primarily complete* function and Weinstein–Marsden's *positive completeness*, is analyzed. Secondly, we consider specifically the time-dependent case. Even though natural bounds are obtained for the growth of the potential in this case, we also explore some alternatives. Finally, we discuss the difficulties of the generalization when the Riemannian metrics are replaced by Finslerian ones, and we provide a simple example for the (standard) finite-dimensional Finsler case.

3.1 Complete Vector Fields on Finsler Banach Manifolds

3.1.1 Elementary Criteria

The properties of the (local) flow ϕ of a vector field X and, in particular, the existence of a flow box around each point, can be found, for example, in [2, p. 192ff], [44, p. 84ff] or [49, Sect. 1.10]. We start with a well-known result (see for example [2, Prop. 4.1.19]).

Proposition 1. *Let X be a vector field on a Banach manifold M, and let $c : [0, b) \to M$ (resp. $[-b, 0) \to M$) be an integral curve of X with $0 < b < +\infty$. Then, c can be extended beyond b as an integral curve of X if and only if there exists a sequence $t_n \to b^-$ such that the sequence $\{c(t_n)\}_n$ (resp. $\{c(-t_n)\}_n$) is convergent in M.*

Proof. The necessity of the condition is obvious. For its sufficiency, let $p \in M$ be the limit of the sequence. The existence of a flow box of X at p ensures the existence of a neighborhood U of p and some $\epsilon > 0$ such that the integral curves of X at any $p' \in U$ are defined on $(-\epsilon, \epsilon)$. So, taking n large so that $b - t_n < \epsilon$ the integral curve through $c(t_n)$ will be defined on $[0, \epsilon)$ and c will be extensible through b.

Accordingly, we will say that an integral curve c of X defined on some interval I of $\mathbb{R}$ is *complete* if it can be extended as an integral curve of X to all $\mathbb{R}$, and X will be complete if so are its integral curves.

Remark 2. (i) This result follows in the infinite-dimensional case as well as in the finite-dimensional one. However, the application in the latter case is easier, as M is then locally compact. For example, Proposition 1 yields directly that, if the support of X is compact (in particular, if M is compact and, thus, finite-dimensional) then X is complete.

(ii) Analogously, one can prove that if a Banach manifold (M, F) admits a C^1-proper map $f : M \to \mathbb{R}$ (i.e. $f^{-1}([a, b])$ is compact for any compact $[a, b] \subset \mathbb{R}$), then a vector field X is complete whenever

$$|X_p(f)| \leq C_1 |f(p)| + C_2 \tag{5}$$

for some $C_1, C_2 > 0$ and all $p \in M$. In fact, (5) implies a bound for the derivative of $\log(C_1|f \circ c| + C_2)$. If the domain of the integral curve c were bounded, a bound for f on c would be obtained too. As f is proper, the result would follow then from Proposition 1 (see [1, 2.1.20] or [2, 4.1.21] for more details). Even though proper maps are well behaved in Banach manifolds (for example, they are closed maps [54]) results as the previous one are used typically in the finite-dimensional case (putting, for example, $f = C_1|x|^2 + C_2$ on a complete Riemannian n-manifold).

The following criterion on completeness for Finsler Banach manifolds holds as in the case of Riemann Hilbert ones or Banach spaces (compare with [1, Prop. 2.1.2] or [2, Prop. 4.1.22]).

Proposition 2. *Let (M, F) be a complete Finsler Banach manifold and X a vector field on M. If $c : I \subset \mathbb{R} \to M$ is an integral curve of X and $F(\dot{c})$ is bounded on bounded subintervals of I, then c is complete.*

Proof. Assume with no loss of generality that $I = [0, b), b < \infty$, let A be the assumed bound and choose $\{t_n\} \nearrow b$. The associated distance d satisfies then:

$$d(c(t_n), c(t_m)) \leq \int_{t_n}^{t_m} F(\dot{c}(t))dt \leq A|t_n - t_m|.$$

So, $\{c(t_n)\}_n$ is a Cauchy sequence, which becomes convergent to some limit p by the completeness of (M, F). Then, Proposition 1 can be applied to $\{c(t_n)\}_n$.

Remark 3 (The Time-Dependent Case). The results in the previous two propositions can be extended to the case when X is time-dependent, and defined for all the values of the time.

More precisely, consider the product manifold $M \times \mathbb{R}$, let $\Pi_{\mathbb{R}} : M \times \mathbb{R} \to \mathbb{R}$, $\Pi_M : M \times \mathbb{R} \to M$ be the natural projections, and denote by t the natural coordinate on $\mathbb{R}$. We say that X is a *time-dependent vector field on* M if it is a smooth section of the pull-back bundle $\Pi_M^\star(TM)$, whose base is $M \times \mathbb{R}$ and each fiber comes from a tangent space to M. Such a vector field yields naturally a (time-independent) vector field $\hat{X}$ on $M \times \mathbb{R}$ which satisfies both, $d\Pi_M \hat{X}_{(p_0,t_0)}$ is naturally identifiable to the natural projection of $X_{(p_0,t_0)}$ on $T_{p_0}M$ and $d\Pi_{\mathbb{R}} \hat{X}_{(p_0,t_0)} = \partial_t|_{t_0}$, for all $(p_0, t_0) \in M \times \mathbb{R}$.

To speak about the integral curves of X makes a natural sense (see for example [44, Ch. IV]) and becomes equivalent to consider the integral curves of $\hat{X}$; in fact, c will be an integral curve of X if and only if $\hat{c} : t \mapsto (c(t), t)$ is an integral curve of $\hat{X}$. So, Proposition 1 is extended directly to a time-dependent X.

To extend Proposition 2, recall that, if (M, F) is a Finsler Banach manifold, then $M \times \mathbb{R}$ admits a natural C^0 Finsler metric $\hat{F}$ obtained as the direct sum of F and the usual one on $\mathbb{R}$ (see Remark 1). Clearly, $\hat{F}$ will be complete if and only if so is F. Moreover, the F-length of the integral curve c of X is bounded on finite intervals if and only so is the $\hat{F}$-length of the integral curve $\hat{c}$ of $\hat{X}$, as required.

3.1.2 Applications

Next, we will apply previous results to simple but general situations. But, previously, we consider the following technical elementary result for future referencing (see for example [66, Lemma 1.1]).

Lemma 1. *Consider the equation*

$$\dot{u} = f(t, u) \quad on \quad [t_0, T), \tag{6}$$

where $f \in C^0(\mathbb{R}^2, \mathbb{R})$ is locally Lipschitz in its second variable, and let $w = w(t)$ be a subsolution of the differential equation i.e.,

$$\dot{w}(t) < f(t, w(t)) \qquad \forall t \in [t_0, T). \tag{7}$$

Then, for every solution $u = u(t)$ of (6) such that $w(t_0) \leq u(t_0)$ we have

$$w(t) < u(t) \quad for\ all \quad t \in (t_0, T). \tag{8}$$

The same conclusion (8) holds if w is only locally Lipschitzian and the inequality (7) occurs when $\dot{w}(t)$ is replaced by some local Lipschitz bound around each t.

The proof follows just recalling that $\Delta := w - u < 0$ close to t_0 by the assumptions and, if there were a first point such that $\Delta(t_1) = 0$, then $\dot{\Delta}(t_1) < 0$ (or an analogous inequality involving a local Lipschitz bound) holds, a contradiction.

Estimates of the Growth for Completeness Let us introduce some auxiliary definitions.

Definition 1. A (locally Lipschitz) function $\alpha : [0, \infty) \to \mathbb{R}$ is *primarily complete* if it is positive, non-decreasing and satisfies:

$$\int_0^\infty \frac{dx}{\alpha(x)} = \infty \tag{9}$$

A vector field X on a Finsler Banach manifold (M, F) is *primarily bounded* if there exists a primarily complete function α, which be called a *bounding function*, such that

$$F(X_p) < \alpha(|p|)) \qquad \forall p \in M. \tag{10}$$

In particular, X *grows at most linearly* if it is primarily bounded by an affine bounding function, i.e.:

$$F(X_p) < C_0 + C_1|p| \qquad \forall p \in M, \tag{11}$$

for some constants $C_0, C_1 > 0$.

Remark 4. The best polynomial candidate for the bounding function α has degree one as, clearly, no polynomial of higher degree can be a primarily complete function. Nevertheless, a slightly faster growth is allowed for non-polynomial functions. For example, α will be primarily complete if it grows as $x \cdot \log x \cdot \log(\log x)$ for large x (see also the discussion in the last part of Section 3.2.1).

Now, we can give a general bound for the completeness of vector fields.

Theorem 1. *Any primarily bounded vector field on a complete Finsler Banach manifold* (M, F) *is complete.*

Proof. Let $c : I \to M$ be an integral curve of X. With no loss of generality, assume $I = [0, b)$, $0 \leq t_0 < t_1 < b$, and choose $p_0 = c(0)$ in the notation introduced in (3). Then:

$$||c(t_1)| - |c(t_0)|| \leq \int_{t_0}^{t_1} F(\dot{c}(s))ds < \int_{t_0}^{t_1} \alpha(|c(s)|)ds, \tag{12}$$

where α is the bounding function. Thus, putting $w(t) = |c(t)|$ we can assume:

$$\dot{w}(t) < \alpha(w(t)),$$

(or the analogous inequality for local Lipschitz constants). The unique inextensible solution w_0 of the equality

$$\dot{w}_0(t) = \alpha(w_0(t)) \qquad w_0(0) = w(0)(= 0)$$

is defined for all $t \in [0, \infty)$, as its inverse is determined as $w \mapsto t(w) = \int_0^w d\bar{w}/\alpha(\bar{w})$ and (9) holds. So, from Lemma 1 one has

$$w(t) < w_0(t) < w_0(b) \qquad \forall t \in (0, b).$$

As α is non-decreasing, equation (10) yields the bound $F(\dot{c}) \leq \alpha(w_0(b))$ so that Proposition 2 is applicable.

Remark 5. By considering on $\mathbb{R}$ a vector field type $X_{x_0} = \alpha(x_0)\partial_x$ one can check the optimality of Theorem 1 and, in particular, the optimality (in the sense discussed in Remark 4) of the at most linear growth of X to ensure completeness. Of course, a vector field with a *superlinear* growth such as $X = y^2\partial_x$ may be complete. In fact, in order to ensure completeness, only the growth of X along the direction of its integral curves becomes relevant. This underlies in the fact that the sum of two complete vector fields X, Y may be incomplete (put $Y = x^2\partial_y$ and X as before) and may suggest more refined hypotheses for completeness in Hilbert spaces (compare with [2, Exercise 2.2H]).

Time-Dependent Case As in the case of the criterions on completeness, Theorem 1 can be extended to the case of a time-dependent vector field X. In fact, the proof works in a completely analogous way (with the observations in Remark 3), if the inequality in (9) is regarded as $F(X_{(p,t)}) < \alpha(|p|)$ for all $(p, t) \in M \times \mathbb{R}$. Nevertheless, one can be a bit more accurate.

Definition 2. A time-dependent vector field X on a Finsler Banach manifold is *primarily bounded along finite times* if there exists a primarily complete function α and a continuous function $C(t) > 0$ such that

$$F(X_{(p,t)}) < C(t)\alpha(|p|) \qquad \forall (p, t) \in M \times \mathbb{R}.$$

In particular, X *grows at most linearly along finite times* when α can be chosen affine or, equivalently, when

$$F(X_{(p,t)}) < C_0(t) + C_1(t)|p| \qquad \forall (p, t) \in M \times \mathbb{R} \tag{13}$$

for some functions $C_0(t), C_1(t) > 0$

Corollary 1. *Let X be a time-dependent vector field on a complete Finsler Banach (M, F). If X is primarily bounded along finite times then it is complete.*

Proof. Reasoning with an integral curve c defined on $[0, b)$ as in the proof of Proposition 2, notice that the inequality (13) for all the pairs $(p, t) \in M \times [0, b]$ also

yields a time independent inequality as (11) with $C_i = \mathrm{Max}_{t\in[0.b]}\{C_i(t)\}, i = 0, 1$. Then, reason as in Remark 3 taking into account that $\hat{X}$ is primarily bounded (on $M \times [0, b]$) if and only if so does X.

3.2 Completeness for 2nd Order Trajectories

3.2.1 General Result on Riemann Hilbert Manifolds

The next result, stated on a Riemann Hilbert manifold (M, g), will summarize those in [1, 17, 23, 33]. To state it, recall that the notion of time-dependent vector field on M in Remark 3 can be directly translated to (continuous, linear) endomorphism fields, which will be regarded here as sections of a fiber bundle on $M \times \mathbb{R}$ with fiber at each $(p, t) \in M \times \mathbb{R}$ equal to the vector space of bounded linear operators $T_{(p,t)}(M \times \mathbb{R}) \to T_{(p,t)}(M \times \mathbb{R})$ which vanish on $(0, \partial_t)_{(p,t)}$. Given such a field E, we will decompose it as $E = S + H$ where S denotes its self-adjoint part ($S = (E + E^\dagger)/2$), and H the skew-adjoint one. A time-dependent or non-autonomous potential means just a smooth map $V : M \times \mathbb{R} \to \mathbb{R}$, then, the notation $\partial V/\partial t : M \times \mathbb{R} \to \mathbb{R}$ makes a natural sense, and $\nabla^M V$ denotes the time dependent vector field on M obtained by taking the gradient of V at each slice $t =$constant with respect to g, i.e., $dV(X(p, t), 0) = g_p(\nabla^M V(p, t), X(p, t))$ for $(X(p, t), 0) \in T_{(p,t)}(M \times \mathbb{R})$. The pointwise norm induced by g in any space of tensor fields will be denoted $\| \cdot \|$.

Theorem 2. *Let (M, g) be a complete Riemann Hilbert manifold, and consider a endomorphism field $E = S + H$, a vector field R and a potential V on M, all of them time-dependent and smooth. Assume that:*

(i) S is uniformly bounded along finite times, i.e., $\| S_{(p,t)} \| \leq C_0(t)$ for all $(p, t) \in M \times \mathbb{R}$,

(ii) R grows at most linearly along finite times, i.e., $\| R_{(p,t)} \| \leq C_0(t) + C_1(t)|p|$ for all $(p, t) \in M \times \mathbb{R}$, and

(iii) both, $-V$ and $|\partial V/\partial t|$ grow at most quadratically along finite times, i.e., they are bounded by $C_0(t) + C_2(t)|p|^2$,

where $C_i(t), i = 0, 1, 2$, denote positive functions. Then, the inextensible solutions of

$$\frac{D\dot{\gamma}}{dt}(t) = E_{(\gamma(t),t)}\,\dot{\gamma}(t) + R_{(\gamma(t),t)} - \nabla^M V(\gamma(t), t), \tag{14}$$

are complete.

Proof. In order to clarify the ideas, the proof is divided into three steps.

Step 1: Reduce the problem to the completeness of a vector field on the tangent bundle. The second order equation (14) allows to define a vector field G on the manifold $T(M \times \mathbb{R})$ such that each solution γ of (14) generates an integral curve

$t \mapsto (\gamma'(t), 1)$ of G. This is standard (see for example [1, Ch. 3] or, for explicit details on the time-dependent case, [17, Section 3.1]) and, so, the problem will be reduced to apply the criterions in Propositions 1 and 2 to G.

Step 2: Find a bound for the velocity of any solution γ of (14), by using the hypotheses (i) to (iii). With no loss of generality, let $\gamma : [0, b) \to M, b < \infty$, be a solution of (14) whose extendability to b is to be determined, let $u(t) = g(\dot\gamma(t), \dot\gamma(t))$ the function to be bounded, and choose the base point $p_0 = \gamma(0)$ for (3). Taking in (14) the product by $\dot\gamma$:

$$\frac{1}{2}\dot u(t) = g(S_{(\gamma(t),t)}\dot\gamma(t), \dot\gamma(t)) + g(R_{(\gamma(t),t)}, \dot\gamma(t)) - \left(\frac{d}{dt}V(\gamma((t), t) - \frac{\partial V}{\partial t}(\gamma((t), t)\right)$$

so that taking pointwise norms and simplifying the notation:

$$\begin{aligned} \tfrac{d}{dt}(\tfrac{1}{2}u + V) &\leq \| S \| u + \| R \| \sqrt{u} + \partial V/\partial t \\ &\leq (\| S \| + 1/2)u + \| R \|^2 /2 + \partial V/\partial t \end{aligned} \tag{15}$$

Using the bounds (i), (ii), (iii) and taking into account that, as the t coordinate is confined in the compact interval $[0, b]$, the t-dependence of these bounds can be dropped:

$$\frac{d}{dt}(u + 2V) \leq A_0 + A_1 u + A_2|\gamma|^2 \tag{16}$$

for some constants $A_0, A_1, A_2 > 0$. Consider the function $l(t) = \int_0^t \sqrt{u}$, $t \in [0, b)$ which provides the length of γ. Clearly:

$$|\gamma(t)|^2 \leq l(t)^2 \qquad \text{and} \qquad \int_0^t l(\bar t)^2 d\bar t \leq b \cdot l(t)^2 \qquad \forall t \in [0, b),$$

the latter as l is nondecreasing. Using these inequalities and integrating in (16):

$$u(t) - A_1 \int_0^t u \leq A_0' - 2V(\gamma(t), t) + A_2 b l(t)^2 < C_0 + C_1 l(t)^2,$$

where A_0', C_0, C_1 are constants (C_0 and C_1 positive), obtained by taking into account the hypothesis (iii). So, putting $v(t) = \int_0^t u$ and relabelling A_1,

$$\dot v < C_0 + C_1 \cdot l^2 + C_2 \cdot v \qquad \text{for some constants} \quad C_0, C_1, C_2 > 0. \tag{17}$$

Now, v can be regarded as a subsolution of a differential equation, and Lemma 1 will be applicable to the solution v_0 of this equation with $v_0(0) = v(0) = 0$ i.e. $v(t) < v_0(t)$ and, taking into account (17):

$$\dot v < C_0 + C_1 \cdot l^2 + C_2 \cdot v_0 = \dot v_0$$

on $(0, b)$. As $u = \dot v$, to bound $\dot v_0$ would suffice.

Notice that v_0 can be written explicitly as:

$$v_0(t) = e^{C_2 t} \int_0^t e^{-C_2 \bar{t}} (C_0 + C_1 l(\bar{t})^2) d\bar{t}$$

so that, using that l is nondecreasing,

$$\dot{v}_0 \leq C_0 + C_1 l^2 + C_2 b e^{C_2 b} (C_0 + C_1 l^2) = A + B l^2 \qquad \text{on } [0, b) \tag{18}$$

for some constants $A, B > 0$. But recall that $\dot{l} = \sqrt{u} < \sqrt{\dot{v}_0}$, that is, l can be also regarded as a subsolution of a differential equation:

$$\dot{l} < \sqrt{A + B \cdot l^2}. \tag{19}$$

So, l is bounded by the corresponding solution ($l(t) < \sqrt{A/B} \cdot \sinh(\sqrt{B} \cdot t$ on $(0, b)$) and, thus, u (regarded either as $\dot{l}^2$ in (19) or as $\dot{v}_0$ in (18)) is bounded, as required.

Step 3: As g is complete, $\dot{\gamma}$ must lie in a compact subset. The aim is to prove the extendability of $\dot{\gamma}$ as an integral curve of the vector field G on $T(M \times \mathbb{R})$ defined in the first step. As a first consequence of the boundedness of u, the completeness of g imply that γ must be convergent in M. Then, it is convenient to distinguish two type of reasonings:

(3a) In the case that M is finite dimensional, the convergence of γ at b, the boundedness of $u = g(\dot{\gamma}, \dot{\gamma})$ and the local compactness of TM, are enough to ensure that $\dot{\gamma}$ lies in a compact subset of TM, so that Proposition 1 is applicable to G.

(3b) In the infinite-dimensional case, the lack of local compactness requires a more elaborated argument. First, the Riemannian metric g on M induces naturally a Riemannian metric $\tilde{g}$ on TM, the *Sasaki metric* [62]. As proven by Ebin [23], $\tilde{g}$ is complete whenever so is g. The vector field G can be written as a sum $G = G_0 + G_1 + G_2$ where G_0 is the geodesic spray and, thus, a horizontal vector field, G_1 is a vertical vector field such that, at each $v_{(p,t)}$, depends only of the value of $R + \nabla^M V$ at (p, t) and G_2 is also a vertical vector which, at each $v_{(p,t)}$, can be identified with $E(v_{(p,t)})$. The convergence of γ yields a bound for $\tilde{g}(G_1, G_1)$ on $\dot{\gamma}$, the boundedness of u implies a bound for $\tilde{g}(G_0, G_0)$ and, then, the boundedness of the operator E implies the boundedness of $\tilde{g}(G_2, G_2)$. So, G is bounded on $\dot{\gamma}$, and Proposition 2 is applicable.

Remark 6. (1) The result can be also sharpened, if one is only interested in the forward or backward completeness of the trajectories (*positive* or *negative completeness*), i.e. the possibility to extend the solutions to an upper or lower unbounded interval type $[a, \infty)$ or $(-\infty, a]$. From the proof is clear that, in order to obtain the extensibility of the trajectories to $+\infty$ (resp. $-\infty$), one

requires only the upper (resp. lower) uniform bound of $g(v, S(v))/g(v, v)$, for $v \in TM \setminus \{0\}$,[4] as well as the upper (resp. lower) bound of $\partial V/\partial t$, instead of the bounds for the norm and absolute value imposed in the hypotheses (i) and (iii).

(2) As a trivial consequence of Theorem 2, if M is compact then all the inextensible trajectories are complete, for any E, R, V.

Primary and Positively Complete Functions The optimal growth allowed either for $-V$ or for $|\partial V/\partial t|$ can be sharpened, by using bounds in the spirit of the *primary* ones, introduced for Theorem 1, which are clearly related to the notion of *positive completeness* introduced by Weinstein and Marsden [68].

Recall that a smooth function $V_0 : [0, \infty) \to \mathbb{R}$ is called *positively complete* if it is non-increasing and satisfies

$$\int_0^{+\infty} \frac{ds}{\sqrt{e - V_0(s)}} = \infty,$$

for some (and then all) constant $e > V_0(0)$ (hence $e > V_0(s)$ for all $s \in [0, +\infty)$) [1, 68]. Extending Weinstein–Marsden notions, we say that a smooth time-dependent function $V : M \times \mathbb{R} \to \mathbb{R}$ is bounded by a positively complete function along finite times if there exists functions $V_0, C : [0, \infty) \to \mathbb{R}$, V_0 positively complete and $C > 0$ such that:

$$V(p, t) \geq C(t)V_0(|p|)) \qquad \forall (p, t) \in M \times \mathbb{R}.$$

The relation between these notions and those used in the last subsection comes from the fact that *a smooth function V_0 is positively complete if and only if $\sqrt{e - V_0}$ is well-defined and primarily complete for some $e > V_0(0)$*. Now, from the proof of Theorem 2, one can easily check:

> Hypotheses (ii) and (iii) in Theorem 2 can be replaced by the following more general one: there exists a primarily complete function α and a positive one C such that R is primarily bounded along finite times by $C \cdot \alpha$ and $-V(p, t), |\partial V/\partial t|(p, t) < C(t)^2\alpha(|p|)^2$ for all $(p, t) \in M \times \mathbb{R}$.

In particular, the quadratic bounds in (iii) can be improved by requiring only bounds[5] by, say, $C_0(t) + C_2(t)|x|^2 \log^2(1 + |x|)$ and the linear bound in (ii) by

[4] This can be rephrased as a bound of the spectrum of S, see [44, Th. 3.10].

[5] These improvements can be also extended to other contexts, as the completeness of certain Finsler metrics in [21].

$\tilde{C}_0(t)+C_1(t)|x|\log(1+|x|)$ (as well as by other functions pointed out in [1, p. 233] or [17, Remark 5(2)]). These bounds might be optimized further, combining them also with better bounds for E.

The Time-Dependence of the Potential V For a non-autonomous potential, the role of the bounds of $\partial V/\partial t$ becomes quite subtler. Notice that one can regard $\nabla^M V$ as a time-dependent vector. Thus:

> If we assume in Theorem 2 that $\nabla^M V$ grows at most linearly along finite times, no bound for $\partial V/\partial t$ is necessary. Nevertheless, such a hypothesis is independent of the one stated in *(iii)*. In fact, in the autonomous case, if $\nabla^M V$ grows at most linearly then $-V$ grows at most quadratically, but, clearly, the converse does not hold.

Other alternative bounds for $\partial V/\partial t$ in Theorem 2 can be explored. For example, assuming by simplicity $R = 0$ in *(ii)*, the result of completeness still holds if we replace *(iii)* by the following two conditions: V is lower bounded at finite times ($V(p,t) \geq -C_0(t)$) and:

$$|\partial V/\partial t| \leq C_1(t)(V(p,t) - C_0(t)) \qquad \forall (p,t) \in M \times \mathbb{R}. \tag{20}$$

In fact, (15) would yield now $d(u+2V)/dt < C(u+2V-B)$ for some constants $C > 0$, $B \in \mathbb{R}$ which depend on the domain $[0,b)$, $b < \infty$. So, $u+2V$ (and, then, u) would be bounded as a subsolution, see [16] for details.

> These new bounds (lower for V plus (20)) are independent of those in *(iii)* because, when V grows fast to infinity, such a growth is allowed for $\partial V/\partial t$ too. So, to find a general optimal bound for $\partial V/\partial t$ (say, extending all previous with some nice geometric interpretation) remains as a natural question.

3.2.2 Notes on the General Finsler Case

Finsler Metrics, Second Order Equations and Strong Convexity In order to extend previous results to the Finslerian setting, notice that the Riemannian metric g in Theorem 2 not only allows to introduce distances and estimates on the growth of tensor fields, but also becomes essential to pose the second-order differential equation (14). Thus, for the Finslerian extension, not only higher differentiability for the Finsler metric F will be required but also its *strong convexity*, to be explained here.

Remark 7. As pointed out in Section 2, the existence of smooth Finsler metrics introduce some restrictions in the infinite dimensional case. In fact, notions such as pseudo-gradients[6] were introduced to avoid those restrictions. Recall that the smoothness of each pointwise norm F_p is required only away from 0 and, thus, it can be characterized as the smoothness of the F_p-unit sphere as a submanifold of the corresponding vector space T_pM. However, the smoothness of F is not enough to introduce connections, covariant derivatives, etc., which appear implicitly in (14).

The triangle inequality implies that, for each norm F_p, $p \in M$, the closed unit ball $\bar{B}_p(0,1)$ is convex, i.e., it contains any segment with endpoints in $\bar{B}_p(0,1)$. If the triangle inequality holds strictly, then the unit sphere is strictly convex, in the sense that each segment with endpoints in $\bar{B}_p(0,1)$ must be entirely contained in the open unit ball $B_p(0,1)$ except, at most, the endpoints. Nevertheless, even in the smooth finite-dimensional case, the unit sphere may be strictly convex but not strongly convex in the following sense.

Recall that the *fundamental tensor* of each norm F_p is the tensor field on $T_pM \setminus \{0\}$ defined as the Hessian h_{v_p} of F_p^2 at each $v_p \in T_pM \setminus \{0\}$. Such a Hessian can be defined by using an affine connection of T_pM if F_p is C^2. Now, consider the slit tangent bundle $TM \setminus \{0\}$ and the tangent bundle TM, as well as the natural projection $\pi : TM \setminus \{0\} \to M$. This maps induces a vector bundle $\pi^*(TM)$ with base $TM \setminus \{0\}$, being its fiber at each $v \in TM \setminus \{0\}$ isomorphic to $T_{\pi(v)}M$. Taking the fundamental tensor for each F_p, $p \in M$, one defines naturally the fundamental tensor field h of F as a tensor field on the vector bundle $\pi^*(TM)$, and F is called *strongly convex* when h becomes a smooth positive definite tensor.

Strong convexity may introduce a new restriction in the infinite-dimensional case, but it is necessary for several purposes, even in the case of n-manifolds (see [37] for details):

- To ensure that geodesics (defined as extremals of the energy functional) are determined univocally by its initial condition (starting point and velocity) at some point. That is, otherwise *geodesics cannot be regarded as solutions of a second order differential equation* nor their velocities yield integral curves on a vector field on TM.
- To ensure (at least in the finite-dimensional case) that the natural Legendre transformation $TM \to TM^*, v_p \mapsto g_{v_p}(v_p, \cdot)$ (which generalizes the metric isomorphism of inner spaces, see (4), but may not be linear) becomes a diffeomorphism. Recall that this map is the fiber derivative associated to the Lagrangian $L = F^2/2$ (see [65, Sect. 3.1], [2, Sect. 3.6]) and, then, the Lagrangian becomes hyper-regular. In this case gradients can be defined, and pseudo-gradients (see the footnote 6) are no longer necessary.
- To define natural connections on the Finsler manifold.

[6] According to Palais [52, Defn. 4.1] (and taking into account Moore's modification [49, p. 50]), a pseudo-gradient for a function V on an open subset U is a locally Lipschitz vector field X such that $\epsilon^2 F_p(X_p)^2 \leq \| dV_p \| \leq \epsilon^{-2} dV_p(X_p)$ for all $p \in U$.

Standard Finsler Case Taking into account the difficulties pointed out above for the general Finsler case, we restrict now to *standard Finsler manifolds* i.e., n-manifolds endowed with a C^∞-smooth and strongly convex Finsler metric. This is the object of study of standard references on Finsler manifolds as, for example,[7] [4, 65]. Some similarities with the Riemannian case appear then:

- A covariant derivative for vector fields on curves exists. Thus, the acceleration of these curves can be defined, extending so the notion of $D\dot{\gamma}/dt$ in the Riemannian case [4, pp. 121–124], [65, Sect. 5.3].
- Non-constant geodesics can be defined as curves with 0 acceleration, they admit a variational characterization and they also determine a (second order equation) vector field G on the slit tangent bundle $TM \setminus \{0\}$ so that the integral curves of G are the curves of velocities of geodesics, [4, Sect. 3.8, 5.3], [65, Sect. 5.1].
- The Finsler metric F provides the fundamental tensor as well as a natural Sasaki type metric on the slit tangent bundle that makes $TM \setminus \{0\}$ a Riemannian manifold [4, p. 35].

Of course, important differences with the Riemannian case remain, because Chern/Rundt connection in Finslerian geometry (as well as Cartan, Hashiguchi or Berwald connections) becomes much subtler than the natural Levi–Civita connection in the Riemannian case.

Bearing in mind these subtleties, one can try to give different Finslerian extensions of Theorem 2. Here, we will consider just the most obvious one, and leave the possibility of obtaining more general results for further developments. To avoid working with Finslerian machinery and work with one of the possible connections, notice that, in the case $R = E = 0$, formula (14) is the Euler–Lagrange equation for the critical curves of the action:

$$\int_a^b \left(\frac{1}{2}F(\dot{\gamma}(t))^2 - V(\gamma(t), t)\right) dt \tag{21}$$

with fixed points $\gamma(a), \gamma(b)$. In Theorem 2, F is the norm of the Riemannian metric but, obviously, functional (14) makes sense for any Finsler metric and, under some conditions as above, its Euler–Lagrange equation can be written as in (14). We say that $\gamma : I \subset \mathbb{R} \to M$ is a *trajectory for the potential* V if its restriction to any compact subinterval $[a, b]$ of I is a critical point of the action functional (21).

Proposition 3. *Let (M, F) be a standard Finsler manifold, and consider a C^1 time-dependent potential $V : M \times \mathbb{R} \to \mathbb{R}$ such that $-V$ and $|\partial V/\partial t|$ grows at most quadratically for finite times. Then, any inextensible trajectory $\gamma : I \subset \mathbb{R} \to M$ for the potential V is complete.*

[7] However, standard Finsler metrics are usually allowed to be non-reversible, see Remark 8.

Proof. Notice first that the problem can be reduced to study the integral curves of a vector field on TM, because, as the Finsler metric is standard, the Lagrangian $L = (F^2/2) - V$ becomes regular (in fact, hyper-regular), see for example [2, Th. 3.5.17, 3.8.3]. Then, putting $u = F(\dot{\gamma})^2$, one has $d(u + 2V)/dt = 2\partial V/\partial t$ and formula (16) holds (with $A_1 = 0$), so that the proof follows as in Theorem 2.

Remark 8. A different direction in the possible generalizations of Theorem 2, is to allow non-reversible Finsler metrics, so that $F(v) \neq F(-v)$ in general. This leads us to consider *generalized distances* (i.e., possibly non-symmetric ones) and then, *forward and backward* geodesics and Cauchy completions, as well as many other subtleties (see [28] and references therein). Nevertheless, the general background for completeness would be maintained for this case. In fact, Proposition 3 can be extended to the non-reversible case. Namely, regarding the hypotheses of completeness for F in the sense of, say, *forward completeness*, and the generalized distance d_F to the base point in the ordering $|p| = d_F(p_0, p)$ (so that the bound for the potential remains formally equal). Then, the technique works also for the non-reversible case, and the conclusion of *forward* completeness still holds.

4 Completeness of Pseudo-Riemannian Geodesics

This section is divided into four parts. The first one tries to orientate the intuition about completeness on indefinite manifolds by recalling some examples. Moreover, the role of incompleteness in relativistic singularity theorems is compared with the role of finite diameter for some Riemannian Myer's-type results. In the second part, we recall some results on completeness for manifolds with a high degree of symmetry. Here, the difference between global symmetries (homogeneous, symmetric spaces) as in Theorems 5 and 6 and local ones (constant curvature, local symmetry) in Theorems 7 and 8 becomes apparent. The third part is focused on plane wave type spacetimes, whose completeness yields a direct link with the Riemannian results of trajectories under potentials (Theorem 9). Previous results suggest some open questions stated in the last part of the section.

In what follows, (M, g) will be a n-manifold endowed with a pseudo-Riemannian metric of index ν, typically a Lorentzian one (i.e., $\nu = 1$ so that the signature is $(-, +, \ldots, +)$). The name of *semi-Riemannian* manifold (instead of pseudo-Riemannian) has been also spread, especially since O'Neill's book [50]. This book is referred to here for general background on pseudo-Riemannian geometry, the review [14] for the specific problem of geodesic completeness, and the book [6] for related Lorentzian results.

4.1 The Pseudo-Riemannian and Lorentzian Settings

Let (M, g) be a pseudo-Riemannian manifold, and $v \in TM$, $v \neq 0$. Extending the nomenclature in General Relativity, v will be called *timelike* (resp. lightlike, spacelike) if $g(v, v) < 0$ (resp. $= 0, > 0$).

4.1.1 Abandoning the Riemannian Intuition

For a pseudo-Riemannian manifold there is no any result analogous to the Hopf–Rinow one and, for example, M may be compact and geodesically incomplete.

Example 1. Consider the Lorentzian metric g on $\mathbb{R}^2$ defined as $g = 2dxdy + \tau(x)dy^2$, where τ is periodic of period 1, $\tau(0) = 0$ and $\tau'(0) \neq 0$. A simple computation shows that the line $x = 0$ can be reparameterized as an incomplete lightlike geodesic. So, the quotient torus $T = \mathbb{R}^2/\mathbb{Z}^2$ inherits an incomplete Lorentzian metric (more refined properties on tori can be found in [59] and references therein).

The previous example also shows that a closed lightlike geodesic may be non-periodic and, then, incomplete. Also as a difference with the Riemannian case, a homogeneous Lorentzian manifold may be incomplete.

Example 2. Consider a half plane of Lorentz–Minkowski space in lightlike coordinates u, v namely $(\mathbb{R}^+ \times \mathbb{R}, g = 2dudv)$. This space is trivially incomplete, and it is homogeneous too, as both, the v-translations and the maps $\Phi_\lambda : (u.v) \mapsto (\lambda u, v/\lambda)$ (for any $\lambda > 0$), are isometries. Recall also that the quotient cylinder obtained from the orbits of the isometry group $\{\Phi_2^m : m \in \mathbb{Z}\}$ is another example of space with a closed incomplete lightlike geodesic (namely, the projection of $u \mapsto (u, 0)$).

4.1.2 Singularity Theorems

Even though at the very beginning of General Relativity incompleteness was regarded as a pathological property for a physical spacetime, the further development of Relativity showed that incompleteness appears commonly under physically realistic conditions. Well-known results in this direction were obtained by Raychaudhuri [56], Penrose [55], Hawking [34], Gannon [31] or, more recently, Galloway and Senovilla [30], amongst others (see the review [63] for general background). We emphasize that the claimed incompleteness here occurs only for geodesics of timelike or lightlike type.[8] Even though it is not totally clear to what

[8]Explicit examples by Kundt [39], Geroch [32, p. 531] and Beem [5] showed the full logical independence among spacelike, timelike and lightlike geodesic completeness.

extent such incomplete geodesics would represent a physical singularity (nor the meaning of the latter, see the classical discussion [32]), the moral in Relativity is that the knowledge of the possible completeness or incompleteness of the underlying Lorentzian manifold becomes an essential property of the spacetime.

As pointed out in [61], perhaps the simplest singularity theorem for researchers interested in connections with Riemannian Geometry is the following one by Hawking, which can be regarded as a support for the physical existence of a *Big Bang*.

Theorem 3. *Let* (M, g) *be a spacetime satisfying the following conditions:*

1. (M, g) *is globally hyperbolic,*
2. *there exists some spacelike Cauchy hypersurface* S *with an infimum* $C > 0$ *of its expansion, that is, such that its mean curvature vector* $\mathbf{H} = H\mathbf{n}$*, where* $\mathbf{n}$ *is the future-directed unit normal, satisfies* $H \geq C > 0$*,*
3. *the timelike convergence condition holds:* $\mathrm{Ric}(v, v) \geq 0$ *for any timelike vector* v*.*

Then, any past-directed timelike curve starting at S *has length at most* $1/C$*.*

The reason is that the proof of this theorem can be regarded as isomorphic to the proof of the following purely Riemannian result:

Theorem 4. *Let* (M, g) *be a Riemannian manifold satisfying:*

1. g *is complete,*
2. *there exists some embedded hypersurface* S *which separates* M *as a disjoint union* $M = M_- \cup S \cup M_+$*, with an infimum* $C > 0$ *of its expansion towards* M_+*, that is, such that its mean curvature vector* $\mathbf{H} = H\mathbf{n}$*, where* $\mathbf{n}$ *is the unit normal which points out* M_-*, satisfies* $H \geq C > 0$*,*
3. $Ric(v, v) \geq 0$ *for every* v*.*

Then, $\mathrm{dist}(p, S) \leq 1/C$ *for every* $p \in M_-$*.*

In fact, this last theorem can be proven by using standard techniques on focal points and Myers' theorem. Such techniques can be extended to the Lorentzian setting by realizing that the roles of each one of the three hypotheses in Theorem 3 is isomorphic in the proof to the corresponding hypothesis in Theorem 4 (in particular, the role of Riemannian completeness is played by global hyperbolicity), see [36] and [48] for full details. The techniques of singularity theorems, however, become much more refined, because of the weakening of causality assumptions, the appearance of genuinely Lorentzian elements such as trapped surfaces and other subtleties, see for example [35] or, more recently, [30].

4.2 Completeness Under Symmetries

After previous considerations, it is clear that some strong assumptions will be required in order to ensure geodesic completeness. We will focus on some types of symmetries.

4.2.1 Killing and Conformal Fields

The simple Examples 1 and 2 of non-complete compact or homogeneous Lorentzian manifolds, make apparent the importance of the following theorem by Marsden [47] (see also [1, 4.2.22]):

Theorem 5 ([47]). *Any compact homogeneous pseudo-Riemannian manifold is geodesically complete.*

Marsden's proof is carried out by proving that TM can be written as the union of compact subsets S_α, each one invariant by the geodesic flow (and, so, Proposition 1 yields directly the result). In fact, if $\mathfrak{g}^*$ is the dual of the Lie algebra of the isometry group, and $P : TM \to \mathfrak{g}^*$ is the momentum map (i.e., $P(v)\xi = g(v, \xi_M)$, where ξ_M is the infinitesimal generator of $\xi \in \mathfrak{g}$), then $S_\alpha = P^{-1}(\alpha)$, for each $\alpha \in \mathfrak{g}^*$.

As proven by Romero and the author [57, 58], this result can be extended in two directions. Firstly, it is not necessary, in order to ensure the completeness of each geodesic γ, that its velocity $\dot\gamma$ remains in a compact subset of TM. In the spirit of Proposition 2, it is enough if it remains in a compact subset when its domain is restricted to bounded intervals. From such an observation, Theorem 5 can be extended to metrics conformal to Marsden's. Secondly, a homogeneous manifold is full of Killing vector fields but if, say, a compact Lorentzian manifold admitted just one *timelike* Killing vector field[9] K, this would be enough. Indeed, as $g(\dot\gamma, K)$ is a constant for any geodesic γ, this (plus the constancy of $g(\dot\gamma, \dot\gamma)$) is sufficient to ensure that $\dot\gamma$ lies in a compact subset. So, from these ideas:

Theorem 6 ([57, 58]). *A compact pseudo-Riemannian manifold (M, g) of index ν is geodesically complete if one of the following properties hold:*

- *(M, g) is (globally) conformal to a homogeneous one, or*
- *(M, g) admits ν timelike conformal vector fields which are pointwise independent.*

The technique also admits extensions to non-compact manifolds, see [57, 60]; for applications to classification of spaceforms, see [38]. Further results on locally homogeneous 3-spaces (involving also the classification of these spaces) can be found in [10, 13, 22].

[9] This case is interesting also for the classification of flat compact Lorentzian manifolds, which are called then *standard*, see [38].

4.2.2 Locally Symmetric and Constant Curvature Manifolds

As a difference with homogeneous spaces, it is easy to check that any *pseudo-Riemannian symmetric space is geodesically complete* (see for example [50, Lemma 8.20]). Nevertheless, even for locally symmetric spaces and, in particular, constant curvature ones, the problem is not as trivial as it may seem. We quote two results which will be relevant in order to state some open questions below. The first one is due to Lafuente:

Theorem 7 ([43]). *For a locally symmetric Lorentzian manifold, the three types of causal completeness (timelike, lightlike and spacelike) are equivalent.*

The second one was proven by Carriére [19] in the flat case and extended by Klinger [41] for manifolds of any constant curvature.

Theorem 8 ([19, 41]). *Any compact Lorentzian manifold of constant curvature is geodesically complete.*

Remark 9. Recall that the proof of this result holds only for Lorentzian signature; as far as we know, the extension of the result to higher signatures is an open problem.

4.3 Riemannian and Lorentzian Interplay: Plane Waves

4.3.1 Plane Waves, pp-Waves and Further Generalizations

Following [15], consider a Lorentzian n-manifold, $n \geq 3$, that can be written globally as $(M = \mathbb{R}^2 \times M_0, g)$ where the natural coordinates of $\mathbb{R}^2$ will be labelled (u, v) and g is written as:

$$g_{(u,v,x)} = -2dudv + H(u,x)du^2 + \Pi_0^\star g_0, \qquad \forall (u,v,x) \in \mathbb{R}^2 \times M_0,$$

being $\Pi_0 : M \to M_0$ the natural projection and g_0 a Riemannian metric on M_0. Here, we will refer to these spaces as M_0p*-waves*. When (M_0, g_0) is just $\mathbb{R}^{n-2}$, these metrics are called *pp-waves* (*plane-fronted waves with parallel rays*), namely, $M = \mathbb{R}^n$,

$$g_{(u,v,x)} = -2du dv + H(u, x^1, \ldots, x^{n-2})du^2 + \sum_{i=1}^{n-2}(dx^i)^2 \quad \forall (u, v, x^1, \ldots, x^{n-2}) \in \mathbb{R}^n \tag{22}$$

Such a pp-wave is called a *plane wave* when H is quadratic in $(x^1, \ldots, x^{n-2})$,

$$H(u, x^1, \ldots, x^{n-2}) = \sum_{i,j=1}^{n-2} A_{ij}(u)x^i x^j .$$

In the particular case $n = 4$ one writes $H(u, x, y) = a(u)\,(x^2 - y^2) + 2\,b(u)\,xy + c(u)\,(x^2 + y^2)$, where a, b, c are arbitrary smooth functions of u. The functions a, b describe the wave profiles of the two linearly independent polarization modes of gravitational radiation, while c describes the wave profile of non-gravitational radiation. When $c = 0$ (vacuum or gravitational plane waves) the Ricci tensor vanishes.

Plane waves are interesting in many physical issues. We remark here that they are also interesting in the framework of *rth-symmetric spaces* $r \geq 2$ (introduced in [64], see [8] for a systematic study). These are pseudo-Riemannian manifolds with rth-covariant derivative of its curvature tensor R equal to 0:

$$\nabla^r R := \nabla \ldots^{(r)} \nabla R \equiv 0.$$

For Riemannian manifolds rth-symmetry implies local symmetry (i.e., $\nabla R = 0$) but proper examples of rth-symmetric spaces can be found in the class of plane waves. In fact, such examples are obtained just regarding the matrix A as a polynomial in u of degree $r - 1$:

$$A_{ij}(u) = a_{ij}^{(r-1)} u^{r-1} + \ldots + a_{ij}^{(1)} u^1 + a_{ij}^{(0)}$$

where $a_{ij}^{(r-1)} \not\equiv 0$; a simple computation shows that $\nabla^r R = 0$ but $\nabla^{r-1} R \neq 0$.

As shown in [8], proper 2nd-symmetric Lorentzian spaces are locally isometric to the product of such a wave (with $r = 2$) and a locally symmetric Riemannian space.

4.3.2 Completeness of M_0p-Waves

A nice relation between the geodesic completeness of a class of Lorentzian manifold and the completeness of Riemannian trajectories for a potential appears in the case of M_0p-waves:

Theorem 9. *A M_0p-wave is geodesically complete if and only if (M_0, g_0) is complete and the trajectories of*

$$\frac{D\dot{\gamma}}{dt}(t) = -\nabla^{M_0} V(\gamma(t), t)$$

are complete for $V = -H/2$.

Thus, under the completeness of the Riemannian part (M_0, g_0), a M_0p-wave is complete if H and $|\partial H/\partial u|$ grows at most quadratically for finite u-times. In particular, all plane waves are geodesically complete.

Proof. The first part is proven in [15, Th. 3.2], by means of a careful equivalence between the Lorentzian geodesics and Riemannian trajectories [15, Prop. 3.1]. So, it is enough to apply Theorem 2.

As emphasized in [26], this type of result also justifies that all physically reasonable pp-waves (that is, those with a qualitative behavior of H as a plane wave, eventually with some possible decay at infinity) will be geodesically complete and, so, they can be regarded as singularity free.

Finally, we state the following very recent result by Leistner and Schliebner on pp-waves. Notice that, for any pp-wave as above (formula (22)), the vector field $V = \partial_v$ is parallel and lightlike, and the curvature tensor R satisfies:

$$R(U, W) = 0 \qquad \text{for all vector fields } U, W \text{ orthogonal to } V. \tag{23}$$

Conversely, any spacetime admitting such a vector field can be written locally as a pp-wave. Now:

Theorem 10 ([45]). *The universal covering of any compact Lorentzian manifold (M, g) which admits a parallel lightlike vector field V satisfying (23), is a geodesically complete pp-wave. In particular, (M, g) is geodesically complete.*

This result goes in the same direction of those for the compact case with constant curvature or (conformal) homogeneity. Nevertheless, the special holonomy derived from the *global* existence of V plays a fundamental role here. So, in principle, it is not enough to assume that the spacetime is just locally isometric to a plane wave (and, so, for example, Carriére's theorem is not re-proved). In fact, the universal covering is taken such that ∂_v is the lift of the globally defined vector field V.

Remark 10. The existence of a complete vector field V fulfilling the hypotheses in Theorem 10, can be also regarded as a generalization of the notion of pp-wave to non-trivial topology. As emphasized in [45], such a generalization may pose some topological subtleties related to Ehlers–Kundt conjecture (see the third question below), loosely suggested in the original article [24].

4.4 Some Open Questions

Taking into account previous considerations, the following questions become natural and are open, as far as we know:

1. Assume that a compact Lorentzian manifold is globally conformal to a manifold of constant curvature. Must it be geodesically complete?

Recall that this poses a possible extension of Theorem 8, which may be expected after the conformal extension in Theorem 6 of Marsden's Theorem 5.

It is also worth pointing out that, for compact manifolds, *lightlike* completeness is a conformal invariant (this is easy to check as lightlike pregeodesics are conformally invariant, and their reparameterizations as geodesics depend on a bounded conformal factor, see [14, Section 2.3] for detailed computations). So, if a counterexample to the question existed, it would be incomplete in some causal sense and complete in the lightlike case. In particular, such a counterexample would prove that Lafuente's Theorem 7 cannot be extended to the conformal case even for compact manifolds. It is also worth pointing out that, if γ is a geodesic for a metric g, then it satisfies an equation type (14) for any conformally related metric $\bar{g}$ (but, in this case, such an equation is posed on a Lorentzian manifold $(M, \bar{g})$).

2. Assume that a pseudo-Riemannian manifold is r-th symmetric. Must the three types of causal completeness be equivalent?

Such a question becomes natural after Lafuente's Theorem 7, especially in the case of Lorentzian 2nd-symmetric spaces, because of their simple classification explained above.

3. Must any complete gravitational (i.e., Ricci flat) pp-wave be a plane wave?

This is a long-standing open problem posed by Ehlers and Kundt [24]. Recall first that all plane waves are complete, even if non-gravitational (Theorem 9). The fact that these waves are gravitational, i.e., Ricci flat, yields a link with complex variable, as this condition is equivalent to the harmonicity of $H(x, u)$ with respect to the variable x (see [27])—notice that the study of the completeness of holomorphic vector fields, become a field of research in its own right which has been handled with specific tools, see for example [11, 12, 29]. Thus, there are both, physical and mathematical motivations for its study [7, 27].

As a last comment, we point out that the completeness of trajectories in a Lorentzian manifold under external forces is an almost open field with rich possibilities [18]; as we have said in the comments to question 1, this includes the equation of geodesics for a conformally related metric. So, even though the physical interpretations of such forces are less apparent in the Lorentzian case than in the Riemannian one, this may be an interesting topic for future research.

Acknowledgements Partially supported by Spanish grants with Feder funds P09-FQM-4496 (J. Andalucía) and MTM2013-47828-C2-1-P (Mineco).

References

1. Abraham, R., Marsden, J.E.: Foundations of Mechanics, 2nd edn. Addison-Wesley Publishing, Boston (1987)
2. Abraham, R., Marsden, J.E., Ratiu, T.: Manifolds, Tensor Analysis and Applications, 2nd edn. Springer, New York (1988)
3. Atkin, C.J.: Geodesic and metric completeness in infinite dimensions. Hokkaido Math. J. **26**, 1–61 (1997)
4. Bao, D., Chern, S.-S., Shen, Z.: An Introduction to Riemann–Finsler Geometry. Graduate Texts in Mathematics, vol. 200. Springer, New York (2000)
5. Beem, J.K.: Some examples of incomplete space-times. Gen. Relativ. Gravitation **7**, 501–509 (1976)
6. Beem, J.K., Ehrlich, P.E., Easley, K.L.: Global Lorentzian Geometry. Monographs Textbooks Pure Applied Mathematics, vol. 202. Dekker, New York (1996)
7. Bičák, J.: Selected solutions of Einstein's field equations: their role in general relativity and astrophysics. In: Schmidt, B.G. (ed.) Einstein's Field Equations and Their Physical Implications (Selected Essays in Honour of Jürgen Ehlers). Springer, Berlin (2000)
8. Blanco, O.F., Sánchez, M., Senovilla, J.M.M.: Structure of second-order symmetric Lorentzian manifolds. J. Eur. Math. Soc. **15**, 595–634 (2013)
9. Bonic, R., Frampton, J.: Smooth functions on Banach manifolds. J. Math. Mech. **15**, 877–898 (1966)
10. Bromberg, S., Medina, A.: Geodesically complete Lorentzian metrics on some homogeneous 3 manifolds. Symmetry Integrability Geom. Methods Appl. **4**, Paper 088, 13 pp. (2008)
11. Brunella, M.: Complete polynomial vector fields on the complex plane. Topology **43**(2), 433–445 (2004)
12. Bustinduy, A., Giraldo, L.: Completeness is determined by any non-algebraic trajectory. Adv. Math. **231**(2), 664–679 (2012)
13. Calvaruso, G.: Homogeneous structures on three-dimensional Lorentzian manifolds. J. Geom. Phys. **57**(4), 1279–1291 (2007)
14. Candela, A.M., Sánchez, M.: Geodesics in semi-Riemannian manifolds: geometric properties and variational tools. In: Alekseevsky, D.V., Baum, H. (eds.) Recent Developments in Pseudo-Riemannian Geometry, Special Volume in the ESI Series on Mathematics and Physics, pp. 359–418. EMS Publishing House, Zürich (2008)
15. Candela, A., Flores, J.L., Sánchez, M.: On general plane fronted waves. Geodesics. Gen. Relativ. Gravitation **35**, 631–649 (2003)
16. Candela, A.M., Romero, A., Sánchez, M.: Remarks on the completeness of plane waves and the trajectories of accelerated particles in Riemannian manifolds. In: Proceedings of International Meeting on Differential Geometry, pp. 27–38. University of Córdoba, Córdoba (2012)
17. Candela, A.M., Romero, A., Sánchez, M.: Completeness of the trajectories of particles coupled to a general force field. Arch. Ration. Mech. Anal. **208**(1), 255–274 (2013)
18. Candela, A.M., Romero, A., Sánchez, M.: Completeness of relativistic particles under stationary magnetic fields. In: Proceedings of XXI International Fall Workshop on Geometry and Physics. Int. J. Geom. Methods Mod. Phys. **10**(8), 1360007, 8 pp. (2013)
19. Carrière, Y.: Autour de la conjecture de L. Markus sur les variétés affines. Invent. Math. **95**, 615–628 (1989)
20. Deimling, K.: Nonlinear Functional Analysis. Springer, Berlin (1985)
21. Dirmeier, A., Plaue, M., Scherfner, M.: Growth conditions, Riemannian completeness and Lorentzian causality. J. Geom. Phys. **62**(3), 604–612 (2012). Erratum ibidem (2013)
22. Dumitrescu, S., Zeghib, A.: Géométries lorentziennes de dimension 3: classification et complétude. Geom. Dedicata **149**, 243–273 (2010)
23. Ebin, D.G.: Completeness of Hamiltonian vector fields. Proc. Am. Math. Soc. **26**, 632–634 (1970)

24. Ehlers, J., Kundt, K.: Exact solutions of the gravitational field equations. In: Witten, L. (ed.) Gravitation: An Introduction to Current Research. Wiley, New York (1962)
25. Ekeland, I.: The Hopf–Rinow theorem in infinite dimension. J. Differ. Geom. **13**, 287–30 (1978)
26. Flores, J.L., Sánchez, M.: Causality and conjugate points in general plane waves. Class. Quantum Gravity **20**(11), 2275–2291 (2003)
27. Flores, J.L., Sánchez, M.: In: Jörg, F., Domenico, G., Perlick, J.W., Volker (Eds.) Analytical and Numerical Approaches to Mathematical Relativity. Springer, Berliin (2006) [ISBN 978-3-540-33484-2]
28. Flores, J.L., Herrera, J., Sánchez M.: Gromov, Cauchy and causal boundaries for Riemannian, Finslerian and Lorentzian manifolds. Memoirs Am. Math. Soc. **226**(1064), 76 or, more precisely: vi+76 (2013)
29. Forstneric, F.: Actions of $(\mathbb{R}, +)$ and $(\mathbb{C}, +)$ on complex manifolds. Math. Zeitschrift **223**, 123–153 (1996)
30. Galloway, G.J., Senovilla J.M.M.: Singularity theorems based on trapped submanifolds of arbitrary co-dimension. Class. Quantum Gravity **27**(15), 152002, 10 pp. (2010)
31. Gannon, D.: Singularities in nonsimply connected space-times. J. Math. Phys. **16**(12), 2364–2367 (1975)
32. Geroch, R.P.: What is a singularity in general relativity. Ann. Phys. (NY) **48**, 526–540 (1970)
33. Gordon, W.B.: On the completeness of Hamiltonian vector fields. Proc. Am. Math. Soc. **26**, 329–331 (1970)
34. Hawking, S.W.: The occurrence of singularities in cosmology. III. Causality and singularities. Proc. R. Soc. Lond. A **300**, 187–201 (1967)
35. Hawking, S.W., Penrose, R.: The singularities of gravitational collapse and cosmology. Proc. R. Soc. Lond. A **314**, 529–548 (1970)
36. Javaloyes, M.A., Sánchez, M.: An Introduction to Lorentzian Geometry and its Applications. Sao Carlos, Rima (2010). ISBN: 978-85-7656-180-4
37. Javaloyes, M.A., Sánchez, M.: On the definition and examples of Finsler metrics. Ann. Sc. Norm. Sup. Pisa, Cl. Sci. **XIII**(5), 813–858 (2014). doi:10.2422/2036-2145.201203_002 (arxiv: 1111.5066)
38. Kamishima, Y.: Completeness of Lorentz manifolds of constant curvature admitting Killing vector fields. J. Differ. Geom. **37**(3), 569–601 (1993)
39. Kundt, W.: Note on the completeness of spacetimes. Z. Physik **172**, 488–489 (1963)
40. Klingenberg, W.: Riemannian Geometry. de Gruyter Studies in Mathematics, 1. Walter de Gruyter & Co., Berlin (1982)
41. Klingler, B.: Complétude des variétés lorentziennes à courbure constante. Math. Ann. **306**, 353–370 (1996)
42. Kriegl, A., Michor, P.W.: The Convenient Setting of Global Analysis. Mathematical Surveys and Monographs, vol. 53. American Mathematical Society, Providence (1997)
43. Lafuente López, J.: A geodesic completeness theorem for locally symmetric Lorentz manifolds. Rev. Mat. Univ. Complut. Madrid **1**, 101–110 (1988)
44. Lang, S.: Differential and Riemannian Manifolds. Graduate Texts in Mathematics, vol. 160, 3rd edn. Springer, New York (1995)
45. Leistner, L., Schliebner, D.: Completeness of compact Lorentzian manifolds with special holonomy. Preprint (arxiv in 2013)
46. Margalef Roig, J., Outerelo Domínguez, E.: Una variedad diferenciable de dimension infinita, separada y no regular. Rev. Matem. Hispanoamericana **42**, 51–55 (1982)
47. Marsden, J.E.: On completeness of homogeneous pseudo-Riemannian manifolds. Indiana Univ. J. **22**, 1065–1066 (1972/73)
48. Morales Alvarez, P., Sánchez, M.: Myers and Hawking theorems: Geometry for the limits of the Universe, preprint U. Granada (2015)
49. Moore, J.D.: Introduction to Global Analysis. University of California Santa Barbara (2010). Available at www.math.ucsb.edu/~moore/globalanalysisshort.pdf

50. O'Neill, B.: Semi-Riemannian Geometry with Applications to Relativity. Pure and Applied Mathematics, vol. 103. Academic, New York (1983)
51. Palais, R.S.: Morse theory on Hilbert manifolds. Topology **2**, 299–340 (1963)
52. Palais, R.S.: Lusternik–Schnirelman theory on Banach manifolds. Topology **5**, 115–132 (1966)
53. Palais, R.S.: Critical point theory and the minimax principle. In: Global Analysis (Proc. Sympos. Pure Math., vol. XV, Berkeley, 1968), pp. 185–212. American Mathematical Society, Providence (1970)
54. Palais, R.S.: When proper maps are closed. Proc. Am. Math. Soc. **24**, 835–836 (1970)
55. Penrose, R.: Gravitational collapse and space-time singularities. Phys. Rev. Lett. **14**, 57–59 (1965)
56. Raychaudhuri, A.K.: Relativistic cosmology I. Phys. Rev. **98**, 1123–1126 (1955)
57. Romero, A., Sánchez, M.: On completeness of certain families of semi-Riemannian manifolds. Geom. Dedicata **53**(1), 103–117 (1994)
58. Romero, A., Sánchez, M.: Completeness of compact Lorentz manifolds admitting a timelike conformal Killing vector field. Proc. Am. Math. Soc. **123**(9), 2831–2833 (1995)
59. Sánchez, M.: Structure of Lorentzian tori with a Killing vector field. Trans. Am. Math. Soc. **349**(3), 1063–1080 (1997)
60. Sánchez, M.: On the geometry of generalized Robertson–Walker spacetimes: geodesics. Gen. Relativ. Gravitation **30**(6), 915–932 (1998)
61. Sánchez, M.: Cauchy hypersurfaces and global Lorentzian geometry. Publ. RSME **8**, 143–163 (2006)
62. Sasaki, S.: On the differential geometry of tangent bundles of Riemannian manifolds. T*ô*hoku Math. J. **10**, 338–354 (1958)
63. Senovilla, J.M.M.: Singularity theorems and their consequences. Gen. Relativ. Gravitation **29**(5), 701–848 (1997)
64. Senovilla, J.M.M.: Second-order symmetric Lorentzian manifolds. I. Characterization and general results. Class. Quantum Gravity **25**(24), 245011, 25 pp. (2008)
65. Shen, Z.: Lectures on Finsler Geometry. World Scientific Publishing, Singapore (2001)
66. Teschl, G.: Ordinary Differential Equations and Dynamical Systems. Graduate Studies in Mathematics, vol. 140. American Mathematical Society, Providence (2012)
67. Warner, F.W.: The conjugate locus of a Riemannian manifold. Am. J. Math. **87**(3), 575–604 (1965)
68. Weinstein, A., Marsden, J.E.: A comparison theorem for Hamiltonian vector fields. Proc. Am. Math. Soc. **26**, 629–631 (1970)

Diffeomorphic Image Matching with Left-Invariant Metrics

Tanya Schmah*, Laurent Risser, and François-Xavier Vialard*

Abstract The geometric approach to diffeomorphic image registration known as *large deformation by diffeomorphic metric mapping* (LDDMM) is based on a left action of diffeomorphisms on images, and a right-invariant metric on a diffeomorphism group, usually defined using a reproducing kernel. We explore the use of left-invariant metrics on diffeomorphism groups, based on reproducing kernels defined in the body coordinates of a source image. This perspective, which we call Left-LDM, allows us to consider non-isotropic spatially-varying kernels, which can be interpreted as describing variable deformability of the source image. We also show a simple relationship between LDDMM and the new approach, implying that spatially-varying kernels are interpretable in the same way in LDDMM. We conclude with a discussion of a class of kernels that enforce a soft mirror-symmetry constraint, which we validate in numerical experiments on a model of a lesioned brain.

*All authors contributed equally to this work.

T. Schmah (✉)
Rotman Research Institute, Baycrest, 3560 Bathurst Street, Toronto, ON, Canada M6A 2E1

Department of Computer Science, University of Toronto, Sandford Fleming Building, 10 King's College Road, Room 3302, Toronto, ON, Canada M5S 3G4
e-mail: tschmah@research.baycrest.org; schmah@cs.toronto.edu

L. Risser
CNRS - Institut de Mathématiques de Toulouse, Université Paul Sabatier, 118 route de Narbonne, 31062 Toulouse Cedex 9, France
e-mail: lrisser@math.univ-toulouse.fr

F.-X. Vialard
Department of Applied Mathematics, Université Paris-Dauphine, CEREMADE UMR CNRS 7534, Place du Maréchal de Lattre de Tassigny, 75775 Paris Cedex 16, France
e-mail: vialard@ceremade.dauphine.fr

D.E. Chang et al. (eds.), *Geometry, Mechanics, and Dynamics*, Fields Institute Communications 73, DOI 10.1007/978-1-4939-2441-7_16

1 Introduction

The geometric point of view on diffeomorphic image matching was pioneered by [10, 31], and has been developed significantly in the last ten years [4, 5, 8, 16, 19, 20, 32]. In its many practical applications to medical imaging, including computational anatomy [23], the approach is known as the Large Deformation Diffeomorphic Metric Mapping framework (LDDMM). A good geometric overview may be found in [5]. Two key elements of this framework are: a right-invariant Riemannian metric on a group of diffeomorphisms; and the left action of this group on images $I : \Omega \to \mathbb{R}^d$ defined by $\phi \cdot I := I \circ \phi^{-1}$. Combining these two elements gives an induced Riemannian metric on the group orbit of a given image I.

In image registration in general, the *inexact matching problem* is, given two images I and J, to find a transformation ϕ that minimises the sum of some measure of the size of ϕ and some measure of image dissimilarity (or error) $E(\phi \cdot I, J)$, such as $\|\phi \cdot I - J\|^2_{L^2}$. In LDDMM, we seek a path of diffeomorphisms $\phi(t)$ starting at Id, with the size of the final diffeomorphism $\phi(1)$ given by the length of the path ϕ defined by the right-invariant Riemannian metric associated with some norm $\|.\|_V$ on a Hilbert space V of smooth vector fields. Thus the fundamental optimisation problem in LDDMM is to minimise

$$\mathscr{J}(\phi) = \frac{1}{2}\int_0^1 \|v(t)\|_V^2 \, \mathrm{d}t + E(\phi(1) \cdot I, J), \tag{1}$$

for a path ϕ with $\phi(0) = Id$, under the constraint

$$\partial_t \phi(t) = v(t) \circ \phi(t), \tag{2}$$

which defines $v(t)$ as the *spatial (Eulerian) velocity* of $\phi(t)$. Note that all minimisers of this functional are geodesics, since they must minimise the first term of (1) for a given $\phi(1)$.

The minimisation problem (1) is well-posed provided that the norm on V is sufficiently strong in terms of smoothness (see [36], Theorem 11.2). The Hilbert space V is usually defined via its reproducing kernel:

$$\|v\|_K^2 = \langle p, K \star p \rangle_{L^2}, \text{ where } v = K \star p\,. \tag{3}$$

A Gaussian kernel is often chosen for computational convenience, or a mixture of Gaussian kernels as in [25, 26].

We note that LDDMM is not the only diffeomorphism-based approach to image matching. There is another family of successful methods, based on exponentiating stationary vector fields [2, 3, 33]. However, unlike these methods, LDDMM is able to draw on concepts in geometry and mechanics such as geodesic distance and momentum, which have been central both to theoretical developments and to recent efficient numerical algorithms [7, 34].

Though not required by the theory, in practice the kernel used in diffeomorphic methods (LDDMM and the other methods cited above) has always been chosen to be translationally-invariant and isotropic. In LDDMM, spatially-varying or non-isotropic ("direction-dependent") kernels have no obvious interpretation, because the norm is defined in Eulerian coordinates, so that as t varies during the deformation, a fixed point in the source image moves through space, and conversely, a fixed point in space will correspond to different points on the source image. Similarly, the directions in a direction-dependent kernel are defined with respect to Eulerian coordinates, not the coordinates of the moving source image. Nonetheless, spatially-varying kernels are potentially of great interest in medical applications, if they can be made to represent spatially-variable (or non-isotropic) deformability of tissue. This is indeed already done in [27] to model sliding conditions between the lungs and the ribs. In general it is well-known that a good choice of kernel (the "regulariser") is essential for optimising registration performance, so that taking into account any spatial variability of the tissue deformability in the kernel will improve the registration.

With this motivation, we propose a new registration framework, which will support natural interpretations of spatially-varying metrics. Left-Invariant LDDMM ("Left-LDM") is analogous to LDDMM but based on a *left*-invariant metric, i.e. based on a norm in the body (Lagrangian) coordinates of the source image. This means that instead of the norm in (1) being applied to the spatial (Eulerian) velocity defined by (2), it is applied to the *convective velocity* defined by

$$\partial_t \phi(t) = d\phi(t) \cdot v(t)\,, \tag{4}$$

where $d\phi(t)$ is the spatial derivative of $\phi(t)$. To emphasize the relationship between the two frameworks, we will refer to LDDMM from now on as "Right-LDM", consistent with the use of the shortened acronym LDM in [16]. The matching problem in Left-LDM is to minimize the same functional as in Right-LDM (1) but under the "new" constraint (4). Note that the convective velocity of a given $\phi(t)$ is the pull-back of the spatial velocity by ϕ_t, i.e. it is just the spatial velocity expressed in body (Lagrangian) coordinates.

Subject to some analytical subtleties explored in Section 2, the solutions $\phi(t)$ are left-geodesics in a diffeomorphism group. The description of left-geodesic flow in terms of the convective velocity is an example of a convective representation of a continuum theory. Convective representations were introduced in [18] for ideal fluid flow, and [29] for elasticity, and the subject has been further developed in [15]. The relationship between left- and right- geodesic flows on a diffeomorphism group was explored earlier in [14].

In the Left-LDM framework, a spatially-varying or non-isotropic kernel makes sense, because it is defined in Lagrangian coordinates, so it can model variable deformability of different parts of the source image. (The norm is carried along by push-forwards with the moving source image.) This opens up possibilities for application-specific regularisation, either hand-tuned or learnt from data.

2 Analytical Setting

We consider the convective velocity constraint, formula (4), and the conditions on $v(t)$ such that it can be integrated to produce the diffeomorphism $\phi(t)$. Such an evolution equation is a partial differential equation that belongs to the class of linear symmetric hyperbolic systems [12]. The usual method for solving such equations consists in using the method of characteristics, which amounts to solve an equation of the type (2) on the inverse of the flow. The equation of characteristics, being equivalent to formula (2), is an ordinary differential equation and can be integrated provided sufficient smoothness assumptions on the *spatial velocity*. For the spatial velocity constraint, a satisfactory answer has been given in [36, Theorems 8.7 and 8.14]: The flow of a time dependent vector field in $L^2([0,1],V)$ is well-defined if there exists a constant $C > 0$ such that for every $v \in V$

$$\|v\|_{1,\infty} \leq C\,\|v\|_V\,, \tag{5}$$

where $\|v\|_{1,\infty}$ is the Banach norm in $W^{1,\infty}(\Omega,\mathbb{R}^d)$. Under this hypothesis, the variational problem (1) is well-posed and the set G_R, defined by[1]

$$G_R := \left\{\phi(1)\,\middle|\,\partial_t\phi(t) = v(t)\circ\phi(t) \text{ and } v \in L^2([0,1],V)\,,\phi(0) = Id\right\}\,, \tag{6}$$

is a group. A similar approach in [11] proves that the flow of $v \in C([0,1],H^s)$ defines an H^s diffeomorphisms for $s > d/2 + 2$. From a variational point of view the former approach is better suited for solving Problem (1). In particular, working with the space $L^2([0,1],V)$ is crucial for proving the existence of a minimizer and therefore we cannot reduce our work to a smooth setting. This is our main motivation for developing the following analytical study. Let us then define the following set,

$$G_L := \left\{\phi(1)\,\middle|\,\partial_t\phi(t) = d\phi(t)\cdot v(t) \text{ and } v \in L^2([0,1],V)\,,\phi(0) = Id\right\}\,. \tag{7}$$

Integrating equation (4) is straightforward in a smooth setting. Indeed, this equation is equivalent to

$$\partial_t\phi^{-1}(t) = -v(t)\circ\phi^{-1}(t)\,. \tag{8}$$

Unfortunately, working with $L^2([0,1],V)$ vector fields, Equation (8) has to be proven true in that context. An example of this issue is the following: with a fixed regularity, for instance the group $Diff^s$ of H^s diffeomorphisms, the inversion map is

[1] In the corresponding definition in [36], v need only be absolutely integrable in time.

only continuous and not differentiable. This comes from the fact that the inversion map $Inv : Diff^s \to Diff^s$ presents a loss of regularity when being differentiated:

$$D\ Inv(\phi)(v) = -d\phi^{-1}(v \circ \phi^{-1})\,. \tag{9}$$

The rest of the section will be devoted to show that equation (4) can be solved via the method of characteristics. Our strategy consists in proving that Equation (8) holds under very weak conditions so that integration of the *convective velocity* equation (4) reduces to the integration of Equation (8).

In what follows, we consider Ω a closed, bounded domain and V a Hilbert space of vector fields u such that both u and du vanish on its boundary, and we suppose that V is embedded in $C^1(\Omega, \mathbb{R}^d)$, i.e. there exists a constant $C > 0$ such that (5) applies for all u. Let us begin with the following lemma:

Lemma 1. *Let $B := C^0([0,1], C^1_\infty(\Omega, \mathbb{R}^d)) \cap H^1([0,1], L^2(\Omega, \mathbb{R}^d))$. Let $\phi \in B$, and denote by ϕ^{-1} the map $t \mapsto \phi_t^{-1}$. If ϕ_t is a diffeomorphism onto Ω for all $t \in [0,1]$, then ϕ^{-1} lies in B.*

Remark 1. The subscript ∞ denotes the use of the sup norm.

Proof. The standard Inverse Function Theorem implies that ϕ_t^{-1} is C^1 for all $t \in [0,1]$. The continuity of ϕ implies the continuity of the map $(t,x) \mapsto \phi_t(x)$, which by a lesser-known version of the Implicit Function Theorem (see [22]) implies the continuity of $t \mapsto \phi_t^{-1}(x)$ for every x. Therefore, by compactness of Ω we have $\phi^{-1} \in C^0([0,1], C^1_\infty(\Omega, \mathbb{R}^d)$.

Let us first suppose that $\phi \in C := C^0([0,1], C^1_\infty(\Omega, \mathbb{R}^d) \cap C^1([0,1], C^0(\Omega, \mathbb{R}^d))$, and that (as before) ϕ_t is a diffeomorphism onto Ω for all $t \in [0,1]$. Then for all $x \in \Omega$ one has by simple differentiation

$$\partial_t \phi_t^{-1}(x) = -[d\phi_t]_{\phi_t^{-1}(x)}(\partial_t \phi_t(\phi_t^{-1}(x)))\,. \tag{10}$$

We aim at proving that $\partial_t \phi_t^{-1}$ belongs to $L^2([0,1], L^2(\Omega, \mathbb{R}^d))$: The first term $[d\phi_t]_{\phi_t^{-1}(x)}$ is continuous (on Ω) and its sup norm is uniformly bounded for $t \in [0,1]$ since $C^0_\infty([0,1], C^1_\infty(\Omega, \mathbb{R}^d))$. By assumption, $\partial_t \phi_t \in L^2(\Omega, \mathbb{R}^d)$ and the right composition with a C^1 diffeomorphism is a bounded linear operator on $L^2(\Omega, \mathbb{R}^d)$ (by a standard change of variable). It follows easily that $\partial_t \phi_t^{-1} \in L^2([0,1], L^2(\Omega, \mathbb{R}^d))$ and $\phi^{-1} \in C$.

We will prove a similar result for any $\phi \in B$: By density of C in B, we consider a sequence $\phi_n \in C$ converging to $\phi \in B$. In particular, we have

$$\phi_{n,T}^{-1}(x) = \int_0^T -[d\phi_{n,t}]_{\phi_{n,t}^{-1}(x)}(\partial_t \phi_{n,t}(\phi_{n,t}^{-1}(x)))\,\mathrm{d}t\,. \tag{11}$$

First, the left-hand side strongly converges in $C^1_\infty(\Omega, \mathbb{R}^d)$ (by the inverse function theorem) and thus in $L^2(\Omega, \mathbb{R}^d)$ to ϕ_T^{-1}.

Second, the right-hand side weakly converges in $L^2(\Omega, \mathbb{R}^d)$ to

$$\int_0^T -[d\phi_t]_{\phi_t^{-1}(x)}(\partial_t \phi_t(\phi_t^{-1}(x)))\,\mathrm{d}t\,.$$

Indeed, let us consider $f \in C^\infty(\Omega, \mathbb{R}^d)$ and calculate the L^2 scalar product

$$\begin{aligned}\langle f, \int_0^T -[d\phi_{n,t}]_{\phi_{n,t}^{-1}(\cdot)}(\partial_t \phi_{n,t}(\phi_{n,t}^{-1}(\cdot)))\,\mathrm{d}t\rangle &= \int_0^T -\langle [d\phi_{n,t}]^*_{\phi_{n,t}^{-1}(\cdot)}(f), \partial_t \phi_{n,t}(\phi_{n,t}^{-1}(\cdot))\rangle\,\mathrm{d}t \\ &= \int_0^T -\langle [d\phi_{n,t}]^{-1*}(f \circ \phi_{n,t}), \partial_t \phi_{n,t}(\cdot)\mathrm{Jac}(\phi_{n,t})\rangle\,\mathrm{d}t\,. \end{aligned} \tag{12}$$

Since f is smooth and Ω compact, f is uniformly Lipschitz and thus $[d\phi_{n,t}]^{-1*}(f \circ \phi_{n,t})$ converges for the sup norm to $[d\phi_t]^{-1*}(f \circ \phi_t)$. The same convergence holds for $\mathrm{Jac}(\phi_{n,t})$ by assumption. This proves the weak convergence on smooth functions, which implies the weak convergence in L^2 (see [35]). Strong and weak limits are equal so that $[d\phi_t]_{\phi_t^{-1}(\cdot)}(\partial_t \phi_t(\phi_t^{-1}(\cdot))) \in L^2([0,1], L^2(\Omega, \mathbb{R}^d))$ is the (time) derivative of ϕ_t^{-1} and the conclusion ensues.

Remark 2. In fact, we could have proven the following stronger result: the inversion map is continuous on an affine subspace $\tilde{B}$ of B defined by $\tilde{B} = \{\phi \in B \mid \phi_t \in Diff\}$ endowed with the Banach norm $\sup(\|\phi\|_{H^1}, \|\phi\|_\infty, \|\phi^{-1}\|_\infty)$. However, the proof would be a little more involved and the result is not needed in what follows.

Proposition 1. *Solutions in B of (4) exist, are unique and are characterized by being solutions of*

$$\partial_t \phi^{-1}(t) = -v(t) \circ \phi^{-1}(t)\,. \tag{13}$$

Proof. The initial condition is $\phi_0 = Id$ together with the assumption $\phi \in B$ imply the existence of a positive real number $T > 0$ such that ϕ_t is a diffeomorphism for $t \in [0, T]$. On this interval, the previous lemma gives that $\phi^{-1} \in B$ and $\partial_t \phi_t = -[d\phi_t]_{\phi_t^{-1}(\cdot)}(\partial_t \phi_t(\phi_t^{-1}(\cdot)))$. Since $\partial_t \phi_t = d\phi(t) \cdot v(t)$, we obtain $\partial_t \phi_t^{-1} = -v(t) \circ \phi^{-1}(t)$. Using the result [36, Theorem 8.7] on flow integration, we obtain the existence and uniqueness of $\phi^{-1} \in B$ satisfying (13). This implies also existence and uniqueness of solutions in B of (4) on $[0, T]$. The extension for all time $t \in [0, 1]$ is straightforward by considering $I = \sup\{T > 0 \mid \forall t < T\,, \phi_t \in Diff\}$. By construction, I is open and the argument above shows that I is non-empty. Last, I is closed since the flow of $-v(t)$ is a diffeomorphism for all time $t \in [0, 1]$ and therefore $I = [0, 1]$.

Remark 3. The definition of the space B could have been a little more general using $W^{1,1}(\Omega, \mathbb{R}^d)$ instead of $H^1(\Omega, \mathbb{R}^d)$. However, it was not necessary regarding the existence of minimizers of functional (1) under *convective velocity* constraint.

In light of this result, we modify the definitions of G_L and G_R to require that $\phi \in B$:

$$G_L := \left\{\phi(1) \in B \,\middle|\, \partial_t \phi(t) = d\phi(t) \cdot v(t) \text{ and } v \in L^2([0,1], V)\right\},$$
$$G_R = \left\{\phi(1) \in B \,\middle|\, \partial_t \phi(t) = u(t) \circ \phi^{-1}(t) \text{ and } u \in L^2([0,1], V)\right\}.$$

Since G_R is closed under inversion, Proposition 1 implies $G_L = G_R$. Note that the sets of paths $\phi(t)$ in the definitions of G_L and G_R do not coincide in general. Indeed, these sets of paths correspond to each other by the inverse map, and this inversion shows a loss of regularity for instance on $Diff^s$. In the rest of the paper, we will use the notation G_V to denote the group $G_L = G_R$, and by abuse of notation, G_L and G_R will denote the set of paths generated under the constraint (4) (and respectively (2)) by elements of $L^2([0,1], V)$.

The structure of G_V is not well-known. In the case of Gaussian kernels, G_V is probably included in an ILH-Lie group in the sense of Omori [24]. In general, it is not known whether G_V admits a differentiable structure. Nonetheless, the group carries natural left- and right- invariant metrics, as defined in the next section, and isometries should be understood as being between metric spaces. In the case of Sobolev spaces, the right-invariant metric is a smooth Riemannian metric, whereas the left-invariant metric is probably not.

Finally, we can now benefit from the existence of minimizers for the functional (1) in the LDDMM framework:

Theorem 1. *If V satisfies assumption (5) and E is continuous w.r.t. uniform convergence of ϕ on every compact set in Ω, then there exists a minimizer in G_V of the functional (1) under the convective velocity constraint (4).*

Proof. This follows from [36, Theorem 11.2].

Note that the theorem applies for the usual sum of squared differences similarity measure:

$$E(\phi) = \|I \circ \phi(1)^{-1} - J\|_{L^2}^2 .$$

3 Left- and Right-Invariant Metrics on Diffeomorphism Groups

Proposition (1) proved that the convective velocity constraint (4) is equivalent to

$$\partial_t \phi^{-1}(t) = -v(t) \circ \phi^{-1}(t) , \tag{14}$$

in a general setting.This equation is simply the spatial velocity constraint (2) for ϕ^{-1}, except with a minus sign. In other words, if the spatial and convective velocities of any path $\phi(t)$ are denoted by v_R^ϕ and v_L^ϕ, respectively, then

$$v_R^{\phi^{-1}} = -v_L^\phi. \tag{15}$$

As a consequence of this simple fact (well-known in a smooth setting), there are close relationships between Left-LDM and Right-LDM.

On G_V a left-invariant metric d_L can be defined by

$$d_L(\phi, Id) = \inf\{\sqrt{\int_0^1 \|v_L^\phi(t)\|_V^2 \, dt} \, : \, \phi(0) = Id \text{ and } \phi(1) = \phi\}. \tag{16}$$

A right-invariant metric d_R can be defined in the same way but using the spatial velocity v_R^ϕ instead of the convective velocity v_L^ϕ. It follows from (15) that

$$d_L(\phi, Id) = d_R(\phi^{-1}, Id). \tag{17}$$

As shown in [31], the distance d_R is well-defined and makes G_V a complete metric space. From (17), it follows that the same is true of d_L. Between any two diffeomorphisms in G_V, there exists a path minimising the distance d_L (*resp.* d_R), and such minimising paths will be called left- (*resp.* right-) geodesics. Note that we have defined geodesics without reference to a Riemannian metric, since we do not know whether G_V even has a smooth structure, as discussed earlier.

The following proposition summarises some elementary properties of these distance metrics, all straightforward consequences of (15) and the definitions.

Proposition 2.

1. *The inverse mapping is an isometry:*

$$(G_V, d_L) \to (G_V, d_R)$$
$$\phi \to \phi^{-1}$$

2. *ϕ is a left-geodesic if and only if ϕ^{-1} is a right-geodesic.*
3. *Left translation is an isometry of (G_V, d_L), and right translation is an isometry of (G_V, d_L).*
4. *The left translation of a left-geodesic is a left-geodesic (and similarly for right-geodesics).*

Remark 4. In the context of fluid dynamics, ϕ is the usual Lagrangian map, and ϕ^{-1} is the "back-to-labels" map. Observation (2) in the above proposition has been exploited before in this context [14].

We now show two correspondences between Left- and Right- LDM.

Lemma 2. *Let $\phi(t)$ be a path of diffeomorphisms with spatial velocity $v_R^\phi(t)$, defined by (2). Define $\psi : t \to \phi(1)\phi^{-1}(1-t)$, and let $v_L^\psi(t)$ be its convective velocity, defined by (4). Then $v_L^\psi(t) = v_R^\phi(1-t)$.*

Proof. From (2) we have, by direct calculation:

$$\partial_t \phi^{-1}(t) = -d\phi^{-1}(t) \cdot v_R^\phi(t)\,,$$

so that

$$\partial_t \phi^{-1}(1-t) = d\phi^{-1}(1-t) \cdot v_R^\phi(1-t)\,,$$

and therefore,

$$\partial_t \psi(t) = d\psi(t) \cdot v_R^\phi(1-t)\,.$$

Thus $v_R^\phi(1-t)$ satisfies the relation (4) that defines $v_L^\psi(t)$.

The following proposition is a direct consequence of the previous lemma. It concerns a generalisation of the matching functional (1), in which the squared path length in the first term is replaced by the integral of a general Lagrangian $l(v(t))$, and the image dissimilarity term $E(\phi(1)\cdot I, J)$ is replaced by a general real-valued function $H(\phi(1))$.

Proposition 3. *Let V and $G = G_L = G_R$ be as defined above. Let $H : G \mapsto \mathbb{R}$ and $l : V \mapsto \mathbb{R}$ be smooth maps. Let v_R^ϕ and v_L^ϕ be the spatial and convective velocities defined by (2) and (4), respectively. We define $\mathscr{F}_R$ on the set of paths in G_R such that $\phi(0) = Id_\Omega$ by*

$$\mathscr{F}_R(\phi(t)) = \int_0^1 \ell(v_R^\phi(t))\,\mathrm{d}t + H(\phi(1))\,. \tag{18}$$

Respectively, $\mathscr{F}_L(\phi)$ is defined on the set of paths in G_L by

$$\mathscr{F}_L(\phi(t)) = \int_0^1 \ell(v_L^\phi(t))\,\mathrm{d}t + H(\phi(1))\,. \tag{19}$$

Then,

$$\mathscr{F}_R(\phi(t)) = \mathscr{F}_L(\phi(1)\phi^{-1}(1-t))\,, \tag{20}$$

and as a consequence, the minimizers of $\mathscr{F}_R$ and $\mathscr{F}_L$ are in one to one bijection by the map $\phi(t) \mapsto \phi(1)\phi^{-1}(1-t)$.

Proof. Let $\psi : t \to \phi(1)\phi^{-1}(1-t)$. Changing the variable $t \mapsto 1-t$, and then applying the Lemma, we have

$$\int_0^1 \ell(v_R^\phi(t))\,\mathrm{d}t = \int_0^1 \ell(v_R^\phi(1-t))\,\mathrm{d}t = \int_0^1 \ell(v_L^\psi(t))\,\mathrm{d}t.$$

Since $\psi(0) = \phi(0) = Id_\Omega$ and $\psi(1) = \phi(1)$, the result follows.

Remark 5.

1. Generically, changing from right- to left- invariant Lagrangian does not change the endpoint of the optimal path.
2. The correspondence also holds for the boundary value problem, *i.e.* when $\phi(1)$ is fixed.
3. One can use a time-dependent Lagrangian $\ell(v,t)$ if $\ell(v,1-t) = \ell(v,t)$ for all $t \in [0,1]$.
4. If the term H is replaced by a path-dependent term, then the result does not hold any more.

A direct application of the previous proposition to the case of the kinetic energy defined by $\ell(v) := \frac{1}{2}\|v\|_V^2$ and $H(\phi) = E(\phi_1 \cdot I, J)$ gives the following corollary. The existence of minimizers for these functionals is guaranteed by [36].

Corollary 1 (Equivalence of Optimal Matches in Left- and Right- LDM). *Consider the problem of minimising*

$$\mathscr{J}(\phi) = \frac{1}{2}\int_0^1 \|v(t)\|_V^2\,\mathrm{d}t + E(\phi_1 \cdot I, J)\,, \tag{21}$$

for $\phi_0 = Id_\Omega$, and with either constraint

$$\partial_t \phi_t = d\phi_t \cdot v_t \qquad \textit{(Left-LDM constraint)} \tag{22}$$

or

$$\partial_t \phi_t = v_t \circ \phi_t \qquad \textit{(Right-LDM constraint).} \tag{23}$$

Then

1. *The optimal endpoint ϕ_1 is the same with either constraint.*
2. *If ϕ_t minimises $\mathscr{J}$ in Left-LDM, then $\psi_t := \phi_{1-t}^{-1} \circ \phi_1$ minimises $\mathscr{J}$ in Right-LDM.*
3. *If ψ_t minimises $\mathscr{J}$ in Right-LDM, then $\phi_t := \psi_1 \circ \psi_{1-t}^{-1}$ minimises $\mathscr{J}$ in Left-LDM.*

Optimal paths in Left-LDM are left-geodesics, while optimal paths in Right-LDM are right-geodesics.

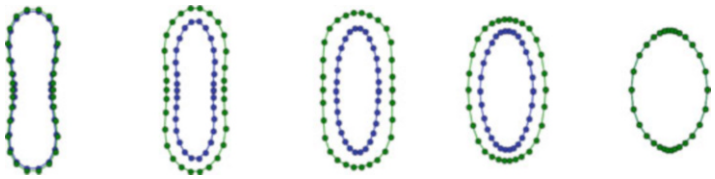

Fig. 1 This figure shows snapshots of two deformations from the left-most source image to the right-most target image. The green curves show the optimal Right-LDM path (a right-geodesic), while blue curves show the optimal Left-LDM path (a left-geodesic). Note that the paths are different, though both arrive at an exact match. The right-metric length of the green geodesic equals the left-metric length of the blue geodesic

In summary, the optimal diffeomorphism ϕ_1 is the same in both approaches, but there are two optimal paths from Id to ϕ_1: one left- and one right- geodesic. These two paths are illustrated in the following diagram.

$$\begin{array}{ccccc} & & \phi_{t_1} & \rightarrow & \phi_{t_2} & & \\ \nearrow & & & & & \searrow & \\ Id & & & & & & \phi_1 \\ \searrow & & & & & \nearrow & \\ & & \phi_{1-t_1}^{-1} \circ \phi_1 & \rightarrow & \phi_{1-t_2}^{-1} \circ \phi_1 & & \end{array}$$

When left- (resp. right-) geodesics act on a image, the resulting paths in shape space are left- (resp. right-) geodesics. An example is given in Figure 1.

4 Geodesic Flow of Left-Invariant Metrics

We have considered minimisers of (1), which are geodesics. We now consider the corresponding initial value problem in which only $\phi(0) = Id$ is fixed. The minimisers $\phi(t)$ evolve according to Euler-Lagrange equations which are equivalent, in the Right-LDM case, to the EPDiff equation [21],

$$\frac{d}{dt}\frac{\partial l}{\partial v} = -\operatorname{ad}_v^* \frac{\partial l}{\partial v}, \tag{24}$$

together with the spatial velocity constraint. This formulation leads to the *momentum representation* of diffeomorphisms, and further to the special *pulson* solutions, which correspond to image landmarks and have applications to optimization schemes [7, 34] and to the statistical description of images [23]. We now discuss the corresponding concepts in Left-LDM.

The first term of (1) with fixed endpoints may be expressed as $\int_0^1 l(v(t))dt$ where l is the *kinetic energy Lagrangian* defined by

$$l(v) := \frac{1}{2}\|v\|_V^2, \tag{25}$$

and $v(t)$ is the convective velocity of $\phi(t)$, defined in (4). The minima of this problem, with given endpoints $\phi(0)$ and $\phi(1)$, are left-geodesics, as defined in the previous section. There is a question of the well-posedness of the boundary value problem that defines these "left-geodesics". However, from the equivalence with Right-LDM shown in Section 3, it follows that the problem *is* well-posed for the same norms for which the corresponding problem in Left-LDM is well-posed. In addition, the Euler-Poincaré equation is available via this equivalence and let us point out that left-reduction is not needed here.

4.1 Euler-Poincaré Equation

Using the equivalence with Right-LDM, under mild conditions on H in (21), left-geodesics minimising (21) satisfy the *left* Euler-Poincaré equation [21],

$$\frac{d}{dt}\frac{\partial l}{\partial v} = \mathrm{ad}_v^* \frac{\partial l}{\partial v}\,. \tag{26}$$

This equation can be expressed in terms of the *convective momentum*,

$$p(t) := \frac{\partial l}{\partial v}\,,$$

as $\frac{d}{dt}p = \mathrm{ad}_v^* p$. In Euclidean coordinates, the Euler-Poincaré equation takes the following form, called *EPDiff-left*,

$$\frac{\partial \mathbf{p}}{\partial t} = \mathrm{ad}_{\mathbf{v}}^* \mathbf{p} := \mathbf{v}\cdot\nabla\mathbf{p} + (\nabla\mathbf{v})^T \cdot \mathbf{p} + \mathbf{p}\,(\mathrm{div}\,\mathbf{v})\,, \tag{27}$$

where $(\nabla\mathbf{v})^T \cdot \mathbf{p} := \sum_j p_j \nabla v^j$. If the norm is defined in terms of a kernel K_σ as in (3), then $v = K_\sigma \star p$ and

$$l = \frac{1}{2}\int_0^1 \langle p(t), K_\sigma \star p(t)\rangle_{L^2}\,\mathrm{d}t. \tag{28}$$

4.2 Conservation Law

Given the convective velocity constraint (4), the left-invariant Euler-Poincaré equation is equivalent to (see [21])

$$0 = \frac{d}{dt}\,\mathrm{Ad}^*_{\phi}\,\frac{\partial l}{\partial v} = \left(\phi^{-1}\right)^*\,p. \tag{29}$$

This is a conservation law, with the conserved quantity being *spatial momentum*,

$$m(t) := \left(\phi^{-1}\right)^*\,p(t) = \left(\phi^{-1}\right)^*\,\frac{\partial l}{\partial v}\,.$$

Note that this reverses the Right-LDM situation, where convective momentum is preserved and spatial momentum evolves according to EPDiff-right.

4.3 Pulsons

Singular "pulson" solutions may be found by making the following ansatz [13],

$$\mathbf{p}(t) = \sum_{a=1}^{N} \mathbf{P}_a(t)\delta\left(\mathbf{x} - \mathbf{Q}_a(t)\right). \tag{30}$$

It is known [17] that this momentum ansatz defines an equivariant momentum map

$$J_{Sing} : T^*Emb(S, R^n) \to \mathscr{X}(R^n)^* \tag{31}$$

called the *singular solution momentum map*, where here S is a finite set of N points indexed by a. It is the momentum map for the cotangent-lift of the left action of $Diff(R^n)$ on $Emb(S, R^n)$. It follows from general theory (see e.g. [21]) that J_{Sing} is a Poisson map with respect to the canonical symplectic form on $T^*Emb(S, R^n)$ and the right Lie-Poisson bracket on $\mathscr{X}(R^n)^*$. Thus the EPDiff-*right* equations pull back to canonical Hamiltonian equations in Q and P, with respect to Hamiltonian

$$H = \sum_{a,b=1}^{N} \left(\mathbf{P}^a(t)\cdot\mathbf{P}^b(t)\right) K\left(\mathbf{Q}^a(t), \mathbf{Q}^b(t)\right).$$

These are the singular pulson solutions discussed in [13] and elsewhere. It also follows, applying a time reversal, that the EPDiff-left equations (27) pull back to

time-reversed canonical Hamiltonian equations in Q and P, with respect to the same Hamiltonian:

$$\frac{\partial}{\partial t}\mathbf{Q}_a(t) = -\sum_{b=1}^{N} \mathbf{P}_b(t)\, K(\mathbf{Q}_a(t), \mathbf{Q}_b(t))$$

$$\frac{\partial}{\partial t}\mathbf{P}_a(t) = \sum_{b=1}^{N} \big(\mathbf{P}_a(t)\cdot \mathbf{P}_b(t)\big)\, \frac{\partial}{\partial \mathbf{Q}_a} K(\mathbf{Q}_a(t), \mathbf{Q}_b(t))\,.$$

These are the equations of the pulson solutions of EPDiff-*left*. Note that they are nearly the same equations as for the pulson solutions of EPDiff-*right*, with two important differences: (i) there is a time-reversal; and (ii) $Q_a(t)$ is *not* the spatial location of particle a at time t, but instead it is an "anti-particle's location" in *body coordinates*, i.e. the location in body coordinates corresponding to a fixed spatial location $Q_a(0)$. This follows from the conservation of spatial momentum. Similar observations apply to higher-dimensional singular solutions (filaments, sheets, etc.).

All of the results in this section can be either verified directly, making minor changes to the well-known proofs for right-geodesics (the flow of EPDiff-right), or deduced from the correspondence between left and right geodesics in Section 3.

5 Spatially Varying Metrics and Non-local Symmetries

Regarding applications, a crucial point consists in defining the metric which can be viewed as a parameter to be tuned accordingly with data. In the classical Right-LDM picture, due to translation and rotation symmetry, the class of metrics is rather small. In contrast, the Left-LDM model enables the use of many more types of kernels. In particular, kernels that incorporate non-local correlations. A striking example is the brain development where a symmetry at large scale between the left and the right parts of the brain can be exploited in order to improve the image matching quality. Of course, it is natural to ask for *soft* symmetry in practical applications rather than perfect symmetry. We give hereafter an explicit example of a kernel satisfying those requirements.

Let us first present the case of perfect symmetry: Let $\Pi : V \mapsto V$ be the symmetry of interest, which is a continuous linear operator on the space of vector fields V that satisfies $\Pi^2 = id$. For instance, in $\mathbb{R}^2$ if $v = (v_1, v_2)$, the example showed in the simulation is $\Pi((v_1, v_2))) = (u_1, u_2)$ where $u_1(x, y) = -v_1(-x, y)$ and $u_2(x, y) = v_2(-x, y)$. The set of vector fields v satisfying the symmetry condition $\Pi(v) = v$ is thus a closed linear subspace denoted by V_1, which may be endowed with the induced norm or alternatively with:

$$\|v_1\|^2_{V_1} = \min_{v\in V} \left\{ \|v\|^2_V \;\middle|\; \frac{1}{2}(v + \Pi(v)) = v_1 \right\}\,. \tag{32}$$

In general, those two norms do not coincide, unless Π is self-adjoint which is the case in our example. We prefer the metric (32) since the kernel associated with that metric is given by:

$$K_{V_1} = \frac{1}{4}(Id + \Pi) \circ K \circ (Id + \Pi^*) \,. \tag{33}$$

Since, in our example, Π is self-adjoint, we can simplify the expression of K_{V_1} to get

$$K_{V_1} = \frac{1}{2}(Id + \Pi) \circ K \,. \tag{34}$$

The above kernel K_{V_1} will produce perfect symmetry which is not desired as mentioned above. However, we can modify it to allow for a variable degree of symmetry. For example, consider the class of kernels

$$K = (Id + c\Pi) \circ K_\sigma \,, \tag{35}$$

where the strength of the symmetry ranges from none at $c = 0$ to perfect symmetry at $c = 1$. It is also natural to introduce a mixture of kernels with different length scales, to account for local discrepancies in the deformation field, *i.e.* which means using

$$K = (Id + c\Pi) \circ K_{\sigma_1} + K_{\sigma_2} \,, \tag{36}$$

where σ_1, σ_2 are the scale parameters of the kernels, for example the standard deviation of the Gaussian kernel. In particular, it is natural to use $\sigma_1 > \sigma_2$ to account for large scale symmetry. Looking at the form of the kernel (36), it is tempting to introduce a spatially varying coefficient that accounts for more or less symmetry or importance of a given kernel. Therefore, the final example of spatially-varying kernel is the following: Let K_i be n kernels and $\chi_i : \Omega \mapsto [0, 1]$ be n smooth functions such that $\sum_{i=1}^n \chi_i = 1$ then we consider

$$K = \sum_{i=1}^{n} \chi_i K_i \chi_i \,. \tag{37}$$

This kernel is associated to the following variational interpretation:

$$\|v\|^2 = \min_{(v_1,\ldots,v_n)\in V_1\times\ldots\times V_n} \left\{ \sum_{i=1}^{n} \|v_i\|_{V_i}^2 \;\middle|\; \sum_{i=1}^{n} \chi_i v_i = v \right\} \,. \tag{38}$$

We note that Formula (38) is a simple generalization of mixtures of kernels, which are explained in detail in [6].

6 Experiments

In the following experiments, we are interested in deformations generated by the Left-LDM model using spatially dependent kernels that incorporate the soft symmetry constraint proposed in Section 5. By the equivalence proven in Section 3, the final deformation is also given by the corresponding Right-LDM model, so all of the numerical results presented below have been computed using the standard gradient descent optimization method for the Right-LDM model detailed in [6].

We registered two images out of the LPBA40 dataset [28]. We considered Subjects 8 and 9 of the dataset. The images were resampled to a resolution of 1 mm and rigidly aligned. We then extracted corresponding 2D slices from the two aligned images. Finally, we simulated a large lesion in the slice from Subject 8. A mask was also constructed, by dilating the original lesion location mask 8 times, each time using a 3×3 structuring element. This mask was used to omit lesioned areas from calculation of the image dissimilarity term, and also to mask the updated momenta before smoothing. Registered images are shown in Fig. 2.

We registered the lesioned images with LDM as described above, using two kinds of kernel: a standard translationally-invariant sum of Gaussian kernels (non-symmetric); and a spatially-varying kernel that softly enforces a left-right symmetry:

1. (non-symmetric) the sum of two Gaussian kernels $K_{\sigma_1} + K_{\sigma_2}$, where $\sigma_1 = 25$ mm and $\sigma_2 = 7$ mm, as in [4, 26].
2. (symmetric) the sum of a large-scale symmetrised kernel with a small-scale Gaussian kernel, $K_{\sigma_1} + c\Pi K_{\sigma_1} + K_{\sigma_2}$, where Π is a reflection about the vertical line dividing the two hemispheres. The values of σ_1 and σ_2 are the same as above, and c takes values 0.1 (weak symmetry), 0.5 or 1.0 (pure symmetry at large scale).

For comparison, we have also performed LDM registration of the *unlesioned* images using kernel (1) without a mask.

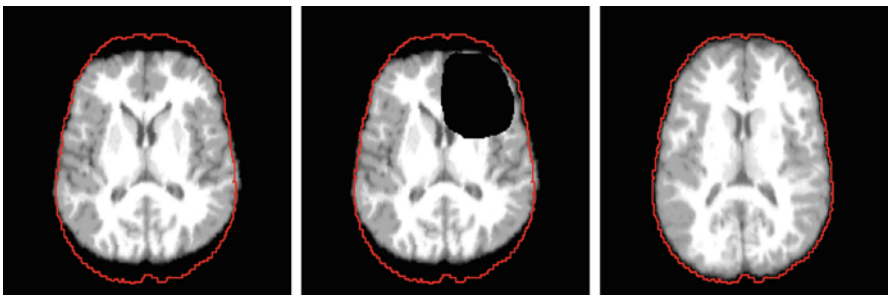

Fig. 2 (From left to right) 2D slice from Subject 8 of the LPBA40 dataset; same slice with a simulated lesion (source image); and corresponding 2D slice from Subject 9 (target image). The *red isoline* represents the surface of Subject 9's brain

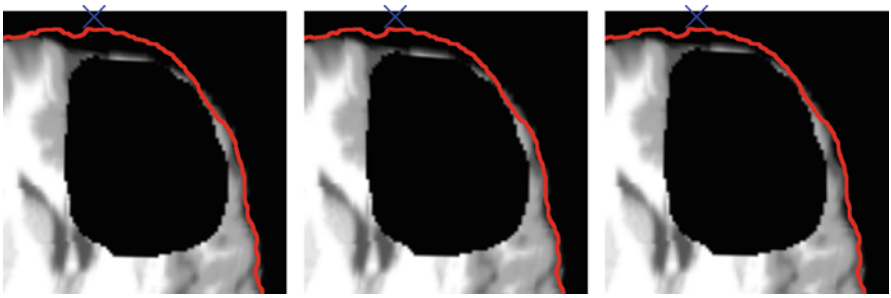

Fig. 3 Source images around the simulated lesion deformed using the registration strategies 1 and 2 of Section 6. From left to right, the registration strategies were: non-symmetric kernel (strategy 1); symmetric kernel (strategy 2) with symmetry weighting factor $c = 0.1$; and symmetric kernel (strategy 2) with symmetry weighting factor $c = 1$ (pure symmetry at large scale). The red isoline (surface of the target) and the blue cross are always at the same location, to visualize the influence of the symmetric kernel

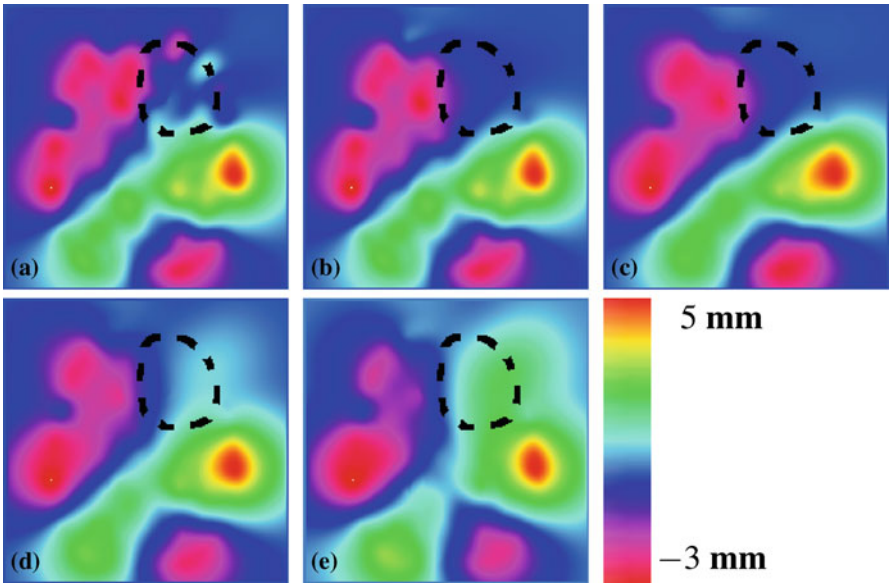

Fig. 4 Deformation magnitude in the x direction (horizontal) estimated using the different registration strategies in Section 6. Results were obtained by registering the images without (a) and with (b–e) the lesion. A mixture of Gaussian kernels was used in (a–b). In (c), (d), (e) a similar mixture of kernels was used, but with a symmetry at the large scale weighted by the factors 0.1, 0.5 and 1, respectively. The dashed curve represents the boundary of the simulated lesion

Deformed images are shown in Fig. 3 and deformation magnitudes in the x direction (horizontal) are shown in Fig. 4. We can see in Fig. 3 that modeling a symmetry in the left and right sides of the brain allows partial compensation for the information missing in the lesion. The deformations estimated in the lesion are

indeed almost only due to the symmetry as clearly emphasized in Fig. 4. It is also interesting to remark that the most similar deformation to the one obtained without the lesion (image (a) in Fig. 4) is not the one obtained using pure symmetry on the large scale (image (e) in Fig. 4), but the one obtained using a factor 0.5 on the symmetry (image (d) in Fig. 4). In this case, the symmetry plausibly compensates for the missing information at a large scale in the lesion but does not penalize too much the estimation of the deformations in the region symmetric to the lesion.

7 Discussion

We have introduced a new perspective on diffeomorphic image matching, based on left- (rather than right-) invariant metrics. For inexact matching with Left-LDM, the optimal diffeomorphism $\phi(1)$ is the same as for Right-LDM (i.e., the usual LDDMM), however there are two different optimal paths from the identity to $\phi(1)$ in the diffeomorphism group: one left- and one right- geodesic. This difference could become significant if a time-dependent similarity measure were used.

In the Left-LDM setting, it is clear that spatially-varying and nonisotropic kernels describe variable deformability properties of the source image. We have shown, in a numerical experiment, the value of spatially-varying kernels as problem-specific regularisation terms in inexact matching. In particular, in a model of a lesioned brain image, we found that a kernel including a large-scale soft symmetry constraint was successful in compensating for missing information in the lesion area.

Through the relationship between Left- and Right- LDM, it also becomes apparent that spatially-varying and directionally-dependent kernels in Right-LDM have an interpretation in terms of local deformability properties of the source image, which has not been remarked upon in the literature.

One very promising avenue for further work is to replace ad-hoc regularisation choices with automatically learnt ones, as has been done by Simpson et al. [30] for global regularisation parameters. Similar methods could be developed for spatially-varying and directionally-dependent regularisation, based on a generative Left-LDM model. Given a template image I, the LDM functional (1) can be interpreted as a log probability density function on pairs of initial vector fields $v(0)$ and images J:

$$\begin{aligned} \log P\,(v(0), J\,|\,I, \lambda, \boldsymbol{\sigma}) &= \log P(v(0)|\boldsymbol{\sigma}) + \log P(J\,|\,v(0), I, \lambda) \\ &= \frac{1}{2}\int_0^1 \|v(t)\|^2_{V_\sigma}\, dt + \frac{\lambda}{2}\|\phi(1)\cdot I - J\|^2_{L^2}, \end{aligned} \tag{39}$$

with the constraint (4) determining $v(t)$ and ϕ from $v(0)$. This could in theory be marginalised over v to get $P(J)$. Both the regularisation parameters σ and the noise parameters λ could be spatially-varying, possibly expressed in terms of labels

associated with the template. A variety of more or less standard methods could be used to optimise the parameters for a population of targets, including Bayesian methods related to those in [1, 9].

References

1. Allassonnière, S., Amit, Y., Trouvé, A.: Towards a coherent statistical framework for dense deformable template estimation. J. R. Stat. Soc. B **69**(1), 3–29 (2007)
2. Arsigny, V., Commowick, O., Pennec, X., Ayache, N.: A log-Euclidean framework for statistics on diffeomorphisms. In: Larsen, R., Nielsen, M., Sporring, J. (eds.) Proceedings of MICCAI'06, vol. 4190, pp. 924–931. Springer, New York (2006)
3. Ashburner, J.: A fast diffeomorphic image registration algorithm. NeuroImage **38**, 95–113 (2007)
4. Beg, M.F., Miller, M.I., Trouvé, A., Younes, L.: Computing large deformation metric mappings via geodesic flows of diffeomorphisms. Int. J. Comput. Vis. **61**(2), 139–157 (2005)
5. Bruveris, M., Gay-Balmaz, F., Holm, D., Ratiu, T.: The momentum map representation of images. J. Nonlinear Sci. **21**(1), 115–150 (2011)
6. Bruveris, M., Risser, L., Vialard, F.: Mixture of kernels and iterated semidirect product of diffeomorphisms groups. Multiscale Model. Simul. **10**(4), 1344–1368 (2012)
7. Cotter, C.J.: The variational particle-mesh method for matching curves. J. Phys. A Math. Theor. **41**(34), 344003 (2008)
8. Cotter, C.J., Holm, D.D.: Continuous and discrete Clebsch variational principles. Found. Comput. Math. **9**, 221–242 (2009)
9. Cotter, C.J., Cotter, S.L., Vialard, F.X.: Bayesian data assimilation in shape registration. Inverse Prob. **29**(4), 045011 (2013)
10. Dupuis, P., Grenander, U., Miller, M.I.: Variational problems on flows of diffeomorphisms for image matching. Q. Appl. Math. **56**, 587–600 (1998)
11. Ebin, D.G., Marsden, J.E.: Groups of diffeomorphisms and the motion of an incompressible fluid. Ann. Math **92**, 102–163 (1970)
12. Fischer, A.E., Marsden, J.E.: The Einstein evolution equations as a first-order quasi-linear symmetric system, I. Commun. Math. Phys. **28**, 1–38 (1972)
13. Fringer, O., Holm, D.: Integrable vs nonintegrable geodesic soliton behavior. Physica D **150**, 237–263 (2001)
14. Gay-Balmaz, F., Ratiu, T.S.: Clebsch optimal control formulation in mechanics. J. Geom. Mech. **3**, 47–79 (2011)
15. Gay-Balmaz, F., Marsden, J.E., Ratiu, T.S.: Reduced variational formulations in free boundary continuum mechanics. J. Nonlinear Sci. **22**, 463–497 (2012)
16. Gay-Balmaz, F., Holm, D.D., Ratiu, T.S.: Geometric dynamics of optimization. Commun. Math. Sci. **11**(1), 163–231 (2013)
17. Holm, D.D., Marsden, J.E.: Momentum maps and measure-valued solutions (peakons, filaments and sheets) for the EPDiff equation. Prog. Math. **232**, 203–235 (2004)
18. Holm, D.D., Marsden, J.E., Ratiu, T.: The Hamiltonian structure of continuum mechanics in material, inverse material, spatial, and convective representations. In: Hamiltonian Structure and Lyapunov Stability for Ideal Continuum Dynamics, vol. 100, pp. 11–124. Presses de l'Université Montréal, Montréal (1986)
19. Holm, D.D., Ratnanather, J.T., Trouvé, A., Younes, L.: Soliton dynamics in computational anatomy. NeuroImage **23**, S170–S178 (2004)
20. Holm, D.D., Trouvé, A., Younes, L.: The Euler-Poincaré theory of metamorphosis. Quart. Appl. Math. **67**, 661–685 (2009)

21. Holm, D.D., Schmah, T., Stoica, C.: Geometric Mechanics and Symmetry: From Finite to Infinite Dimensions. Clarendon Press, Oxford (2009)
22. Kudryavtsev, L.: Implicit function. Encyclopedia of Mathematics (2011). http://www.encyclopediaofmath.org
23. Miller, M., Qiu, A.: The emerging discipline of computational functional anatomy. NeuroImage **45**, S16–S39 (2009)
24. Omori, H.: Infinite Dimensional Lie Transformation Groups. Lecture Notes in Mathematics, vol. 427. Springer, Berlin (1974)
25. Risser, L., Vialard, F.X., Wolz, R., Holm, D.D., Rueckert, D.: Simultaneous fine and coarse diffeomorphic registration: application to the atrophy measurement in Alzheimer's disease. In: MICCAI 2010. Lecture Notes in Computer Science, vol. 6362, pp. 610–617. Springer, Berlin (2010)
26. Risser, L., Vialard, F.X., Wolz, R., Murgasova, M., Holm, D.D., Rueckert, D.: Simultaneous multi-scale registration using large deformation diffeomorphic metric mapping. IEEE Trans. Med. Imaging **30**(10), 1746–1759 (2011)
27. Risser, L., Vialard, F.X., Baluwala, H.Y., Schnabel, J.A.: Piecewise-diffeomorphic image registration: application to the motion estimation between 3D CT lung images with sliding conditions. Med. Image Anal. **17**, 182–193 (2013)
28. Shattuck, D.W., Mirza, M., Adisetiyo, V., Hojatkashani, C., Salamon, G., Narr, K.L., Poldrack, R.A., Bilder, R.M., Toga, A.W.: Construction of a 3D probabilistic atlas of human cortical structures. NeuroImage **39**, 1064–1080 (2008)
29. Simo, J.C., Marsden, J.E., Krishnaprasad, P.S.: The Hamiltonian structure of nonlinear elasticity: the material, spatial and convective representations of solids, rods and plates. Arch. Ration. Mech. Anal. **104**, 125–183 (1988)
30. Simpson, I., Schnabel, J., Groves, A., Andersson, J., Woolrich, M.: Probabilistic inference of regularisation in non-rigid registration. NeuroImage **59**(3), 2438–2451 (2012)
31. Trouvé, A.: Diffeomorphic groups and pattern matching in image analysis. Int. J. Comput. Vis. **28**, 213–221 (1998)
32. Trouvé, A., Younes, L.: Metamorphoses through Lie group action. Found. Comput. Math. **5**, 173–198 (2005)
33. Vercauteren, T., Pennec, X., Perchant, A., Ayache, N.: Diffeomorphic demons: efficient non-parametric image registration. NeuroImage **45**(1 Suppl.), S61–S72 (2009)
34. Vialard, F.X., Risser, L., Rueckert, D., Cotter, C.J.: Diffeomorphic 3D image registration via geodesic shooting using an efficient adjoint calculation. Int. J. Comput. Vision **97**(2), 229–241 (2012)
35. Yosida, K.: Functional Analysis. Die Grundlehren der Mathematischen Wissenschaften in Einzeldarstellungen, vol. 123. Springer, Berlin/New York (1965)
36. Younes, L.: Shapes and Diffeomorphisms. Springer, New York (2010)

Normal Forms for Lie Symmetric Cotangent Bundle Systems with Free and Proper Actions

Tanya Schmah and Cristina Stoica

Abstract We consider free and proper cotangent-lifted symmetries of Hamiltonian systems. For the special case of $G = SO(3)$, we construct symplectic slice coordinates around an arbitrary point. We thus obtain a parameterisation of the phase space suitable for the study of dynamics near relative equilibria, in particular for the Birkhoff-Poincaré normal form method. For a general symmetry group G, we observe that for the calculation of the truncated normal forms, one does not need an explicit coordinate transformation but only its higher derivatives at the relative equilibrium. We outline an iterative scheme using these derivatives for the computation of truncated Birkhoff-Poincaré normal forms.

1 Introduction

The Birkhoff-Poincaré normal form is one of the main tools used in studying local bifurcation and stability for dynamical systems. It is a method based on applying coordinate transformations that simplify the jets of a vector field at an equilibrium, up to a certain order. For Hamiltonian vector fields, the transformations applied must be symplectic, or more generally Poisson, so that the truncated vector field preserves its structure. We will not report here on the importance and usefulness of normal forms in relation, for instance, to bifurcation and stability theory; the interested reader may consult, for instance, [4] and references therein, as well as [12].

For Lie symmetric systems, relative equilibria play an important rôle in dynamics, analogous to the rôle that equilibria play for generic vector fields. A very common first step in dynamical studies near relative equilibria is to use a *slice*

T. Schmah (✉)
Rotman Research Institute, Baycrest, 3560 Bathurst Street, Toronto, ON, Canada M6A 2E1

Department of Computer Science, University of Toronto, Sandford Fleming Building, 10 King's College Road, Room 3302, Toronto, ON, Canada M5S 3G4
e-mail: tschmah@research.baycrest.org; schmah@cs.toronto.edu

C. Stoica
Department of Mathematics, Wilfrid Laurier University, 75 University Avenue West, Waterloo, ON, Canada N2L 3C5
e-mail: cstoica@wlu.ca

D.E. Chang et al. (eds.), *Geometry, Mechanics, and Dynamics*, Fields Institute Communications 73, DOI 10.1007/978-1-4939-2441-7_17

theorem to pass to a coordinate system that separates directions along and transversal to the group orbit. Indeed, if the symmetry group G acts freely and properly, then in a sufficiently small neighborhood of an orbit Gz_0, the phase space is isomorphic to the *slice bundle* $G \times S$ where S, called the *slice*, is a subspace of the tangent space at z_0 that is transversal to Gz_0. (For the non-free case, as well as a characterisation of normal forms near relative equilibria, see [10].) This local model of the action of G on the phase space is actually "semi-global" in the sense that it is global "in the G direction" but local "in the transverse direction".

In these coordinates, a relative equilibrium $z(t)$ corresponds to $(\exp(t\omega), 0)$ and the dynamics takes the form

$$\dot{g} = g f_G(s), \qquad \dot{s} = f_S(s)\,,$$

where $f_S : S \to S$ and $f_G : S \to \mathfrak{g}$. Thus, locally, the dynamics in the slice $\dot{s} = f_S(s)$ drives the dynamics in the group (or "drift") directions $\dot{g} = g f_G(s)$.

In the case of Lie symmetric Hamiltonian systems, the dynamics may be split into the "drift" and "slice" directions as above, but it must also accommodate the additional Hamiltonian structure. By Noether's theorem, the symmetry group G provides the Hamiltonian system with conserved quantities, called momenta. The symplectic manifold is therefore partitioned into flow-invariant level sets of the momenta. The way these level sets intersect the slice can be complicated, especially when G is non-abelian and the relative equilibrium has non-trivial isotropy (the *non-free action* case). This leads to a nontrivial structure on the slice bundle, which in turn induces a nontrivial structure on the slice equations, [22, 23].

For calculating Birkhoff-Poincaré normal forms near relative equilibria of Hamiltonian systems, a natural approach is to try to transfer the machinery from the case of canonical Hamiltonian systems near an equilibrium. For many dynamical studies, it is sufficient to consider a single symplectic reduced space at a single momentum level μ_0, in which the original relative equilibrium z_0 corresponds to an equilibrium.

In the case of cotangent-bundle systems T^*Q, coordinates on the symplectic reduced space suitable for the normal form computation may be found by applying a slice theorem in the configuration space: Q is locally modelled as $G \times S$, where S is an "internal-shape space" direction transverse to the group orbit Gq_0. Then the symplectic reduced space may be identified with $\mathcal{O}_{\mu_0} \times T^*S$ (where $\mathcal{O}_{\mu_0}$ is the coadjoint orbit through μ_0), with the KKS and canonical symplectic forms. This point of view is pursued in [5] and [6]; see also [15].

However it is not always sufficient to consider only a single symplectic reduced space, or a single momentum level set. In particular, the analysis of symmetry-breaking perturbations requires symmetry-adapted local coordinates for the entire phase space that simultaneously place the group action, its momentum map and the symplectic form in simple forms. For symplectic actions, the Hamiltonian slice theorem of Marle [11] and Guillemin and Sternberg [8] (see Theorem 2 below) achieves this goal, modelling the phase space as $G \times \mathfrak{g}^*_{\mu_0} \times N_s$ (for free actions), where N_s is the symplectic normal space. In these symplectic slice coordinates,

the momentum level set $J^{-1}(\mu_0)$ becomes $G_{\mu_0} \times \{0\} \times N_s$, where G_{μ_0} is the isotropy group of μ_0 with respect to the co-adjoint action; so the corresponding symplectic reduced space may be symplectically embedded in the unreduced space as $\{e, 0\} \times N_s$. For free actions on cotangent bundles, $N_s \cong T_{\mu_0}\mathcal{O}_{\mu_0} \times T^*S$, for S a slice in configuration space, with KKS and canonical symplectic forms, which illustrates the connection with the approach in the previous paragraph.

The applicability of the Hamiltonian slice theorem is obstructed by the lack of a constructive proof. Practically, one does not know the change of coordinates, known as the *symplectic tube*, which renders the desired structure. This explicit change of coordinates has been found in only two special cases: (i) cotangent-lifted actions where $G_{\mu_0} = G$ (this happens, for instance, at zero momentum and for abelian Lie groups) [24]; and (ii) free cotangent-lifted actions of $G = SO(3)$, which we present here in Sections 2.3 and 2.4.

In this paper we outline an algorithm for the computation of truncated Birkhoff-Poincaré normal forms near a relative equilibrium, for Lie symmetric cotangent bundle systems with free and proper actions. The splitting of the phase space and the associated change of coordinates are explicitly given for $SO(3)$-symmetric systems. The general algorithm, for any symmetry group G, is based on an iterative scheme which allows the calculation of the truncated normal form up to any desired order. At its core, our method relies on the observation that for the calculation of the truncated normal forms one does not need an explicit coordinate transformation but only its derivatives at the equilibrium/relative equilibrium. We thank Mark Roberts making this key observation in a discussion about 10 years ago.

For the dynamics on $T^*SO(3)$, the coordinates we have obtained for the reduced space coincide with the *regularised* Serret-Andoyer-Deprit coordinates used in celestial mechanics (see [3] and references therein); however, we retrieved these coordinates via a different path and this was crucial for arriving at a methodology for the general case. Our slice parameterisation uses a global description for the reconstruction (attitude) variable $R(t) \in G$. (We use the word "attitude" in analogy to its use in rigid body dynamics.) In concrete applications, it is likely that a local coordinate system will be used. For example, for $SO(3)$, if an explicit local coordinate system is sought, Serret-Andoyer-Deprit is probably the best choice, because they are action-angle coordinates with a very simple relation to Euler angles.

We also compare the splitting of the phase space used for the computations of the normal forms with those used in the Reduced Energy Momentum Method (REM) [12, 25], the latter citation being to Jerry Marsden's "blue book". We respond to one of Jerry's questions stated on page 104 of that book:

It is also of interest to link the normal forms here (i.e., in the REM) *with those in singularity theory. In particular, can one use the forms here as first terms in higher order normal forms?*

In short, the answer is no: while the REM splittings are very useful when looking for sufficient conditions for stability with minimal computational effort, they do not

organise the symplectic form in a convenient form for the Birkhoff-Poincaré normal form method. We expand on this subject in Section 5.

This paper is organised as follows. In Section 2 we investigate the free action of a Lie group G on T^*G by cotangent lifts, arriving at a general *Tube Condition* given in Proposition 1. (Some technical details from this section appear in the Appendix.) We then focus on the special case of $G = SO(3)$ and succeed in constructing an explicit symplectic tube around an arbitrary point, see Theorem 3. We use this to construct a symplectic tube for any free cotangent-lifted action of $SO(3)$ on an arbitrary manifold, see Section 2.4. In Section 3 we offer the equations of motion in slice coordinates for dynamics on $T^*SO(3)$ and for cotangent bundle rotationally invariant systems, including the case of simple mechanical systems. In Section 4 we outline the algorithm for calculating truncated Birkhoff-Poincaré normal forms for general free and proper actions. Section 5 comments on the relationship between the splittings used in these normal forms and those in the Reduced Energy Momentum method.

2 Slice Coordinates

2.1 Lie Symmetries of Hamiltonian Systems

For general background information on Lie symmetries, see [9]. In what follows, gothic letters will always denote Lie algebras of the Lie groups with corresponding latin letters. Let G act on M, with the action of $g \in G$ on $z \in M$ denoted by gz. The corresponding infinitesimal action of $\xi \in \mathfrak{g}$ on z is denoted by ξz. The *isotropy subgroup* of a point $z \in M$ is $G_z := \{g \in G \mid gz = z\}$. The adjoint action of G on $\mathfrak{g}$ is denoted by Ad, and the infinitesimal adjoint action by ad. The *coadjoint* action of G on $\mathfrak{g}^*$ is the inverse dual to the adjoint action, $g\nu = \mathrm{Ad}^*_{g^{-1}}\,\nu$. The infinitesimal coadjoint action is given by $\xi \cdot \nu = -\mathrm{ad}^*_\xi\,\nu$. For any $\mu \in \mathfrak{g}^*$, the notation G_μ will always denote the isotropy subgroup of G with respect to the coadjoint action, that is $G_\mu := \{g \in G \mid \mathrm{Ad}^*_{g^{-1}}\,\mu = g\}$. The notation introduced is summarised in the following table.

$\mathfrak{g}$	Lie algebra of a Lie group G
gz	Action of $g \in G$ on z
ξz	Infinitesimal action of $\xi \in \mathfrak{g}$ on z
Ad_g	Adjoint action of $g \in G$ on $\mathfrak{g}$
$\mathrm{Ad}^*_{g^{-1}}$	Coadjoint action of $g \in G$ on $\mathfrak{g}^*$
ad_ξ	Infinitesimal adjoint action of $\xi \in \mathfrak{g}$ on $\mathfrak{g}$
$-\mathrm{ad}^*_\xi$	Infinitesimal coadjoint action of $\xi \in \mathfrak{g}$ on $\mathfrak{g}^*$
G_μ	Isotropy subgroup of μ w.r.t. coadjoint action

Suppose G acts symplectically on a symplectic manifold (M, Ω). Recall that any function $F : M \to \mathbf{R}$ defines a Hamiltonian vector field X_F by $i_{X_F}\Omega = dF$, in other words $\Omega(X_F(z), v) = dF(v)$ for every $v \in T_z^*M$. A *momentum map* is a function $J : M \to \mathfrak{g}^*$ satisfying $X_{J_\xi}(z) = \xi z$ for every $\xi \in \mathfrak{g}$ and $z \in M$, where $J_\xi : M \to \mathbf{R}$ is defined by $J_\xi(z) = \langle J(z), \xi \rangle$. If the G action has an Ad^*-equivariant momentum map J, then it is called *globally Hamiltonian.*

The *coadjoint orbit* through any $\mu \in \mathfrak{g}^*$ is the orbit of μ with respect to the coadjoint action, $\mathcal{O}_\mu := \{\mathrm{Ad}^*_{g^{-1}}\mu : g \in G\}$. The *Kostant-Kirillov-Souriau (KKS)* symplectic forms on any coadjoint orbit $\mathcal{O}_\mu$ are given by

$$\Omega^{\pm}_{\mathcal{O}_\mu}(\nu)\left(-\mathrm{ad}^*_{\eta_1}\nu, -\mathrm{ad}^*_{\eta_2}\nu\right) = \pm\langle \nu, [\eta_1, \eta_2]\rangle \ . \tag{1}$$

The momentum map of the coadjoint action of G on $\mathcal{O}_\mu$ with respect to $\Omega^{\pm}_{\mathcal{O}_\mu}$ (the "$\pm$KKS forms") is $J_{\mathcal{O}_\mu}(\nu) = \pm\nu$. It can be shown that the KKS forms are always G-invariant.

Let N_s be the *symplectic normal space* at z,

$$N_s(z) := \ker dJ(z)/\mathfrak{g}_\mu z\,,$$

where $\mathfrak{g}_\mu z := \{\xi z : \xi \in \mathfrak{g}_\mu\}$ The restriction of $\Omega(z)$ to $\ker dJ(z)$ has kernel $\mathfrak{g}_\mu z$, by the Reduction Lemma [1], so it descends to a reduced symplectic bilinear form on $N_s(z)$. For free and proper actions, this space is isomorphic to the tangent at $[z]$ to the symplectic reduced space $J^{-1}(\mu)/G_\mu$ (see [12]).

We now give limited versions of Palais' slice theorem [18, 19] and the Hamiltonian Slice Theorem of Marle, Guillemin and Sternberg [8, 11], treating only the case of free actions (for ease of exposition).

Theorem 1 ("Palais' Slice Theorem" for Free Actions [18, 19]). *Let G be a Lie group acting properly, smoothly and freely on a manifold M, and let $z \in M$. Choose a local Riemannian metric around z (such a metric always exists), let N be the orthogonal complement to $\mathfrak{g}z$, and let $\exp_z$ be the corresponding Riemannian exponential based at z. Then there exists a neighbourhood S of 0 in N such that the map*

$$\begin{aligned} \tau : G \times (S \subset N) &\to M \\ (g, s) &\longmapsto g \exp_z s \end{aligned}$$

is a G-equivariant diffeomorphism. (Such a τ is called a tube.) If M is a vector space and G acts linearly, then the "$exp_z s$" in the formula for τ may be replaced by "$z + s$", and τ is a G-equivariant diffeomorphism for any choice of an H-invariant neighbourhood S of 0 for which τ is injective.

Suppose that G acts *symplectically* on a manifold (M, Ω), with Ad^*-equivariant momentum map J. We would like to find a *symplectic* tube $\tau : G \times N \to M$, for

some N, with respect to some simple or "natural" symplectic form on $G \times N$. The Hamiltonian Slice Theorem, also known as the Marle-Guillemin-Sternberg normal form [2, 8], accomplishes this, for actions that are not necessarily free. We present the theorem now only for free actions. Let $z \in M$ and $\mu = J(z)$, and let G_μ be the isotropy group of μ with respect to the coadjoint action. (Note that μ is a specific momentum value, corresponding to the μ_0 in the Introduction; we have dropped the subscript 0 for ease of notation.) Let N_s be the *symplectic normal space* at z. We define a symplectic form on $G \times \left(\mathfrak{g}_\mu^* \times N_s\right)$. First, choose a specific G-invariant splitting $\mathfrak{g} = \mathfrak{g}_\mu \oplus \mathfrak{g}_\mu^\perp$. Define Ω_T and Ω_μ on $G \times \mathfrak{g}_\mu^*$ by

$$\Omega_T(g,\nu)\left((\xi_1,\dot{\nu}_1),(\xi_2,\dot{\nu}_2)\right) =< \mu, [\xi_1,\xi_2] >$$
$$\Omega_0(g,\nu)\left((\xi_1,\dot{\nu}_1),(\xi_2,\dot{\nu}_2)\right) = \langle \nu, [\xi_1,\xi_2]\rangle + < \dot{\nu}_2, \xi_1^\mu > - < \dot{\nu}_1, \xi_2^\mu >,$$

where ξ_1^μ and ξ_2^μ are the $\mathfrak{g}_\mu$ components of ξ_1 and ξ_2. Third, let Ω_{N_s} be the reduced symplectic bilinear form on N_s (defined above). Then $\Omega_Z := \Omega_T + \Omega_0 + \Omega_{N_s}$ is a presymplectic form on $G \times \mathfrak{g}_\mu^* \times N_s$. It can be shown that there exists a G-invariant neighbourhood Y of $[e,0,0]$ in $G \times \mathfrak{g}_\mu^* \times N_s$ in which Ω_Z is symplectic. Let Ω_Y be the restriction of Ω_Z to Y. Finally, note that there is left G-action on Y given by $g'(g,\nu,\rho) = (g'g,\nu,\rho)$ It is easy to check that this is symplectic with respect to Ω_Y.

Theorem 2 (Hamiltonian Slice Theorem for Free Actions[1] [2, 8]). *In the above context, there exists a symplectic tube from $Y \subset G \times \mathfrak{g}_\mu^* \times N_s$ to M that maps $(e,0,0)$ to z. The momentum map of the G action on Y is*

$$J_Y(g,\nu,\rho) = \mathrm{Ad}^*_{g^{-1}}(\mu + \nu).$$

No general constructive proof of this theorem is known, even for free actions. However a constructive proof is given in [24] for the special case of a cotangent-lifted action, not necessarily free, for which $G_\mu = G$.

2.2 Symplectic Slices for the Cotangent Bundle of a Lie Group

We now consider the special case of G acting on T^*G by the cotangent lift of left multiplication. We left-trivialise T^*G, meaning that we identify it with $G \times \mathfrak{g}^*$ via the map $p \in T_gG \mapsto (g,\mu) := (g, g^{-1}p)$, with $g^{-1}p := D\Phi_g(e)^*(p)$. We seek a constructive symplectic tube based at a general $(g,\mu) \in G \times \mathfrak{g}^*$ satisfying the conditions of the Hamiltonian Slice Theorem (Theorem 2). Without loss of

[1] In the full Hamiltonian Slice Theorem, at a point z with non-trivial isotropy group G_z, the model space is $G \times_{G_z} \left(\mathfrak{g}_\mu^* \times N_s\right)$, and J_Y has an extra term.

generality, we will assume $g = e$ (the identity). We will also assume that $\mu \neq 0$, since in the case $\mu = 0$ we have $G_\mu = G$ and a trivial symplectic normal space, so Theorem 2 is trivial.

Using left-trivialisation, the canonical symplectic form becomes:

$$\Omega_c(e,\mu)\left((\xi_1,\rho_1),(\xi_2,\rho_2)\right) = <\mu,[\xi_1,\xi_2]> + <\rho_2,\xi_1> - <\rho_1,\xi_2>.$$

The G action on T^*G becomes $h(g,\nu) = (hg,\nu)$, which has momentum map $J(g,\nu) = \mathrm{Ad}^*_{g^{-1}}\nu$. Note that J is Ad^*-equivariant) and

$$DJ(e,\mu)\cdot(\xi,\rho) = \xi\cdot\mu + \rho = -\operatorname{ad}^*_\xi \mu + \rho. \tag{2}$$

Fix a $\mu \in \mathfrak{g}^*$, $\mu \neq 0$. Choose a G-invariant Riemannian metric on $\mathfrak{g}$, and let $\mathfrak{g}_\mu^\perp$ be the orthogonal complement of $\mathfrak{g}_\mu$. Define

$$N_1 := \left\{\left(\eta, \operatorname{ad}^*_\eta \mu\right) : \eta \in \mathfrak{g}_\mu^\perp\right\}. \tag{3}$$

It follows from (2) that N_1 is a complement to $\mathfrak{g}_\mu z$ in $\ker DJ(z)$. Therefore N_1 is isomorphic to the symplectic normal space $N_s(z)$, with the reduced symplectic bilinear form on $N_s(z)$ corresponding to the restriction of $\Omega_c(z)$ to N_1.

Lemma 1. *The following is a linear symplectomorphism from N_1 (with the restricted canonical symplectic form) to $T_\mu\mathcal{O}_\mu$ with the KKS form $\Omega^-_{\mathcal{O}}(\mu)$,*

$$L : \left(\eta, \operatorname{ad}^*_\eta \mu\right) \mapsto \operatorname{ad}^*_\eta \mu\,.$$

Proof.

$$\begin{aligned}
\Omega_c\left(\left(\eta_1, \operatorname{ad}^*_{\eta_1}\mu\right), \left(\eta_2, \operatorname{ad}^*_{\eta_2}\mu\right)\right) &= <\mu,[\eta_1,\eta_2]> + <\operatorname{ad}^*_{\eta_2}\mu,\eta_1> \\
&\quad - <\operatorname{ad}^*_{\eta_1}\mu,\eta_2> \\
&= -\langle\mu,[\eta_1,\eta_2]\rangle = \Omega^-_{\mathcal{O}}(\mu)\left(\operatorname{ad}^*_{\eta_1}\mu, \operatorname{ad}^*_{\eta_2}\mu\right) \\
&= \left(L^*\Omega^-_{\mathcal{O}}(\mu)\right)\left(\left(\eta_1, \operatorname{ad}^*_{\eta_1}\mu\right), \left(\eta_2, \operatorname{ad}^*_{\eta_2}\mu\right)\right).
\end{aligned}$$

The result follows by equivariance of L and invariance of the two symplectic forms.

We identify $N_s(z) \cong N_1 \cong T_\mu\mathcal{O}_\mu$ via this lemma, so that the reduced symplectic form Ω_{N_s} is identified with $\Omega^-_{\mathcal{O}}(\mu)$.

We seek a constructive version of the Hamiltonian Slice Theorem (for free actions) in this context. That is, we wish to construct a G-equivariant local diffeomorphism

$$\Phi : G \times \mathfrak{g}_\mu^* \times N \longrightarrow G \times \mathfrak{g}^*,$$
$$(e, 0, 0) \mapsto (e, \mu),$$

such that $\Phi^* \Omega_c = \Omega_Y := \Omega_T + \Omega_0 + \Omega_N$, where

$$\begin{aligned}
\Omega_T(g,\nu,\rho)\left((\xi_1,\dot\nu_1,\dot\rho_1),(\xi_2,\dot\nu_2,\dot\rho_2)\right) &= <\mu,[\xi_1,\xi_2]>,\\
\Omega_0(g,\nu,\rho)\left((\xi_1,\dot\nu_1,\dot\rho_1),(\xi_2,\dot\nu_2,\dot\rho_2)\right) &= \langle\nu,[\xi_1,\xi_2]\rangle + <\dot\nu_2,\xi_1^\mu> \\
&\quad - <\dot\nu_1,\xi_2^\mu>, \qquad (4)\\
\Omega_N(g,\nu,\rho)\left((\xi_1,\dot\nu_1,\mathrm{ad}^*_{\zeta_1}\mu),(\xi_2,\dot\nu_2,\mathrm{ad}^*_{\zeta_2}\mu)\right) &= -\langle\mu,[\zeta_1,\zeta_2]\rangle .
\end{aligned}$$

The following proposition, proven in the Appendix, characterises the symplectic tubes that appear in the Hamiltonian Slice Theorem (Theorem 2).

Proposition 1 (Tube Condition). *$\Phi^* \Omega_c = \Omega_Y$ if and only if*

$$\Phi(g,\nu,\mathrm{ad}^*_\eta\,\mu) = \left(gF(\nu,\eta)^{-1}, \mathrm{Ad}^*_{F(\nu,\eta)^{-1}}(\mu+\nu)\right)$$

for some $F : \mathfrak{g}_\mu^* \times \mathfrak{g}_\mu^\perp \to G$ such that $F(0,0) = e$ and

$$\begin{aligned}
&\left\langle \mu+\nu, \left[F(\nu,\eta)^{-1}\left(DF(\nu,\eta)\cdot(\dot\nu_1,\zeta_1)\right), F(\nu,\eta)^{-1}\left(DF(\nu,\eta)\cdot(\dot\nu_2,\zeta_2)\right)\right]\right\rangle\\
&\quad + \left\langle \dot\nu_2, F(\nu,\eta)^{-1}\left(DF(\nu,\eta)\cdot(\dot\nu_1,\zeta_1)\right)\right\rangle - \left\langle \dot\nu_1, F(\nu,\eta)^{-1}\left(DF(\nu,\eta)\cdot(\dot\nu_2,\zeta_2)\right)\right\rangle\\
&= \langle\mu,[\zeta_1,\zeta_2]\rangle .
\end{aligned}$$

We have not found a general construction for a symplectic tube valid for all Lie groups G, and indeed we do not expect that one will ever be found. However we noticed, as explained in the Appendix, that the restriction of the Tube Condition to the subspace $\{0\} \times \{0\} \times N$ is reminiscent of the condition in the following lemma, which is proven in the Appendix.

Lemma 2. *Let $\varphi : T_\mu \mathscr{O}_\mu \to \mathscr{O}_\mu$ be of the form $\varphi(-\mathrm{ad}^*_\eta\,\mu) = f(\eta)\mu$ for some $f : \mathfrak{g}_\mu^\perp \to G$. Then φ preserves the $-$KKS symplectic form if and only if*

$$\begin{aligned}
\langle\mu,[\zeta_1,\zeta_2]\rangle &= \left\langle f(\eta)\mu, \left[(Df(\eta)\cdot\zeta_1)\, f(\eta)^{-1}, (Df(\eta)\cdot\zeta_2)\, f(\eta)^{-1}\right]\right\rangle\\
&= \left\langle \mu, \left[f(\eta)^{-1}\left(Df(\eta)\cdot\zeta_1\right), f(\eta)^{-1}\left(Df(\eta)\cdot\zeta_2\right)\right]\right\rangle \qquad (5)
\end{aligned}$$

for all $\eta, \zeta_1, \zeta_2 \in \mathfrak{g}_\mu^\perp$.

This was the inspiration that led to the constructive slice theorem in the next section.

2.3 A Constructive Slice Theorem for $T^*SO(3)$

For the reason outlined above, we consider maps $\varphi : T_\mu\mathcal{O}_\mu \to \mathcal{O}_\mu$ such that $\varphi(\mathbf{0}) = \mu$ and $D\varphi(\mathbf{0})$ is the identity, that preserve the $-$KKS form. The KKS forms for $SO(3)$, for any μ, are $\frac{1}{\|\mu\|}$ times the signed area form on $\mathcal{O}_\mu \cong S^2$, with the sign corresponding to the outward-pointing normal for the $+$KKS form, and the inward-pointing normal for the $-$KKS form. Thus a map $\varphi : T_\mu\mathcal{O}_\mu \to \mathcal{O}_\mu$ that preserves the $\pm$KKS form is just an area-preserving map from $\mathbb{R}^2$ to $S^2(\|\mu\|)$, where $S^2(\|\mu\|)$ is the sphere of radius $\|\mu\|$ centred at the origin.

Without loss of generality, we consider $\mu = (0, 0, \mu_z)$, with $\mu_z > 0$. Consider the usual polar coordinates (r, θ) on the plane and spherical coordinates (θ, ϕ) on the unit sphere, where θ is usual angle coordinate in the xy-plane, and ϕ is the angle from the positive z axis. Note that the signed area $d\theta \wedge \mathrm{d}\phi$ is the $-$KKS form. We seek an area-preserving map $\varphi : T_\mu\mathcal{O}_\mu \to \mathcal{O}_\mu$, such that $\varphi(\mathbf{0}) = \mu$ and $D\varphi(\mathbf{0}) = Id$, and require also that φ be equivariant with respect to G_μ, which consists of rotations around the z axis. We make an Ansatz that φ preserves θ. It can be shown that the unique φ satisfying all of these requirements is given by

$$\phi = 2 \arcsin\left(\frac{r}{2\|\mu\|}\right).$$

To write this in the form of Lemma 2, $\varphi\left(-\mathrm{ad}^*_\eta\,\mu\right) = \mathrm{Ad}^*_{f(\eta)^{-1}}\,\mu$, we define

$$f(\eta) := \exp\left(2 \arcsin\left(\frac{\|\eta\|}{2}\right)\frac{\eta}{\|\eta\|}\right).$$

where exp be the usual matrix exponential.

Comparing (37) and (38) in the Appendix, we may guess that a factor involving $\|\mu\|/\|\mu + \nu\|$ should be inserted in order to produce a symplectic tube. The solution may be discovered by trial and error, however we will proceed systematically from the Ansatz

$$F(\nu, \eta) = \exp\left(h(\nu, \eta)\,\frac{\eta}{\|\eta\|}\right), \tag{6}$$

for some real-valued h. Note that the term $F(\nu, \eta)^{-1}\,(DF(\nu, \eta) \cdot (\dot{\nu}, \zeta))$ that appears in the Tube Condition in Proposition 1 takes the following form when $\dot{\nu} = 0$,

$$F(\nu, \eta)^{-1}\,(DF(\nu, \eta) \cdot (0, \zeta)) = \exp\left(-\hat{\mathbf{v}}\right)\left.\frac{d}{dt}\right|_{t=0} \exp\left(\hat{\mathbf{v}} + t\,\hat{\mathbf{w}}\right),$$

where $\hat{\mathbf{v}} := h(\nu, \eta)\frac{\eta}{\|\eta\|}$ and $\hat{\mathbf{w}} := h(\nu, \eta)\frac{\zeta}{\|\eta\|}$, and the hat map $\mathbf{v} \mapsto \hat{\mathbf{v}}$ is defined by

$$\hat{\mathbf{v}} = \begin{pmatrix} 0 & -v_3 & v_2 \\ v_3 & 0 & -v_1 \\ -v_2 & v_1 & 0 \end{pmatrix}.$$

We compute this quantity with the aid of **Rodrigues' rotation formula** (see [13]):

$$\exp(\hat{\mathbf{v}}) = I + \frac{\sin\|\mathbf{v}\|}{\|\mathbf{v}\|}\hat{\mathbf{v}} + \frac{1-\cos\|\mathbf{v}\|}{\|\mathbf{v}\|^2}\hat{\mathbf{v}}^2 = I + \frac{\sin\|\mathbf{v}\|}{\|\mathbf{v}\|}\hat{\mathbf{v}} + \frac{2\sin^2\frac{\|\mathbf{v}\|}{2}}{\|\mathbf{v}\|^2}\hat{\mathbf{v}}^2.$$

Lemma 3. *For general orthogonal* $\mathbf{v}$ *and* $\mathbf{w}$*,*

$$\exp(-\hat{\mathbf{v}})\left.\frac{d}{dt}\right|_{t=0}\exp(\hat{\mathbf{v}} + t\hat{\mathbf{w}}) = \frac{\sin\|\mathbf{v}\|}{\|\mathbf{v}\|}\hat{\mathbf{w}} - \frac{2\sin^2\frac{\|\mathbf{v}\|}{2}}{\|\mathbf{v}\|^2}(\mathbf{v}\times\mathbf{w})\hat{}. \tag{7}$$

Proof. By the naturality property of exp, and the fact that $R\hat{\mathbf{w}}R^{-1} = (R\mathbf{w})\hat{}$, it suffices to prove the claim for $\mathbf{v} = (v_x, 0, 0)$ and $\mathbf{w} = (0, w_y, 0)$. This is a straightforward calculation.

Lemma 4. *If* $\eta, \zeta \in \mathfrak{g}_\mu^\perp$ *and* ζ *is perpendicular to* η*, then*

$$F(\nu,\eta)^{-1}\left(DF(\nu,\eta)\cdot(\dot\nu,\dot\zeta)\right) = \frac{\sin h}{\|\eta\|}\hat{\zeta} - \frac{2\sin^2\frac{h}{2}}{\|\eta\|^2}(\eta\times\zeta)\hat{},$$

and $\eta\times\zeta \in \mathfrak{g}_\mu$.

Proof. $\left.\frac{d}{dt}\right|_{t=0}\|\eta + t\zeta\| = 0$ and $\left.\frac{d}{dt}\right|_{t=0}\frac{\eta+t\zeta}{\|\eta+t\zeta\|} = \frac{\zeta}{\|\eta\|}$. Then

$$DF(\nu,\eta)\cdot(0,\zeta) = \left.\frac{d}{dt}\right|_{t=0}\exp\left(h(\nu,\eta)\frac{\eta}{\|\eta\|} + t\,h(\nu,\eta)\frac{\zeta}{\|\eta\|}\right).$$

From (7), with $\hat{\mathbf{v}} = h(\nu,\eta)\frac{\eta}{\|\eta\|}$ and $\hat{\mathbf{w}} = h(\nu,\eta)\frac{\zeta}{\|\eta\|}$,

$$\begin{aligned} F(\nu,\eta)^{-1}\left(DF(\nu,\eta)\cdot(\dot\nu,\dot\zeta)\right) &= \exp(-\hat{\mathbf{v}})\left.\frac{d}{dt}\right|_{t=0}\exp(\hat{\mathbf{v}}+t\hat{\mathbf{w}}) \\ &= \frac{\sin\|\mathbf{v}\|}{\|\mathbf{v}\|}\hat{\mathbf{w}} - \frac{2\sin^2\frac{\|\mathbf{v}\|}{2}}{\|\mathbf{v}\|^2}(\mathbf{v}\times\mathbf{w})\hat{} \\ &= \frac{\sin h}{h}\hat{\mathbf{w}} - \frac{2\sin^2\frac{h}{2}}{h^2}(\mathbf{v}\times\mathbf{w})\hat{} \\ &= \frac{\sin h}{\|\eta\|}\hat{\zeta} - \frac{2\sin^2\frac{h}{2}}{\|\eta\|^2}(\eta\times\zeta)\hat{}. \end{aligned}$$

Since $\eta, \zeta \in \mathfrak{g}_\mu^\perp$ and $\eta \perp \zeta$, it follows that $\eta\times\zeta \in \mathfrak{g}_\mu$.

We now calculate the Tube Condition in Proposition 1 under the Ansatz (6). The following lemma covers the case of ζ_1, ζ_2 both parallel to η, which includes the case of $\zeta_1 = \zeta_2 = 0$ (the "$\dot{\nu} - \dot{\nu}$" case). Though motivated by our study of the $SO(3)$ case, the following lemma applies to general G. It is proven in the Appendix.

Lemma 5. *Suppose* $F(\nu, \eta) = \exp\left(h(\nu, \eta)\, \dfrac{\eta}{\|\eta\|}\right)$, *for some* $h : \mathfrak{g}_\mu^* \times \mathfrak{g}_\mu^\perp \to \mathbb{R}$. *Then the Tube Condition in Proposition 1 is automatically satisfied (regardless of the definition of* h*) for all* $(\dot{\nu}_1, \zeta_1), (\dot{\nu}_2, \zeta_2)$ *such that* ζ_1 *and* ζ_2 *are parallel to* η.

From this and the bilinearity of Condition (37) in the Appendix, we are left with three cases to check.

Case: ζ_1 and ζ_2 both perpendicular to η. In this case, ζ_1 and ζ_2 are parallel to each other, and

$$\begin{aligned}
&\left\langle \mu + \nu, \left[F(\nu,\eta)^{-1} \left(DF(\nu,\eta)\cdot(0,\zeta_1)\right), F(\nu,\eta)^{-1}\left(DF(\nu,\eta)\cdot(0,\zeta_2)\right)\right]\right\rangle \\
&= \left\langle \mu + \nu, \left(\frac{\sin h}{\|\eta\|}\,\zeta_2\right) \times \left(\frac{2\sin^2\frac{h}{2}}{\|\eta\|^2}\,(\eta\times\zeta_1)\right) - \left(\frac{\sin h}{\|\eta\|}\,\zeta_1\right) \times \left(\frac{2\sin^2\frac{h}{2}}{\|\eta\|^2}\,(\eta\times\zeta_2)\right)\right\rangle \\
&= 0 = \langle \mu, [\zeta_1, \zeta_2]\rangle\,.
\end{aligned}$$

Therefore the Tube Condition in Proposition 1 is satisfied, for any h.

Case: $\dot{\nu}_1 = \dot{\nu}_2 = 0$, ζ_1 is parallel to η and ζ_2 is perpendicular to η. By Lemma 4,

$$\begin{aligned}
&\left\langle \mu + \nu, \left[F(\nu,\eta)^{-1} \left(DF(\nu,\eta)\cdot(0,\zeta_1)\right), F(\nu,\eta)^{-1}\left(DF(\nu,\eta)\cdot(0,\zeta_2)\right)\right]\right\rangle \\
&= \left\langle \mu + \nu, \left(\frac{\partial h}{\partial \eta}(\nu,\eta)\cdot\zeta_1\right)\frac{\eta}{\|\eta\|} \times \left(\frac{\sin h}{\|\eta\|}\,\zeta_2 - \frac{2\sin^2\frac{h}{2}}{\|\eta\|^2}\,(\eta\times\zeta_2)\right)\right\rangle \\
&= \left\langle \mu + \nu, \left(\frac{\partial h}{\partial \eta}(\nu,\eta)\cdot\zeta_1\right)\frac{\eta}{\|\eta\|} \times \left(\frac{\sin h}{\|\eta\|}\right)\zeta_2\right\rangle \\
&= \pm\|\mu+\nu\|\left(\frac{\partial h}{\partial \eta}(\nu,\eta)\cdot\zeta_1\right)\left(\frac{\sin h}{\|\eta\|}\right)\|\zeta_2\|,
\end{aligned}$$

where the sign is the sign of $\mu\cdot(\eta\times\zeta_2)$.

For the Tube Condition in Proposition 1 to be satisfied, this must equal $\mu\cdot\zeta_1\times\zeta_2 = \pm\|\mu\|\|\zeta_1\|\|\zeta_2\|$ for all ζ_1, ζ_2, which occurs if and only if

$$\operatorname{sgn}(\zeta_1\cdot\eta)\|\mu+\nu\|\left(\frac{\partial h}{\partial \eta}(\nu,\eta)\cdot\zeta_1\right)\left(\frac{\sin h}{\|\eta\|}\right) = \|\mu\|\|\zeta_1\|. \tag{8}$$

If we further assume that h depends on η only through $\|\eta\|$, then (8) becomes:

$$\|\mu+\nu\|\frac{\partial h}{\partial\|\eta\|}(\nu,\|\eta\|)\left(\frac{\sin h}{\|\eta\|}\right) = \|\mu\|. \tag{9}$$

Case: $\zeta_1 = 0$ and ζ_2 is perpendicular to η.

$$\begin{aligned}
&\left\langle \mu + \nu, \left[F(\nu,\eta)^{-1} \left(DF(\nu,\eta) \cdot (\dot\nu_1, 0) \right), F(\nu,\eta)^{-1} \left(DF(\nu,\eta) \cdot (0, \zeta_2) \right) \right] \right\rangle \\
&\quad + \left\langle \dot\nu_2, F(\nu,\eta)^{-1} \left(DF(\nu,\eta) \cdot (\dot\nu_1, 0) \right) \right\rangle - \left\langle \dot\nu_1, F(\nu,\eta)^{-1} \left(DF(\nu,\eta) \cdot (0, \zeta_2) \right) \right\rangle \\
&= \left\langle \mu + \nu, \left(\left(\frac{\partial h}{\partial \nu}(\nu,\eta)\, \dot\nu_1 \right) \frac{\eta}{\|\eta\|} \right) \times \left(\frac{\sin h}{\|\eta\|}\, \zeta_2 \right) \right\rangle \\
&\quad + \left\langle \dot\nu_1, \frac{2 \sin^2 \frac{h}{2}}{\|\eta\|^2} \left(\eta \times \zeta_2 \right) \right\rangle \\
&= \pm \left[\|\mu + \nu\| \left(\frac{\partial h}{\partial \nu}(\nu,\eta)\, \dot\nu_1 \right) (\sin h)\, \frac{\|\zeta_2\|}{\|\eta\|} + 2 \dot\nu_1 \left(\sin^2 \frac{h}{2} \right) \frac{\|\zeta_2\|}{\|\eta\|} \right],
\end{aligned}$$

where the sign is the sign of $\mu \cdot (\eta \times \zeta_2)$.

For the Tube Condition in Proposition 1 to be satisfied, this expression must equal zero, for all $\dot\nu_1$. If $h(\nu,\eta) \neq 0$, a factor of $\sin(h/2)$ cancels, giving the equivalent condition

$$\|\mu + \nu\| \frac{\partial h}{\partial \nu} \cos \frac{h}{2} + \sin \frac{h}{2} = 0, \tag{10}$$

Theorem 3. *Let*

$$\Phi(g, \nu, \mathrm{ad}^*_\eta\, \mu) = \left(g F(\nu,\eta)^{-1}, \mathrm{Ad}^*_{F(\nu,\eta)^{-1}} (\mu + \nu) \right),$$

where

$$F(\nu,\eta) = \exp\left(2 \arcsin\left(\frac{1}{2} \|\eta\| \sqrt{\frac{\|\mu\|}{\|\mu + \nu\|}} \right) \frac{\eta}{\|\eta\|} \right).$$

Then $\Phi^* \Omega_c = \Omega_Y$. The domain of definition of Φ is $SO(3) \times \left(U \subset \mathfrak{so}(3)^*_\mu \times T_\mu \mathcal{O}_\mu \right)$, where

$$U = \left\{ \left(\nu, \mathrm{ad}^*_\eta\, \mu \right) : \nu > -\|\mu\| \text{ and } \|\eta\| < 2 \sqrt{\frac{\|\mu + \nu\|}{\|\mu\|}} \right\}.$$

Proof. Let $x = \|\eta\| \sqrt{\frac{\|\mu\|}{\|\mu+\nu\|}}$, and

$$h(\nu, \|\eta\|) = 2 \arcsin \frac{x}{2} = 2 \arcsin\left(\frac{1}{2} \|\eta\| \sqrt{\frac{\|\mu\|}{\|\mu + \nu\|}} \right).$$

Then $dh/dx = 2/\sqrt{4-x^2} = 1/\cos(h/2)$, so

$$\frac{\partial h}{\partial \nu}\cos\frac{h}{2} = \frac{-\|\eta\|}{2\|\mu+\nu\|}\sqrt{\frac{\|\mu\|}{\|\mu+\nu\|}},$$

which implies that (10) is satisfied. Also,

$$\frac{\partial h}{\partial \|\eta\|}\sin h = 2\sin\frac{h}{2}\sqrt{\frac{\|\mu\|}{\|\mu+\nu\|}} = \frac{\|\eta\|\|\mu\|}{\|\mu+\nu\|},$$

so (9) is satisfied.

Remark 1. The restriction of Φ to a level set defined by $(R,\nu) = (Id,\nu_0)$ has as its image an open neighbourhood of $\mu+\nu_0$ in the coadjoint orbit $\mathcal{O}_{\mu+\nu_0}$, which is a sphere and is isomorphic to the symplectic reduced space at $\mu+\nu_0$. For any choice of ν_0, the neighbourhood covers almost the entire sphere, excluding only the antipodal point $-(\mu+\nu_0)$.

Remark 2. This Φ has a limited uniqueness property. From the Tube Condition in Proposition 1, any symplectic tube must of be expressed in terms of an F as stated in the theorem. Any F can be expressed as the exponential of some function $\mathfrak{g}^*_\mu \times \mathfrak{g}^\perp_\mu \mapsto \mathfrak{g}$. If that function is of the form $h(\nu,\|\eta\|)\,\eta/\|\eta\|$, then the two conditions (9) and (10) are sufficient to determine $h(\nu,\|\eta\|)$.

2.4 Actions of SO(3) on Arbitrary Configuration Spaces

The results of the previous section can be used to construct symplectic slices for any free and proper cotangent-lifted action of $SO(3)$ on T^*Q, for arbitrary Q.

Proposition 2. *Suppose $SO(3)$ acts freely on a manifold Q, and by cotangent lifts on T^*Q. Let*

$$\begin{aligned}\tau : SO(3)\times(S\subset N) &\to Q\\ (R,s) &\longmapsto R\exp_{q_0} s\end{aligned}$$

be the tube given by Theorem 1 (Palais' Slice Theorem). Let $\Phi : SO(3)\times\mathfrak{so}(3)^*_\mu \times T_\mu\mathcal{O}_{\mu_0} \to SO(3)\times\mathfrak{so}(3)^*$ be defined as in Theorem 3. Then the following composition

$$\begin{aligned}SO(3)\times\mathfrak{so}(3)^*_\mu\times T_\mu\mathcal{O}_\mu\times T^*S &\overset{(\Phi,\mathrm{id})}{\to} SO(3)\times\mathfrak{so}(3)^*\times T^*S \cong T^*(SO(3)\times S)\\ &\overset{T^*\tau^{-1}}{\to} T^*Q \qquad (11)\end{aligned}$$

(where the central isomorphism is left-trivialisation) is an $SO(3)$-equivariant symplectomorphism with respect to the canonical symplectic form on T^*Q and the symplectic form Ω_Y defined in (4).

In the case $Q = \mathbb{R}^n$, we have $\tau(R, s) = R(q_0+s)$. We now explain the cotangent lift $T^*\tau^{-1}$ that appears in (11). Writing $q := R(q_0+s)$, the tangent space T_qQ splits into the direct sum of two subspaces:

$$\begin{aligned} \mathfrak{so}(3)q &:= \{\xi q : \xi \in \mathfrak{so}(3)\} && \text{(“group direction”, tangent to } Gq\text{)}, \\ RN &:= \{Rv : v \in N\} && \text{(“slice direction”).} \end{aligned}$$

The cotangent space T^*_qQ has a corresponding splitting into $\mathfrak{so}(3)^*$ (group direction) and RN^* (slice direction); note that $(RN)^* = R(N^*)$. The tangent lift of τ is given by

$$(\xi, \dot{s}) \in T_{(R,s)}(SO(3) \times S) \mapsto R\left(\xi(q_0 + s) + \dot{s}\right) \in T_qQ, \tag{12}$$

where $R(\xi(q + s))$ is in the group direction and $R\dot{s}$ is in the slice direction, and we have used left-trivialisation to write $(R, \xi) \in SO(3) \times \mathfrak{so}(3) \cong T(SO(3)$. The cotangent lift $T^*\tau^{-1}$, also has two components, in the group and slice directions:

$$(\mu, \sigma) \in T^*_{(R,s)}(SO(3) \times S) \mapsto (\alpha_\mu(q) + R\sigma) \in T^*_qQ,$$

where $\alpha_\mu(q) \in (\mathfrak{so}(3)q)^*$ and $R\sigma \in RN^*$. To define these components explicitly, we pair them with the components of a general tangent vector. Since τ is a diffeomorphism, all such tangent vectors can be expressed in the form (12). We have

$$\left\langle \alpha_\mu(q) + R\sigma, R\left(\xi(q + s) + \dot{s}\right)\right\rangle := \langle \mu, \xi\rangle + \langle \sigma, \dot{s}\rangle,$$

i.e.

$$\begin{aligned} \left\langle \alpha_\mu(q), R\left(\xi(q + s)\right)\right\rangle &:= \langle \mu, \xi\rangle, \quad \text{and} \\ \langle R\sigma, R\dot{s}\rangle &:= \langle \sigma, \dot{s}\rangle. \end{aligned}$$

A similar strategy allows one to construct symplectic slices for some *non-free* actions of $SO(3)$ on general cotangent bundles. However we leave this topic for a later paper.

3 Dynamics in Slice Coordinates

3.1 Dynamics on $T^*SO(3)$

In this section we describe the motion on $T^*SO(3)$ in normal form coordinates near a fixed non-zero momentum $(0,0,\mu_0) \in \mathbb{R}^3 \simeq so(3)^*$. We identify $T_{\mu_0}\mathscr{O}_{\mu_0}$ with $so(3)^{\perp}_{\mu_0}$ via $\mathrm{ad}^*_\eta\, \mu_0 \mapsto \eta$. Then the $SO(3)$-equivariant symplectomorphism given by Theorem 3 takes the form

$$\Phi : SO(3) \times so(3)^*_{\mu_0} \times so(3)^{\perp}_{\mu_0} \to SO(3) \times so(3)^*$$
$$\Phi(R,\nu,\eta) = \Big(R\,(F(\nu,\eta))^{-1},\ F(\nu,\eta)(\mu_0+\nu)\Big)$$

with

$$F(\nu,\eta) = \exp\left(\theta\,\frac{\hat{\eta}}{\|\eta\|}\right) \quad \text{where} \quad \sin\frac{\theta}{2} = \frac{1}{2}\|\eta\|\sqrt{\frac{\|\mu_0\|}{\|\mu_0+\nu\|}}\,. \tag{13}$$

Specifically, one has the change of variables

$$SO(3) \times so(3)^*_{\mu_0} \times so(3)^{\perp}_{\mu_0} \to SO(3) \times so(3)^*$$
$$(R,\nu,\eta) \to \Phi(R,\nu,\eta) := (S,\mu)$$

where

$$\mu_1 = \eta_y\sqrt{\mu_0(\mu_0+\nu)\left(1-\frac{\mu_0}{4(\mu_0+\nu)}(\eta_x^2+\eta_y^2)\right)} \tag{14}$$

$$\mu_2 = -\eta_x\sqrt{\mu_0(\mu_0+\nu)\left(1-\frac{\mu_0}{4(\mu_0+\nu)}(\eta_x^2+\eta_y^2)\right)} \tag{15}$$

$$\mu_3 = (\mu_0+\nu) - \frac{1}{2}\mu_0(\eta_x^2+\eta_y^2) \tag{16}$$

and $S = RF(\nu,\eta)^{-1}$. The symplectic form on $SO(3)\times so(3)^*_{\mu_0}\times so(3)^{\perp}_{\mu_0}$ is given by

$$\Omega_Y(R,\nu,\eta) = \begin{bmatrix} (\mu_0+\nu)\mathbb{J} & 0 & 0 \\ 0 & \mathbb{J} & 0 \\ 0 & 0 & -\mu_0\mathbb{J} \end{bmatrix}$$

where we use the notation $\mathbb{J} := \begin{bmatrix} 0 & 1 \\ 1 & 0 \end{bmatrix}$. Note that this matrix does not depend on η. In (R, ν, η) coordinates the (spatial) momentum map $J(S, \mu) = S\mu$ reads:

$$J\,(R, \nu, \eta) = R\,(\mu_0 + \nu\,).$$

It is useful to recall that in slice coordinates the Marsden-Weinstein reduced spaces at (R, ν, η), which are $J^{-1}\,(R(\mu_0 + \nu))\,/SO(3)^*_{R(\mu_0+\nu)}$, are all isomorphic to the linear space $T_{\mu_0}\mathcal{O}_{\mu_0} \cong so(3)^{\perp}_{\mu_0}$. The symplectic leaves $\mathcal{O}_{\mu_0+\nu} = S^2(\|\mu_0 + \nu\|)$ of $so(3)^*$ are modelled (locally) as canonical linear spaces, and "indexed" by ν.

Consider now a Hamiltonian $\tilde{H}(S, \mu)$ on $SO(3)\times so(3)^*$. Applying the change of coordinates given by Φ, we have: $H(R, \nu, \eta) := (\tilde{H} \circ \Phi)(R, \nu, \eta)$ and the equations of motion become

$$\begin{bmatrix} \xi_x \\ \xi_y \\ \\ \xi_z \\ \dot{\nu} \\ \\ \dot{\eta}_x \\ \dot{\eta}_y \end{bmatrix} = \begin{bmatrix} 0 & \frac{1}{\mu_0+\nu} & 0 & 0 & 0 & 0 \\ -\frac{1}{\mu_0+\nu} & 0 & 0 & 0 & 0 & 0 \\ \\ 0 & 0 & 0 & 1 & 0 & 0 \\ 0 & 0 & -1 & 0 & 0 & 0 \\ \\ 0 & 0 & 0 & 0 & 0 & -\frac{1}{\mu_0} \\ 0 & 0 & 0 & 0 & \frac{1}{\mu_0} & 0 \end{bmatrix} \begin{bmatrix} \left(R^{-1}\partial_R H\right)_x \\ \left(R^{-1}\partial_R H\right)_y \\ \\ \left(R^{-1}\partial_R H\right)_z \\ \partial_\nu H \\ \\ \partial_{\eta_x} H \\ \partial_{\eta_y} H \end{bmatrix} \tag{17}$$

where $\xi = R^{-1}\dot{R} \in so(3)$. In particular, if H is $SO(3)$-invariant and $h(\nu, \eta) := H(\cdot\,, \nu, \eta)$, we have

$$\dot{\nu} = 0 \tag{18}$$

$$\dot{\eta} = -\frac{1}{\mu_0}\mathbb{J}\,\nabla_\eta h \tag{19}$$

with reconstruction equations:

$$R(t)^{-1}\dot{R}(t) = \xi(t) = \begin{pmatrix} 0 \\ 0 \\ \left.\frac{\partial h}{\partial \nu}\right|_{(\nu(t),\eta(t))} \end{pmatrix}. \tag{20}$$

Note that this reconstructs $R(t)$, not the body's attitude $S(t)$. At a given time t_1, once $\nu(t_1)$, $\eta(t_1)$ and $R(t_1)$ have been calculated by integrating (18), (19) and (20), the attitude can be computed simply as

$$S(t_1) = R(t_1)F(\nu(t_1), \eta(t_1))^{-1}.$$

A *relative equilibrium* is a steady motion in a group direction. In the original left-trivialised coordinates (S, μ), a relative equilibrium with velocity ξ_0 is a trajectory of the form $S(t) = \exp(t\xi_0)S_0$ with μ constant. In slice coordinates, μ constant is equivalent to ν and η constant, and in this case $S(t) = R(t)F^{-1}(\nu_0, \eta_0)$ implies $R(t) = \exp(t\xi_0)R_0$. Thus in slice coordinates, a relative equilibrium with velocity ξ_0 is a trajectory in which η is an equilibrium of (19) and the velocity $\xi(t)$ given by (20) has the constant value ξ_0.

Since $\nu = const. = \nu_0$, the reduced Hamiltonian depends dynamically on η only, whereas ν_0 affects the motion as an external parameter. Thus $h(\eta; \nu_0)$ is a one degree of freedom canonical system on a symplectic vector space. The phase curves for (19) fill in the $so(3)^{\perp}_{\mu_0}$-phase plane as level sets of the energy integral $h(\eta; \nu_0) = const.$ In particular, any $SO(3)$-invariant system on $T^*SO(3)$ is integrable.

Note that the reconstruction equation (20) reduces to reconstruction on the Abelian group $SO(3)_{\mu_0}$ and it leads to rotations about the z-axis. Specifically, if $\eta(t)$ is a solution for (19), then

$$R(t) = \begin{bmatrix} \cos\theta(t) & -\sin\theta(t) & 0 \\ \sin\theta(t) & \cos\theta(t) & 0 \\ 0 & 0 & 1 \end{bmatrix} \tag{21}$$

where

$$\theta(t) = \frac{\partial h}{\partial \nu}\Big|_{(\nu_0, \eta(t))}.$$

3.2 The Euler-Poinsot Rigid Body

The Hamiltonian of the Euler-Poinsot (free) rigid body is (see, for instance, [13]):

$$h(\mu_1, \mu_2, \mu_3) = \frac{1}{2}\left(\frac{\mu_1}{\mathbb{I}_1} + \frac{\mu_2}{\mathbb{I}_2} + \frac{\mu_3}{\mathbb{I}_3}\right)$$

where $\mathbb{I}_i$ are the principal moments of inertia. Using the formulae (14)–(16) the Hamiltonian h reads:

$$h(\nu, \eta) := \frac{1}{2}(\mu_0 + \nu)\left[\mu_0\left(1 - \frac{\mu_0}{4(\mu_0 + \nu)}\left(\eta_x^2 + \eta_y^2\right)\right)\left(\frac{\eta_x^2}{\mathbb{I}_2} + \frac{\eta_y^2}{\mathbb{I}_1}\right) + \left(1 - \frac{\mu_0}{2(\mu_0 + \nu)}\left(\eta_x^2 + \eta_y^2\right)\right)^2 \frac{(\mu_0 + \nu)}{\mathbb{I}_3}\right] \tag{22}$$

One may deduce easily the stability criteria, as well as sketch the Marsden-Weinstein reduced phase-space at any momentum $(\mu_0 + \nu)$; see Figure 1. The

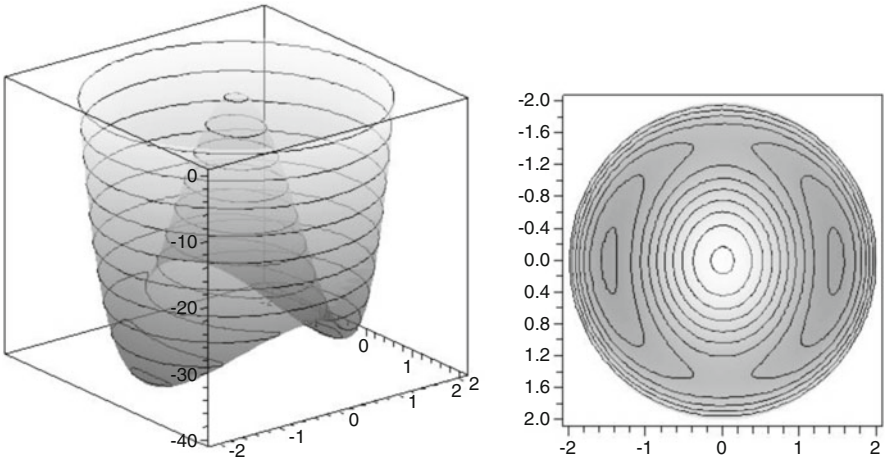

Fig. 1 The Marsden-Weinstein reduced phase-space for the free rigid body in slice coordinates. By (19), we have $\nu = \nu_0 = const$. The phase curves are retrieved as the level sets of the Hamiltonian $h(\eta_x, \eta_y; \nu_0)$. Left: 3-d view. Right: top view

super-integrability of the Euler-Poinsot rigid body (that is the case when $\mathbb{I}_1 = \mathbb{I}_2$) is transparent, as h becomes a function of $|\eta|^2$ only.

Is is known that the rigid body accepts a canonical action-angle description as given by Serret-Deprit-Andoyer coordinates. A comprehensive description of these coordinates and their generalisation to *regularised* coordinate charts which cover the co-adjoint sphere minus the antipodal point of the relative equilibrium $(0, 0, \mu_0)$ can be found in [3, Section 4] and the references therein. A direct comparison of the slice and the *regularised* Serret-Deprit-Andoyer coordinates shows that they provide *identical* parametrisations of $T_{\mu_0}\mathcal{O}_{\mu_0} \equiv so(3)^{\perp}_{\mu_0}$. Specifically, (η_x, η_y) are in fact regularised Serret-Andoyer-Deprit coordinates. The slice parameterisation uses a global attitude description R(t). If an explicit local coordinate system is sought, Serret-Deprit-Andoyer is probably the best choice, because they are action-angle coordinates with a very simple relation to Euler angles. The relationship between the two parametrisations will be discussed in detail in future work.

3.3 Cotangent-Bundle Rotationally Invariant Systems

Consider a $SO(3)$-invariant Hamiltonian system $H : T^*Q \to \mathbb{R}$ and let $(q_0, p_0) \in T^*Q$ be a point on a relative equilibrium with group velocity ξ and momentum μ_0. We apply now Proposition 2 where (q_0, p_0) is the base point of the Palais tube. It follows that in a neighbourhood of (q_0, p_0) the phase space is symplectomorphic to

$SO(3) \times so(3)^*_{\mu_0} \times so(3)^\perp_{\mu_0} \times T^*S$, where we identified $T_{\mu_0}\mathcal{O}_{\mu_0} \equiv so(3)^\perp_{\mu_0}$. Since the Hamiltonian is $SO(3)$ invariant, in slice coordinates

$$(R, \nu, \eta, s, \sigma) \in SO(3) \times so(3)^*_{\mu_0} \times so(3)^\perp_{\mu_0} \times T^*S \tag{23}$$

it can be written as $h = h(\nu, \eta, s, \sigma)$. The equations of motion take the form

$$\dot{\nu} = 0 \tag{24}$$

$$\dot{\eta} = -\frac{1}{\mu_0}\,\mathbb{J}\,\partial_\eta h\,, \qquad \begin{pmatrix} \dot{s} \\ \\ \dot{\sigma} \end{pmatrix} = \mathbb{J} \begin{pmatrix} \frac{\partial h}{\partial s} \\ \\ \frac{\partial h}{\partial \sigma} \end{pmatrix} \tag{25}$$

whereas the reconstruction equation is

$$\dot{R} = R \begin{pmatrix} 0 \\ 0 \\ \frac{\partial h}{\partial \nu}\,. \end{pmatrix} \tag{26}$$

The reconstruction equation can be integrated to give rotations about the z axis by angle:

$$\theta(t_0) = \int_0^{t_0} \frac{\partial h}{\partial \nu}\Big|_{(\nu_0, \eta(t), s(t), \sigma(t))} dt. \tag{27}$$

We consider relative equilibria at $(\nu, \eta, s, \sigma) = (\nu_0, 0, 0, 0)$, with velocity

$$\xi_0 := \begin{pmatrix} 0 \\ 0 \\ \\ \frac{\partial h}{\partial \nu}\Big|_{(\nu_0,0,0,0)} \end{pmatrix}. \tag{28}$$

By construction the Marsden-Weinstein reduced space at μ_0 is locally symplectomorphic to the canonical vector space $so(3)^\perp_{\mu_0} \times T^*S$, and the dynamics are given by the reduced Hamiltonian $h_{\mu_0}(\eta, s, \sigma) := h(0, \eta, s, \sigma)$. In this model of the reduced space, the relative equilibrium q_0 becomes the origin.

Recall that a simple mechanical system is a system with a Hamiltonian $H : T^*Q \to \mathbb{R}$ of the form

$$H(q, p_q) = \frac{1}{2}\mathbb{K}^{-1}(p_q, p_q) + V(q) \tag{29}$$

for some G-invariant Riemannian metric $\mathbb{K}$, and some G-invariant potential $V : Q \to \mathbb{R}$. We assume that G acts properly. The dynamics on T^*Q may be specialised easily this case. We take Q a finite dimensional vector space which, without loss of generality, we consider to be an open subset of $\mathbb{R}^n$.

Fix $q_0 \in Q$ and let N be the orthogonal complement to the group orbit through q_0. By Palais' slice theorem, there is a neighbourhood S of $0 \in N$ such that the map $\tau : SO(3) \times S \to Q$, $(R, s) \mapsto R(q_0 + s)$ is a diffeomorphism onto its image. The cotangent lift of τ defines local coordinates $(R, \xi, s, \dot{s})$ on TQ, (R, μ, s, σ) on T^*Q, as explained in Section 2.4. Since the Riemannian metric $\mathbb{K}$ and the potential V are both $SO(3)$-invariant, they are independent of R in these coordinates. We write $\mathbb{K}(s)$ in block form in coordinates $(\xi, \dot{s})$ as follows (this defines $\mathbb{I}$, $\mathbb{C}$ and m):

$$\mathbb{K}(s) = \begin{bmatrix} \mathbb{I}(s) & \mathbb{C}(s) \\ \mathbb{C}^T(s) & m(s) \end{bmatrix}$$

and define $\mathbb{A} := \mathbb{I}^{-1}\mathbb{C}$ and $\mathbb{M} := m - \mathbb{C}^T\mathbb{I}^{-1}\mathbb{C}$. With these definitions, it can be shown that the Hamiltonian takes the following form,

$$h(\mu, s, \sigma) = \frac{1}{2}\,\mu^T \mathbb{I}^{-1}\,\mu + \frac{1}{2}(\sigma - \mathbb{A}^T\mu)^T \mathbb{M}^{-1}(\sigma - \mathbb{A}^T\mu) + V(s). \tag{30}$$

This is a special case, for free actions, of a more general result in [23, Section 6]. In the case of N-body problems (molecules), the corresponding Hamiltonian is deduced in [15] and [5]. The relative equilibria conditions are [23]

$$\begin{aligned} &\sigma = \mathbb{A}^T(s)\mu \\ &\mu \times \left(\mathbb{I}^{-1}(s)\,\mu\right) = 0 \\ &\frac{\partial}{\partial s}\left(V(s) + \mu^T \mathbb{I}^{-1}(s)\,\mu\right) = 0\,. \end{aligned}$$

Assume that $((0, 0, \mu_0), s_0, \sigma_0)$ is a relative equilibrium, as determined by the above equations, and let $(q_0, p_0) \simeq (Id, (0, 0, \mu_0), s_0, \sigma_0)$. Now we express the Hamiltonian (30) in the slice coordinates given by (14)–(16), obtaining

$$h : so(3)_{\mu_0} \times so(3)^{\perp}_{\mu_0} \times T^*S \to \mathbb{R}\,, \quad h = h(\nu, \eta, s, \sigma)\,.$$

The equations of motion are given by (24)–(26).

3.4 On the Nekhoroshev's Estimates Near a Relative Equilibrium

Recall that in [16] Nekhoroshev showed that under a perturbation of order ε, the actions of an arbitrary orbit of a quasi-convex integrable Hamiltonian vary at order ε^b over a time interval of order $\exp(\varepsilon^{-a})$, where a and b are positive numbers which depend on the number of degrees of freedom and the steepness of the Hamiltonian. For Hamiltonians near an elliptic equilibrium, under certain hypothesis, analogous

estimates are found by [7, 21] and [17]. Specifically, (under the right conditions) the actions $I = (I_1, I_2, \ldots, I_n)$ of a Hamiltonian system near an elliptic equilibrium fulfill

$$|I(t) - I(0)| < C\varepsilon^a \qquad \text{for } |t| < D_1 \exp(D_2 \varepsilon^{-a})$$

where a, C, D_1, D_2 are constants independent of ε.

The Nekhoroshev long term stability of the perturbed Euler-Poinsot rigid-body near a relative equilibrium (proper rotation) was treated in a series of excellent papers by Benettin, Fassò et al. (see [3] and references therein). In particular, the authors show that for a perturbed rigid body, the proper rotations around the symmetry axis are Nekhoroshev stable.

Recall from Section 3.2 that our slice coordinates for the reduced space correspond to the regularised Serret-Andoyer-Deprit coordinates used by Benettin, Fassò et al. This suggests that our slice coordinates for general rotationally-invariant cotangent-bundle systems may be useful for addressing long-term stability of RE. Specifically, one may look for conditions under which motions that start near an elliptic RE (i.e., an elliptic equilibrium in the reduced space) are Nekhoroshev long term stable with respect to a small symmetry-breaking perturbation.

4 Birkhoff-Poincaré Normal Forms Near a Relative Equilibrium

4.1 Rotationally Invariant Cotangent Bundle Systems

Consider a canonical symplectic manifold (P, Ω_c), a Hamiltonian $H : P \to \mathbb{R}$ and z_0 an equilibrium of the dynamics induced by H. Denote by $\hat{H}^{(i)}$ the homogeneous polynomial of degree i as obtained from the Taylor expansion of H around z_0. The truncated normal form of order k is defined as the k-jet of the Hamiltonian written in some (new) coordinates $\hat{H}$

$$j^k \hat{H} = \hat{H}^{(2)} + \hat{H}^{(3)} + \ldots + \hat{H}^{(k)}$$

which fulfills

$$\left\{ \hat{H}^{(2)}, \hat{H}^{(i)} \right\} = 0 \qquad \text{for all } i = 2, 3, \ldots k$$

The method itself consists in obtaining the property above by applying iteratively changes of coordinates as given by the time-1 Hamiltonian flow X_F^1 where F is a homogeneous polynomial of degree k found by solving the *homological* equation

$$\hat{H}^{(k)} + \left\{ \hat{H}^{(2)}, F \right\} = 0$$

A detailed exposition of Hamiltonian normal forms can be found in [4] (see also [14]).

The classical method of Birkhoff-Poincaré normal forms near an equilibrium can now be applied to the study of dynamics near relative equilibria in the reduced space in the case of rotationally invariant systems. Indeed, since a relative equilibrium is an equilibrium in the reduced space, and since the reduced space is endowed with a canonical form, one may immediately apply the standard theory.

We will not report here on the importance and usefulness of normal forms in relation, for instance, to bifurcation and stability theory (the interested reader may consult, for instance, [4] and references therein, as well as [12]). In the context of cotangent bundles systems with $SO(3)$ symmetry, very recent applications can be found in [5] and [6]; here, since the normal forms are calculated directly on the reduced space, there is no need of a canonical embedding in the full space.

4.2 The General Case

All of the theory in Section 3 can be generalised to arbitrary Lie groups, i.e., to proper, cotangent-lifted free actions of any G on T^*G. A key difference is that we have no general formula for the symplectic tube Φ, and do not expect to find one. Thus we do not expect to be able to write H explicitly in slice coordinates (though this might be possible in special cases). Nonetheless, the equations of motion in the slice have almost the same form as in (18) and (19). If G_μ is compact, the equations of motion are

$$\dot{\nu} = \mathrm{ad}^*_{\frac{\partial h}{\partial \nu}} \nu, \tag{31}$$

$$\dot{\eta} = -\frac{1}{\mu_0} \mathbb{J} \nabla_\eta h, \tag{32}$$

with the first equation reducing to $\dot{\nu} = 0$ whenever G_μ is abelian. The reconstruction equation takes the same form as before:

$$R(t)^{-1} \dot{R}(t) = \frac{\partial h}{\partial \nu}. \tag{33}$$

The case of non-compact G_μ is dealt with in [22]. For simple mechanical systems, the relative equilibrium conditions given in Section 3.3 have a generalisation in [23].

It is clear that if an explicit formula for the symplectic tube $\Phi : G \times \mathfrak{g}_\mu \times N \to G \times \mathfrak{g}^*$ exists, then this can be composed with the original Hamiltonian to express it in slice coordinates, and this Hamiltonian can then be differentiated as needed. However, a key observation is that, to obtain a truncated normal form of order k, it is not necessary to have an explicit formula for $\hat{H}$; all that is required is its truncated series expansion. In particular, to obtain such a truncation in slice coordinates one

needs only the derivatives of Φ at $(e, 0, 0)$ up to order k. These can be obtained using the Tube Condition in Proposition 1, which for reader's convenience we re-write:

$\Phi^* \Omega_c = \Omega_Y$ if and only if

$$\Phi(g, \nu, \mathrm{ad}^*_\eta \mu) = \left(gF(\nu, \eta)^{-1}, \mathrm{Ad}^*_{F(\nu,\eta)^{-1}} (\mu + \nu) \right)$$

for some $F : \mathfrak{g}^*_\mu \times \mathfrak{g}^\perp_\mu \to G$ *such that* $F(0, 0) = e$ *and, for all* $\nu, \eta, \nu_i, \zeta_i$,

$$\begin{aligned} &\left\langle \mu + \nu, \left[F(\nu, \eta)^{-1} \left(DF(\nu, \eta) \cdot (\dot\nu_1, \zeta_1) \right), F(\nu, \eta)^{-1} \left(DF(\nu, \eta) \cdot (\dot\nu_2, \zeta_2) \right) \right] \right\rangle \\ &+ \left\langle \dot\nu_2, F(\nu, \eta)^{-1} \left(DF(\nu, \eta) \cdot (\dot\nu_1, \zeta_1) \right) \right\rangle - \left\langle \dot\nu_1, F(\nu, \eta)^{-1} \left(DF(\nu, \eta) \cdot (\dot\nu_2, \zeta_2) \right) \right\rangle \\ &= \langle \mu, [\zeta_1, \zeta_2] \rangle \, . \end{aligned}$$

For any specific matrix Lie group G, this condition can be solved directly for $DF(0, 0)$, while implicit differentiation of the same condition allows the *iterative* calculation of higher derivatives to the desired order. Note that there may not be unique solutions to these equations, since the symplectic tube is in general not unique. Different choices of solutions will lead to different normal forms, all valid.

Note that the Lie symmetry group need not be compact, either in the Tube Condition in Proposition 1 or in Lemma 5. In particular, one can apply the methodology outlined here for $G = SE(3)$ for which an interesting case study is given by the so-called full two body problem, that is, two spatially extended bodies, (two asteroids), in gravitational interaction. We intend to investigate such problems in the future.

5 Relationship to Reduced Energy Momentum Method

We consider the relationship between the symplectic slice coordinates studied here and the Reduced Energy Momentum (REM) method [12, 25]. The general Energy-Momentum Method [20] concerns a relative equilibrium z_e, with velocity ξ_e, of a G-symmetric Hamiltonian system. The method gives sufficient conditions for for a kind of equivariant nonlinear stability called G_{μ_e}-stability, where $\mu_e = J(z_e)$. The main condition is that the *augmented Hamiltonian* defined by $H_{\xi_e}(z) = H(z) - \langle J(z), \xi_e \rangle$ be definite on some (and hence any) subspace $\mathscr{S}$ of $\ker dJ(z_e)$ that is transverse to $\mathfrak{g}_{\mu_e} z_e$.

Consider a simple mechanical system on T^*Q, with Hamiltonian as in (29) and G acting properly, with relative equilibrium $z_e = (q_e, p_e)$. The REM reduces the main condition of the Energy-Momentum method to two simple tests of definiteness on subspaces of $T_{q_e} Q$. This provides a computationally cheap way to prove nonlinear stability in some cases. The proof of the REM relies on a particular choice of the subspace $\mathscr{S}$ mentioned above, and a particular splitting of that subspace that block-diagonalises $d^2 H_{\xi_e}$. We compute some of these spaces in coordinates given the Palais slice theorem for the action of G on Q. Let S be a slice in Q at q_e with

respect to the given metric. Without loss of generality we assume S is a vector space, so that

$$T^*Q \cong T^*(G \times S) \cong \mathfrak{g} \oplus \mathfrak{g}^* \oplus S \oplus S^*,$$

where we use left-trivialisation on T^*G. The relative equilibrium in the new coordinates is $z_e = (e, \mu, 0, 0)$. Restricting the Riemannian metric at $q_e = (e, 0)$ to the subspace $\mathfrak{g} \oplus \{0\}$ of $T_e(G \times S) \cong \mathfrak{g} \oplus S$ gives an inner product on $\mathfrak{g}$, with respect to which we take the complement $\mathfrak{g}^{\perp}$.[2] We calculate the spaces $\mathscr{V} \subset T_{(e,0)}Q$ and $\mathscr{S} \subset \ker dJ(z_e)$ in the Reduced Energy-Momentum method as presented in [12]:

$$\begin{aligned} J(g, \nu, s, \sigma) &= \mathrm{Ad}^*_{g^{-1}} \nu, \\ \ker dJ(e, \mu, 0, 0) &= \{(\eta, \mathrm{ad}^*_\eta \mu) : \eta \in \mathfrak{g}\} \oplus S \oplus S^*, \\ T_{z_e}(G_\mu z_e) = \mathfrak{g}_\mu z_e &= \mathfrak{g}_\mu \oplus \{0\} \oplus \{0\} \oplus \{0\}, \\ \mathscr{V} &:= \big(\mathfrak{g}_\mu (e, 0)\big)^{\perp} = \big(\mathfrak{g}_\mu \oplus \{0\}\big)^{\perp} = \mathfrak{g}_\mu^{\perp} \oplus S, \end{aligned}$$

where the last equality is due to the definition of the inner product on $\mathfrak{g}$, and

$$\begin{aligned} \mathscr{S} &:= \{\delta z \in \ker DJ(z_e) : T\pi_Q \cdot \delta z \in \mathscr{V}\} \\ &= \{(\eta, \mathrm{ad}^*_\eta \mu) : \eta \in \mathfrak{g}_\mu^{\perp}\} \oplus S \oplus S^* \\ &= N_1 \oplus S \oplus S^*, \end{aligned}$$

where N_1 is as in (3). Since $\mathscr{S}$ is a complement to $\mathfrak{g}_\mu z_e$ in $\ker DJ(z_e)$, it is a realisation of the symplectic normal space N_s, and in fact it is the same as the realisation that appears in the constructive symplectic slice theorem in Section 2.4 (recall that $N_1 \cong T_\mu \mathscr{O}_\mu \cong \mathfrak{g}_\mu^{\perp}$). The REM splits $\mathscr{S}$ further:

$$\mathscr{S} = \mathscr{S}_{RIG} \oplus \mathscr{W}_{INT} \oplus \mathscr{W}^*_{INT}.$$

We will not fully calculate these spaces here, but the following can easily be checked:

$$\begin{aligned} \mathscr{S}_{RIG} &= N_1 \oplus \{0\} \oplus \{0\}, \\ \mathscr{W}_{INT} &\leq \mathfrak{g}_\mu^{\perp} \oplus \mathfrak{g}^* \oplus S \oplus \{0\}, \\ \mathscr{W}^*_{INT} &= \{0\} \oplus \{0\} \oplus \{0\} \oplus S^*. \end{aligned} \tag{34}$$

[2] This inner product need not be invariant with respect to the adjoint action of G_μ on $\mathfrak{g}$. One of the conditions of the Energy-Momentum Method is that $\mathfrak{g}$ admits a G_{μ_e}-invariant inner product.

The REM works in part because this splitting of $\mathscr{S}$ block-diagonalises the augmented Hamiltonian.

In contrast, the Hamiltonian Slice Theorem block-diagonalises the *symplectic form*, and it does so at every point z, not just z_e. In symplectic slice coordinates, the symplectic form block-diagonalises with respect to the two-way splitting $\left(\mathfrak{g} \oplus \mathfrak{g}_\mu^*\right) \oplus N_s$, where

$$N_s \cong N_1 \oplus S \oplus S^* \cong T_\mu \mathscr{O}_\mu \oplus S \oplus S^* \tag{35}$$

and Ω_{N_s} has the following form with respect to this splitting:

$$\begin{bmatrix} \Omega_{KKS} & 0 & 0 \\ 0 & 0 & I \\ 0 & -I & 0 \end{bmatrix}. \tag{36}$$

Thus the total symplectic form block-diagonalises with respect to the the 3-way splitting $\left(\mathfrak{g} \oplus \mathfrak{g}_\mu^*\right) \oplus N_1 \oplus (S \oplus S^*)$.

The REM and the constructive Hamiltonian Slice Theorem both make use of the same realisation of the symplectic normal space, $\mathscr{S} = N_1 \oplus S \oplus S^*$, but while the slice theorem uses the canonical 3-way splitting $N_1 \oplus S \oplus S^*$, the REM uses the splitting in (34). The two splittings do share one common subspace, $\{0\} \oplus \{0\} \oplus \{0\} \oplus S^*$, however there the similarities end. The splitting in the REM is chosen to block-diagonalise the augmented Hamiltonian, leading to a stability condition defined directly on configuration space. The splitting in the constructive Hamiltonian Slice Theorem puts the symplectic form into block form, but not the augmented Hamiltonian, and is not associated with a convenient condition for nonlinear stability.

For the specific purpose of proving stability of a relative equilibrium of a simple mechanical system, the REM is a superb tool. Symplectic slice coordinates are general-purpose symmetry-adapted coordinates on phase space that block-diagonalise the symplectic form at every z, leading to a normal form for the Hamiltonian equations given in (31), (32) and (33). The simple form of these equations, and the fact that (32) is the reduced Hamiltonian system, make these coordinates ideal for computing Birkhoff-Poincaré normal forms.

Acknowledgements CS was supported by an NSERC Discovery grant. This work was completed during a research stay at the Otter Lake Science Institute in Ontario. Also, we thank the referee for many useful comments.

Appendix

This appendix contains proofs of three results in the main text. The main result is Proposition 1 (the "Tube Condition") in Section 2.2, which gives a necessary and sufficient condition for a map Φ from $G \times \mathfrak{g}_\mu^* \times N_s$ to $G \times \mathfrak{g}^*$ to be symplectic. This proposition is used in Section 2.3 to construct an explicit symplectic tube when $G = SO(3)$, and it is also a key ingredient in the algorithm outlined in Section 4 for computing Birkhoff-Poincaré normal forms for arbitrary G.

In the statement of the proposition, Ω_c is the canonical symplectic form on T^*G, which is identified by left-trivialisation with $G \times \mathfrak{g}^*$. The symplectic form Ω_Y is the form on $Y := G \times \mathfrak{g}_\mu^* \times N_s$ that appears in the Hamiltonian Slice Theorem (Theorem 2). This symplectic form is stated more explicitly in (4), using the identification of N_s with $T_\mu \mathcal{O}_\mu$ that appears earlier in the same section.

Restatement of Proposition 1 (Tube Condition) $\Phi^* \Omega_c = \Omega_Y$ if and only if

$$\Phi(g, \nu, \mathrm{ad}_\eta^* \mu) = \left(g F(\nu, \eta)^{-1}, \mathrm{Ad}^*_{F(\nu,\eta)^{-1}} (\mu + \nu) \right)$$

for some $F : \mathfrak{g}_\mu^* \times \mathfrak{g}_\mu^\perp \to G$ such that

$$\begin{aligned} &\left\langle \mu + \nu, \left[F(\nu,\eta)^{-1} \left(DF(\nu,\eta) \cdot (\dot\nu_1, \zeta_1) \right), F(\nu,\eta)^{-1} \left(DF(\nu,\eta) \cdot (\dot\nu_2, \zeta_2) \right) \right] \right\rangle \\ &+ \left\langle \dot\nu_2, F(\nu,\eta)^{-1} \left(DF(\nu,\eta) \cdot (\dot\nu_1, \zeta_1) \right) \right\rangle - \left\langle \dot\nu_1, F(\nu,\eta)^{-1} \left(DF(\nu,\eta) \cdot (\dot\nu_2, \zeta_2) \right) \right\rangle \\ &= \langle \mu, [\zeta_1, \zeta_2] \rangle . \end{aligned}$$

Proof. The most general formula for a G-equivariant Φ is

$$\Phi(g, \nu, \mathrm{ad}_\eta^* \mu) = (g F_1(\nu, \eta), F_2(\nu, \eta)) .$$

We consider the condition $\Phi^* \Omega_c = \Omega_Y$. Since

$$D\Phi(g, \nu, \mathrm{ad}_\eta^* \mu) \cdot (\xi, 0, 0,) = \left(\mathrm{Ad}^*_{F_1^{-1}(\nu,\eta)} \xi, 0 \right),$$

it follows that, for all ξ_1, ξ_2,

$$\begin{aligned} &\left(\Phi^* \Omega_c \right) (e, \nu, \mathrm{ad}_\eta^* \mu) \left((\xi_1, 0, 0) (\xi_2, 0, 0) \right) = \Omega_Y (e, \nu, \mathrm{ad}_\eta^* \mu) \left((\xi_1, 0, 0) (\xi_2, 0, 0) \right) \\ &\Leftrightarrow \left\langle F_2 \left(\nu, \mathrm{ad}_\eta^* \mu \right), \left[\mathrm{Ad}_{F_1^{-1}(\nu,\eta)} \xi_1, \mathrm{Ad}_{F_1^{-1}(\nu,\eta)} \xi_2 \right] \right\rangle = \langle \mu + \nu, [\xi_1, \xi_2] \rangle \\ &\Leftrightarrow \left\langle \mathrm{Ad}^*_{F_1^{-1}(\nu,\eta)} F_2 \left(\nu, \mathrm{ad}_\eta^* \mu \right), [\xi_1, \xi_2] \right\rangle = \langle \mu + \nu, [\xi_1, \xi_2] \rangle . \end{aligned}$$

Hence this condition is true for all ξ_1, ξ_2 if and only if

$$F_2 \left(\nu, \mathrm{ad}_\eta^* \mu \right) = \mathrm{Ad}^*_{F_1(\nu,\eta)} (\mu + \nu) .$$

Let $F = F_1^{-1}$. We will use the notation $F(\nu,\eta)\nu := \mathrm{Ad}^*_{F(\nu,\eta)^{-1}}\,\nu$, so

$$\Phi(g,\nu,\mathrm{ad}^*_\eta\,\mu) = \left(gF(\nu,\eta)^{-1}, F(\nu,\eta)\,(\mu+\nu)\right),$$

with first derivative:

$$\begin{aligned} D\Phi(g,\nu,\mathrm{ad}^*_\eta\,\mu)\cdot(\xi,\dot\nu,\mathrm{ad}^*_\zeta\,\mu) \\ = (\mathrm{Ad}_{F(\nu,\eta)}\,\xi - (DF(\nu,\eta)\cdot(\dot\nu,\zeta))\,F(\nu,\eta)^{-1}, \\ (DF(\nu,\eta)\cdot(\dot\nu,\zeta))\,(\mu+\nu) + F(\nu,\eta)\,\dot\nu). \end{aligned}$$

(using left-trivialisation in the first component). Hence,

$$\begin{aligned} &(\Phi^*\Omega_c)(e,\nu,\mathrm{ad}^*_\eta\,\mu)((\xi_1,\dot\nu_1,\mathrm{ad}^*_{\zeta_1}\,\mu)(\xi_2,\dot\nu_2,\mathrm{ad}^*_{\zeta_2}\,\mu)) \\ &= \Omega_c(gF(\nu,\eta)^{-1}, F(\nu,\eta)(\mu+\nu)) \\ &\quad((\mathrm{Ad}_{F(\nu,\eta)}\,\xi_1 - (DF(\nu,\eta)\cdot(\dot\nu_1,\zeta_1))F(\nu,\eta)^{-1}, \\ &\qquad (DF(\nu,\eta)\cdot(\dot\nu_1,\zeta_1))(\mu+\nu) + F(\nu,\eta)\,\dot\nu_1), \\ &\qquad (\mathrm{Ad}_{F(\nu,\eta)}\,\xi_2 - (DF(\nu,\eta)\cdot(\dot\nu_2,\zeta_2))F(\nu,\eta)^{-1}, \\ &\qquad (DF(\nu,\eta)\cdot(\dot\nu_2,\zeta_2))(\mu+\nu) + F(\nu,\eta)\,\dot\nu_2)) \\ &= \langle F(\nu,\eta)(\mu+\nu), \\ &[\mathrm{Ad}_{F(\nu,\eta)}\,\xi_1 - (DF(\nu,\eta)\cdot(\dot\nu_1,\zeta_1))F(\nu,\eta)^{-1}, \\ &\qquad \mathrm{Ad}_{F(\nu,\eta)}\,\xi_2 - (DF(\nu,\eta)\cdot(\dot\nu_2,\zeta_2))F(\nu,\eta)^{-1}]\rangle \\ &\quad + \langle(DF(\nu,\eta)\cdot(\dot\nu_2,\zeta_2))(\mu+\nu) + F(\nu,\eta)\,\dot\nu_2, \\ &\qquad \mathrm{Ad}_{F(\nu,\eta)}\,\xi_1 - (DF(\nu,\eta)\cdot(\dot\nu_1,\zeta_1))F(\nu,\eta)^{-1}\rangle \\ &\quad - \langle(DF(\nu,\eta)\cdot(\dot\nu_1,\zeta_1))(\mu+\nu) + F(\nu,\eta)\,\dot\nu_1, \\ &\qquad \mathrm{Ad}_{F(\nu,\eta)}\,\xi_2 - (DF(\nu,\eta)\cdot(\dot\nu_2,\zeta_2))F(\nu,\eta)^{-1}\rangle. \end{aligned}$$

To verify the condition $\Phi^*\Omega_c = \Omega_Y$, we must consider all pairs of tangent vectors $(\xi_i,\dot\nu_i,\zeta_i)$. By linearity, it suffices to consider only tangent vectors where two of these three components are zero. Thus there are 9 types of tangent vector pairs to consider, which reduce to 6 types by skew-symmetry. The $\xi-\xi$ case has already been considered above, with the conclusion that the pull-back condition is automatically satisfied for arbitrary F. This same conclusion will now be shown to apply in the $\xi-\dot\nu$ and $\xi-\zeta$ cases. Finally, we will combine the remaining 3 cases into one $(\nu,\zeta)-(\nu,\zeta)$ case, which will lead to the Tube Condition in Proposition 1.

Case $\xi - \dot{\nu}$:

$$\begin{aligned}
&\left(\Phi^* \Omega_c\right)(e, \nu, \mathrm{ad}^*_\eta\, \mu)\left((\xi_1, 0, 0)\,(0, \dot{\nu}_2, 0)\right)\\
&= \left\langle F\,(\nu, \eta)\,(\mu + \nu), \left[\mathrm{Ad}_{F(\nu,\eta)}\,\xi_1, -\left(DF(\nu, \eta)\cdot(\dot{\nu}_2, 0)\right) F(\nu, \eta)^{-1}\right]\right\rangle\\
&\quad + \left\langle \left(DF(\nu, \eta)\cdot(\dot{\nu}_2, 0)\right)(\mu + \nu) + F(\nu, \eta)\,\dot{\nu}_2, \mathrm{Ad}_{F(\nu,\eta)}\,\xi_1\right\rangle\\
&= \left\langle F\,(\nu, \eta)\,(\mu + \nu), \left[\left(DF(\nu, \eta)\cdot(\dot{\nu}_2, 0)\right) F(\nu, \eta)^{-1}, \mathrm{Ad}_{F(\nu,\eta)}\,\xi_1\right]\right\rangle\\
&\quad + \left\langle \left(DF(\nu, \eta)\cdot(\dot{\nu}_2, 0)\right)(\mu + \nu), \mathrm{Ad}_{F(\nu,\eta)}\,\xi_1\right\rangle\\
&\quad + \left\langle F(\nu, \eta)\,\dot{\nu}_2, \mathrm{Ad}_{F(\nu,\eta)}\,\xi_1\right\rangle
\end{aligned}$$

Using explicit notation for the coadjoint action gives:

$$\begin{aligned}
&\left\langle \mathrm{Ad}^*_{F(\nu,\eta)^{-1}}(\mu + \nu), \mathrm{ad}_{\left(DF(\nu,\eta)\cdot(\dot{\nu}_2,0)\right)F(\nu,\eta)^{-1}}\left(\mathrm{Ad}_{F(\nu,\eta)}\,\xi_1\right)\right\rangle\\
&\quad + \left\langle -\mathrm{Ad}^*_{F(\nu,\eta)^{-1}}\,\mathrm{ad}^*_{F(\nu,\eta)^{-1}\left(DF(\nu,\eta)\cdot(\dot{\nu}_2,0)\right)}(\mu + \nu), \mathrm{Ad}_{F(\nu,\eta)}\,\xi_1\right\rangle\\
&\quad + \left\langle \mathrm{Ad}^*_{F(\nu,\eta)^{-1}}\,\dot{\nu}_2, \mathrm{Ad}_{F(\nu,\eta)}\,\xi_1\right\rangle\\
&= \left\langle \mathrm{Ad}^*_{F(\nu,\eta)^{-1}}(\mu + \nu), \mathrm{ad}_{\left(DF(\nu,\eta)\cdot(\dot{\nu}_2,0)\right)F(\nu,\eta)^{-1}}\left(\mathrm{Ad}_{F(\nu,\eta)}\,\xi_1\right)\right\rangle\\
&\quad - \left\langle \mathrm{ad}^*_{\left(DF(\nu,\eta)\cdot(\dot{\nu}_2,0)\right)F(\nu,\eta)^{-1}}\left(\mathrm{Ad}^*_{F(\nu,\eta)^{-1}}(\mu + \nu)\right), \mathrm{Ad}_{F(\nu,\eta)}\,\xi_1\right\rangle\\
&\quad + \langle \dot{\nu}_2, \xi_1\rangle\\
&= \langle \dot{\nu}_2, \xi_1\rangle\\
&= \Omega_Y(e, \nu, \mathrm{ad}^*_\eta\, \mu)\left((\xi_1, 0, 0)\,(0, \dot{\nu}_2, 0)\right), \qquad \text{for all } \xi_1, \dot{\nu}_2
\end{aligned}$$

automatically, for all functions F.

Case $\xi - \zeta$:

$$\begin{aligned}
&\left(\Phi^* \Omega_c\right)(e, \nu, \mathrm{ad}^*_\eta\, \mu)\left((\xi_1, 0, 0), \left(0, 0, \mathrm{ad}^*_{\zeta_2}\,\mu\right)\right)\\
&= \left\langle F\,(\nu, \eta)\,(\mu + \nu), \left[\mathrm{Ad}_{F(\nu,\eta)}\,\xi_1, -\left(DF(\nu, \eta)\cdot(0, \zeta_2)\right) F(\nu, \eta)^{-1}\right]\right\rangle\\
&\quad + \left\langle \left(DF(\nu, \eta)\cdot(0, \zeta_2)\right)(\mu + \nu), \mathrm{Ad}_{F(\nu,\eta)}\,\xi_1\right\rangle\\
&= 0\\
&= \Omega_Y(e, \nu, \mathrm{ad}^*_\eta\, \mu)\left((\xi_1, 0, 0)\,(0, 0, \zeta_2)\right), \qquad \text{for all } \xi_1, \zeta_2
\end{aligned}$$

automatically, for all functions F.

Case $(\dot{\nu},\zeta)-(\dot{\nu},\zeta)$ (three cases combined)

$$
\begin{aligned}
&\left(\Phi^{*}\Omega_{c}\right)(e,\nu,\mathrm{ad}_{\eta}^{*}\,\mu)\left(\left(0,\dot{\nu}_{1},\mathrm{ad}_{\zeta_{1}}^{*}\,\mu\right)\left(0,\dot{\nu}_{2},\mathrm{ad}_{\zeta_{2}}^{*}\,\mu\right)\right)\\
&=\left\langle F\,(\nu,\eta)\,(\mu+\nu),\left[(DF(\nu,\eta)\cdot(\dot{\nu}_{1},\zeta_{1}))\,F(\nu,\eta)^{-1},\right.\right.\\
&\qquad\left.\left.(DF(\nu,\eta)\cdot(\dot{\nu}_{2},\zeta_{2}))\,F(\nu,\eta)^{-1}\right]\right\rangle\\
&\quad-\left\langle(DF(\nu,\eta)\cdot(\dot{\nu}_{2},\zeta_{2}))\,(\mu+\nu),(DF(\nu,\eta)\cdot(\dot{\nu}_{1},\zeta_{1}))\,F(\nu,\eta)^{-1}\right\rangle\\
&\quad+\left\langle(DF(\nu,\eta)\cdot(\dot{\nu}_{1},\zeta_{1}))\,(\mu+\nu),(DF(\nu,\eta)\cdot(\dot{\nu}_{2},\zeta_{2}))\,F(\nu,\eta)^{-1}\right\rangle\\
&\quad-\left\langle F(\nu,\eta)\,\dot{\nu}_{2},(DF(\nu,\eta)\cdot(\dot{\nu}_{1},\zeta_{1}))\,F(\nu,\eta)^{-1}\right\rangle\\
&\quad+\left\langle F(\nu,\eta)\,\dot{\nu}_{1},(DF(\nu,\eta)\cdot(\dot{\nu}_{2},\zeta_{2}))\,F(\nu,\eta)^{-1}\right\rangle.
\end{aligned}
$$

Using explicit notation for the coadjoint action gives:

$$
\begin{aligned}
&\left(\Phi^{*}\Omega_{c}\right)(e,\nu,\mathrm{ad}_{\eta}^{*}\,\mu)\left(\left(0,\dot{\nu}_{1},\mathrm{ad}_{\zeta_{1}}^{*}\,\mu\right)\left(0,\dot{\nu}_{2},\mathrm{ad}_{\zeta_{2}}^{*}\,\mu\right)\right)\\
&=\left\langle\mathrm{Ad}_{F(\nu,\eta)^{-1}}^{*}(\mu+\nu),\left[(DF(\nu,\eta)\cdot(\dot{\nu}_{1},\zeta_{1}))\,F(\nu,\eta)^{-1},\right.\right.\\
&\qquad\left.\left.(DF(\nu,\eta)\cdot(\dot{\nu}_{2},\zeta_{2}))\,F(\nu,\eta)^{-1}\right]\right\rangle\\
&\quad-\left\langle\mathrm{ad}_{(DF(\nu,\eta)\cdot(\dot{\nu}_{2},\zeta_{2}))F(\nu,\eta)^{-1}}^{*}\left(\mathrm{Ad}_{F(\nu,\eta)^{-1}}^{*}(\mu+\nu)\right),\right.\\
&\qquad\left.(DF(\nu,\eta)\cdot(\dot{\nu}_{1},\zeta_{1}))\,F(\nu,\eta)^{-1}\right\rangle\\
&\quad+\left\langle\mathrm{ad}_{(DF(\nu,\eta)\cdot(\dot{\nu}_{1},\zeta_{1}))F(\nu,\eta)^{-1}}^{*}\left(\mathrm{Ad}_{F(\nu,\eta)^{-1}}^{*}(\mu+\nu)\right),\right.\\
&\qquad\left.(DF(\nu,\eta)\cdot(\dot{\nu}_{2},\zeta_{2}))\,F(\nu,\eta)^{-1}\right\rangle\\
&\quad-\left\langle\dot{\nu}_{2},F(\nu,\eta)^{-1}\,(DF(\nu,\eta)\cdot(\dot{\nu}_{1},\zeta_{1}))\right\rangle\\
&\quad+\left\langle\dot{\nu}_{1},F(\nu,\eta)^{-1}\,(DF(\nu,\eta)\cdot(\dot{\nu}_{2},\zeta_{2}))\right\rangle\\
&=-\left\langle\mathrm{Ad}_{F(\nu,\eta)^{-1}}^{*}(\mu+\nu),\left[(DF(\nu,\eta)\cdot(\dot{\nu}_{1},\zeta_{1}))\,F(\nu,\eta)^{-1},\right.\right.\\
&\qquad\left.\left.(DF(\nu,\eta)\cdot(\dot{\nu}_{2},\zeta_{2}))\,F(\nu,\eta)^{-1}\right]\right\rangle\\
&\quad-\left\langle\dot{\nu}_{2},F(\nu,\eta)^{-1}\,(DF(\nu,\eta)\cdot(\dot{\nu}_{1},\zeta_{1}))\right\rangle+\left\langle\dot{\nu}_{1},F(\nu,\eta)^{-1}\,(DF(\nu,\eta)\cdot(\dot{\nu}_{2},\zeta_{2}))\right\rangle\\
&=-\left\langle\mu+\nu,\left[F(\nu,\eta)^{-1}\,(DF(\nu,\eta)\cdot(\dot{\nu}_{1},\zeta_{1}))\,,F(\nu,\eta)^{-1}\,(DF(\nu,\eta)\cdot(\dot{\nu}_{2},\zeta_{2}))\right]\right\rangle\\
&\quad-\left\langle\dot{\nu}_{2},F(\nu,\eta)^{-1}\,(DF(\nu,\eta)\cdot(\dot{\nu}_{1},\zeta_{1}))\right\rangle+\left\langle\dot{\nu}_{1},F(\nu,\eta)^{-1}\,(DF(\nu,\eta)\cdot(\dot{\nu}_{2},\zeta_{2}))\right\rangle.
\end{aligned}
$$

We need this to equal

$$\Omega_Y(e,\nu,\mathrm{ad}^*_\eta\,\mu)\left(\left(0,\dot\nu_1,\mathrm{ad}^*_{\zeta_1}\,\mu\right)\left(0,\dot\nu_2,\mathrm{ad}^*_{\zeta_2}\,\mu\right)\right) = -\langle\mu,[\zeta_1,\zeta_2]\rangle\,,$$

for all $\nu,\dot\nu_1,\dot\nu_2\in\mathfrak{g}^*_\mu$, for all $\eta,\zeta_1,\zeta_2\in\mathfrak{g}^\perp$. This proves the Tube Condition.

Remark 3. We note the three special cases that were combined in the "$(\dot\nu,\zeta)-(\dot\nu,\zeta)$" case above:

Case $\dot\nu-\dot\nu$: When $\dot\zeta_1=\dot\zeta_2=0$, the condition in the proposition is equivalent to:

$$\begin{aligned}&\left\langle\mu+\nu,\left[F(\nu,\eta)^{-1}\left(DF(\nu,\eta)\cdot(\dot\nu_1,0)\right),F(\nu,\eta)^{-1}\left(DF(\nu,\eta)\cdot(\dot\nu_2,0)\right)\right]\right\rangle\\&+\left\langle\dot\nu_2,F(\nu,\eta)^{-1}\left(DF(\nu,\eta)\cdot(\dot\nu_1,0)\right)\right\rangle-\left\langle\dot\nu_1,F(\nu,\eta)^{-1}\left(DF(\nu,\eta)\cdot(\dot\nu_2,0)\right)\right\rangle=0.\end{aligned}$$

Note that a sufficient condition is that $(DF(\nu,\eta)\cdot(\dot\nu_1,0))$ is a multiple of $(DF(\nu,\eta)\cdot(\dot\nu_2,0))$ and $F(\nu,\eta)^{-1}\left(DF(\nu,\eta)\cdot(\dot\nu_1,0)\right)\in\mathfrak{g}^\perp_\mu$ for all $\dot\nu_1,\dot\nu_2\in\mathfrak{g}^*_\mu$.

Case $\dot\nu-\zeta$: When $\dot\zeta_1=\dot\nu_2=0$, the condition in the proposition is equivalent to:

$$\begin{aligned}&-\left\langle(\mu+\nu),\left[F(\nu,\eta)^{-1}\left(DF(\nu,\eta)\cdot(\dot\nu_1,0)\right),F(\nu,\eta)^{-1}\left(DF(\nu,\eta)\cdot(0,\zeta_2)\right)\right]\right\rangle\\&+\left\langle\dot\nu_1,F(\nu,\eta)^{-1}\left(DF(\nu,\eta)\cdot(0,\zeta_2)\right)\right\rangle=0\end{aligned}$$

all $\dot\nu_1,\zeta_2$, since $\Omega_Y(e,\nu,\mathrm{ad}^*_\eta\,\mu)\left((0,\dot\nu_1,0),(0,0,\zeta_2)\right)=0$.

Case $\zeta-\zeta$: When $\dot\nu_1=\dot\nu_2=0$, the condition in the proposition is equivalent to:

$$\begin{aligned}&\left\langle\mu+\nu,\left[F(\nu,\eta)^{-1}\left(DF(\nu,\eta)\cdot\ (0,\zeta_1)\right),F(\nu,\eta)^{-1}\left(DF(\nu,\eta)\cdot\ (0,\zeta_2)\right)\right]\right\rangle\\&=\langle\mu,[\zeta_1,\zeta_2]\rangle\,.\end{aligned}\tag{37}$$

The last case above may be compared with the following:

Restatement of Lemma 2 Let $\varphi:T_\mu\mathscr{O}_\mu\to\mathscr{O}_\mu$ be of the form $\varphi(-\mathrm{ad}^*_\eta\,\mu)=f(\eta)\mu$ for some $f:\mathfrak{g}^\perp_\mu\to G$. Then φ preserves the $-$KKS symplectic form if and only if

$$\begin{aligned}\langle\mu,[\zeta_1,\zeta_2]\rangle&=\left\langle f(\eta)\mu,\left[(Df(\eta)\cdot\zeta_1)\,f(\eta)^{-1},(Df(\eta)\cdot\zeta_2)\,f(\eta)^{-1}\right]\right\rangle\\&=\left\langle\mu,\left[f(\eta)^{-1}\left(Df(\eta)\cdot\zeta_1\right),f(\eta)^{-1}\left(Df(\eta)\cdot\zeta_2\right)\right]\right\rangle\end{aligned}\tag{38}$$

for all $\eta,\zeta_1,\zeta_2\in\mathfrak{g}^\perp_\mu$.

Proof. $D\varphi(-\mathrm{ad}^*_\eta\,\mu)\cdot\left(-\mathrm{ad}^*_\zeta\,\mu\right)=(Df(\eta)\cdot\zeta)\,\mu$ (using the "hat" map for μ), which corresponds to

$$-\mathrm{ad}^*_{(Df(\eta)\cdot\zeta_1)\,f(\eta)^{-1}}\left(\mathrm{Ad}^*_{f(\eta)^{-1}}\,\mu\right),$$

so

$$\begin{aligned}
&\left(\varphi^*\Omega^-_{KKS}\right)\left(-\operatorname{ad}^*_\eta\mu\right)\left(-\operatorname{ad}^*_{\zeta_1}\mu,-\operatorname{ad}^*_{\zeta_2}\mu\right)\\
&\quad=\Omega^-_{KKS}(f(\eta)\mu)\left((Df(\eta)\cdot\zeta_1)\,\mu,(Df(\eta)\cdot\zeta_2)\,\mu\right)\\
&\quad=\Omega^-_{KKS}(\operatorname{Ad}^*_{f(\eta)^{-1}}\mu)\left(\operatorname{ad}^*_{(Df(\eta)\cdot\zeta_1)f(\eta)^{-1}}\left(\operatorname{Ad}^*_{f(\eta)^{-1}}\mu\right),\right.\\
&\qquad\left.\operatorname{ad}^*_{(Df(\eta)\cdot\zeta_2)f(\eta)^{-1}}\left(\operatorname{Ad}^*_{f(\eta)^{-1}}\mu\right)\right)\\
&\quad=\left\langle\operatorname{Ad}^*_{f(\eta)^{-1}}\mu,\left[(Df(\eta)\cdot\zeta_1)\,f(\eta)^{-1},(Df(\eta)\cdot\zeta_2)\,f(\eta)^{-1}\right]\right\rangle\\
&\quad=\left\langle\mu,\left[\operatorname{Ad}_{f(\eta)^{-1}}\left((Df(\eta)\cdot\zeta_1)\,f(\eta)^{-1}\right),\operatorname{Ad}_{f(\eta)^{-1}}\left((Df(\eta)\cdot\zeta_2)\,f(\eta)^{-1}\right)\right]\right\rangle\\
&\quad=\left\langle\mu,\left[f(\eta)^{-1}\,(Df(\eta)\cdot\zeta_1),\,f(\eta)^{-1}\,(Df(\eta)\cdot\zeta_2)\right]\right\rangle
\end{aligned}$$

The similarity of conditions (37) and (38) led to the discovery of an explicit construction of a symplectic tube for $G=SO(3)$, see Section 2.3.

Finally, we prove Lemma 5 in Section 2.3. This lemma concerns an Ansatz that is motivated by our consideration of the $SO(3)$ case. However, the lemma is valid for all Lie groups.

Restatement of Lemma 5 Suppose $F(\nu,\eta)=\exp\left(h(\nu,\eta)\,\frac{\eta}{\|\eta\|}\right)$, for some $h:\mathfrak{g}^*_\mu\times\mathfrak{g}^\perp_\mu\to\mathbb{R}$. Then the Tube Condition in Proposition 1 is automatically satisfied (regardless of the definition of h) for all $(\dot\nu_1,\zeta_1),(\dot\nu_2,\zeta_2)$ such that ζ_1 and ζ_2 are parallel to η.

Proof. For arbitrary $f:\mathbb{R}\to M(n,\mathbb{R})$, if $f'(0)$ is a multiple of $f(0)$ then they commute, so

$$\left.\frac{d}{dt}\right|_{t=0}\exp(f(t))=\left.\frac{d}{dt}\right|_{t=0}\exp\left(f(0)+tf'(0)\right)=\exp(f(0))\,f'(0)\tag{39}$$

$$=f'(0)\exp(f(0)).\tag{40}$$

Let $f(t)=h\left((\nu,\eta)+t(\dot\nu,\zeta)\right)\frac{\eta}{\|\eta\|}$. If ζ is parallel to η then $\dfrac{\eta+t\zeta}{\|\eta+t\zeta\|}=\dfrac{\eta}{\|\eta\|}$, so

$$\begin{aligned}
DF(\nu,\eta)\cdot(\dot\nu,\zeta)&=\left.\frac{d}{dt}\right|_{t=0}F\left((\nu,\eta)+t(\dot\nu,\zeta)\right)\\
&=\left.\frac{d}{dt}\right|_{t=0}\exp\left(h\left((\nu,\eta)+t(\dot\nu,\zeta)\right)\frac{\eta}{\|\eta\|}\right)\\
&=\left.\frac{d}{dt}\right|_{t=0}\exp(f(t))
\end{aligned}$$

$$
\begin{aligned}
&= f'(0)\exp\left(f(0)\right)\\
&= \left(Dh(\nu,\eta)\cdot(\dot{\nu},\zeta)\right)\frac{\eta}{\|\eta\|}F(\nu,\eta)\\
&= F(\nu,\eta)\left(Dh(\nu,\eta)\cdot(\dot{\nu},\zeta)\right)\frac{\eta}{\|\eta\|}.
\end{aligned}
$$

Thus if ζ_1 and ζ_2 are parallel to η,

$$\left[F(\nu,\eta)^{-1}\left(DF(\nu,\eta)\cdot\left(\dot{\nu}_1,\zeta_1\right)\right),F(\nu,\eta)^{-1}\left(DF(\nu,\eta)\cdot\left(\dot{\nu}_2,\zeta_2\right)\right)\right]=0$$

and

$$\left\langle\dot{\nu}_i,F(\nu,\eta)^{-1}\left(DF(\nu,\eta)\cdot\left(\dot{\nu}_j,\zeta_j\right)\right)\right\rangle=0,$$

for all $i,j=1,2$. Therefore the Tube Condition in Proposition 1 holds.

References

1. Abraham, R., Marsden, J.: Foundations of Mechanics, 2nd edn. Addison-Wesley, Redwood (1978)
2. Bates, L., Lerman, E.: Proper group actions and symplectic stratified spaces. Pac. J. Math. **181**(2), 201–229 (1997)
3. Benettin, G., Fassò, F., Guzzo, M.: Long term stability of proper rotations of the perturbed Euler rigid body. Commun. Math. Phys. **250**, 133–160 (2004)
4. Broer, H.W.: Normal forms in perturbation theory. In: Meyers, R. (ed.) Encyclopaedia of Complexity and System Science. Springer, New York (2009)
5. Çiftçi, U., Waalkens, H.: Phase space structures governing reaction dynamics in rotating molecules. Nonlinearity **25**(3), 791 (2012)
6. Çiftçi, U., Waalkens, H., Broer, H.W.: Cotangent bundle reduction and Poincaré-Birkhoff normal forms. Physica D **268**, 1–13 (2014)
7. Fassò, F., Guzzo, M., Benettin, G.: Nekhoroshev-stability of elliptic equilibria of Hamiltonian systems. Commun. Math. Phys. **197**, 347–360 (1998)
8. Guillemin, V., Sternberg, S.: A normal form for the moment map. In: S. Sternberg (ed.) Differential Geometric Methods in Mathematical Physics. Mathematical Physics Studies, vol. 6. Reidel, Dordrecht (1984)
9. Holm, D.D., Schmah, T., Stoica, C.: Geometric Mechanics and Symmetry: From Finite to Infinite Dimensions. Oxford University Press, Oxford (2009)
10. Lamb, J., Melbourne, I.: Normal forms theory for relative equilibria and relative periodic solutions. Trans. AMS **359**(9), 4537–4556 (2007)
11. Marle, C.M.: Modèle d'action hamiltonienne d'un groupe de Lie sur une variété symplectique. Rendiconti del Seminario Matematico, Università e Politecnico, Torino **43**(2), 227–251 (1985)
12. Marsden, J.: Lectures on Mechanics. London Mathematical Society Lecture Note Series, vol. 174. Cambridge University Press, Cambridge (1992)
13. Marsden, J., Ratiu, T.: Introduction to Mechanics and Symmetry: A Basic Exposition of Classical Mechanical Systems, 2nd edn. Springer, New York (1999)

14. Montaldi, J., Ratiu, T. (eds.): Geometric Mechanics and Symmetry: The Peyresq Lectures. London Mathematical Society Lecture Notes Series, vol. 306. Cambridge University Press, Cambridge (2005)
15. Montaldi, J., Roberts, M.: Relative equilibria of molecules. Nonlinear Sci. **9**, 53–88 (1999)
16. Nekhoroshev, N.: An exponential estimate of the time of stability of nearly-integrable hamiltonian systems. Russ. Math. Surv. **32**, 1–65 (1977)
17. Niederman, L.: Nonlinear stability around an elliptic equilibrium point in a Hamiltonian system. Nonlinearity **11**(6), 1465–1479 (1998)
18. Ortega, J.P., Ratiu, T.: Momentum Maps and Hamiltonian Reduction. Progress in Mathematics. Birkhäuser, Boston (2004)
19. Palais, R.: On the existence of slices for actions of non-compact Lie groups. Ann. Math. **73**, 295–323 (1961)
20. Patrick, G.W.: Relative equilibria in hamiltonian systems: the dynamic interpretation of nonlinear stability on a reduced phase space. J. Geom. Phys. **9**, 111–119 (1992)
21. Pöschel, J.: On Nekhoroshev's estimate at an elliptic equilibrium. Int. Math. Res. Not. **4**, 203–215 (1999)
22. Roberts, M., Wulff, C., Lamb, J.: Hamiltonian systems near relative equilibria. J. Differ. Eq. **179**, 562–604 (2002)
23. Roberts, M., Schmah, T., Stoica, C.: Relative equilibria in systems with configuration space isotropy. J. Geom. Phys. **56**, 762–779 (2006)
24. Schmah, T.: A cotangent bundle slice theorem. Differ. Geom. Appl. **25**, 101–124 (2007)
25. Simo, J., Lewis, D., Marsden, J.: Stability of relative equilibria. Part I: the reduced energy momentum method. Arch. Ration. Mech. Anal. **115**, 15–59 (1991)

Polite Actions of Non-compact Lie Groups

Larry Bates and Jędrzej Śniatycki

Abstract Based mainly on examples of interest in mechanics, we define the notion of a polite group action. One may view this as not only trying to give a more general notion than properness of a group action, but also to more fully understand the role of invariant functions in describing just about everything of interest in reduction.

We show that a polite action of a symmetry group of a dynamical system admits reduction and reconstruction.

1 Introduction

Dirac's seminal 1950 paper [6] showed how to construct a reduced bracket on a Hamiltonian system with constraints, but did not focus on constraints generated by the action of a symmetry group. The first significant theory of reduction of a Hamiltonian system with symmetry was given by Meyer in 1973 [9], and this was followed by work of Marsden and Weinstein a year later [8]. Since then there has been a veritable flood of papers endeavouring to understand reduction and various forms of singular behaviour. For example, many of these works have studied what happens when the action of the symmetry group is not free and quotient spaces are not manifolds. It is probably fair to say that a reasonably complete reduction theory now exists in the case that the group action is proper (see, for example, [2, 5, 11–13]). Here we make the case that since there are interesting, important examples in mechanics where the symmetry group does not act properly, a less restrictive notion of group action warrants consideration.

This paper defines the notion of a *polite* action, and gives some examples. In addition, it proves that a polite action of the symmetry group of a dynamical system admits reduction and reconstruction. This means that the dynamical vector field projects to a vector field on a reduced space, and that the original dynamics can be recovered from the dynamics on the reduced space. This is all done in the context of vector fields and differential equations on manifolds.

L.M. Bates • J. Śniatycki (✉)
Department of Mathematics, University of Calgary, Calgary, AB, Canada T2N 1N4
e-mail: bates@ucalgary.ca; sniatyck@ucalgary.ca

D.E. Chang et al. (eds.), *Geometry, Mechanics, and Dynamics*, Fields Institute Communications 73, DOI 10.1007/978-1-4939-2441-7_18

Since the possibility exists that our notion of a polite action is not the last word on group actions in mechanics, we hope that, in the spirit of this commemorative volume, others will provide even better solutions to the problem of 'what's next'.

2 Motivating Examples

The following examples motivate why one needs to deal with problems where the group action is not proper, so that strictly speaking the usual reduction theories do not apply.

1. The one-dimensional harmonic oscillator. Here the Hamiltonian is $h(p,q) = \frac{1}{2}p^2 + \frac{1}{2}q^2$ on the phase space $P = T^*\mathbb{R}$. All solutions of Hamilton's equations are periodic with period 2π. The Hamiltonian flow ϕ_t is

$$\phi_t \begin{pmatrix} q_0 \\ p_0 \end{pmatrix} = \begin{pmatrix} \cos t & \sin t \\ -\sin t & \cos t \end{pmatrix} \begin{pmatrix} q_0 \\ p_0 \end{pmatrix}.$$

   The action of $\mathbb{R}$ on P is not proper but is indistinguishable from the free proper action of the compact group $\mathbb{R}/2\pi\mathbb{Z}$.
2. The stiff spring. The Hamiltonian is, for $\epsilon > 0$,

$$h(q,p) = \frac{1}{2}p^2 + \frac{1}{2}q^2 + \frac{\epsilon}{4}q^4.$$

   Hamilton's equations yield Duffing's equation $q'' + q + \epsilon q^3 = 0$. This implies that the solution may be written in terms of the Jacobi elliptic function cn as

$$q(t) = \mathrm{cn}\left(\sqrt{1+\epsilon}\, t; \sqrt{\frac{\epsilon}{2(1+\epsilon)}}\right).$$

   Here the parameters are chosen so that $q(t)$ solves the initial value problem

$$q'' + q + \epsilon q^3 = 0, \qquad q(0) = 1, \quad q'(0) = 0,$$

   for $\epsilon > 0$. It follows that the period τ is

$$\begin{aligned} \tau &= \frac{4}{\sqrt{1+\epsilon}} K\left(\sqrt{\frac{\epsilon}{2(1+\epsilon)}}\right), \\ &= 2\pi\left(1 - \frac{3}{8}\epsilon + \frac{57}{256}\epsilon^2 + \cdots\right), \end{aligned}$$

   where $K(k)$ is the complete elliptic integral of the first kind. It is now easy to solve for other initial conditions to find the period as a function of the energy h

and ϵ. The Hamiltonian flow ϕ_t, which is an action of $\mathbb{R}$ on $P = T^*\mathbb{R}$ is still periodic, but not proper. In this case there is no *fixed* subgroup G of $\mathbb{R}$ with the flow ϕ_t being a proper $\mathbb{R}/G$ action (although we can do this individually for each orbit). However, it is common practice in mechanics to rescale the Hamiltonian vector field X_h by the period τ to produce a new vector field $Y = \tau X_h$, all of whose integral curves are periodic of period 1. It is a theorem that the resulting vector field Y is still a Hamiltonian vector field, and we produce a new variable called the action (see, for example [4]). In this way a free proper action ψ_t of the compact group SO(2) is associated to the original nonproper action ϕ_t by setting $\psi_t := \phi_{\tau t}$.

3. The champagne bottle. The Hamiltonian in this case is

$$h = \frac{1}{2}(p_1^2 + p_2^2) + (q_1^2 + q_2^2)^2 - (q_1^2 + q_2^2)$$

on the phase space $P = T^*\mathbb{R}^2$. This is a completely integrable system because of the rotational invariance. The Hamiltonian h, together with the angular momentum j gives the construction of action variables (I_1, I_2) that generate a torus action whose orbits contain the original quasiperiodic trajectories of the Hamiltonian. In this way, a proper group action is associated to the non-proper Hamiltonian action of $\mathbb{R}^2$ associated to the flow of the commuting Hamiltonian vector fields of the energy and the angular momentum (see [3] for more details). However, what is interesting in this case is that the construction of the actions is only local because of the presence of an obstruction called monodromy preventing the torus group action being globally well-defined (see [1]).

4. A nonabelian example. We construct an oriented S^3 bundle over $\mathbb{R}^3\backslash\{0\}$. The fiber S^3 is diffeomorphic to the group Spin(3), but the bundle is not a principal bundle. In a sense, we may view this example as a simply-connected version of the previous example.

   To start, consider the two copies of the trivial bundle $D^2 \times S^3$, which we think of as local trivializations of our bundle over the upper and lower hemispheres of the sphere S^2. Viewing S^3 as the unit sphere in $\mathbb{R}^4$, we consider the gluing map from one hemisphere to another as a map from the equator into $\mathrm{Diff}^+(S^3)$. By a theorem of Hatcher [7], this diffeomorphism group retracts onto the orthogonal group SO(4). The orthogonal group is diffeomorphic to the product SO(3) × Spin(3), and has fundamental group $\mathbb{Z}_2$. The transition map from one hemisphere to the other is given by the map

$$S^1 \longrightarrow \mathrm{SO}(4) : \phi \longrightarrow \begin{pmatrix} \cos\phi & -\sin\phi & 0 & 0 \\ \sin\phi & \cos\phi & 0 & 0 \\ 0 & 0 & 1 & 0 \\ 0 & 0 & 0 & 1 \end{pmatrix}.$$

This map is a generator of the fundamental group of SO(4) because the matrix represented by the upper left 2×2 block is a generator of the fundamental group of SO(2), and we have the natural inclusions

$$\mathrm{SO}(2) \hookrightarrow \mathrm{SO}(3) \hookrightarrow \mathrm{SO}(4)$$

and thus a surjection in homotopy $\pi_1(\mathrm{SO}(2)) \longrightarrow \pi_1(\mathrm{SO}(4))$. This implies that the bundle is not a trivial bundle.

Observe that the south pole $(0, 0, 0, 1)$ on the sphere S^3 is fixed by the transition map, and this implies that the map $S^2 \longrightarrow$ 'south pole' is a global section of the bundle. This fact, together with the nontriviality of the bundle implies that the bundle is not a principal Spin(3) bundle, as any principal bundle with a global section must be globally trivial.

Reviewing this example from the point of view of classifying spaces suggests that many more such examples may be constructed by considering Spin(3) bundles over the four-sphere S^4.

The bundle constructed here may be given a symplectic structure by embedding the sphere S^2 into $\mathbb{R}^3 \backslash 0$ in the usual way. In more detail, let S^2 be $x_1^2 + x_2^2 + x_3^2 = 1$, and ψ_1, ψ_2, ψ_3 be the usual left-invariant one-forms on Spin(3). Then the form

$$\omega = \psi_1 \wedge \psi_2 + d(z(x_3)\psi_3) + dx_1 \wedge dx_2$$

is a symplectic form on our bundle where $z(x_3)$ is a function that satisfies 1) $z'(x_3) > 0$ for all x_3, and 2) $|z(x_3)| < 1$ for all x_3. For example, we may take $z(x) = x/\sqrt{1 + x^2}$.

5. Consider the Hamiltonian system given by the motion of the free particle in space (you can take any dimension $n \geq 2$ for space). The Euclidean group $\mathrm{SE}(n)$ acts in a Hamiltonian way on the phase space $T^*\mathbb{R}^n$ and preserves the level set $h^{-1}(1/2)$, which are the straight lines parameterized by arclength. We are of course taking the Hamiltonian to be $h = |p|^2/2$. The components of the momentum map for the Euclidean group are the linear and angular momentum, and as they commute with the Hamiltonian, they induce an action on the quotient space $\bar{P} := h^{-1}(1/2)/\sim$, where the $\sim$ represents the quotient by the Hamiltonian flow $\phi_t(q, p) = (q + tp, p)$. The quotient manifold $\bar{P}$, which is the space of oriented lines in $\mathbb{R}^n$, is naturally endowed with a symplectic structure, as follows from the reduction theorem. Furthermore, the action of the Euclidean group on the quotient $\bar{P}$ is Hamiltonian. This action is not fixed point free and is not proper, as the stability subgroup of a point in the quotient contains the subgroup which corresponds to the translations along the line that it represents. More precisely, the space of lines is the homogeneous space $\mathrm{SE}(n)/(\mathrm{SO}(n-1) \times \mathbb{R}) \sim T^*S^n$. This construction is used when studying the Radon transform, as it involves integration along lines.

3 Polite Actions

Consider a Hamiltonian system (P, ω, h) invariant under the action ϕ of a connected Lie group G. Given a closed subgroup H of G, define

$$P_H := \{p \in P \mid G_p = H\}.$$

Denote by N^H the normalizer of H in G; that is

$$N^H = \{n \in G \mid n^{-1}hn \in H \text{ for all } h \in H\}.$$

The normalizer is a closed subgroup of G.

Lemma 1. *The action of N^H on P preserves P_H.*

Proof. For $p \in P_H$, and $n \in N^H$, the isotropy group G_{np} of np is given by

$$\begin{aligned} G_{np} &= \{g \in G \mid gnp = np\} \\ &= \{g \in G \mid n^{-1}gnp = p\} \\ &= \{g \in G \mid n^{-1}gn \in H\}. \end{aligned}$$

In other words, $g \in G_{np}$ if and only if $h = n^{-1}gn \in H$. Therefore, $g = nhn^{-1} \in H$, and $G_{np} = H$. Hence, $np \in P_H$. Thus, the action of N^H on P preserves P_H.

Since the action of N^H on P preserves P_H, it induces an action of N^H on P_H. Let $G_H = N^H/H$. Since H is closed in G, it is closed in N^H, and G_H is a Lie group. Moreover, there is an action

$$G_H \times P_H \to P_H : ([n], p) = np,$$

where $[n]$ is the equivalence class of n in $G_H = N^H/H$.

Warning: The group G_H is *not* a subgroup of the group G.

Proposition 1. *The action of G_H on P_H is free.*

Proof. For $g \in N^H$, suppose $[g] \in G_H$ preserves a point $p \in P_H$; that is $gp = p$. This means that $g \in G_p = H$. Therefore, $[g]$ is the identity in G_H.

Definition 1. The action of G on P is polite if for each closed subgroup H of G, the set P_H is a manifold and the action of G_H on P_H is proper.

4 Examples of Polite Actions

It is straightforward to check that the group action in all of the following examples (except the third) is polite.

Example 1. The actions in the motivating Examples 1, 2, 3, 5 are all polite.

Example 2. Every action of a compact group is polite because it is proper.

Example 3. The $\mathbb{R}$ action generated by the flow of the vector field $X = \sin x\, \partial_x + \cos x\, \partial_y$ on the plane is free but not polite.

Example 4. The coadjoint action of a compact connected Lie group is polite because this is just the action of the (finite) Weyl group N^H/H on a coadjoint orbit cross an interval.

Example 5. The co-adjoint action of $\mathrm{SL}(2,\mathbb{R})$.

There are three co-adjoint orbits of interest, which we can label as parabolic, hyperbolic and elliptic since the group is semi-simple. The elliptic and hyperbolic ones correspond to Cartan subalgebras, so the corresponding stability groups are self-normalizing. The only nontrivial case is the parabolic one, and here the normalizer is the Borel subgroup which we may take as the upper triangular matrices. The quotient N^H/H in this case acts by dilations on the cone (translations along the ruling), and the action is again seen to be proper.

Example 6. A special class of solvable groups of type $\mathfrak{S}$.

Following Nomizu [10], we say that a group G belongs to the class $\mathfrak{S}$ if the Lie algebra $\mathfrak{g}$ of the Lie group G contains a codimension one commutative ideal $\mathfrak{a}$ and an element Y with the property that $[Y, X] = X$ for all X in the ideal $\mathfrak{a}$. Let $X_1, \ldots, X_n$ be a basis for $\mathfrak{a}$, and let $X_1^*, \ldots, X_n^*, Y^*$ be the corresponding dual basis in the dual space $\mathfrak{g}^*$. Let (a, b) be an element in the half-space $\mathbb{R}^+ \times \mathbb{R}$, and consider the point $\mu = aX_1^* + bY^* \in \mathfrak{g}^*$. Then the non-zero infinitesimal generators of the co-adjoint action are generated by

$$\mathrm{ad}^*_{X_1}|_\mu = -a\frac{\partial}{\partial Y^*}, \qquad \mathrm{ad}^*_{Y}|_\mu = -a\frac{\partial}{\partial X_1^*}.$$

This implies that the co-adjoint orbit through the point μ is the two-dimensional open half plane spanned by Y^* and μ. It follows that the Lie algebra $\mathfrak{h} = \mathrm{span}\{X_2, \ldots, X_n\}$, and hence that the isotropy group $H \sim \mathbb{R}^{n-1}$. Thus the normalizer $N^H = G$ and

$$N^H/H \sim \mathrm{Aff}^+(1,\mathbb{R})$$

acts freely, transitively and properly on the co-adjoint orbit through μ. Note that the action is just the usual action of the affine group on the half-plane.

In light of the previous two examples we make the following

Conjecture 1. The coadjoint action of a Lie group on the dual of its Lie algebra is polite for any group in which the coadjoint orbits are locally closed.

5 Reduction and Reconstruction of Polite Symmetries

We consider a dynamical system given by a smooth vector field X on a manifold P, called the phase space of the system. Evolutions of our dynamical system are integral curves $\gamma : I \to P$ of X, where I is an interval in $\mathbb{R}$.

Let $\phi : G \times P \to P$ be an action of a Lie group G on P. We say that G is a symmetry group of our dynamical system if the action ϕ preserves the vector field X. The *reduced phase space* is the space $\bar{P} = P/G$ of G-orbits in P endowed with a differential structure

$$C^\infty(\bar{P}) = \{f : \bar{P} \to \mathbb{R} \mid \rho^* f \in C^\infty(P)^G\},$$

where $\rho : P \to \bar{P}$ is the orbit map and $C^\infty(P)^G$ is the ring of G-invariant smooth functions on P. It should be noted that the orbit space $\bar{P}$ has two topologies: the quotient space topology and the differential space topology. Here, we take the differential space topology.[1] The reduced dynamical system is the derivation $\rho_* X$ of $C^\infty(\bar{P})$ defined by

$$\rho^*((\rho_* X)(f)) = X(\rho^* f) \tag{1}$$

for every $f \in C^\infty(\bar{P})$.

Proposition 2. *For every integral curve $\gamma : I \to P$ of X, the curve $\rho \circ \gamma : I \to \bar{P} : t \mapsto \rho(\gamma(t))$ satisfies the equation*

$$\frac{d}{dt} f(\rho(\gamma(t))) = ((\rho_* X)(f))(\rho(\gamma(t))) \tag{2}$$

for each $f \in C^\infty(\bar{P})$ and $t \in I$.

Proof. It follows from equation (1) that

$$\begin{aligned} \frac{d}{dt} f(\rho(\gamma(t))) &= \frac{d}{dt}((\rho^* f)(\gamma(t)) = (X(\rho^* f))(\gamma(t)) \\ &= \rho^*((\rho_* X)(f))(\gamma(t)) = ((\rho_* X)(f))(\rho(\gamma(t))). \end{aligned}$$

Equation (2) is called the *reduced equation*. A curve $\rho \circ \gamma : I \to \bar{P}$ satisfying the reduced equation gives a reduced evolution of the system. Given a reduced evolution $\bar{\gamma} : I \to \bar{P}$ of the system, the process of finding integral curves γ of X such that $\rho \circ \gamma = \bar{\gamma}$ is called *reconstruction*. If the action ϕ of G on P is free and proper, the reduced equation as well as equations involved in reconstruction are ordinary differential equations on manifolds.

[1] For applications of the theory of differential spaces to reduction of symmetries see [13].

Definition 2. An action $\phi : G \times P \to P$ that preserves a vector field X on P admits reduction and reconstruction if the reduced equation and equations involved in reconstruction can be presented as differential equations on manifolds.

Theorem 1. *A polite action $\phi : G \times P \to P$ that preserves a vector field X on P admits reduction and reconstruction.*

We shall prove this theorem by a sequence of propositions.

Proposition 3. *Let X be a vector field on P that is invariant under a polite action of a Lie group G on P. For each closed subgroup H of G, the flow of X preserves P_H.*

Proof. Let $\exp tX$ be the local one-parameter group of local diffeomorphisms of P generated by X, and H be a closed subgroup of G. For each $g \in H$ we have

$$g \exp tXg^{-1} = \exp tX,$$

because X is G-invariant and $H \subseteq G$. Hence, for each $p \in P_H$ and $g \in H$,

$$g \exp tX(p) = \exp tXgp = \exp tX(p),$$

which implies that $\exp tX(p) \in P_H$.

Let $\bar{P}_H = \rho(P_H)$ and $\rho_H : P_H \to \bar{P}_H$ be the restriction of ρ to P_H. The following diagram

$$\begin{array}{ccc} & \overset{\iota_H}{} & \\ P_H & \hookrightarrow & P \\ {\scriptstyle \rho_H}\downarrow & & \downarrow{\scriptstyle \rho} \\ \bar{P}_H & \hookrightarrow & \bar{P} \\ & {\scriptstyle \epsilon_H} & \end{array}$$

where the horizontal arrows are the inclusion maps, commutes.

The space $\bar{P}_H$ has the differential structure

$$C_1^\infty(\bar{P}_H) = \{h : \bar{P}_H \to \mathbb{R} |\ \rho_H^* h \in C^\infty(P_H)\}$$

and a differential structure $C_2^\infty(\bar{P}_H)$ generated by the restrictions to $\bar{P}_H$ of smooth functions on $\bar{P}$.

Proposition 4. *The differential structures $C_2^\infty(\bar{P}_H)$ and $C_1^\infty(\bar{P}_H)$ are related by the inclusion*

$$C_2^\infty(\bar{P}_H) \subseteq C_1^\infty(\bar{P}_H).$$

If the action of G on P is improper, $C_2^\infty(\bar{P}_H)$ may be a proper subset of $C_1^\infty(\bar{P}_H)$.

Proof. If $f \in C^\infty(\bar{P})$, then $\epsilon_H^* f = f_{|\bar{P}_H} \in C_2(\bar{P}_H)$. On the other hand, $\rho^* f \in C^\infty(P)$ and the restriction of $\rho^* f$ to P_H is an N^H-invariant smooth function $(\rho^* f)_{|P_H} = \iota_H^* \rho^* f$ on P_H. Moreover, $\rho \circ \iota_H = \epsilon_H \circ \rho_H$ implies that $\iota_H^* \rho^* f = \rho_H^* \epsilon_H^* f$. Therefore, $\epsilon_H^* f \in C_1^\infty(\bar{P}_H)$.

Suppose now that $h : \bar{P}_H \to \mathbb{R}$ is such that, for every $r \in \bar{P}_H$, there exists a neighbourhood U_r of r in $\bar{P}_H$ and a function $f_r \in C^\infty(\bar{P})$ such that $\epsilon_H^* f_{r|U_r} = h_{|U_r}$. By definition of the differential structure generated by a family of functions, $f_r \in C_2^\infty(\bar{P}_H)$. We have shown above that $\epsilon_H^* f_r \in C_1^\infty(\bar{P}_H)$. Hence, $f_{r|\bar{P}_H \cap U_r} = f_{r|U_r}$, which implies

$$C_2^\infty(\bar{P}_H) \subseteq C_1^\infty(\bar{P}_H).$$

On the other hand, suppose that $h \in C_1^\infty(\bar{P}_H)$, which means that $\rho_H^* h \in C^\infty(P_H)^H$. The set

$$P_{(H)} = \{gp \in P \mid g \in G,\ p \in P_H\}$$

is the union of the orbits of G through points in P_H. We can extend the H-invariant function $\rho_H^* h$ on P_H to a G-invariant function k on $P_{(H)}$. If the action of G on P is not proper, we have no guarantee that a G-invariant function k on $P_{(H)}$ extends to a G-invariant function on P, as may be seen in the following example. Let X be the planar vector field

$$X = \sin x\, \partial_x + \cos x\, \partial_y.$$

Since X has bounded norm in the plane (so has a complete flow) and is invariant by translations of 2π in both the x and y directions, X generates an $\mathbb{R}$-action on the torus $\mathbb{R}^2/(2\pi\mathbb{Z}\times 2\pi\mathbb{Z})$ This action is not free only on the two circular orbits through $[(0,0)]$ and $[(\pi,0)]$, and the isotropy group H for these orbits in this case is $2\pi\mathbb{Z}$. Any function that is locally constant on each circle need not extend to an invariant function on the entire torus unless it has the same value on each circle, because the pair of circles are the alpha and omega limit sets of every other trajectory on the torus.

Hence, if the action is not proper, $C_2^\infty(\bar{P}_H)$ may be a proper subset of $C_1^\infty(\bar{P}_H)$.

In the following we shall consider $\bar{P}_H$ with the differential structure $C_1^\infty(\bar{P}_H)$.

Proposition 5. *For each closed subgroup H of G, $\bar{P}_H$ with the differential structure $C_1^\infty(\bar{P}_H)$ is diffeomorphic to P_H/G_H.*

Proof. The differential structure $C_2^\infty(\bar{P}_H)$ of $\bar{P}_H$ consists of pushforwards of N_H-invariant smooth functions on P_H. However, a function $f \in C^\infty(P_H)$ is N_H-invariant if and only if it is G_H-invariant. But the differential structure of P_H/G_H consists of G_H-invariant functions on P_H. Hence, the differential structures of $\bar{P}_H$ and P_H/G_H coincide.

By Proposition 3, for each closed subgroup H of G, the flow $\exp tX$ of the invariant vector field X preserves P_H. The politeness of the action of G on P ensures that P_H is a manifold and that the action of G_H on P_H is proper. Proposition 1 ensures that the action of G_H on P_H is free. Hence, P_H/G_H is a quotient manifold of P_H, and P_H has the structure of a left principal G_H-bundle over P_H/G_H. This implies that both the reduction and the reconstruction of the restriction of X to P_H is the same as in the case of a free and proper action. This completes the proof of Theorem 1.

References

1. Bates, L.: Monodromy in the champagne bottle. J. Appl. Math. Phys. (ZAMP) **42**, 837–847 (1991)
2. Bates, L., Lerman, E.: Proper group actions and symplectic stratified spaces. Pac. J. Math. **181**, 201–229 (1997)
3. Bates, L., Śniatycki, J.: On action-angle variables. Arch. Ration. Mech. Anal. **120**, 337–343 (1992)
4. Bates, L., Śniatycki, J.: On the period-energy relation. Proc. Am. Math. Soc. **114**(3), 877–878 (1992)
5. Cushman, R., Bates, L.: Global Aspects of Classical Integrable Systems. Birkhauser, Basel (1997)
6. Dirac, P.: Generalized hamiltonian dynamics. Can. J. Math. **2**, 129–148 (1950)
7. Hatcher, A.: A proof of the Smale conjecture. Ann. Math. **117**(3), 553–607 (1983)
8. Marsden, J., Weinstein, A.: Reduction of symplectic manifolds with symmetry. Rep. Math. Phys. **5**, 121–130 (1974)
9. Meyer, K.: Symmetries and integrals in mechanics. In: Peixoto, M. (ed.) Dynamical Systems, pp. 259–272. Academic, New York (1973)
10. Nomizu, K.: Left-invariant Lorentz metrics on L ie groups. Osaka J. Math. **16**, 143–150 (1979)
11. Ortega, J.-P., Ratiu, T.: Momentum Maps and Hamiltonian Reduction. Birkhauser, Boston (2003)
12. Sjamaar, R., Lerman, E.: Stratified symplectic spaces and reduction. Ann. Math. **134**, 375–422 (1991)
13. Śniatycki, J.: Differential Geometry of Singular Spaces and Reduction of Symmetries. Cambridge University Press, Cambridge (2013)

Geometric Computational Electrodynamics with Variational Integrators and Discrete Differential Forms

Ari Stern, Yiying Tong, Mathieu Desbrun, and Jerrold E. Marsden

In memory of Jerry, our colleague, mentor, and friend.
— A.S., Y.T., and M.D.

Abstract In this paper, we develop a structure-preserving discretization of the Lagrangian framework for electrodynamics, combining the techniques of *variational integrators* and *discrete differential forms*. This leads to a general family of variational, multisymplectic numerical methods for solving Maxwell's equations that automatically preserve key symmetries and invariants. In doing so, we show that Yee's finite-difference time-domain (FDTD) scheme and its variants are multisymplectic and derive from a discrete Lagrangian variational principle. We also generalize the Yee scheme to unstructured meshes, not just in space but in 4-dimensional spacetime, which relaxes the need to take uniform time steps or even to have a preferred time coordinate. Finally, as an example of the type of methods that can be developed within this general framework, we introduce a new *asynchronous variational integrator* (AVI) for solving Maxwell's equations. These results are illustrated with some prototype simulations that show excellent numerical behavior and absence of spurious modes, even for an irregular mesh with asynchronous time stepping.

A. Stern (✉)
Department of Mathematics, Washington University, St. Louis, MO 63130, USA
e-mail: astern@math.wustl.edu

Y. Tong
Department of Computer Science and Engineering, Michigan State University, East Lansing, MI 48824, USA
e-mail: ytong@msu.edu

M. Desbrun
Department of Computing and Mathematical Sciences, California Institute of Technology, Pasadena, CA 91125, USA
e-mail: mathieu@caltech.edu

J.E. Marsden
California Institute of Technology, Pasadena, CA 91125, USA

D.E. Chang et al. (eds.), *Geometry, Mechanics, and Dynamics*, Fields Institute Communications 73, DOI 10.1007/978-1-4939-2441-7_19

1 Introduction

The Yee scheme (also known as finite-difference time-domain, or FDTD) was introduced by Yee [48] in 1966, but it remains to this day one of the most successful numerical methods used in the field of computational electromagnetics, particularly in the area of microwave problems. Although it is not a "high-order" method, it is still preferred for many applications because it preserves important structural features of Maxwell's equations that other methods fail to capture. Among these distinguishing attributes are the exact preservation of a discrete version of the Gauss constraint $\nabla \cdot \mathbf{D} = \rho$, and discrete stationarity of electrostatic solutions of the form $\mathbf{E} = -\nabla\phi$ (cf. Rylander et al. [39], Taflove and Hagness [41]). In this paper, we show that these desirable properties are direct consequences of the variational and discrete differential structure of the Yee scheme, which mirrors the geometry of Maxwell's equations. Moreover, we will show how to construct other variational methods, which share these same numerical properties while being applicable to more general domains.

1.1 Variational Integrators and Symmetry

Geometric numerical integrators have been used primarily for the simulation of classical mechanical systems, where features such as symplecticity, conservation of momentum, and conservation of energy are essential (cf. Hairer et al. [18]). Among these, *variational integrators* are developed by discretizing the Lagrangian variational principle of a system, and then requiring that numerical trajectories satisfy a discrete version of Hamilton's stationary-action principle. These methods are automatically symplectic, and they exactly preserve discrete momenta associated to symmetries of the Lagrangian: for instance, systems with translational invariance will conserve a discrete linear momentum, those with rotational invariance will conserve a discrete angular momentum, etc. In addition, variational integrators exhibit good long-time energy behavior, without artificial numerical damping. (For a comprehensive overview of variational integrators in mechanics, see Marsden and West [30].)

This variational approach was extended to discretizing general multisymplectic field theories, with an application to nonlinear wave equations, in Marsden et al. [31, 32], which developed the multisymplectic approach for continuum mechanics. Building on this work, Lew et al. [28] introduced *asynchronous variational integrators* (AVIs), which allow different time step sizes to be chosen at individual elements of the spatial mesh, while still preserving the same variational and geometric structure as uniform-time-stepping schemes. These methods were implemented and shown to be not only practical, but in many cases superior to existing methods for problems such as nonlinear elastodynamics. Some further developments are given in Lew et al. [29].

While there have been attempts to apply the existing AVI theory to computational electromagnetics, these efforts encountered a fundamental obstacle: the key symmetry of Maxwell's equations is not rotational or translational symmetry, as in mechanics, but a *differential gauge symmetry*. Without taking additional care to preserve this differential structure, even variational integrators cannot be expected to preserve the symmetries and invariants of Maxwell's equations. We demonstrate how to overcome this obstacle by combining variational methods with discrete differential forms and operators. This gauge structure also turns out to be important for numerical performance, and its preservation is one of the hallmarks of the Yee scheme.

1.2 Preserving Differential Structure and Gauge Symmetry

As motivation, consider the basic relation $\mathbf{B} = \nabla \times \mathbf{A}$, where $\mathbf{B}$ is the magnetic flux and $\mathbf{A}$ is the magnetic vector potential. Because of the vector calculus identities $\nabla \cdot \nabla \times \; = \; 0$ and $\nabla \times \nabla \; = \; 0$, this equation has two immediate and important consequences. First, $\mathbf{B}$ is automatically divergence-free. Second, any transformation $\mathbf{A} \mapsto \mathbf{A} + \nabla f$ has no effect on $\mathbf{B}$; this describes a gauge symmetry, for which the associated conserved momentum is $\nabla \cdot \mathbf{D} - \rho$ (which vanishes, by Gauss's law). A similar argument also explains the invariance of electrostatic solutions, since $\mathbf{E} = -\nabla \phi$ is curl-free and invariant under constant shifts in the scalar potential ϕ. Therefore, a proper variational integrator for electrodynamics should also preserve a discrete analog of these differential identities.

This can be done by viewing the objects of electromagnetics not as vector fields, but as *differential forms* in 4-dimensional spacetime, as is typically done in the literature on classical field theory. Using Discrete Exterior Calculus (DEC) as the framework to discretize these differential forms, we find that the resulting variational integrators automatically respect discrete differential identities such as $\mathrm{d}^2 = 0$ (which encapsulates the previous div-curl-grad relations) and Stokes' theorem. Consequently, they also respect the gauge symmetry of Maxwell's equations, and therefore preserve the associated discrete momentum.

1.3 Numerical Consequences of Geometry

The Yee scheme, as we will show, is a method of precisely this type, which gives a new explanation for many of its previously observed *a posteriori* numerical qualities. For instance, one of its notable features is that the electric field $\mathbf{E}$ and magnetic field $\mathbf{H}$ do not live at the same discrete space or time locations, but at separate nodes on a staggered lattice. The reason why this particular setup leads to improved numerics is not obvious: if we view $\mathbf{E}$ and $\mathbf{H}$ simply as vector fields in 3-space—the exact same type of mathematical object—why shouldn't they live at

the same points? In fact, traditional finite element method (FEM) approaches do exactly this, resulting in a "nodal" discretization. However, from the perspective of differential forms in spacetime, it becomes clear that the staggered-grid approach is more faithful to the structure of Maxwell's equations: as we will see, **E** and **H** come from objects that are dual to one another (the spacetime forms F and $G = *F$), and hence they naturally live on two staggered, dual meshes.

The argument for this approach is not merely a matter of theoretical interest: the geometry of Maxwell's equations has important practical implications for numerical performance. For instance, the vector-field-based discretization, used in nodal FEM, results in spurious 3-D artifacts due to its failure to respect the underlying geometric structure. The Yee scheme, on the other hand, produces resonance spectra in agreement with theory, without spurious modes (cf. Rylander et al. [39], Taflove and Hagness [41]). Furthermore, it has been shown in Haber and Ascher [17] that staggered-grid methods can be used to develop fast numerical methods for electrodynamics, even for problems in heterogeneous media with highly discontinuous material parameters such as conductivity and permeability.

By developing a structure-preserving, geometric discretization of Maxwell's equations, not only can we better understand the Yee scheme and its characteristic advantages, but we can also construct more general methods that share its desirable properties. This family of methods includes the "Yee-like" scheme of Bossavit and Kettunen [7], which presented the first extension of Yee's scheme to unstructured grids (e.g., simplicial meshes rather than rectangular lattices). General methods like these are highly desirable: rectangular meshes are not always practical or appropriate to use in applications where domains with curved and oblique boundaries are needed (see Clemens and Weiland [8]). By allowing general discretizations while still preserving geometry, one can combine the best attributes of the FEM and Yee schemes.

1.4 Contributions

Using DEC as a structure-preserving, geometric framework for general discrete meshes, we obtain the following results:

1. The Yee scheme is actually a variational integrator: that is, it can be obtained by applying Hamilton's principle of stationary action to a discrete Lagrangian.
2. Consequently, the Yee scheme is multisymplectic and preserves discrete momentum maps, analogous to the conserved quantities in continuum electrodynamics. In particular, the Gauss constraint is understood as a discrete momentum map of this integrator, while the preservation of electrostatic potential solutions corresponds to the identity $\mathrm{d}^2 = 0$, where d is the discrete exterior derivative operator.
3. We also create a foundation for more general schemes, allowing for arbitrary discretizations of spacetime, not just uniform time steps on a spatial mesh.

One such scheme, introduced here, is a new asynchronous variational integrator (AVI) for Maxwell's equations, where each spatial element is assigned its own time step size and evolves "asynchronously" with its neighbors. This means that one can choose to take smaller steps where greater refinement is needed, while still using large steps for other elements. Since this allows for local (rather than global) refinement, an AVI can be computationally efficient and numerically stable with fewer total iterations. In addition to the AVI scheme, we briefly sketch how fully covariant spacetime integrators for electrodynamics can be implemented, without even requiring a $3 + 1$ split into space and time components.

1.5 Outline

We will begin by reviewing Maxwell's equations, first introducing their differential forms expression from a Lagrangian variational principle, and next showing how this is equivalent to the familiar vector calculus formulation. We will then motivate the use of DEC for computational electromagnetics, explaining how electromagnetic quantities can be modeled using discrete differential forms and operators on a spacetime mesh. These DEC tools will then be used to set up the discrete Maxwell's equations, and to show that the resulting numerical algorithm yields the Yee and Bossavit-Kettunen schemes as special cases, as well as a new AVI method. Finally, we will demonstrate that the discrete Maxwell's equations can also be derived from a discrete variational principle, and will explore its other discrete geometric properties, including multisymplecticity and momentum map preservation.

2 Maxwell's Equations

This section quickly reviews the differential forms approach to electromagnetism, in preparation for the associated discrete formulation given in the next section. For more details, the reader can refer to Bossavit [5], Gross and Kotiuga [16].

2.1 From Vector Fields to Differential Forms

Maxwell's equations, without free sources of charge or current, are traditionally expressed in terms of four vector fields in 3-space: the electric field $\mathbf{E}$, magnetic field $\mathbf{H}$, electric flux density $\mathbf{D}$, and magnetic flux density $\mathbf{B}$. To translate these into the language of differential forms, we begin by replacing the electric field with a 1-form E and the magnetic flux density by a 2-form B. These have the coordinate expressions

$$E = E_x\,\mathrm{d}x + E_y\,\mathrm{d}y + E_z\,\mathrm{d}z$$
$$B = B_x\,\mathrm{d}y \wedge \mathrm{d}z + B_y\,\mathrm{d}z \wedge \mathrm{d}x + B_z\,\mathrm{d}x \wedge \mathrm{d}y,$$

where $\mathbf{E} = (E_x, E_y, E_z)$ and $\mathbf{B} = (B_x, B_y, B_z)$. The motivation for choosing E as a 1-form and B as a 2-form comes from the integral formulation of Faraday's law,

$$\oint_C \mathbf{E} \cdot \mathrm{d}\mathbf{l} = -\frac{\mathrm{d}}{\mathrm{d}t} \int_S \mathbf{B} \cdot \mathrm{d}\mathbf{A},$$

where $\mathbf{E}$ is integrated over curves and $\mathbf{B}$ is integrated over surfaces. Similarly, Ampère's law,

$$\oint_C \mathbf{H} \cdot \mathrm{d}\mathbf{l} = \frac{\mathrm{d}}{\mathrm{d}t} \int_S \mathbf{D} \cdot \mathrm{d}\mathbf{A},$$

integrates $\mathbf{H}$ over curves and $\mathbf{D}$ over surfaces, so we can likewise introduce a 1-form H and a 2-form D.

Now, $\mathbf{E}$ and $\mathbf{B}$ are related to $\mathbf{D}$ and $\mathbf{H}$ through the usual constitutive relations

$$\mathbf{D} = \epsilon \mathbf{E}, \qquad \mathbf{B} = \mu \mathbf{H}.$$

As shown in Bossavit and Kettunen [7], we can view ϵ and μ as corresponding to Hodge operators $*_\epsilon$ and $*_\mu$, which map the 1-form "fields" to 2-form "fluxes" in space. Therefore, this is compatible with viewing E and H as 1-forms, and D and B as 2-forms.

Note that in vacuum, with $\epsilon = \epsilon_0$ and $\mu = \mu_0$ constant, one can simply express the equations in terms of $\mathbf{E}$ and $\mathbf{B}$, choosing appropriate geometrized units such that $\epsilon_0 = \mu_0 = c = 1$, and hence ignoring the distinction between $\mathbf{E}$ and $\mathbf{D}$ and between $\mathbf{B}$ and $\mathbf{H}$. This is typically the most familiar form of Maxwell's equations, and the one that most students of electromagnetism first encounter. In this presentation, we will restrict ourselves to the vacuum case with geometrized units; for geometric clarity, however, we will always distinguish between the 1-forms E and H and the 2-forms D and B.

Finally, we can incorporate free sources of charge and current by introducing the charge density 3-form $\rho\,\mathrm{d}x \wedge \mathrm{d}y \wedge \mathrm{d}z$, as well as the current density 2-form $J = J_x\,\mathrm{d}y \wedge \mathrm{d}z + J_y\,\mathrm{d}z \wedge \mathrm{d}x + J_z\,\mathrm{d}x \wedge \mathrm{d}y$. These are required to satisfy the continuity of charge condition $\partial_t \rho + \mathrm{d}J = 0$, which can be understood as a conservation law.

2.2 The Faraday and Maxwell 2-Forms

In Lorentzian spacetime, we can now combine E and B into a single object, the Faraday 2-form

$$F = E \wedge \mathrm{d}t + B.$$

There is a theoretical advantage to combining the electric field and magnetic flux into a single spacetime object: this way, electromagnetic phenomena can be described in a relativistically covariant way, without favoring a particular split of spacetime into space and time components. In fact, we can turn the previous construction around: take F to be the fundamental object, with E and B only emerging when we choose a particular coordinate frame. Taking the Hodge star of F, we also get a dual 2-form

$$G = *F = H \wedge \mathrm{d}t - D,$$

called the Maxwell 2-form. The equation $G = *F$ describes the dual relationship between E and B on one hand, and D and H on the other, that is expressed in the constitutive relations.

2.3 The Source 3-Form

Likewise, the charge density ρ and current density J can be combined into a single spacetime object, the source 3-form

$$\mathcal{J} = J \wedge \mathrm{d}t - \rho.$$

Having defined $\mathcal{J}$ in this way, the continuity of charge condition simply requires that $\mathcal{J}$ be closed, i.e., $\mathrm{d}\mathcal{J} = 0$.

2.4 Electromagnetic Variational Principle

Let A be the electromagnetic potential 1-form, satisfying $F = \mathrm{d}A$, over the spacetime manifold X. Then define the 4-form Lagrangian density

$$\mathcal{L} = -\frac{1}{2}\mathrm{d}A \wedge *\mathrm{d}A + A \wedge \mathcal{J},$$

and its associated action functional

$$S[A] = \int_X \mathcal{L}.$$

Now, let α be a variation of A vanishing on the boundary ∂X. Then the variation of the action functional along α is

$$\begin{aligned}\mathbf{d}S[A]\cdot\alpha &= \left.\frac{\mathrm{d}}{\mathrm{d}\epsilon}\right|_{\epsilon=0} S[A+\epsilon\alpha] \\ &= \int_X (-\mathrm{d}\alpha\wedge *\mathrm{d}A + \alpha\wedge \mathcal{J}) \\ &= \int_X \alpha\wedge(-\mathrm{d}*\mathrm{d}A + \mathcal{J})\,,\end{aligned}$$

where in this last equality we have integrated by parts, using the fact that α vanishes on the boundary. Hamilton's principle of stationary action requires this variation to be equal to zero for arbitrary α, thus implying the electromagnetic Euler-Lagrange equation,

$$\mathrm{d}*\mathrm{d}A = \mathcal{J}. \tag{1}$$

2.5 Variational Derivation of Maxwell's Equations

Since $G = *F = *\mathrm{d}A$, clearly (1) is equivalent to $\mathrm{d}G = \mathcal{J}$. Furthermore, since $\mathrm{d}^2 = 0$, it follows that $\mathrm{d}F = \mathrm{d}^2A = 0$. Hence, Maxwell's equations with respect to the Maxwell and Faraday 2-forms can be written as

$$\mathrm{d}F = 0, \tag{2}$$

$$\mathrm{d}G = \mathcal{J}. \tag{3}$$

Suppose now that we choose the standard coordinate system (x, y, z, t) on Minkowski space $X = \mathbb{R}^{3,1}$, and define E and B through the relation $F = E\wedge \mathrm{d}t + B$. Then a straightforward calculation shows that (2) is equivalent to

$$\nabla\times\mathbf{E} + \partial_t\mathbf{B} = 0, \tag{4}$$

$$\nabla\cdot\mathbf{B} = 0. \tag{5}$$

Likewise, if $G = *F = H\wedge\mathrm{d}t - D$, then (3) is equivalent to

$$\nabla\times\mathbf{H} - \partial_t\mathbf{D} = \mathbf{J}, \tag{6}$$

$$\nabla\cdot\mathbf{D} = \rho. \tag{7}$$

Hence this Lagrangian, differential forms approach to Maxwell's equations is strictly equivalent to the more classical vector calculus formulation in smooth spacetime. However, in discrete spacetime, we will see that the differential form version is *not* equivalent to an arbitrary vector field discretization, but rather implies a particular choice of discrete objects.

2.6 Generalized Hamilton-Pontryagin Principle for Maxwell's Equations

We can also derive Maxwell's equations by using a mixed variational principle, similar to the Hamilton-Pontryagin principle introduced by Yoshimura and Marsden [49] for classical Lagrangian mechanics. To do this, we treat A and F as separate fields, while G acts as a Lagrange multiplier, weakly enforcing the constraint $F = \mathrm{d}A$. Define the extended action to be

$$S[A, F, G] = \int_X \left[-\frac{1}{2} F \wedge *F + A \wedge \mathcal{J} + (F - \mathrm{d}A) \wedge G \right].$$

Then, taking the variation of the action along some α, ϕ, γ (each vanishing on ∂X), we have

$$\begin{aligned} \mathbf{d}S[A, F, G] \cdot (\alpha, \phi, \gamma) &= \int_X [-\phi \wedge *F + \alpha \wedge \mathcal{J} + (\phi - \mathrm{d}\alpha) \wedge G + (F - \mathrm{d}A) \wedge \gamma] \\ &= \int_X [\alpha \wedge (\mathcal{J} - \mathrm{d}G) + \phi \wedge (G - *F) + (F - \mathrm{d}A) \wedge \gamma]. \end{aligned}$$

Therefore, setting this equal to zero, we get the equations

$$\mathrm{d}G = \mathcal{J}, \qquad G = *F, \qquad F = \mathrm{d}A.$$

This is precisely equivalent to Maxwell's equations, as derived above. However, this approach provides some additional insight into the geometric structure of electromagnetism: the gauge condition $F = \mathrm{d}A$ and constitutive relations $G = *F$ are *explicitly included in the equations of motion*, as a direct result of the variational principle.

2.7 Reducing the Equations

When solving an initial value problem, it is not necessary to use all of Maxwell's equations to evolve the system forward in time. In fact, the curl equations (4) and (6) automatically conserve the quantities $\nabla \cdot \mathbf{B}$ and $\nabla \cdot \mathbf{D} - \rho$. Therefore, the divergence equations (5) and (7) can be viewed simply as constraints on initial conditions, while the curl equations completely describe the time evolution of the system.

There are a number of ways to see why we can justify eliminating the divergence equations. A straightforward way is to take the divergence of equations (4) and (6). Since $\nabla \cdot \nabla \times = 0$, we are left with

$$\partial_t (\nabla \cdot \mathbf{B}) = 0, \qquad \partial_t (\nabla \cdot \mathbf{D}) + \nabla \cdot \mathbf{J} = \partial_t (\nabla \cdot \mathbf{D} - \rho) = 0.$$

Therefore, if the divergence constraints are satisfied at the initial time, then they are satisfied for all time, since the divergence terms are constant.

Another approach is to notice that Maxwell's equations depend only on the exterior derivative $\mathrm{d}A$ of the electromagnetic potential, and not on the value of A itself. Therefore, the system has a *gauge symmetry*: any gauge transformation $A \mapsto A + \mathrm{d}f$ leaves $\mathrm{d}A$, and hence Maxwell's equations, unchanged. Choosing a time coordinate, we can then partially fix the gauge so that the electric scalar potential $\phi = A\,(\partial/\partial t) = 0$ (the so-called Weyl gauge or temporal gauge), and so A has only spatial components. In fact, these three remaining components correspond to those of the usual vector potential $\mathbf{A}$. The reduced Euler-Lagrange equations in this gauge consist only of (6), while the remaining gauge symmetry $\mathbf{A} \mapsto \mathbf{A} + \nabla f$ yields a momentum map that automatically preserves $\nabla \cdot \mathbf{D} - \rho$ in time. Equations (4) and (5) are automatically preserved by the identity $\mathrm{d}^2 A = 0$; they are not actually part of the Euler-Lagrange equations. A more detailed exposition of these calculations will be given in Subsection 5.2.

3 Discrete Forms in Computational Electromagnetics

In this section, we give a quick review of the fundamental objects and operations of Discrete Exterior Calculus (DEC), a structure-preserving calculus of discrete differential forms. By construction, DEC automatically preserves a number of important geometric structures, and hence it provides a fully discrete analog of the tools used in the previous section to express the differential form version of Maxwell's equations. In subsequent sections, we will use this framework to formulate Maxwell's equations discretely, emulating the continuous version.

3.1 Rationale Behind DEC for Computational Electromagnetics

Modern computational electromagnetics began in the 1960s, when the finite element method (FEM), based on *nodal basis functions*, was used successfully to discretize the differential equations governing 2-D static problems formulated in terms of a scalar potential. Unfortunately, the initial success of the FEM approach appeared unable to carry over to 3-D problems without spurious numerical artifacts. With the introduction of *edge elements* by Nédélec [34] came the realization that a better discretization of the geometric structure of Maxwell's electromagnetic theory was key to overcoming this obstacle (see Gross and Kotiuga [16] for more historical details). Mathematical tools developed by Weyl and Whitney in the 1950s, in the context of algebraic topology, turned out to provide the necessary foundations on which robust numerical techniques for electromagnetics can be built, as detailed in Bossavit [5].

3.2 Discrete Differential Forms and Operators

In this section, we show how to define differential forms and operators on a discrete mesh, in preparation to use this framework for computational modeling of classical fields. By construction, the calculus of discrete differential forms automatically preserves a number of important geometric structures, including Stokes' theorem, integration by parts (with a proper treatment of boundaries), the de Rham complex, Poincaré duality, Poincaré's lemma, and Hodge theory. Therefore, this provides a suitable foundation for the coordinate-independent discretization of geometric field theories. In subsequent chapters, we will also use these discrete differential forms as the space of fields on which we will define discrete Lagrangian variational principles.

The particular "flavor" of discrete differential forms and operators we will be using is known as Discrete Exterior Calculus, or DEC for short (see Desbrun et al. [10], Hirani [23], Leok [26]). Guided by Cartan's exterior calculus of differential forms on smooth manifolds, DEC is a discrete calculus developed, *ab initio*, on discrete manifolds, so as to maintain the covariant nature of the quantities involved. This computational tool is based on the notion of discrete chains and cochains, used as basic building blocks for compatible discretizations of important geometric structures such as the de Rham complex. The chain and cochain representations are not only attractive from a computational perspective due to their conceptual simplicity and elegance; as we will see, they also originate from a theoretical framework defined by Whitney [46], who introduced the Whitney and de Rham maps between simplicial cochains and Lipschitz differential forms, thereby inducing an isomorphism between simplicial cohomology and de Rham cohomology.

Other approaches to the discretization of differential forms include the calculus of differential chains (or chainlets) of Harrison [19, 20], Harrison and Pugh [21], as well as the Finite Element Exterior Calculus (FEEC) of Arnold et al. [1, 2]. In particular, FEEC has proven to be a powerful framework for obtaining numerical-analytic results about stability and convergence, particularly for elliptic problems in Euclidean domains. An extension of FEEC to Riemannian submanifolds embedded in Euclidean space was also obtained by Holst and Stern [24]. Since computational electrodynamics concerns hyperbolic problems on Lorentzian spacetime manifolds, the purely combinatorial nature of DEC allows it to be adapted to this setting with relatively little additional complication, although it would be interesting to study the extension of the aforementioned approaches to this setting as well.

3.2.1 Primal and Dual Meshes

DEC is concerned with problems in which the smooth n-dimensional manifold X is replaced by a discrete mesh—precisely, by a cell complex that is manifold, admits a metric, and is orientable. The simplest example of such a mesh is a finite simplicial complex, such as a triangulation of a 2-dimensional surface. We will generally denote the complex by $\mathcal{K}$, and a cell in the complex by σ.

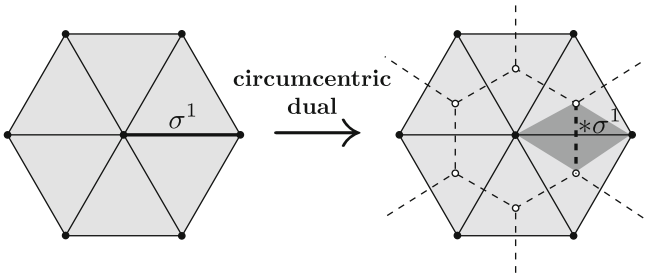

Fig. 1 Given a 2-D simplicial mesh (left), we can construct its circumcentric dual mesh, called the Voronoi diagram of the primal nodes (right). In bold, we show one particular primal edge σ^1 (left) and its corresponding dual edge $*\sigma^1$ (right); the convex hull of these cells $\text{CH}(\sigma^1, *\sigma^1)$ is shaded dark grey

Given a mesh $\mathcal{K}$, one can construct a *dual mesh* $*\mathcal{K}$, where each primal k-cell σ corresponds to a dual $(n-k)$-cell $*\sigma$. ($*\mathcal{K}$ is "dual" to $\mathcal{K}$ in the combinatorial sense of a graph dual.) One way to do this is as follows: place a dual vertex at the circumcenter of each n-simplex, then connect two dual vertices by an edge wherever the corresponding n-simplices share an $(n-1)$-simplex, and so on. This is called the *circumcentric dual*, and it has the important property that primal and dual cells are automatically orthogonal to one another, which is advantageous when defining a pseudo-inner product (as we will see later in this section). For example, the circumcentric dual of a Delaunay triangulation, with the Euclidean metric, is its corresponding Voronoi diagram (see Figure 1). For more on the dual relationship between Delaunay triangulations and Voronoi diagrams, a standard reference is O'Rourke [36]. A similar construction of the circumcenter can be carried out for higher-dimensional Euclidean simplicial complexes, as well as for simplicial meshes in Minkowski space. Note that, in both the Euclidean and Lorentzian cases, the circumcenter may actually lie *outside* the simplex if it has a very bad aspect ratio, underscoring the importance of mesh quality for good numerical results [33].

There are alternative ways to define the dual mesh—for example, placing dual vertices at the barycenter rather than the circumcenter—but we will use the circumcentric dual unless otherwise noted. Note that a refined definition of the dual mesh, where dual cells at the boundary are restricted to $\mathcal{K}$, is discussed in Subsection 3.3 to allow proper enforcement of boundary conditions in computational electromagnetics.

3.2.2 Discrete Differential Forms

The fundamental objects of DEC are discrete differential forms. A discrete k-form α^k assigns a real number to each oriented k-dimensional cell σ^k in the mesh $\mathcal{K}$. (The superscripts k are not actually required by the notation, but they are often useful as

reminders of what order of form or cell we are dealing with.) This value is denoted by $\langle \alpha^k, \sigma^k \rangle$, and can be thought of as the value of α^k "integrated over" the element σ^k, i.e.,

$$\langle \alpha, \sigma \rangle \equiv \int_\sigma \alpha.$$

For example, 0-forms assign values to vertices, 1-forms assign values to edges, etc. We can extend this to integrate over discrete paths by linearity: simply add the form's values on each cell in the path, taking care to flip the sign if the path is oriented opposite the cell. Formally, these "paths" of k-dimensional elements are called *chains*, and discrete differential forms are *cochains*, where $\langle \cdot, \cdot \rangle$ is the pairing between cochains and chains.

Differential forms can be defined either on the mesh $\mathcal{K}$ or on its dual $*\mathcal{K}$; we will refer to these as *primal forms* and *dual forms* respectively. Note that there is a natural correspondence between primal k-forms and dual $(n-k)$-forms, since each primal k-cell has a dual $(n-k)$-cell. This is an important property that will be used below to define the discrete Hodge star operator.

3.2.3 Exterior Derivative

The discrete exterior derivative d is constructed to satisfy Stokes' theorem, which in the continuous sense is written

$$\int_\sigma \mathrm{d}\alpha = \int_{\partial\sigma} \alpha.$$

Therefore, if α is a discrete differential k-form, then the $(k+1)$-form $\mathrm{d}\alpha$ is defined on any $(k+1)$-chain σ by

$$\langle \mathrm{d}\alpha, \sigma \rangle = \langle \alpha, \partial\sigma \rangle ,$$

where $\partial\sigma$ is the k-chain boundary of σ. For this reason, d is often called the *coboundary* operator in cohomology theory.

3.2.4 Diagonal Hodge Star

The discrete Hodge star transforms k-forms on the primal mesh into $(n-k)$-forms on the dual mesh, and vice-versa. In our setup, we will use the so-called diagonal (or mass-lumped) approximation of the Hodge star [5] because of its simplicity, but note that higher-order accurate versions can be substituted. Given a discrete form α, its *Hodge star* $*\alpha$ is defined by the relation

$$\frac{1}{|*\sigma|}\langle *\alpha, *\sigma\rangle = \kappa(\sigma)\frac{1}{|\sigma|}\langle \alpha, \sigma\rangle ,$$

where $|\sigma|$ and $|*\sigma|$ are the volumes of these elements, and κ is the causality operator, which equals $+1$ when σ is spacelike and -1 otherwise. For more information on alternative discrete Hodge operators, the reader may refer to, e.g., Arnold et al. [1, 2], Auchmann and Kurz [3], Harrison [20], Hiptmair [22], Tarhasaari et al. [42], Wang et al. [45].

3.2.5 Pseudo-Inner Product

Define the pseudo-inner product $(\cdot, \cdot)$ between two primal k-forms to be

$$\begin{aligned}(\alpha, \beta) &= \sum_{\sigma^k} \kappa(\sigma)\binom{n}{k}\frac{|\mathrm{CH}(\sigma, *\sigma)|}{|\sigma|^2}\langle \alpha, \sigma\rangle \langle \beta, \sigma\rangle \\ &= \sum_{\sigma^k} \kappa(\sigma)\frac{|*\sigma|}{|\sigma|}\langle \alpha, \sigma\rangle \langle \beta, \sigma\rangle\end{aligned}$$

where the sum is taken over all k-dimensional elements σ, and $\mathrm{CH}(\sigma, *\sigma)$ is the diamond-shaped region defined as the signed union of the n-dimensional convex hulls of the primal vertices of σ and each boundary element of the dual cell $*\sigma$, see Figure 1. (On a spacelike mesh, this is a true inner product, since $\kappa(\sigma) = 1$ for all σ. Otherwise, it is merely a pseudo-inner product, as it fails to be positive-definite.) The final equality holds as a result of using the circumcentric dual, since σ and $*\sigma$ are orthogonal to one another, and hence $|\mathrm{CH}(\sigma, *\sigma)| = \binom{n}{k}^{-1}|\sigma|\,|*\sigma|$. (Indeed, this is one of the advantages of using the circumcentric dual, since one only needs to store volume information about the primal and dual cells themselves, and not about these primal-dual convex hulls.) This pseudo-inner product can be expressed in terms of $\alpha \wedge *\beta$, as in the continuous case, for a particular choice of the discrete primal-dual wedge product; see Desbrun et al. [9].

Note that, since we have already defined a discrete version of the operators d and $*$, we immediately have a discrete codifferential $\delta = \mathrm{d}^*$. See Figure 2 for a visual diagram of primal and dual discrete forms, along with the corresponding operators $\mathrm{d}, *, \delta$, for the case where $\mathcal{K}$ is a 3-D tetrahedral mesh.

3.2.6 Implementation of DEC

DEC can be implemented simply and efficiently using linear algebra. A k-form α can be stored as a vector, where its entries are the values of α on each k-cell of the mesh. That is, given a list of k-cells σ_i^k, the entries of the vector are $\alpha_i = \langle \alpha, \sigma_i^k\rangle$. The exterior derivative d, taking k-forms to $(k+1)$-forms, is then represented as

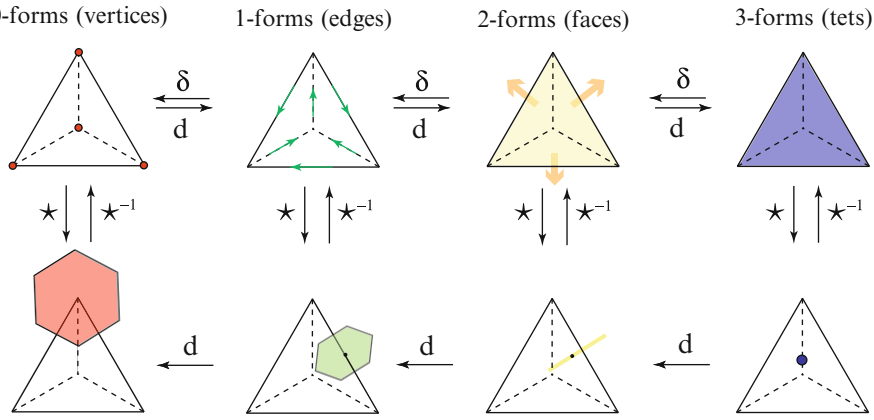

Fig. 2 This figure is an illustration of discrete differential forms and operators on a 3-D simplicial mesh. In the top row, we see how a discrete k-form lives on k-cells of the primal mesh, for $k = 0, 1, 2, 3$; the bottom row shows the location of the corresponding dual $(n-k)$-forms on the dual mesh. The differential operators d and δ map "horizontally" between k and $(k+1)$ forms, while the Hodge star $*$ and its inverse $*^{-1}$ map "vertically" between primal and dual forms

a matrix: in fact, it is precisely the signed *incidence matrix* between k-cells and $(k+1)$-cells in the mesh, with sparse entries ± 1. The Hodge star taking primal k-forms to dual $(n-k)$-forms becomes a square matrix, and in the case of the diagonal Hodge star, it is the diagonal matrix with entries $\kappa\left(\sigma_i^k\right) \frac{\left|*\sigma_i^k\right|}{\left|\sigma_i^k\right|}$. The discrete pseudo-inner product is then simply the Hodge star matrix taken as a quadratic form.

Because of this straightforward isomorphism between DEC and linear algebra, problems posed in the language of DEC can take advantage of existing numerical linear algebra codes. For more programming details, refer to Bell and Hirani [4], Elcott and Schröder [11].

3.3 Initial and Boundary Values with DEC

Particular care is required to properly enforce initial and boundary conditions on the discrete spacetime boundary $\partial\mathcal{K}$. For example, in electrodynamics, we may wish to set initial conditions for E and B at time t_0; however, while B is defined on $\partial\mathcal{K}$ at t_0, E is not. In fact, as we will see, E lives on edges that are extruded between the time slices t_0 and t_1, so unless we modify our definitions, we can only initialize E at the half-step $t_{1/2}$. (This half-step issue also arises with the standard Yee scheme.) There are some applications where it may be acceptable to initialize E and B at separate times (for example, when the fields are initialized randomly and integrated for a long time to compute a resonance spectrum), but we wish to be able to handle

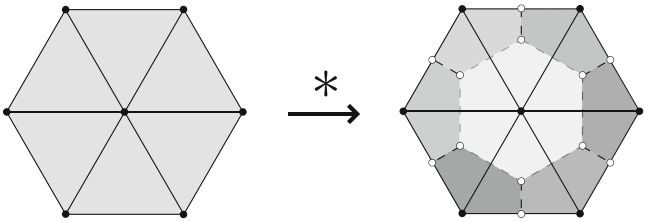

Fig. 3 In this 2-D example, the dual mesh is properly defined near the boundary by adding dual vertices on the boundary edges. The restricted Voronoi cells of the primal boundary vertices (shaded at right) thus have boundaries containing both dual edges (dashed lines) *and* primal boundary half-edges

the more general case. Although our previous exposition of DEC thus far applies anywhere away from a boundary, notions as simple as "dual cell" need to be defined carefully on or near $\partial\mathcal{K}$.

For a primal mesh $\mathcal{K}$, the dual mesh $*\mathcal{K}$ is defined as *the Voronoi dual of* $\mathcal{K}$ *restricted to* $\mathcal{K}$. This truncates the portion of the dual cells extending outside of $\mathcal{K}$; compare Figure 3 with the earlier Figure 1. This new definition results in the addition of a dual vertex at the circumcenter of each boundary $(n-1)$-simplex, in addition to the interior n-simplices as previously defined. To complete the dual mesh $*\mathcal{K}$, we add a dual edge between adjacent dual vertices on the boundary, as well as between dual boundary vertices and their neighboring interior dual vertices, and proceed similarly with higher-dimensional dual cells. For intuition, one can imagine the $(n-1)$-dimensional boundary to be a vanishingly thin n-dimensional shell. That is, each boundary $(k-1)$-simplex can be thought of as a prismal k-cell that has been "squashed flat" along the boundary normal direction. This process is quite similar to the use of "ghost cells" at the boundary, as is commonly done for finite volume methods (see LeVeque [27]). Note that these additional dual cells provide the boundary $\partial\mathcal{K}$ with its own dual mesh $*(\partial\mathcal{K})$. In fact, the boundary of the dual is now equal to the dual of the boundary, i.e., $\partial(*\mathcal{K}) = *(\partial\mathcal{K})$. Returning to the example of initial conditions on E and B, we recall that E is defined on extruded faces normal to the time slice t_0. Therefore, thanks to the proper restriction of the Voronoi diagram to the domain, we can now define E on *edges* in $\partial\mathcal{K}$ at time t_0, where these edges can be understood as vanishingly thin faces (i.e., extruded between some $t_{-\epsilon}$ and t_0 for $\epsilon \to 0$). Notice finally that with this construction of $*\mathcal{K}$, there is a dual relationship between Dirichlet conditions on the dual mesh and Neumann conditions on the primal mesh, e.g., between primal fields and dual fluxes, as expected.

3.4 Discrete Integration by Parts with Boundary Terms

With the dual mesh properly defined, dual forms can now be defined on the boundary. Therefore, the discrete duality between d and δ can be generalized to include nonvanishing boundary terms. If α is a primal $(k-1)$-form and β is a primal k-form, then

$$(\mathrm{d}\alpha, \beta) = (\alpha, \delta\beta) + \langle \alpha \wedge *\beta, \partial\mathcal{K} \rangle \,. \tag{8}$$

In the boundary integral, α is still a primal $(k-1)$-form on $\partial\mathcal{K}$, while $*\beta$ is an $(n-k)$-form taken on the boundary dual $*(\partial\mathcal{K})$. Formula (8) is readily proved using the familiar method of discrete "summation by parts," and thus agrees with the integration by parts formula for smooth differential forms.

4 Implementing Maxwell's Equations with DEC

In this section, we explain how to obtain numerical algorithms for solving Maxwell's equations with DEC. To do so, we proceed in the following order. First, we find a sensible way to define the discrete forms F, G, and $\mathcal{J}$ on a spacetime mesh. Next, we use the DEC version of the operators d and $*$ to obtain the discrete Maxwell's equations. While we have not yet shown that these equations are variational in the discrete sense, we show later in Section 5 that the Lagrangian derivation of the smooth Maxwell's equations also holds with the DEC operators, in precisely the same way. Finally, we discuss how these equations can be used to define a numerical method for computational electromagnetics.

In particular, for a rectangular grid, we show that our setup results in the traditional Yee scheme. For a general triangulation of space with equal time steps, the resulting scheme will be Bossavit and Kettunen's scheme. We then develop an AVI method where each spatial element can be assigned a different time step, and the time integration of Maxwell's equations can be performed on the elements asynchronously. Finally, we comment on the equations for fully generalized spacetime meshes, e.g., an arbitrary meshing of $\mathbb{R}^{3,1}$ by 4-simplices.

Note that the idea of discretizing Maxwell's equations using spacetime cochains was mentioned in, e.g., Leok [26], as well as in a paper by Wise [47] taking the more abstract perspective of higher-level "p-form" versions of electromagnetism and category theory.

4.1 Rectangular Grid

Suppose that we have a rectangular grid in $\mathbb{R}^{3,1}$, oriented along the axes (x, y, z, t). To simplify this exposition (although it is not necessary), let us also suppose that the grid has uniform space and time steps $\Delta x, \Delta y, \Delta z, \Delta t$. (Note that the DEC setup applies directly to a non-simplicial rectangular mesh, since an n-rectangle has a well-defined circumcenter.)

4.1.1 Setup

Since F is a 2-form, its values should live on 2-faces in this grid. Following the continuous expression of F,

$$\begin{aligned} F = {} & E_x \, \mathrm{d}x \wedge \mathrm{d}t + E_y \, \mathrm{d}y \wedge \mathrm{d}t + E_z \, \mathrm{d}z \wedge dt \\ & + B_x \, \mathrm{d}y \wedge \mathrm{d}z + B_y \, \mathrm{d}z \wedge \mathrm{d}x + B_z \, \mathrm{d}x \wedge \mathrm{d}y, \end{aligned}$$

and due to the tensor product nature of the regular grid, the exact assignment of each 2-face becomes simple: *the six components of F correspond precisely to the six types of 2-faces in a 4-D rectangular grid*. Simply assign the values $E_x \Delta x \Delta t$ to faces parallel to the xt-plane, $E_y \Delta y \Delta t$ to faces parallel to the yt-plane, and $E_z \Delta z \Delta t$ to faces parallel to the zt-plane. Likewise, assign $B_x \Delta y \Delta z$ to faces parallel to the yz-plane, $B_y \Delta z \Delta x$ to faces parallel to the xz-plane, and $B_z \Delta x \Delta y$ to faces parallel to the xy-plane. This is pictured in Figure 4.

Let us look at these values on the faces of a typical 4-rectangle $[x_k, x_{k+1}] \times [y_l, y_{l+1}] \times [z_m, z_{m+1}] \times [t_n, t_{n+1}]$. To simplify the notation, we can index each value of F by the midpoint of the 2-face on which it lives: for example, $F|^{n+\frac{1}{2}}_{k+\frac{1}{2},l,m}$ is stored on the face $[x_k, x_{k+1}] \times \{y_l\} \times \{z_m\} \times [t_n, t_{n+1}]$, parallel to the xt-plane. Hence, the following values are assigned to the corresponding faces:

$$\begin{aligned} xt\text{-face} &: E_x|^{n+\frac{1}{2}}_{k+\frac{1}{2},l,m} \, \Delta x \Delta t \\ yt\text{-face} &: E_y|^{n+\frac{1}{2}}_{k,l+\frac{1}{2},m} \, \Delta y \Delta t \\ zt\text{-face} &: E_z|^{n+\frac{1}{2}}_{k,l,m+\frac{1}{2}} \, \Delta z \Delta t \\ yz\text{-face} &: B_x|^{n}_{k,l+\frac{1}{2},m+\frac{1}{2}} \, \Delta y \Delta z \\ xz\text{-face} &: B_y|^{n}_{k+\frac{1}{2},l,m+\frac{1}{2}} \, \Delta z \Delta x \\ xy\text{-face} &: B_z|^{n}_{k+\frac{1}{2},l+\frac{1}{2},m} \, \Delta x \Delta y. \end{aligned}$$

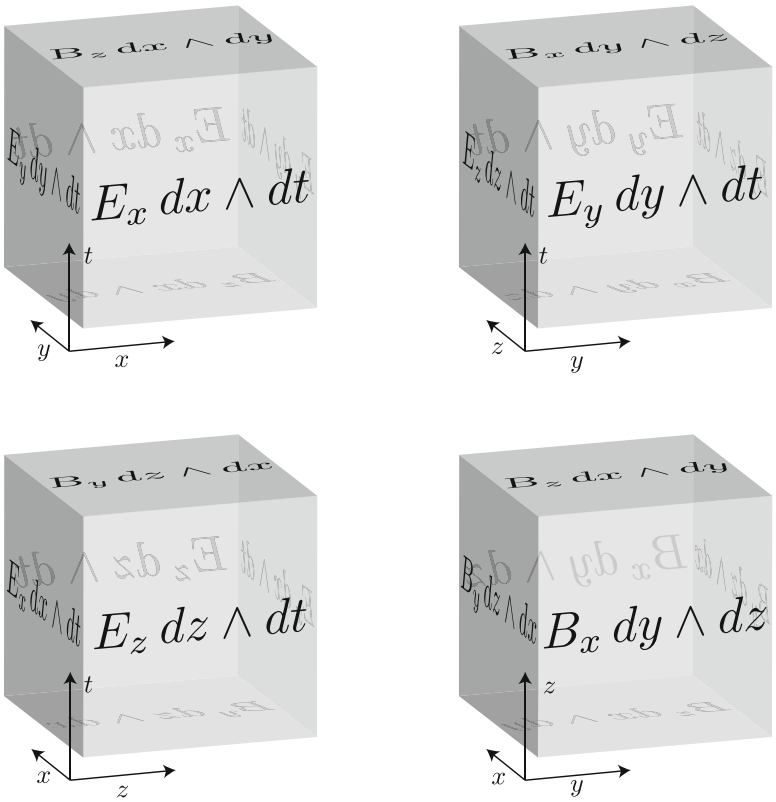

Fig. 4 Values of F are stored on the primal 2-faces of a 4-D rectangular grid. Shown here are the three mixed space/time 3-cells, and the one purely spatial 3-cell (lower right)

We see that a "staggered grid" arises from the fact that E and B naturally live on 2-faces, not at vertices or 4-cells.

4.1.2 Equations of Motion

The discrete equations of motion are, as in the continuous case, given formally by

$$\mathrm{d}F = 0, \qquad \mathrm{d}G = \mathcal{J},$$

where now these equations are interpreted in the sense of DEC. Let us first look at the DEC interpretation of $\mathrm{d}F$. Since $\mathrm{d}F$ is a discrete 3-form, it takes values on the 3-faces of each 4-rectangle. Its values are as follows:

$$
\begin{aligned}
xyt\text{-face} : &- \left(E_x|^{n+\frac{1}{2}}_{k+\frac{1}{2},l+1,m} - E_x|^{n+\frac{1}{2}}_{k+\frac{1}{2},l,m} \right) \Delta x \Delta t \\
&+ \left(E_y|^{n+\frac{1}{2}}_{k+1,l+\frac{1}{2},m} - E_y|^{n+\frac{1}{2}}_{k,l+\frac{1}{2},m} \right) \Delta y \Delta t \\
&+ \left(B_z|^{n+1}_{k+\frac{1}{2},l+\frac{1}{2},m} - B_z|^{n}_{k+\frac{1}{2},l+\frac{1}{2},m} \right) \Delta x \Delta y,
\end{aligned}
$$

$$
\begin{aligned}
xzt\text{-face} : &- \left(E_x|^{n+\frac{1}{2}}_{k+\frac{1}{2},l,m+1} - E_x|^{n+\frac{1}{2}}_{k+\frac{1}{2},l,m} \right) \Delta x \Delta t \\
&+ \left(E_z|^{n+\frac{1}{2}}_{k+1,l,m+\frac{1}{2}} - E_z|^{n+\frac{1}{2}}_{k,l,m+\frac{1}{2}} \right) \Delta z \Delta t \\
&- \left(B_y|^{n+1}_{k+\frac{1}{2},l,m+\frac{1}{2}} - B_y|^{n}_{k+\frac{1}{2},l,m+\frac{1}{2}} \right) \Delta x \Delta z,
\end{aligned}
$$

$$
\begin{aligned}
yzt\text{-face} : &- \left(E_y|^{n+\frac{1}{2}}_{k,l+\frac{1}{2},m+1} - E_y|^{n+\frac{1}{2}}_{k,l+\frac{1}{2},m} \right) \Delta y \Delta t \\
&+ \left(E_z|^{n+\frac{1}{2}}_{k,l+1,m+\frac{1}{2}} - E_z|^{n+\frac{1}{2}}_{k,l,m+\frac{1}{2}} \right) \Delta z \Delta t \\
&+ \left(B_x|^{n+1}_{k,l+\frac{1}{2},m+\frac{1}{2}} - B_x|^{n}_{k,l+\frac{1}{2},m+\frac{1}{2}} \right) \Delta y \Delta z,
\end{aligned}
$$

$$
\begin{aligned}
xyz\text{-face} : &\quad \left(B_x|^{n}_{k+1,l+\frac{1}{2},m+\frac{1}{2}} - B_x|^{n}_{k,l+\frac{1}{2},m+\frac{1}{2}} \right) \Delta y \Delta z \\
&+ \left(B_y|^{n}_{k+\frac{1}{2},l+1,m+\frac{1}{2}} - B_y|^{n}_{k+\frac{1}{2},l,m+\frac{1}{2}} \right) \Delta x \Delta z \\
&+ \left(B_z|^{n}_{k+\frac{1}{2},l+\frac{1}{2},m+1} - B_z|^{n}_{k+\frac{1}{2},l+\frac{1}{2},m} \right) \Delta x \Delta y.
\end{aligned}
$$

Setting each of these equal to zero, we arrive at the following four equations:

$$
\frac{B_x|^{n+1}_{k,l+\frac{1}{2},m+\frac{1}{2}} - B_x|^{n}_{k,l+\frac{1}{2},m+\frac{1}{2}}}{\Delta t} = \frac{E_y|^{n+\frac{1}{2}}_{k,l+\frac{1}{2},m+1} - E_y|^{n+\frac{1}{2}}_{k,l+\frac{1}{2},m}}{\Delta z} - \frac{E_z|^{n+\frac{1}{2}}_{k,l+1,m+\frac{1}{2}} - E_z|^{n+\frac{1}{2}}_{k,l,m+\frac{1}{2}}}{\Delta y},
$$

$$
\frac{B_y|^{n+1}_{k+\frac{1}{2},l,m+\frac{1}{2}} - B_y|^{n}_{k+\frac{1}{2},l,m+\frac{1}{2}}}{\Delta t} = \frac{E_z|^{n+\frac{1}{2}}_{k+1,l,m+\frac{1}{2}} - E_z|^{n+\frac{1}{2}}_{k,l,m+\frac{1}{2}}}{\Delta x} - \frac{E_x|^{n+\frac{1}{2}}_{k+\frac{1}{2},l,m+1} - E_x|^{n+\frac{1}{2}}_{k+\frac{1}{2},l,m}}{\Delta z}
$$

$$
\frac{B_z|^{n+1}_{k+\frac{1}{2},l+\frac{1}{2},m} - B_z|^{n}_{k+\frac{1}{2},l+\frac{1}{2},m}}{\Delta t} = \frac{E_x|^{n+\frac{1}{2}}_{k+\frac{1}{2},l+1,m} - E_x|^{n+\frac{1}{2}}_{k+\frac{1}{2},l,m}}{\Delta y} - \frac{E_y|^{n+\frac{1}{2}}_{k+1,l+\frac{1}{2},m} - E_y|^{n+\frac{1}{2}}_{k,l+\frac{1}{2},m}}{\Delta x}
$$

and

$$\frac{B_x|^n_{k+1,l+\frac{1}{2},m+\frac{1}{2}} - B_x|^n_{k,l+\frac{1}{2},m+\frac{1}{2}}}{\Delta x} + \frac{B_y|^n_{k+\frac{1}{2},l+1,m+\frac{1}{2}} - B_y|^n_{k+\frac{1}{2},l,m+\frac{1}{2}}}{\Delta y} + \frac{B_z|^n_{k+\frac{1}{2},l+\frac{1}{2},m+1} - B_z|^n_{k+\frac{1}{2},l+\frac{1}{2},m}}{\Delta z} = 0. \quad (9)$$

These equations are the discrete version of the equations

$$\partial_t \mathbf{B} = -\nabla \times \mathbf{E}, \qquad \nabla \cdot \mathbf{B} = 0.$$

Moreover, since E and B are differential forms, this can also be seen as a discretization of the *integral version* of Maxwell's equations as well. Because DEC satisfies a discrete Stokes' theorem, this automatically preserves the equivalence between the differential and integral formulations of electrodynamics.

Doing the same with the equation $\mathrm{d}G = \mathcal{J}$, evaluating on dual 3-faces this time, we arrive at four more equations:

$$\frac{D_x|^{n+\frac{1}{2}}_{k+\frac{1}{2},l,m} - D_x|^{n-\frac{1}{2}}_{k+\frac{1}{2},l,m}}{\Delta t} = \frac{H_z|^n_{k+\frac{1}{2},l+\frac{1}{2},m} - H_z|^n_{k+\frac{1}{2},l-\frac{1}{2},m}}{\Delta y} - \frac{H_y|^n_{k+\frac{1}{2},l,m+\frac{1}{2}} - H_y|^n_{k+\frac{1}{2},l,m-\frac{1}{2}}}{\Delta z} - J_x|^n_{k+\frac{1}{2},l,m},$$

$$\frac{D_y|^{n+\frac{1}{2}}_{k,l+\frac{1}{2},m} - D_y|^{n-\frac{1}{2}}_{k,l+\frac{1}{2},m}}{\Delta t} = \frac{H_x|^n_{k,l+\frac{1}{2},m+\frac{1}{2}} - H_x|^n_{k,l+\frac{1}{2},m-\frac{1}{2}}}{\Delta z} - \frac{H_z|^n_{k+\frac{1}{2},l+\frac{1}{2},m} - H_z|^n_{k-\frac{1}{2},l+\frac{1}{2},m}}{\Delta x} - J_y|^n_{k,l+\frac{1}{2},m},$$

$$\frac{D_z|^{n+\frac{1}{2}}_{k,l,m+\frac{1}{2}} - D_z|^{n-\frac{1}{2}}_{k,l,m+\frac{1}{2}}}{\Delta t} = \frac{H_y|^n_{k+\frac{1}{2},l,m+\frac{1}{2}} - H_y|^n_{k-\frac{1}{2},l,m+\frac{1}{2}}}{\Delta x} - \frac{H_x|^n_{k,l+\frac{1}{2},m+\frac{1}{2}} - H_x|^n_{k,l-\frac{1}{2},m+\frac{1}{2}}}{\Delta y} - J_z|^n_{k,l,m+\frac{1}{2}},$$

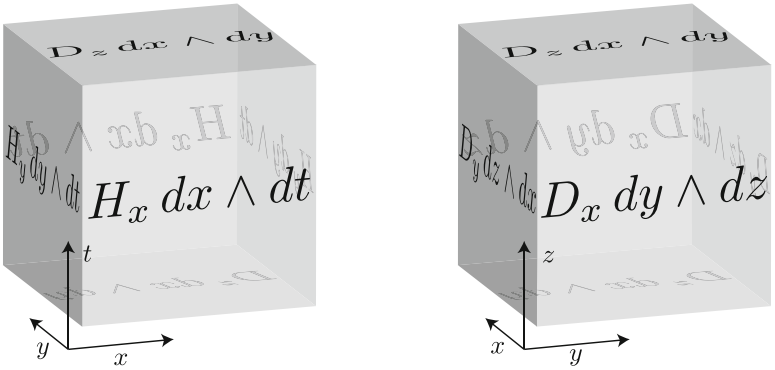

Fig. 5 Values of $G = *F$ are stored on dual 2-faces in a rectangular grid. Shown here are a mixed space/time dual 3-cell (left), corresponding to a spacelike primal edge; and a purely spatial dual 3-cell (right), corresponding to a timelike primal edge. There are also two other mixed space/time cells, as in Figure 4, that are not shown here

and

$$\frac{D_x|^{n+\frac{1}{2}}_{k+\frac{1}{2},l,m} - D_x|^{n+\frac{1}{2}}_{k-\frac{1}{2},l,m}}{\Delta x} + \frac{D_y|^{n+\frac{1}{2}}_{k,l+\frac{1}{2},m} - D_y|^{n+\frac{1}{2}}_{k,l-\frac{1}{2},m}}{\Delta y} + \frac{D_z|^{n+\frac{1}{2}}_{k,l,m+\frac{1}{2}} - D_z|^{n+\frac{1}{2}}_{k,l,m-\frac{1}{2}}}{\Delta z} = \rho|^{n+\frac{1}{2}}_{k,l,m}. \tag{10}$$

This results from storing G on the dual grid, as shown in Figure 5. This set of equations is the discrete version of

$$\partial_t \mathbf{D} = \nabla \times \mathbf{H} - \mathbf{J}, \qquad \nabla \cdot \mathbf{D} = \rho.$$

After eliminating the redundant divergence equations (9) and (10) (see Subsection 5.2 for details) and making the substitutions $\mathbf{D} = \epsilon\mathbf{E}$, $\mathbf{B} = \mu\mathbf{H}$, the remaining equations are precisely the Yee scheme, as formulated in Rylander et al. [39, p. 73].

4.2 Unstructured Spatial Mesh with Uniform Time Steps

We now consider the case of an unstructured grid in space, but with uniform steps in time as advocated in, e.g., Bossavit and Kettunen [6]. Suppose that, instead of a rectangular grid for both space and time, we have an arbitrary space discretization on which we would like to take uniform time steps. (For example, we may be given

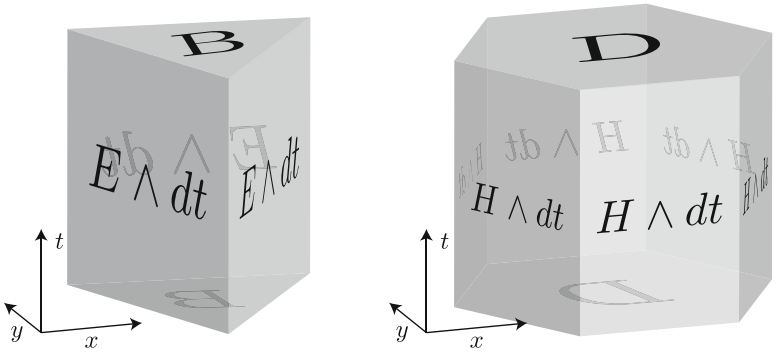

Fig. 6 For an unstructured spatial mesh, F is stored on primal 2-faces (left), while $G = *F$ is stored on dual 2-faces (right). Shown here are the values on mixed space/time 3-cells (the purely spatial 3-cells, which correspond to the divergence equations and do not contribute to the equations of motion, are not shown)

a tetrahedral mesh of the spatial domain.) This mesh contains two distinct types of 2-faces. First, there are triangular faces that live entirely in the space mesh at a single position in time. Every edge of such a face is spacelike—that is, it has positive length—so the causality operator defined in Subsection 3.2 takes the value $\kappa = 1$. Second, there are rectangular faces that live between time steps. These faces consist of a single spacelike edge extruded by one time step. Because they have one timelike edge, these faces satisfy $\kappa = -1$. Again, the circumcentric-dual DEC framework applies directly to this type of mesh, since the prismal extrusion of a 3-simplex still has a well-defined circumcenter.

4.2.1 Setup

Again, we can characterize the discrete values of F by looking at the continuous expression

$$F = E \wedge \mathrm{d}t + B.$$

Therefore, let us assign B to the purely spacelike faces and $E\Delta t$ to the mixed space/time faces. Looking at $G = *F$ shows that mixed dual faces should store $H\Delta t$ and spacelike dual faces should store D; see Figure 6.

4.2.2 Equations of Motion

As in Bossavit [5], we can store the values of each differential form over every spatial element in an array, using the method described in Subsection 3.2. This leads to the arrays B^n and H^n at whole time steps n, and $E^{n+1/2}$ and $D^{n+1/2}$ at

half time steps. Let d_1 denote the edges-to-faces incidence matrix for the spatial domain. That is, d_1 is the matrix corresponding to the discrete exterior derivative, taken only in space, from primal 1-forms to primal 2-forms. Similarly, the transpose d_1^T corresponds to the exterior derivative from spatial dual 1-forms to dual 2-forms. Then the equation $\mathrm{d}F = 0$, evaluated on all prismal 3-faces becomes

$$\frac{B^{n+1} - B^n}{\Delta t} = -\mathrm{d}_1 E^{n+1/2}.$$

Likewise, the equation $\mathrm{d}G = \mathcal{J}$, evaluated on all space/time 3-faces in the dual mesh, becomes

$$\frac{D^{n+1/2} - D^{n-1/2}}{\Delta t} = \mathrm{d}_1^T H^n - J^n.$$

We can also evaluate $\mathrm{d}F = 0$ and $\mathrm{d}G = \mathcal{J}$ on spacelike 3-faces, e.g, tetrahedra; these simply yield the discrete versions of the divergence conditions for B and D, which can be eliminated.

Therefore, the DEC scheme for such a mesh is equivalent to Bossavit and Kettunen's Yee-like scheme; additionally, when the spatial mesh is taken to be rectangular, this integrator reduces to the standard Yee scheme. However, we now have solid foundations to extend this integrator to handle asynchronous updates for improved efficiency.

4.3 Unstructured Spatial Mesh with Asynchronous Time Steps

Instead of choosing the same time step size for every element of the spatial mesh, as in the previous two sections, it is often more efficient to assign each element its own, optimized time step, as done in Lew et al. [28] for problems in elastodynamics. In this case, rather than the entire mesh evolving forward in time simultaneously, individual elements advance one-by-one, asynchronously—hence the name *asynchronous variational integrator* (AVI). As we will prove in Section 5, this asynchronous update process will maintain the variational nature of the integration scheme. Here, we again allow the spatial mesh to be unstructured.

4.3.1 Setup

After choosing a primal space mesh, assign each spatial 2-face (e.g., triangle) σ its own discrete time set

$$\Theta_\sigma = \left\{ t_\sigma^0 < \cdots < t_\sigma^{N_\sigma} \right\}.$$

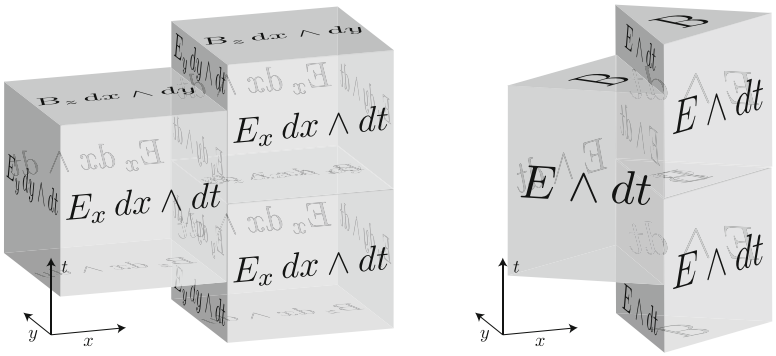

Fig. 7 Shown here is part of an AVI mesh, for a rectangular spatial mesh (left) and for an unstructured spatial mesh (right). The different heights of the spacetime prisms reflect the fact that elements can take different time steps from one another. Moreover, these time steps can be asynchronous, as seen in the mismatch between the horizontal faces

For example, one might assign each face a fixed time step size $\Delta t_\sigma = t_\sigma^{n+1} - t_\sigma^n$, taking equal time steps *within* each element, but with Δt varying *across* elements. We further require for simplicity of explanation that, except for the initial time, no two faces take the same time step: that is, $\Theta_\sigma \cap \Theta_{\sigma'} = \{t_0\}$ for $\sigma \neq \sigma'$.

In order to keep proper time at the edges e where multiple faces with different time sets meet, we let

$$\Theta_e = \bigcup_{\sigma \ni e} \Theta_\sigma = \left\{ t_e^0 \leq \cdots \leq t_e^{N_e} \right\}.$$

Therefore the mixed space-time 2-faces, which correspond to the edge e extruded over a time step, are assigned the set of intermediate times

$$\Theta'_e = \left\{ t_e^{1/2} \leq \cdots \leq t_e^{N_e - 1/2} \right\},$$

where $t_e^{k+1/2} = (t_e^{k+1} + t_e^k)/2$. The values stored on a primal AVI mesh are shown in Figure 7.

Since $\Theta_e \supset \Theta_\sigma$ when $e \subset \sigma$, each spatial edge e takes more time steps than any one of its incident faces σ; as a result, it is not possible in general to construct a circumcentric dual on the entire spacetime AVI mesh, since the mesh is not prismal and hence the circumcenter may not exist. Instead, we find the circumcentric dual to the *spatial* mesh, and assign the same time steps to the primal and dual elements

$$\Theta_{*\sigma} = \Theta_\sigma, \qquad \Theta_{*e} = \Theta_e.$$

This results in well-defined primal and dual cells for each 2-element in spacetime, and hence a Hodge star for this order. (A Hodge star on k-forms for $k \neq 2$ is not needed to formulate Maxwell's equations.)

4.3.2 Equations of Motion

The equation $\mathrm{d}F = 0$, evaluated on a mixed space/time 3-cell, becomes

$$\frac{B_\sigma^{n+1} - B_\sigma^n}{t_\sigma^{n+1} - t_\sigma^n} = -\mathrm{d}_1 \sum \left\{ E_e^{m+1/2} : t_\sigma^n < t_e^{m+1/2} < t_\sigma^{n+1} \right\}. \tag{11}$$

Similarly, the equation $\mathrm{d}G = \mathcal{J}$ becomes

$$\frac{D_e^{m+1/2} - D_e^{m-1/2}}{t_e^{m+1/2} - t_e^{m-1/2}} = \mathrm{d}_1^T \left(H_\sigma^n \, \mathbb{I}_{\{t_\sigma^n = t_e^m\}} \right) - J_e^m, \tag{12}$$

where $\mathbb{I}_{\{t_\sigma^n = t_e^m\}}$ is the indicator function "picking out" the incident face that lives at the same time step as edge e, i.e., equaling 1 when face σ has $t_\sigma^n = t_e^m$ for some n, and 0 otherwise.

Solving an initial value problem can then be summarized by the following update loop:

1. Pick the minimum time t_σ^{n+1} where B_σ^{n+1} has not yet been computed.
2. Advance B_σ^{n+1} according to (11).
3. Update $H_\sigma^{n+1} = *_\mu^{-1} B_\sigma^{n+1}$.
4. Advance $D_e^{m+3/2}$ on neighboring edges $e \subset \sigma$ according to (12).
5. Update $E_e^{m+3/2} = *_\epsilon^{-1} D_e^{m+3/2}$.

4.3.3 Iterative Time Stepping Scheme

As detailed in Lew et al. [28] for elastodynamics, the explicit AVI update scheme can be implemented by selecting mesh elements from a priority queue, sorted by time, and iterating forward. However, as written above, the scheme is not strictly iterative, since (12) depends on past values of E. This can be easily fixed by rewriting the AVI scheme to advance in the variables A and E instead, where the potential A effectively stores the cumulative contribution of E to the value of B on neighboring faces. Compared to the AVI for elasticity, A plays the role of the positions $\mathbf{x}$, while E plays the role of the (negative) velocities $\dot{\mathbf{x}}$. The algorithm is given as pseudocode in Figure 8. Note that if all elements take uniform time steps, the AVI reduces to the Bossavit–Kettunen scheme.

4.3.4 Numerical Experiments

We first present a simple numerical example demonstrating the good energy behavior of our asynchronous integrator. The AVI was used to integrate in time over a 2-D rectangular cavity with perfectly electrically conducting (PEC) boundaries, so

```
// Initialize fields and priority queue
for each spatial edge e do
    A_e ← A_e^0, E_e ← E_e^{1/2}, τ_e ← t_0 // Store initial field values and times
for each spatial face σ do
    τ_σ ← t_0
    Compute the next update time t_σ^1
    Q.push(t_σ^1, σ) // Push element onto queue with its next update time

// Iterate forward in time until the priority queue is empty
repeat
    (t, σ) ← Q.pop() // Pop next element σ and time t from queue
    for each edge e of element σ do
        A_e ← A_e − E_e(t − τ_e) // Update neighboring values of A at time t
    if t < final-time then
        B_σ ← d_1 A_e
        H_σ ← ∗_μ B_σ
        D_e ← ∗_ε E_e
        D_e ← D_e + d_1(e, σ) H_σ(t − τ_σ)
        E_e ← ∗_ε D_e
        τ_σ ← t // Update element's time
        Compute the next update time t_σ^next
        Q.push(t_σ^next, σ) // Schedule σ for next update
until (Q.isEmpty())
```

Fig. 8 Pseudocode for the asynchronous variational integrator (AVI), implemented using a priority queue data structure for storing and selecting the elements to be updated

that E vanishes at the boundary of the domain. The initial values of E were chosen randomly, so as to excite all frequency modes, and integrated for 8 seconds. Each spatial element was given a time step equal to 1/10 of the stability-limiting time step determined by the Courant–Friedrichs–Lewy (CFL) condition.

This simulation was performed for two different spatial discretizations. The first is a uniform discretization, so that each element has identical time step size, which coincides exactly with the Yee scheme. The second discretization randomly partitioned the x- and y-axes, so that each element has completely unique spatial dimensions and time step size, and so the update rule is truly asynchronous. The energy plot for the uniform Yee discretization is shown in Figure 9, while the energy for the random discretization is shown in Figure 10. Even for a completely random, irregular mesh, the AVI method displays near-energy preservation qualities. Such numerical behavior stems from the variational nature of the integrator, which will be detailed in Section 5.

In addition, we tested the performance of the AVI method with regard to computing the resonant frequencies of a 3-D rectangular cavity, but using an *unstructured* tetrahedral spatial mesh. While the resonant frequencies are relatively simple to compute analytically, nodal finite element methods are well known to produce *spurious modes* for this type of simulation. By contrast, as shown in Figure 11, the AVI simulation produces a resonance spectrum consistent with electromagnetic

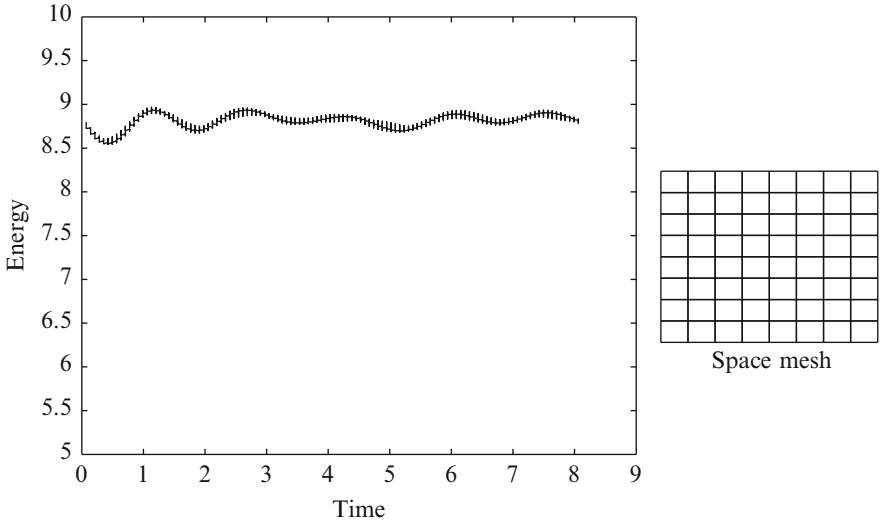

Fig. 9 Energy vs. time for the AVI with uniform space and time discretization. This is the special case where the AVI reproduces the Yee scheme—which is well known to have good energy conservation properties, as seen here (the vertical "tick marks" on the plot show where the elements become synchronized, since they take uniform time steps)

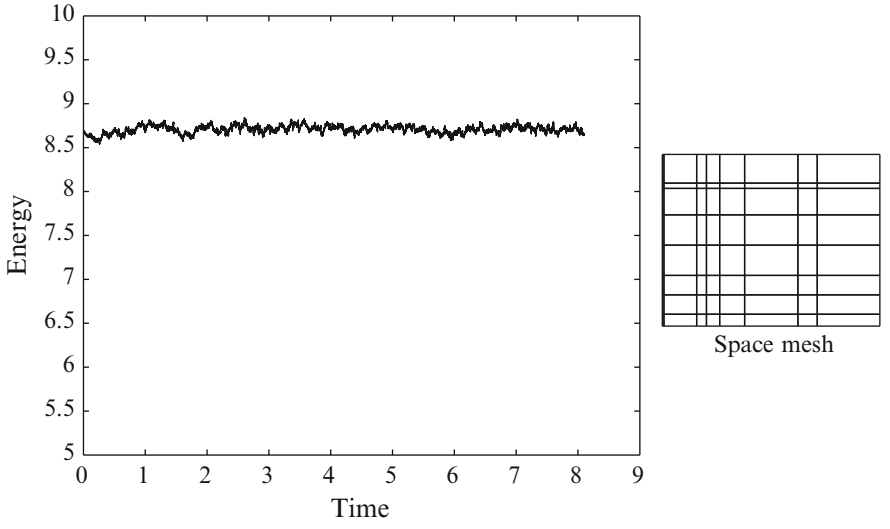

Fig. 10 Energy vs. time for the AVI with random spatial discretization and fully asynchronous time steps. Despite the lack of regularity in the mesh and time steps, the AVI maintains the good energy behavior displayed by the Yee scheme

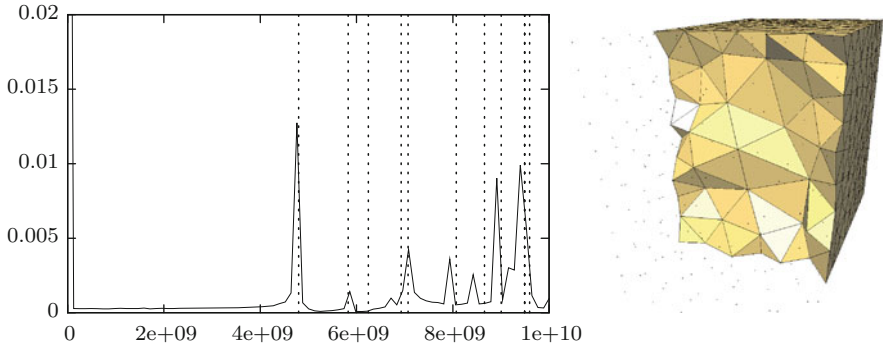

Fig. 11 To produce the power spectrum shown at left, the electric field E was initialized with random data (to excite all frequencies) and integrated forward in time, measuring the field strength at a particular sample point for every time step, and then performing a discrete Fourier transform. The locations of the amplitude "spikes" are consistent with the analytic resonant frequencies, shown by the dashed vertical lines. The spatial mesh, shown at right, was refined closer to the boundary, and coarser in the interior, allowing the AVI to produce this result with fewer total steps than uniform-time-stepping would require

theory. Furthermore, by refining the mesh close to the spatial boundary, while using a coarser discretization in the interior, we were able to achieve these results with less computational effort than a uniformly fine mesh would require, since the time steps were selected to be proportional to the respective element sizes.

4.4 Fully Unstructured Spacetime Mesh

Finally, we look at the most general possible case: an arbitrary discretization of spacetime, such as a simplicial 4-complex. Such a mesh is completely relativistically covariant, so that F cannot be objectively separated into the components E and B without a coordinate frame. In most engineering applications, relativistic effects are insignificant, so a $3 + 1$ mesh (as in the previous subsections) is almost always adequate, and avoids the additional complications of spacetime mesh construction. Still, we expect that there are scientific applications where a covariant discretization of electromagnetism may be very useful. For example, many implementations of numerical general relativity (using Regge calculus for instance) are formulated on simplicial 4-complexes; one might wish to simulate the interaction of gravity with the electromagnetic field, or charged matter, on such a mesh.

4.4.1 Spacetime Mesh Construction

First, a quick caution on mesh construction: since the Lorentz metric is not positive definite, it is possible to create edges that have length 0, despite connecting two distinct points in $\mathbb{R}^{3,1}$ (so-called "null" or "lightlike" edges). Meshes containing such edges are degenerate—akin to a Euclidean mesh containing a triangle with two identical points. In particular, the DEC Hodge star is undefined for 0-volume elements (due to division by zero). Even without 0-volume elements, it is still possible for a spacetime mesh to violate causality, so extra care should be taken. Methods to construct causality-respecting spacetime meshes over a given spatial domain can be found in, e.g., Erickson et al. [12] and Thite [43, 44].

When the mesh contains no inherent choice of a time direction, there is no canonical way to split F into E and B. Therefore, one must set up the problem by assigning values of F directly to 2-cells (or equivalently, assigning values of A to 1-cells). For initial boundary value problems, one might choose to have the initial and final time steps be prismal, so that E and B can be used for initial and final values, while the internal discretization is general.

4.4.2 Equations of Motion

The equations $\mathrm{d}F = 0$ and $\mathrm{d}G = \mathcal{J}$ can be implemented directly in DEC. Since this mesh is generally unstructured, there is no simple algorithm as the ones we presented above. Instead, the equations on F results in a sparse linear system which, given proper boundary conditions, can be solved globally with direct or iterative solvers. However, it is clear that the previous three examples that the methods of Yee, Bossavit–Kettunen, and our AVI integrator are special cases where the global solution is particularly simple to compute via synchronous or asynchronous time updates.

4.4.3 Mesh Construction and Energy Behavior

It is known that, while variational integrators in mechanics do not preserve energy exactly, they have excellent energy behavior, in that it tends to oscillate close to the exact value. This is only true, however, when the integrator takes time steps of uniform size; adaptive and other non-uniform stepping approaches can give poor results unless additional measures are taken to enforce good energy behavior. (See [18, Chapter VIII] for a good discussion of this problem for mechanics applications.)

Therefore, there is no reason to expect that *arbitrary* meshes of spacetime will yield energy results as good as the Yee, Bossavit–Kettunen, and AVI schemes. However, if one is taking a truly covariant approach to spacetime, "energy" is not even defined without specifying a time coordinate. Likewise, one would not necessarily expect good energy behavior from the other methods with respect to an arbitrary transformation of spatial coordinates. Which sort of mesh to choose is thus highly application-dependent.

5 Theoretical Results

In this section, we complete our exposition with a number of theoretical results about the discrete and continuous Maxwell's equations. In particular, we show that the DEC formulation of electrodynamics derives from a discrete Lagrangian variational principle, and that this formulation is consequently multisymplectic. Furthermore, we explore the gauge symmetry of Maxwell's equations, and detail how a particular choice of gauge eliminates the equation for $\nabla \cdot \mathbf{D} - \rho$ from the Euler–Lagrange equations, while preserving it automatically as a momentum map.

Theorem 1. *The discrete Maxwell's equations are precisely the discrete Euler–Lagrange equations corresponding to the discrete Lagrangian density* $\mathcal{L}_d = -\frac{1}{2}\mathrm{d}A \wedge *\mathrm{d}A + A \wedge \mathcal{J}$. *Consequently, the numerical methods of Section 4 are variational integrators.*

Proof. The idea of this proof is to emulate the derivation of the continuous Maxwell's equations from Section 2. Interpreting this in the sense of DEC, we will obtain the discrete Maxwell's equations.

Given a discrete 1-form A and dual source 3-form $\mathcal{J}$, the discrete action functional S_d is defined by

$$S_d[A] = \langle \mathcal{L}_d, \mathcal{K} \rangle = \left\langle -\frac{1}{2}\mathrm{d}A \wedge *\mathrm{d}A + A \wedge \mathcal{J}, \mathcal{K} \right\rangle.$$

Then, taking a discrete 1-form variation α vanishing on the boundary $\partial\mathcal{K}$, the corresponding variation of the action is

$$\mathbf{d}S_d[A] \cdot \alpha = \langle -\mathrm{d}\alpha \wedge *\mathrm{d}A + \alpha \wedge \mathcal{J}, \mathcal{K} \rangle = \langle \alpha \wedge (-\mathrm{d}*\mathrm{d}A + \mathcal{J}), \mathcal{K} \rangle .$$

Note that we used the bold $\mathbf{d}$ to indicate that we are differentiating over the *smooth space of discrete forms* A, as opposed to differentiating over discrete spacetime, for which we use d. Setting this equal to 0 for all variations α, the resulting discrete Euler–Lagrange equations are therefore $\mathrm{d}*\mathrm{d}A = \mathcal{J}$. Defining the discrete 2-forms $F = \mathrm{d}A$ and $G = *F$, this implies $\mathrm{d}F = 0$ and $\mathrm{d}G = \mathcal{J}$, the discrete Maxwell's equations.

5.1 Multisymplecticity

The concept of *multisymplecticity* for Lagrangian field theories was developed in Marsden et al. [31], where it was shown to arise from the boundary terms for general variations of the action, i.e., those not restricted to vanish at the boundary. (This work had its roots in the fabled *GIMMSY* project of Gotay et al. [14, 15].) As originally presented, the Cartan form $\theta_{\mathcal{L}}$ is an $(n+1)$-form, where the

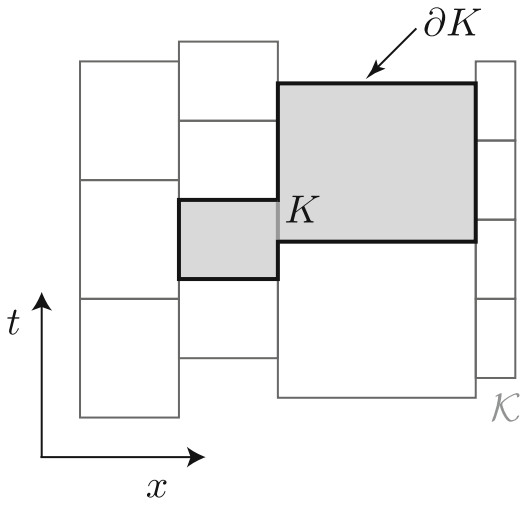

Fig. 12 To illustrate the discrete multisymplectic form formula (14), we have here a 2-D asynchronous-time mesh $\mathcal{K}$, where the shaded region is an arbitrary subcomplex $K \subset \mathcal{K}$. Given any two variations α, β of the field, and the multisymplectic form $\omega_{\mathcal{L}_d}$, the formula states that $\omega_{\mathcal{L}_d} \cdot \alpha \cdot \beta$ vanishes when integrated over the boundary ∂K (shown in bold)

n-dimensional boundary integral is then obtained by contracting $\theta_{\mathcal{L}}$ with a variation. The multisymplectic $(n+2)$-form $\omega_{\mathcal{L}}$ is then given by $\omega_{\mathcal{L}} = -\mathbf{d}\theta_{\mathcal{L}}$. Contracting $\omega_{\mathcal{L}}$ with two arbitrary variations gives an n-form that vanishes when integrated over the boundary, a result called the *multisymplectic form formula*, which results from the identity $\mathbf{d}^2 = 0$. In the special case of mechanics, where $n = 0$, the boundary consists of the initial and final time points; hence, this implies the usual result that the symplectic 2-form ω_L is preserved by the time flow.

Alternatively, as communicated to us by Patrick [37], one can view the Cartan form $\theta_{\mathcal{L}}$ as an n-form-valued 1-form, and the multisymplectic form $\omega_{\mathcal{L}}$ as an n-form-valued 2-form. Therefore, one simply evaluates these forms on tangent variations to obtain a boundary integral, rather than taking contractions. These two formulations are equivalent on smooth spaces. However, we will adopt Patrick's latter definition, since it is more easily adapted to problems on discrete meshes: $\theta_{\mathcal{L}_d}$ and $\omega_{\mathcal{L}_d}$ remain smooth 1- and 2-forms, respectively, but their n-form values are now taken to be discrete. See Figure 12 for an illustration of the discrete multisymplectic form formula.

Theorem 2. *The discrete Maxwell's equations satisfy the multisymplectic form formula* $\langle \omega_{\mathcal{L}_d} \cdot \alpha \cdot \beta, \partial K \rangle = 0$*, for all variations* α, β *of the discrete* 1*-form* A *and all subcomplexes* $K \subset \mathcal{K}$*. Consequently, the numerical methods of Section 4 are multisymplectic.*

Proof. Let $K \subset \mathcal{K}$ be an arbitrary subcomplex, and consider the restricted discrete action functional $s_d = S_d|_K$. Suppose now that we take a discrete variation α, *without* requiring it to vanish on the boundary ∂K. Then variations of the restricted action contain an additional boundary term

$$\mathbf{d}s_d[A] \cdot \alpha = \langle \alpha \wedge (-\mathrm{d} * \mathrm{d}A + \mathcal{J}), K \rangle + \langle \alpha \wedge * dA, \partial K \rangle .$$

Restricting to the space of potentials A that satisfy the discrete Euler–Lagrange equations, the first term vanishes, leaving only

$$\mathbf{d}s_d[A]\cdot\alpha = \langle \alpha \wedge *\mathrm{d}A, \partial K\rangle \tag{13}$$

Then we can express the *Cartan form* $\theta_{\mathcal{L}_d}$ by

$$\theta_{\mathcal{L}_d}\cdot\alpha = \alpha \wedge *\mathrm{d}A.$$

Since $\theta_{\mathcal{L}_d}$ takes a tangent vector α and produces a discrete 3-form on the boundary of the subcomplex, it is a *smooth 1-form taking discrete* 3*-form values*. Now, since the *space of discrete forms* is itself actually continuous, we can take the exterior derivative in the smooth sense on both sides of (13). Evaluating along another first variation β (again, restricted to the space of Euler–Lagrange solutions), we then get

$$\mathbf{d}^2 s_d[A]\cdot\alpha\cdot\beta = \langle \mathbf{d}\theta_{\mathcal{L}_d}\cdot\alpha\cdot\beta, \partial K\rangle\,.$$

Finally, using the multisymplectic form defined by $\omega_{\mathcal{L}_d} = -\mathbf{d}\theta_{\mathcal{L}_d}$ and the fact that $\mathbf{d}^2 s_d = 0$, we get the relation

$$\langle \omega_{\mathcal{L}_d}\cdot\alpha\cdot\beta, \partial K\rangle = 0 \tag{14}$$

for all variations α, β, which completes the proof.

5.2 Gauge Symmetry Reduction and Covariant Momentum Maps

We now explore the symmetry of Maxwell's equations under gauge transformations. This symmetry allows us to reduce the equations by eliminating the time component of A (for some chosen time coordinate), effectively fixing the electric scalar potential to zero. Because this is an incomplete gauge, there is a remaining gauge symmetry, and hence a conserved momentum map. This conserved quantity turns out to automatically preserve the Gauss constraint $\nabla\cdot\mathbf{D} = \rho$, which justifies its elimination from the Euler–Lagrange equations. These calculations are done in the formal language of differential forms and exterior calculus, and hence the results apply equally well to the continuum and discrete cases of electrodynamics.

5.3 Choosing a Gauge

Because Maxwell's equations only depend on $\mathrm{d}A$, they are invariant under gauge transformations of the form $A \mapsto A + \mathrm{d}f$, where f is any scalar function on spacetime. If we fix a time coordinate, we can now choose the Weyl gauge, so that the time component $A_t = 0$. Therefore, we can assume that

$$A = A_x\,\mathrm{d}x + A_y\,\mathrm{d}y + A_z\,\mathrm{d}z.$$

In fact, A_x, A_y, A_z are precisely the components of the familiar vector potential $\mathbf{A} = A^\sharp$.

5.4 Reducing the Equations

Having fixed the gauge and chosen a time coordinate, we can now define two new "partial exterior derivative" operators, d_t (time) and d_s (space), where $\mathrm{d} = \mathrm{d}_t + \mathrm{d}_s$. Since A contains no $\mathrm{d}t$ terms, $\mathrm{d}_s A$ is a 2-form containing only the space terms of $\mathrm{d}A$, while $\mathrm{d}_t A$ contains the terms involving both space and time. That is,

$$\mathrm{d}_t A = E \wedge \mathrm{d}t, \qquad \mathrm{d}_s A = B.$$

Restricted to this subspace of potentials, the Lagrangian density then becomes

$$\begin{aligned}\mathcal{L} &= -\frac{1}{2}\,(\mathrm{d}_t A + \mathrm{d}_s A) \wedge *\,(\mathrm{d}_t A + \mathrm{d}_s A) + A \wedge \mathcal{J} \\ &= -\frac{1}{2}\,(\mathrm{d}_t A \wedge *\mathrm{d}_t A + \mathrm{d}_s A \wedge *\mathrm{d}_s A) + A \wedge J \wedge \mathrm{d}t\end{aligned}$$

Next, varying the action along a restricted variation α that vanishes on ∂X,

$$\begin{aligned}\mathbf{d}S[A]\cdot\alpha &= \int_X (\mathrm{d}_t\alpha \wedge D - \mathrm{d}_s\alpha \wedge H \wedge \mathrm{d}t + \alpha \wedge J \wedge \mathrm{d}t) \\ &= \int_X \alpha \wedge (\mathrm{d}_t D - \mathrm{d}_s H \wedge \mathrm{d}t + J \wedge \mathrm{d}t)\,.\end{aligned} \tag{15}$$

Setting this equal to zero by Hamilton's principle, one immediately gets Ampère's law as the sole Euler–Lagrange equation. The divergence constraint $\mathrm{d}_s D = \rho$, corresponding to Gauss's law, has been eliminated via the restriction to the Weyl gauge.

5.4.1 Noether's Theorem and Preservation of the Gauss Constraint

Let us restrict A to be an Euler–Lagrange solution in the Weyl gauge, but remove the previous requirement that variations α be fixed at the initial time t_0 and final time t_f. Then, varying the action along this new α, the Euler–Lagrange term disappears, but we now pick up an additional boundary term due to integration by parts

$$\mathbf{d}S[A]\cdot\alpha = \int_\Sigma \alpha\wedge D\Big|_{t_0}^{t_f},$$

where Σ denotes a Cauchy hypersurface of X, corresponding to the spatial domain. If we vary along a gauge transformation $\alpha = \mathrm{d}_s f$, then this becomes

$$\mathbf{d}S[A]\cdot\mathrm{d}_s f = \int_\Sigma \mathrm{d}_s f\wedge D\Big|_{t_0}^{t_f} = -\int_\Sigma f\wedge \mathrm{d}_s D\Big|_{t_0}^{t_f}$$

Alternatively, plugging $\alpha = \mathrm{d}_s f$ into (15), we get

$$\mathbf{d}S[A]\cdot\mathrm{d}_s f = \int_X \mathrm{d}_s f\wedge J\wedge \mathrm{d}t = -\int_X f\wedge \mathrm{d}_s J\wedge \mathrm{d}t = -\int_X f\wedge \mathrm{d}_t\rho = -\int_\Sigma f\wedge\rho\Big|_{t_0}^{t_f}.$$

Since these two expressions are equal, and f is an arbitrary function, it follows that

$$(\mathrm{d}_s D-\rho)\big|_{t_0}^{t_f} = 0.$$

This indicates that $\mathrm{d}_s D-\rho$ is a conserved quantity, a momentum map, so if Gauss's law holds at the initial time, then it holds for all subsequent times.

5.5 *Boundary Conditions and Variational Structure*

It should be noted that the variational structure and symmetry of Maxwell's equations may be affected by the boundary conditions that one chooses to impose. There are many boundary conditions that one can specify independent of the initial values, such as the PEC condition used in the numerical example in Subsection 4.3. However, one can imagine more complicated boundary conditions where which the boundary interacts nontrivially with the interior of the domain—such as dissipative or forced boundary conditions, where energy/momentum is removed from or added to the system. In these cases, one will obviously *not* conclude that total charge is conserved, but more generally that the *change* in charge is related to the flux through the spatial boundary. This is because, in the momentum map derivation above, the values of f on the initial time slice causally affect its values on the spatial boundary at intermediate times, not just on the final time slice. Thus, the spatial part of ∂X cannot be neglected for arbitrary boundary conditions.

6 Conclusion

The continued success of the Yee scheme for many applications of computational electrodynamics, for over four decades, illustrates the value of structure-preserving numerical integrators for Maxwell's equations. Recent advances by, among others, Bossavit and Kettunen, and Gross and Kotiuga, have demonstrated the important role of compatible spatial discretization using differential forms, allowing for Yee-like schemes that apply on generalized spatial meshes. In this paper, we have extended this approach by considering discrete forms on *spacetime*, encapsulating both space and time discretization, and have derived a general family of geometric numerical integrators for Maxwell's equations. Furthermore, since we have derived these integrators from a discrete variational principle, the resulting methods are provably multisymplectic and momentum-map-preserving, and they experimentally show correct global energy behavior. Besides proving the variational nature of well-known techniques such as the Yee and Bossavit–Kettunen schemes, we have also introduced a new asynchronous integrator, so that time step sizes can be taken non-uniformly over the spatial domain for increased efficiency, while still maintaining the desirable variational and energy behavior of the other methods.

6.1 Future Work

One promising avenue for future work involves increasing the order of accuracy of these methods by deriving higher-order discrete Hodge star operators. While this would involve redefining the Hodge star matrix to be non-diagonal, the discrete Maxwell's equations would remain formally the same, and hence there would be no change in the variational or multisymplectic properties proven here. In particular, Stern [40] discusses the construction of a spectrally accurate spatial Hodge star, which might make these geometric schemes competitive for applications where non-variational spectral codes are currently favored.

Additionally, the recent work of Kale and Lew [25] has shown that AVIs can be implemented as parallel algorithms for solid mechanics simulations. This uses the fact that, due to the asynchronous update procedure, an element does not need information from every one of its neighbors at every time step, which lessens the need for communication among parallel nodes. The resulting parallel AVIs, or PAVIs, can therefore take advantage of parallel computing architecture for improved efficiency. This approach might be valuable in the case of our electromagnetic AVI.

While we have experimentally observed the fact that variational integrators exhibit near-energy conservation, little is known about this behavior from a theoretical standpoint. In the case of ODEs in mechanics, backward error analysis has shown that these methods exactly integrate a nearby smooth Hamiltonian system, although not much is known about how this relates to the discrete variational principle on the Lagrangian side. Some initial work has been done

in Oliver et al. [35] to understand, also by a backward error analysis approach, why discrete multisymplectic methods also display good energy behavior.

Finally, variational methods using discrete spacetime forms may be developed for field theories other than electromagnetism. Recent work by Gawlik et al. [13], Pavlov et al. [38] has proposed an extension to fluid dynamics through discretization of the infinite-dimensional diffeomorphism group. Another promising candidate is numerical general relativity. One may be able to adapt our work to these field theories to derive numerical methods for, e.g., gravity coupled with an electromagnetic field, or the dynamics of a charged or magnetic fluid.

Acknowledgements We would like to thank several people for their inspiration and suggestions. First of all, Alain Bossavit for suggesting many years ago that we take the present DEC approach to computational electrodynamics, and for his excellent lectures at Caltech on the subject. Second, Michael Ortiz and Eva Kanso for their ongoing interactions on related topics and suggestions. We also thank Doug Arnold, Uri Ascher, Robert Kotiuga, Melvin Leok, Adrian Lew, and Matt West for their feedback and encouragement. In addition, the 3-D AVI simulations shown in Figure 11 were programmed and implemented by Patrick Xia, as part of a Summer Undergraduate Research Fellowship at Caltech supervised by M.D. and A.S.

A.S. was partially supported by a Gordon and Betty Moore Foundation fellowship at Caltech, and by NSF grant CCF-0528101. Y.T. and M.D. were partially supported by NSF grants CCR-0133983 and DMS-0453145 and DOE contract DE-FG02-04ER25657. J.E.M. was partially supported by NSF grant CCF-0528101.

References

1. Arnold, D.N., Falk, R.S., Winther, R.: Finite element exterior calculus, homological techniques, and applications. Acta Numer. **15**, 1–155 (2006). doi:10.1017/S0962492906210018
2. Arnold, D.N., Falk, R.S., Winther, R.: Finite element exterior calculus: from Hodge theory to numerical stability. Bull. Am. Math. Soc. (N.S.) **47**(2), 281–354 (2010). doi:10.1090/S0273-0979-10-01278-4
3. Auchmann, B., Kurz, S.: A geometrically defined discrete Hodge operator on simplicial cells. IEEE Trans. Magn. **42**(4), 643–646 (2006). doi:10.1109/TMAG.2006.870932
4. Bell, N., Hirani, A.N.: PyDEC: software and algorithms for discretization of exterior calculus. ACM Trans. Math. Softw. **39**(1), 3:1–3:41 (2012). doi:10.1145/2382585.2382588
5. Bossavit, A.: Computational Electromagnetism: Variational Formulations, Complementarity, Edge Elements. Academic, San Diego (1998)
6. Bossavit, A., Kettunen, L.: Yee-like schemes on a tetrahedral mesh, with diagonal lumping. Int. J. Numer. Modell. **12**(1–2), 129–142 (1999). doi:10.1002/(SICI)1099-1204(199901/04)12:1/2<129::AID-JNM327>3.0.CO;2-G
7. Bossavit, A., Kettunen, L.: Yee-like schemes on staggered cellular grids: a synthesis between FIT and FEM approaches. IEEE Trans. Magn. **36**(4), 861–867 (2000). doi:10.1109/20.877580
8. Clemens, M., Weiland, T.: Magnetic field simulation using conformal FIT formulations. IEEE Trans. Magn. **38**(2), 389–392 (2002). doi:10.1109/20.996104
9. Desbrun, M., Hirani, A.N., Marsden, J.E.: Discrete exterior calculus for variational problems in computer vision and graphics. In: Proceedings of the 42nd IEEE Conference on Decision and Control (CDC), vol. 5, pp. 4902–4907. IEEE Press, Washington (2003). doi:10.1109/CDC.2003.1272393

10. Desbrun, M., Kanso, E., Tong, Y.: Discrete differential forms for computational modeling. In: Discrete Differential Geometry, Oberwolfach Semin., vol. 38, pp. 287–324. Birkhäuser, Basel (2008). doi:10.1007/978-3-7643-8621-4_16
11. Elcott, S., Schröder, P.: Building your own DEC at home. In: ACM SIGGRAPH 2006 Courses, SIGGRAPH '06, pp. 55–59. ACM, New York (2006). doi:10.1145/1185657.1185666
12. Erickson, J., Guoy, D., Sullivan, J., Üngör, A.: Building spacetime meshes over arbitrary spatial domains. Eng. Comput. **20**(4), 342–353 (2005). doi:10.1007/s00366-005-0303-0
13. Gawlik, E.S., Mullen, P., Pavlov, D., Marsden, J.E., Desbrun, M.: Geometric, variational discretization of continuum theories. Physica D **240**(21), 1724–1760 (2011). doi:10.1016/j.physd.2011.07.011
14. Gotay, M.J., Isenberg, J., Marsden, J.E.: Momentum maps and classical relativistic fields. Part 1: covariant field theory (1997). arXiv:physics/9801019
15. Gotay, M.J., Isenberg, J., Marsden, J.E.: Momentum maps and classical relativistic fields. Part II: canonical analysis of field theories (2004). arXiv:math-ph/0411032
16. Gross, P.W., Kotiuga, P.R.: Electromagnetic Theory and Computation: A Topological Approach. Mathematical Sciences Research Institute Publications, vol. 48. Cambridge University Press, Cambridge (2004)
17. Haber, E., Ascher, U.M.: Fast finite volume simulation of 3D electromagnetic problems with highly discontinuous coefficients. SIAM J. Sci. Comput. **22**(6), 1943–1961 (2001). doi:10.1137/S1064827599360741
18. Hairer, E., Lubich, C., Wanner, G.: Geometric Numerical Integration: Structure-Preserving Algorithms for Ordinary Differential Equations. Springer Series in Computational Mathematics, vol. 31, 2nd edn. Springer, Berlin (2006). doi:10.1007/3-540-30666-8
19. Harrison, J.: Isomorphisms of differential forms and cochains. J. Geom. Anal. **8**(5), 797–807 (1998). doi:10.1007/BF02922671. Dedicated to the memory of Fred Almgren
20. Harrison, J.: Geometric Hodge star operator with applications to the theorems of Gauss and Green. Math. Proc. Camb. Philos. Soc. **140**(1), 135–155 (2006). doi:10.1017/S0305004105008716
21. Harrison, J., Pugh, H.: Topological aspects of differential chains. J. Geom. Anal. **22**(3), 685–690 (2012). doi:10.1007/s12220-010-9210-8
22. Hiptmair, R.: Discrete Hodge operators. Numer. Math. **90**(2), 265–289 (2001). doi:10.1007/s002110100295
23. Hirani, A.N.: Discrete exterior calculus. Ph.D. thesis, California Institute of Technology (2003). http://resolver.caltech.edu/CaltechETD:etd-05202003-095403
24. Holst, M., Stern, A.: Geometric variational crimes: Hilbert complexes, finite element exterior calculus, and problems on hypersurfaces. Found. Comput. Math. **12**(3), 263–293 (2012). doi:10.1007/s10208-012-9119-7
25. Kale, K.G., Lew, A.J.: Parallel asynchronous variational integrators. Int. J. Numer. Methods Eng. **70**(3), 291–321 (2007). doi:10.1002/nme.1880
26. Leok, M.: Foundations of computational geometric mechanics. Ph.D. thesis, California Institute of Technology (2004). http://resolver.caltech.edu/CaltechETD:etd-03022004-000251
27. LeVeque, R.J.: Finite Volume Methods for Hyperbolic Problems. Cambridge Texts in Applied Mathematics. Cambridge University Press, Cambridge (2002)
28. Lew, A., Marsden, J.E., Ortiz, M., West, M.: Asynchronous variational integrators. Arch. Ration. Mech. Anal. **167**(2), 85–146 (2003). doi:10.1007/s00205-002-0212-y
29. Lew, A., Marsden, J.E., Ortiz, M., West, M.: Variational time integrators. Int. J. Numer. Methods Eng. **60**(1), 153–212 (2004). doi:10.1002/nme.958
30. Marsden, J.E., West, M.: Discrete mechanics and variational integrators. Acta Numer. **10**, 357–514 (2001). doi:10.1017/S096249290100006X
31. Marsden, J.E., Patrick, G.W., Shkoller, S.: Multisymplectic geometry, variational integrators, and nonlinear PDEs. Commun. Math. Phys. **199**(2), 351–395 (1998). doi:10.1007/s002200050505

32. Marsden, J.E., Pekarsky, S., Shkoller, S., West, M.: Variational methods, multisymplectic geometry and continuum mechanics. J. Geom. Phys. **38**(3-4), 253–284 (2001). doi:10.1016/S0393-0440(00)00066-8
33. Mullen, P., Memari, P., de Goes, F., Desbrun, M.: HOT: Hodge-optimized triangulations. ACM Trans. Graph. **30**(4), 103:1–103:12 (2011). doi:10.1145/2010324.1964998
34. Nédélec, J.C.: Mixed finite elements in $\mathbb{R}^3$. Numer. Math. **35**(3), 315–341 (1980). doi:10.1007/BF01396415
35. Oliver, M., West, M., Wulff, C.: Approximate momentum conservation for spatial semidiscretizations of semilinear wave equations. Numer. Math. **97**(3), 493–535 (2004). doi:10.1007/s00211-003-0488-3
36. O'Rourke, J.: Computational Geometry in C, 2nd edn. Cambridge University Press, Cambridge (1998)
37. Patrick, G.W.: Geometric classical field theory. Personal communication (2004)
38. Pavlov, D., Mullen, P., Tong, Y., Kanso, E., Marsden, J.E., Desbrun, M.: Structure-preserving discretization of incompressible fluids. Physica D **240**(6), 443–458 (2011). doi:10.1016/j.physd.2010.10.012
39. Rylander, T., Ingelström, P., Bondeson, A.: Computational Electromagnetics. Texts in Applied Mathematics, vol. 51, 2nd edn. Springer, New York (2013). doi:10.1007/978-1-4614-5351-2
40. Stern, A.: Geometric discretization of Lagrangian mechanics and field theories. Ph.D. thesis, California Institute of Technology (2009). http://resolver.caltech.edu/CaltechETD:etd-12312008-173851
41. Taflove, A., Hagness, S.C.: Computational Electrodynamics: The Finite-Difference Time-Domain Method, 3rd edn. Artech House Inc., Boston (2005)
42. Tarhasaari, T., Kettunen, L., Bossavit, A.: Some realizations of a discrete Hodge operator: a reinterpretation of finite element techniques. IEEE Trans. Magn. **35**(3), 1494–1497 (1999). doi:10.1109/20.767250
43. Thite, S.: Spacetime meshing for discontinuous Galerkin methods. Ph.D. thesis, University of Illinois at Urbana-Champaign (2005). http://hdl.handle.net/2142/11078
44. Thite, S.: Adaptive spacetime meshing for discontinuous Galerkin methods. Comput. Geom. **42**(1), 20–44 (2009). doi:10.1016/j.comgeo.2008.07.003
45. Wang, K., Weiwei, Tong, Y., Desbrun, M., Schröder, P.: Edge subdivision schemes and the construction of smooth vector fields. ACM Trans. Graph. **25**(3), 1041–1048 (2006). doi:10.1145/1141911.1141991
46. Whitney, H.: Geometric Integration Theory. Princeton University Press, Princeton (1957)
47. Wise, D.K.: p-form electromagnetism on discrete spacetimes. Class. Quantum Gravity **23**(17), 5129–5176 (2006). doi:10.1088/0264-9381/23/17/004
48. Yee, K.S.: Numerical solution of inital boundary value problems involving Maxwell's equations in isotropic media. IEEE Trans. Ant. Prop. **14**(3), 302–307 (1966). doi:10.1109/TAP.1966.1138693
49. Yoshimura, H., Marsden, J.E.: Dirac structures in Lagrangian mechanics. II. Variational structures. J. Geom. Phys. **57**(1), 209–250 (2006). doi:10.1016/j.geomphys.2006.02.012

Hamel's Formalism and Variational Integrators

Kenneth R. Ball and Dmitry V. Zenkov

Abstract Hamel's formalism is a representation of Lagrangian mechanics obtained by measuring the velocity components relative to a frame that generically is not induced by configuration coordinates. The use of this formalism often leads to a simpler representation of dynamics. Utilizing the variational discretization approach, this paper develops a discrete Hamel's formalism with applications to nonholonomic integrators.

1 Introduction

This paper introduces the discrete Hamel formalism along with some of its applications. Besides being of a pure theoretical interest, this development is motivated by restoring the concept of ideal constraints in the discrete setting and by an attempt to better understand structural stability of variational and nonholonomic integrators. A loss of structural stability has been recently observed in [25, 26, 34].

Hamel's formalism is a version of Lagrangian mechanics in which the velocity components are measured relative to a set of independent vector fields on the configuration space. These vector fields are not associated with configuration coordinates and therefore do not commute, leading to the so-called 'bracket terms' in the equations of motion.

One of the reasons for using Hamel's formalism is that the Euler–Lagrange equations written in generalized coordinates, while universal, are not always the best tool for analyzing the dynamics of mechanical systems. For example, it is difficult to study the motion of the Euler top if the Euler–Lagrange equations (either intrinsically or in generalized coordinates) are used to represent the dynamics. On the other hand, the use of the angular velocity components relative to a body frame pioneered by Euler [13] results in a much simpler representation of dynamics. Euler's approach led to the development of the Euler–Poincaré equations by Lagrange [24] for reasonably general Lagrangians on the rotation group and by Poincaré [35] for arbitrary Lie groups (see [27] for details and history). An extension

K.R. Ball • D.V. Zenkov (✉)
Department of Mathematics, North Carolina State University, Raleigh, NC 27695, USA
e-mail: krball@ncsu.edu; dvzenkov@ncsu.edu

D.E. Chang et al. (eds.), *Geometry, Mechanics, and Dynamics*, Fields Institute Communications 73, DOI 10.1007/978-1-4939-2441-7_20

of this formalism from Lie groups to arbitrary configuration manifolds was carried out by Hamel [16]. Hamel's formalism is especially useful in nonholonomic mechanics. See e.g. [5, 30, 33] for the history and contemporary exposition of Hamel's formalism.

Discrete Lagrangian mechanics is obtained by discretizing Hamilton's variational principle. This approach leads to symplectic- and, for systems with symmetry, momentum-preserving integrators. By discretizing the Lagrange–d'Alembert principle, nonconservative forces (see Kane et al. [20] and Marsden and West [28]) and nonholonomic constraints (see Cortés and Martínez [12]) can be incorporated as well. Recall that, in the continuous-time setting, the dynamics of a Lagrangian system with nonholonomic constraints may be reformulated as the dynamics of an unconstrained system by adding the constraint reaction force. See Suslov [37] and Chetaev [11] for details and precise statements. However, as pointed out in Cortés and Martínez [12], the discretizations of these two representations, as a rule, are not the same, which makes the versions of the discrete Lagrange–d'Alembert principle of [20, 28] and [12] incompatible. In other words, the notion of an ideal constraint of continuous-time mechanics is not retained by the discretization of Cortés and Martínez.

Following the variational discretization approach, we develop discrete Hamel's formalism by discretizing Hamilton's principle for Hamel's equations. The principal difficulty in extending this program to Hamel's setting is caused by the bracket terms, as a discrete analogue of the Jacobi–Lie bracket is known only for left- or right-invariant vector fields on Lie groups (Moser and Veselov [32], Marsden, Pekarsky, and Shkoller [29], Bobenko and Suris [6, 7]). In this paper we resolve the bracket term discretization issue for systems on vector spaces.

When a continuous-time system is discretized, we first select the vector fields that are used to measure the velocity components, and then set up the discrete variational principle. In general, the outcome is a somewhat different discrete dynamical system than the outcome of the usual variational discretization procedure. Remarkably, a modification of our formalism for systems with nonholonomic constraints resolves, at least for Chaplygin systems, the ideal constraint issue of Cortés and Martínez. That is, the discrete Lagrange–d'Alembert principle for Hamel's equations in the presence of nonholonomic constraints is identical to the discrete Lagrange–d'Alembert principle of Kane et al. [20] and Marsden and West [28] written after replacing the constraints with their reactions.

Our formalism also contributes to the study of structural stability of nonholonomic integrators. Recently, Lynch and Zenkov [25, 26] discovered that the nonholonomic integrator of Cortés and Martínez, in general, is not structure-preserving, as it is capable of changing the dimension and stability of manifolds of relative equilibria of continuous-time systems. A similar effect was observed in the holonomic setting in [34]. This lack of structural stability is a serious issue as it alters the α- and ω-limit sets, thus making the asymptotic dynamics of the integrator different from the asymptotic dynamics of the underlying continuous-time system. Such an integrator, in principle, is not suitable for long-term numerical simulations of continuous-time nonholonomic systems. Discrete Hamel's equations are certain

to preserve the manifolds of relative equilibria and their stability, and thus are a better candidate for good quality long-term integrators.

The paper is organized as follows: Continuous-time Lagrangian mechanics and Hamel's formalism, Hamilton's variational principle, and discrete mechanics are reviewed in Sections 2–4. Discrete Hamel's formalism is introduced in Section 5. Applications of discrete Hamel's formalism to nonholonomic mechanics and to global energy-momentum numerical integration of the spherical pendulum are exposed in Sections 6 and 7.

2 Lagrangian Mechanics

Lagrangian mechanics provides a systematic approach to deriving the equations of motion as well as establishes the equivalence of force balance and variational principles.

2.1 The Euler–Lagrange Equations

A ***Lagrangian mechanical system*** is specified by a smooth manifold Q called the ***configuration space*** and a function $L : TQ \to \mathbb{R}$ called the ***Lagrangian***. In many cases, the Lagrangian is the kinetic minus potential energy of the system, with the kinetic energy defined by a Riemannian metric and the potential energy being a smooth function on the configuration space Q. If necessary, non-conservative forces can be introduced (e.g., gyroscopic forces that are represented by terms in L that are linear in the velocity), but this is not discussed in detail in this paper.

In local coordinates $q = (q^1, \ldots, q^n)$ on the configuration space Q we write $L = L(q, \dot{q})$. The dynamics is given by the ***Euler–Lagrange equations***

$$\frac{d}{dt}\frac{\partial L}{\partial \dot{q}^i} = \frac{\partial L}{\partial q^i}, \quad i = 1, \ldots, n. \tag{1}$$

These equations were originally derived by Lagrange [24] in 1788 by requiring that simple force balance be *covariant*, i.e. expressible in arbitrary generalized coordinates. A variational derivation of the Euler–Lagrange equations, namely ***Hamilton's principle*** (see Theorem 1 below), came later in the work of Hamilton [17, 18] in 1834/35.

Let $q(t)$, $a \le t \le b$, be a smooth curve in Q. A ***variation*** of the curve $q(t)$ is a smooth map $\beta : [a, b] \times [-\varepsilon, \varepsilon] \to Q$ that satisfies the condition $\beta(t, 0) = q(t)$. This variation gives rise to the vector field

$$\delta q(t) = \left.\frac{\partial \beta(t, s)}{\partial s}\right|_{s=0} \tag{2}$$

along the curve $q(t)$.

Theorem 1. *The following statements are equivalent:*

(i) *The curve $q(t)$, where $a \leq t \leq b$, is a critical point of the* ***action functional***

$$\int_a^b L(q, \dot{q})\, dt$$

on the space of curves in Q connecting q_a to q_b on the interval $a \leq t \leq b$, where we choose variations of the curve $q(t)$ that satisfy the condition $\delta q(a) = \delta q(b) = 0$.

(ii) *The curve $q(t)$ satisfies the Euler–Lagrange equations* (1).

We point out here that this principle assumes that a variation of the curve $q(t)$ induces the variation $\delta\dot{q}(t)$ of its velocity according to the formula

$$\delta\dot{q}(t) := \frac{d}{dt}\delta q(t).$$

For more details and a proof, see e.g. [2, 27], and Theorem 2 below.

3 Lagrangian Mechanics in Non-coordinate Frames

In this section we discuss the continuous-time Hamel formalism and a relevant variational principle, following the exposition of [5].

3.1 The Hamel Equations

In many cases the Lagrangian and the equations of motion have a simpler structure when the velocity components are measured against a frame that is not necessarily induced by system's local configuration coordinates. An example of such a system is the rigid body.

Let $q = (q^1, \ldots, q^n)$ be local coordinates on the configuration space Q and $u_i \in TQ$, $i = 1, \ldots, n$, be smooth independent *local* vector fields on Q defined in the same coordinate neighborhood hereafter denoted U. In certain cases, some or all of u_i can be chosen to be *global* vector fields on Q. The components of u_i relative to the coordinate-induced basis $\partial/\partial q^j$ are written as ψ_i^j; that is,

$$u_i(q) = \psi_i^j(q)\frac{\partial}{\partial q^j},$$

where $i, j = 1, \ldots, n$.

Let $\xi = (\xi^1, \ldots, \xi^n) \in \mathbb{R}^n$ be the components of the velocity vector $\dot{q} \in TQ$ relative to the frame $u(q) = (u_1(q), \ldots, u_n(q))$, i.e.,

$$\dot{q} = u(q) \cdot \xi, \tag{3}$$

where, by definition,

$$u(q) \cdot \xi := \xi^i u_i(q). \tag{4}$$

When convenient, we reverse the order of factors in (4), i.e., we assume that

$$u(q) \cdot \xi = \xi \cdot u(q).$$

The Lagrangian of the system written in the local coordinates (q, ξ) on the velocity phase space TQ reads

$$l(q, \xi) := L(q, u(q) \cdot \xi). \tag{5}$$

The coordinates (q, ξ) are a Lagrangian analogue of non-canonical variables in Hamiltonian dynamics.

Given two elements $\xi, \zeta \in \mathbb{R}^n$, define the antisymmetric bracket operation $[\cdot, \cdot]_q : \mathbb{R}^n \times \mathbb{R}^n \to \mathbb{R}^n$ by

$$u(q) \cdot [\xi, \zeta]_q = \big[u(q) \cdot \xi, u(q) \cdot \zeta\big],$$

where $[\cdot, \cdot]$ is the Jacobi–Lie bracket of vector fields on Q. That is, $[\xi, \zeta]_q$ consists of the components of $[u_i \xi^i, u_j \zeta^j](q)$ relative to the frame $u_1, \ldots, u_n$.

Therefore, each tangent space $T_q U$ is isomorphic to the Lie algebra $W_q := (\mathbb{R}^n, [\cdot, \cdot]_q)$, and the tangent bundle TU is diffeomorphic to a Lie algebra bundle over U.

The ***dual*** of $[\cdot, \cdot]_q$ is, by definition, the operation $[\cdot, \cdot]_q^* : W_q \times W_q^* \to W_q^*$ given by

$$\langle [\xi, \alpha]_q^*, \zeta \rangle := \langle \alpha, [\xi, \zeta]_q \rangle.$$

Define the ***structure functions*** $c_{ij}^a(q)$ by the equations

$$[u_i(q), u_j(q)] = c_{ij}^a(q) u_a(q),$$

$i, j, a = 1, \ldots, n$. These quantities vanish if and only if the vector fields $u_i(q)$, $i = 1, \ldots, n$, commute.

Viewing u_i as vector fields on TQ whose fiber components equal 0, one defines the directional derivatives $u_i[l]$ for a function $l : TQ \to \mathbb{R}$ in a usual way. It is straightforward to show that

$$u_i[l] = \psi_i^j \frac{\partial l}{\partial q^j}.$$

For a frame $u = (u_1, \ldots, u_n)$, define $u[l]$ by the formula

$$u[l] = (u_1[l], \ldots, u_n[l]).$$

The evolution of the variables (q, ξ) is governed by the ***Hamel equations***

$$\frac{d}{dt}\frac{\partial l}{\partial \xi^j} = c_{ij}^a \xi^i \frac{\partial l}{\partial \xi^a} + u_j[l], \tag{6}$$

coupled with equation (3). If $u_i = \partial/\partial q^i$, equations (6) become the Euler–Lagrange equations (1). Equations (6) were introduced in [16] (see also [33] and [5] for details and some history).

3.2 Hamilton's Principle for Hamel's Equations

The variational derivation of Hamel's equations in this section mostly follows [5]. We refer the readers to [27] for the related history of the development of variational principles for the Euler–Lagrange, Euler–Poincaré, and Hamel equations, and to [1] for the Hamilton–Pontryagin principle for the Hamel equations.

Theorem 2 (Zenkov, Bloch, and Marsden [5]). *Let $L : TQ \to \mathbb{R}$ be a Lagrangian and l be its representation in local coordinates (q, ξ). Then, the following statements are equivalent:*

(i) *The curve $q(t)$, where $a \le t \le b$, is a critical point of the action functional*

$$\int_a^b L(q, \dot{q})\, dt \tag{7}$$

on the space of curves in Q connecting q_a to q_b on the interval $[a, b]$, where we choose variations of the curve $q(t)$ that satisfy $\delta q(a) = \delta q(b) = 0$.

(ii) *The curve $q(t)$ satisfies the Euler–Lagrange equations*

$$\frac{d}{dt}\frac{\partial L}{\partial \dot{q}} = \frac{\partial L}{\partial q}.$$

(iii) *The curve* $(q(t), \xi(t))$ *is a critical point of the functional*

$$\int_a^b l(q, \xi)\, dt \tag{8}$$

with respect to variations $\delta\xi$*, induced by the variations*

$$\delta q = u(q) \cdot \zeta \equiv u_i(q)\zeta^i, \tag{9}$$

and given by

$$\delta\xi = \dot{\zeta} + [\xi, \zeta]_q.^{1} \tag{10}$$

(iv) *The curve* $(q(t), \xi(t))$ *satisfies the Hamel equations*

$$\frac{d}{dt}\frac{\partial l}{\partial \xi} = \left[\xi, \frac{\partial l}{\partial \xi}\right]_q^* + u[l]$$

coupled with the equations $\dot{q} = u(q) \cdot \xi \equiv \xi^i u_i(q)$.

For the early development of these equations see [35] and [16].

Proof. The equivalence of (i) and (ii) is proved by computing the variation of the action functional (7):

$$\delta \int_a^b L(q, \dot{q})\, dt = \int_a^b \left(\frac{\partial L}{\partial q}\delta q + \frac{\partial L}{\partial \dot{q}}\delta\dot{q}\right) dt = \int_a^b \left(\frac{\partial L}{\partial q} - \frac{d}{dt}\frac{\partial L}{\partial \dot{q}}\right) \delta q\, dt.$$

Recall that we denote the components of $\delta q(t)$ relative to the frame $u(q(t)) = (u_1(q(t)), \ldots, u_n(q(t)))$ by $\zeta(t) = (\zeta^1(t), \ldots, \zeta^n(t))$; that is,

$$\delta q(t) = u(q(t)) \cdot \zeta(t) \equiv u_i(q(t))\zeta^i(t).$$

To prove the equivalence of (i) and (iii), we first compute the quantities $\delta\dot{q}$ and $d(\delta q)/dt$. Using the definition (2) of the field δq, one concludes that

$$\delta u_a(q(t)) = \left.\frac{\partial u_a(\beta(t, s))}{\partial s}\right|_{s=0} = \zeta \cdot u[u_a] = \delta q[u_a] \equiv \zeta^b u_b[u_a]. \tag{11}$$

Similarly,

$$\frac{d}{dt}u_b(q(t)) = \dot{q}[u_b] = \xi \cdot u[u_b] \equiv \xi^a u_a[u_b].$$

[1] If Q is a Lie group, this formula is derived in Bloch, Krishnaprasad, Marsden, and Ratiu [4].

Next,

$$\delta\dot{q} = \delta u(q(t)) \cdot \xi(t) + u(q(t)) \cdot \delta\xi(t),$$

$$\frac{d(\delta q)}{dt} = \frac{du(q(t))}{dt} \cdot \zeta(t) + u(q(t)) \cdot \dot{\zeta}(t).$$

Equivalently, in coordinates,

$$\delta\dot{q} = \delta\left(\xi^i(t)u_i(q(t))\right) = \delta\xi^i(t)u_i(q(t)) + \xi^i(t)\frac{\partial u_i}{\partial q^j}\delta q^j,$$

$$\frac{d(\delta q)}{dt} = \frac{d}{dt}\left(\zeta^i(t)u_i(q(t))\right) = \dot{\zeta}^i(t)u_i(q(t)) + \zeta^i(t)\frac{\partial u_i}{\partial q^j}\dot{q}^j.$$

Since $\delta\dot{q} = d(\delta q)/dt$, we obtain

$$u(q(t)) \cdot \left(\delta\xi(t) - \dot{\zeta}(t)\right) = \xi^i(t)\zeta^j(t)\big(u_i(q(t))[u_j(q(t))] - u_j(q(t))[u_i(q(t))]\big)$$

$$= \xi^i(t)\zeta^j(t)[u_i(q(t)), u_j(q(t))] \equiv \big[u(q(t)) \cdot \xi(t), u(q(t)) \cdot \zeta(t)\big],$$

which implies formula (10).

To prove the equivalence of (iii) and (iv), we use the above formula and compute the variation the functional (8):

$$\begin{aligned}\delta\int_a^b l(q,\xi)\,dt &= \int_a^b \left(\frac{\partial l}{\partial q}\delta q + \frac{\partial l}{\partial \xi}\delta\xi\right)dt \\ &= \int_a^b \left(\zeta \cdot u[l] + \frac{\partial l}{\partial \xi}\left(\dot{\zeta} + [\xi,\zeta]_{q(t)}\right)\right)dt \\ &= \int_a^b \left(u[l] + \left[\xi, \frac{\partial l}{\partial \xi}\right]^*_{q(t)} - \frac{d}{dt}\frac{\partial l}{\partial \xi}\right)\zeta\,dt.\end{aligned}$$

The latter vanishes if and only if the Hamel equations are satisfied. □

3.3 *Remarks on the Frame Selection*

As discussed in [2, 3], and [5], constraints and symmetry naturally define subbundles of the velocity phase space TQ. For underactuated mechanical systems, the controlled directions define a subbundle of the momentum phase space T^*Q. It may be beneficial to select a frame in such a way that suitable subframes of the

frame and its dual span the mentioned subbundles. Such frames lead to a simpler representation of dynamics and clarify the structure of the mechanical system under consideration (subsystems, interconnections, etc.).

4 Discrete Mechanics

A discrete analogue of Lagrangian mechanics can be obtained by discretizing Hamilton's principle; this approach underlies the construction of variational integrators. See Marsden and West [28], and references therein, for a more detailed discussion of discrete mechanics.

A key notion is that of the ***discrete Lagrangian***, which is a map $L^d : Q \times Q \to \mathbb{R}$ that approximates the action integral along an exact solution of the Euler–Lagrange equations joining the configurations $q_k, q_{k+1} \in Q$,

$$L^d(q_k, q_{k+1}) \approx \operatorname*{ext}_{q \in C([0,h],Q)} \int_0^h L(q, \dot{q})\, dt,$$

where $C([0,h], Q)$ is the space of curves $q : [0,h] \to Q$ with $q(0) = q_k$, $q(h) = q_{k+1}$, and ext denotes extremum.

In the discrete setting, the action integral of Lagrangian mechanics is replaced by an ***action sum***

$$S^d(q_0, q_1, \ldots, q_N) = \sum_{k=0}^{N-1} L^d(q_k, q_{k+1}),$$

where $q_k \in Q$, $k = 0, 1, \ldots, N$, is a finite sequence in the configuration space. The equations are obtained by the ***discrete Hamilton principle***, which extremizes the discrete action given fixed endpoints q_0 and q_N. Taking the extremum over $q_1, \ldots, q_{N-1}$ gives the ***discrete Euler–Lagrange equations***

$$D_1 L^d(q_k, q_{k+1}) + D_2 L^d(q_{k-1}, q_k) = 0 \tag{12}$$

for $k = 1, \ldots, N-1$. Here and below, $D_i F$ denotes the partial derivative of the function F with respect to its ith input. Equations (12) implicitly define the ***update map*** $\Phi : Q \times Q \to Q \times Q$, where $\Phi(q_{k-1}, q_k) = (q_k, q_{k+1})$ and $Q \times Q$ replaces the velocity phase space TQ of continuous-time Lagrangian mechanics.

In the case that Q is a vector space, it may be convenient to use $(q_{k+1/2}, v_{k,k+1})$, where $q_{k+1/2} = \frac{1}{2}(q_k + q_{k+1})$ and $v_{k,k+1} = \frac{1}{h}(q_{k+1} - q_k)$, as a state of a discrete

mechanical system. In such a representation, the discrete Lagrangian becomes a function of $(q_{k+1/2}, v_{k,k+1})$, and the discrete Euler–Lagrange equations read

$$\tfrac{1}{2}\big(D_1L^d(q_{k-1/2}, v_{k-1,k}) + D_1L^d(q_{k+1/2}, v_{k,k+1})\big) + \tfrac{1}{h}\big(D_2L^d(q_{k-1/2}, v_{k-1,k}) - D_2L^d(q_{k+1/2}, v_{k,k+1})\big) = 0.$$

These equations are equivalent to the variational principle

$$\delta S^d = \sum_{k=0}^{N-1} \big(D_1L^d(q_{k+1/2}, v_{k,k+1})\,\delta q_{k+1/2} + D_2L^d(q_{k+1/2}, v_{k,k+1})\,\delta v_{k,k+1}\big) = 0, \tag{13}$$

where the variations $\delta q_{k+1/2}$ and $\delta v_{k,k+1}$ are induced by the variations δq_k and are given by the formulae

$$\delta q_{k+1/2} = \tfrac{1}{2}\big(\delta q_{k+1} + \delta q_k\big), \quad \delta v_{k,k+1} = \tfrac{1}{h}\big(\delta q_{k+1} - \delta q_k\big).$$

The discrete Hamel formalism introduced below may be interpreted as a generalization of the representation (13) of discrete mechanics.

5 Discrete Hamel's Equations

In the rest of the paper we assume that Q is a vector space. Start with a sequence of configurations $\{q_k\}_{k=0}^N$. Given a parameter $\tau \in [0, 1]$, define the points $q_{k+\tau} := (1-\tau)q_k + \tau q_{k+1}$ for each $0 \le k \le N-1$. The velocity components relative to the frame $u(q)$ at $q_{k+\tau}$ are denoted $\xi_{k,k+1} = (\xi^1_{k,k+1}, \dots, \xi^n_{k,k+1})$. Similar to [8, 22], the phase space for the suggested discretization of Hamel's equation is the tangent bundle TQ. In local coordinates (q, ξ) on TQ, the discrete Lagrangian $l^d : TQ \to \mathbb{R}$ reads $l^d = l^d(q_{k+\tau}, \xi_{k,k+1})$. To discretize a continuous-time system, we suggest the following procedure:

(i) Select a frame $u(q)$ and identify the continuous-time Lagrangian $l(q, \xi)$, as in (5).
(ii) Construct the discrete Lagrangian using the formula

$$l^d(q_{k+\tau}, \xi_{k,k+1}) = hl(q_{k+\tau}, \xi_{k,k+1}).$$

The action sum then is

$$s^d = \sum_{k=0}^{N-1} l^d(q_{k+\tau}, \xi_{k,k+1}), \tag{14}$$

which is an approximation of the action integral (8) of the continuous-time system.

Given $\tau \in [0,1]$, define $\zeta_{k+\tau}$ by the formula

$$\zeta_{k+\tau} = (1-\tau)\zeta_k + \tau\zeta_{k+1}. \tag{15}$$

The quantities ζ_k, ζ_{k+1}, and $\zeta_{k+\tau}$ will be used below to establish the discrete analogues of the variation formulae (9) and (10).

Define the ***discrete conjugate momentum*** by

$$\mu_{k,k+1} := D_2 l^d(q_{k+\tau}, \xi_{k,k+1}). \tag{16}$$

Below, we use the notations

$$u_{k+\tau} := u(q_{k+\tau}),\ \ l^d_{k+\tau} := l^d(q_{k+\tau}, \xi_{k,k+1}),\ \ u\big[l^d\big]_{k+\tau} := u\big[l^d\big](q_{k+\tau}, \xi_{k,k+1}),$$

etc.

Theorem 3. *The sequence* $\big(q_{k+\tau}, \xi_{k,k+1}\big) \in TQ$ *satisfies the* ***discrete Hamel equations***

$$\begin{aligned}&\tfrac{1}{h}\big(\mu_{k-1,k} - \mu_{k,k+1}\big) + \tau u\big[l^d\big]_{k-1+\tau} + (1-\tau)u\big[l^d\big]_{k+\tau}\\ &\quad + \tau\big[\xi_{k-1,k}, \mu_{k-1,k}\big]^*_{q_{k-1+\tau}} + (1-\tau)\big[\xi_{k,k+1}, \mu_{k,k+1}\big]^*_{q_{k+\tau}} = 0\end{aligned} \tag{17}$$

if and only if

$$\delta s^d = \delta \sum_{k=0}^{N-1} l^d(q_{k+\tau}, \xi_{k,k+1}) = 0,$$

where

$$\delta q_{k+\tau} = u(q_{k+\tau}) \cdot \zeta_{k+\tau}, \tag{18}$$

$$\delta\xi_{k,k+1} = \tfrac{1}{h}\big(\zeta_{k+1} - \zeta_k\big) + \big[\xi_{k,k+1}, \zeta_{k+\tau}\big]_{q_{k+\tau}}. \tag{19}$$

Here $\zeta_0 = \zeta_N = 0$, *and* $\zeta_{k+\tau}$ *is defined in* (15), $k = 0, \ldots, N-1$.

In order to obtain a complete system of equations, one supplements (17) with a discrete analogue of the kinematic equation $\dot{q} = u(q) \cdot \xi$. There is a certain freedom in doing that. For now, we assume this discrete analogue to be

$$\frac{\Delta q_k}{h} = u_{k+\tau} \cdot \xi_{k,k+1}.$$

We will use a different discretization of the kinematic equation to construct an integrator for the spherical pendulum in Section 7.

In the coordinate form, the discrete Hamel equations and the formulae for variations read

$$\frac{1}{h}\left(\mu_{k-1,k;j} - \mu_{k,k+1;j}\right) + \tau u_j \left[l^d\right]_{k-1+\tau} + (1-\tau) u_j \left[l^d\right]_{k+\tau}$$
$$+ \tau c^a_{ij}(q_{k-1+\tau})\xi^i_{k-1,k}\mu_{k-1,k;a} + (1-\tau)c^a_{ij}(q_{k+\tau})\xi^i_{k,k+1}\mu_{k,k+1;a} = 0,$$

and

$$\delta q^i_{k+\tau} = \psi^i_b(q_{k+\tau})\zeta^b_{k+\tau},$$
$$\delta\xi^b_{k,k+1} = \frac{1}{h}\left(\zeta^b_{k+1} - \zeta^b_k\right) + c^b_{ij}(q_{k+\tau})\,\xi^i_{k,k+1}\zeta^j_{k+\tau},$$

respectively.

Remark. Unlike the continuous-time case, the formulae for variations (18) and (19) *cannot* be derived in a manner presented in the proof of Theorem 2. The situation here is somewhat similar to the issue encountered and resolved by Chetaev in his work [10] on the equivalence of the Lagrange–d'Alembert and Gauss principles for systems with nonlinear nonholonomic constraints. Recall that Chetaev's approach was to *define* variations in such a way that the two principles become equivalent.

Proof. Using formulae (18) and (19) and computing the variation of the action sum (14), one obtains

$$\begin{aligned}
\delta s^d &= \sum_{k=0}^{N-1} D_1 l^d(q_{k+\tau},\xi_{k,k+1})\,\delta q_{k+\tau} + D_2 l^d(q_{k+\tau},\xi_{k,k+1})\,\delta\xi_{k,k+1}\\
&= \sum_{k=0}^{N-1} \left\langle D_1 l^d_{k+\tau}, u_{k+\tau}\cdot\zeta_{k+\tau}\right\rangle\\
&\qquad + \left\langle D_2 l^d_{k+\tau}, (\zeta_{k+1}-\zeta_k)/h + \left[\xi_{k,k+1},\zeta_{k+\tau}\right]_{q_{k+\tau}}\right\rangle\\
&= \sum_{k=1}^{N-1} \left\langle \tfrac{1}{h}(\mu_{k-1,k}-\mu_{k,k+1}),\zeta_k\right\rangle\\
&\qquad + \left\langle u\left[l^d\right]_{k+\tau} + \left[\mu_{k,k+1},\xi_{k,k+1}\right]^*_{q_{k+\tau}}, (1-\tau)\zeta_k + \tau\zeta_{k+1}\right\rangle\\
&= \sum_{k=1}^{N-1} \left\langle \tfrac{1}{h}(\mu_{k-1,k}-\mu_{k,k+1}),\zeta_k\right\rangle + \left\langle \tau u\left[l^d\right]_{k-1+\tau} + (1-\tau)u\left[l^d\right]_{k+\tau},\zeta_k\right\rangle\\
&\qquad + \left\langle \tau\left[\mu_{k-1,k},\xi_{k-1,k}\right]^*_{q_{k-1+\tau}} + (1-\tau)\left[\mu_{k,k+1},\xi_{k,k+1}\right]^*_{q_{k+\tau}},\zeta_k\right\rangle.
\end{aligned}$$

Thus, vanishing of δs^d for arbitrary ζ_k, $k = 1, \ldots, N-1$, is equivalent to discrete Hamel's equations (17). □

The formulae for variations (18) and (19) in the discrete setting are motivated by the following observations. First, recall that in the continuous-time setting the formula (10) for $\delta\xi$ follows from the formula

$$\delta(u \cdot \xi) - \frac{d}{dt}(u \cdot \zeta) = 0. \tag{20}$$

A discrete analogue of $\delta(u \cdot \xi)$ is relatively straightforward to obtain. Indeed, using the formula

$$\delta q_{k+\tau} = u_{k+\tau} \cdot \zeta_{k+\tau} \equiv u_{k+\tau} \cdot \big((1-\tau)\zeta_k + \tau\zeta_{k+1})\big)$$

and the interpretation of the operator δ as a directional derivative, just like in formula (11), one obtains

$$\delta u_{k+\tau} = \big(\zeta_{k+\tau} \cdot u[u]\big)_{k+\tau},$$

and therefore

$$\begin{aligned}\delta(u_{k+\tau} \cdot \xi_{k+1}) &= \delta u_{k+\tau} \cdot \xi_{k,k+1} + u_{k+\tau} \cdot \delta\xi_{k,k+1} \\ &= u_{k+\tau} \cdot \delta\xi_{k,k+1} + \big(\zeta_{k+\tau} \cdot u\big[\xi_{k,k+1} \cdot u\big]\big)_{k+\tau}.\end{aligned}$$

However, a discrete analogue of the formula $\frac{d}{dt}(u \cdot \zeta)$ is not immediately available, as the operation of time differentiation is not intrinsically present in the discrete setting. A workaround that we suggest is to view the transition from q_k to q_{k+1} as a motion along a straight line segment at a uniform rate:

$$q_{k+\tau} = (1-\tau)q_k + \tau q_{k+1}, \quad 0 \le \tau \le 1, \tag{21}$$

so that $q_{k+\tau} = q_k$ when $\tau = 0$ and $q_{k+\tau} = q_{k+1}$ when $\tau = 1$. Since the time step is h, the analogue of continuous-time velocity is $\Delta q_k / h$. From (21),

$$\frac{\Delta q_k}{h} = \frac{1}{h}\frac{dq_{k+\tau}}{d\tau},$$

leading to an interpretation of the operator

$$\frac{1}{h}\frac{d}{d\tau}$$

as a discrete analogue of time differentiation of continuous-time mechanics.

The discrete analogue of the term $\frac{d}{dt}(u \cdot \zeta)$ thus is

$$\begin{aligned}\frac{1}{h}\frac{d}{d\tau}\big(u_{k+\tau} \cdot \zeta_{k+\tau}\big) &= \frac{1}{h}\frac{du_{k+\tau}}{d\tau} \cdot \zeta_{k+\tau} + u_{k+\tau} \cdot \frac{1}{h}\frac{d\zeta_{k+\tau}}{d\tau} \\ &= u_{k+\tau} \cdot \frac{1}{h}\frac{d\zeta_{k+\tau}}{d\tau} + \big(\xi_{k,k+1} \cdot u\big[\zeta_{k+\tau} \cdot u\big]\big)_{k+\tau} \\ &= u_{k+\tau} \cdot \frac{\zeta_{k+1} - \zeta_k}{h} + \big(\xi_{k,k+1} \cdot u\big[\zeta_{k+\tau} \cdot u\big]\big)_{k+\tau}.\end{aligned}$$

Summarizing, the discrete analogue of (20) reads

$$u_{k+\tau} \cdot \delta\xi_{k,k+1} = u_{k+\tau} \cdot \frac{\zeta_{k+1} - \zeta_k}{h} + \big[u \cdot \xi_{k,k+1}, u \cdot \zeta_{k+\tau}\big]_{q_{k+\tau}},$$

which implies formula (19) for variation $\delta\xi$.

6 Hamel's Formalism and Nonholonomic Integrators

In this section we study some of the structure-preserving properties of discrete Hamel's formalism in the presence of velocity constraints.

6.1 The Lagrange–d'Alembert Principle

Assume now that there are *velocity constraints* imposed on the system. We confine our attention to constraints that are homogeneous in the velocity. Accordingly, we consider a configuration space Q and a distribution $\mathcal{D}$ on Q that describes these constraints. Recall that a distribution $\mathcal{D}$ is a collection of linear subspaces of the tangent spaces of Q; we denote these spaces by $\mathcal{D}_q \subset T_qQ$, one for each $q \in Q$. A curve $q(t) \in Q$ is said to ***satisfy the constraints*** if $\dot{q}(t) \in \mathcal{D}_{q(t)}$ for all t. This distribution is, in general, *nonintegrable*; i.e., the constraints are, in general, ***nonholonomic***.[2]

Consider a Lagrangian $L : TQ \to \mathbb{R}$. The equations of motion are given by the following ***Lagrange–d'Alembert principle***.

[2]Constraints are nonholonomic if and only if they cannot be rewritten as *position* constraints.

Definition 1. The ***Lagrange–d'Alembert equations of motion*** for the system are those determined by

$$\delta \int_a^b L(q, \dot{q})\, dt = 0,$$

where we choose variations $\delta q(t)$ of the curve $q(t)$ that satisfy $\delta q(a) = \delta q(b) = 0$ and $\delta q(t) \in \mathcal{D}_{q(t)}$ for each $t \in [a, b]$.

This principle is supplemented by the condition that the curve $q(t)$ itself satisfies the constraints. Note that we take the variation *before* imposing the constraints; that is, we do not impose the constraints on the family of curves defining the variation. This is well known to be important to obtain the correct mechanical equations (see [23] and [3] for discussions and references).

6.2 Ideal Constraints

As discussed in e.g. Suslov [37] and Chetaev [11], it is assumed in classical mechanics that the constraints imposed on the system can be replaced with the ***reaction forces***. This means that after the forces are imposed on the *unconstrained* system, the constraint distribution becomes a *conditional invariant manifold* of the *forced unconstrained* Lagrangian system whose dynamics on this invariant manifold is identical to that of the constrained system.

Definition 2. Constraints (either holonomic or nonholonomic) are called ***ideal*** if their reaction forces at each $q \in Q$ belong to the null space $\mathcal{D}_q^\circ \subset T_q^* Q$ of $\mathcal{D}_q$.

As shown in Suslov [37] and Chetaev [11], the reaction forces of ideal constraints are defined uniquely at each state $(q, \dot{q}) \in TQ$.

In summary, for a system subject to ideal constraints, the forced dynamics is equivalent to the Lagrange–d'Alembert principle. We refer the reader to books [37] and [11] for a more detailed exposition and history of the concept of ideal constraints.

6.3 The Constrained Hamel Equations

Given a system with velocity constraints, that is, a Lagrangian $L : TQ \to \mathbb{R}$ and constraint distribution $\mathcal{D}$, select the independent local vector fields

$$u_i : Q \to TQ, \quad i = 1, \ldots, n,$$

such that $\mathcal{D}_q = \text{span}\{u_1(q), \ldots, u_m(q)\}$, $m < n$. Each $\dot{q} \in TQ$ can be uniquely written as

$$\dot{q} = u(q) \cdot \xi^{\mathcal{D}} + u(q) \cdot \xi^{\mathcal{U}}, \tag{22}$$

where $u(q) \cdot \xi^{\mathcal{D}}$ is the component of $\dot{q}$ along $\mathcal{D}_q$ and $u(q) \cdot \xi^{\mathcal{U}}$ is the complementary component. Similarly, each $a \in T^*Q$ can be uniquely decomposed as

$$a = a_{\mathcal{D}} \cdot u^*(q) + a_{\mathcal{U}} \cdot u^*(q),$$

where $a_{\mathcal{D}} \cdot u^*(q)$ is the component of a along the dual of $\mathcal{D}_q$, where $a_{\mathcal{U}} \cdot u^*(q)$ is the complementary component, and where $u^*(q) \in T^*Q \times \cdots \times T^*Q$ denotes the dual frame of $u(q)$. Using the decomposition (22), the constraints read

$$\xi = \xi^{\mathcal{D}} \quad \text{or} \quad \xi^{\mathcal{U}} = 0. \tag{23}$$

Similar to (22), we write

$$\delta q = u(q) \cdot \zeta = u(q) \cdot \zeta^{\mathcal{D}} + u(q) \cdot \zeta^{\mathcal{U}}.$$

Recall that $\delta q(t) \in \mathcal{D}_{q(t)}$, which is equivalent to

$$\zeta = \zeta^{\mathcal{D}} \quad \text{or} \quad \zeta^{\mathcal{U}} = 0. \tag{24}$$

The Lagrange–d'Alembert principle in combination with (24) proves the following theorem:

Theorem 4. *The dynamics of a system with velocity constraints is represented by the* ***constrained Hamel equations***

$$\left(\frac{d}{dt} \frac{\partial l}{\partial \xi} - \left[\xi^{\mathcal{D}}, \frac{\partial l}{\partial \xi} \right]_q^* - u[l] \right)_{\mathcal{D}} = 0, \quad \xi^{\mathcal{U}} = 0,$$

coupled with the kinematic equation

$$\dot{q} = u(q) \cdot \xi^{\mathcal{D}}.$$

The ***constrained Lagrangian*** is the restriction of the Lagrangian to the constraint distribution. Thus, using Hamel's formalism, the constrained Lagrangian reads

$$l_c\left(q, \xi^{\mathcal{D}}\right) = l\left(q, \xi^{\mathcal{D}}, 0\right) \equiv l(q, \xi)|_{\xi^{\mathcal{U}}=0}.$$

It is straightforward to check that an alternative form of the constrained Hamel equations is

$$\frac{d}{dt}\frac{\partial l_c}{\partial \xi^{\mathcal{D}}} - \left(\left[\xi^{\mathcal{D}}, \frac{\partial l}{\partial \xi}\right]^*_q\right)_{\mathcal{D}} - u_{\mathcal{D}}[l_c] = 0, \quad \xi^{\mathcal{U}} = 0. \tag{25}$$

6.4 Continuous-Time Chaplygin Systems

As an important special case, consider ***commutative Chaplygin systems***, which are nonholonomic systems with a commutative symmetry group H, $\dim H = n - m$, and subject to the condition that at each $q \in Q$ the tangent space $T_q Q$ is the direct sum of the fiber of the constraint distribution and the tangent space to the orbit $\mathrm{Orb}_H(q)$ of H through q:

$$T_q Q = \mathcal{D}_q \oplus T_q \mathrm{Orb}_H(q). \tag{26}$$

To avoid technical difficulties, assume that the group H acts freely and properly on the configuration space Q, so that $\pi : Q \to Q/H$ is a principal fiber bundle, where π is the projection. Elements of Q/H and H are denoted x and s, respectively.

Following [3], define an ***Ehresmann connection*** by requiring that $\mathcal{D}_q$ and $T_q \mathrm{Orb}_H(q)$ are the ***horizontal and vertical spaces*** at $q \in Q$, respectively. These spaces are denoted H_q and V_q.

In other words, the nonholonomic kinematic constraints provide an Ehresmann connection on the principal bundle $\pi : Q \to Q/H$. Under the assumptions made above, the equations of motion drop to the reduced space $\mathcal{D}/H$, which in this special case is the same as $T(Q/H)$.

Recall that an Ehresmann connection A on a bundle Q is a *vertical-valued* one-form that is a *projection*; i.e., $A_q : T_q Q \to V_q$ is a linear map for each $q \in Q$ and $A(v) = v$ for all $v \in V_q$. In the bundle coordinates (x, s) introduced above, the form A reads

$$A = \omega^a \frac{\partial}{\partial s^a}, \quad \text{where} \quad \omega^a(q) = A^a_\alpha(x)\, dx^\alpha + ds^a, \tag{27}$$

where $\alpha = 1, \ldots, m$ and $a = m + 1, \ldots, n$. Recall also that the horizontal space $H_q = \ker A_q$, so that $T_q Q = H_q \oplus V_q$, in full agreement with (26).

The ***curvature*** of A is the vertical-valued two-form defined by

$$B(X, Y) = -A([\mathrm{hor}\, X, \mathrm{hor}\, Y]),$$

where hor X and hor Y are the horizontal parts of the vectors $X, Y \in T_q Q$. In the bundle coordinates (x, s),

$$B(X, Y) = B^a_{\alpha\beta} X^\alpha Y^\beta \frac{\partial}{\partial s^a},$$

where

$$B^a_{\alpha\beta} = \frac{\partial A^a_\alpha}{\partial r^\beta} - \frac{\partial A^a_\beta}{\partial r^\alpha}.$$

Recall that the constrained Lagrangian is the restriction of the Lagrangian onto the constraint distribution: $L_c = L|_{\mathcal{D}}$. For Chaplygin systems, L and L_c naturally reduce to the functions on TQ/H and $\mathcal{D}/H$, respectively. In the bundle coordinates (x, s), this simply means that L is independent of s,[3] i.e., $L = L(x, \dot{x}, \dot{s})$, and the constrained Lagrangian reads

$$L_c(x, \dot{x}) = L(x, \dot{x}, -A(x)\,\dot{x}).$$

The equations of motion for Chaplygin systems,

$$\frac{d}{dt}\frac{\partial L_c}{\partial \dot{x}} - \frac{\partial L_c}{\partial x} = \left\langle \frac{\partial L}{\partial \dot{s}}, \mathbf{i}_{\dot{x}}\, B \right\rangle, \tag{28}$$

or, in coordinates,

$$\frac{d}{dt}\frac{\partial L_c}{\partial \dot{x}^\alpha} - \frac{\partial L_c}{\partial x^\alpha} = -\frac{\partial L}{\partial \dot{s}^a} B^a_{\alpha\beta} \dot{x}^\beta,$$

$\alpha, \beta = 1, \ldots, m$, $a = m+1, \ldots, n$, were first derived, through a coordinate calculation, by Chaplygin in [9]. They are called the ***Chaplygin equations***.

Following [30], we now obtain equations (28) using Hamel's formalism. Recall that connection (27) is defined by the constraint distribution. Equivalently, the constraints read

$$\dot{s} + A(x)\,\dot{x} = 0.$$

Associated with the constraint distribution are the vector fields

$$u_\alpha = \operatorname{hor} \partial_{x^\alpha} = \partial_{x^\alpha} - A^a_\alpha \partial_{s^a} \quad \text{and} \quad u_a = \partial_{s^a}. \tag{29}$$

[3] For a noncommutative symmetry group, L depends on $(s, \dot{s})$ through the combination $s^{-1}\dot{s}$.

Using this frame,

$$\dot{q} = \dot{x}^\alpha u_\alpha + (\dot{s}^a + A^a_\alpha \dot{x}^\alpha) u_a,$$

$\alpha = 1, \ldots, m, a = m+1, \ldots, n$, or, equivalently,

$$\xi^{\mathcal{D}} = \dot{x}, \quad \xi^{\mathcal{U}} = \dot{s} + A(x)\,\dot{x}, \quad \dot{q} = u_{\mathcal{D}} \cdot \xi^{\mathcal{D}} + u_{\mathcal{U}} \cdot \xi^{\mathcal{U}},$$

and

$$l(x, \xi) = L\left(x, \xi^{\mathcal{D}}, \xi^{\mathcal{U}} - A(x)\xi^{\mathcal{D}}\right), \quad l_c\left(x, \xi^{\mathcal{D}}\right) = L\left(x, \xi^{\mathcal{D}}, -A(x)\xi^{\mathcal{D}}\right). \tag{30}$$

Evaluating the Jacobi–Lie brackets of the fields (29), one obtains

$$[u_\alpha, u_\beta] = \left(\frac{\partial A^a_\alpha}{\partial x^\beta} - \frac{\partial A^a_\beta}{\partial x^\alpha}\right)\frac{\partial}{\partial s^a} \equiv B^a_{\alpha\beta}\frac{\partial}{\partial s^a}, \quad [u_\alpha, u_a] = [u_a, u_b] = 0,$$

which implies

$$\left(\left[\xi^{\mathcal{D}}, \frac{\partial l}{\partial \xi}\right]^*_q\right)_{\mathcal{D}} = \left\langle \frac{\partial L}{\partial \dot{s}}, \mathbf{i}_{\dot{x}}\, B \right\rangle,$$

and thus (28) are just the constrained Hamel equations (25). Recall that B is the curvature of the form A.

An important remark is that, from Chaplygin's prospective, equations (28) are the Euler–Lagrange equations on the configuration space Q/H subject to a nonconservative force

$$\left\langle \frac{\partial L}{\partial \dot{s}}, \mathbf{i}_{\dot{x}}\, B \right\rangle.$$

This force may be interpreted as a shape component of the constraint reaction.

Another important remark is that $\dot{x}^\alpha$ in the classical literature are viewed as the reduced configuration velocities, whereas from the point of view of Hamel's formalism $\dot{x}^\alpha$ represent the velocity components along the non-commuting fields $u_\alpha, \alpha = 1, \ldots, m$.

6.5 *Discrete Nonholonomic Systems*

Discrete nonholonomic systems (nonholonomic integrators) were introduced by Cortés and Martínez in [12].

Let Q be a configuration space. According to Cortés and Martínez, a ***discrete nonholonomic mechanical system*** on Q is characterized by:

(i) A discrete Lagrangian $L^d : Q \times Q \to \mathbb{R}$;
(ii) A constraint distribution $\mathcal{D}$ on Q;
(iii) A ***discrete constraint manifold*** $\mathcal{D}^d \subset Q \times Q$ which has the same dimension as $\mathcal{D}$ and satisfies the condition $(q, q) \in \mathcal{D}^d$ for all $q \in Q$.

The dynamics is given by the following ***discrete Lagrange–d'Alembert principle*** (see [12]):

$$\sum_{k=1}^{N-1} \Big(D_1 L^d(q_k, q_{k+1}) + D_2 L^d(q_{k-1}, q_k) \Big) \delta q_k = 0, \ \delta q_k \in \mathcal{D}_{q_k}, \ (q_k, q_{k+1}) \in \mathcal{D}^d.$$

As pointed out in [14, 15], the discrete constraint manifold should be carefully selected when a continuous-time nonholonomic system is discretized. For the details on the properties of discrete nonholonomic systems we refer the reader to papers [12, 14, 15, 31]. In a recent paper [22], a somewhat different approach to discretizing nonholonomic systems has been suggested.

Cortés and Martínez also study the dynamics of discrete Chaplygin systems. In particular, given a continuous-time Chaplygin system, they discretize the *Euler–Lagrange equations with constraint reactions*, and conclude that, in general, the resulting discrete system is inconsistent with the outcome of their discrete Lagrange–d'Alembert principle. In other words, *the concept of ideal constraints is not acknowledged by their discretization procedure*.

Lynch and Zenkov [25, 26] proved that the discrete dynamics defined by the Lagrange–d'Alembert principle of Cortés and Martínez may lack *structural stability*. For example, it is possible for the discretization of a continuous-time Chaplygin system to change the dimension and/or stability of manifolds of relative equilibria of the said continuous-time system.

Below, we shall show that a different definition of the discrete Lagrange–d'Alembert principle exists that is free of the aforementioned issues. In particular, the dimension and stability of manifolds of relative equilibria are kept intact if this new version of the Lagrange–d'Alembert principle is utilized.

6.6 Hamel's Formalism for Discrete Nonholonomic Systems

Recall that the Lagrange–d'Alembert principle for continuous-time nonholonomic systems assumes that the variation of action is carried out before imposing the constraints. The outcome is the constrained Hamel equations, as discussed in Section 6.3. In a similar manner, we accept that the dynamics of a discrete nonholonomic system is determined by the ***discrete Lagrange–d'Alembert principle***, obtained by *first* taking the variation of the discrete action (14) using variations (18)

and (19) subject to the discrete analogue of (24), and *then* imposing the discrete constraints. We emphasize that the definition of the discrete Lagrange–d'Alembert principle given here *is not* the same as the definition of Cortés and Martínez reproduced in Section 6.5.

In the continuous-time setting, the constraints are represented by formula (23). We thus suggest that, under the same assumptions on the frame selection as in Section 6.3, the discrete constraints are

$$\xi_{k,k+1} = \xi^{\mathcal{D}}_{k,k+1} \quad \text{or} \quad \xi^{\mathcal{U}}_{k,k+1} = 0.$$

The discrete analogue of (24) is

$$\zeta_k = \zeta^{\mathcal{D}}_k \quad \text{or} \quad \zeta^{\mathcal{U}}_k = 0.$$

Arguing like in Section 6.3, one proves the discrete analogue of Theorem 4:

Theorem 5. *The dynamics of a discrete system with velocity constraints is given by the* ***constrained discrete Hamel equations***

$$\begin{aligned} &\tfrac{1}{h}\left(\mu_{k-1,k} - \mu_{k,k+1}\right)_{\mathcal{D}} + \left(\tau u\left[l^d\right]_{k-1+\tau} + (1-\tau)u\left[l^d\right]_{k+\tau}\right)_{\mathcal{D}} \\ &\quad + \left(\tau\left[\xi^{\mathcal{D}}_{k-1,k}, \mu_{k-1,k}\right]^*_{q_{k-1+\tau}} + (1-\tau)\left[\xi^{\mathcal{D}}_{k,k+1}, \mu_{k,k+1}\right]^*_{q_{k+\tau}}\right)_{\mathcal{D}} = 0, \end{aligned} \tag{31}$$

where $\mu_{k,k+1}$ *is given by formula* (16).

Of a special interest is the value $\tau = 1/2$, in which case one verifies that the order of approximation of (31) is 2.

6.7 Discrete Chaplygin Systems

Given a continuous-time Chaplygin system, we construct its discretization by utilizing the discrete Hamel formalism. Using the frame (29) and the continuous-time Lagrangians (30) introduced in Section 6.4, the discrete Lagrangian and the discrete constrained Lagrangian read

$$\begin{aligned} l^d(x_{k+\tau}, \xi_{k,k+1}) &= hl(x_{k+\tau}, \xi_{k,k+1}), \\ l^d_c\left(x_{k+\tau}, \xi^{\mathcal{D}}_{k,k+1}\right) &= l^d\left(x_{k+\tau}, \xi^{\mathcal{D}}_{k,k+1}\right) \equiv hl_c\left(x_{k+\tau}, \xi^{\mathcal{D}}_{k,k+1}\right). \end{aligned}$$

The dynamics is then given by equation (31), with

$$(\mu_{k,k+1})_{\mathcal{D}} = D_2 l^d_c\left(x_{k+\tau}, \xi^{\mathcal{D}}_{k,k+1}\right) \equiv D_2 l^d(x_{k+\tau}, \xi_{k,k+1})|_{\xi^{\mathcal{U}}_{k,k+1}=0}$$

and $\mu_{k,k+1}$ defined as in (16).

We now convert the dynamics into a discrete analogue of the Chaplygin equations (28). Following the general discretization procedure, we obtain the formulae

$$\xi^{\mathcal{D}}_{k,k+1} = \Delta x_k/h, \quad \xi^{\mathcal{U}}_{k,k+1} = \Delta s_k/h + A(x_{k+\tau})\Delta x_k/h.$$

Then, invoking (30), it is straightforward to see that

$$\begin{aligned} l^d(x_{k+\tau}, \xi_{k,k+1}) &= hl(x_{k+\tau}, \xi_{k,k+1}) \\ &= hL\left(x_{k+\tau}, \xi^{\mathcal{D}}_{k,k+1}, \xi^{\mathcal{U}}_{k,k+1} - A(x_{k+\tau})\xi^{\mathcal{D}}_{k,k+1}\right) \end{aligned} \tag{32}$$

and

$$\begin{aligned} l^d_c\left(x_{k+\tau}, \xi^{\mathcal{D}}_{k,k+1}\right) &= l^d\left(x_{k+\tau}, \xi^{\mathcal{D}}_{k,k+1}\right) = hl_c\left(x_{k+\tau}, \xi^{\mathcal{D}}_{k,k+1}\right) \\ &= hL_c\left(x_{k+\tau}, \xi^{\mathcal{D}}_{k,k+1}\right) = hL_c(x_{k+\tau}, \Delta x_k/h) \\ &= hL(x_{k+\tau}, \Delta x_k/h, -A(x_{k+\tau})\Delta x_k/h), \end{aligned} \tag{33}$$

where $L(x, \dot{x}, \dot{s})$ is the Lagrangian of the continuous-time Chaplygin system. From formulae (32), (33), and (29), one obtains

$$\begin{aligned} \mu_{k,k+1} &= D_2 l^d(x_{k+\tau}, \xi_{k,k+1}), \\ (\mu_{k,k+1})_{\mathcal{D}} &= D_2 l^d_c\left(x_{k+\tau}, \xi^{\mathcal{D}}_{k,k+1}\right) \\ &= hD_2 L_c\left(x_{k+\tau}, \xi^{\mathcal{D}}_{k,k+1}\right) = hD_2 L_c(x_{k+\tau}, \Delta x_k/h), \\ (\mu_{k,k+1})_{\mathcal{U}} &= D_3 l^d\left(x_{k+\tau}, \xi^{\mathcal{D}}_{k,k+1}, \xi^{\mathcal{U}}_{k,k+1}\right) \\ &= hD_3 L\left(x_{k+\tau}, \xi^{\mathcal{D}}_{k,k+1}, \xi^{\mathcal{U}}_{k,k+1} - A(x_{k+\tau})\xi^{\mathcal{D}}_{k,k+1}\right) \\ &= hD_3 L(x_{k+\tau}, \Delta x_k/h, \Delta s_k/h). \end{aligned}$$

Next, since we utilize the frame (29) just like in the continuous-time setting, the formula

$$\begin{aligned} \left(\left[\xi^{\mathcal{D}}_{k,k+1}, \mu_{k,k+1}\right]^*_{q_{k+\tau}}\right)_{\mathcal{D}} &= \left\langle \mu_{k,k+1}, \mathbf{i}_{\xi^{\mathcal{D}}_{k,k+1}} B_{q_{k+\tau}} \right\rangle \\ &= \left\langle (\mu_{k,k+1})_{\mathcal{U}}, \mathbf{i}_{\xi^{\mathcal{D}}_{k,k+1}} B_{q_{k+\tau}} \right\rangle = \left\langle (\mu_{k,k+1})_{\mathcal{U}}, \mathbf{i}_{\Delta x_k/h} B_{q_{k+\tau}} \right\rangle \\ &= \left\langle hD_3 L(x_{k+\tau}, \Delta x_k/h, -A(x_{k+\tau})\Delta x_k/h), \mathbf{i}_{\Delta x_k/h} B_{q_{k+\tau}} \right\rangle \end{aligned}$$

is established with an aid of the arguments of Section 6.4. To keep the formulae shorter, we write the latter expression as

$$\left\langle hD_3 L, \mathbf{i}_{\Delta x_k/h} B \right\rangle_{k+\tau}.$$

Finally,

$$\begin{aligned}\left(u[l^d](q_{k+\tau}, \xi_{k,k+1})\right)_{\mathcal{D}} &= D_1 l^d \left(x_{k+\tau}, \xi^{\mathcal{D}}_{k,k+1}\right) \\ &= D_1 l^d_c \left(x_{k+\tau}, \xi^{\mathcal{D}}_{k,k+1}\right) = h D_1 L_c(x_{k+\tau}, \Delta x_k / h).\end{aligned}$$

Summarizing, the dynamics of the discrete Chaplygin system reads

$$\begin{aligned}\tfrac{1}{h}\left((D_2 L_c)_{k+\tau} - (D_2 L_c)_{k-1+\tau}\right) &= \tau (D_1 L_c)_{k-1+\tau} + (1-\tau)(D_1 L_c)_{k+\tau} \\ &+ \tau \left\langle D_3 L, \mathbf{i}_{\Delta x_{k-1}/h}\, B\right\rangle_{k-1+\tau} + (1-\tau)\left\langle D_3 L, \mathbf{i}_{\Delta x_k/h}\, B\right\rangle_{k+\tau}, \end{aligned} \tag{34}$$

where $(D_i L_c)_{k+\tau} := D_i L_c(x_{k+\tau}, \Delta x_k / h)$. Remarkably, the discrete Chaplygin equations (34) are identical to the discretization of continuous-time Chaplygin equations (28) viewed as forced Euler–Lagrange dynamics. For more details on this latter discretization of the Chaplygin equations see [12] and [26].

6.8 Stability

In this section we link up stability of relative equilibria of Chaplygin systems with structural stability of nonholonomic integrators.

Consider a commutative Chaplygin system characterized by the Lagrangian L and constraint distribution $\mathcal{D}$, as discussed in Section 6.4. Assume that the dynamics of the Chaplygin system (28) is invariant with respect to the action of a commutative group G on Q/H.[4] Often such a situation is the result of the original system being invariant with respect to the semidirect product $G \circledS H$ of the groups G and H. The elements of the group G are denoted g, and we assume that the action of G on Q/H is free and proper, so that Q/H has the structure of a principal fiber bundle with the structure group G. Thus, locally, there exist the bundle coordinates $x = (r, g)$ on Q/H.

Under certain assumptions (see e.g. [21] and [39]), the dynamics has a manifold (whose dimension equals $\dim G$) of relative equilibria. These relative equilibria are the solutions of (28) that in the bundle coordinates (r, g) read

$$r = r_e, \quad \dot{g} = \eta_e.$$

As established in Karapetyan [21], some of these relative equilibria may be *partially asymptotically stable*. Karapetyan justifies stability using the center manifold stability analysis, which, for nonholonomic systems under consideration, reduces

[4] The general noncommutative setting is not studied in this paper and will be the subject of a future publication.

to verifying that the nonzero spectrum of linearization of (28) at the relative equilibrium of interest belongs to the left half-plane.[5]

Partially asymptotically stable relative equilibria are a part of the ω-limit set of dynamics (28). Similarly, relative equilibria that become partially asymptotically stable after the time reversal are a part of the α-limit set of dynamics (28).

It is important for a long-term numerical integrator to preserve the manifold of relative equilibria and their stability types. Indeed, if the limit sets of an integrator are different from the limit sets of the continuous-time dynamics, this integrator will not adequately simulate the continuous-time dynamics over long time intervals.

As shown in [25, 26], the discrete Lagrange–d'Alembert principle of Cortés and Martínez may produce discretizations that fail to preserve the manifold of relative equilibria. For instance, it may change the dimension of this manifold, thus changing the structure of the limit sets. Informally, the origin of this effect can be explained as follows: The discrete Lagrange–d'Alembert principle of Cortés and Martínez is capable of introducing reactions that correspond to non-ideal constraints. A typical example would be a reaction force with a dissipative component, whose discrete counterpart causes the aforementioned changes of relative equilibria.

A relative equilibrium of a discrete Chaplygin system (34) with commutative symmetry is a solution

$$r_k = \text{const}, \quad \Delta g_k = \text{const}.$$

Assume now that $\tau = 1/2$ in equations (34). Let $h > 0$ be the time step.

Theorem 6 (Lynch and Zenkov [25, 26]). *Discretization* (34)[6] *preserves the manifold of relative equilibria of the continuous-time Chaplygin system; that is, $r_k = r_e$, $\Delta g_k = h\eta_e$ is a relative equilibrium of the discretization* (34) *if and only if $r = r_e$, $\dot{g} = \eta_e$ is a relative equilibrium of the continuous-time system. The conditions for partial asymptotic stability of the equilibria of the continuous-time system and of its discretization are the same.*

Summarizing, the discrete Lagrange–d'Alembert principle proposed in this paper ensures the necessary conditions for structural stability of the associated nonholonomic integrator.

[5]The stability analysis of relative equilibria of nonholonomic systems has a long history, starting form the results of Walker [38] and Routh [36]; see [39] for some of this history and for the energy-momentum method for nonholonomic systems.

[6]Equations (34) were derived in [25, 26] without the use of the discrete Hamel formalism.

7 The Spherical Pendulum

Here we outline the results of Zenkov, Leok, and Bloch [40] on the applications of the discrete Hamel formalism to the energy-momentum-preserving integrator for the spherical pendulum.

7.1 The Spherical Pendulum as a Degenerate Rigid Body

Consider a spherical pendulum whose length is r and mass is m. We view the pendulum as a point mass moving on the sphere of radius r centered at the origin of $\mathbb{R}^3$. The development here is based on the representation

$$\dot{\boldsymbol{\mu}} = \boldsymbol{\mu} \times \boldsymbol{\xi} + mg\,\boldsymbol{\gamma} \times \boldsymbol{a}, \tag{35}$$

$$\dot{\boldsymbol{\gamma}} = \boldsymbol{\gamma} \times \boldsymbol{\xi} \tag{36}$$

of pendulum's dynamics; that is, the pendulum is viewed as a rigid body rotating about a fixed point. This rigid body is of course *degenerate*, with the inertia tensor $\mathcal{I} = \operatorname{diag}\{mr^2, mr^2, 0\}$. Here $\boldsymbol{\xi}$ is the angular velocity of the pendulum, $\boldsymbol{\mu}$ is its angular momentum, $\boldsymbol{\gamma}$ is the unit vertical vector (and thus the constraint $\|\boldsymbol{\gamma}\| = 1$ is imposed), and $\boldsymbol{a}$ is the vector from the origin to the center of mass, which for the pendulum is its bob, all written relative to the body frame. Throughout the rest of the paper, the boldface characters represent three-dimensional vectors. The kinetic and potential energies of the pendulum are

$$K = \tfrac{1}{2}\langle \boldsymbol{\mu}, \boldsymbol{\xi} \rangle \equiv \tfrac{1}{2}\langle \mathcal{I}\,\boldsymbol{\xi}, \boldsymbol{\xi} \rangle, \quad U = mg\langle \boldsymbol{\gamma}, \boldsymbol{a} \rangle \equiv mgr\gamma^3,$$

and the Lagrangian reads

$$l(\boldsymbol{\xi}, \boldsymbol{\gamma}) = \tfrac{1}{2}\langle \mathcal{I}\,\boldsymbol{\xi}, \boldsymbol{\xi} \rangle - mg\langle \boldsymbol{\gamma}, \boldsymbol{a} \rangle. \tag{37}$$

This Lagrangian is invariant with respect to rotations about $\boldsymbol{\gamma}$, and therefore the vertical component of the *spatial angular momentum* is conserved.

There are two independent components in the vector equation (35). We emphasize that the representation (35) and (36) of the dynamics of the pendulum, though redundant, eliminates the use of local coordinates on the sphere, such as spherical coordinates. Spherical coordinates, while being a nice theoretical tool, introduce artificial singularities at the north and south poles. That is, the equations of motion written in spherical coordinates have denominators vanishing at the poles, but this has nothing to do with the physics of the problem and is solely caused by the geometry of the spherical coordinates. Thus, the use of spherical coordinates in calculations is not advisable.

Another important remark is that the length of the vector $\boldsymbol{\gamma}$ is a *conservation law* of equations (35) and (36), and thus adding the constraint $\|\boldsymbol{\gamma}\| = 1$ *does not* result in a system of differential-algebraic equations. The latter are known to be a nontrivial object for numerical integration.

Equations (35) and (36) may be interpreted in a number of ways. In the above, we viewed them as the dynamics of a degenerate rigid body. Since the moment of inertia relative to the direction of the vector $\boldsymbol{a}$ is zero, the third component of the body angular momentum vanishes,

$$\mu_3 = \frac{\partial l}{\partial \xi^3} = 0,$$

and thus there are only two nontrivial equations in (35). Thus, one needs five equations to capture the pendulum dynamics. This reflects the fact that rotations about the direction of the pendulum have no influence on the pendulum's motion.

The dynamics then can be simplified by setting

$$\xi^3 = 0, \tag{38}$$

which leads to an interpretation of equations (35) and (36) as the dynamics of the *heavy Suslov top*[7] with a rotationally-invariant inertia tensor and constraint (38).

Summarizing, the dynamics becomes

$$\dot{\boldsymbol{\mu}} = mg\boldsymbol{\gamma} \times \boldsymbol{a}, \quad \dot{\boldsymbol{\gamma}} = \boldsymbol{\gamma} \times \boldsymbol{\xi}, \quad \langle \boldsymbol{\xi}, \boldsymbol{a} \rangle = 0. \tag{39}$$

These equations are in fact the constrained Hamel equations, the reconstruction equation, and the constraint, written in the redundant configuration coordinates $\boldsymbol{\gamma} = (\gamma^1, \gamma^2, \gamma^3)$; see [40] for details. Recall that the length of $\boldsymbol{\gamma}$ is the conservation law, so that the constraint $\|\boldsymbol{\gamma}\| = 1$ does not need to be imposed, but the appropriate level set of the conservation law has to be selected.

Our discretization is based on this point of view, i.e., the discrete dynamics will be written in the form of discrete Hamel's equations. The discrete dynamics will posses the discrete version of the conservation law $\|\boldsymbol{\gamma}\| = \text{const}$, so that the algorithm should be capable, in theory, of preserving the length of $\boldsymbol{\gamma}$ up to machine precision.

7.2 Variational Discretization for the Spherical Pendulum

The integrator for the spherical pendulum is constructed by discretizing equations (39).

[7] See [33, 37], and [2] for the Suslov top.

Let the positive real constant h be the time step. Applying the mid-point rule to (37), the discrete Lagrangian is computed to be

$$l^d(\boldsymbol{\xi}_{k,k+1}, \boldsymbol{\gamma}_{k+1/2}) = \tfrac{h}{2}\langle \mathcal{I}\,\boldsymbol{\xi}_{k,k+1}, \boldsymbol{\xi}_{k,k+1}\rangle - hU(\boldsymbol{\gamma}_{k+1/2}).$$

Here $\boldsymbol{\xi}_{k,k+1} = (\xi^1_{k,k+1}, \xi^2_{k,k+1}, 0)$ is the discrete analogue of the angular velocity $\boldsymbol{\xi} = (\xi^1, \xi^2, 0)$ and $\boldsymbol{\gamma}_{k+1/2} = \frac{1}{2}(\boldsymbol{\gamma}_{k+1} + \boldsymbol{\gamma}_k)$. The discrete dynamics then reads

$$\tfrac{1}{h}\,\mathcal{I}\left(\boldsymbol{\xi}_{k,k+1} - \boldsymbol{\xi}_{k-1,k}\right) = mg\big(\boldsymbol{\gamma}_{k+1/2} + \boldsymbol{\gamma}_{k-1/2}\big) \times \boldsymbol{a}, \tag{40}$$

$$\tfrac{1}{h}\big(\boldsymbol{\gamma}_{k+1/2} - \boldsymbol{\gamma}_{k-1/2}\big) = \tfrac{1}{2}\big(\boldsymbol{\gamma}_{k+1/2} + \boldsymbol{\gamma}_{k-1/2}\big) \times \tfrac{1}{2}\big(\boldsymbol{\xi}_{k,k+1} + \boldsymbol{\xi}_{k-1,k}\big). \tag{41}$$

We reiterate that there is a certain flexibility in setting up the discrete analogue (41) of the continuous-time reconstruction equation (36). Our choice may be justified in a number of ways, one of them being energy conservation by the discrete dynamics.

The structure-preserving properties of the proposed integrator for the spherical pendulum are summarized in the following theorem.

Theorem 7 (Zenkov, Leok, and Bloch [40]). *The discrete spherical pendulum dynamics* (40) *and* (41) *preserves the energy, the vertical component of the spatial angular momentum, and the length of* $\boldsymbol{\gamma}$.

We refer the readers to [40] for the proof and details.

7.3 Simulations

Here we present simulations of the dynamics of the spherical pendulum using the integrator constructed in Section 7.2. For simulations, we select the parameters of the system and the time step to be

$$m = 1 \text{ kg}, \quad r = 9.8 \text{ m}, \quad h = .2 \text{ s}.$$

The trajectory of the bob of the pendulum with the initial conditions

$$\xi^1_0 = .6 \text{ rad/s}, \qquad \xi^2_0 = 0 \text{ rad/s}, \tag{42}$$

$$\gamma^1_0 = .3 \text{ m}, \qquad \gamma^2_0 = .2 \text{ m}, \qquad \gamma^3_0 = -\sqrt{1 - \big(\gamma^1_0\big)^2 - \big(\gamma^2_0\big)^2}\ \text{m} \tag{43}$$

is shown in Figure 1a. As expected, it reveals the quasiperiodic nature of pendulum's dynamics.

Figure 1b shows pendulum's trajectory that crosses the equator. This simulation demonstrates the global nature of the algorithm, and also seems to do a good job of hinting at the geometric conservation properties of the method.

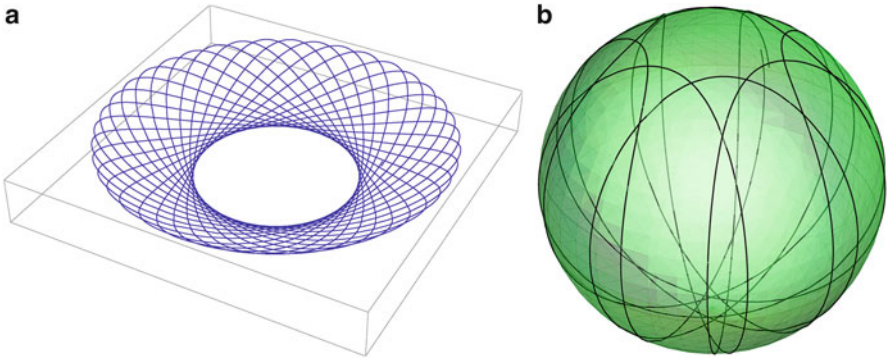

Fig. 1 Trajectories of the pendulum calculated with the Hamel integrator. (**a**) Pendulum's trajectory on S^2 for initial conditions (42) and (43). (**b**) Pendulum's trajectory on S^2 that crosses the equator

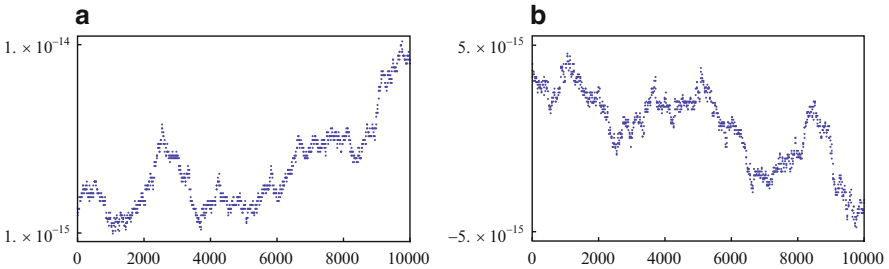

Fig. 2 Numerical properties of the Hamel integrator for the pendulum. (**a**) Preservation of the length of $\boldsymbol{\gamma}$. (**b**) Conservation of energy

Theoretically, if one solves the nonlinear equations exactly, and in the absence of numerical roundoff error, the Hamel variational integrator should exactly preserve the length constraint and the energy. In practice, Figure 2a demonstrates that $\|\boldsymbol{\gamma}\|$ stays to within unit length to about 10^{-14} after 10,000 iterations. Figure 2b demonstrates numerical energy conservation, and the energy error is to about $5 \cdot 10^{-15}$ after 10,000 iterations. Indeed, one notices that the energy error tracks the length error of the simulation, which is presumably due to the relationship between the length of the pendulum and the potential energy of the pendulum. The drift in both appear to be due to accumulation of numerical roundoff error, and could possibly be reduced through the use of compensated summation techniques.

For the comparison of the Hamel integrator with simulations using the generalized Störmer–Verlet method and the RATTLE method see [40]. We point out here that the energy error for the Hamel integrator is smaller than those of the Störmer–Verlet and RATTLE methods.

8 Conclusions

This paper introduced the discrete Hamel formalism and demonstrated its utility in nonholonomic mechanics. Future work will include further study of the properties of this formalism, as well as the development of discrete Hamel's formalism on manifolds in general, and on Lie groups and homogeneous spaces as important special cases. It would be also interesting to relate the discrete Hamel formalism to the results of Iglesias et al. [19].

Acknowledgements The authors would like to thank Jerry Marsden for his inspiration and helpful discussions in the beginning of this work, and the reviewers for useful remarks. The research of DVZ was partially supported by NSF grants DMS-0604108, DMS-0908995 and DMS-1211454. The research of KRB was partially supported by NSF grants DMS-0604108 and DMS-0908995. DVZ would like to acknowledge support and hospitality of Mathematisches Forschungsinstitut Oberwolfach, the Fields Institute, and the Beijing Institute of Technology, where a part of this work was carried out.

References

1. Ball, K., Zenkov, D.V., Bloch, A.M.: Variational structures for Hamel's equations and stabilization. In: Proceedings of the 4th IFAC, pp. 178–183 (2012)
2. Bloch, A.M.: Nonholonomic Mechanics and Control. Interdisciplinary Applied Mathematics, vol. 24. Springer, New York (2003)
3. Bloch, A.M., Krishnaprasad, P.S., Marsden, J.E., Murray, R.: Nonholonomic mechanical systems with symmetry. Arch. Ration. Mech. Anal. **136**, 21–99 (1996)
4. Bloch, A.M., Krishnaprasad, P.S., Marsden, J.E., Ratiu, T.S.: The Euler–Poincaré equations and double bracket dissipation. Commun. Math. Phys. **175**, 1–42 (1996)
5. Bloch, A.M., Marsden, J.E., Zenkov, D.V.: Quasivelocities and symmetries in nonholonomic systems. Dyn. Syst. Int. J. **24**(2), 187–222 (2009)
6. Bobenko, A.I., Suris, Yu.B.: Discrete Lagrangian reduction, discrete Euler–Poincaré equations, and semidirect products. Lett. Math. Phys. **49**, 79–93 (1999)
7. Bobenko, A.I., Suris, Yu.B.: Discrete time Lagrangian mechanics on Lie groups, with an application to the Lagrange top. Commun. Math. Phys. **204**(1), 147–188 (1999)
8. Bou-Rabee, N., Marsden, J.E.: Hamilton–Pontryagin integrators on Lie groups part I: Introduction and structure-preserving properties. Found. Comput. Math. **9**(2), 197–219 (2009)
9. Chaplygin, S.A.: On the motion of a heavy body of revolution on a horizontal plane. Phys. Sect. Imperial Soc. Friends Phys. Anthropol. Ethnograph. **9**, 10–16 (1897) (in Russian)
10. Chetaev, N.G.: On Gauss' principle. Izv. Fiz-Mat. Obsc. Kazan. Univ. Ser. 3 **6**, 68–71 (1932–1933) (in Russian)
11. Chetaev, N.G.: Theoretical Mechanics. Springer, New York (1989)
12. Cortés, J., Martínez, S.: Nonholonomic integrators. Nonlinearity **14**, 1365–1392 (2001)
13. Euler, L.: Decouverte d'un nouveau principe de Mecanique. Mémoires de l'académie des sciences de Berlin **6**, 185–217 (1752)
14. Fedorov, Yu.N., Zenkov, D.V.: Discrete nonholonomic LL systems on Lie groups. Nonlinearity **18**, 2211–2241 (2005)
15. Fedorov, Yu.N., Zenkov, D.V.: Dynamics of the discrete Chaplygin sleigh. Discrete Continuous Dyn. Syst. (extended volume), 258–267 (2005)

16. Hamel, G.: Die Lagrange–Eulersche Gleichungen der Mechanik. Z. Math. Phys. **50**, 1–57 (1904)
17. Hamilton, W.R.: On a general method in dynamics, part I. Philos. Trans. R. Soc. Lond. **124**, 247–308 (1834)
18. Hamilton, W.R.: On a general method in dynamics, part II. Philos. Trans. R. Soc. Lond. **125**, 95–144 (1835)
19. Iglesias, D., Marrero, J.C., Martín de Diego, D., Martínez, E.: Discrete nonholonomic Lagrangian systems on Lie groupoids. J. Nonlinear Sci. **18**(3), 221–276 (2008)
20. Kane, C., Marsden, J.E., Ortiz, M., West, M.: Variational integrators and the Newmark algorithm for conservative and dissipative mechanical systems. Int. J. Numer. Math. Eng. **49**(10), 1295–1325 (2000)
21. Karapetyan, A.V.: On the problem of steady motions of nonholonomic systems. J. Appl. Math. Mech. **44**, 418–426 (1980)
22. Kobilarov, M., Marsden, J.E., Sukhatme, G.S.: Geometric discretization of nonholonomic systems with symmetries. Discrete Continuous Dyn. Syst. Ser. S **3**(1), 61–84 (2010)
23. Kozlov, V.V.: The problem of realizing constraints in dynamics. J. Appl. Math. Mech. **56**(4), 594–600 (1992)
24. Lagrange, J.L.: Mécanique Analytique. Chez la Veuve Desaint (1788)
25. Lynch, C., Zenkov, D.: Stability of stationary motions of discrete-time nonholonomic systems. In: Kozlov, V.V., Vassilyev, S.N., Karapetyan, A.V., Krasovskiy, N.N., Tkhai, V.N., Chernousko, F.L. (eds.) Problems of Analytical Mechanics and Stability Theory. Collection of Papers Dedicated to the Memory of Academician Valentin V. Rumyantsev, pp. 259–271. Fizmatlit, Moscow (2009) (in Russian)
26. Lynch, C., Zenkov, D.V.: Stability of relative equilibria of discrete nonholonomic systems with semidirect symmetry. Preprint (2010)
27. Marsden, J.E., Ratiu, T.S.: Introduction to Mechanics and Symmetry. Texts in Applied Mathematics, vol. 17, 2nd edn. Springer, New York (1999)
28. Marsden, J.E., West, M.: Discrete mechanics and variational integrators. Acta Numerica **10**, 357–514 (2001)
29. Marsden, J.E., Pekarsky, S., Shkoller, S.: Discrete Euler–Poincaré and Lie–Poisson equations. Nonlinearity **12**, 1647–1662 (1999)
30. Maruskin, J.M., Bloch, A.M., Marsden, J.E., Zenkov, D.V.: A fiber bundle approach to the transpositional relations in nonholonomic mechanics. J. Nonlinear Sci. **22**(4), 431–461 (2012)
31. McLachlan, R., Perlmutter, M.: Integrators for nonholonomic mechanical systems. J. Nonlinear Sci. **16**, 283–328 (2006)
32. Moser, J., Veselov, A.: Discrete versions of some classical integrable systems and factorization of matrix polynomials. Commun. Math. Phys. **139**(2), 217–243 (1991)
33. Neimark, Ju.I., Fufaev, N.A.: Dynamics of Nonholonomic Systems. Translations of Mathematical Monographs, vol. 33. AMS, Providence, RI (1972)
34. Peng, Y., Huynh, S., Zenkov, D.V., Bloch, A.M.: Controlled Lagrangians and stabilization of discrete spacecraft with rotor. Proc. CDC **51**, 1285–1290 (2012)
35. Poincaré, H.: Sur une forme nouvelle des équations de la mécanique. CR Acad. Sci. **132**, 369–371 (1901)
36. Routh, E.J.: Treatise on the Dynamics of a System of Rigid Bodies. MacMillan, London (1860)
37. Suslov, G.K.: Theoretical Mechanics, 3rd edn. GITTL, Moscow–Leningrad (1946) (in Russian)
38. Walker, G.T.: On a dynamical top. Q. J. Pure Appl. Math. **28**, 175–184 (1896)
39. Zenkov, D.V., Bloch, A.M., Marsden, J.E.: The energy-momentum method for the stability of nonholonomic systems. Dyn. Stab. Syst. **13**, 128–166 (1998)
40. Zenkov, D.V., Leok, M., Bloch, A.M.: Hamel's formalism and variational integrators on a sphere. Proc. CDC **51**, 7504–7510 (2012)